BIOTECHNOLOGY: PHARMACEUTICAL ASPECTS

Current Trends in Monoclonal Antibody Development and Manufacturing

Edited by
Steven J. Shire
Wayne Gombotz
Karoline Bechtold-Peters
James Andya

Springer

AAPS PRESS

Biotechnology: Pharmaceutical Aspects

For other titles published in this series, go to
www.springer.com/series/7364

Biotechnology: Pharmaceutical Aspects

Volume I: *Pharmaceutical Profiling in Drug Discovery for Lead Selection*
R.T. Borchardt, E.H. Kerns, C.A. Lipinski, D.R. Thakker, B. Wang

Volume II: *Lypophilization of Biopharmaceuticals*
H.R. Constantino, M.J. Pikal

Volume III: *Methods for Structural Analysis of Protein Pharmaceuticals*
W. Jiskoot, D.J.A. Crommelin

Volume IV: Optimizing *the "Drug-Like" Properties of Leads in Drug Discovery*
R.T. Borchardt, E.H. Kerns, M.J. Hageman, D.R. Thakker, J.L. Stevens

Volume V: *Prodrugs: Challenges and Rewards, Parts 1 and 2*
V.J. Stella, R.T. Borchardt, M.J. Hageman, R. Oliyai, H. Maag, J.W. Tilley

Volume VI: *Solvent Systems and Their Selection in Pharmaceutics and Biopharmaceutics*
P. Augustijns, M.E. Brewster

Volume VII: *Drug Absorption Studies: In Situ, In Vitro and In Silico Models*
C. Ehrhardt, K.J. Kim

Volume VIII: *Immunogenicity of Biopharmaceuticals*
M. van de Weert, E. H. Møller

Volume IX: *Advances in Bioactivation Research*
A. Elfarra

Volume X: *Nanotechnology in Drug Delivery*
M. M. de Villiers, P. Aramwit, G. S. Kwon

Volume XI: *Current Trends in Monoclonal Antibody Development and Manufacturing*
S.J. Shire, W. Gombotz, K. Bechtold-Peters, J. Andya

Current Trends in Monoclonal Antibody Development and Manufacturing

Edited by

Steven J. Shire
Genentech, Inc.,
San Francisco, CA
USA

Wayne Gombotz
Omeros Corporation
Seattle, WA
USA

Karoline Bechtold-Peters
Boehringer Ingelheim
Pharma, Biberach
Germany

James Andya
Genentech, Inc.,
San Francisco, CA
USA

Springer

AAPS PRESS

Editors
Steven J. Shire
Genentech, Inc.,
San Francisco, CA
USA

Karoline Bechtold-Peters
Boehringer Ingelheim
Pharma, Biberach
Germany

Wayne Gombotz
Omeros Corporation
Seattle, WA
USA

James Andya
Genentech, Inc.,
San Francisco, CA
USA

ISBN 978-0-387-76642-3 e-ISBN 978-0-387-76643-0
DOI 10.1007/978-0-387-76643-0
Springer New York Dordrecht Heidelberg London

Library of Congress Control Number: 2009938432

Preface

Monoclonal antibodies (MAbs) have rapidly developed into one of the major tools in our arsenal for fighting human diseases. Currently, about 25% of the biological therapeutics that are being developed are MAbs or some form thereof. This book was initially planned as a formulation/analytical volume on MAb development, but the editors realizing the huge proliferation of development of MAbs felt that therapeutics might be better served with a book that touches on a variety of topics essential to the development of this exciting class of drugs. Hopefully you, the reader, will concur with this assessment and appreciate the efforts of all our contributors to this volume. Thus, this book represents a compilation of chapters that summarizes some of the recent progress in the pharmaceutical development of MAbs. It is divided into several different sections that span design of MAbs to the upstream and downstream processing steps required for production and manufacture of MAb therapeutics.

A summary of novel techniques used to humanize MAbs by Dennis along with a chapter on design of single-domain antigen-binding fragments by Ghassabeh et al. are presented in the section on "Design of Therapeutic Antibodies." The former addresses some new ways that MAbs are being engineered to reduce the potential of the immune response to murine-derived MAbs. The latter deals with the novel design of single heavy chain MAb fragments with comparable affinity to their related full-length MAbs, but that may be less costly to produce.

In the section on "Expression and Production of MAbs" some of the latest advances in the use of mammalian cell culture systems to produce therapeutic MAbs are discussed. The first chapter of this section by Bleck discusses a versatile transfection technology utilizing replication deficient retroviral vectors that allows for rapid expression of MAbs in different mammalian cell types. The second chapter by Heath describes the experiences and advances made in mammalian cell culture technology at Amgen. Their goal is to develop a cell culture platform for process development of MAbs to increase speed to market while minimizing resource commitments during early phase development.

This section is followed by two chapters on recovery and purification technologies that emphasize the efforts to develop and scale-up chromatographic processes. The first chapter in this section by Myers et al. discusses a case study involving the challenges and issues of scale-up and transfer of the chimeric MAb Remicade to a second manufacturing site. A detailed account is provided on the process changes that occurred during transfer and the changes that were made to ensure comparability of the products produced at the two

facilities. The second chapter by Walter and Gottschalk addresses the recent uses of disposable devices for tangential flow filtration (TFF) and chromatography for downstream MAb processing. Advantages and limitations of the technology over fixed stainless steel equipment are discussed with an emphasis on the cost of using disposables.

In the section on "Formulation and Delivery" two previously well-cited review publications are reproduced. The first chapter in this section by Daugherty and Mrsny reviews the general challenges of formulating complex biomolecules such as MAbs and then discusses potential administration by several delivery routes. The second chapter by Shire et al. reviews the challenges of developing and manufacturing high concentration MAb formulations for SC administration. The third chapter in the section by Bechtold-Peters summarizes innovative alternate approaches to lyophilization for the production of formulated bulk and solid dosage forms of therapeutic MAbs.

Recent progress and experience in the analysis of these complex biomolecules is presented in the section entitled "Analytics and Specification Setting for MAbs." The first chapter by Klakamp, reproduced from a previous publication, discusses the use of BiaCore and KinExA technologies to characterize binding affinities and kinetics of binding of MAbs to their therapeutic targets. This chapter summarizes the technologies as well as the challenges and limitations of the methods. The second chapter in this section by Harris et al. discusses the contributions to microheterogeneity of MAbs. In particular, glycosylation and covalent modifications as well as experimental modalities to characterize these modifications are reviewed. This chapter is followed by a review of the use of analytical ultracentrifugation (AUC) by Andya et al. to characterize fragmentation and aggregation of MAbs. This chapter also includes suggested methods to improve the precision of the AUC measurements. The final chapter in this section by Harn et al. explores the use of several biophysical methods to characterize and compare MAbs from different biotechnology companies. This chapter demonstrates that the use of different biophysical methods combined with changes in solution conditions such as temperature, pH, and ionic strength can provide a sensitive way to monitor conformational stability of MAbs.

The next section deals with MAb pharmacokinetic and immunogenicity issues. In particular, the first chapter by Raju discusses the complex role of glycosylation of MAbs and how the glycosylation can impact potential degradation of the protein backbone by proteases. The second chapter by Stas et al. discusses the potential for immunogenic responses to the administered MAbs, and the risks for altered pharmacokinetics. General strategies and methods to assess immunogenicity during MAb development are also reviewed.

The final section of this book deals with new classes as well as production methods of MAbs. The first chapter by Yansura and Reilly discuss novel technology to express recombinant derived full-length MAbs in *E. coli*, which may have advantages in cost and faster production rates. The second chapter in this section by Senter addresses the development of drug-conjugated MAbs for cancer therapy whereby the MAb is used to target a small molecule drug to a specific site on a cancer cell resulting in greater specific activity with lower systemic toxicity. This chapter discusses the challenges of choosing an appropriate linker chemistry that is sufficiently stable to minimize cytotoxic drug exposure during MAb circulation, but is still capable of releasing the drug once the MAb is internalized into the target cell.

As mentioned earlier, we decided to expand the scope of this volume and hopefully we have been successful in touching on the many aspects of MAb development and manufacture. The successful completion of this book was made possible by the assistance of a large number of people to whom we are very grateful. In particular, we wish to thank and acknowledge the contributions from many in the industry and academia who took time from their very busy schedules to share their expertise with all of us. We also want to thank the publisher, in particular Kathleen Lyons and Renata Hutter for their wonderful support.

San Francisco, CA — Steven J. Shire
Seattle, WA — Wayne Gombotz
Biberach, Germany — Karoline Bechtold-Peters
San Francisco, CA — James Andya

Contents

Contributors

C. Allan
RegeneRx Biopharmaceuticals, Bethesda, MD, USA

James D. Andya
Early Stage Pharmaceutical Development, Genentech, Inc.,
South San Francisco, CA, USA

Joann Bannon
Centocor Research & Development, Malvern, PA, USA

John E. Battersby
Protein Analytical Chemistry Department, Genentech, Inc.
S. San Francisco, CA, USA

Karoline Bechtold-Peters
Boehringer Ingelheim Pharma GmbH & Co. KG, Biberach, Germany

Corinne Bensimon
Canadian Molecular Imaging Center of Excellence (CMICE), MDS Nordion,
University of Ottawa Heart Institute, Ottawa, ON, Canada

Gregory T. Bleck
Cell Line Engineering, Gala Biotech, A Catalent Pharma Solutions
Company, Middleton, WI, USA

Edward T. Chin
Analytical Chemistry, Genentech, Inc., South San Francisco, CA, USA

Armando J. Cordoba
Protein Analytical Chemistry, Genentech, Inc., South San Francisco,
CA, USA

Ann L. Daugherty
Genentech, Inc., South San Francisco, CA, USA

Mark S. Dennis
Department of Antibody Engineering, Genentech, Inc., South San Francisco, CA, USA

Andrew W. Drake
Amgen Fremont, Inc., Fremont, CA, USA

Y. Gansemans
Algonomics NV, Gent-Zwijnaarde, Belgium

Gholamreza Hassanzadeh Ghassabeh
VIB, Flanders Institute for Biotechnology, Vrije Universiteit Brussel, Brussels, Belgium

Wayne Gombotz
Omeros Corporation, Seattle, WA, USA

Uwe Gottschalk
Sartorius-Stedim Biotech GmbH, Göttingen, Germany

N. Harn
Department of Pharmaceutical Chemistry, University of Kansas, Lawrence, KS, USA

Reed J. Harris
Protein Analytical Chemistry Department, Genentech, Inc., South San Francisco, CA, USA

Carole Heath
Process Development, Amgen Inc., Seattle, WA, USA

Andy J.S. Jones
Analytical Chemistry, Genentech, Inc., South San Francisco, CA, USA

Camille Keating
ImClone Systems, Branchburg, NJ, USA

Rodney G. Keck
Protein Analytical Chemistry, Genentech, Inc., South San Francisco, CA, USA

Scott L. Klakamp
Takeda San Francisco, S. San Francisco, CA USA

I. Lasters
Algonomics NV, Gent-Zwijnaarde, Belgium

Victor T. Ling
Protein Analytical Chemistry, Genentech, Inc., South San Francisco, CA, USA

Jun Liu
Late Stage Pharmaceutical and Processing Development, Genentech, Inc.
S. San Francisco, CA USA

Frank Macchi
Protein Analytical Chemistry, Genentech, Inc., South San Francisco, CA, USA

Melinda Marian
Clinical and Experimental Pharmacology, Genentech, Inc.,
South San Francisco, CA, USA

C. Russell Middaugh
Department of Pharmaceutical Chemistry, University of Kansas, Lawrence,
KS, USA

R.J. Mrsny
Department of Pharmacy & Pharmacology, Epithelial Cell Biology,
University of Bath, Bath, UK

Serge Muyldermans
VIB, Flanders Institute for Biotechnology, Vrije Universiteit Brussel,
Brussels, Belgium

Michele M. Myers
Centocor Research & Development, Radnor, PA, USA

David G. Myszka
Center for Biomolecular Interaction Analysis, University of Utah,
Salt Lake City, UT, USA

Donald S. Neblock
Centocor Research & Development, Malvern, PA, USA

M. Perkins
Human Genome Sciences, Rockville, MD, USA

T. Shantha Raju
Discovery Research, Centocor R&D Inc., Radnor, PA, USA

Russell Redshaw BSc, MBA,
Science and Technology Partnerships, MDS Nordion, Ottawa,
ON, Canada

Dorothea E. Reilly
Early Stage Cell Culture, Genentech, Inc., South San Francisco,
CA, USA

Dirk Saerens
VIB, Flanders Institute for Biotechnology, Vrije Universiteit Brussel,
Brussels, Belgium

Peter D. Senter
Seattle Genetics, Inc., Bothell, WA, USA

Zahra Shahrokh
Department of Pharmaceutical and Analytical Development, Transkaryotic Therapies, Cambridge, MA, USA

Steven J. Shire
Late Stage Pharmaceutical and Processing Development, Genentech, Inc., South San Francisco, CA, USA

Bao-Jen Shyong
Protein Analytical Chemistry, Genentech, Inc., South San Francisco, CA, USA

Don Sinclair
Clinical PK/PD, Genentech, Inc., South San Francisco, CA, USA

T. Spitznagel
Human Genome Sciences, Rockville, MD, USA

P. Stas
Algonomics NV, Gent-Zwijnaarde, Belgium

Joachim K. Walter
emergene AG, Teufen, Switzerland

Peter W. Wojciechowski
Advanced Technologies and Regenerative Medicine, LLC, Raynham, MA, USA

Daniel G. Yansura
Antibody Engineering, Genentech, Inc., South San Francisco, CA, USA

Chapter 1

Introduction

Wayne R. Gombotz and Steven J. Shire

1. Overview of Monoclonal Antibodies

Monoclonal antibodies (MAbs) are one of the fastest growing classes of all pharmaceutical products. In 2007, a total of 26 therapeutic MAbs were approved in the U.S. market (Table 1-1), which was valued at more than $12,612 million (Frost & Sullivan 2008). Currently, more than 200 MAbs are in clinical study with more than 600 in preclinical development (Reuters 2008). They play a major role in treating a wide variety of diseases including cancer, infectious disease, allergy, autoimmune disease and inflammation. MAbs now belong to a well-established drug class, that has a high success rate from first in human studies to regulatory approval: Typically 25% (Reichert et al. 2005), which compares favorably with the 11% success rate for small molecule drugs (Kola and Landis 2004).

Monoclonal antibodies are produced in the following main forms:

- Murine – 100% mouse protein
- Chimeric – approximately 65% human and 35% mouse protein
- Humanized – 95% human and 5% mouse protein
- Fully human – 100% human protein

All full length MAbs approved to date have been produced in mammalian cells. Common production cell types include Chinese hamster ovary (CHO) cells, NS0 mouse myeloma cells and hybridoma cells. The PERC6 cell line has been recently introduced as new mammalian expression system for MAbs although, a commercial product has yet to be approved.

In addition to full length MAbs, the development of antibody fragments is growing in clinical importance (Carter 2006). Antibody fragments possess several attributes that differ from full length MAbs, and these may offer potential advantages in some clinical settings. In imaging applications, antibody fragments can penetrate tumors more efficiently and are cleared more rapidly from the body than full length MAbs, ultimately giving rise to improved tumor-to-non-tumor binding ratios (Wu and Senter 2005). Antibody

From: *Current Trends in Monoclonal Antibody Development and Manufacturing,*
Biotechnology: Pharmaceutical Aspects, DOI 10.1007/978-0-387-76643-0_1,
Edited by: S.J. Shire et al.

Table 1-1. Commercial monoclonal antibody products approved in the United States.

Brand name	Molecule	Type of MAb and MW	Year approved	Company	Indication	Administration route
Avastin	Bevacizumab	Humanized IgG1, 149 kDa	2004	Genentech	Metastatic carcinoma of colon or rectum, binds VEGF	IV infusion
Bexxar	Tositumomab and I-131 Tositumomab	Murine IgG2λ, 150 kDa	2003	Corixa and GSK	CD20 positive follicular NonHodgkin's lymphoma	IV infusion
Campath	Alemtuzmab	Humanized IgG1k, 150 kDa	2001	Ilex Oncology; Millenium and Berlex	B-cell chronic lymphocytic leukemia	IV infusion
CEA-Scan	Acrituomab	Murine Fab, 50 kDa	1996	Immunomedics	Imaging agent for colorectal cancer	IN infusion or injection
Cimzia	Certolizumab pegol	Humanized Fab' fragment bound to PEG, 91 kDa	2008	UCB Pharma	Crohn's disease	SC
Erbitux	Centuximab	Chimeric IgG1k, 152 kDa	2004	ImClone and BMS	Treatment of EGFR-expressing colorectal carcinoma	IV infusion
Herceptin	Trastuzumab	Humanized IgG1k, 170 kDa	1998	Genentech	Metastatic breast cancer with tumor overexpression of HER2 protein	IV infusion
Humira	Adalimumab	Human IgG1k, 148 kDa	2002	CAT and Abbott	RA patients not responding to DMARDs. Blocks TNF-alpha	SC
Lucentis	Ranibizumab	Humanized IgG1k fragment, 48 kDa	2006	Genentech	Age-related wet macular degeneration	Intravitreal injection
Mylotarg	Gemtuzumab ozogamicin	Humanized IgG4k conjugated to calicheamicin	2000	Celltech and Wyeth	Treatment of CD33 positive acute myeloid leukemia	IV infusion
OncoScint	Satumomab pendetide	Murine IgG1k conjugated to GYK-DTPA	1992	Cytogen	Imaging agent for colorectal and ovarian cancer	IV injection
Orthoclone OKT	Muromomab-CD3	Murine IgG2a, 170 kDa	1986	Ortho Biotech	Reversal of acute kidney transplant rejection (anti CD3-antigen)	IV Injection
ProstaScint	Indium-111 capromab pendetide	Murine IgG1k conjugated to GYK-DTPA	1996	Cytogen	Imaging for prostate cancer	IV injection
Raptiva	Efalizumab	Humanized IgG1k	2003	Xoma and Genentech	Chronic moderate to severe plaque psoriasis, binds to CD11a subunit of LFA-1	SC

Remicade	Infliximab	Chimeric, 70% corresponds to human IgG1 heavy chain and human kappa light chain constant region, 149 kDa	1998	Centocor	RA and Crohn's disease, binds TNF alpha	IV infusion
ReoPro	Abciximab	Chimeric Fab, 48 kDa	1994	Centocor and Lilly	Reduction of acute blood clot related complications	IV injection and infusion
Rituxan	Riruximab	Chimeric IgG1k with murine light and heavy chain variable region, 145 kDa	1997	IDEC and Genentech	NonHodgkin's lymphoma, binds to anti CD20-antigen	IV infusion
Simulect	Basiliximab	Chimeric IgG1k, 144 kDa	1998	Novartis	Prevention of acute kidney transplant rejection, IL-2 receptor antagonist	IV injection and infusion
Soliris	Eculizumab	Humanized IgG2/IgG4, 148 kDa	2007	Alexion	Treatment of paroxysmal nocturnal hemoglobinuria (PNH)	IV infusion
Synagis	Palivizumab	Humanized IgG1k, 148 kDa	1998	MedImmune	Prevention replication of respiratory syncytial virus (RSV)	IM injection
Tysarbi	Natalizumab	Humanized IgG4k	2004	Biogen IDEC	MS relapse	IV infusion
Vectibix	Panitumumab	Human IgG2k, 147 kDa	2006	Amgen	Treatment of patients with EGFr-expressing metastatic colorectal cancer	IV injection
Verluma	Nofetumomab	Murine Fab	1996	Boehringer Ingelheim and Dupont Merk	Imaging agent for lung cancer	IV injection
Xolair	Omalizumab	Humanized IgG1k, 149 kDa	2003	Genentech with Novartis and Tanox	Asthma	SC
Zenapax	Daclizumab	Humanized IgG1, 144 kDa	1997	Roche	Prophylaxis of acute organ rejection in patients receiving renal transplants	IV infusion
Zevalin	Ibritumomab-Tiuxetan	Murine IgG1k-covalenrtly linked to Tiuxetan, 148 kDa	2002	IDEC	NonHodgkin's lymphoma, binds to CD20 antigen and irradiates cells with Ytterium-90	IV infusion

fragments provide a simple way to avoid Fc-dependent cell-effector functions. After pegylation, these fragments can exhibit a wide range of pharmacokinetic properties. Since they are much smaller in size and less complex in structure than full length MAbs, antibody fragments can be expressed and produced in non-mammalian systems such as *E. coli*, resulting in a significant reduction in the cost of goods.

2. Advantages of MAbs as Drugs

There are a number of reasons why MAbs have become increasingly popular for commercial development. The action of MAbs is highly specific, binding to a single antigen, leading to fewer side effects than conventional drugs. MAbs can also be conjugated to another therapeutic entity such as a toxin or radioisotope. The delivery of this entity to a target site can reduce potential side effects. Radioisotope-labeled MAbs can be used as both therapeutic and imaging agents. Advances in molecular biology and protein engineering have enabled the rapid development of highly specific MAbs with high binding affinities for their targets. MAb fragments and MAbs with different isotypes can also be produced to provide control over the pharmacokinetics and effector function of the drug product.

3. Challenges with MAb Development

Prior to the approval of the first full-length MAb therapeutic, Orthoclone OKT3 in 1986, this class of protein therapeutics did not have a high success rate for commercialization. In many of the early clinical trials, patients had immune reactions due to generation of their own antibodies to the administered MAbs (Ezzell et al. 2001). Much of this occurred because, the early MAbs were made with hybridoma technology and were of mouse origin. Furthermore, it was found that dosing was fairly high, on the order of mg/kg, presenting significant challenges for manufacturing and commercialization. The emergence of MAbs as a major class of protein biotechnology drugs, reflects the development of humanization technology, and highly efficient and cost effective mammalian cell culture production and recovery methods. Humanization technology involves incorporation of murine (mouse) residues responsible for binding to target into a human immunoglobulin framework, which after further protein engineering refinement, often results in immunoglobulin sequences as high as 95% human origin. Such humanized therapeutic MAbs are preferred for chronic administration, since the risk of generation of human anti-mouse antibodies (HAMA response) is reduced. The development of high yield processes meets the needs of large markets coupled with chronic and high dosing regimens. Currently, a majority of approved MAbs is administered by the intravenous (IV) route, but indications that involve treatment on an outpatient basis or at home will require alternate routes such as subcutaneous (SC) and intramuscular (IM). The development of SC formulations for MAbs will pose additional challenges for the pharmaceutical scientist to develop high concentration (>100 mg/mL) formulations that can be manufactured with adequate stability, and that can be easily administered (Shire et al. 2004). Future development of MAbs will include using the antibodies to specifically deliver drugs or toxins and kill targeted cells. These so-called “conjugated antibodies” may lead to

additional formulation, and manufacturing challenges involving development of appropriate linkers, that remain stable until delivery to the target.

References

Carter P (2006) Potent antibody therapeutics by design. Nat Rev 6:343–357

Ezzell C (2001) Magic bullets fly again. Sci Am 285:34–41

Frost & Sullivan (2008) Technical Report #N167-52, U.S. Biotechnology Therapeutic Monoclonal Antibodies Market

Kola I, Landis J (2004) Can the pharmaceutical industry reduce attrition rates? Nat Rev Drug Discov 3:711–715

Reichert JM, Rosensweig CJ, Faden LB, Dewitz MC (2005) Monoclonal antibody successes in the clinic. Nat Biotechnol 23:1073–1078

http://www.Reuters.com Number of monoclonal antibody products in development nearly tripled in last decade, According to Tufts Center for the Study of Drug Development, March 11, 2008

Shire SJ, Shahrokh Z, Liu J (2004) Challenges in the development of high protein concentration formulations. J Pharm Sci 93:1390–1402

Wu AM, Senter PD (2005) Arming antibodies: prospects and challenges for immunoconjugates. Nat Biotechnol 23:1137–1146

Part I

Design Of Therapeutic MABS

Chapter 2

CDR Repair: A Novel Approach to Antibody Humanization

Mark S. Dennis

Abbreviations

CDRs	Complementarity determining regions
Fab	Antigen binding fragment consisting of the light chain and the variable and first constant domains of the heavy chain
HAMA	Human anti-mouse antibodies
VH	Variable heavy domain
VL	Variable light domain

Hybridoma technology has enabled the rapid production of a large number of monoclonal antibodies with interesting biological properties. Their use in a therapeutic setting, however, can lead to the generation of a human anti-mouse antibody (HAMA) response in patients despite the high degree of sequence similarity shared between human and mouse antibodies. This has prompted efforts to make hybridoma antibodies appear more human through the construction of chimeras, (Morrison et al. 1984) and through a process known as antibody humanization (Riechmann et al. 1988; Verhoeyen et al. 1988).

The modular nature of antibodies makes the swapping of domains a relatively simple process. A chimera consisting of the mouse variable heavy (VH) and variable light (VL) domains recombinantly fused to human heavy and light constant domains is a simple way to reduce HAMA response. Yet, despite 60–75% homology to human, murine variable domains may still elicit a HAMA response.

Humanization is a process used to further reduce the content of murine residues in the variable domains. Each VL and VH domain adapts the immunoglobulin fold and presents three loops protruding from one end, called complimentarity determining regions or CDRs, for interaction with antigen. The rest of the variable domain functions as a framework to support and stabilize the conformation of these CDRs. The transfer of the six CDR loops from murine variable domains to human variable frameworks is considered a CDR graft (Jones et al. 1986). Compared to the chimera, this

From: *Current Trends in Monoclonal Antibody Development and Manufacturing,*
Biotechnology: Pharmaceutical Aspects, DOI 10.1007/978-0-387-76643-0_2,
Edited by: S.J. Shire et al.

step further reduces the amount of murine sequence present. Unfortunately, a loss in binding affinity is generally incurred during this process and so additional engineering steps may be required (Riechmann et al. 1988; Foote and Winter 1992).

Fig. 2-1a provides a simple conceptual image of the differences between murine, chimeric and humanized antibodies. Due to the high homology

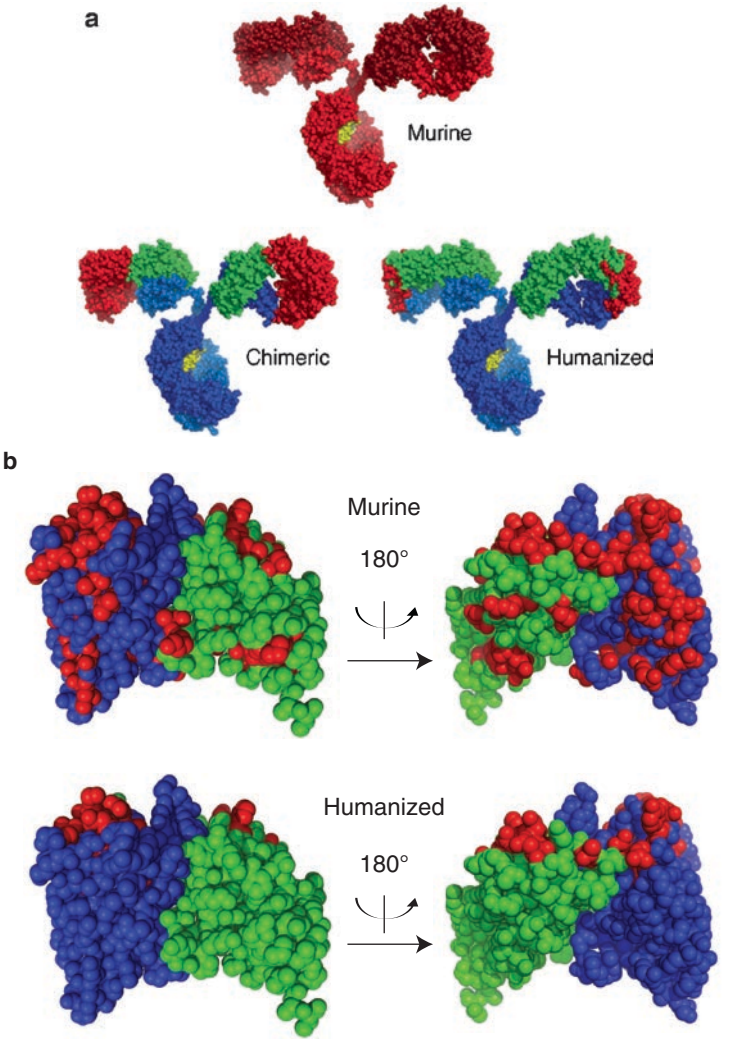

Fig. 2-1. A comparison of murine, chimeric and humanized antibodies. (**a**) A conceptual representation of murine, chimeric and humanized antibodies with amino acid residues derived from the murine antibody are depicted in *red*. The chimera consists of murine VL and VH domains (*red*) fused to human constant light (*green*) and constant heavy (*blue*) domains. The humanized antibody consists entirely of human light (*green*) and heavy (*blue*) chain sequence with exception of the six CDR sequences that have been transferred from the murine antibody (*red*). (**b**) Differences between murine 4D5 and humanized 4D5 (1FVC (Berman et al. 2000)) variable domains are depicted in a way that takes into account sequence identity between murine and human sequences. In this representation, the CDR sequences are oriented at the *top* of the image. The sequence of CDR-H3 is highly variable and is not included in this depiction

between murine and human variable domains, however, this representation is somewhat misleading. Residues that are identical between mouse and human should ideally be excluded from a calculation of an antibody's "human-ness." The variable domains of murine 4D5 and humanized 4D5 (trastuzumab) are depicted in Fig. 2-1b. Both the murine and humanized sequences are compared to their closest human germline, respectively, and residues that differ are colored in red. Here, the degree to which murine residues are reduced by humanization is actually greater than what is suggested in Fig. 2-1a, since many of the CDR residues from the respective germline are identical. In either representation, however, humanization clearly reduces the number of murine residues.

Multiple approaches, discussed below, have been described for improving the success of making a CDR graft, that retains the original antigen binding properties or for restoring binding affinity to the CDR graft. Each of these methods requires an appreciation for the structural components inherent in the antibody variable domains.

1. Important Considerations

Antibody variable domains share a high degree of sequence and structural homology across species and across germlines (Padlan 1994); however, while a few changes in variable domain sequence can have only a very subtle influence on the structure, they can have a profound impact on antigen binding (Eigenbrot et al. 1993). When humanizing an antibody, there are three important factors to consider, each of which can influence antigen binding: delineation of the CDRs, the choice of a human acceptor framework and positions that differ between murine and human frameworks that can influence CDR structure and affect antigen binding. These components are also important when humanizing antibodies from other species (e.g. rat, rabbit or hamster). How each of these factors is utilized can depend upon the humanization method used, nevertheless each should be considered.

Historically and conceptually, there have been three approaches that define the CDRs. The first, a sequence based definition, arose as antibody sequences became available. Kabat and Wu compared multiple variable domain sequences and recognized that the hypervariable regions in antibodies were likely to determine antigen specificity (Wu and Kabat 1970; Kabat and Wu 1971). As antibody X-ray structures were determined, it became apparent that these hypervariable regions mapped to loops with a limited number of conformations extending from the immunoglobulin variable domain β-sandwich. This led Chothia and Lesk to develop a structural definition for CDRs, and propose a set of canonical CDR conformations that were based upon loop length and a few key residues directing main-chain conformation (Chothia and Lesk 1987; Chothia et al. 1989). Later, as multiple antibody–antigen complex structures were determined, yet another definition of the CDRs emerged based upon residues found to be in contact with antigen (MacCallum et al. 1996). While all three of these CDR definitions generally map to similar locations within the VL and VH domains, there are slight differences as to where each CDR starts and stops (Fig. 2-2). The largest discrepancies are at the beginning of CDR-L1, where both the sequence and structural definitions include residues, that are not commonly observed to be in contact with antigen, and the

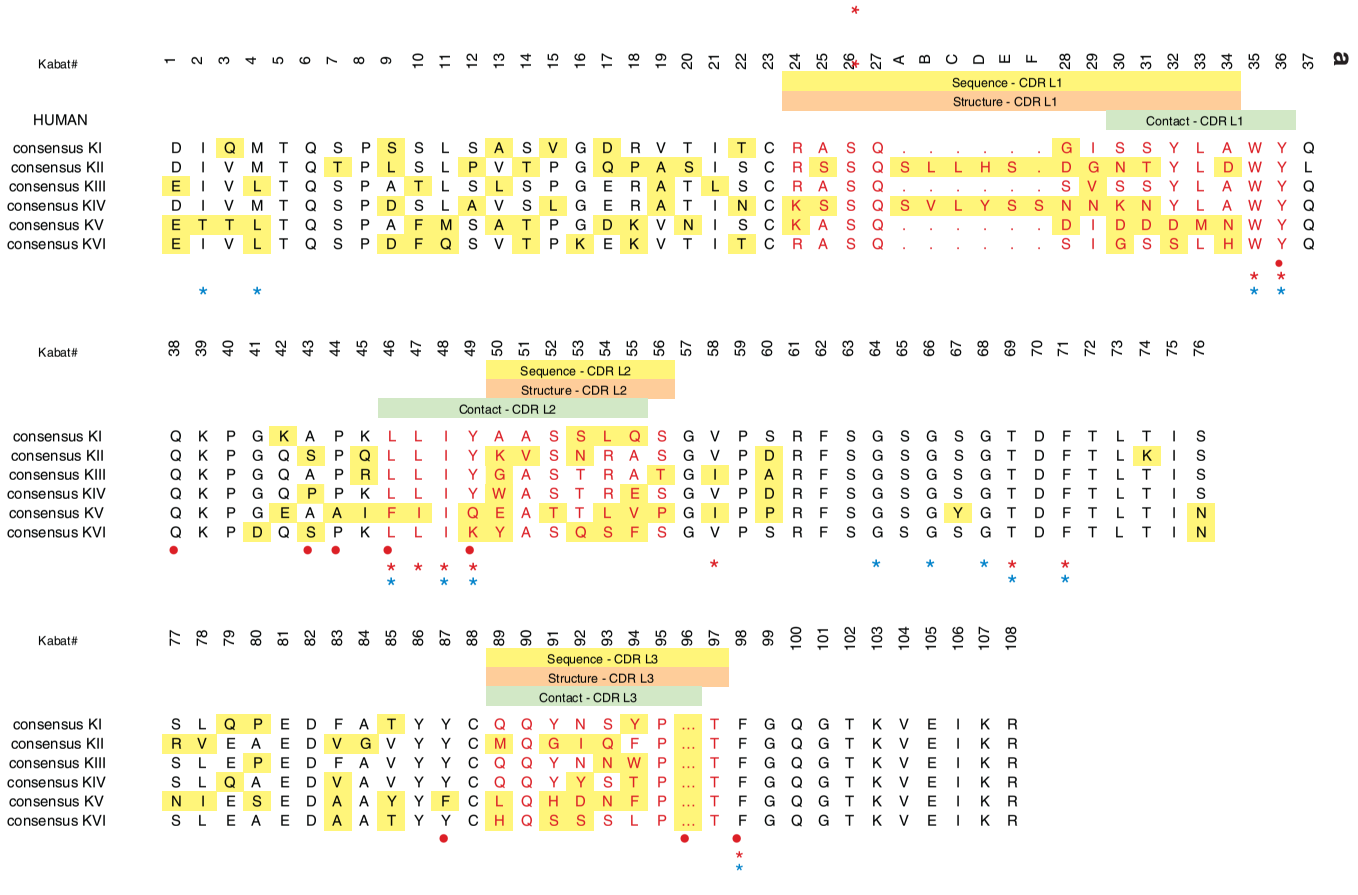

Fig. 2-2. CDR delineation, residues in the VL–VH interface and vernier positions in human consensus variable domains. Human consensus variable domain sequences representing each VL_{kappa} and VH subgroup (derived from Honegger 2007) are shown numbered according to Kabat (Kabat et al. 1991). Non-homologous residues between the consensus sequences are *shaded*. CDR locations in (**a**) VL (CDR-L1, CDR-L2, and CDR-L3) and

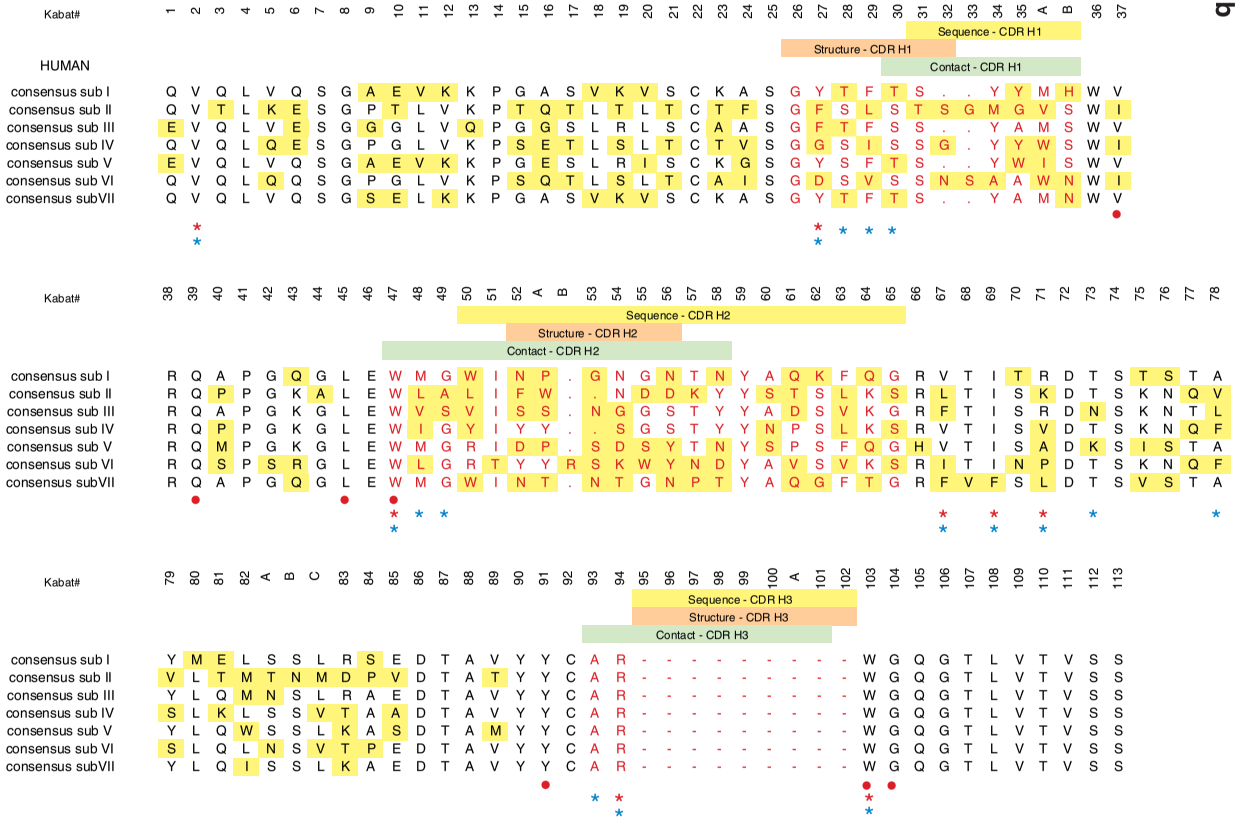

Fig. 2-2. (continued) (**b**) VH (CDR-H1, CDR-H2, and CDR-H3) delineated by sequence hypervariability (*yellow bar* (Kabat and Wu 1971; Kabat et al. 1991)), loop structure (*orange bar* (Chothia and Lesk 1987)) or antigen contact (*green bar* (MacCallum et al. 1996)) are depicted, as well as the location of vernier positions defined by Foote and Winter (1992) (*blue star*) or Padlan (limited to those observed in greater than 70% of studied antibody structures and having at least six van der Waals contacts, *red star* (Padlan 1994)). Residues potentially affecting the VL–VH interface are indicated by a *red dot* (those observed in greater than 80% of studied antibody structures (Padlan 1994))

end of CDR-H2, which contains hypervariable sequence, but is neither part of the protruding loop nor commonly found in antigen contacts.

Another important consideration is the human acceptor framework to be used for a particular humanization for which there are several schools of thought. A common approach is to identify and graft the CDRs into the human germline, that is most homologous to the murine sequence. This has an advantage that the framework environment presenting the CDRs is minimally changed. Related to this, the CDRs may also be grafted into a calculated human consensus framework sequence, based upon the most homologous human germline subgroup (Fig. 2-2). In either case, the choice of framework can be made based upon the overall homology of the variable domain (Queen et al. 1989) or just homology within the framework (Wu et al. 1999) or just within the CDRs (Tan et al. 2002; Hwang et al. 2005). Using homology to select a human framework has a disadvantage in that each humanization can result in a new VL and VH combination. Additional engineering steps may be required to optimize the large VL/VH interface for each combination.

An alternate strategy is to utilize a single stable framework that has been validated in the clinic for generating the CDR graft, regardless of the parent antibody sequence. For example, the $VL_{kappa\ I}$ and VH_{III} consensus frameworks are derived from the most abundant human VL and VH subclasses and has been used to humanize a number of murine antibodies (Carter et al. 1992; Presta et al. 1993, 1997, 2001; Werther et al. 1996; Adams et al. 2006). Utilizing a previously validated framework may reduce the likelihood of protein stability or manufacturing problems and, thereby facilitate clinical development.

CDRs do not function independently on the rest of the antibody. They consist of residues that interact with antigen, but also include residues that interact with the framework and neighboring CDRs. How CDRs are presented and structurally supported by the framework is critical to their ability to interact with antigen. The VL–VH interface is mostly composed of framework residues, yet this interface is also influenced by certain CDR positions. Vernier positions provide a foundation for the CDRs; they can directly influence framework–CDR interactions and as a result can affect antigen binding (Foote and Winter 1992). In addition, other positions that influence VL/VH domain interactions or on occasion are involved in unusual antigen contacts can also play an important role. An analysis of antibody crystal structures has suggested that there are about 30 positions distributed throughout the variable domains that have the potential to influence CDR packing and function (Foote and Winter 1992; Padlan 1994). These are noted in Fig. 2-2 and are illustrated in Fig. 2-3. Depending upon the human acceptor framework selected, these positions will differ from the parent antibody. Further, the importance of any particular vernier position will vary depending on the antibody/antigen system. The interaction between vernier positions and CDR anchor residues (CDR residues that interact with the framework) is often the source of humanization problems, and the identification of the optimal combination of vernier positions can be a major challenge.

2. Humanization Approaches

Typically, the first step during humanization is to generate a CDR graft in which, the CDRs (or some portion of the CDRs (Kashmiri et al. 2005)) are grafted onto a human acceptor framework. As mentioned previously, this

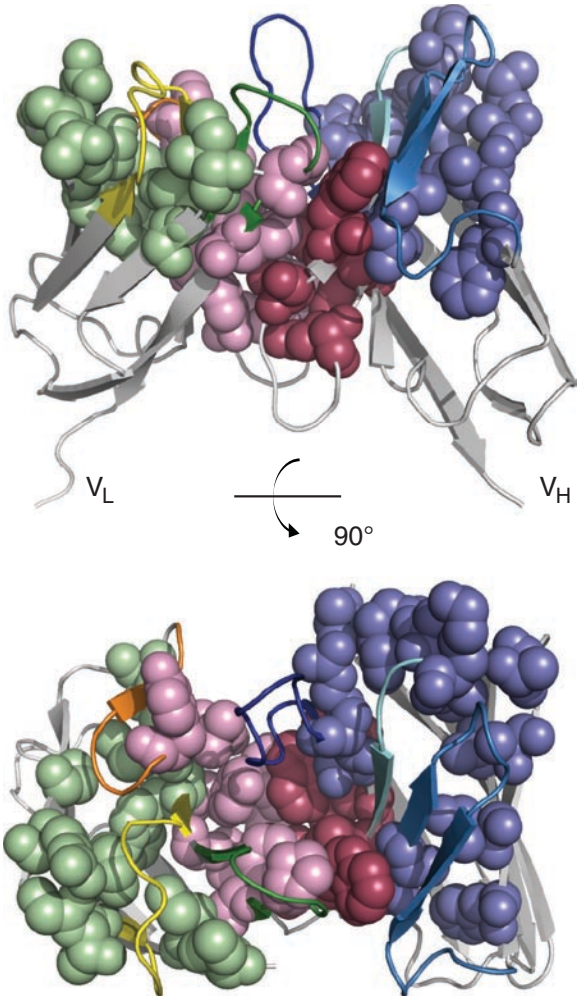

Fig. 2-3. A structural representation of variable domain vernier positions. CDRs are colored (CDR-L1 is *yellow*, CR-L2 is *orange*, CDR-L3 is *dark green*, CDR-H1 is *light blue*, CDR-H2 is *blue* and CDR-H3 is *dark blue*) on the VL and VH framework (*white*). The side chains of vernier positions (*green* for VL and *blue* for VH) and domain interface positions (*pink* for VL and *salmon* for VH) from Fig. 2-2 are depicted using spheres. Humanized 4D5 (1FVC (Berman et al. 2000)) was used as the model (Eigenbrot et al. 1993)

often results in partial or complete loss of antigen binding. The most common approach to restoring high affinity binding is to identify and replace key residues in the human acceptor framework with residues from the parent antibody. Molecular modeling has frequently been used to identify potentially inappropriate packing between CDR anchor residues and vernier positions. Alternatively, the appropriate combination of framework changes can be derived empirically through combinatorial techniques (Baca et al. 1997; Rader et al. 2000; Lee et al. 2004). These approaches attempt to reestablish the original CDR/framework environment by utilizing information gained from the parent murine framework to incorporate changes into the human acceptor framework. This approach to repair the acceptor framework (framework repair)

has been used quite successfully (Kettleborough et al. 1991; Carter et al. 1992; Presta et al. 1993, 1997, 2001; Werther et al. 1996; Tsurushita et al. 2005; Adams et al. 2006) and has been relied on careful modeling of the human and murine variable domains. Several iterations may be required to identify the minimal set of murine positions that need to be substituted into the human framework.

Framework repair can be facilitated by the selection of an appropriate framework from the most homologous human germline, or a consensus framework (Fig. 2-2) that is derived from the most homologous human subgroup (Tsurushita et al. 2005). This method enables the retention of many potentially important vernier residues by default. An alternative approach is to utilize only CDR sequence homology for framework selection, thus identifying a framework that is capable of presenting the proper canonical CDR structure, regardless of sequence variations in the framework (Tan et al. 2002; Hwang et al. 2005).

In contrast to framework repair, recent work in our laboratory suggests that, affinity can also be reestablished in the CDR graft by making changes within the CDRs; thus, this approach is termed CDR repair. CDR repair seeks to identify changes within the CDRs that can alleviate inappropriate CDR anchor residue interaction with framework vernier positions, and thus restore favorable interactions with antigen. Alternatively, rather than resolving inappropriate CDR interactions with the framework, CDR repair may also identify CDR changes that interact directly or modify interactions with antigen to improve binding. The challenge of this approach is that unlike framework repair, where solutions are derived from the parent framework, the solutions required for CDR repair are not immediately obvious and thus a combinatorial approach is required.

CDR repair was used to facilitate the humanization of antibodies in the examples that follow. For each humanization, a single consensus VL ($VL_{kappa\ I}$) and VH (VH_{III}) framework has been used even though the parent antibodies have higher homology to other human germline subgroups. The consensus $VL_{kappa\ I}/VH_{III}$ framework is stable and suitable for manufacturing and has been clinically validated in a number of marketed therapeutics (Carter et al. 1992; Presta et al. 1993, 1997; Werther et al. 1996). A combination of the sequence (Kabat and Wu 1971; Kabat et al. 1991), structural (Chothia and Lesk 1987) and contact (MacCallum et al. 1996) CDR definitions were used for the CDR graft. Thus in VL, CDR-L1 is defined as positions 24–36, CDR-L2 includes positions 46–56, and CDR-L3 includes positions 89–97. In VH, CDR-H1 consists of positions 26–35b, CDR-H2 includes 47–65 and CDR-H3 includes 93–102 (Fig. 2-2)[1] We have found that the inclusion of residues defined by the contact CDR definition is frequently important to restore antigen binding. Following the identification of a suitable humanized candidate, these positions can be changed back to the human sequence to assess their importance.

Following the construction and evaluation of the initial CDR graft, should additional affinity be needed, a number of strategies can be employed and are illustrated in the following examples.

[1]The Kabat numbering system for positions in the variable domain is used throughout (Kabat et al. 1991).

3. Humanization Methods

Antigen binding affinity can be re-established and in many cases it can be improved over the parent antibody, following the generation of a CDR graft by introduction of mutations into the framework or CDRs. Identification of favorable mutations is most easily achieved by combinatorial methods such as phage or ribosome display; however, to maintain the properties inherent in the parent antibody, the introduction of mutations should be minimized. Further, to mitigate immunogenic risk, the choice of acceptable amino acid substitutions should be guided by the diversity of amino acids observed naturally at particular amino acid positions (Kabat et al. 1991; Johnson and Wu 2001).

The vernier positions listed in Fig. 2-2, derived through modeling and experimentation, provide a good starting place but are not meant as an all-inclusive list. The inclusion of murine residues at these positions can improve antibody function, however, due to potential immunogenic risk, the identification of a minimal set is desired. Variants can be generated incorporating one murine vernier position at a time to identify those that influence binding, followed by combinations of those identified as important. Unfortunately, combined vernier position changes are not necessarily additive, and the search for an optimum combination can be difficult. Alternatively, all murine vernier positions can be added and then removed one (or a few) at a time to identify those that are not important. Obviously, this approach can be tedious and modeling is often performed to guide residue selection. Careful framework selection to incorporate many vernier positions a priori, can facilitate this approach and may lead to CDR grafts with higher starting affinities.

Methods reported for introducing diversity into a CDR graft are numerous. For example, libraries can be generated by DNA shuffling using the murine and human DNA to generate hybrid proteins from which, variants with improved binding can be selected; alternatively, error prone PCR can infuse random mutations throughout the CDRs and framework (Maynard et al. 2002; Schlapschy et al. 2004; Wang et al. 2004; Oliphant et al. 2005). CDR diversity can also be introduced in a modular fashion by cassette mutagenesis (Knappik et al. 2000) or site-directed mutatgenesis (Sidhu et al. 2004); however, since the CDR regions comprise approximately 60 residues, the sequence space that can actually be sampled in a diverse library is limited. Further, antigen binding characteristics inherent in the transferred CDRs may be lost upon the introduction of unrestrained CDR diversity.

Soft-randomization is a technique that enables mutation of several positions (such as an entire CDR sequence) while maintaining a bias towards the parent sequence. Soft-randomization is easily accomplished by phage display using Kunkel mutagenesis, where mutation can be introduced using a poisoned oligonucleotide. The flanking regions of the oligonucleotides anneal to the single stranded DNA template, while the region to be soft randomized is synthesized using 70% of the proper base (that coding for the wild-type DNA sequence) and 10% each of the other three bases. Following mutagenesis, the resulting "poisoned" codon will then code for the wild-type amino acid approximately 50% of the time while allowing all other 19 amino acids to be introduced at a lower frequency (Gallop et al. 1994). This mutagenesis approach can be employed on one CDR at a time or on all six CDRs simultaneously.

The following example describes the humanization of a rat anti-β7 antibody (Fib504 (Andrew et al. 1994)). This antibody blocks the adhesion of α4β7 positive lymphocytes to MAdCAM-1, VCAM-1 and fibronectin and may have therapeutic utility in inflammatory bowel disease by blocking lymphocyte migration to the gut (Kelsen et al. 2004).

A CDR graft of Fib504 was generated using the $VL_{kappa\ I}/VH_{III}$ framework (Fig. 2-4a, b); however, this CDR graft had no detectible binding affinity for α4β7 despite the use of a broad definition for the CDRs. Using a Fab form of the CDR graft as a template, a framework toggle phage library was generated by Kunkel mutageneis (Baca et al. 1997). The library was designed to offer either rat or human amino acid residues at vernier positions that differed between the two frameworks. After panning against a detergent solubilized form of α4β7, a change to the rat framework amino acid at position 78 in VH (L78F) was highly selected while the frequency of rat or human amino acids at other positions was unbiased. This single framework change, incorporated into the graft (graft.v2), restored binding to within 23-fold of the chimera.

To further improve the affinity, graft.v2 was used as a template for a soft randomization library that incorporated all six CDRs simultaneously. Random sequences from the initial unselected library are shown in Fig. 2-4c. Note that the library members have mutations localized to the CDR regions, not all CDRs are mutated (many clones have less than six oligonucleotides incorporated) and that introduced mutations reflect an underlying bias towards the initial CDR graft sequence. Unique sequences recovered after four rounds of selection against antigen are shown in Fig. 2-4d. All of the heavily mutated sequences exemplified in Fig. 2-4c were lost, and only clones containing a very similar change in CDR-L1 were selected and remained in the final pool. Surprisingly, the single change Y32L in CDR-L1 nearly restored antigen binding, and an additional change T31D improved binding affinity by threefold compared to the parent antibody. Mutagenesis of the final humanized clone to assess the importance of residues residing within the contact CDR definition suggests that, the inclusion of K49 in VL was critical to the success of this humanization since K49Y resulted in a greater than tenfold loss in binding. The VH mutation M94R resulted in a twofold increase in the dissociation rate for the Fab, however this difference was not detected when reformatted as an IgG.

CDR repair has been successful for many other antibodies. For example, a CDR graft of a mouse anti-IgE antibody (MaE11) also exhibited no affinity for its antigen, but was humanized using CDR repair. The CDR graft of MaE11 was used as a template to generate a soft randomized library of all six CDRs simultaneously from which highly focused changes in CDR-H1 were identified. Many clones incorporating W35L in this CDR were found to completely restore IgE binding (Fig. 2-5). By comparison, the framework repair approach, that was used previously (Presta et al. 1993), required three vernier framework changes (identical regions were transferred in both CDR grafts) to achieve similar results in the marketed Xolair® anti-IgE antibody (omalizumab).

The small number of amino acid changes required to re-establish binding in these two examples was surprising, and suggests that even simpler mutagenesis strategies can be effective. For example, a small combinatorial library that targets each CDR individually is likely to be successful, allowing libraries with higher diversity to be generated. In addition, libraries that target one

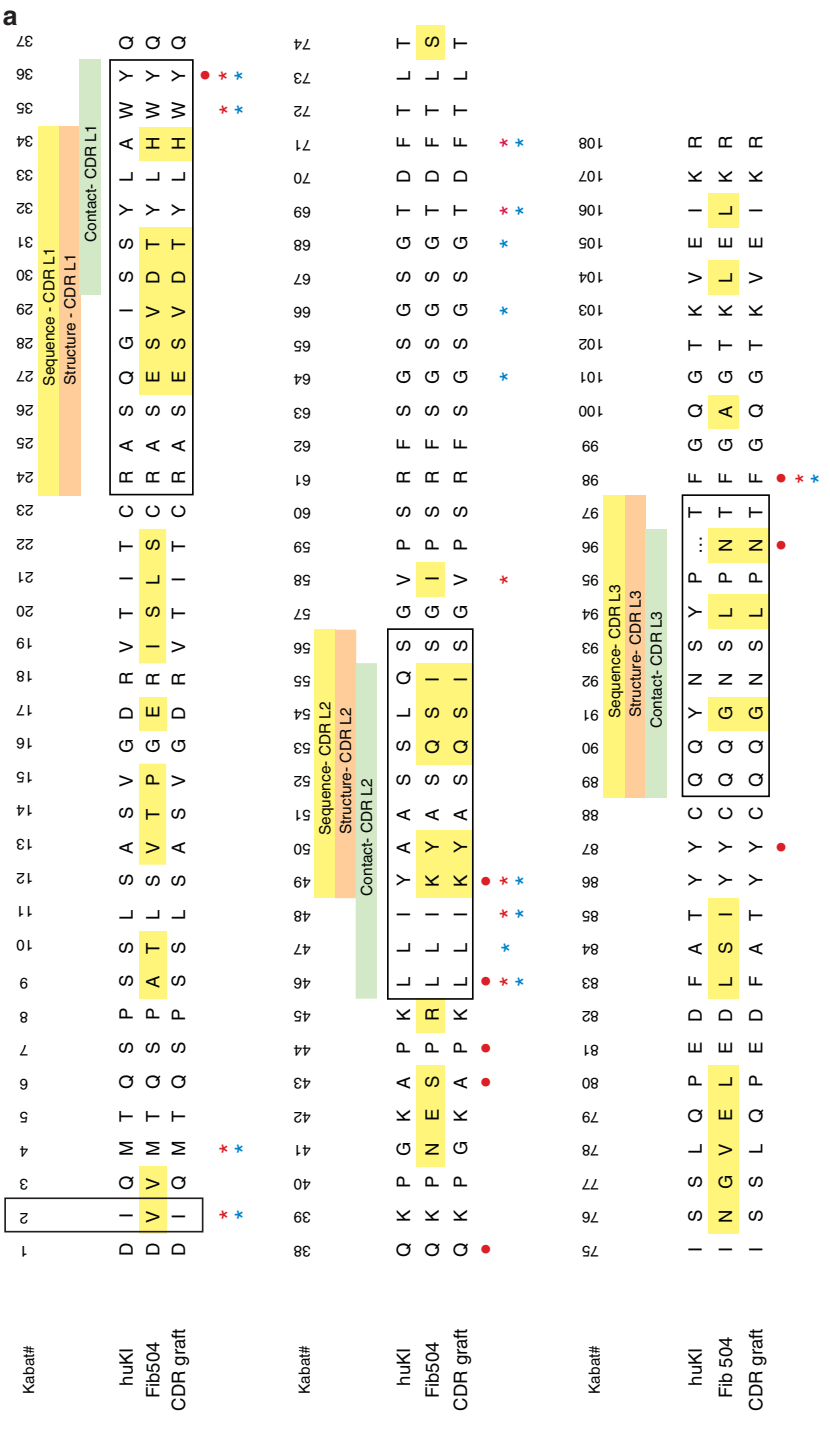

Fig. 2-4. Humanization of the rat monoclonal Fib504. Alignment of the human (**a**) $VL_{kappa\,I}$ consensus or

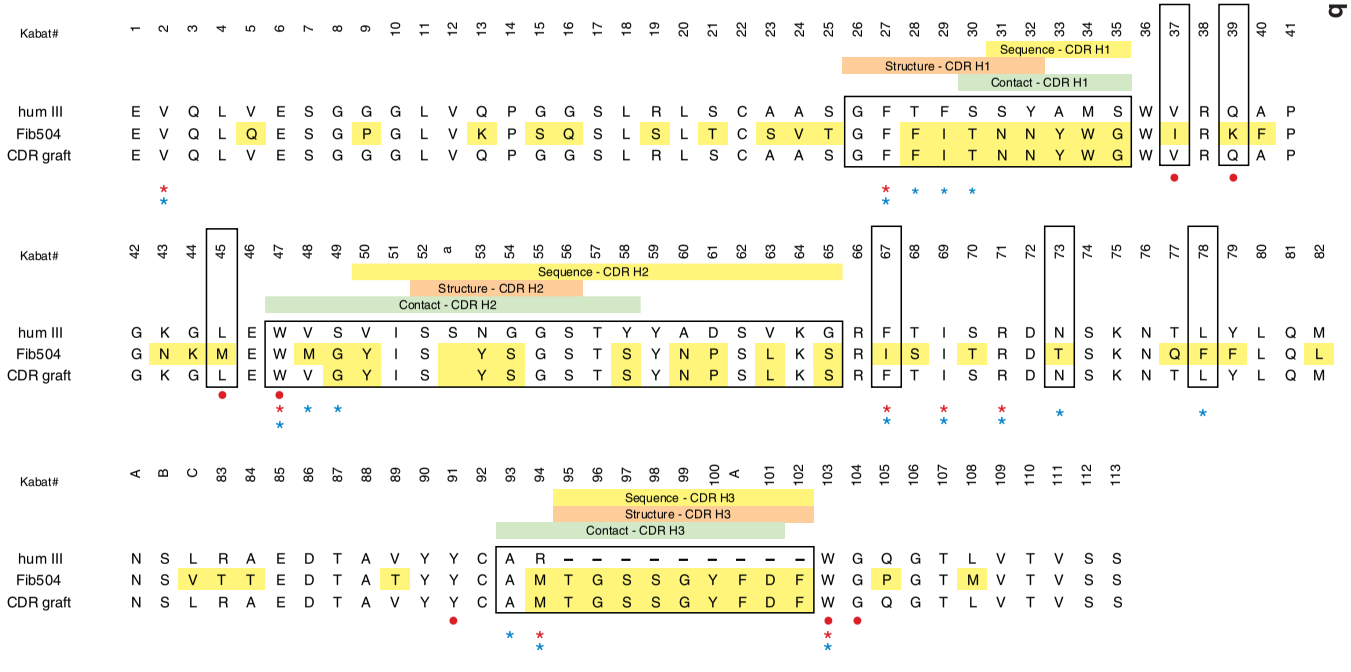

Fig. 2-4. (continued) (**b**) VH_{III} consensus with the variable domain sequences from Fib504, delineation of CDR regions and design of the Fib504 CDR graft. Vernier positions are stared as described in Fig. 2-2. Vernier positions that were toggled between rat and human amino acid residues are *boxed*.

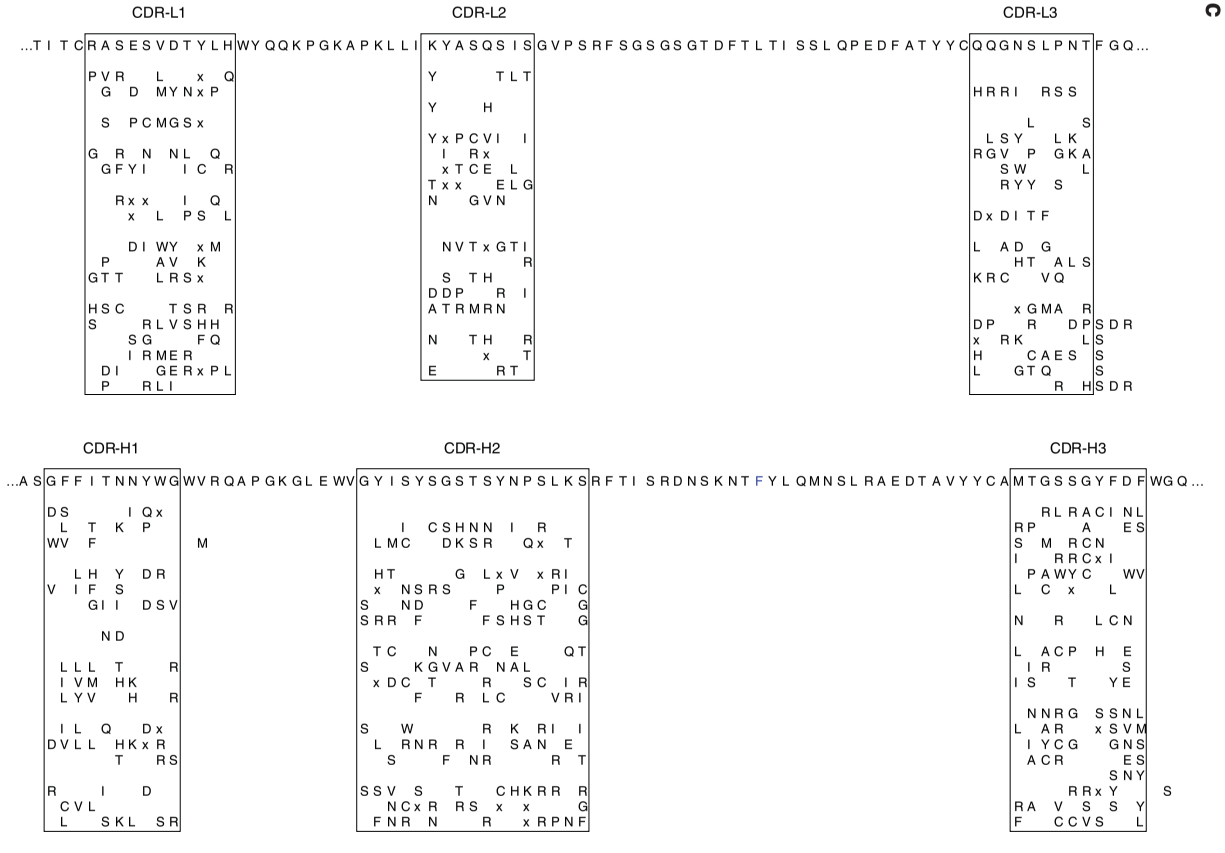

Fig. 2-4. (continued) (**c**) Random sequences selected from an initial unselected soft randomized library that targeted mutations to all six CDRs simultaneously are shown, compared to the amino acid sequence of CDR graft.v2 that served as the mutagenesis template. Targeted CDR sequences are *boxed*. Only positions that were mutated in the library samples during soft randomization are shown.

d

CDR L1

24	25	26	27	28	29	30	31	32	33	34	fold	
R	A	S	E	S	V	D	T	Y	L	H	1	chimera
											ND	graft
											23	graft.v2
								I				
							D	L	V			
							D	L			0.3	
							N	L				
							P	L				
							S	L			0.8	
	S		D				S	L	V			
				D				L				
				N				L				
								L			2.1	

Fig. 2-4. (continued) (**d**) Following four rounds of selection against antigen, ten unique clones were identified. All had changes limited to CDR-L1 and are shown compared with the original CDR-L1 sequence (*top*). Selected clones were expressed as Fab and binding to β7 was assessed using surface plasmon resonance. Affinity is expressed as variant (K_d)/chimera (K_d)

CDR H1

26	27	28	29	30	31	32	33	34	35	35a	fold	
G	Y	S	I	T	S	G	Y	S	W	N	1	chimera
											ND	graft
				S	G			H	L		1.8	
				S	G			R	L		1	
		I						K	L		1.8	
	N							K	L		1.5	
							H	K	L		1.5	
								K	L		0.5	
								N	L		1.5	
									L	H	0.8	

Fig. 2-5. Changes identified during CDR repair of an E25 CDR graft that restore binding to IgE. All six CDRs in the MaE11 CDR graft were soft randomized simultaneously. Following four rounds of selection against IgE, eight unique clones were identified each of which had sequence differences limited to CDR-H1. Phage clones were assessed for IgE binding using a competitive phage ELISA (Li et al. 2000). Affinity is expressed as variant (IC_{50})/chimera (IC_{50})

position at a time have the potential to identify the single most useful change. These can be generated through multiple small-scale mutagenesis reactions, that target each of the approximately 60 CDR residues individually offering all 20 possible amino acids; 60 mutagenesis reactions can then be pooled to form a "single position library" and panned against antigen. A single position library ensures that any CDR repair solution selected from the phage library

will have only a single mutation. Like any humanization approach, introduced changes have the potential to modify antibody–antigen interaction, thus careful subsequent analysis of antibody function is important.

Assigning the effect of CDR mutations to those that repair interactions with the framework, or to those that provide more favorable interactions with antigen can be difficult, and will require a significant structural investigation. Nevertheless, antibodies humanized by CDR repair in these two examples recapitulate the properties, both affinity and function, of the parent antibody and demonstrate that very small changes in the CDR have profound effects (Kettleborough et al. 1991; Eigenbrot et al. 1993). Comparison of the CDR sequences in these examples to homologous variable domains whose tertiary structures have been determined (2D7T was used for Fib504, 1CF8 and 1KB9 were used for MaE11 (Berman et al. 2000)) suggests that these selected mutations affect a remodeling of CDR interactions both with the framework and potentially with antigen. In the Fib504 example, both newly selected positions are anticipated to be solvent exposed. While this suggests the modification of interactions with β7, an influence of these changes on the conformations of CDR-L2 (at position 50) and CDR-L3 (at positions 91 and 92) cannot be ruled out. In contrast, W35L in CDR-H1 of the MaE11 CDR graft should be completely buried and interacting with vernier positions 24 and 78 in VH as well as CDR-H2 (at position 51) and CDR-H3 (at position 94). Thus, this selected mutation likely modifies framework-CDR interactions. Other antibodies humanized by this method in our laboratory have resulted in the selection of multiple solutions, often targeting different locations that restore, or in many cases improve binding affinity. These examples suggest that for the most part, grafted CDRs can be transferred from one framework to another without problem; however a slight mismatch, even as little as a hydroxyl group, can affect binding by ten or more fold. CDR repair enables the rapid identification of solutions to these disruptive interactions, allowing them to be fixed with surprisingly few sequence changes.

In situations where humanization by CDR repair alone is unable to restore binding affinity, or the loss of some other property of the parent antibody, a scan of the vernier residues that differ between the CDR graft and the parent antibody can identify one or two framework positions that cannot be compensated by CDR changes. The framework toggle library approach discussed above is a rapid way to identify these positions. In addition, not all antigens lend themselves to phage selection. Multi-spanning transmembrane proteins, for example, may only be available in a native form on a cell surface. Here, an analysis of differing vernier framework positions in VL and VH (i.e. framework repair) may be the only approach available to restore binding.

By combining both CDR repair and framework repair approaches, we have found that the overall number of changes incorporated into a humanized antibody can be reduced. To date, over a dozen antibodies have been humanized using this approach with a single $VL_{kappa\ I}/VH_{III}$ framework. For 13 antibodies humanized by framework repair alone using the same $VL_{kappa\ I}/VH_{III}$ framework, an average of 7.5 ± 3.4 residues were incorporated into the CDR graft whereas, the combined approach required alteration of only 4.4 ± 2.5 residues. The broader definition of CDRs that incorporates sequence hypervariability, structural considerations and regions that are known to contact antigen resulted in roughly one third of the CDR grafts, having no loss in binding while, the

rest suffered a tenfold or greater loss in binding affinity. CDR repair alone restored antigen binding affinity in the majority of these with less than three amino acid changes in a particular CDR. In fact, binding affinity was improved an average of sixfold. The location of the amino acid changes was antibody dependent with a nearly equal distribution across all six CDRs. Importantly, a wide selection of murine antibodies of distant homology have all been humanized using the same $VL_{kappa\ I}/VH_{III}$ framework containing a nearly constant set of vernier residues.

4. Antibody Properties

Aside from binding affinity, there are many other properties of antibodies that must be monitored during humanization. The equilibrium constant (K_d) for example, is related to the kinetics of association (k_a) and dissociation (k_d). While the success of humanization is often reported as restoring the equilibrium constant, the underlying kinetics may differ, and may be very important in particular in vivo systems. Binding affinity is also influenced by avidity for some antigens; bivalent binding may boost the apparent affinity by over 1,000-fold or cooperative binding may have little affect on apparent affinity. Avidity can be critical depending upon whether the target is a soluble antigen, or on the cell surface. Monitoring the ability of a Fab displayed on phage to bind antigen can be misleading, if the humanized clones behave differently when reformatted into IgG. Thus, performance of the IgG should also be monitored during the humanization process.

Generally, antibodies are selected for humanization due to some function they provide. They may act as agonists that dimerize a receptor or antagonists that block ligand–receptor interactions; they may be used to deliver a therapeutic agent through conjugation or induce ADCC or CDC through Fc effector functions. Occasionally, these properties can be lost during humanization, if the combining site of the parent antibody is not fully reproduced on the newly humanized antibody. These properties must also be carefully monitored during the humanization process.

5. Minimizing Immunogenic Potential

The purpose of antibody humanization is to make a murine antibody appear human, but what does the sequence of a human antibody look like? This is a particularly important consideration for CDR repair, where often multiple solutions, each having different amino acid changes that improve binding, may be obtained. Only changes that are compatible with canonical CDR structure should be considered (Chothia et al. 1989). In addition, comparisons to human germline sequences can be used as a guide for selecting a variant with the lowest immunogenic risk (Kabat et al. 1991). When considering the origin of a mature naturally occurring antibody, it becomes apparent that the CDR regions, while initially appearing hypervariable across a group of aligned variable domain sequences, are in fact well defined. Each CDR sequence is linked to its originating germline and as a result CDR sequences (e.g. CDR-L1, CDR-L2 and part of CDR-L3) are generally linked until the joining region in VL or the diversity segment in VH. Thus when considering which amino

acids are commonly observed at a given position within a particular CDR, the context of the rest of the CDR should also be considered.

Positions that differ in sequence between a mouse and human variable domain are typically distributed evenly with about 30 differences per variable domain. Humanization can reduce these by half with the remaining differences concentrated in the CDR regions (Fig. 2-1b). In comparison, mature antibodies have only about six sporadically distributed somatic mutations per variable domain with half of these targeted towards CDR regions (Clark et al. 2006). While the entire humanized variable domain may not match any specific germline, peptides that may be presented on MHC molecules should look relatively similar to those from naturally occurring antibodies.

Aside from the antibody itself, many additional factors may significantly influence immunogenic potential. These include route of administration, dose and dose frequency, formulation, degree of aggregation, antibody stability and pharmacokinetics, the targeted antigen, therapeutic indication, and the patient's immune status. While these problems cannot be anticipated, it is incumbent upon the antibody engineer to eliminate as much potential risk from the antibody sequence as possible.

Biological research is greatly facilitated by the ability to rapidly generate and screen large numbers of high affinity antibodies from hybridomas. While the advent of synthetic antibody phage libraries and "fully human" antibodies from genetically engineered mice have the potential to further reduce differences from germline, once having generated and validated a murine hybridoma antibody with desired properties, humanization is likely to remain the simplest path forward. Further, humanization and antibody engineering enable the ability to choose well-characterized frameworks that are stable for manufacturing and storage.

6. Conclusions

Monoclonal antibodies are an increasingly important class of therapeutics that can be recruited to target specific antigens and engineered to perform specific functions in vivo. Humanization technologies have made it possible to use murine antibodies, that can be easily generated as a starting point for developing these therapeutics. Despite the high homology between mouse and human antibodies, the transfer of variable domain CDRs to a new human framework often results in a loss of antigen binding affinity due to changes in the environment supporting the CDRs. Alterations, most easily identified through combinatorial means, are frequently required in order to repair the interactions between the human acceptor framework and CDRs. Framework repair and CDR repair can both be used to alter CDR-framework interactions from either side of this interface. CDR repair has an added potential to modify antigen interactions that can improve binding affinity.

In practice, each antibody humanization is unique and presents its own challenges. Both framework repair and CDR repair are effective approaches to restore antigen binding following the transfer of CDRs to a human framework, and should lead to the successful generation of humanized antibodies, that retain antigen binding affinity and biological properties of parental monoclonal antibodies.

Acknowledgment. I gratefully recognize the contributions made by the oligonucleotide synthesis and DNA sequencing groups at Genentech who have made this work possible. I also thank all current and former members of the Protein Engineering and Antibody Engineering Departments at Genentech for discussions and their contributions to the development of phage display methods, and antibody humanization technologies and especially, Henry Lowman for his support.

References

Adams CW, Allison DE, Flagella K, Presta L, Clarke J, Dybdal N, McKeever K, Sliwkowski MX (2006) Humanization of a recombinant monoclonal antibody to produce a therapeutic HER dimerization inhibitor, pertuzumab. Cancer Immunol Immunother 55:717–727

Andrew DP, Berlin C, Honda S, Yoshino T, Harnann A, HoIzmann B, Kilshaw PJ, Butcher EC (1994) Distinct but overlapping epitopes are involved in α4β7-mediated adhesion to vascular cell adhesion molecule-1, mucosal addressin-1, fibronectin, and lymphocyte aggregation. J Immunol 153:3847–3861

Baca M, Presta LG, O'Connor SJ, Wells JA (1997) Antibody humanization using monovalent phage display. J Biol Chem 272:10678–10684

Berman HM, Westbrook J, Feng Z, Gilliland G, Bhat TN, Weissig H, Shindyalov IN, Bourne PE (2000) The protein data bank. Nucleic Acids Res 28:235–242

Carter P, Presta LG, Gorman CM, Ridgway JBB, Henner D, Wong WLT, Rowland AM, Kotts C, Carver ME, Shepard MH (1992) Humanization of an anti-P185HER2 antibody for human cancer therapy. Proc Natl Acad Sci U S A 89:4285

Chothia C, Lesk AM (1987) Canonical structures for the hypervariable regions of immunoglobulins. J Mol Biol 196:901–917

Chothia C, Lesk AM, Tramontano A, Levitt M, Smith-Gill SJ, Air G, Sheriff S, Padlan EA, Davies D, Tulip WR, Colman PM, Spinelli S, Alzari PM, Poljak RJ (1989) Conformations of immunoglobulin hypervariable regions. Nature 342:877

Clark LA, Ganesan S, Papp S, van Vlijmen HWT (2006) Trends in antibody sequence changes during the somatic hypermutation process. J Immunol 177:333–340

Eigenbrot C, Randal M, Presta LG, Carter P, Kossiakoff AA (1993) X-ray structures of the antigen-binding domains from three variants of humanized anti-P185HER2 antibody 4d5 and comparison with molecular modeling. J Mol Biol 229:969–995

Foote J, Winter G (1992) Antibody framework residues affecting the conformation of hypervariable loops. J Mol Biol 224:487–499

Gallop MA, Barrett RW, Dower WJ, Fodor SPA, Gordon EM (1994) Applications of combinatorial technologies to drug discovery. 1. Background and peptide combinatorial libraries. J Med Chem 37:1233–1251

Honegger A (2007) AHo's amazing atlas of antibody anatomy. http://www.bioc.unizh.ch/antibody. Assessed June 2007

Hwang WYK, Almagro JC, Buss TN, Tan P, Foote J (2005) Use of human germline genes in a CDR homology-based approach to antibody humanization. Methods 36:35–42

Johnson G, Wu TT (2001) Kabat database and its applications: future directions. Nucleic Acids Res 29:205–206

Jones PT, Dear PH, Foote J, Neuberger MS, Winter G (1986) Replacing the complementarity-determining regions in a human antibody with those from a mouse. Nature 321:522–525

Kabat EA, Wu TT (1971) Attempts to locate complementarity determining residues in the variable positions of light and heavy chains. Ann N Y Acad Sci 190:382–393

Kabat EA, Wu TT, Perry HM, Gottesman KS, Foeller C (1991) Sequences of proteins of immunological interest. Public Health Service, National Institutes of Health, Bethesda

Kashmiri SVS, Pascalis RD, Gonzales NR, Schlom J (2005) SDR grafting – a new approach to antibody humanization. Methods 36:25–34

Kelsen J, Agnholt J, Falborg L, Nieslen JT, Romer JL, Hoffmann HJ, Dahlerup JF (2004) ^{111}Indium-labelled human gut-derived T cells from healthy subjects with strong in vitro adhesion to MAdCAM-1 show no detectable homing to the gut *in vivo*. Clin Exp Immunol 138:66–74

Kettleborough CA, Saldanha J, Heath VJ, Morrison CJ, Bendig MM (1991) Humanization of a mouse monoclonal antibody by CDR-grafting: the importance of framework residues on loop conformation. Protein Eng 4:773

Knappik A, Ge L, Honegger A, Pack P, Fischer M, Wellnhofer G, Hoess A, Wolle J, Pluckthun A, Virnekas B (2000) Fully synthetic human combinatorial antibody libraries (HuCAL) based on modular consensus frameworks and CDRs randomized with trinucleotides. J Mol Biol 296:57–86

Lee UH, Son JH, Lee JJ, Kwon B, Park JW, Kwon BS (2004) Humanization of antagonistic anti-human 4-1bb monoclonal antibody using a phage-displayed combinatorial library. J Immunother 27:201–210

Li B, Fuh G, Meng G, Xin X, Gerritsen ME, Cunningham B, de Vos AM (2000) Receptor-selective variants of human vascular endothelial growth factor. J Biol Chem 275:29823–29828

MacCallum RM, Martin ACR, Thornton JT (1996) Antibody–antigen interactions: contact analysis and binding site topography. J Mol Biol 262:732–745

Maynard JA, Maassen CBM, Leppla SH, Brasky K, Patterson JL, Iversone BL, Georgiou G (2002) Protection against anthrax toxin by recombinant antibody fragments correlates with antigen affinity. Nat Biotechnol 20:597–601

Morrison SL, Johnson MJ, Herzenberg LA, Oi VT (1984) Chimeric human antibody molecules: mouse antigen-binding domains with human constant region domains. Proc Natl Acad Sci U S A 81:6851–6855

Oliphant T, Engle M, Nybakken GE, Doane C, Johnson S, Huang LH, Gorlatov S, Mehlhop E, Marri A, Chung KM, Ebel GD, Kramer LD, Fremont DHF, Diamond MS (2005) Development of a humanized monoclonal antibody with therapeutic potential against West Nile virus. Nat Med 11:522–530

Padlan EA (1994) Anatomy of the antibody molecule. Mol Immunol 31:169–217

Presta LG, Lahr SJ, Shields RL, Porter JP, Gorman CM, Fendly BM, Jardieu PM (1993) Humanization of an antibody directed against IgE. J Immunol 151:2623–2632

Presta LG, Chen H, O'Connor SJ, Chisholm V, Meng YG, Krummen L, Winkler M, Ferrara N (1997) Humanization of an anti-vascular endothelial growth factor monoclonal antibody for the therapy of solid tumors and other disorders. Cancer Res 57:4593–4599

Presta LG, Sims P, Meng YG, Moran P, Bullens S, Bunting S, Schoenfeld J, Lowe D, Lai J, Rancatore P, Iverson M, Lim M, Chisholm V, Kelley RF, Riederer M, Kirchhofer D (2001) Generation of a humanized, high affinity anti-tissue factor antibody for use as a novel antithrombotic therapeutic. Thromb Haemost 85:379–389

Queen C, Schneider WP, Selick HE, Payne PW, Landolfi NF, Duncan JF, Avdalovic NM, Levitt M, Junghans RP, Waldmann TA (1989) A humanized antibody that binds to the interleukin 2 receptor. Proc Natl Acad Sci U S A 86:10029–10033

Rader C, Ritter G, Nathan S, Elia M, Gout I, Jungbluth AA, Cohen LS, Welt S, Old LJ, Barbas CF III (2000) The rabbit antibody repertoire as a novel source for the generation of therapeutic human antibodies. J Biol Chem 275:13668–13676

Riechmann L, Clark M, Waldmann H, Winter G (1988) Reshaping human antibodies for therapy. Nature 332:323–327

Schlapschy M, Gruber H, Gresch O, Schafer C, Renner C, Pfreundschuh M, Skerra A (2004) Functional humanization of an anti-CD30 Fab fragment for the immunotherapy of Hodgkin's lymphoma using an in vitro evolution approach. Protein Eng Des Sel 17:847–860

Sidhu SS, Li B, Chen Y, Fellouse FA, Eigenbrot C, Fuh G (2004) Phage-displayed antibody libraries of synthetic heavy chain complementarity determining regions. J Mol Biol 338:229–310

Tan P, Mitchell DA, Buss TN, Holmes MA, Anasetti C, Foote J (2002) "Superhumanized" antibodies: reduction of immunogenic potential by complementarity-determining region grafting with human germline sequences: application to an anti-CD28. J Immunol 169:1119–1125

Tsurushita N, Hinton PR, Kumar S (2005) Design of humanized antibodies: from anti-Tac to Zenapax. Methods 36:69–83

Verhoeyen M, Milstein C, Winter G (1988) Reshaping human antibodies: grafting an antilysozyme activity. Science 239:1534–1536

Wang X-BW, Zhou B, Yin C-C, Lin Q, Huang H-L (2004) A new approach for rapidly reshaping single-chain antibody *in vitro* by combining DNA shuffling with ribosome display. J Biochem 136:19–28

Werther WA, Gonzalez TN, O'Connor SJ, McCabe S, Chan B, Hotaling T, Champe M, Fox JA, Jardieu PM, Berman PW, Presta LG (1996) Humanization of an anti-lymphocyte function-associated antigen (LFA-1) monoclonal antibody and reengineering of the humanized antibody for binding to rhesus LFA-1. J Immunol 157:4986–4995

Wu TT, Kabat EA (1970) An analysis of the sequences of the variable regions of Bence Jones proteins and myeloma light chains and their implications for antibody complementarity. J Exp Med 132:211–250

Wu H, Nie Y, Huse WD, Watkins JD (1999) Humanization of a murine monoclonal antibody by simultaneous optimization of framework and CDR residues. J Mol Biol 294:151–162

Chapter 3

Nanobodies, Single-Domain Antigen-Binding Fragments of Camelid Heavy-Chain Antibodies

Gholamreza Hassanzadeh Ghassabeh, Serge Muyldermans, and Dirk Saerens

Abbreviations

CH	Constant domain of the heavy chain
Fab	Fragment antigen binding
Fv	Fragment variable
H	Heavy chain
HCAb	Heavy-chain antibody
L	Light chain
scFv	Single chain fragment variable
VH	Variable domain of the heavy chain of the conventional antibodies
VHH	Variable domain of the heavy chain of the heavy-chain antibodies
VL	Variable domain of the light chain of the conventional antibodies

1. Introduction

Antibodies or immunoglobulins are glycoproteins produced by B-cells and play a central role in host immune defense. Antibodies can be elicited virtually against any substance. Moreover, the immune response to any given antigen can be diverse, comprising different antibodies exhibiting different affinities and/or epitope specificities. Due to their antigen specificity, high affinity and almost the limitless repertoire diversity, antibodies have placed themselves among the most attractive reagents for both fundamental and applied sciences.

Conventional antibodies are multimers of heavy (H) and light (L) chains, each chain consisting of variable (V) and constant (C) domains (Porter 1973; Padlan 1994). Naturally, in a conventional antibody, the variable region of the light chain (VL) and the variable region of the heavy chain (VH) combine to make the antigen binding site, although, in some cases, the heavy chain alone can also bind antigen (Utsumi and Karush 1964). The constant domains of antibodies are not involved in antigen recognition; the heavy chain constant regions CH2 and CH3 (Fc) are responsible for effector functions, which trigger the elimination of antigens (Fig. 3-1a) (Dwek et al. 1984; Burton 1985).

From: *Current Trends in Monoclonal Antibody Development and Manufacturing,*
Biotechnology: Pharmaceutical Aspects, DOI 10.1007/978-0-387-76643-0_3,
Edited by: S.J. Shire et al.

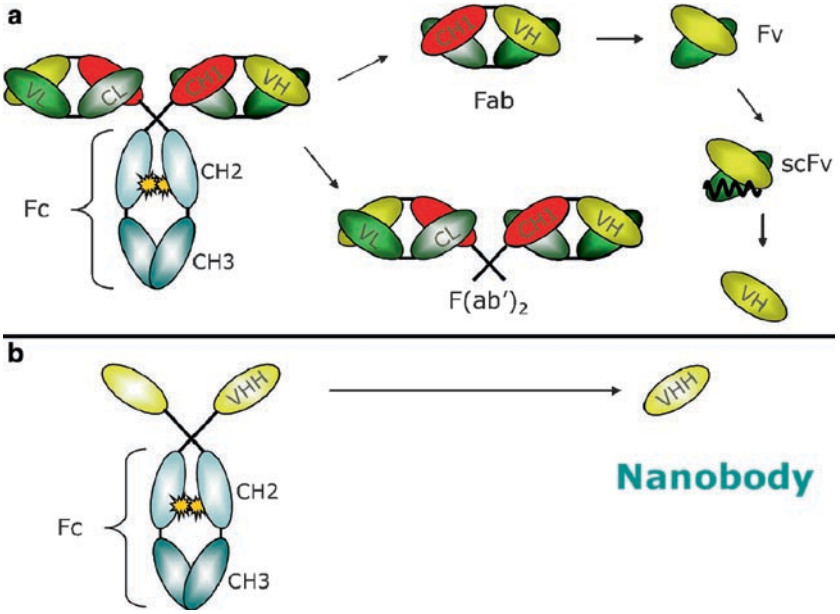

Fig. 3-1. Schematic presentation of the camelid conventional (**a**) and heavy-chain (**b**) IgGs and the antigen-binding fragments thereof. The entire light chain and the CH1 domain are absent in HCAbs. When compared to conventional antibodies that require both VH and VL to bind antigen optimally, the HCAbs bind their target antigen by virtue of one single domain, termed VHH or Nanobody

Since the constant domains of antibodies are not directly involved in the recognition of antigen, a range of smaller antibody fragments such as Fab, $F(ab')_2$, Fv and scFv, which retain the antigen-binding activity, have been designed (Fig. 3-1a). As compared with the whole antibody molecules, such smaller antibody formats, expressed in microorganisms, are more cost-effective to produce, have a faster organ clearance (Milenic et al. 1991; Wu and Senter 2005), penetrate the solid tumors more efficiently (Yokota et al. 1992), and are more suitable for structural analysis (McManus and Riechmann 1991; Riechmann et al. 1991). However, the generation of antibody fragments from conventional antibodies has faced technical difficulties such as low expression yields in heterologous systems and aggregation.

In the early 1990s, we discovered, by serendipity, that the antibody repertoire of camelids contains antibodies consisting of only heavy chains (Fig. 3-1b) (Hamers-Casterman et al. 1993). These antibodies are referred to as heavy-chain antibodies (HCAbs). Despite the absence of light chain in camelid HCAbs, these antibodies not only display an extensive antigen-binding repertoire, but also their binding affinities for their cognate antigens are in the range of affinities that are described for conventional antibodies. The antigen-binding domains of camelid HCAbs consist of only one domain, termed VHH (variable domain of the heavy chain of the heavy-chain antibodies) (Fig. 3-1b). As we will discuss later on, this feature offers a number of technological advantages in the generation of engineered antibodies, as compared with conventional antibodies which require both the variable domain of the heavy

chain (VH), and that of the light chain (VL) to bind antigen optimally. These technological advantages together with small size, recognition of unique epitopes, high affinity, high solubility, high stability and high expression yields in heterologous expression systems have combined to make Nanobodies an interestingly useful class of molecules for various applications including diagnosis and therapy.

In this chapter, we focus on the unique features of Nanobodies and demonstrate their potential applications as a novel class of antibody derivatives in different fields.

2. Heavy-Chain Antibodies

By definition, heavy-chain antibodies (HCAbs) are antibodies consisting of heavy chains only. Functional HCAbs are present in nurse and wobbegong sharks, in ratfish and in camelids (camels, dromedaries and llamas) (Hamers-Casterman et al. 1993; Greenberg et al. 1995; Rast et al. 1998; Nuttall et al. 2001). It seems that HCAbs, at least in camelids, are not derived from remnants of a putative primordial HCAb form, but are the result of more recent evolutionary changes occurring in conventional antibodies. The shared properties of HCAbs across different taxa can therefore be explained by convergent evolution due to similar constraints (Nguyen et al. 2002).

The HCAbs have also been described in human as a pathological disorder termed "heavy chain disease." These human HCAbs are devoid of light chain, lacking the first constant domain (CH1) and parts of the variable region (VH), fail to bind antigen and are consequently non-functional (Fleischman et al. 1962; Franklin et al. 1964; Seligmann et al. 1979; Cogne et al. 1989).

Considerable parts of IgGs in the sera of camelids are dimers of heavy chain. In contrast to HCAbs in the case of heavy chain disease, the camelid HCAbs are functional antigen-binding entities which associate with antigen by virtue of one single domain termed VHH (Hamers-Casterman et al. 1993). The VHHs are also called Nanobody, a term inspired by their small size (2.5 nm diameter and about 4 nm height). Here, we refer to VHHs as Nanobodies, wherever the antigen specificities of the VHHs are known.

Isolated heavy chains (H) of the conventional antibodies are not usually soluble unless they pair with light chains via the CH1 and VH domains (Roholt et al. 1964; Seligmann et al. 1979; Chothia et al. 1985; Padlan 1994). The camelid HCAbs lack the entire CH1 domain. The sequences encoding the CH1 domain are present in the dromedary and llama genomes, but are removed during mRNA splicing, possibly due to a point mutation in the consensus splicing signal at the 3′ end of the CH1 exon (Nguyen et al. 1999; Woolven et al. 1999). The CH1 domain is the binding site for the heavy-chain chaperoning protein BiP which prevents the secretion of antibody heavy chains from endoplasmic reticulum (ER). Replacement of BiP by light chain triggers the antibody secretion (Hendershot et al. 1987; Hendershot 1990; Hamers-Casterman et al. 1993). Therefore, the lack of CH1 domain may account for the immediate secretion of camelid HCAbs in the absence of light chain.

The Fc part of the camelid HCAbs contains sequences that, in conventional antibodies, mediate the effector functions, suggesting that HCAbs exert the conventional effector functions (Atarhouch et al. 1997; Nguyen et al. 1999).

2.1 Antigen-Binding Repertoire of Camelid HCAbs

Random association of heavy (H) and light (L) chains contributes considerably to the expansion of the conventional antibody repertoire. The lack of light chain in HCAbs raises the question as to whether HCAbs repertoire bears an extensive antigen-binding complexity. This was addressed initially by the analysis of the immune response of dromedaries naturally infected with *Trypanosoma evansi*. This revealed a very diverse HCAbs response against different proteins of this parasite (Hamers-Casterman et al. 1993). Since then, our work and that of others clearly established the possibility to raise diverse HCAbs against various antigens and showed that the isolated Nanobodies derived from camelid HCAbs target a broad range of epitopes on the cognate antigens (Ghahroudi et al. 1997; Lauwereys et al. 1998, Van der Linden et al. 2000a; Cortez-Retamozo et al. 2004; Saerens et al. 2004; Hulstein et al. 2005; De Genst et al. 2006; Klooster et al. 2007).

The VHHs are encoded by a large set of V gene segments (42 gene segments encoding 33 unique sequences) which are distinct from the V gene segments coding for VHs. The frequency of mutation hotspots and DNA recombination signal sequences is higher in VHH germline sequences than in VH germline genes (Nguyen et al. 1999, 2000). Moreover, as compared with VHs, VHHs have on average longer complementarity determining regions (CDRs) and their antigen-binding loops display a larger structural repertoire (Muyldermans et al. 1994; Decanniere et al. 1999, 2000; Nguyen et al. 2000). The average CDR3 length in mouse and human is, respectively, 9 and 12 amino acids (Wu et al. 1993), whereas, the CDR3 of VHHs from dromedaries has usually a length of 16–18 amino acids (Muyldermans et al. 1994; Nguyen et al. 2000). In dromedaries, the CDR1 of VHHs is extended to include additional amino acid residues which are part of framework 1 in VHs (Nguyen et al. 2000). It is tempting to suggest that the high frequency of mutation hotspots and recombination signal sequences, the long CDRs and the expanded structural repertoire of antigen-binding loops of Nanobodies contribute to VHHs repertoire complexity and compensate, at least in part, for the lack of VH–VL combinatorial diversity. However, not all the above-mentioned features are necessarily required to achieve repertoire diversity. For example, a large fraction of VHHs in llamas have a short CDR3 of about six amino acids (Vu et al. 1997; Harmsen et al. 2000), and yet these animals exhibit a complex Nanobody repertoire.

2.2 Induction of HCAb Response

The procedures to elicit HCAbs in camelids are, in principle, similar to those in use to raise conventional antibodies in other animals: for example, an initial subcutaneous inoculation of antigen in complete Freunds adjuvant followed by 5–6 weekly boosts in incomplete Freunds adjuvant, using 50–500 μg antigen per injection (Lauwereys et al. 1998). We have also raised HCAbs against various antigens using Gerbu adjuvant LQ # 3000 (Gerbu Biotechnik GmbH, Germany). Heavy-chain antibodies can also be obtained by subcutaneous injection of whole cells (10^8 cells in PBS per injection) (our unpublished data). Other procedures involving other types of adjuvant or with different boost intervals as well as DNA-prime protein-boost protocol have also been successfully used to raise an HCAb response (Ladenson et al. 2006; Koch-Nolte

et al. 2007; Maass et al. 2007). To make the immunization cost effective, an animal can be injected simultaneously with several antigens (Lauwereys et al. 1998; Van der Linden et al. 2000a).

It is worth noting that, although the present data support the idea that virtually HCAbs can be raised against any antigen, the HCAbs and conventional antibodies elicited against complex antigens such as natural infections can differ in terms of antigens which they recognize. For instance, Van der Linden et al. (2000a) reported that HCAbs and conventional antibodies from an llama immunized with *S. mutans* lysate exhibited different antigen recognition patterns.

3. Isolation of Antigen-Specific Nanobodies

3.1. Isolation of Polyclonal Nanobodies

Polyclonal mono- and bi-valent Nanobodies (VHH and VHH_2) can be obtained by the proteolysis of the HCAbs.

From an immunized dromedary, Lauwereys et al. (1998) prepared polyclonal monovalent Nanobodies containing α-amylase-specific binders. In this study, the HCAb isotype IgG3 obtained by Protein G chromatography was digested with endo-Glu V8 protease and then the Nanobodies were separated from the Fc part by chromatography on Protein A which retains the Fc part. It should, however, be kept in mind that some of the dromedary and a large fraction of the llama Nanobodies bind Protein A. This class of Nanobodies cannot therefore be separated from the Fc fraction by using Protein A.

Bivalent Nanobodies (VHH_2) can be obtained by digestion of IgG3 with pepsin, trypsin or papain which cleaves the hinge region mainly after the first disulfide bond linking the γ3 heavy chains (Hamers and Muyldermans 1998).

Although the above examples demonstrate the feasibility to obtain polyclonal Nanobodies from IgG3, methods for the generation of polyclonal Nanobodies from the HCAb IgG2 isotype remain to be developed.

3.2. Isolation of Monoclonal Nanobodies

The most commonly used approach to identify monoclonal antigen-specific antibody fragments is the panning of phage display libraries (Winter et al. 1994; Hoogenboom et al. 1998; Hoogenboom and Chames 2000; Dufner et al. 2006). We adapted the phage display technology for the cloning of the VHH repertoire, and for the isolation of monoclonal antigen-specific Nanobodies (Ghahroudi et al. 1997; Lauwereys et al. 1998). Others have used the ribosome display to construct a VHH library and to select hapten-specific Nanobodies (Yau et al. 2003).

Immune, non-immune, synthetic as well as semi-synthetic libraries can all serve as sources of monoclonal Nanobodies. However, while the affinities of Nanobodies isolated from immune libraries are usually in the nanomolar range (Lauwereys et al. 1998; Spinelli et al. 2000; Cortez-Retamozo et al. 2004; Saerens et al. 2004; Hulstein et al. 2005; De Genst et al. 2006; Klooster et al. 2007), Nanobodies obtained from synthetic and non-immune libraries have often micromolar affinities (Davies and Riechmann 1996; Tanha et al. 2001; Yau et al. 2003; Groot et al. 2006; Stewart et al. 2007). Therefore, Nanobodies isolated from libraries other than immune libraries might require

further optimization (e.g. in vitro affinity maturation) before use (Yau et al. 2005; Goldman et al. 2006). Despite this shortcoming, the non-immune and synthetic libraries represent interesting alternatives to immune libraries in some cases, for example, when the amount of antigen is limited or the antigen is non-immunogenic or toxic to dromedaries and llamas.

As compared with the cloning of the antigen-binding repertoire of conventional antibodies, cloning Nanobody repertoire offers some technological advantages as follows. The antigen binding by conventional antibodies usually relies on both VH and VL, and construction of libraries of conventional antibodies involves random association of VHs and VLs. Therefore, very large libraries are required to obtain all possible VH–VL combinations, of which some may represent the original VH–VL pairing generated in vivo. For example, starting with a B-cell population representing 10^6 different VHs and 10^6 different VLs, a library of at least 10^{12} independent colonies is required to generate all possible VH–VL pairs. Obviously, random VH–VL pairing can generate novel VH–VL combinations which, as pairs, were not present in the original B-cell population used for library construction. Some of these novel pairs may bind antigen specifically, but usually have sub-optimal affinity and stability.

Taking into account that the HCAbs bind their target antigens by virtue of only one single domain, construction of large immune libraries to trap the antigen-specific Nanobodies has been proven unnecessary (Lauwereys et al. 1998; Alvarez-Reuda et al. 2007).

Construction of libraries of antigen-binding repertoire of conventional antibodies is also complicated by the existence of multiple VH and VL gene families, each requiring a specific set of primers for PCR amplification. On the contrary, all VHHs belong to one single subfamily, namely subfamily III (Vu et al. 1997; Nguyen et al. 1998, 2000). Therefore, one pair of primers is sufficient to amplify the entire VHH repertoire.

Since the sticky behavior of isolated VHs can result in the enrichment of non-specific clones during panning (Davies and Riechmann 1995), it is important to exclude the VHs from the VHH repertoire prior to cloning. To achieve this, we first use a pair of primers, of which one binds to the leader signal sequences of both VHs and VHHs and the other anneals to the CH2 exons of all γ genes. This yields two types of PCR fragments that differ in size: the longer fragments contain the CH1 exon and are derived from the conventional antibodies, while the shorter fragments lack the CH1 exon and are derived from the HCAbs. The two types of PCR fragments are separated by agarose gel electrophoresis, and the shorter fragments are excised from the gel and used for further PCR to construct the VHH library (Nguyen et al. 2001). Alternatively, the VHs can be excluded from the VHH pool by using a primer that exclusively anneals to the hinge region of the HCAb (Van der Linden et al. 2000a).

Identification of antigen-specific binders from VHH libraries can be achieved by direct screening of the individual colonies (without prior enrichment via panning). It has been demonstrated that the percentage of antigen-specific clones in VHH libraries from immunized animals can reach 1% (Ghahroudi et al. 1997) or even 20% (Frenken et al. 2000). However, the extremely low frequency of antigen-specific clones in non-immune libraries makes direct screening inappropriate. To enrich for specific binders, the VHH

phage display libraries are subjected to one to four rounds of panning prior to the analysis of individual colonies. The advantage of panning by phage display is that, by proper design of the selection procedure, it is possible to select for Nanobodies with specific properties such as those with highest affinity, greater stability and/or better expression yield.

4. Interesting Features of Nanobodies

Although there have been few reports describing the successful isolation of functional VH domains from conventional antibodies (Ward et al. 1989; Cai and Garen 1997; Reiter et al. 1999; Tanaka et al. 2003), the use of VHs is usually hampered by their low affinity, low expression yields, poor solubility and low stability (Davies and Riechmann 1995; Kortt et al. 1995; Reiter et al. 1999), features which make VHs inferior to Nanobodies. Here, we elaborate on the features of Nanobodies which make them ideal small recognition units, as compared to VHs.

4.1. High Expression Yields and Ease of Purification

The possibility to express Nanobodies in different expression systems has already been established. We routinely obtain about 5–10 mg pure protein per liter of *E. coli* culture in shaker flasks (Ghahroudi et al. 1997). Others have reported even higher yields in *E. coli* shake flask cultures (Rahbarizadeh et al. 2005). Production levels of Nanobodies in *Saccharomyces cerevisiae* have been as high as 9.3 mg/L/$OD_{660\ nm}$ in shaker flasks. This suggests that, it is feasible to achieve production levels higher than 1 g/L in a high density fermentation with ODs of over 100 (40–80 g dry weight per liter) (Frenken et al. 2000). Expression of a hapten-specific Nanobody fused to peroxidase in *Aspergillus awamori* in shake-flask cultures yielded up to 30 mg/L fusion proteins secreted to the medium, and this could be increased to about 200 mg/L in preliminary fermentation experiments without any optimization (Joosten et al. 2005). An initial attempt to express a lysozyme-specific Nanobody in plant plastids resulted in a semi-lethal phenotype (Magee et al. 2004). However, later on, a study suggested that this undesirable effect could have been due to the type of expression system used (Magee et al. 2007). Functional Nanobodies expressed in tobacco plants have been shown to constitute up to about 1.6% of the total leave soluble protein fraction (Rajabi-Memari et al. 2006; Ismaili et al. 2007), demonstrating the feasibility to use transgenic plants as an economic source of Nanobodies.

Nanobodies can be purified following various procedures. Van der Linden et al. (1999) reported that a simple ultrafiltration of yeast culture supernatants using membranes with cut-off limits of 50 and 5 kDa, respectively, resulted in a purity of 80–90%. Bacterial periplasmic extracts, obtained by a simple osmotic shock (Skerra and Plückthun 1988), provide Nanobodies that are pure enough for applications such as ELISA and Western blot.

Inclusion of a C-terminal His_6-tag allows the easy purification of Nanobodies by Immobilized Metal Affinity Chromatography (IMAC) using Ni-NTA columns. If necessary, the Nanobodies can be further purified from the fractions obtained via IMAC, for example, by ion exchange or gel filtration chromatography.

This usually results in purities that satisfy most applications (Lauwereys et al. 1998; Alvarez-Reuda et al. 2007).

Nearly all VHs which belong to subfamily III bind protein A (Sasso et al. 1991; Potter et al. 1996). This characteristic has been exploited for the purification of Nanobodies (Ghahroudi et al. 1997; van der Linden et al. 1999; Frenken et al. 2000). The advantage of this method is that it selects for the properly folded domains. However, not all properly folded Nanobodies bind protein A (Ghahroudi et al. 1997).

Recently, Olichon et al. (2007) demonstrated the feasibilty to purify Nanobodies by a simple one-step heat treatment. The heat treatment did not affect the Nanobodies functionality. The purities and the yields of Nanobodies obtained after heating were as high as those of the samples purified by IMAC (Olichon et al. 2007).

4.2. High Stability, High Solubility and High Affinity

Nanobodies retain more than 80% of their original binding activity after prolonged incubation at 37°C (Ghahroudi et al. 1997), and bind antigen specifically during and/or after incubation at temperatures as high as 90°C (van der Linden et al. 1999, 2000b; Goldman et al. 2006; Ladenson et al. 2006). Although the presence of a disulfide bond between the CDRs in some Nanobodies contributes to their stability (Davies and Riechmann 1996; Ghahroudi et al. 1997), the functionality of Nanobodies over long periods of time or at extreme temperatures is attributed to their ability to properly refold after unfolding (Perez et al. 2001; Ewert et al. 2002). In contrast to Nanobodies, thermal denaturation of VHs is not readily reversible and results in aggregation (Ewert et al. 2002). The unfolding of Nanobodies by guanidinium chloride and urea is also fully reversible (Dumoulin et al. 2002).

The high stability and the reversible folding make Nanobodies attractive for applications such as biosensors and affinity purification, where harsh conditions are encountered.

In contrast to VHs, Nanobodies are highly soluble. Nanobodies can be concentrated to 10–20 mg/mL without any aggregation (Ghahroudi et al. 1997; Conrath et al. 2005). The superior solubility of Nanobodies is, in part, due to amino acid adaptations in framework-2, which render Nanobodies more hydrophilic (Muyldermans et al. 1994; Desmyter et al. 1996; Spinelli et al. 1996; Vu et al. 1997). The well-conserved VH residues V42, G49, L50 and W52 constitute a hydrophobic area which is the VL binding site (numbering is according to IMGT; http://imgt.cines.fr). In the absence of VL, the exposure of this hydrophobic area to aqueous environment results in stickiness and aggregation of VHs. In VHHs, the above residues are usually replaced by F42 or Y42, E49, R50 and G52, making this area more hydrophilic (Muyldermans et al. 1994; Vu et al. 1997; Maass et al. 2007). Camelization of human VHs as well as Nanobody humanization has clearly established that the above amino acid substitutions contribute to Nanobodies solubility (Davies and Riechmann 1994, 1995; Tanha et al. 2001; Conrath et al. 2005). Substitutions of other framework amino acids such as L11, which in conventional antibodies contact the CH1 domain, might also enhance Nanobody solubility by increasing its hydrophilicity (Nieba et al. 1997; Muyldermans 2001).

The VHHs framework amino acid substitutions are encoded in the germline, and are not the result of somatic hypermutation (Nguyen et al. 1998).

Mechanisms other than increased hydrophilicity of the frameworks may also account for the increased solubility of Nanobodies. For example, in some Nanobodies, the CDR3 loop folds over the region which in conventional antibodies constitutes the VL-interacting surface of a VH, thereby shielding any remaining hydrophobic patch from the aqueous solution (Desmyter et al. 1996, 2001; De Genst et al. 2006).

The lack of VL contribution to antigen binding by Nanobodies may bring into question the binding affinities of Nanobodies. With the data now available for a large number of Nanobodies raised against many antigens of different nature, it is well established that the binding affinities of Nanobodies are in the range reported for scFvs. The affinities of Nanobodies isolated from immune libraries are often in the low nanomolar or sub-nanomolar range (Lauwereys et al. 1998; Spinelli et al. 2000; Cortez-Retamozo et al. 2004; Saerens et al. 2004; Hulstein et al. 2005; De Genst et al. 2006; Klooster et al. 2007). The functional affinities (avidities) of Nanobodies can be increased by generating bivalent Nanobodies. Interestingly, although Nanobodies from non-immune libraries do not usually have high binding affinities, it is still possible to obtain Nanobodies with nanomolar affinities from such libraries (Goldman et al. 2006; Verheesen et al. 2006a, b). It is worth mentioning that the success rate of isolation of high affinity antibodies from non-immune libraries is directly correlated with the library size.

4.3. Alternative Epitope Recognition

The paratopes of conventional antibodies raised against protein antigens and haptens are, respectively, planar and concave (Webster et al. 1994; Padlan 1996). These topographies are not suited for binding into antigen grooves and cavities. As a consequence, conventional antibodies usually avoid targeting clefts.

Grooves and cavities play a critical role in many biological processes as they are often involved in interactions between molecules. In enzymes, for example, the catalytic site is often located in large and deep clefts (Lakowski et al. 1996). Therefore, the ability to obtain specific binders to epitopes within the clefts is of particular interest.

In contrast to conventional antibodies that are rarely competitive enzyme inhibitors, a considerable fraction of camelid HCAbs, raised against carbonic anhydrase, α-amylase and lysozyme, competitively inhibit the target enzymes (Lauwereys et al. 1998; De Genst et al. 2006). In line with these findings, a large number of enzyme-specific inhibitory monoclonal Nanobodies, many of which are competitive inhibitors, have been isolated from immune and synthetic libraries (Martin et al. 1997; Lauwereys et al. 1998; Conrath et al. 2001; Jobling et al. 2003; De Genst et al. 2006; Koch-Nolte et al. 2007).

Competitive inhibition of enzymes by Nanobodies suggests that the catalytic site of the enzymes constitutes the epitope recognized by these Nanobodies. We demonstrated that, in the case of a lysozyme-specific Nanobody, the CDR3 protrudes from the paratope, penetrates into the active site of the enzyme, and inhibits the enzyme activity by mimicking carbohydrate substrate (Desmyter et al. 1996; Transue et al. 1998). Desmyter et al. (2002) reported that the competitive inhibition of α-amylase by a Nanobody involved mainly the interaction between CDR2 and the enzyme active site, while the role of CDR3 in this process was minimal.

Collectively, the above data suggest that Nanobodies recognize epitopes that are not immunogenic for conventional antibodies. This has been further supported by comparing the crystal structures of Nanobodies–lysozyme complexes with those of conventional antibodies–lysozyme complexes (De Genst et al. 2006).

Significantly, Nanobodies also recognize epitopes (e.g. planar epitopes) recognized by conventional antibodies (Decanniere et al. 1999; Desmyter et al. 2001; Dumoulin et al. 2003; Loris et al. 2003; De Genst et al. 2006).

5. Applications of Nanobodies

At present, the possibility to use Nanobodies as enzyme inhibitors (Martin et al. 1997; Lauwereys et al. 1998; Conrath et al. 2001; De Genst et al. 2006; Koch-Nolte et al. 2007), as affinity ligands (Klooster et al. 2007), as intrabodies (Jobling et al. 2003; Gueorguieva et al. 2006; Rothbauer et al. 2006; Verheesen et al. 2006a), as probes in biosensors (Pleschberger et al. 2004; Huang et al. 2005a; Saerens et al. 2005), and as tools to trace antigens in live cells (Rothbauer et al. 2006) and to study protein–protein interactions (Huang et al. 2005b) has been demonstrated. Owing to their small size and reduced complexity of paratopes, Nanobodies are ideal candidates to design small peptide mimetics (Marquardt et al. 2006). Nanobodies can also be used in consumer products. For example, Nanobodies prevent infection of lactic acid bacteria by phage, thereby accelerating fermentation in cheese production (Ledeboer et al. 2002; de Haard et al. 2005) or they can prevent dandruff when supplied in shampoo (Dolk et al. 2005). Obviously, the discussion of all Nanobodies applications is irrelevant to this chapter, and therefore, we herein focus only on their potential applications to improve human and animal health.

5.1. Nanobodies in Cancer Diagnosis and Therapy

More than 85% of human cancers are solid tumors (Beckman et al. 2007). In most solid tumors, to obtain a maximal therapeutic effect, the necessary first step is the access of sufficient amounts of the therapeutic antibody to various regions of the tumor (Tunggal et al. 1999). The transfer of macromolecules in tumors is mainly by diffusion and the speed of diffusion through tumors is inversely proportional to molecular size (Nugent and Jain 1984; Clauss and Jain 1990; Pluen et al. 2001). In agreement with this, small antibody fragments penetrate the solid tumors more efficiently than the whole antibody molecule (Yokota et al. 1992; Graff and Wittrup 2003).

On the other hand, in order to increase target-to-background signal ratios for high detection sensitivities in imaging, and also to reduce non-specific toxic effects of antibody conjugates, the unbound antibodies should, be cleared rapidly from the non-target organs. When compared to the whole antibody molecule, the small antibody fragments have a faster clearance rate (Milenic et al. 1991; Wu and Senter 2005).

Based on the above-described criteria, the very small size of Nanobodies makes them suitable for in vivo imaging and tumors.

In a mouse model, we demonstrated that Nanobodies selectively and effectively accumulated in bulky tumors as well as in metastatic lesions, rapidly yielding high tumor-to-non-target organ ratios. The excess of these

Nanobodies were quickly cleared from the circulation (Cortez-Retamozo et al. 2002). In a Nanobody directed enzyme prodrug therapy setting using prodrug cephalosporin mustard, intravenous administration of an anti-carcinoembryonic antigen Nanobody fused to β-lactamase resulted in complete eradication of established LS 174T human adenocarcinoma xenografts (Fig. 3-2d) (Cortez-Retamozo et al. 2004). This Nanobody–enzyme conjugate localized preferentially in tumors and cleared from the systemic circulation so rapidly that there was no need for clearance agents prior to prodrug administration (Cortez-Retamozo et al. 2004). Recently, Roovers et al. (2007) identified Nanobodies that competed with epidermal growth factor (EGF) for binding to EGF receptor (EGFR), and reported that these Nanobodies inhibited the growth of A431-derived solid tumors, demonstrating the feasibility to use untagged Nanobodies to cure cancer.

Although fast clearance is a desirable feature for in vivo imaging of tumors, it might be of interest to increase the serum half-life of antibody fragments for therapy in order to improve efficacy, to reduce the dose or frequency of

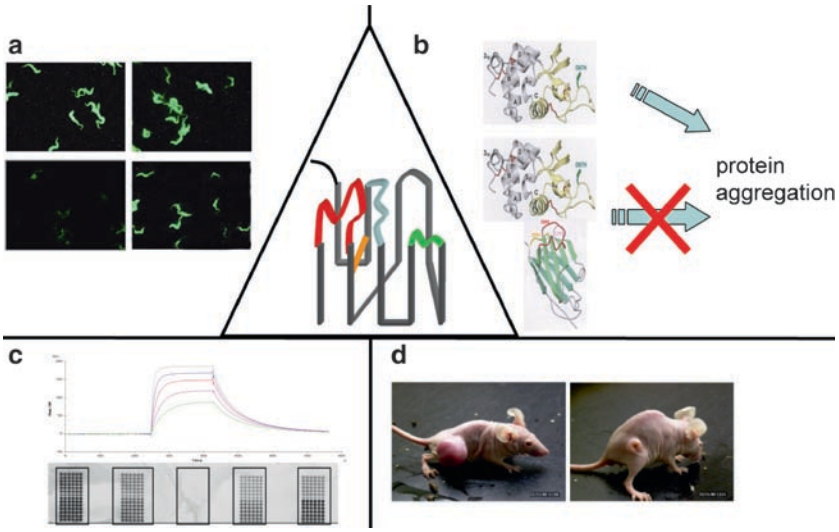

Fig. 3-2. Some of the Nanobodies applications. The structure within the *triangle* is the schematic presentation of a Nanobody structure with CDR1, CDR2, CDR3 and the conserved disulfide bridge in *blue*, *green*, *red* and *orange*, respectively. (**a**) Detection of live trypanosomes with three different His_6-tagged Nanobodies specific for the trypanosomes variable surface glycoprotein (*top panels* and the *bottom right panel*). The *bottom left panel* is negative control (an irrelevant Nanobody). A mouse anti-His antibody and an FITC-labeled anti-mouse monoclonal antibody were used as primary and secondary antibodies, respectively. (**b**) Prevention of protein aggregation. *Top*: A human lysozyme variant prone to aggregation forms fibrils. *Bottom*: The same protein in complex with a Nanobody fails to form fibrils. (**c**) Detection of antigen. *Top*: Sensogram of the real-time biosensor using hPSA as antigen and an hPSA-specific Nanobody as probe. *Bottom*: Microarrays for the detection of lysozyme using an irrelevant Nanobody (*middle panel*), a lysozyme-specific Nanobody (*left panel*), and its different mutants with reduced affinities, as compared with the Nanobody used in the *left panel*. (**d**) Nanobody directed enzyme prodrug therapy of cancer. *Left panel*: The bulky subcutaneous tumor in the flank of a mouse not subjected to treatment. *Right panel*: A mouse bearing a similar tumor but subjected to treatment (Cortez-Retamozo et al. 2004)

administration (Carter 2006). Different strategies such as PEGylation or fusion to peptides and proteins with affinity for the long-lived serum albumin have proven effective in increasing the half-lives of antibody fragments (Chapman et al. 1999; Chapman 2002; Dennis et al. 2002). Several studies have demonstrated the feasibility to use these approaches in order to tune the half-lives of Nanobodies to fit the application (Harmsen et al. 2005, 2007; Coppieters et al. 2006; Roovers et al. 2007). It is worth noting that PEGylation is very expensive and the usefulness of these approaches in clinics remains to be demonstrated.

Nanobodies can also be used as probes to develop biosensors for various applications including cancer diagnosis (Fig. 3-2c). We generated several Nanobodies specific for human prostate-specific antigen (hPSA) (Saerens et al. 2004). When immobilized onto various surfaces, these Nanobodies detect clinically relevant concentrations of hPSA, and determine the ratios of different hPSA isoforms (Pleschberger et al. 2004; Huang et al. 2005a; Saerens et al. 2005). Taking into account the harsh probe regeneration conditions, as compared with other antibody fragments, Nanobodies are the preferred antibody format for biosensor applications due to their higher stability and folding reversibility.

Bacteria such as *Bifodobacterium*, *Clostridium* and *Salmonella* replicate within solid tumors, and have been used for tumor-specific delivery of therapeutic genes (Pawelek et al. 2003; Mengesha et al. 2007). The efficiency of tumor colonization by bacteria can be increased by the display of tumor-specific antibody fragments on their surface (Bereta et al. 2007). In a similar way, tropism-modified measles virus has been generated, that exclusively targets ovarian tumors (Hasegawa et al. 2006). Since Nanobodies expressed on the surface of bacteria retain their antigen-binding activity (Veiga et al. 2004; Pant et al. 2006), Nanobodies may represent a new class of molecules for improving the tumor-specificity of bacteria and viruses.

5.2. Nanobodies Applications in Other Diseases

Besides their use in cancer diagnosis and therapy, Nanobodies offer alternatives to diagnostic and therapeutic tools presently used in other areas of human and animal health.

We demonstrated that a Nanobody specific for trypanosome variant surface glycoprotein (VSG) penetrates the dense VSG coat in live parasites to access its cryptic epitope. This Nanobody detected the parasite in blood smears with high selectivity and sensitivity (Fig. 3-2a) (Stijlemans et al. 2004), founding the ground for diagnosis. Administration of a conjugate consisting of this Nanobody and truncated apolipoprotein L-I resulted in complete cure of disease in a mouse model of human African trypanosomiasis (Baral et al. 2006). In a similar study, a Nanobody was used to direct an antimicrobial enzyme to *Streptococcus mutans*, resulting in the killing of the bacteria (Szynol et al. 2004). Daily oral administration of an untagged Nanobody specific for *S. mutans* significantly reduced the development of dental caries in a rat model, which mimic the clinical situation in patients with xerostomia, suggesting that Nanobodies can be used to prevent the development of dental caries (Krüger et al. 2006).

In a murine arthritis model, antagonistic anti-TNF-α Nanobodies exhibited an excellent therapeutic efficiency. In this report, Nanobodies were more potent than the conventional antibodies that are already in use for the treatment of rheumatoid arthritis (Coppieters et al. 2006).

Intracellularly expressed Bax-specific Nanobodies, conferring resistance against oxidative-stress-induced apoptosis, formed a basis to develop Nanobody-based therapeutics for degenerative diseases such as stroke which involve oxidative stress (Gueorguieva et al. 2006). A study reporting detoxification of LPS in whole blood by an anti-LPS Nanobody introduced Nanobodies as potential candidates for the prevention of LPS-mediated sepsis (El Khattabi et al. 2006).

In a mouse model of rotavirus-induced diarrhea, oral administration of rotavirus-specific Nanobodies or *Lactobacillus paracasei* expressing one of these Nanobodies on their surface largely reduced the duration and severity of diarrhea and viral load, demonstrating the feasibility to use Nanobodies for the treatment of diarrhea (Pant et al. 2006; van der Vaart et al. 2006).

The negative impact of protein aggregation disorders such as Alzheimer's and Parkinson's diseases is constantly increasing, as the population especially that of the developed world is aging. Preliminary studies reveal that Nanobodies are attractive therapeutic options for such disorders, since Nanobodies can prevent protein aggregation and, even more interesting, they can clear the already existing aggregates (Fig. 3-2b) (Dumoulin et al. 2003; Verheesen et al. 2006a).

Of note, the potential problem of Nanobody antigenicity has to be dealt with, whenever Nanobodies are to be used in humans. For example, it might be necessary to humanize Nanobodies prior to use in humans.

6. Conclusion

Since their discovery, the interest in the use of Nanobodies has been growing increasingly. The examples described here clearly demonstrate the usefulness of Nanobodies in many areas, in particular, in human and animal health. Of particular interest is the use of Nanobodies for applications where large amounts of antibody, high stability, high solubility and recognition of epitopes usually not antigenic for conventional antibodies are added values. With the first Nanobody already in phase I clinical trials, and several others close to this stage (http://www.ablynx.com), Nanobodies are advancing towards putting into test their promise as a novel class of therapeutics.

References

Alvarez-Reuda N, Behar G, Ferré V, Pugnière M, Roquet F, Gastinel L, Jacquot C, Aubry J, Baty D, Barbet J, Birklè S (2007) Generation of llama single-domain antibodies against methotrexate, a prototypical hapten. Mol Immunol 44:1680–1690

Atarhouch T, Bendahman N, Hamers-Casterman C, Hamers R, Muyldermans S (1997) cDNA sequence coding for the constant region of the dromedary γ3 heavy chain antibody. J Camel Pract Res 4:177–182

Baral TN, Magez S, Stijlemans B, Conrath K, Vanhollebeke B, Pays E, Muyldermans S, De Baetselier P (2006) Experimental therapy of African trypanomisis with a nanobody-conjugated human trypanolytic factor. Nat Med 12:580–584

Beckman RA, Weiner LM, Davis HM (2007) Antibody constructs in cancer therapy. Cancer 109:170–179

Bereta M, Hayhurst A, Gajda M, Chorobik P, Targosz M, Marcinkiewicz J, Kaufman HL (2007) Improving tumor targeting and therapeutic potential of *Salmonella* VNP20009 by displaying cell surface CEA-specific antibodies. Vaccine 25:4183–4192

Burton DR (1985) Immunoglobulin G: functional sites. Mol Immunol 22:161–206

Cai X, Garen A (1997) Comparison of fusion phage libraries displaying VH or single-chain Fv antibody fragments derived from the antibody repertoire of a vaccinated melanoma patient as a source of melanoma-specific targeting molecules. Proc Natl Acad Sci U S A 94:9261–9266

Carter PJ (2006) Potent antibody therapeutics by design. Nat Rev Immunol 6:343–357

Chapman AP (2002) PEGylated antibodies and antibody fragments for improved therapy: a review. Adv Drug Deliv Rev 54:531–545

Chapman AP, Antoniw P, Spitali M, West S, Stephens S, King DJ (1999) Therapeutic antibody fragments with prolonged in vivo half-lives. Nat Biotechnol 17:780–783

Chothia C, Novotny J, Bruccoleri R, Karplus M (1985) Domain association in immunoglobulin molecules. The packing of variable domains. J Mol Biol 186:651–663

Clauss MA, Jain RK (1990) Interstitial transport of rabbit and sheep antibodies in normal and neoplastic tissues. Cancer Res 50:3487–3492

Cogne M, Preud'homme JL, Guglielmi P (1989) Immunoglobulins gene alterations in human heavy chain disease. Res Immunol 140:487–502

Conrath KE, Lauwereys M, Galleni M, Matagne A, Frere JM, Kinne J, Wyns L, Muyldermans S (2001) Beta-lactamase inhibitors derived from single-domain antibody fragments elicited in *Camelidae*. Antimicrob Agents Chemother 45: 2807–2812

Conrath K, Vincke C, Stijlemans B, Schymkowitz J, Decanniere K, Wyns L, Muyldermans S, Loris R (2005) Antigen binding and solubility effects upon the veneering of a camel VHH in framework-2 to mimic VH. J Mol Biol 350:112–125

Coppieters K, Dreier T, Silence K, de Haard H, Lauwereys M, Casteels P, Beirnaert E, Jonckheere H, Van de Wiele C, Staelens L et al (2006) Formatted anti-tumor necrosis factor alpha VHH proteins derived from camelids show superior potency and targeting to inflamed joints in a murine model of collagen-induced arthritis. Arthritis Rheum 54:1856–1866

Cortez-Retamozo V, Lauwereys M, Hassanzadeh GG, Gobert M, Conrath K, Muyldermans S, de Baetselier P, Revets H (2002) Efficient tumor targeting by single-domain antibody fragments of camels. Int J Cancer 98:456–462

Cortez-Retamozo V, Backmann N, Senter PD, Wernery U, De baetselier P, Muyldermans S, Revets H (2004) Efficient cancer therapy with a nanobody-based conjugate. Cancer Res 64:2853–2857

Davies J, Riechmann L (1994) 'Camelising' human antibody fragments: NMR studies on VH domains. FEBS Lett 339:285–290

Davies J, Riechmann L (1995) Antibody VH domains as small recognition units. Biotechnology 13:475–479

Davies J, Riechmann L (1996) Single antibody domains as small recognition units: design and in vitro antigen selection of camelized, human VH domains with improved protein stability. Protein Eng 9:531–537

De Genst E, Silence K, Decanniere K, Conrath K, Loris R, Kinne J, Muyldermans S, Wyns L (2006) Molecular basis for the preferential cleft recognition by dromedary heavy-chain antibodies. Proc Natl Acad Sci U S A 103:4586–4591

de Haard HJW, Bezemer S, Ledeboer AM, Müller WH, Boender PJ, Moineau S, Coppelmans M-C, Verkleij AJ, Frenken LGJ, Verrips CT (2005) Llama antibodies against a lactococcal protein located at the tip of the phage tailprevent phage infection. J Bacteriol 187:4531–4541

Decanniere K, Desmyter A, Lauwereys M, Ghahroudi MA, Muyldermans S, Wyns L (1999) A single-domain antibody fragment in complex with RNase A: non-canonical loop structures and nanomolar affinity using two CDR loops. Structure 7:361–370

Decanniere K, Muyldermans S, Wyns L (2000) Canonical antigen binding loop structures: more structures, more canonical classes? J Mol Biol 300:83–91

Dennis M, Zhang M, Meng YG, Kadkhodayan M, Kirchhofer D, Combs D, Damico LA (2002) Albumin binding as a general strategy for improving the pharmacokinetics of proteins. J Biol Chem 277:35035–35043

Desmyter A, Transue TR, Ghahroudi MA, Dao Thi MH, Poortmans F, Hamers R, Muyldermans S, Wyns L (1996) Crystal structure of a camel single-domain VH antibody fragment in complex with lysozyme. Nat Struct Biol 3:803–811

Desmyter A, Decanniere K, Muyldermans S, Wyns L (2001) Antigen specificity and high affinity binding provided by one single loop of a camel single-domain antibody. J Biol Chem 276:26285–26290

Desmyter A, Spinelli S, Payan F, Lauwereys M, Wyns L, Muyldermans S, Cambillau C (2002) Three cameli VHH domains in complex with porcine α-amylase. J Biol Chem 277:23645–23650

Dolk E, van der Vaart M, Hulsik DL, Vriend G, de Haard H, Spinelli S, Cambillau C, Frenken L, Verrips T (2005) Isolation of llama antibody fragments for prevention of dandruff by phage display in shampoo. Appl Environ Microbiol 71:442–450

Dufner P, Jermutus L, Minter RR (2006) Harnessing phage and ribosome display for antibody optimization. Trends Biotechnol 24:523–529

Dumoulin M, Conrath K, van Meirhaeghe A, Meersman F, Heremans K, Frenken LGJ, Muyldermans S, Wyns L, Matagne A (2002) Single-domain antibody fragments with high conformational stability. Protein Sci 11:500–515

Dumoulin M, Last AM, Desmyter A, Decanniere K, Canet D, Larsson G, Spencer A, Archer DB, Sasse J, Muyldermans S et al (2003) A camelid antibody fragment inhibits the formation of amyloid fibrils human lysozyme. Nature 424:783–788

Dwek RA, Sutton BJ, Perkins SJ, Rademacher TW (1984) Structure–function relationships in immunoglobulins. Biochem Soc Symp 49:123–136

El Khattabi M, Adams H, Heezius E, Hermans P, Detmers F, Maassen B, van der Ley P, Tommassen J, Verrips T, Stam J (2006) Llama single-chain antibody that blocks lipopolysaccharide binding and signaling: prospects for therapeutic applications. Clin Vaccine Immunol 13:1079–1086

Ewert S, Cambillau C, Conrath K, Pluckthun A (2002) Biophysical properties of camelid V(HH) domains compared to those of human V(H)3 domains. Biochemistry 41:3628–3636

Fleischman JB, Pain RH, Porter RR (1962) Reduction of γ-globulins. Arch Biochem Biophys 1:174–180

Franklin EC, Lowenstein J, Bigelow B, Meltzer M (1964) Heavy chain disease. A new disorder of serum γ-globulins: report of the first case. Am J Med 37:332–350

Frenken LG, van der Linden RH, Hermans PW, Bos JW, Ruuls RC, de Geus B, Verrips CT (2000) Isolation of antigen specific llama VHH antibody fragments and their high level secretion by *Saccharomyces cerevisiae*. J Biotechnol 78:11–21

Ghahroudi MA, Desmyter A, Wyns L, Hamers R, Muyldermans S (1997) Selection and identification of single domain antibody fragments from camel heavy-chain antibodies. FEBS Lett 414:521–526

Goldman ER, Anderson GP, Liu JL, Delehanty JB, Sherwood LJ, Osborn LE, Cummins LB, Hayhurst A (2006) Facile generation of heat-stable antiviral and antitoxin single domain antibodies from a semisynthetic llama library. Anal Chem 78:8245–8255

Graff CP, Wittrup KD (2003) Theoretical analysis of antibody targeting of tumor spheroids: importance of dosage for penetration, and affinity for retention. Cancer Res 63:1288–1296

Greenberg AS, Avila D, Hughes M, Hughes A, Mckinney EC, Flajnik MF (1995) A new antigen receptor gene family that undergoes rearrangement and extensive somatic diversification in sharks. Nature 374:168–173

Groot AJ, Verheesen P, Westerlaken EJ, Gort EH, van der Groep P, Bovenschen N, van der Wall E, van Diest PJ, Shvarts A (2006) Identification by phage display of single-domain antibody fragments specific for the ODD domain in hypoxia-inducible factor 1alpha. Lab Invest 86:345–356

Gueorguieva D, Li S, Walsh N, Mukerji A, Tanha J, Pandey S (2006) Identification of single-domain, Bax-specific intrabodies that confer resistance to mammalian cells against oxidative-stress-induced apoptosis. FASEB J 20:2636–2638

Hamers R, Muyldermans S (1998) Immunology of the camels and llamas. In: Pastoret PP, Griebel P, Bazin H, Govaerts A (eds) Handbook of vertebrate immunology. Academic, San Diego, CA, pp 421–438

Hamers-Casterman C, Atarhouch T, Muyldermans S, Robinson G, Hamers C, Bajyana Songa E, Bendahman N, Hamers R (1993) Naturally occurring antibodies devoid of light chains. Nature 363:446448

Harmsen MM, Ruuls RC, Nijman IJ, Niewold TA, Frenken LGJ, de Geus B (2000) Llama heavy-chain V regions consist of at least four distinct subfamilies revealing novel sequence features. Mol Immunol 37:579–590

Harmsen MM, Van Slot CB, Fijten HP, Van Setten MC (2005) Prolonged in vivo residence times of llama single-domain antibody fragments in pigs by binding to porcine immunoglobulins. Vaccine 23:4926–4934

Harmsen MM, van Slot CB, Fijten HP, van Keulen L, Rosalia RA, Weerdmeester K, Cornelissen AH, De Bruin MG, Eblé PL, Dekker A (2007) Passive immunization of guinea pigs with llama single-domain antibody fragments against foot-and-mouth disease. Vet Microbiol 120:193–206

Hasegawa K, Nakamura T, Harvey M, Ikeda Y, Oberg A, Figini M, Canevari S, Hartmann LC, Peng KW (2006) The use of a tropism-modified measles virus in folate receptor-targeted virotherapy of ovarian cancer. Clin Cancer Res 12:6170–6178

Hendershot LM (1990) Immunoglobulin heavy chain and binding protein complexes are dissociated in vivo by light chain addition. J Cell Biol 111:829–837

Hendershot LM, Bole D, Köhler G, Kearney JF (1987) Assembly and secretion of heavy chains that do not associate posttranslationally with immunoglobulin heavy chain-binding protein. J Cell Biol 104:761–767

Hoogenboom HR, Chames P (2000) Natural and designer binding sites made by phage display technology. Immunol Today 21:371–378

Hoogenboom HR, de Bruine AP, Hufton SE, Hoet RMA, Arends JW, Roovers RC (1998) Antibody phage display technology and its applications. Immunotechnology 4:309–318

Huang L, Reekmans G, Saerens D, Friedt JM, Frederix F, Francis L, Muyldermans S, Campitelli A, Van Hoof C (2005a) Prostate-specific antigen immunosensing based on mixed self-assembled monolayers, camel antibodies and colloidal gold enhanced sandwich assays. Biosens Bioelectron 21:483–490

Huang Y, Verheesen P, Roussis A, Frankhuizen W, Ginjaar J, Haldane F, Laval S, Anderson LVB, Verrips T, Frants RR et al (2005b) Protein studies in dysferlinopathy patients using llama-derived antibody fragments selected by phage display. Eur J Hum Genet 13:721–730

Hulstein JJJ, de Groot PG, Silence K, Veyradier A, Fijnheer R, Lenting PJ (2005) A novel nanobody that detects the gain-of-function phenotype of von Willebrand factor in ADAMTS13 deficiency and von Willebrand disease type 2B. Blood 106:3035–3042

Ismaili A, Jalali-Javaran M, Rasaee MJ, Rahbarizadeh F, Forouzandeh-Moghadam M, Memari HR (2007) Production and characterization of anti-(mucin MUC1) single-domain antibody in tobacco (*Nicotiana tabacum cultivar Xanthi*). Biotechnol Appl Biochem 47:11–19

Jobling SA, Jarman C, Teh MM, Holmberg N, Blake C, Verhoeyen ME (2003) Immunomodulation of enzyme function in plants by single-domain antibody fragments. Nat Biotechnol 21:77–80

Joosten V, Roelofs MS, van den Dries N, Goosen T, Verrips CT, van den Hondel CA, Lokman BC (2005) Production of bifunctional proteins by *Aspergillus awamori*: llama variable heavy chain antibody fragment (VHH) R9 coupled to *Arthromyces ramosus* peroxidase (ARP). J Biotechnol 120:347–359

Klooster R, Maassen BTH, Stam JC, Hermans PW, ten Haaft MR, Detmers FJM, de Haard HJ, Post JA, Verrips CT (2007) Improved anti-IgG and HSA affinity ligands: clinical application of VHH antibody technology. J Immunol Methods 324:1–12

Koch-Nolte F, Reyelt J, Schössow B, Schwarz N, Scheuplein F, Rothenburg S, Haag F, Alzogaray V, Cauerhff A, Goldbaum FA (2007) Single domain antibodies from

llama effectively and specifically block T cell ecto-ADP-ribosyltransferase ART2.2 in vivo. FASEB J 21:3490–3498
Kortt AA, Guthrie RE, Hinds MG, Power BE, Ivancic N, Caldwell JB, Gruen LC, Norton RS, Hudson PJ (1995) Solution properties of *Escherichia coli*-expressed VH domain of anti-neuraminidase antibody NC41. J Protein Chem 14:167–178
Krüger C, Hultberg A, Marcotte H, Hermans P, Bezemer S, Frenken LG, Hammarström L (2006) Therapeutic effect of llama derived VHH fragments against Streptococcus mutans on the development of dental caries. Appl Microbiol Biothecnol 72:732–737
Ladenson RC, Crimmins DL, Landt Y, Ladenson JH (2006) Isolation and characterization of a thermally stable recombinant anti-caffeine heavy-chain antibody fragment. Anal Chem 78:4501–4508
Lakowski RA, Luscombe NM, Swindells MB, Thornton JM (1996) Protein clefts in molecular recognition and function. Protein Sci 5:2438–2452
Lauwereys M, Ghahroudi MA, Desmyter A, Kinne J, Hölzer W, De Genst E, Wyns L, Muyldermans S (1998) Potent enzyme inhibitors derived from dromedary heavy-chain antibodies. EMBO J 17:3512–3520
Ledeboer AM, Bezemer S, de Haard JJW, Schaffers IM, Verrips CT, van Vliet C, Düsterhöft E-M, Zoon P, Moineau S, Frenken LGJ (2002) Preventing phage lysis of *Lactococcus lactis* in cheese production using a neutralizing heavy-chain antibody fragment from llama. J Dairy Sci 85:1376–1382
Loris R, Marianovsky I, Lah J, Laeremans T, Engelberg-Kulka H, Glaser G, Muyldermans S, Wyns L (2003) Crystal structure of the intrinsically flexible addiction antidote MazE. J Biol Chem 278:28252–28257
Maass DR, Sepulveda J, Pernthaner A, Shoemaker CB (2007) Alpaca (*Lama pacos*) as a convenient source of recombinant camelid heavy chain antibodies (VHHs). J Immunol Methods 324:13–25
Magee AM, Coyne S, Murphy D, Horvath EM, Medgyesy P, Kavanagh TA (2004) T7 RNA polymerase-directed expression of an antibody fragment transgene in plastids causes a semi-lethal pale-green seedling phenotype. Transgenic Res 13:325–337
Magee AM, MacLean D, Gray JC, Kavanagh TA (2007) Disruption of essential plastid gene expression caused by T7 RNA polymerase-mediated transcription of plastid transgenes during early seedling development. Transgenic Res 16:415–428
Marquardt A, Muyldermans S, Przybylski M (2006) A synthetic camel anti-lysozyme peptide antibody (peptibody) with flexible loop structure identified by high-resolution affinity mass spectrometry. Chem Eur J 12:1915–1923
Martin F, Volpari C, Steinkuhler C, Dimasi N, Brunetti M, Biasiol G, Altamura S, Cortese R, De Francesco R, Sollazzo M (1997) Affinity selection of a camelized VH domain antibody inhibitor of hepatitis C virus NS3 protease. Protein Eng 10: 607–614
McManus S, Riechmann L (1991) Use of 2D NMR, protein engineering, and molecular modeling to study the hapten-binding site of an antibody Fv fragment against 2-phenyloxazolone. Biochemistry 30:5851–5857
Mengesha A, Dubois L, Chiu RK, Paesmans K, Wouters BG, Lambin P, Theys J (2007) Potential and limitations of bacterial-mediated cancer therapy. Front Biosci 12:3880–3891
Milenic DE, Yokota T, Filpula DR, Finkelman MA, Dodd SW, Wood JF, Whitlow M, Snoy P, Schlom J (1991) Construction, binding properties, metabolism, and tumor targeting of a single-chain Fv derived from the pancarcinoma monoclonal antibody CC49. Cancer Res 51:6363–6371
Muyldermans S (2001) Single domain camel antibodies: current status. Rev Mol Biotechnol 74:277–302
Muyldermans S, Atarhouch T, Saldanha J, Barbosa JA, Hamers R (1994) Sequence and structure of VH domain from naturally occurring camel heavy chain immunoglobulins lacking light chains. Protein Eng 7:1129–1135
Nguyen VK, Muyldermans S, Hamers R (1998) The specific variable domain of camel heavy-chain antibodies is encoded in the germline. J Mol Biol 257:413–418

Nguyen VK, Hamers R, Wyns L, Muyldermans S (1999) Loss of splice consensus signal is responsible for the removal of the entire CH1 domain of the functional camel IgG2A heavy-chain antibodies. Mol Immunol 36:515–524

Nguyen VK, Hamers R, Wyns L, Muyldermans S (2000) Camel heavy-chain antibodies: diverse germline VHH and specific mechanisms enlarge the antigen-binding repertoire. EMBO J 19:921–931

Nguyen VK, Desmyter A, Muyldermans S (2001) Functional heavy-chain antibodies in camelidae. Adv Immunol 79:261–296

Nguyen VK, Su C, Muyldermans S, van der Loo W (2002) Heavy-chain antibodies in *camelidae*; a case of evolutionary innovation. Immunogenetics 54:39–47

Nieba L, Honegger A, Krebber C, Plückthun A (1997) Disrupting the hydrophobic patches at the antibody variable/constant domain interface: improved in vivo folding and physical characterization of an engineered scFv fragment. Protein Eng 10:435–444

Nugent LJ, Jain RK (1984) Extravascular diffusion in normal and neoplastic tissues. Cancer Res 44:238–244

Nuttall SD, Krishnan UV, Hattarki M, De Gori R, Irving RA, Hudson PJ (2001) Isolation of the new antigen receptor from wobbegong sharks, and use as a scaffold for the display of protein loop libraries. Mol Immunol 38:313–326

Olichon A, Schweizer D, Muyldermans S, de Marco A (2007) Heating as a rapid purification method for recovering correctly-folded thermotolerant VH and VHH domains. BMC Biotechnol 7:7

Padlan EA (1994) Anatomy of the antibody molecule. Mol Immunol 31:169–217

Padlan EA (1996) X-ray crystallography of antibodies. Adv Protein Chem 49:57–133

Pant N, Hultberg A, Zhao Y, Svensson L, Pan-Hammarström Q, Johansen K, Pouwels PH, Ruggeri FM, Hermans P, Frenken L et al (2006) Lactobacilli expressing variable domain of llama heavy-chain antibody fragments (lactobodies) confer protection against rotavirus-induced diarrhea. J Infect Dis 194:1580–1588

Pawelek JM, Low KB, Bermudes D (2003) Bacteria as tumor-targeting vectors. Lancet Oncol 4:548–556

Perez JM, Renisio JG, Prompers JJ, van Platerink CJ, Cambillau C, Darbon H, Frenken LGJ (2001) Thermal unfolding of a llama antibody fragment: a two-state reversible process. Biochemistry 40:74–83

Pleschberger M, Saerens D, Weigert S, Sleytr UB, Muyldermans S, Sára M, Egelseer EM (2004) An S-layer heavy chain camel antibody fusion protein for generation of a nanopatterned sensing layer to detect the prostate-specific antigen by surface plasmon resonance technology. Bioconjug Chem 15:664–671

Pluen A, Boucher Y, Ramanujan S, McKee TD, Gohongi T, di Tomaso E, Brown EB, Izumi Y, Campbell RB, Berk DA et al (2001) Role of tumor-host interactions in interstitial diffusion of macromolecules: cranial versus subcutaneous tumors. Proc Natl Acad Sci U S A 98:4628–4633

Porter RR (1973) Structural studies of immunoglobulins. Science 180:713–716

Potter KN, Li Y, Capra JD (1996) Staphylococcal protein A simultaneously interacts with framework region 1, complementarity determining region 2 and framework region 3 on human VH3-encoded Igs. J Immunol 157:2982–2988

Rahbarizadeh F, Rasaee MJ, Forouzandeh-Moghadam M, Allameh AA (2005) High expression and purification of the recombinant camelid anti-MUC1 single domain antibodies in *Escherichia coli*. Protein Expr Purif 44:32–38

Rajabi-Memari H, Jalali-Javaran M, Rasaee MJ, Rahbarizadeh F, Forouzandeh-Moghadam M, Esmaili A (2006) Expression and characterization of a recombinant single-domain monoclonal antibody against MUC1 mucin in tobacco plants. Hybridoma (Larchmt) 25:209–215

Rast JP, Amemiya CT, Litman RT, Strong SJ, Litman GW (1998) Distinct patterns of IgH structure and organization in a divergent lineage of chrondrichthyan fishes. Immunogenetics 47:234–245

Reiter Y, Schuck P, Boyd LF, Plaksin D (1999) An antibody single-domain phage display library of a native heavy chain variable region: isolation of functional single-domain VH molecules with a unique interface. J Mol Biol 290:685–698

Riechmann L, Cavanagh J, McManus S (1991) Uniform labeling of a recombinant antibody Fv-fragment with ^{15}N and ^{13}C for heteronuclear NMR spectroscopy. FEBS Lett 287:185–188

Roholt O, Onoue K, Pressman D (1964) Specific combination of H and L chains of rabbit γ-globulins. Proc Natl Acad Sci U S A 51:173–178

Roovers RC, Laeremans T, Huang L, de Taeye S, Verkleij AJ, Revets H, de Haard HJ, van Bergen en Henegouwen PMP (2007) Efficient inhibition of EGFR signaling and of tumor growth by antagonistic anti-EGFR Nanobodies. Cancer Immunol Immunother 56:303–317

Rothbauer U, Zolghadr K, Tillib S, Nowak D, Schermelleh L, Gahl A, Backman N, Conrath K, Muyldermans S, Cardoso MC, Leonhardt H (2006) Targeting and tracing antigens in live cells with fluorescent nanobodies. Nat Methods 3:887–889

Saerens D, Kinne J, Bosmans E, Wernery U, Muyldermans S, Conrath K (2004) Single domain antibodies derived from dromedary lymph node and peripheral blood lymphocytes sensing conformational variants of prostate-specific antigen. J Biol Chem 279:51965–51972

Saerens D, Frederix F, Reekmans G, Conrath K, Jans K, Brys L, Huang L, Bosmans E, Maes G, Borghs G, Muyldermans S (2005) Engineering camel single-domain antibodies and immobilization chemistry for human prostate-specific antigen sensing. Anal Chem 77:7547–7555

Sasso EH, Silverman GJ, Mannik M (1991) Human IgA and IgG F(ab′)2 that bind to staphylococcal protein A belong to the VHIII subgroup. J Immunol 147:1877–1883

Seligmann M, Mihaesco E, Preud'homme JL, Danon F, Brouet JC (1979) Heavy chain diseases: current findings and concepts. Immunol Rev 48:145–167

Skerra A, Plückthun A (1988) Assembly of functional immunoglobulin Fv fragment in *Escherichia coli*. Science 240:1038–1041

Spinelli S, Frenken L, Bourgeois D, de Ron L, Bos W, Verrips T, Anguille C, Cambillau C, Tegoni M (1996) The crystal structure of a llama heavy chain variable domain. Nat Struct Biol 3:752–757

Spinelli S, Frenken LG, Hermans P, Verrips T, Brown K, Tegoni M, Cambillau C (2000) Camelid heavy-chain variable domains provide efficient combining sites to haptens. Biochemistry 39:1217–1222

Stewart CS, MacKenzie CR, Hall JC (2007) Isolation, characterization and pentamerization of α-cobrotoxin specific single-domain antibodies from a naïve phage display library: preliminary findings for antivenom development. Toxicon 49:699–709

Stijlemans B, Conrath K, Cortez-Retamozo V, Van Xong H, Wyns L, Senter P, Revets H, De Baetselier P, Muyldermans S, Magez S (2004) Efficient targeting of conserved cryptic epitopes of infectious agents by single domain antibodies. J Biol Chem 279:1256–1261

Szynol A, de Soet JJ, Sieben-van Tuyl E, Bos JW, Frenken LG (2004) Bactericidal effects of a fusion protein of llama heavy-chain antibodies coupled to glucose oxidase on oral bacteria. Antimicrob Agents Chemother 48:3390–3395

Tanaka T, Lobato MN, Rabbitts TH (2003) Single domain intracellular antibodies: a minimal fragment for direct in vivo selection of antigen-specific intrabodies. J Mol Biol 331:1109–1120

Tanha J, Xu P, Chen Z, Ni F, Kaplan H, Narang SA, MacKenzie CR (2001) Optimal design features of camelized human single-domain antibody libraries. J Biol Chem 276:24774–24780

Transue TR, De Genst E, Ghahroudi MA, Wyns L, Muyldermans S (1998) Camel single-domain antibody inhibits enzyme by mimicking carbohydrate substrate. Proteins Struct Funct Genet 32:515–522

Tunggal JK, Cowan DS, Shaikh H, Tannock IF (1999) Penetration of anticancer drugs through solid tissue: a factor that limits the effectiveness of chemotherapy for solid tumors. Clin Cancer Res 5:1583–1586

Utsumi S, Karush F (1964) The subunits of purified rabbit antibody. Biochemistry 3:1329–1338

Van der Linden RHJ, Frenken L, de Gues B, Harmsen MM, Ruuls RC, Stok W, de Ron L, Wilson S, Davis P, Verrips T (1999) Comparison of physical chemical properties of llama VHH antibody fragments and mouse monoclonal antibodies. Biochim Biophys Acta 1431:37–46

Van der Linden R, de Geus B, Stok W, Bos W, van Wassenaar D, Verrips T, Frenken L (2000a) Induction of immune responses and molecular cloning of the heavy chain antibody repertoire of Lama glama. J Immunol Methods 240:185–195

Van der Linden R, de Geus B, Frenken L, Peters H, Verrips T (2000b) Improved production and function of llama heavy chain antibody fragments by molecular evolution. J Biotechnol 80:261–270

Van der Vaart JM, Pant N, Wolvers D, Bezemer S, Hermans PW, Bellamy K, Sarker SA, van der Logt CPE, Svensson L, Verrips CT et al (2006) Reduction in morbidity of rotavirus induced diarrhea in mice by yeast produced monovalent llama-derived antibody fragments. Vaccine 24:4130–4137

Veiga E, de Lorenzo V, Fernández LA (2004) Structural tolerance of bacterial autotransporters for folded passenger protein domains. Mol Microbiol 52:1069–1080

Verheesen P, de Kluijver A, van Koningsbruggen S, de Brij M, de Haard H, van Ommen CJB, van der Maarel SM, Verrips T (2006a) Prevention of oculopharyngeal muscular dystrophy-associated aggregation of nuclear poly(A)-binding protein with a single-domain intracellular antibody. Hum Mol Genet 15:105–111

Verheesen P, Roussis A, de Haard HJ, Groot AJ, Stam JC, den Dunnen JT, Frants RR, Verkleij AJ, Verrips CT, van der Maarel SM (2006b) Reliable and controllable antibody fragment selections from camelid non-immune libraries for target validation. Biochim Biophys Acta 1764:1307–1319

Vu KB, Ghahroudi MA, Wyns L, Muyldermans S (1997) Comparison of llama VH sequences from conventional and heavy chain antibodies. Mol Immunol 34:1121–1131

Ward ES, Güssow D, Griffiths AD, Jones PT, Winter G (1989) Binding activities of a repertoire of single immunoglobulin variable domains secreted from *Escherichia coli*. Nature 341:544–546

Webster DM, Henry AH, Rees AR (1994) Antibody–antigen interactions. Curr Opin Struct Biol 4:123–129

Winter G, Griffiths AD, Hawkins RE, Hoogenboom HR (1994) Making antibodies by phage display technology. Annu Rev Immunol 12:433–455

Woolven BP, Frenken L, van der Logt P, Nicholls PJ (1999) The structure of the llama heavy chain constant genes reveals a mechanism for heavy-chain antibody formation. Immunogenetics 50:98–101

Wu AM, Senter PD (2005) Arming antibodies: prospects and challenges for immunoconjugates. Nat Biothecnol 23:1137–1146

Wu TT, Johnson G, Kabat EA (1993) Length distribution of CDR H3 in antibodies. Proteins Struct Funct Genet 16:1–7

Yau KY, Groves MA, Li S, Sheedy C, Lee H, Tanha J, MacKenzie CR, Jermutus L, Hall JC (2003) Selection of hapten-specific single-domain antibodies from a non-immunized llama ribosome display library. J Immunol Methods 281:161–175

Yau KY, Dubuc G, Li S, Hirama T, MacKenzie CR, Jermutus L, Hall JC, Tanha J (2005) Affinity maturation of a V(H)H by mutational hotspot randomization. J Immunol Methods 297:213–224

Yokota T, Milenic DE, Whitlow M, Schlom J (1992) Rapid tumor penetration of a single-chain Fv and comparison with other immunoglobulin forms. Cancer Res 52:3402–3408

Part II

Expression and Production of MABS

Chapter 4

GPEx® A Flexible Method for the Rapid Generation of Stable, High Expressing, Antibody Producing Mammalian Cell Lines

Gregory T. Bleck

1. Introduction

A versatile system has been developed, which is capable of transferring genes of interest into a wide variety of mammalian host cells and offers a number of advantages over the other methods for production of antibodies. These advantages include; (1) Shorter timelines, (2) Improved consistency, (3) Higher specific productivities, (4) Better genetic stabilities, (5) Increased flexibility and (6) Ability to work on any cell line.

The GPEx® method utilizes replication defective retroviral vectors, derived from Moloney Murine Leukemia virus (MLV) and pseudotyped with Vesicular Stomatitis Virus Glycoprotein (VSV-G), to stably insert single copies of genes at multiple genomic locations into dividing cells. Retrovectors deliver genes coded as RNA that, after entering the cell, are reverse transcribed to DNA and integrated stably into the genome of the host cell. Two enzymes, reverse transcriptase and integrase, provided transiently in the vector particle, perform this function. These integrated genes are maintained through subsequent cell divisions as if they were endogenous cellular genes. By controlling the number of retrovector particles accessing the cell, multiple gene insertion (desirable for high yielding cell cultures) can be achieved without any of the traditional amplification steps. This chapter describes the use of the GPEx® technology for transferring genes into Chinese Hamster Ovary (CHO) cells, for the purpose of consistently producing cell lines with high antibody production levels in a short amount of time (Fig. 4-1).

2. Benefits of the GPEx® Cell Line Development Technology for Production of Antibodies

1. Can be used insert genes into a wide variety of cell lines

The method utilizes VSV-G as an envelope on the retrovector particles. This envelope protein allows the retrovectors to insert genes into all mammalian cells, in addition to numerous other cell types, due to its ability to bind to

From: *Current Trends in Monoclonal Antibody Development and Manufacturing,* Biotechnology: Pharmaceutical Aspects, DOI 10.1007/978-0-387-76643-0_4, Edited by: S.J. Shire et al.

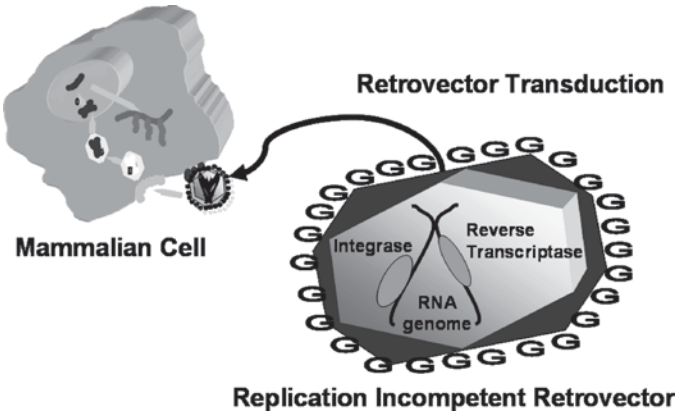

Fig. 4-1. GPEx® cell line engineering

various membrane phospholipids and glycolipids (Schlegel et al. 1983; Burns et al. 1993; Yee et al. 1994). On some occasions, an antibody you make may bind to specific antigens present on the cell surface or in the cell cytoplasm of your production cell type, causing a problem with cell growth or viability. In these instances, a cell type lacking that particular antigen can then be used as a production cell line.

2. Each copy of the transgene is inserted at a different genomic location

Retrovector gene insertions occur at unique locations in the cell genome, with a single copy of the gene being inserted at each independent site. Unlike most other methods of transgene insertion that are undefined "passive" processes, each insertion by a retrovector is an "active" process that is modulated by the integrase enzyme (Andrake and Skalka 1996). This unique insertion process eliminates the occurrence of "head-to-tail" multiple-single-loci transgene inserts in these cell lines. This type of genetic insertion is extremely stable and cell lines generated by this method do not require detailed testing of stability before the production of the master cell bank.

3. Transgene inserts target "open" or "active" regions of the cell genome

The MLV retrovectors have been shown to preferentially insert into or around the transcription start point of genes (Wu et al. 2003; Mitchell et al. 2004). This preference for transcriptionally "active" regions of the genome allows for higher, more consistent levels of expression per copy of the gene inserted as compared to other methods of gene insertion. Antibody producing cell clones generated by this method are extremely consistent, and only a few hundred clones are screened to identify high expressing master cell bank candidate clones.

4. No need for antibiotic selection or use of toxic compounds for gene amplification

Due to the extremely high gene insertion efficiency of the GPEx® process, no selectable markers (e.g. neomycin, blasticidin, hygromycin, or puromycin resistance genes) are needed for cell line generation. This has a number of advantages over other cell line development methods, including reduced costs

for culturing cells, no additional taxing of the cells due to production of the selectable marker, and reduced time to clonal cell line selection. The high transduction efficiency and the ability to do repeat cell transductions generate high copy number cell lines using this process, eliminating the need to amplify gene copy number by adding toxic compounds such as methotrexate. Re-transduction of cells yields clonal lines with copy numbers ranging from 25 to 250.

5. Straightforward addition of extra genes to cell pools or previously developed cell lines

The high transduction efficiency, coupled with no antibiotic selection requirement, allows easy addition of one or more genes to newly developed or already established cell lines. For antibodies, heavy and light chains are easily titrated to the correct gene ratio to yield maximum antibody production and efficient antibody formation. Gene ratio titering can be accomplished through specific screening during clonal selection or an individual transduction of a specific chain, if required.

6. High-expressing cell population prior to clonal selection

After the completion of initial transductions, cell pools are available for small to large scale production. These cell pools have been expanded up to 100-L scale for production. Typical antibody producing cell pools will secrete antibody at levels of 500–1000 mg/L at this early stage in the development process (prior to selection of a high-expressing clone). Milligrams to multi-gram quantities of antibody are produced from these cell pools.

3. Generation of Antibody Producing Cell Lines

The data presented in this chapter are from a number of GPEx® generated CHO cell lines producing various antibodies. GPEx® cell line development was conducted using the methods and materials outlined below.

3.1. Gene Constructs

The backbone vector used for all cell line development is shown in Fig. 4-2. Since the system is based on an RNA virus, and gene introns would be removed during retrovector production, only cDNA's are used in the system.

LTR 1 = Moloney Murine Leukemia Virus Long Terminal Repeat (Non-Protein Coding)
PR = Moloney Murine Leukemia Virus Viral Packaging Region (Non-Protein Coding)
Promoter = Cytomegalovirus Immediate Early Gene Promoter Region
RP = Recombinant Protein Coding Region
RESE = RNA Export and Stability Element (Non-Protein Coding)
LTR 2 = Moloney Murine Leukemia Virus Long Terminal Repeat/Poly-Adenylation Signal (Non-Protein Coding)

Fig. 4-2. Transgene expression construct. Genetic elements are not drawn to scale

The internal promoter controls expression of the transgene, the RESE element assists with RNA export from the nucleus to the cytoplasm, and the poly-adenylation signal is contained within LTR2. The transgene of interest for each project is cloned into the backbone vector and subsequently used for retrovector production. For antibody cell line development, the heavy chain and light chain genes are each cloned as individual gene constructs. Each of the genomic inserts generated with the GPEx® process contain all genetic elements shown in Fig. 4-2.

3.2. Retrovector Production

Retrovectors are produced in a human embryonic kidney cell line, (HEK 293) that has been transformed to constitutively express the MLV *gag*, *pro* and *pol* genes (Burns et al. 1993). This cell line has been master cell banked and fully characterized in detail. Most importantly, the 293 packaging cell line does not contain the MLV envelope (*env*) gene or the MLV packaging region such that in the absence of the transgene construct, which provides the viral RNA packaging region, and an envelope gene, the 293 packaging line produces particles consisting of the required structural elements and enzymes, but these particles are not active since they lack an envelope and an RNA genome.

To create active retrovector particles containing the transgene of interest, a plasmid containing the expression construct (Fig. 4-2) and a plasmid encoding the VSV-G gene are introduced into the 293 cells via calcium-phosphate transfection (Ausubel et al. 1996). The expression construct becomes the RNA genome of the retrovector. The VSV-G envelope causes pseudotyping of the retrovector, allowing the retrovectors to become capable of cell transduction. Expression of the VSV-G gene by the cells is a terminal event resulting in syncytium formation, and ultimately, cell death. However, for a period of about 3 days, the 293 packaging cell line-transgene construct-VSV-G system produces high titers of active retrovector particles (Fig. 4-3). The high titer vector is then concentrated by ultracentrifugation, and used for cell transductions.

3.3. Cell Culture

A master cell bank of the CHO-S cell line (Invitrogen, Carlsbad, CA) was the source for all cell line development outlined in this report. Cells were cultured in serum-free PFCHO LS medium (HyClone, Logan, UT) for all described work; however, 2% fetal bovine serum (HyClone, Logan, UT) is added to the culture medium for approximately 10–14 days during the limited dilution cloning step. Cells are typically cultured at 37°C and 5% CO_2. Cell counts and viabilities are estimated using the Cedex system (Innovatis, Bielefeld, Germany). Fed-batch culture is performed using commercially available supplements (HyClone, Logan, UT, Invitrogen, Carlsbad, CA).

3.4. Cell Line Development

Cell lines expressing antibodies are produced as shown in Fig. 4-4. Transductions are performed at a multiplicity of infection of at least 1,000 retrovector particles per cell. For generation of antibody producing cell lines, an initial transduction of CHO cells are performed using a retrovector containing the light chain (LC) gene. The LC expressing pool of cells are then transduced

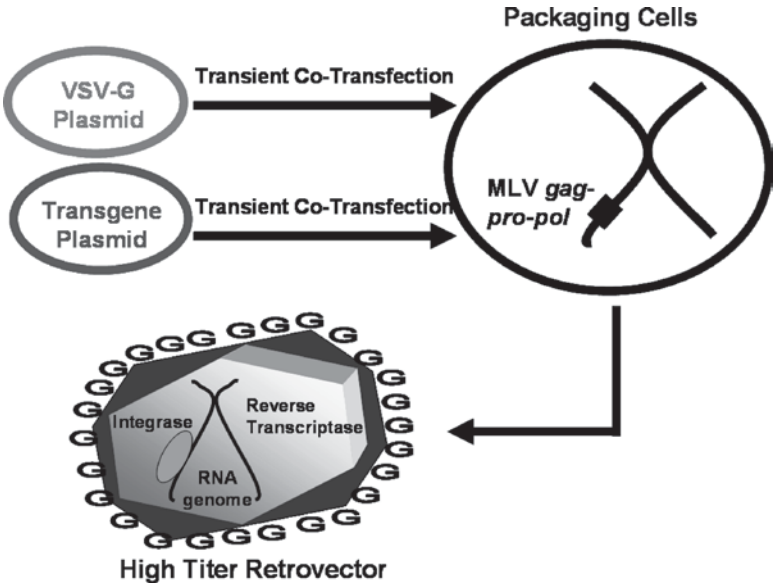

Fig. 4-3. Retrovector production process

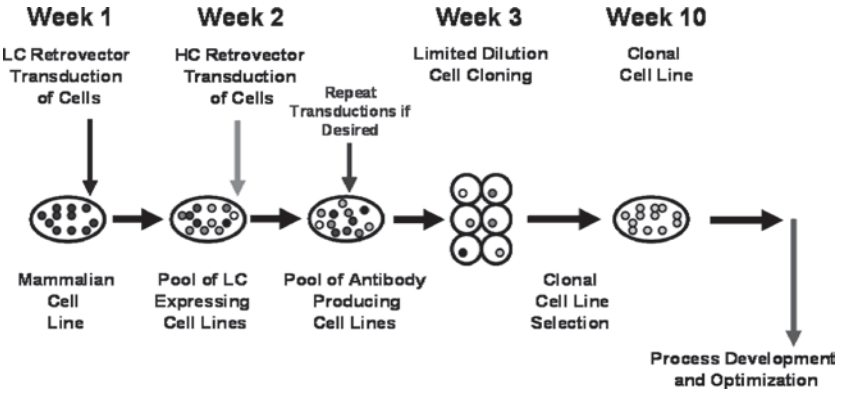

Fig. 4-4. Antibody cell line development method

with a retrovector containing the heavy chain (HC) gene. Upon completion of a single transduction, both LC and HC transductions in the case of antibodies, the resulting pool of cells produces functional antibody for analysis. Single cell clones are isolated from the cell pool using limited dilution cloning. Approximately 300–500 clonal lines are screened for production levels and various protein specific characteristics.

3.5. Transgene and mRNA Analysis

DNA or RNA are isolated from cells in log growth phase. A quantitative real-time PCR based assay is used to estimate the number of gene copies inserted in the cell lines. The MLV packaging region of each gene insert is used as the target sequence to estimate the total number of transgene insertions.

The β-1,4-galactosyltransferase-1 gene is used as an endogenous marker gene to control for the amount of genomic DNA in each reaction. The gene index is calculated by subtracting the transgene assay threshold cycle from the control assay threshold cycle.

A similar quantitative real-time PCR assay along with a reverse transcription step is used to determine the level of HC and LC mRNA being expressed. A portion of the constant region of the HC and LC are used to determine HC and LC mRNA levels respectively. The glyceraldehyde-3-phosphate dehydrogenase (GAPDH) gene is used as a control mRNA for the CHO cell lines. Isolated RNA is reverse transcribed and three quantitative real-time PCR (HC, LC, control) reactions are run in triplicate. Similar to the assays performed with genomic DNA, a transgene mRNA index value is calculated by subtracting the sample threshold cycle number for the either the HC or LC assays from the control GAPDH assay threshold cycle value.

3.6. Protein Analysis

Protein levels were determined using ELISA or Protein A-HPLC based assays specific for each individual antibody.

4. Antibody Screening from Pooled Cell Lines

For antibody screening, a major impact on the project timeline is the ability to quickly identify a product candidate and subsequently produce a high expressing cell line for that product. The advent of various computer based protein design methodologies and antibody discovery technologies for development of antibody therapeutics has resulted in large numbers of antibody variants that must be screened in order to identify the best clinical candidate.

For these antibody variant candidates, proper screening requires milligram to gram levels of protein production in a mammalian cell for testing of the candidate material. Preferentially, this material is produced in the same cell type that will be used to produce the master cell bank for the selected antibody variant. This testing is initially performed in vitro, but in many instances, animal studies are required for identification of the best potential clinical candidate. Animal studies can require multi-gram levels of the antibody variants. Production and screening of these variants and selection of a final clinical candidate is a time consuming process in most research groups, and is generally in conflict with what are now common aggressive timelines for moving products forward into the clinic. Typically, the initial variants are produced from a transient expression system, and then after clinical candidate selection, the cell line development process is restarted, a stable cell line is produced, and the final clinical candidate is master cell banked for manufacturing. The GPEx® technology allows antibody variants to be screened as part of the manufacturing cell line generation process. Milligram to multi-gram levels of protein are produced from an initial stable pool of cells for variant characterization and selection. Final clonal cell line selection from this pooled line either proceeds in parallel with variant in vitro/in vivo screening, or after clinical candidate selection has been completed. This method of variant selection eliminates the need for a total re-start in cell line development after the clinical candidate has been identified, since the pooled cell line is the starting material for clonal selection. The pooled cell lines are grown in fed-batch culture conditions at the

100-mL–100-L scale resulting in milligrams to grams of antibody depending on the scale of production. Final antibody titers from the cell pool culture that ranges from 500 to 1000 mg/L for typical antibodies.

5. Clonal Cell Line Development

A second major impact to antibody clinical development timelines, is the speed to get to a master cell bank (MCB) for the candidate antibody. The GPEx® process takes 5 months to obtain a high expressing MCB candidate line using a cDNA encoding the heavy and light chain genes as the starting material (Fig. 4-5). A pooled antibody producing cell line is used for limited dilution cloning to isolate 300–500 clones, the top twenty clones are selected based on protein production in 96-well plates. Fourteen-day protein production and specific productivity results from triplicate T150-flasks are then used to narrow the number of clones to the top 3–5 candidates. These clones are subsequently moved into process development for production analysis under generic fed-batch culture that conditions to select the master cell bank candidate clone. These candidate clones in generic fed-batch conditions typically produce titers of 1–2 g/L and have specific productivities of 25–70 pg/cell/day. Specific productivities for the last nine different antibody producing cell lines that have been generated using GPEx® are shown in Fig. 4-6.

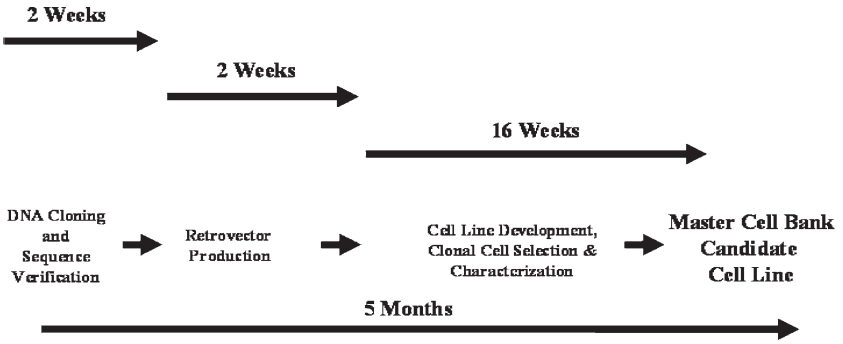

Fig. 4-5. Process timeline from cDNA to the start of master cell banking

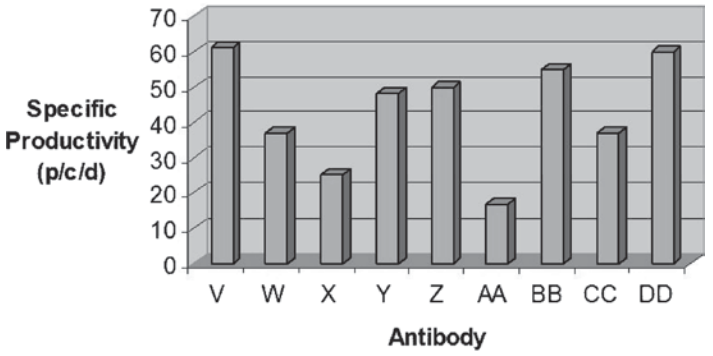

Fig. 4-6. Specific productivities in picograms/cell/day for the last nine GPEx® produced antibody expressing cell lines

Table 4-1. Gene index of the pooled Antibody K cell line after each transduction cycle.

Pooled cell line	Gene index
LC/HC Transduction 1	4.93
LC/HC Transduction 2	7.20
LC/HC Transduction 3	7.93
LC/HC Transduction 4	8.53

Table 4-2. Fourteen-day fed-batch T-flask production of the top Antibody K clone isolated from each transduction cycle pool.

Clonal cell line	Protein (mg/L)
LC/HC Transduction 1	914
LC/HC Transduction 2	1,028
LC/HC Transduction 3	1,376
LC/HC Transduction 4	1,640

6. Pooled Cell Line Re-transduction

For some antibodies, a single transduction cycle (one heavy chain and one light chain transduction) appears to achieve a cell line with maximum genetic potential and adding additional gene copies does not improve cell line production. However, with other antibodies, adding more gene copies via repeated transductions or modifying the ratio of heavy and light chain expression does improve the cell line productivity, allowing a cell line with maximum genetic potential to be produced. An example of this is Antibody K. Four successive cycles of a light chain transduction followed by a heavy chain transduction were completed on a pool of cells. After each cycle, a portion of the cell pool was used for limited dilution cloning and clonal selection. A sample of the cells was also taken for analysis of transgene number. Average gene copy indexes for the cell pool after each cycle are shown in Table 4-1. The highest producing clone isolated from each of the four transduction cycles was analyzed for antibody production in generic fed-batch conditions. Cells were cultured under static conditions in triplicate T150 flasks for 14 days. Final titers of the cultures were compared (Table 4-2). In the case of Antibody K, repeated transductions not only increased the number of transgene inserts, it improved the production levels of the cell clones.

7. Clonal Cell Line Stability

Genetic and expression stability are important metrics used to evaluate any cell line development method. For cell lines produced with amplification type methods, specific reduction in the amount of LC mRNA over extended culture has been observed (Strutzenberger et al. 1999) as well as dramatic decreases in the number of transgene copies present and subsequent mRNA levels when no selection pressure was applied. In addition, major stability differences

between clones have been observed (Kim et al. 1998; Barnes et al. 2004). Many of the stability issues with these types of methods are hypothesized to be caused by having multiple copies of a gene construct inserted at a single genetic locus. During cell mitosis, homologous recombination can occur at the locus, causing a reduction in the number of gene copies at this site and a subsequent decrease mRNA and protein production. The GPEx® technology allows such consistent stability for typical projects, where cell lines are not analyzed for stability until after the master cell bank is generated. This greatly reduces production timelines and gets antibodies into clinical trial much faster. The expanding use of real-time PCR for evaluation of cell lines has made stability analysis much more quantitative and easier to perform.

Final production cell lines expressing seven different antibodies were analyzed for their stability. A cell bank for each cell line was designated as generation 0 for the purpose of the study. Cells were continuously cultured by serial passage from generation 0 to approximately generation 60. At the end of the experiment, samples of cells from generation 0 and generation 60 were used for DNA and RNA isolation. Real-time PCR analysis of the DNA showed no significant difference between the number of transgenes at generation 0 and generation 60 for any of the lines (Fig. 4-7). Both HC and LC mRNA levels were also estimated at the two time points for each of the cell lines. Again, there was no significant difference in either HC or LC chain mRNA levels over the extended culture (Figures 4-8 and 4-9).

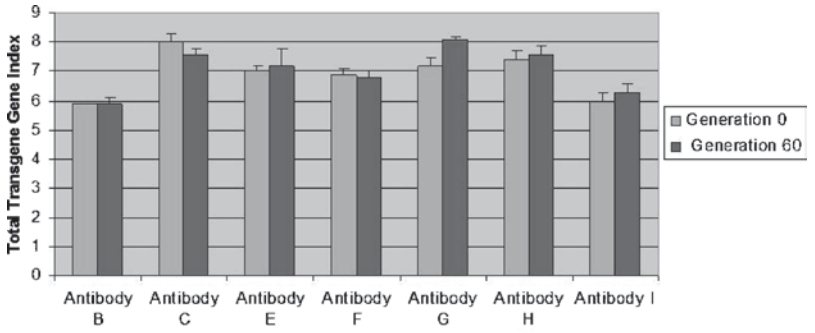

Fig. 4-7. Total transgene estimates before and after 60 generations in culture for seven different antibody producing cell lines

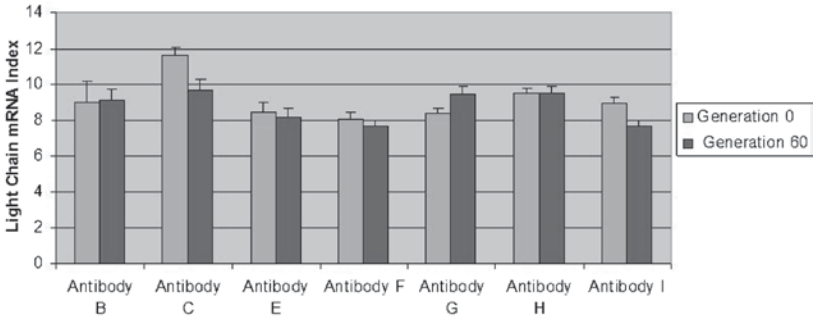

Fig. 4-8. Antibody light chain transgene mRNA expression before and after 60 generations in culture for seven different cell lines

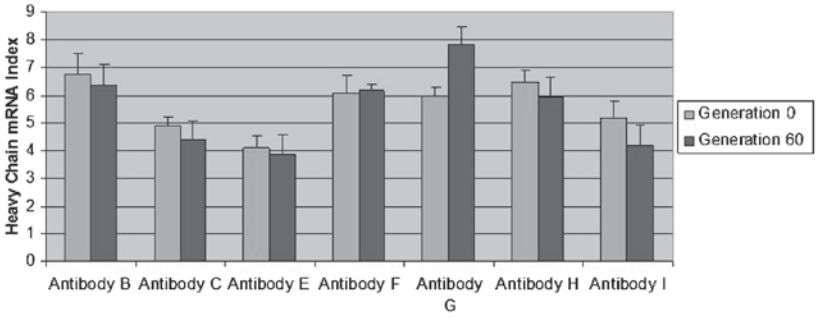

Fig. 4-9. Antibody heavy chain transgene mRNA expression before and after 60 generations in culture for seven different cell lines

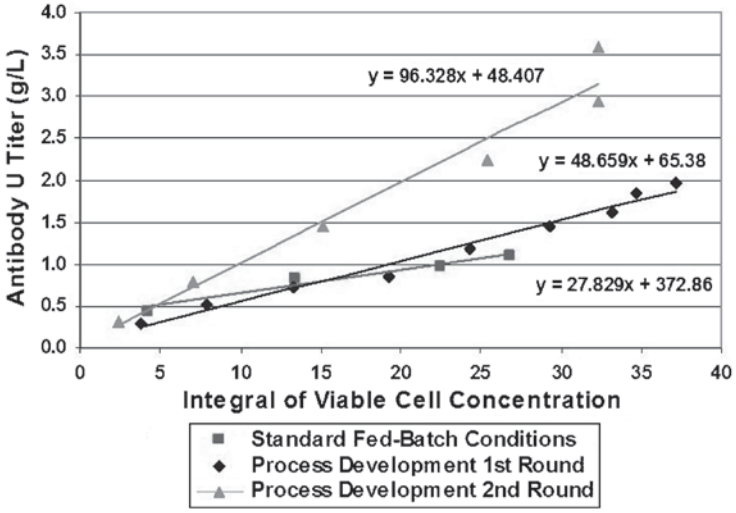

Fig. 4-10. Three different fed-batch production runs of an antibody U producing cell line. The graph shows a plot of antibody titer versus integral of viable cell concentration. The slope of each line corresponds to the specific productivity (pg/cell/day) for each of the three production runs

8. Upstream Process Development of Antibody Cell Lines

Continuing advances in media, supplements, culture vessels, temperature shifts, pH modifications and numerous other methods allow upstream process development to potentially be a never ending source of yield improvement. The fact that optimal culture conditions are unique to each individual cell line, and that detailed upstream process development takes much time and resources make it imperative that the MCB candidate cell line has maximum genetic potential for producing the antibody of interest before starting upstream development. This allows the MCB candidate not only to be used for clinical development, but also have yields needed for commercial production and a process in place for that production. An example of upstream process development on a GPEx® cell line (Antibody U) is shown in Fig. 4-10.

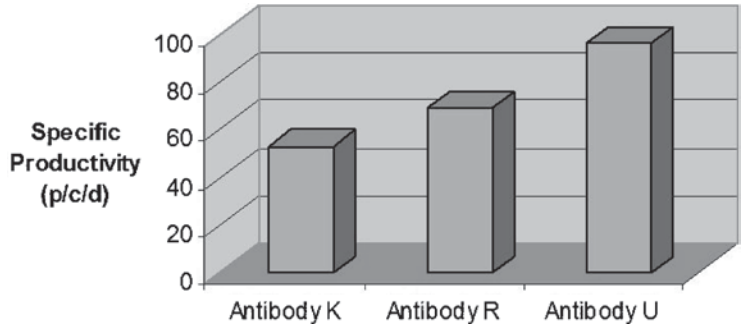

Fig. 4-11. Fed-batch specific productivities of three cell lines after 8 weeks of upstream process development

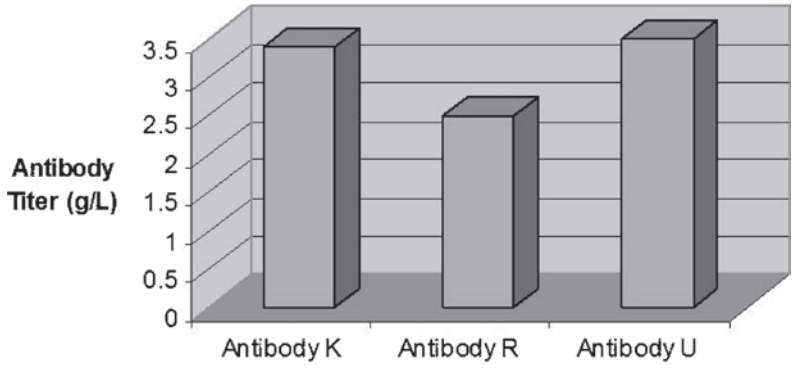

Fig. 4-12. Final fed-batch antibody titers of three cell lines after 8 weeks of upstream process development

Two rounds of process development were performed on the Antibody U cell line. Each round took 4 weeks and improvements were observed after each round. Figures 4-11 and 4-12 show the specific productivity and final production titer of three GPEx® master cell bank lines after two rounds of upstream process development.

9. Conclusions

The GPEx® method of cell line engineering is an extremely flexible, fast and consistent process, that has distinct advantages over other cell line development methods, and can significantly shorten the time from research/development to clinic for antibodies. Large quantities of recombinant antibody can be produced from pooled cell lines along the path to candidate cell line selection, which in turn shortens timelines and eliminates the need for separate, large-scale transient transfection experiments. The lack of an antibiotic selection step and high transduction efficiency allows a master cell bank candidate cell line to be produced 5 months after the start of a project. The consistent genetic stability of these cell lines is unique when compared to other cell line development methods that result in multiple copy gene inserts and eliminates

the need for early testing of stability. GPEx® cell lines producing antibodies consistently express at levels of 2–4 g/L in fed-batch bioreactor manufacturing with minimal upstream process development. Finally, the ease with which genes can be added and titrated into cells permits the genetic potential of each individual cell line to be fully maximized.

References

Andrake MD, Skalka AM (1996) Retroviral integrase, putting the pieces together. J Biol Chem 271(33):19633–19636

Barnes LM, Bentley CM, Dickson AJ (2004) Molecular definition of predictive indicators of stable protein expression in recombinant NS0 myeloma cells. Biotechnol Bioeng 85(2):115–121

Burns JC, Friedmann T, Driever W, Burrascano M, Yee JK (1993) Vesicular stomatitis virus G glycoprotein-pseudotyped retroviral vectors: concentration to a very high titer and efficient gene transfer into mammalian and nonmammalian cells. Proc Natl Acad Sci U S A 90:8033–8037

Kim NS, Kim SJ, Lee GM (1998) Clonal variability within dihydrofolate reductase-mediated gene amplified Chinese hamster ovary cells: stability in the absence of selection pressure. Biotechnol Bioeng 60(6):679–688

Mitchell RS, Beitzel BF, Schroder ARW, Shinn P, Chen H, Berry CC, Ecker JR, Bushman FD (2004) Retroviral DNA, integration: ASLV, HIV and MLV show distinct target site preferences. PLoS Biol 2(8):1127–1137

Pear W (1996) Transient transfection methods for preparation of high-titer retroviral supernatants. In: Current protocols in molecular biology, vol 2, edited by Ausubel FM, Brent R, Kingston RE, Moore DD, Seidman JG, Smith JA, Struhl K. Wiley, New York, 9.11.1–9.11.18

Schlegel R, Tralka TS, Willingham MC, Pastan I (1983) Inhibition of VSV binding and infectivity by phosphatidylserine: is phosphatidylserine a VSV-binding site? Cell 32:639–646

Strutzenberger K, Borth N, Kunert R, Steinfellner W, Katinger H (1999) Changes during subclone development and ageing of human antibody-producing recombinant CHO cells. J Biotechnol 69:215–226

Wu X, Li Y, Crise B, Burgess SM (2003) Transcription start regions in the human genome are favored targets for MLV integration. Science 300:1749–1751

Yee JK, Friedmann T, Burns JC (1994) Generation of high-titer pseudotyped retroviral vectors with very broad host range. Methods Cell Biol 43:99–112

Chapter 5

Advancing Our Cell Culture Platform: Incorporating Lessons Learned and New Technologies

Carole Heath

Abbreviations

CE-SDS	Capillary electrophoresis sodium dodecyl sulfate
CHO	Chinese hamster ovary
cIEF	Capillary isoelectric focusing
DHFR	Dihydrofolate reductase
DOE	Design of experiments
GMP	Good manufacturing practice
HMW	High molecular weight
HTS	High throughput screening
IND	Investigational new drug
LMW	Low molecular weight
MAb	Monoclonal antibody
P&AS	Process and Analytical Sciences
QbD	Quality by design
SEC	Size exclusion chromatography
SE-HPLC	Size exclusion high performance liquid chromatography

1. Introduction

The success of a few monoclonal antibody (MAb) products has made recombinant MAbs the fastest growing therapeutic for a broad range of indications. To quickly move these molecules into the clinic, several of the larger biotechnology companies, including Amgen, have designed and implemented a platform approach to process development for some or all of their products. Amgen initiated development of a platform approach for MAbs soon after the acquisition of Immunex, allowing the company to take advantage of the historical experience from two process development organizations.

In essence, the platform is an approach that leverages similarities across MAbs and integrates the core competencies of multiple functional areas

From: *Current Trends in Monoclonal Antibody Development and Manufacturing,*
Biotechnology: Pharmaceutical Aspects, DOI 10.1007/978-0-387-76643-0_5,
Edited by: S.J. Shire et al.

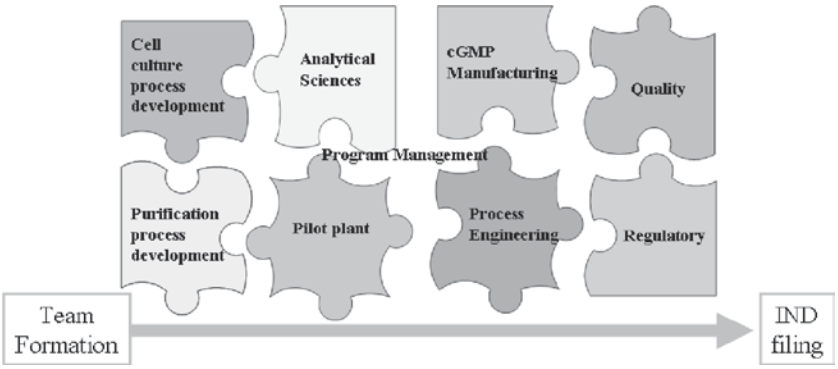

Fig. 5-1. Amgen's platform is an integrated approach that applies core competencies from many functional areas, allowing simultaneous progression of multiple project teams through the development life cycle

(Fig. 5-1). Several project teams can simultaneously move programs through the development life-cycle, from team formation to Investigational New Drug (IND) filing. Creating and applying a platform approach has allowed Process and Analytical Sciences (P&AS) at Amgen to reduce project cycle times for Phase I molecules, improve resource efficiency, reduce expenses and expand our portfolio of candidates in development. Other departments at Amgen, such as Manufacturing, Quality and Regulatory, have also realized time and resource savings because platform processes are very similar from one molecule to another, which allows these groups to use documented templates across the MAb portfolio. Adopting a consistent approach for MAbs also improves the ease of development and manufacturing at multiple sites, an important consideration for a multi-site organization such as Amgen.

2. Implementing a Platform

Prior to Amgen's development of a platform, process development was lengthy and unpredictable. With each new molecule, the lead scientist often re-invented the wheel by exploring/optimizing many parameters in a long series of experiments. The pre-platform approach made it difficult to predict both development time and performance, which created planning problems for groups outside of P&AS because they did not know what to expect and when. With a platform, on the other hand, management can easily assign and rotate project teams, schedule pilot-scale and Good Manufacturing Practice (GMP) runs, ensure adequate supplies of qualified raw materials, and even plan for clinical studies because the outcomes and timing are predictable and have a high likelihood of success.

Although generic, the platform provides some flexibility while building in quality and manufacturability from the start. Most of the operating parameters are predefined with a limited subset that requires some selection or optimization. In Amgen's experience, a fully defined process is not feasible because of differences in performance observed for different MAbs that are the natural consequences of the biophysical and biochemical attributes resulting from unique protein sequences.

3. Components of the Platform

For the Cell Science and Technology group at Amgen, the primary goals of the platform are to create a stable cell line, define a cell culture process from thaw to harvest, and supply material to other departments (e.g., Purification Process Development and Pharmaceutics) for their development activities. Desired characteristics of the cell line are rapid growth and high expression of antibody. The cell culture process must be reproducible, meet titer and final viability targets, and meet in-process targets for product quality. The platform has been designed with ease of manufacturing, consistency and scalability in mind. These factors are critical for transfer of the cell line and process to our pilot-scale plants for generating the toxicology and Phase I study materials.

The upstream platform is divided into three main sections: creation of the cell line, cell culture process definition, and harvest. Details of each are described in the following sections.

3.1. Creation of the Cell Line

The process development platform begins with a robust expression system. For Amgen, the host of choice is a serum-free clonal cell line derived from Chinese Hamster Ovary (CHO) DXB11 with a proprietary vector system. The cells are transfected, selected, and allowed to recover before amplification of pools over a range of methotrexate levels. Some pools are re-amplified to encourage greater expression. The amplified pools are analyzed for growth, viability and productivity; based on these results, the best pools are then cloned. Clone screening begins with a high-throughput analysis of growth and titer, followed by production culture in shake flasks. The final screen of the most promising clones occurs in bioreactors, using design of experiments (DOE) methods that expose the clones to a range of culture conditions to test for robustness. The final and backup clones are chosen based on the growth, viability, expression and product quality data.

3.2. Cell Culture Process Definition

Much of the cell culture process from thaw to production is defined by the platform. For example, unless there is an issue with growth or viability that calls for optimization, the seed train conditions (e.g., format, seeding density, medium, culture duration, etc.) are prescribed by the platform eliminating the need for any experimentation on these steps. The cell culture team will still optimize a few parameters in the fed-batch production step because of molecule and cell line differences. Although the seeding density, format, and culture duration are set, scientists explore the responses to limited ranges of pH and temperature, and select from a restricted number of media and feed recipes. As we improve the formulations, however, the media choices will become limited as well. All other raw materials are fixed to avoid last minute changes for Amgen's Manufacturing, Quality and Supply Chain departments.

3.3. Harvest

The harvest platform is jointly owned by the cell culture and purification functional areas because the unit operation involves cells, and it significantly impacts subsequent downstream processing. The cell culture fluid containing

the product is harvested from the cells and other debris by centrifugation and depth filtration. Essentially all of the centrifugation and depth filtration operating conditions are fixed with the platform approach. The depth filter throughput, however, does have an acceptable range to account for variability in the quality of the cell culture centrate that can result from differences in cell mass and viability in the production bioreactor. The depth filter area is limited by available equipment in the non-GMP and GMP production facilities.

4. Platform Metrics

Since implementation, over a dozen Mabs have gone through platform development at Amgen. Overall performance metrics show that Amgen's platform has been a success. A plot of titers shows acceptable results across the portfolio of MAbs, especially compared to pre-platform processes (Fig. 5-2). After implementation of the platform, all MAbs except two met or exceeded the initial titer target for Phase I processes; even the two that missed were only slightly below the target. The data also demonstrated that the incorporating technology improvements into the platform can raise the bar even for early phase processes. We recently raised the titer target by 50%, and we expect to increase it again soon with our most recent platform improvements.

Another important metric is scalability of the process. Scale-up performance for four typical molecules demonstrates comparable titer performance from bench-scale bioreactors to pilot-scale non-GMP and GMP production tanks (Fig. 5-3). In addition to scalability of titer, other parameters such as growth, viability and metabolic indicators also result in comparable performance across scales.

The Cell Culture, Purification and Analytical Sciences groups all track performance metrics and how well each molecule fits their respective platforms. For many molecules, the fit to the upstream platform is excellent (i.e., no adjustments needed), while more molecules are classified as "good" fits (i.e., require some

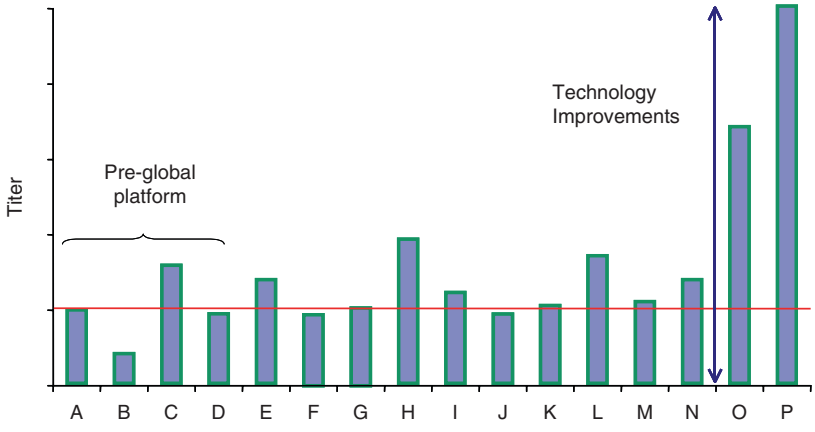

Fig. 5-2. Performance metrics show that the platform results in acceptable titers across the antibody portfolio. Improved media and feed formulations result in higher titers for more recent molecules. Each *letter* refers to a different molecule

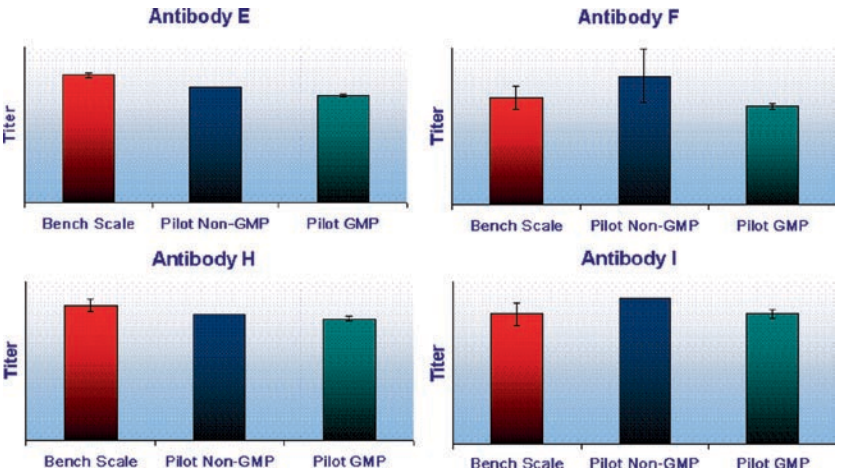

Fig. 5-3. Performance metrics show that the platform results in a scalable process with consistent titer performance from bench to pilot scales

Table 5-1. Qualitative assessment of goodness of platform fit by upstream, downstream and analytical sciences functional areas shows that platform fit is fairly consistent across molecules. (Note that each letter represents a different molecule and that the letters represent the same antibodies as in Figures 5.2 and 5.3.)

	Upstream		Downstream		Analytical	
Excellent (no tweaks)	D	G	H		E	F
	H	I	I		K	L
	L	N	L			
	P					
Good (minor tweaks)	E	F	D	E	D	G
	K	O	F	G	H	I
			K	P	P	
Moderate (significant tweaks)	J		J	N	J	N
			O		O	

minor modifications) for the Purification and Analytical groups (Table 5-1). A likely reason behind this difference in the degree of goodness of fit is that typically the structure of the molecule will have a greater impact on purification performance and analytical development than on cell line growth and expression. In most cases (shown in Table 5-1), the molecules that require significant adjustments ("moderate" fit) are not just problematic for one functional area, but have fit issues with one or both of the other areas as well.

5. Platform Challenges

Despite our efforts to make the platform conditions generic, they were not a perfect fit for all antibody molecules, requiring the scientists, on some occasions, to make minor or even major modifications to achieve adequate

performance. This often results in a longer timeline. Depending on what adjustments are made, the resulting process may also present some new conditions to the pilot plants, affecting their workloads and timelines as well. On the positive side, the learnings from the non-fitting molecules contributed to our understanding of antibodies and cell lines as well as the platform itself.

Our challenges to date have included low titer, low final viability, and product quality attributes that are outside the in-process targets. Product quality outside the targets is usually the result of high levels of aggregates, host cell proteins, product isoforms and/or partially processed carbohydrate moieties. Methods to address some of these challenges are described below.

5.1. Example 1: Titer Target Not Met

The cell line for one of our early molecules produced a titer significantly below the initial target. Because of the low titer, additional runs would have been needed to supply material for other development groups (purification, pharmaceutics, etc.), toxicology studies and Phase I clinical studies. The latter two would have been particularly expensive in terms of time and money.

Generally speaking, there are several options for improving titer. One option is to expand the test ranges of parameters beyond what is allowed by the platform, e.g., seeding density, pH, temperature, and culture duration. Some of these, however, such as increasing the seeding density or the culture duration may not be feasible or even possible because of limitations in the seed train or plant scheduling, respectively. Since developing a new medium is time consuming, a second option is to use different base and/or feed media, such as alternative in-house proprietary media or commercially-available media. Another possibility could be the addition of inducers, growth factors, or other additives, but this option assumes extensive prior knowledge or experience; otherwise, time-consuming screening and experimentation are required with no guarantee of a positive outcome.

In this case, all of the above options were investigated in a relatively short period of time in screening studies. Although parameter exploration was limited, the combination of increased culture duration and altered feed strategy resulted in a titer that was close to the desired target and an acceptable product quality profile. Exploring additional options might have resulted in higher titer, but the impact to the timeline would have been significant. That type of in-depth exploratory work can be done during the development of commercial process. Because this was an early molecule and the platform has been updated three times since then, we have yet to see if it works any better if/when this molecule goes through commercial phase development or if this was just a problematic molecule/cell line.

5.2. Example 2: High Turbidity in Feed Stream to Purification

The molecule implicated in Example 1 also caused difficulties downstream. The first step in purification is a Protein A column, which follows the centrifugal harvest and depth filtration steps. We traced the high turbidity observed in the Protein A eluate for this molecule to high levels of host cell protein impurities that precipitate at low pH. Our first approach to address this problem was to change the cell culture conditions. Separate attempts to shorten the culture duration and to induce precipitation in the bioreactor prior to

centrifugation and depth filtration did not reduce the turbidity of the Protein A eluate. Instead, increasing the depth filter surface area to exploit its adsorptive properties in front of the Protein A column significantly reduced the turbidity of the eluate resulting in acceptable process performance and product quality for the Phase I clinical runs.

5.3. Example 3: Analytical Size Exclusion Chromatography Pre-peak

In another case, changing to a different analytical size exclusion chromatography (SEC) column method resulted in an unexpected product quality profile. With the original column method, the high molecular weight (HMW) peak was quickly followed by the much larger main peak. With a different column method, on the other hand, a front shoulder or "pre-peak" appeared between the HMW and main peaks. Our concern about a possible new and unidentified species was compounded by the observation that the level of the pre-peak was not stable but changed over time.

Subsequent studies identified the pre-peak as a monomeric product variant or isoform with a similar activity as the main peak. Bioreactor studies have shown that the pre-peak occurs at a consistent percentage during cell culture, and that the pre-peak is not an artifact of downstream processing. Experiments have shown that exposure of the unprocessed bulk to light results in a rapid increase in the level of pre-peak, identifying for us a means of controlling the level of pre-peak in the product.

5.4. Example 4: Variable *N*-Glycans

Amgen scientists have observed that the mannose type and level sometimes varies between MAbs and/or for a given MAb under different operating conditions. For one molecule, the level of high mannose varied significantly from one clone to another. With the final clone of the same cell line, the amount of high mannose also varied significantly during the process development activities. Further study showed that the culture osmolality had a significant impact on high mannose level. To maintain a consistent level of high mannose from run to run, we limited the process osmolality to a target range. Both these observations demonstrated that there can be a clone-to-clone dependency, as well as process impact, on the levels of different glycosylation species. Testing for product quality at the clone selection stage and imposing limits to culture parameters, such as osmolality, can control the level and variability of glycan species for MAbs.

These case studies demonstrate that the platform cannot be generic in every respect because of differences between molecules. When possible, we have taken that information and used it to improve the platform. This process is described in the next section.

6. Evolving the Platform

The platform is not a static set of procedures. Lessons learned from our development and manufacturing history across an array of molecules, including information from the above case studies, are fed back into the platform during a yearly review process. Technology advances are also incorporated during the annual review process. Each functional area is responsible for assembling the

data supporting a proposed change to the platform as well as for undertaking a critical review of the pros, cons and any possible risks of proposed changes.

Once the P&AS functional areas have done their own critical review of proposed changes to the platform, other Amgen departments (e.g., Manufacturing Science, Quality, Legal, and Regulatory) review and comment on the acceptability of the proposed changes based on potential impacts to their organizations. Adding a new raw material to the cell culture platform that increases cell growth and may affect levels of host cell protein, for example, requires review by several departments, including, but not limited to, Purification, Sourcing, Legal and Quality.

A couple of the upstream changes that have been made since we put the platform in place are aimed at improving our practice of Quality by Design (QbD). One change is a method for improving our clone selection process, and the other is to increase our understanding of the design space of our production process. During clone selection, we have increased the level of testing to ensure that we select the best clone not only for growth and productivity, but also for product quality. An example of the range in product quality test results across eleven clones is shown in Table 5-2. Early analytical screening can help select out potentially problematic clones such as those producing high levels of aggregate or high mannose. More recently, we have begun testing clones for their sensitivity to process variability in parameters such as pH, temperature and osmolality.

While we do little process optimization during early phase development, we do conduct experiments to explore the design space during or after clone selection. Using DOE, we set up reactor studies to map the operational space for some of the parameters that are likely to vary during processing, potentially affecting product quality. At this stage, we only explore those parameters needed to ensure robust operation for the early phase clinical runs.

Table 5-2. Product analytics vary across clones of the same molecule.

	SE-HPLC			cIEF			CE-SDS
Clone	% HMW	% Main	% LMW	% Acidic	% Main	% Basic	% Glyco-form
1	14.0	86.0	0.0	37.9	55.9	6.2	19.9
2	7.6	92.4	0.0	30.9	65.9	3.3	13.4
3	9.7	90.3	0.0	27.8	66.6	5.5	8.5
4	7.0	93.0	0.0	29.5	65.7	4.8	11.6
5	3.4	96.6	0.0	30.3	63.0	6.6	8.0
6	4.4	95.6	0.0	31.7	61.9	6.4	16.0
7	5.9	94.1	0.0	31.9	62.2	5.9	17.6
8	8.2	91.8	0.0	29.5	67.5	3.0	10.3
9	11.1	88.7	0.2	25.5	68.7	5.8	7.0
10	6.9	93.0	0.1	30.2	65.5	4.3	10.5
11	10.1	89.7	0.2	30.2	66.1	3.7	11.9
Average	8.0	91.9	0.0	30.5	64.5	5.1	12.2

SE-HPLC size exclusion high performance chromatography; *cIEF* capillary isoelectric focusing; *HMW* high molecular weight; *LMW* low molecular weight; *CE-SDS* capillary electrophoresis sodium dodecyl sulfate

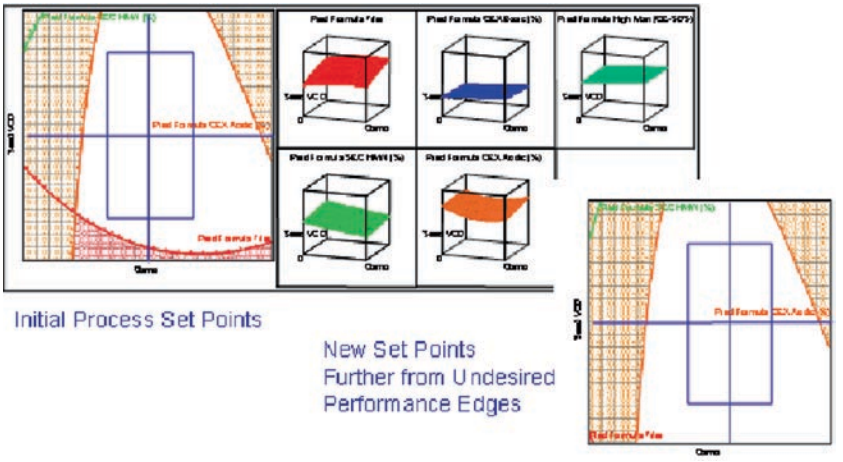

Fig. 5-4. DOE has improved our understanding of the process design space and has helped guide us to selection of more robust parameter set points. The *left hand side* of the figure shows the operating space (*box*) in proximity to an undesired titer region (*bottom crosshatch*). Mapping the responses to a variety of process inputs allows us to choose an operating space that is further from undesired outputs, as demonstrated in the diagram on the *right hand side*

Further in-depth study of a broader spectrum of parameters occurs during later phase development (Fig. 5-4) when process optimization and robustness are critical. Generic process knowledge gained and lessons learned during the later phase development can, however, be cycled back to the early phase development platform for application to future molecules.

Other changes in the platform include improvements to the media toolbox by replacing older media formulations with higher performing, more manufacturing-friendly media and feeds. These advances have come out of a technology focus area at Amgen, which we have applied to the early development platform and our commercial development efforts, resulting in significant titer increases.

7. Vision for the Future

As Amgen moves more molecules through our pipeline, we have developed a more thorough understanding of the relationships between the antibody biochemistry and processing characteristics. In the short term, this has led to a series of improvements in the platform that have allowed us to increase our success rate, increase yields, and shorten our timelines. We expect that Amgen's platform of the not-too-distant future will include more antibody engineering, allowing us to tailor our antibody products so that they are active, high-yielding, safe, and manufacturing-friendly from the start. An antibody database project, now in its infancy, will help to move Amgen in that direction.

Along these lines, we are currently exploring ways of improving our candidate selection techniques. In cases where we have multiple candidates with similar bioactivity, we perform a molecule assessment to assist with candidate

selection. We expect this step to be valuable, not only for early clinical work, but also for later commercial phase development efforts. Because the development life cycle of an antibody product is lengthy, applying knowledge gained from commercial molecules back into our molecule assessment and platform will be slow, but important.

Another step in improving Amgen's platform is high throughput screening (HTS), where we can test many more conditions at the same time than previously feasible. We currently use HTS to screen several hundreds of clones for growth and titer, but we should soon have the capability to expand the screening to include a variety of culture conditions, with the goal of improving our ability to select robust cell lines. HTS is a powerful tool because it affords us the opportunity to screen large numbers of clones under relevant and hopefully predictive conditions, such as high osmolality, during production. During later phase development, HTS will prove valuable for medium optimization, process optimization and robustness, and commercial process troubleshooting.

Finally, we are also rapidly progressing towards single-cycle development for some or all of our MAb products. As the platform evolves, we find that fewer and fewer upstream parameters require optimization during early phase development. As we move closer to eliminating the need for process optimization after clone selection for early phase processes, we will only expend significant time and resources on process development for molecules that are destined for Phase III studies. This development work can occur immediately or with some delay after clone selection, giving us greater flexibility and efficiency in allocating resources to process development.

8. Conclusions

Amgen has established a flexible, generic platform and applied it to multiple product candidates. We have instituted a review and revision process to capitalize on new technologies and lessons learned from our antibody history. Successful implementation of the platform has enabled a substantial increase in the number of candidates in process development, greater resource efficiencies in P&AS and other departments, and improved speed to clinic. Ultimately, we will evolve the platform to a single cycle of development.

Acknowledgments. The author thanks Thomas Seewoester, Victor Fung, Brian Hubbard, and the Cell Science & Technology Groups in Seattle, WA and Thousand Oaks, CA for contributions to this article.

Part III

Recovery and Purification

Chapter 6

Addressing Changes Associated with Technology Transfer: A Case Study

Michele M. Myers, Camille Keating, Joann Bannon, Donald S. Neblock, and Peter W. Wojciechowski

1. Introduction

REMICADE® is a chimeric monoclonal antibody directed against TNF-α. It was the first drug product in the class of TNF-α inhibitors approved for use in humans. It is a lyophilized formulation of the drug substance, infliximab, and is approved for the treatments of autoimmune disorders including rheumatoid arthritis, Crohn's disease, ankylosing spondylitis, and psoriatic arthritis.

Production of REMICADE was first approved in 1998 at Centocor's Leiden, The Netherlands, facility. Soon after approval of the Leiden manufacturing facility, plans to scale-up and add a second manufacturing site in Malvern, Pennsylvania, were initiated. Comparability of the products prepared at the two facilities was demonstrated. The FDA approved the Malvern facility in April 2002. It was approved by the EMEA in 2003.

After production of the comparability batches in Malvern, additional work was required to optimize the Malvern process. Product breakthrough was observed during the cation exchange chromatography step of the downstream process. After a thorough investigation, the appropriate process modification was implemented and validated for use in the downstream production process.

This chapter provides a history of the technology transfer and scale-up, the investigation required to understand product breakthrough experienced during the downstream cation exchange chromatography process, and the corrective actions taken. Process improvements were implemented to eliminate breakthrough in the Malvern process. The case provides an example of how upstream process changes, defined during technology transfer, resulted in the need for downstream process improvements at the receiving site.

2. Defined Process Changes

An overview of the REMICADE production process is shown in Fig. 6-1. The infliximab drug substance is manufactured by continuous perfusion cell culture. The expansion of the antibody secreting cells and production of the

From: *Current Trends in Monoclonal Antibody Development and Manufacturing,* Biotechnology: Pharmaceutical Aspects, DOI 10.1007/978-0-387-76643-0_6, Edited by: S.J. Shire et al.

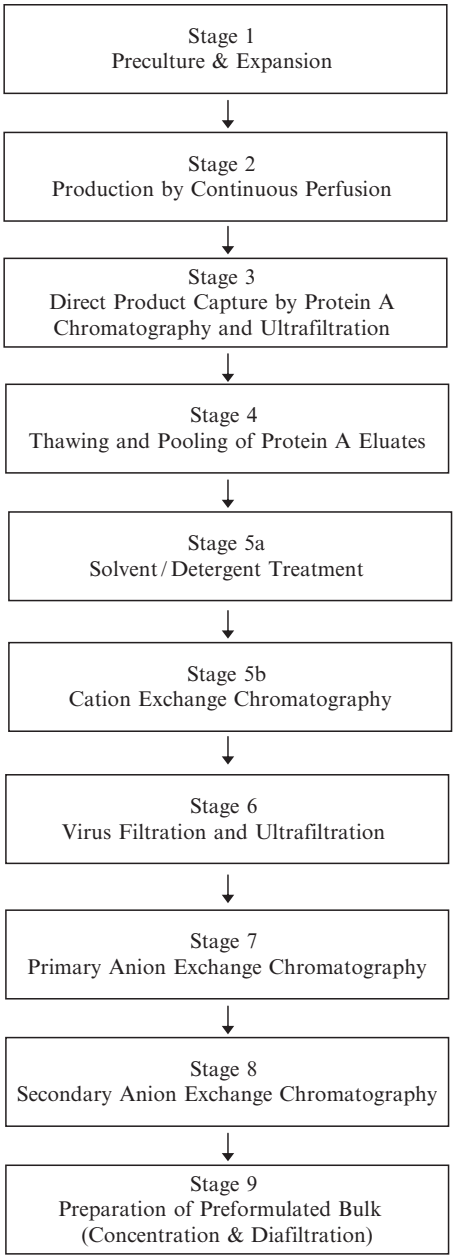

Fig. 6-1. Schematic overview of the REMICADE production process. Each stage of the production process is shown. Stages 1–3 are considered part of the upstream production process. Stages 4–9 are considered part of the downstream production process

chimeric monoclonal antibody occur in the first two manufacturing stages: preculture and expansion (Stage 1) and large scale cell culture production by continuous perfusion (Stage 2). REMICADE is purified and formulated to PreFormulated Bulk (PFB) from cell supernatant (harvest) in Stages 3–9 of the manufacturing process as shown in Fig. 6-1.

Purification of infliximab begins with the filtration of clarified harvest material and the purification of the IgG by Protein A affinity chromatography. It is during this purification step that the vast majority of impurities including viruses, media components, and host cell species are removed. The purified material in the eluted product stream is frozen and stored prior to pooling for the subsequent downstream purification steps.

In the first stage of the downstream purification process (Stage 4), Protein A purified monoclonal antibody is thawed, pooled, pH adjusted, and filtered in preparation for solvent/detergent (S/D) viral inactivation, the first dedicated viral clearance step in Stage 5a. Cation exchange chromatography at Stage 5b is designed to remove the S/D reagents. In Stage 6, the eluted product from Stage 5b is diluted and undergoes a second, dedicated viral clearance step by tangential flow filtration (TFF). The resulting product stream is concentrated by ultrafiltration. In Stages 7 and 8, two anion exchange chromatography steps are used to polish the product. In the final stage, Stage 9, product is concentrated and diafiltered into a buffer containing stabilizers to prepare the preformulated bulk drug substance, which is frozen for storage and shipping to the drug product manufacturing site. The overall purification process (Stages 4–9) has been shown to be effective for the removal/inactivation of lipid-enveloped and nonenveloped viruses and in the removal of protein impurities, residual DNA and reagents introduced by the manufacturing process.

Process changes were implemented during technology transfer from the Leiden production facility to Malvern manufacturing. Select process changes implemented in the Malvern manufacturing facility are summarized in Table 6-1. The majority of the changes were made to accommodate a scale-up of the process in the Malvern facility. The production bioreactors and the

Table 6-1. Select process changes implemented in the new REMICADE production facility.

Process step	Process change
Stage 1: Preculture and expansion	The number of working cell bank vials used for production of a batch is increased in Malvern
	The volume of the perfusion seed bioreactor is increased in Malvern
Stage 2: Production by continuous perfusion	The volume of the production bioreactor is increased in Malvern
	An internal spin filter is used for cell retention in Leiden
	An external spin filter is used in Malvern
	Supernatant is stored at 8–14°C after clarification in Leiden
	Supernatant is stored unclarified at 2–8°C in Malvern
Stage 3: Direct product capture by Protein A chromatography and concentration by ultrafiltration	Protein A columns of one bed height are used in Leiden
	Protein A columns with different bed heights are used in Malvern
	In Leiden, the flow rate used for the wash step after loading is equivalent to that used for loading
	In Malvern, the flow rate used for the wash step after loading is not equivalent to the load flow rate
	In Leiden, the permeate collected during concentration of product is used to flush the UF skid
	In Malvern, buffer is used to flush the UF skid after concentration of product

(continued)

Table 6-1. (continued)

Process step	Process change
Stage 4: Thawing and pooling of DPC eluates	The amount of product thawed for production of a down stream batch is increased in Malvern
Stage 5: Solvent/detergent treatment and cation exchange chromatography	The column volume is increased in Malvern
Stage 6: Viresolve filtration and ultrafiltration	Membrane filter area is increased in Malvern
Stage 7: Primary anion exchange chromatography	The column volume is increased in Malvern
Stage 8: Secondary anion exchange chromatography	The column volume is increased in Malvern
Stage 9: Preparation of PFB	Membrane filter area is increased in Malvern

downstream purification process were scaled-up twofold. Other changes were implemented to take advantage of the capabilities of new equipment, new technologies, and the new facility.

The continuous perfusion cell culture process (Stage 2) was improved in the Malvern facility through the use of external spin filters to separate cell culture harvest from biomass in the reactors. External spin filters were implemented in Malvern to permit change out of the filters during production, if clogging were to occur. External spin filters also have an advantage over internal spin filters because the speeds of the agitator in the bioreactor and the spin filter are independent. Internal spin filters, used in the Leiden facility, are mounted concentric with the agitator shaft in the bioreactor, and they rotate at the same speed as the agitator. Clogging of internal spin filters typically results in termination of the bioreactor.

3. Comparability of the Malvern Process

All Malvern manufacturing process changes, defined during technology transfer, were in place during production of four comparability lots beginning in October 2000. In-process controls and specifications employed in the Malvern manufacturing facility are identical to those used in the Leiden manufacturing facility. In addition to meeting the routine in-process and release testing specifications, process validation studies were conducted to demonstrate comparability of the processes and products manufactured in Malvern and Leiden.

Comparability of the processes was demonstrated at laboratory and production scales. Critical cell culture outputs, product stability during harvest hold, and impurity clearance throughout the process used in Malvern were shown to be comparable to the Leiden process. Viral clearance and host cell protein and DNA clearance were also shown to be comparable in the Malvern and Leiden production facilities.

Comparability of the four PreFormulated Bulk (PFB) lots manufactured in Malvern was demonstrated through routine release testing, including purity and potency testing, stability studies, and side-by-side biochemical characterization with six lots of PFB manufactured in Leiden. Three of the Leiden lots analyzed as part of the comparability studies were prepared in the

same time frame as those prepared in Malvern (2001). The other three Leiden PFB lots were manufactured during the original Leiden process validation in 1997 and 1998. The characterization tests included peptide mapping, circular dichroism, oligosaccharide mapping, mass spectrometry, and sedimentation velocity analytical ultracentrifugation. All results demonstrated that the product prepared in Malvern manufacturing was comparable to the PFB prepared in the Leiden facility.

4. The Need for an Additional Process Improvement

Cation exchange chromatography is performed during Stage 5 of the REMICADE production process after solvent/detergent viral inactivation of the product. The solvent/detergent is removed from the product by flowing through the column while product binds to the cation resin. During production in Malvern manufacturing, however, product was occasionally observed in the effluent from the column during the loading phase of the chromatography.

A Malvern cation exchange chromatogram showing no breakthrough is provided in Fig. 6-2. A slight, expected increase in absorbance is observed as product is loaded on the column, while solvent and detergent flow through and are directed to waste (Load, Fig. 6-2). After loading, a decrease in absorbance is observed (Wash, Fig. 6-2) as the column is washed with at least three column volumes of equilibration buffer. The absorbance then increases as protein is eluted (Elution, Fig. 6-2) from the column with higher ionic strength buffer. After the product has eluted, the column is flushed with strip buffer, generating another peak in absorbance (Strip, Fig. 6-2), prior to regeneration and storage (not shown in chromatogram).

An example of a chromatogram generated when breakthrough was observed during the chromatography in Malvern manufacturing is shown in Fig. 6-3. An increase in absorbance is observed during the column-loading phase. The absorbance was attributed to the presence of product, which did not bind to the column and was directed to waste.

Product breakthrough during the cation exchange chromatography had no impact on product quality. Process improvements were, however, required to

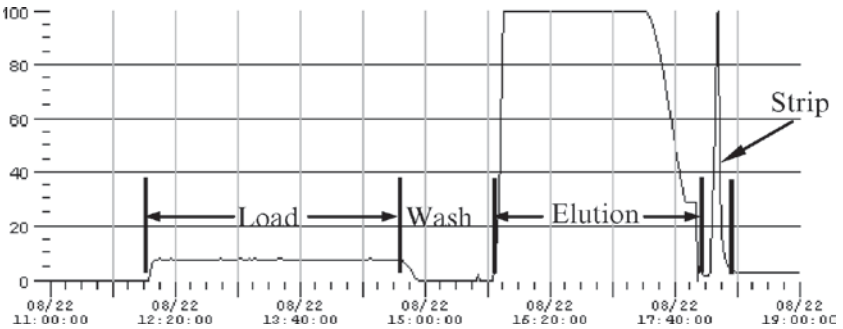

Fig. 6-2. Chromatogram generated during cation exchange chromatography. Absorbance at 280 nm, as percent full scale, is shown as a function of time. The approximate starting and stopping points of the load, wash, elution and strip phases of the chromatography are noted

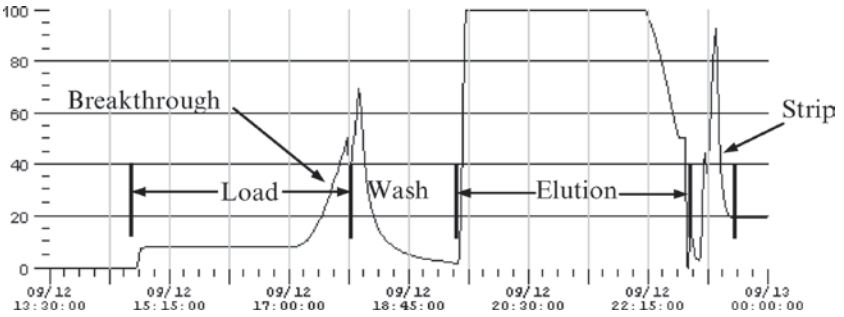

Fig. 6-3. Chromatogram generated during cation exchange chromatography in which product breakthrough has occurred. Absorbance at 280 nm, as percent full scale, is shown as a function of time. The approximate starting and stopping points of the load, wash, elution and strip phases of the chromatography are noted. The increase in absorbance observed at the end of the loading phase of the chromatography is indicative of product breakthrough, as noted

optimize the production process. A thorough investigation was conducted to understand the cause of breakthrough during the cation exchange chromatography and determine the appropriate process modification to optimize the capacity and yield of the step.

4.1. Investigation of Product Breakthrough

Resin capacity for IgG and column packing were first evaluated to verify acceptable capacity of the resin throughout its defined lifetime and the integrity of the packed column used in production. The efficiency of the column pack, calculated as the height equivalent to a theoretical plate (HETP) and asymmetry factor (Af) after injection of acetone on the column, was found to be acceptable and consistent throughout the use of the columns. Resin capacity for IgG, evaluated using a representative scaled-down model, was also found to be acceptable at the end of the resin lifetime. The integrity of the column packing and the resin were, therefore, not considered the primary root causes for product breakthrough.

After elimination of column packing and resin capacity as the root cause of the problem, flow distribution within the chromatography column was evaluated. The ability of the product to contact all of the resin within the column is critical to product binding. Flow distribution was evaluated within the manufacturing column by adding a water rinse step after elution of product. During the load, wash, and elution phases of the cation exchange chromatography, flow is directed over the column from the bottom to the top. The flow is then reversed for application of strip buffer. In the study, water was applied to the column before the direction of flow was reversed for the strip phase of the chromatography. In this way, the distribution of flow was evaluated at a point in the process that is most like the flow distribution experienced during column loading. The conductivity profile generated was compared to profiles generated when the column had been shown to be clean, after regeneration of the column, and after storage.

The conductivity profiles observed after regeneration and storage of the column were as expected. Sigmoid-shaped conductivity profiles were observed.

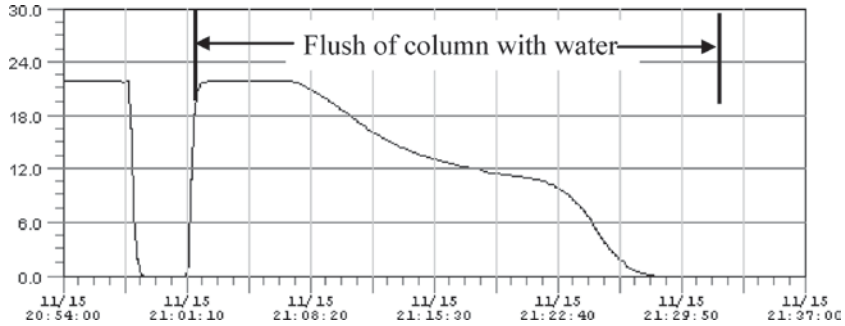

Fig. 6-4. Conductivity profile observed during water flush after elution of product. The conductivity (in mS) is shown as a function of time during the water flush that was performed after product elution, prior to regeneration of the column. The approximate starting and stopping points of the WFI flush are shown. The decrease and increase in conductivity observed before and directly after 21:01:10 h was caused by flushing the system with the column in bypass. The decrease in conductivity observed after approximately 21:08:20 h was caused by introduction of water to the column previously equilibrated in buffer containing sodium chloride

The profiles were characteristic of those expected for a well-packed column in which proper flow distribution was achieved. A representative conductivity profile generated from the water flush applied after elution is shown in Fig. 6-4. The data show a decrease in conductivity between approximately 21:08:20 h and 21:29:50 h as the column, equilibrated in elution buffer containing 200 mM sodium chloride, was flushed with water. The irregular, nonsigmoid shape of the conductivity profile generated by the water flush indicates that the flow distribution within the column was not uniform during the product loading and elution phases of the chromatography.

The most plausible cause of the poor flow distribution observed in the cation exchange column was deposition of precipitate observed in the product feed stream prior to cation exchange chromatography. The precipitate, composed of aggregated IgG, blocked the frit and disrupted the flow in the column. Breakthrough of product was expected to have resulted from the poor flow distribution and the inability of all the product to contact and bind to the resin in the column.

4.2. Investigation of Precipitate in the Feed Stream

The precipitate was found to be composed primarily of insoluble aggregated IgG. It is first observed in the product feed stream after purification by Protein A chromatography and pH adjustment from neutral to acidic pH. Intermediate product generated in Leiden manufacturing contains less precipitate than that generated in Malvern manufacturing. Differences between the Malvern and Leiden upstream manufacturing processes were evaluated to determine the cause of greater product aggregation in Malvern manufacturing. Studies were performed to identify the upstream process change, or changes, that resulted in the increase in precipitate observed in the downstream intermediate.

In the first study, cell culture harvest samples from Malvern manufacturing were taken (a) directly from the bioreactor, (b) after the external spin filter, and

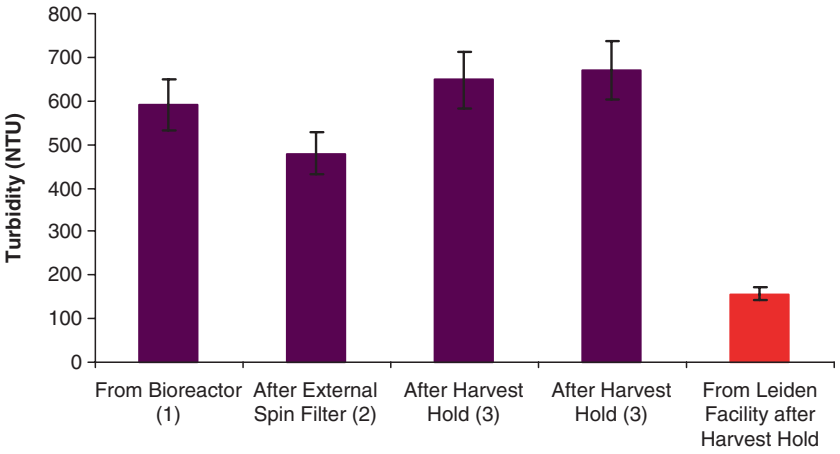

Fig. 6-5. Turbidity of cation exchange chromatography feed stream. The maximum turbidity of product (in Nephelometric turbidity units, NTU), purified at laboratory scale, is shown for material derived from the Malvern manufacturing process directly from the bioreactor (1), after the external spin filter (2), and two samples collected after harvest hold (3). Turbidity is also shown for material derived from the Leiden manufacturing process after harvest hold

(c) after harvest hold. A sample was also taken after harvest hold in Leiden manufacturing. All samples were Protein A purified using a laboratory scale model of the Leiden production process. The product from the laboratory scale preparations was then analyzed to determine the amount of turbidity. The results are shown in Fig. 6-5. All samples derived from Malvern manufacturing harvest (taken directly from the bioreactor, after the external spin filter and after harvest hold) resulted in intermediate with equivalent precipitate formation (as indicated by approximately equivalent turbidity behavior). Significantly less turbidity was observed in the sample derived from Leiden manufacturing. The study results indicate that conditions used during production cell culture (Stage 2) or farther upstream (Stage 1: pre-culture and expansion) in the Malvern process cause the formation of precipitate observed downstream in the process.

A subsequent study indicated that there were no significant trends in the turbidity of intermediate derived from the early, middle, or late stages of either Leiden or Malvern production bioreactors. The turbidity observed in an intermediate sample derived from a Malvern seed reactor was less than that observed for samples derived from Malvern production bioreactors and similar to that observed for sample derived from Leiden production bioreactors. Malvern seed reactors and Leiden production bioreactors are of the same volume, and both use internal spin filters for the separation of harvest from biomass. Malvern production bioreactors use external spin filters and are of a larger volume than those used in the Leiden process. The observation suggests that differences in the upstream scale-up or the cell separation device may play a role in the higher turbidity observed downstream in product generated in Malvern.

5. Impact of Product Breakthrough and Precipitate in the Feed Stream

Clearance of process impurities, routine in-process and release testing, analysis of the product during comparability studies, and product stability were evaluated to assess the impact of product breakthrough and precipitate in the feed stream. The ability to clean the cation exchange column was also considered, given that product breakthrough was caused by the deposition of precipitate on the frit of the column.

Clearance of impurities was not adversely affected by product breakthrough observed in Malvern manufacturing. Cation exchange chromatography is primarily responsible for removal of solvent and detergent reagents. Cation chromatography has also been validated for removal of 1 log of residual host cell proteins. Impurity clearance during cation exchange chromatography occurs in two ways. Some impurities, such as solvent and detergent reagents, flow through the column, while product binds to the resin. Other impurities are resolved from the product by remaining bound to the resin after elution of the product from the column. Both modes of purification were unaffected by product breakthrough.

Data supporting impurity clearance were obtained by testing the process intermediate after the cation exchange step of the process. No significant differences were observed for clearance of impurities regardless of whether breakthrough had occurred during processing. Specifically, the clearance of solvent and detergent reagents by the Malvern manufacturing process was shown to be comparable to that observed in the Leiden process. In addition, all Malvern batches processed have met the in-process specifications for aggregate content after cation exchange chromatography. The data confirmed that there is no impact to product purity or the impurity clearance capability of the cation exchange chromatography process as a result of breakthrough.

No differences in release testing results were observed for PFB batches prepared in Malvern manufacturing regardless of whether product breakthrough was observed during production. In addition, all four comparability batches produced in 2000 and 2001 were subjected to biochemical characterization tests. Product breakthrough was observed during production of one of the four batches. No differences were observed in the results of the biochemical analyses, demonstrating that product breakthrough had no impact on the quality of the PFB.

To further examine the impact of product breakthrough, the stability of PFB prepared in Malvern manufacturing was evaluated at −40 and 5°C for batches with and without product breakthrough. Purity, identity, and activity of the product were determined for up to 24 months. The results of these studies show that all batches of PFB, including batches in which product breakthrough was observed during cation exchange chromatography, met all acceptance criteria. These data demonstrate that there is no product quality impact as a result of breakthrough or upstream process differences between Malvern and Leiden.

Since the root cause of product breakthrough was attributed to deposition of precipitate on the frit of the column, the ability to clean the production column

was of particular interest. During column cleaning (strip and regeneration), the direction of flow (top-to-bottom) is reversed from that for loading through elution (bottom-to-top) to provide effective cleaning of the column and the bottom frit. Cleaning was demonstrated by validation during production of the first three batches and through periodic performance of mock elution cleaning qualification runs throughout the lifetime of the columns.

6. Defining the Process Improvement

While the product quality assessment demonstrated that there was no impact on the validated impurity clearance of the process or biochemical characteristics of the product due to breakthrough during the cation exchange chromatography, the presence of breakthrough impacted production capacity for the cation exchange chromatography step. Each breakthrough occurrence resulted in unrecovered product that was diverted to waste during loading. Further, for a larger average batch size, occurrence of breakthrough was more frequent, thereby limiting the effective capacity of the column to less than that of its resin binding capacity. Finally, batches exhibiting breakthrough also often exhibited a longer or wider elution profile, requiring a larger volume of elution buffer on average for product collection. This also limited batch size capacity due to buffer volume and tank volume constraints.

To improve flow distribution and eliminate breakthrough, it was proposed to implement in-line filtration of the feed stream prior to the cation exchange column in Malvern manufacturing. The addition of filters was not implemented in Leiden manufacturing, where a lower level of precipitate is observed in the process and the chromatography is not experiencing breakthrough or other signs of sub-optimal flow distribution due to precipitate.

Implementation of the filters in the Malvern manufacturing process was governed by existing change control procedures. Laboratory scale studies were first conducted to identify the appropriate filters for use in the process and define the required filter membrane area for production. A laboratory scale feasibility study, using a qualified scaled-down model, was conducted to assess the compatibility of the process and the product with the filters. The study demonstrated that there was no adverse impact on the process or product by the introduction of in-line filtration prior to the cation exchange column. Studies were also conducted to evaluate the compatibility of the filters with the process feed stream (i.e. to verify the integrity of the filters after contact with the process feed stream) and to identify extractable substances that may be removed from the filters during processing. After all laboratory scale studies returned acceptable results, manufacturing scale process validation was conducted with the filters in place.

After discussions with the FDA, the implementation of filters in the production process was submitted as a CBE-30 that was subsequently downgraded to a change reportable in the REMICADE annual report. The EMEA and the Canadian Health Authority approved the change within 3 months of the Type II and Notifiable Change regulatory filings, respectively. Since implementation of the filters in Malvern manufacturing in February 2006, no product breakthrough has been observed. In addition, the efficiency of the cation exchange step has improved in Malvern manufacturing. The average volume of the eluate from the column has decreased by more than 25%.

7. Conclusions

Changes to the production process may be unavoidable during technology transfer and scale-up. Process changes due to new equipment, technology, and facilities are expected. Performance issues associated with process changes can be addressed during process startup. Acceptable product quality and comparability must then be demonstrated during process validation. Ideally, all process changes and optimization occur concurrently with technology transfer and startup, prior to validation. In reality, the need for further process improvements is not always readily apparent prior to validation. After technology transfer, additional process characterization and investigation may be required to understand all aspects of the production process and the inherent interactions of the process steps. Under change control procedures, a continuous cycle of demonstrating product quality and incrementally improving process performance can then be utilized.

Scale-up and technology transfer of the REMICADE production process from Leiden to Malvern manufacturing were accompanied by a number of defined process changes. Comparability of the products produced at the two manufacturing sites was demonstrated through a number of studies during process validation. Although the product was not impacted, changes implemented upstream in the Malvern process impacted downstream production capacity and yield. After a thorough root cause investigation and product quality assessment, the appropriate process modification was identified and implemented at the Malvern manufacturing site. Addressing the changes associated with, and resulting from, technology transfer improved the capacity and yield for the downstream production process.

Acknowledgments. The authors gratefully acknowledge Larry Doolittle, Paul Gahr, and Karen Fixler for their contributions to the project and Timothy Laverty for useful discussions.

Chapter 7

Concepts for Disposables in Biopharmaceutical Manufacture

Joachim K. Walter and Uwe Gottschalk

1. Introduction

The biopharmaceutical manufacturing industry has had a long relationship with stainless steel, and even a decade ago it would have been hard to imagine the industry embracing a new concept that could make stainless steel redundant. Even so, the tide is turning, and disposable concepts are on the rise (Sinclair and Monge 2004). Disposable equipment became popular for upstream production in the 1990s, with the advent of "single-use" media bags and bioreactors, and the use of disposable capsules for sterile filtration (Meyeroltmanns et al. 2005). Over the next few years, disposable concepts also began to appear in downstream processing. Initially, this was restricted to buffer bags and devices for normal flow filtration, including virus filtration and guard filters for chromatographic columns, but gradually more complex concepts have been introduced, including disposable devices for tangential flow filtration and chromatography (Walter 1998; Ransohoff 2004; Gottschalk 2006). The current importance of disposable concepts in downstream processing was demonstrated in a recent industry survey, in which 37% of respondents considered cost-effective disposables to be important for addressing downstream process capacity issues in 2006, when compared to 24% in 2005 (BioPlan BioProcess Technology Consultants 2005, 2006).

What is the attraction of disposables and what do they potentially contribute to biopharmaceutical manufacturing? Are they more convenient, more cost effective? Are they suitable for cGMP processes? What are their major advantages and limitations? Are they scalable? Although the answers are still debated, there is now plenty of information from different biopharmaceutical production campaigns to show that disposables offer real and tangible advantages over fixed stainless steel equipment under many different circumstances. This chapter will address the questions listed above and provide case studies demonstrating the benefits of "going disposable" in biomanufacturing.

From: *Current Trends in Monoclonal Antibody Development and Manufacturing,*
Biotechnology: Pharmaceutical Aspects, DOI 10.1007/978-0-387-76643-0_7,
Edited by: S.J. Shire et al.

2. The Rationale for Single-Use Concepts

At first glance, disposables appear wasteful and unnecessary, like taking fresh plastic bags at the supermarket for each shopping trip rather than re-using a sturdier container. However, this analogy breaks down when one considers the constraints under which biomanufacturing processes must labor to ensure that the resulting active pharmaceutical ingredient is safe, pure, homogeneous and suitable for clinical use. The re-usable shopping bag might not turn out to be so convenient if it had to be washed and sterilized before each trip, and if that cleaning had to be validated professionally!

The most commonly cited benefit for the single-use concept is the elimination of potential cross-contamination between production batches or even between batches of different products. Over the last few years, the industry has seen a significant shift towards the adoption of disposable bioprocess components because unlike stainless steel systems they do not need to be disassembled, steamed, cleaned and reassembled between batches. Instead, components can be supplied as sterile, process-ready modules which are used once and then discarded (Sinclair and Monge 2004; Ransohoff 2004).

In general, the handling of unit operations is simplified by the employment of ready-to-use disposables, and this is probably the only type of disposable unit that provides the full advantage to biopharmaceutical manufacturing operations. The additional costs of replacing disposable components are offset many times over by the cost savings brought about by eliminating cleaning-in-place (CIP) and steaming-in-place (SIP) procedures, validation studies and the associated record keeping. Furthermore, disposable components greatly increase the flexibility of production since they facilitate rapid and inexpensive product changeovers with minimal risk of cross-contamination. Although some of the equipment used for downstream processing still needs to be cleaned (e.g. rotary lobe pumps and mechanical valves), such procedures can be carried out using higher concentrations of chemicals at higher temperatures, therefore significantly reducing process down-time.

Integrated biopharmaceutical fluid-handling steps include media preparation, fermentation, cell harvesting, clarification, product capture and polishing, virus clearance, ultrafiltration and final sterile filtration. All these unit operations, which formerly relied on stainless steel components, can now be carried out using disposable modules. By switching to a single-use concept, the industry aims to reduce or eliminate the most time-consuming and expensive process steps, ultimately shortening the time to market. Additionally, the regulatory bodies focus on critical production steps such as CIP/SIP (European Commission Enterprise Directorate General 2001; FDA 2004, 2006) and these are the very steps that can be eliminated by the single-use concept.

3. Counting the Cost

The obvious question regarding the use of disposables is how the costs compare to hard-piped components. Although there are obvious savings in up-front investment in equipment, cleaning and validation, is this cancelled out by the greater consumption of consumables, not least the disposable modules themselves? For example, how does the cost of

replacing a filter for each process batch compare to the lifetime costs of cleaning and reassembling a permanent filtration device over many process runs?

There is no definitive answer to such generic questions. It is only possible to compare costs for specific process operations, and at specific scales. As an example, we can compare the relative costs of column chromatography and disposable membrane adsorbers for polishing in antibody manufacture. Conventional columns are more economical at low scales; costs break even at a load of approximately 2 kg of antibody per liter of resin. However at higher scales single use membrane adsorbers can be significantly more economical. This reflects not only the cost of equipment, cleaning, validation and consumables, but also the reduced buffer volumes, the reduction in labor required for column assembly and packing, the reduced requirement for water-for-injection (WFI), less process down time, and the higher productivity of the membrane adsorber in this particular setting. The footprint of disposable devices is generally smaller than fixed counterparts with significant knock-on effects in terms of facility layout and design. All the extra buffers required to wash and re-equilibrate fixed equipment need to be stored and prepared somewhere, increasing the overall costs in terms of facility planning and space requirements. Therefore, the use of disposables cannot be evaluated alone, but must be considered in the context of which unit operations are used, their efficiency, scalability and economy. Perhaps one of the most important concepts, often overlooked, is that the use of disposables allows process trains to be assembled rapidly from modules, and scaled up efficiently. A hard-piped process that could take years to finalize can be assembled from disposable modules in a matter of weeks (Gottschalk 2005).

According to cGMP standards, raw materials and equipment in direct contact with the product need to be dedicated, which makes the most expensive hardware prohibitive for limited production campaigns. Typical hardware might include chromatography columns and resins, filters, filter holders, process control systems, buffer storage tanks, and peripheral utilities such as pumps, valves, piping and monitoring equipment. Disposables can be dedicated not only to a specific product, but to a single batch, and therefore dramatically reduce the initial capital investment in limited campaigns. These fixed costs, as well as savings, are likely to be made in terms of reduced lead time for equipment acquisition and qualification, low maintenance and, as stated above, the absence of cleaning requirements. Time is money in biopharmaceutical manufacturing, and clipping the time taken to develop a final process by weeks or months can reap rewards years downstream by extending the useful life of patents and ensuring that market demands are rapidly fulfilled.

In addition to up-front (fixed) costs, which currently drive the industry, there are also operational costs that can be reduced by using disposables (Mora et al. 2006). Such costs include labor, off-line analysis, chemicals and WFI, buffers, and the costs of waste treatment and disposal. While disposable options do not eliminate such costs, they can reduce them significantly. A cost comparison is presented later for column chromatography vs. disposable membrane adsorbers and the surprising result is that even with the costs of the disposable membranes included, the actual running costs of a disposable production campaign are still lower than those of traditional columns over a 10-year production cycle (Mora et al. 2006).

4. Validation

From a cost perspective, the second largest investment after the hardware is the cost of qualification of equipment and validation of procedures in order to make hardware and processes available for cGMP manufacturing. Typically, extensive cleaning validation has to be performed in order to allow the re-use of the equipment for different production batches. Where multipurpose use of the equipment is required for different products, even more extensive studies have to be performed to exclude any potential cross-contamination between products. This is critical for those drugs with significant effects at very low doses, e.g. cytokines (CPMP 1996).

Disposables therefore provide an opportunity to circumvent extensive qualification and validation of cleaning procedures for equipment including piping. Single-use components are available for instant use, i.e. they are pre-sanitized and pyrogen-free. Even so, certain disposable modules must undergo appropriate validation steps to ensure their suitability and safety. For example, the FDA recommends that all sterile filters are properly validated for full bacterial retention (which means in practice withstanding a challenge of 10^7 colony forming units of *Brevundomonas diminuta*, a bacterial species chosen because of its small size, per square cm of filter, while retaining integrity under authentic process conditions) (FDA 1987). At the same time, the filter must not remove any important components of the formulation and must not release "extractables." The latter is an important challenge because filters usually come with manufacturer's data showing the level of extractables in water, but independent validation must be carried out if the filtered drug product contains solvents or other components that are likely to change the quantity or quality of extractables (Stone et al. 1994; Reif et al. 1996; Weitzmann 1997).

The requirement for sterility of single-use equipment depends on the stage of processing, e.g. fermentation or downstream processing or on the type of product to be manufactured. The downstream processing of biopharmaceutical proteins is typically performed in a sanitary, low bioburden but not sterile environment, whereas the purification of virus vaccines and plasmids may require sterile handling. In any case, suitable disposables eliminate the need for CIP or SIP, and pre-assembled single-use equipment reduces further the potential of operator error and thus contributes to increased process robustness (Immelmann et al. 2005). The savings in resources – both time and personnel – significantly help to reduce turnover time and in this manner, allow the installment of additional project(s) without investment in new resources, utilities and facility space. Savings also will be made by reduced analytical costs: as there are no analytical assays for proof of cleaning required, there is no need to develop, qualify, validate and perform individual assays for each new product. One potential negative aspect is that the manufacturing process becomes reliant on the manufacturer of disposable modules, and if the supply fails then the process grinds to a halt. It is therefore important to enter into discussions with suppliers well in advance of the process coming on line to ensure the availability of the necessary resources, as we discuss in detail below.

5. Logistics and Environmental Impact

Successful and efficient manufacturing requires seamless logistics, particularly in terms of production components and materials. Good process economics requires production to be *lean*, i.e. the correct components must be available on demand, but stocks must be limited to conserve storage space and avoid tying up capital that could be invested in the value stream. A lot of up-front investment is required for stainless steel components so, to a certain extent, the flexibility of capital resources is limited when using a hard-piped production system. Similarly, the availability of equipment for CIP and SIP needs to be factored in when looking at the economics of stainless steel. If a CIP station fails, the availability of clean equipment can become critical, particularly if only a limited number of replacements are available.

Single-use components tend to avoid such problems because the demand for different modules can usually be predicted based on the intended production campaigns. It is beneficial to maintain a small surplus stock of single-use components such as filters, or media bags, etc., but this binds much less capital than analogous replacement stainless steel equipment and would be anticipated as a normal line in the consumables budget. Even where there is critical failure and/or an availability crisis, it is much easier to source disposable equipment and have it shipped to the production facility than would be the case for a steel bioreactor or chromatography column.

One issue raised by the throw-away nature of disposable modules is the impact on the environment, bringing us back to the plastic shopping bag analogy mentioned above. The plastic modules are discarded after each production run and are incinerated, which surely must be much worse for the environment than re-using components hundreds of times. Careful analysis, however, shows that the opposite is true. Because of the demands of working under cGMP, the cleaning and validation required between batches in a conventional production train is much heavier in its consumption of chemicals, water and energy than the equivalent disposable technology. Although it would be a mistake to regard disposables arrogantly, as an environmentally-friendly concept per se, it is by far the friendliest option when compared to the traditional approach.

6. Limitations of the Disposable Concept

Although disposables are often beneficial in terms of efficiency, economy and resource management, no-one claims that they can provide the solution to all manufacturing issues and there are still many situations, in which re-usable equipment remains the best choice (DiBlasi et al. 2006). Disposable unit operations are available for almost all conceivable unit operations at smaller scales (<50 L harvest reactor volume) and perhaps this is even true for pilot-scale operations. However, at process scale, the cost of manufacturing some types of disposable equipment becomes unsupportable, meaning that the hard-piped alternative is better value, even with the attendant cleaning and validation (e.g. centrifuges). In some cases, this simply reflects the relative cost of disposable

modules when compared to the cost of stainless steel equipment averaged over the larger number of production runs possible before replacement is required. In other cases, the performance of disposable modules fails to match that of fixed equipment at process scale. However, there has been a noticeable trend toward the availability of larger disposable modules, driven by increasing acceptance at smaller scales, and the realization that further development and improvement will reap economic rewards in the long term by overcoming process bottlenecks.

7. Upstream Production

Disposable bioprocessing systems have been used widely for the preparation, filtration, storage and delivery of media (Sinclair and Monge 2004). This avoids the use of large steel tanks that have to be cleaned and inspected on a regular basis, allowing the process to be fed continuously with medium and also saving valuable space. Several formats of disposable fermenters are available in which agitation is based on rocking, stirring or orbital shaking (De Jesusa et al. 2004; Baldi et al. 2005; Stettler et al. 2006; Muller et al. 2007). Most systems comprise a holding device, which is fitted with disposable plastic bags. Powdered medium is mixed with purified water using an overhead mixer, and a peristaltic pump then pumps the medium from the lined tank, through a sterilizing grade capsule filter, into a pre-sterilized disposable storage bag. The medium may then be delivered directly to the bioreactor, or stored in a cooler for use at a later date. Disposable storage bags may be fitted with a variety of connectors that facilitate aseptic or sterile connection to the bioreactor. Following delivery of media to the reactor, the disposable bag may be steamed off or may be disconnected aseptically using a tube sealer (Sinclair and Monge 2004). In addition to the typical scenario described above, a number of further disposable concepts have been developed for the media preparation area. In one example, media are mixed in bulk and then filtered and divided into aliquots through a manifold linked to up to 20 disposable storage bags. These bags may be disconnected from the manifold, aseptically and stored for use at a later date. The advantage of this system is that a single filter connection is used to fill multiple bags. Hence media and buffers can be prepared in larger quantities as a single batch and, after they have been aliquoted into appropriate volumes and qualified for storage time, they can be used for different operations as appropriate. This minimizes the use of resources for the documentation of media and buffer preparation and analytical release testing. Media may also be heated or cooled in plastic tanks fitted with disposable storage bags for temperature-controlled delivery to the bioreactor.

Bioreactors and fermenters are typically the most challenging modules in upstream manufacturing due to the complexity of their operation and the number of parameters that must be monitored, controlled and integrated. These parameters include temperature, pH and oxygen saturation, the delivery of liquid media and gasses, the mixing of bioreactor contents, and the harvesting of desired products. Any special components that may be required for highly sophisticated processes usually have their own cleaning and maintenance requirements. Because of this complexity, only low-level processes have thus far been established in disposable bioreactors, e.g. seeding cultures, and the upper limit in terms of scale is currently 1,000 L. Even so, the disposable reactors that have been introduced promise to reduce down time, eliminate

the need for pre-fermentation sterilization, improve the handling of bioreactor contents, and – perhaps most importantly of all – facilitate changeovers between cell lines without the typical cleaning and validation procedures.

8. Downstream Processing: Initial Recovery

After the fermentation cycle, cell harvesting and clarification is followed by product capture, polishing (including viral clearance) and product filling, all of which have been streamlined through the use of disposable modules. For cell harvesting and debris removal, disposable filtration systems offer many advantages over their hard-piped counterparts in addition to the general benefits of single-use components listed above. These include the ease of scale up, the availability of pre-sterilized filters that can be integrated directly into production lines, and the fact that abolishing the use of (opaque) stainless steel housings makes it possible to observe the filter in action, and thus identify any potential problems such as foaming or air-locking before the rest of the production line can be affected. The switch from hard-piped steel filters to disposables has been facilitated by the development of disposable filtration systems that use the same cartridges as those used with the stainless steel housings. The increased flexibility afforded by disposables also means that several filters can be arranged in series or in parallel, according to the batch size and the throughput of the bioreactor.

Cell removal and clarification are often achieved by centrifugation and/or lenticular filtration (Prashad and Tarrach 2006), and the first disposable lenticular filters became available recently in the form of Millipore's Pod System (Millipore Corp., Bedford, MA, USA). This combines two distinct separation technologies in an adsorptive depth filter to enhance filter capacity and retention, while compressing multiple filtration steps into one efficient operation. Scale up is achieved by inserting multiple Pods into a holder, with formats allowing 1–5 or 5–30 Pods as required.

Further purification steps focus on bringing the process volume down – an area where crossflow filtration is the technology of choice because the build up of filter cake (the gel layer) on the membrane is slower than in the case for normal-flow filtration devices. Crossflow filters therefore result in extended operating times, but this advantage can be lost if the membranes need to be cleaned regularly. Disposable crossflow filtration devices are now widely used in the vaccine industry, where sterile filtration of the final product is not possible. Disposable hardware and consumable components improve safety by preventing cross-contamination, eliminate CIP steps and validation work, reduce the volume of water used during production (because washing and rinsing is no longer necessary), reduce chemicals use, and improve yield by eliminating the possibility of membrane degradation through long-term use. All these factors help to reduce costs and time to market.

9. Downstream Processing: Chromatography

In traditional chromatography, a steel column is packed with a resin (stationary phase) comprising porous beads made of a polysaccharide, mineral or synthetic matrix conjugated to specific functional groups exploiting different separative principles (Desai et al. 2000). A mixture of components in the feed

is percolated through the resin, and the differing affinity of feed components for the functional groups of the resin facilitates separation, either by retaining the target and eluting contaminants (retention) or vice versa (flow-through). Although column chromatography is the key enabling technology in all bioseparation processes, and large re-useable columns are required for bind and elute steps, membrane-based disposable concepts can be more economical at process scales for flow-through (polishing) operations. Here, oversized columns are necessary to accommodate the throughput, which has a direct impact on facility layouts, costs and infrastructure because the space and buffer volumes for all steps, including preparation and cleaning, also have to be adapted. Membrane chromatography employs thin, synthetic, porous membranes that are generally multilayered in a small cartridge, significantly reducing the footprint of the operation. Membranes have equivalent functional groups to corresponding resins, but they do not need packing, checking, cleaning, re-filling or routine maintenance, and fouled or exhausted modules can be replaced with new ones with minimal process down-time.

A typical example showing the advantages of membrane adsorbers is flow-through anion exchange chromatography, as used during the purification of monoclonal antibodies for the removal of high-molecular-weight contaminants such as DNA and viruses. Such molecules do not readily diffuse into the pores of traditional resins (Fig. 7-1a), resulting in mass transfer resistance and lower efficiency. Accordingly, most polishing steps relying on column chromatography require dramatically oversized columns. In contrast, solutes find their binding sites on membrane adsorbers mainly by convection, while pore diffusion is minimal (Fig. 7-1b). These hydrodynamic benefits provide the opportunity to operate membrane adsorber at much greater flow rates than columns, considerably reducing buffer consumption and shortening the overall process time by up to 100-fold (Walter 1998). To stay with the example of removing DNA from a protein product, polishing with an anion exchange membrane can be conducted with a membrane bed height of 4 mm at flow rates of more than 600 cm/h. Under these processing conditions the membrane

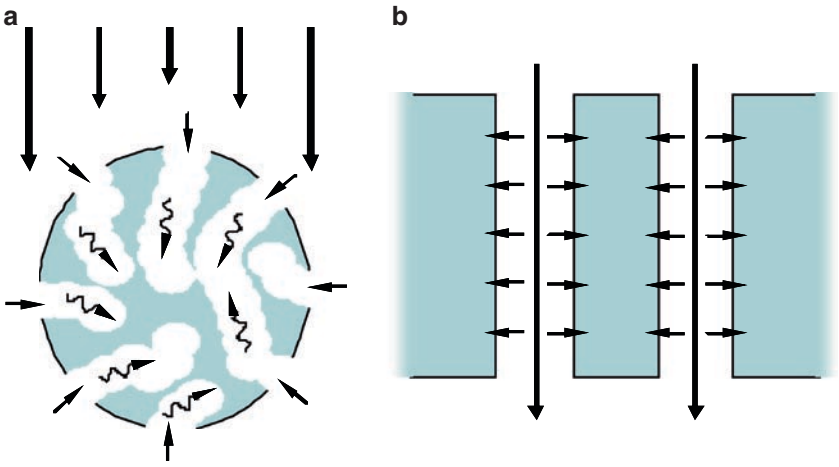

Fig. 7-1. Mechanistic comparison of solute transport in (**a**) packed-bed and (**b**) membrane chromatography. *Thick arrows* represent bulk convection, *thin arrows* represent film diffusion and *curly arrows* represent pore diffusion

Table 7-1. Scale up with SingleSep Q membrane chromatography. Parameters such as frontal surface area, bed volume, flow rate and static binding capacity scale up in a linear fashion (assuming constant bed height of 4 mm). Normalized dynamic BSA binding capacity remains constant at a given breakthrough (values shown at 10 and 100%, see also Fig. 7-2). Data from Sartorius-Stedim Biotech.

	Frontal surface area (cm^2)	Scale-up factor for flow rate	Rec. flow rate (L/min)	Bed volume (mL)	Min. static binding capacity (g) (release test)	Dynamic capacity at 10% (mg/mL)	Dynamic capacity at 100% (mg/mL)
Nano	2.4	1	0.03	1	0.03	22.5	39
5″	160	66	1.9	70	2.0	19.5	30
10″	450	187	5.0	180	5.3	20.5	29.5
20″	900	375	10	360	10.5	20.5	35
30″	1,350	562	15	540	15.8	20.5	37.5
Mega	4,050	1,687	45	1,620	47		

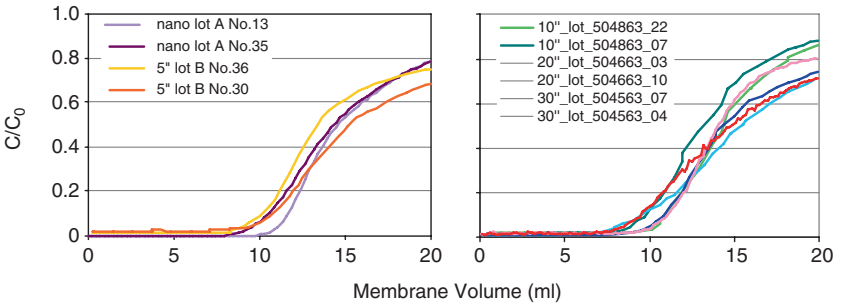

Fig. 7-2. Dynamic binding capacities of SingleSep Q membrane chromatography devices represented by breakthrough values as percentage of total load (C/C_0) against membrane volume (mL). Individual *curves* represent selected lots of different sized devices ranging from nano to 30″. Data from Sartorius-Stedim Biotech

pores still provide adequate binding capacity for large biomolecules such as viruses and DNA (Gottschalk 2005; Gottschalk et al. 2006).

The importance of flexibility in process assembly has already been discussed, but it is pertinent to focus on scalability. Flexibility is most noticeable during scale-up, since disposable devices are generally modular and available in a number of different sizes, and scaling up simply involves swapping one module for another with a higher capacity. As shown in Table 7-1, an important advantage of membrane chromatography is the linear scale up for important parameters such as frontal surface area, bed volume, flow rate and static binding capacity, while normalized dynamic capacity remains fairly constant at 10% or complete breakthrough (Fig. 7-2).

10. Economic and Performance Case Study

The first generation of membrane adsorbers suffered from problems related to both adsorptive capacity and device performance, e.g. low loading capacity, membrane fouling and suboptimal fluid distribution leading to a substantial performance loss during scale-up (Gebauer et al. 1997). However, these issues have been largely addressed by the development of improved surface

chemistries and the design of membrane devices that optimize performance. In the process scale operations, 15-layer devices are commonly deployed and these achieve excellent contaminant removal and viral clearance (Table 7-2). These performance studies confirm that both columns and disposable membrane adsorbers are capable of trace contaminant removal and virus clearance. The main difference between the two formats is disposability and load capacity at flow rates acceptable for large-scale manufacturing. With performance assured, the remaining question is how disposable membrane devices compare columns in terms of fixed (capital) costs and variable (running) costs.

Capacity and disposability are the critical factors to consider, when calculating unit operation costs for new processes. Although membrane devices clearly have a higher throughput, a direct comparison of resins and membranes based on volume shows that membranes are more expensive. This must be balanced, however, against the reduced size of membrane devices, which also reduces buffer requirements, makes the process time shorter and includes all the other benefits from a disposable technology as stated earlier (Mora et al. 2006). Cost models have been proposed by several authors (Sinclair and Monge 2002; Zhou 2006; Lim et al. 2007) and show that cost analysis must be carried out before a rational choice between the two chromatography formats can be made. Ideally, a cost model should segregate all direct and indirect costs into four major categories – capital equipment, consumable equipment and media, consumable chemicals and materials, and labor (Fig. 7-3). As expected, the

Table 7-2. Membrane chromatography spiking study with four model viruses. Test substance was a human monoclonal antibody (5–9 g/L), pH 7.2; 4 mS/cm; 1% spike; 450–600 cm/h. Data from Gottschalk et al. (2006).

Virus	Size (nm)	LRV (run 1)	LRV (run 2)	Virus recovery (%)
MVM	16–25	6.03 ± 0.21	6.03 ± 0.20	100
Reo-3	75–80	7.00 ± 0.31	6.94 ± 0.24	100
MuLV	80–110	5.35 ± 0.23	5.52 ± 0.27	>70
PRV	150–250	5.58 ± 0.28	5.58 ± 0.22	100

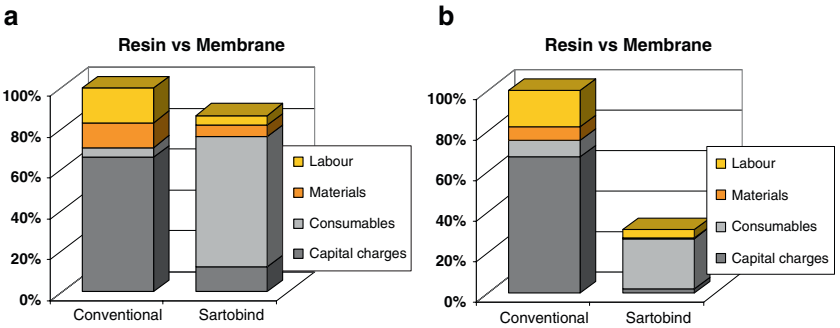

Fig. 7-3. Comparative results from a cost model comparing traditional and membrane chromatography, showing each component (labor, materials, consumables and capital charges) as a percentage of the total cost of column chromatography (which is fixed arbitrarily at 100% so that the savings brought about by membrane chromatography can be shown as a percentage cost reduction per batch). Costs break even at a load capacity of 2 kg/L (**a**) and at 10 kg/L (**b**) membranes cost only 20% as much per batch as running a column

major cost factors in column chromatography are the fixed capital costs of the equipment, and the significant costs of buffer preparation and consumption, whereas for membrane chromatography the consumable equipment and membranes are the predominant cost drivers. Therefore, we see an economy of scale effect for disposable devices that cannot be replicated by column chromatography, where the consumption of resins and buffers increases linearly with the production scale. Hence columns are more economical at low loading capacities, where the resins enjoy a longer life cycle, but costs break even at a load capacity of 2 kg/L and as the capacity increases, so does the relative benefit of membrane devices. At a capacity of 10 kg/L, traditional columns are five times more expensive than their disposable counterparts.

11. Conclusions

Single use and disposable equipment is widely accepted and well-established in the biopharmaceutical industry at process scales of up to several thousand liters. The application of this concept can save a significant investment in hardware, if the intention is limited use for individual applications, e.g. a limited number of process batches. However, the example of disposable membrane chromatography for removal of trace impurities in antibody polishing illustrate potential savings throughout the lifetime of a production campaign by providing superior economy. Single use equipment is attractive for cGMP applications, as it is provided ready to use. Thus it can save valuable labor costs, particularly in terms of cleaning and validation. Single use equipment may help significantly to reduce the turnover time between campaigns. Additional projects can be implemented instead, thus increasing the profitability of the facility. However, the use of disposable concepts should always be considered on a case-by-case basis, taking into account individual properties of the manufacturing facility, its infrastructure and the technical details of all processes.

References

Baldi L, Muller N, Picasso S, Jacquet R, Girard P, Thanh HP, Derow E, Wurm FM (2005) Transient gene expression in suspension HEK-293 cells: application to large-scale protein production. Biotechnol Prog 21:148–153

BioPlan BioProcess Technology Consultants (2005) Third Annual Report and Survey of Biopharmaceutical Manufacturing Capacity and Production, 2005

BioPlan BioProcess Technology Consultants (2006) Fourth Annual Report and Survey of Biopharmaceutical Manufacturing Capacity and Production

CPMP (1996) Note for guidance on virus validation studies. The design, continuation and interpretation of studies validating the inactivation and removal of viruses. CPMP/BWP/268/95

Curling J (2007) Process chromatography: five decades of innovation. BioPharm Int (Suppl):10–19

De Jesusa MJ, Girard P, Michaela Bourgeois M, Baumgartner G, Jacko B, Amstutz H, Wurm FM (2004) TubeSpin satellites: a fast track approach for process development with animal cells using shaking technology. Biochem Eng J 17:217–223

Desai MA, Rayner M, Burns M, Bermingham D (2000) Application of chromatography in the downstream processing of biomolecules. In: Desai MA (ed) Downstream processing of proteins: methods and protocols. Methods in , vol 9. pp 73–94

DiBlasi K, Jornitz MW, Gottschalk U, Priebe PM (2006) Disposable biopharmaceutical processes – myth or reality? BioPharm Int 2–10

European Commission Enterprise Directorate General (2001) Working Party on Control of Medicines and Inspections. EU Guide to Good Manufacturing Practice, vol 4, Annex 15, July 2001, Cleaning Validation (Source: http://ec.europa.eu/enterprise/pharmaceuticals/eudralex/vol-4/pdfs-m/v4_an16_200408_en.pdf)

FDA (1987) Guideline on sterile drug products produced by aseptic processing. FDA, Rockville, MD

FDA (2004) Equipment cleaning and maintenance. Code of Federal Regulations (CFR) Part 211.67 Title 21 Rev. 25 May 2004, FDA, Rockville, MD (Source: http://www.accessdata.fda.gov)

FDA (2006) Guide to inspections validation of cleaning processes. FDA, Rockville, MD (Source: http://www.fda.gov/ora/inspect_ref/igs/valid.html)

Gebauer K, Thommes J, Kula M (1997) Plasma protein fractionation with advanced membrane adsorbents. Biotechnol Bioeng 54:181–189

Gottschalk U (2005) New and unknown challenges facing biomanufacturing. BioPharm Int 18:24–28

Gottschalk U (2006) The Renaissance of protein purification. Biopharm Intl June (suppl):8–9

Gottschalk U (2008) Biochromatography in antibody manufacturing: the good, the bad and the ugly. Biotechnol Prog (in press)

Gottschalk U, Lamproye A, Zhou J, Sinclair A, Reif O-W (2006) An integrated platform for robust virus and contaminant removal in biomanufacturing. Recovery of Biological Products XII, Phoenix, Arizona, April 2–7, 2006

Immelmann A, Kellings K, Stamm O, Tarrach K (2005) Validation and quality procedures for virus and prion removal in biopharmaceuticals. BioProcess Int 3:38–45

Lim JAC, Sinclair A, Kim DS, Gottschalk U (2007) Economic benefits of single-use membrane chromatography in polishing. A cost of goods model. BioProcess Int 5:60–64

Meyeroltmanns F, Schmitz J, Nazlee M (2005) Disposable bioprocess components and single-use concepts for optimized process economy in biopharmaceutical production. Bioprocess Int 3:60–66

Mora J, Sinclair A, Delmdahl N, Gottschalk U (2006) Disposable membrane chromatography. Performance analysis and economic cost model. Bioprocess Int 4(Suppl):38–43

Muller N, Derouazi M, Van Tilborgh F, Wulhfard S, Hacker DL, Jordan M, Wurm FM (2007) Scalable transient gene expression in Chinese hamster ovary cells in instrumented and non-instrumented cultivation systems. Biotechnol Lett 29:703–711

Prashad M, Tarrach K (2006) Depth filtration aspects for the clarification of CHO cell derived biopharmaceutical feed streams. FISE 9:28–30

Ransohoff T (2004) Disposable chromatography: current capabilities and future possibilities. BPD North Carolina Biotechnology Center, 18 Nov 2004

Reif OW, Solkner P, Rupp J (1996) Analysis and evaluation of filter cartridge extractables for validation of pharmaceutical downstream processing. J Pharm Sci Technol 50:399–407

Sinclair A, Monge M (2002) Quantitative economic evaluation of single use disposables in bioprocessing. Pharm Eng 22:20–34

Sinclair A, Monge M (2004) Biomanufacturing for the 21st century: designing a concept facility based on single-use systems. BioProcess Int 2:26–31

Stettler M, Jaccard N, Hacker D, De Jesus M, Wurm FM, Jordan M (2006) New disposable tubes for rapid and precise biomass assessment for suspension cultures of mammalian cells. Biotechnol Bioeng 95:1228–1233

Stone TE, Goel V, Leszczak J (1994) Methodology for analysis of extractables: a model stream approach. J Pharm Technol 18:116–121

Walter JK (1998) Strategies and considerations for advanced economy in downstream processing of biopharmaceutical proteins. In: Subramanian G (ed) Bioseparation and bioprocessing. Processing, quality and characterization, economics, safety and hygiene. Wiley VCH, New York, pp 447–460

Weitzmann KH (1997) The use of model solvents for evaluating extractables from filters used to process pharmaceutical products. Pharm Technol 21:73–79

Zhou J (2006) Disposable anionic membrane chromatography. IBC Technology Transfer for Biopharmaceuticals, Carlsbad, CA 2006

Part IV

Formulation and Delivery

Chapter 8

Formulation and Delivery Issues for Monoclonal Antibody Therapeutics

Ann L. Daugherty and Randall J. Mrsny

1. Introduction

Therapeutic and diagnostic antibodies have become the fastest growing area of biopharmaceutical applications. There are now 18 monoclonal antibodies on the market and over 100 in clinical trials, which highlights the significance of these therapeutics and the advances made in antibody engineering. Further, by 2008, engineered antibodies are projected to be the source of over a third of the revenues from biotechnology (Baker 2005; Reichert et al. 2005).

A few seminal events that have led to the current and projected prominence of antibodies as biopharmaceuticals include the identification of methods to generate murine monoclonal versions of antibodies (Kohler and Milstein 1975), the cloning of human antibody sequences to allow for humanization of murine monoclonal antibodies through complementary-determining region (CDR) grafting (Jones et al. 1986), and even the establishment of fully humanized systems to generate monoclonal antibodies (Peterson 2005). With the sequential identification of these technological advances, antibodies for therapeutic and prophylactic indications have moved from fully murine, to partially murine (mostly human), and to completely human constructions. Added to these events, dramatic advances in production have led to the ability to prepare monoclonal antibodies at scales that can provide sufficient material at costs that make this area appealing to pharmaceutical companies. One important outcome of these various advances is a greater potential to use antibody drugs in chronic settings, tremendously expanding their biopharmaceutical applications.

The majority of currently approved antibody drugs address previously unmet medical needs in the areas of cancer and inflammation. These indications came from practical considerations related to earlier forms of murine and partially murine antibody therapeutics; the first monoclonal to be approved (OKT-3®, muromonab-CD3) was approved in 1986 for a single

Reprinted from Advanced Drug Delivery Reviews 58(5-6): 686–43, 2006, with permission from Elsevier.

From: *Current Trends in Monoclonal Antibody Development and Manufacturing,* Biotechnology: Pharmaceutical Aspects, DOI 10.1007/978-0-387-76643-0_8, Edited by: S.J. Shire et al.

treatment regimen to protect from life-threatening tissue rejection following kidney transplant (Chatenoud 2003). Adverse reactions due to acute immunogenicity problems that develop because of the delivery of a nonself protein limited the use of OKT-3® to only acute application (Merluzzi et al. 2000; Presta 2002). Subsequent partially murine antibodies such as Panorex® (17-1A), Zevalin® (ibritumomab tiuxetan), and Bexxar® (tositumomab) were approved for a limited number of administrations to cancer patients who had failed frontline therapies (Reichert et al. 2005). With the advent of fully humanized antibodies, chronic therapeutic or prophylactic applications for infectious agents have become a realistic clinical option (Reichert et al. 2005). Another critical aspect to the success of antibodies as therapeutic agents involves improved methods to express, purify, and characterize these proteins (Stockwin and Holmes 2003). In general, antibody therapeutics are large (typically >150 kDa), complex in nature (most are glycosylated) and must be administered in stoichiometric rather than in catalytic quantities (nearly a gram per dose is required for many antibodies to be effective). Production and purification scales have thus reached levels of production that were previously assumed impossible in biotech companies (Bogard et al. 1989). Novel concerns then related to the development of stable formulations and delivery strategies for such large amounts of a complex molecule. Understanding product instability with regard to physicochemical and thermodynamic events becomes more and more critical to ensure market success (Atkinson and Klum 2001). The required high concentrations of antibodies in these formulations reduced the need to add a carrier protein, as is the case where in serum albumin is commonly added in formulations of highly potent proteins such as erythropoietin alpha (Epogen®) and Factor VIII (Kogenate®) to enhance stability and reduce loss to vial surfaces. Simultaneously, the large amounts of an antibody protein used in these formulations allowed degradation products to be more readily detectable, particularly when using the highly sensitive methods designed for evaluating hormone biotherapeutics.

Finally, the ability to prepare large quantities of an antibody that could be administered for chronic therapy resulted in a plethora of new and novel applications (Stockwin and Holmes 2003; Bogard et al. 1989) involving the delivery of chemotherapeutics, radionuclides, and imaging agents – to name a few. New issues, related to identifying stable formulations such as high concentration formulations that might reduce the volume of antibody administrations, arose in the move from intravenous infusions to the realm of subcutaneous injection strategies. In some cases, the combination of agents with antibodies produced conflicting stability profiles. Additionally, potential new indications for antibody drugs increased the desire to find novel methods for sustained release, intracellular targeting (Lackey et al. 2002), or delivery via methods not involving an injection. Thus, as is the case in most scientific advances, technological advances opened up possibilities for therapeutic opportunities that were not possible previously as well as for a totally new set of problems that required solving. In this review, we have attempted to identify the major issues associated with formulating and delivering antibody drugs, to recognize challenges already identified, accompanied when possible by solutions, as well as to discuss concerns that will need to be addressed in the future as the use of antibody drugs continues to evolve.

2. Antibody Characteristics Relevant for Formulation and Delivery

The human body produces several classes of antibodies that appear to perform specific functions under different conditions and at discrete anatomic sites. Most of the currently approved antibody-based drugs are of the IgG1 class (Grainger 2004) and are glycosylated on the Fc (fragment crystallizable) domain. Glycosylation has been shown to participate in specific cell response events mediated by antibodies (Imai et al. 2005; Siberil et al. 2005; Wright and Morrison 1994): antibody-dependent cell-mediated cytotoxicity (ADCC) and complement-dependent cell-mediated cytotoxicity (CDCC) through receptor recognition events. Individual glycoforms of antibodies can provide improved efficacies for certain clinical outcomes (Jefferis 2005). In general, IgG1 and IgG3 antibodies are effective at initiating ADCC, while IgG2 readily fixes complement but is poor at inducing ADCC. IgG4 appears to be inefficient at both ADCC and CDCC (Grainger 2004). Interestingly, antibodies can be re-engineered to increase their capacity to recruit complement (Idusogie et al. 2001) or to adjust their affinities to the various classes of Fc receptors and thus ADCC function through mutation of specific amino acids within the Fc domain (Shields et al. 2001). Molecular engineering has also provided a spectrum of new antibodies (Fig. 8-1). Other chapters in this issue delve

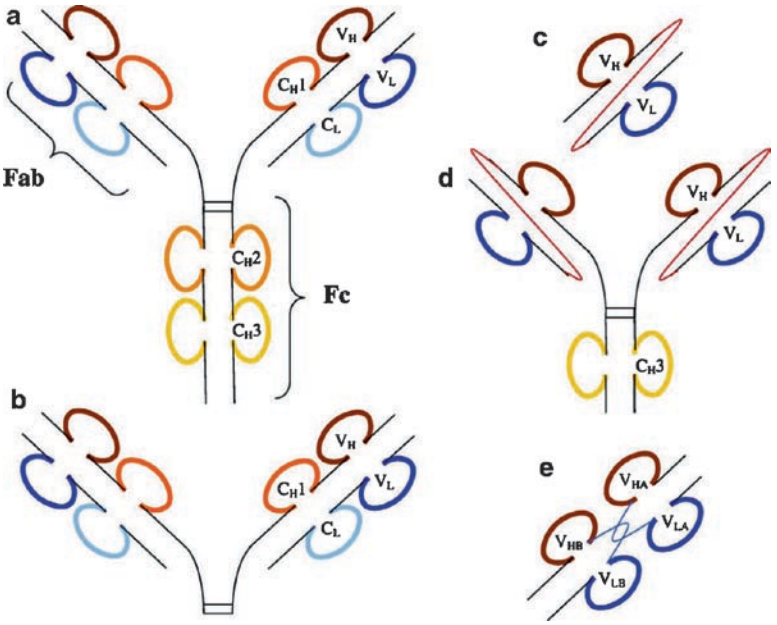

Fig. 8-1. General antibody structure and some antibody-based protein constructions. a) Human antibodies have a common framework that can be described as Fc (fragment crystallizable) and Fab (fragment antigen binding) domains that are derived from the folded structure of heavy (H) and light (L) chain proteins. Multiple constant (C) regions on both the H and L chain proteins are donated as are the variable (V) segments involved in antigen-specific recognition. b) Removal of the Fc domain produces a F(ab)2 structure. c) Single chain structures of the antigen binding region (scFv) can be prepared by themselves or d) in a construct that includes Fc domain elements. e) Bi-specific antibody elements (diabodies) can be prepared to bring two different antigens into close proximity. C_H, heavy chain constant regions; C_L, light chain constant region; V_H, heavy chain variable region; V_L, light chain variable region

deeply into the many characteristics of antibodies that make them remarkable and diversely applicable treatment agents: ligand binding properties, effector functions and potential for modification in their design. Other chapters will also address applications of newly engineered antibody-like molecules that move beyond the realm of intact, full-length IgG antibodies. The current review focuses primarily on IgG1 since this is where the majority of published information exists for antibody drug formulation and delivery.

Antibodies, due to their large size (being greater than the filtration cut-off size of the kidney) and their ability to be sequestered for periods of time from the blood, via interactions with FcRn receptors present on endothelial cells, can have extended serum profiles in the range of weeks. A number of engineered antibody-like molecules are now being examined for therapeutic applications (Wu and Senter 2005). Some engineered fragments, such as diabodies and minibodies, are much smaller than intact, full-length IgG1 and have very different properties of systemic distribution and clearance. Additionally, methods to prepare other antibody types such as dimeric secretory IgA (Corthesy 2003) and methods to prepare antibodies using nonmammalian cell systems, such as plants (Ma et al. 1998), from the eggs of chimeric chickens (Zhu et al. 2005) and from transgenic animals (Lonberg 2005), are now being explored by academic and industrial groups. As these new approaches gain prominence, more information will be acquired about their unique requirements for successful formulation and delivery. At present, however, there is little information on formulation approaches for antibodies produced using these production processes.

3. General Concerns for Antibody Formulations

Owing to their proteinacous nature, antibodies present generic formulation issues that are similar for most protein therapeutics (Atkinson and Klum 2001). Proteins, in general, can be degraded under conditions when they are exposed to heat, freezing, light, pH extremes, agitation, sheer-stress, some metals, and organic solvents. With ever advancing analytical technologies, the ability to assess the physicochemical and thermodynamic instability of antibody drugs has also led to the identification of several events that are more specific to the unique nature of this particular class of proteins: variations in Fc glycosylation, partial heavy chain C-terminal Lys processing, Fc methionine oxidation, hinge-region cleavage, and glycation of Lys residues (Harris 2005). In addition to these issues is the difficulty of preparing dosing materials that might have protein concentrations in the range of 100 mg/ml or greater. Since early preclinical assessment is so critical to successful identification of a new biotherapeutic product, general preformulation strategies are usually employed for initial studies with new antibody drugs. An initial formulation effort will likely employ an isotonic, non-hemolytic, slightly acidic solution that can be administered by intravenous infusion or subcutaneous injection in studies employing a relevant animal model. In some cases, some stability information for the antibody drug can be obtained from initial in silico and in vivo testing during this preclinical phase that aids in the selection of a formulation that is used in clinical trials (Bazin et al. 1994).

Since most early preclinical studies attempt to emulate the delivery strategy that will be used in the clinic, initial studies frequently identify problems with either the initial preformulation approach and/or stability issues with the antibody drug itself. In the case of the formulation, protein precipitation can occur

with refrigerated storage or with repeated freeze–thaw cycles, events that may be facilitated by an inappropriate pH or buffer selection. Analysis of antibody drugs stored in this initial preformulation system may also identify unstable sites within the protein or its linkage to attached molecules (chemotherapeutics, imagining agents, etc.). In the case of the antibody, this information is frequently evaluated to determine if re-engineering of the protein could be performed, for example, to provide greater thermodynamic stability or folding efficiency (Ewert et al. 2004). Such changes in the Fc region are typically conservative, but might act to modify Fc receptor binding properties to provide a different biological outcome (Demarest et al. 2004; Hodoniczky et al. 2005). Amino acid substitutions can also be made within the Fv region to improve thermal stability (Yasui et al. 1994), but such changes might also alter antigen binding specificity (Rudikoff et al. 1982).

4. Stability Issues for Antibody formulations

If one examines the amino acid sequences for currently approved IgG1-based antibody drugs, it becomes quite clear that only a small segment of these proteins are dramatically different from one another, being the Fv segments that are involved in antigen binding. It should be pointed out, however, that there are some minor differences in conserved regions as well. A priori, one might assume that by finding a stable formulation for one of these antibody drugs, such a formulation would be good for most if not all, similar antibodies. If this were borne out by experience, there would be no need for a review such as this. Instead, each antibody seems to have a unique personality related to its requirements for stability, a phenomenon derived from the fact that the small differences between these antibodies are focused on surface-exposed amino acid differences that stipulate antigen specificity. Thus, the interfacial surface of each antibody drug is unique and thus requires specific formulation components to provide maximal stability and retention of activity.

Probably the most important aspect of identifying a successful antibody drug formulation is in the identification of truly detrimental alterations rather than all of the modifications that might occur. Although, from a regulatory standpoint, it may be beneficial to understand all of the potential degradation events associated with an antibody formulation, it is the recognition of a stability-indicating parameter (or several parameters) that allows the formulation scientist to focus in on what is critical to development of a successful product. Here, a series of physicochemical and bioanalytical assays can be used to identify these parameters (Mire-Sluis 2001). Although in vivo bioassays may ultimately be required to validate a stability-indicating formulation parameter, the most critical tools at the disposal of the formulation scientist are rapid and reproducible assays to measure protein changes due to oxidation, deamidation, aggregation, fragmentation, and other forms of chemical modification that could lead to a loss of function of the antibody drug.

4.1. Oxidation

Methionine and cysteine residues are frequently a site of oxidation in protein drugs, and this is also the case for antibody drugs (Kroon et al. 1992). In the case of antibody-based drugs, specific methionine residues within the Fc

domain may be prone to oxidation, resulting in the production of methionine sulfoxide (Harris 2005). While cysteines are present in the Fc framework as disulfide pairs, unpaired cysteines in the variable region may also be sites of oxidation. Besides methionine and cysteine residues, oxidation of histidine, tyrosine, tryptophan, and phenylalanine residues can also occur (Griffiths 2000). A number of methods can be used to monitor oxidation of amino acid residues. As a starting point, the number of reactive protein thiols can be monitored using reagents such as 5,5′-dithionitrobenzoic acid or iodoacethyl dansylcadaverine (Hasegawa et al. 2005), providing a simple readout on the number of protein thiols per protein. Total amino acid analysis can also be used to monitor reductions in methionine, tyrosine, and phenylalanine residues. Tryptic digestion and peptide separation by liquid chromatography followed by mass spectroscopy analysis (LC-MS) can be used to identify specific sites of amino acid oxidation.

A careful study of methionine oxidation has been performed for the humanized monoclonal antibody that recognizes the *her2/neu* gene product. For this protein, it was determined that a methionine at position 255 in at heavy chain of the Fc region was the primary site of oxidation and that a methionine at position 431 could also oxidize under more aggressive conditions. In this study, a chromatography assay was used to detect oxidation events following papain digestion to separate Fab and Fc segments of the antibody (Shen et al. 1996). Another study on the stability of this same protein provides a valuable template for dealing with antibody oxidation: identification of a critical oxidation event, validation of a robust assay for monitoring that event, and comparison of formulation parameters to determine conditions that facilitate oxidation. Addition of antioxidants or stoichiometric levels of free methionine or thiosulfate were found to reduce the extent of oxidation in formulations of this antibody (Lam et al. 1997).

Issues associated with administration of oxidized forms of an antibody may extend beyond concerns of reduced efficacy. Systemic lupus erythematosus (SLE) is a disease characterized by the induction of antidouble-stranded DNA antibodies. Studies have shown that increased levels of markers of protein oxidation, including those of methionine sulfoxide and 3-nitrotyrosine, correlated with SLE disease activity (Morgan et al. 2005). Additionally, oxidative modifications of antibodies isolated from synovial fluid samples collected from patients with rheumatoid arthritis suggested alteration of histidine, methionine, tyrosine, and cysteine residues (Jasin 1993). While no direct causal association is shown or implied, these observations bring attention to the issue that we do not fully understand the clinical impact of antibody oxidation events.

4.2. Deamidation

Glutamine and asparagine residues show a propensity for deamidation (Robinson et al. 1970). Both light and heavy chains of antibodies can undergo deamidation of these amino acids (Mimura et al. 1995), and deamidation events are considered to be one of the major sources of charge heterogeneity of monoclonal antibodies (Zhang and Czupryn 2003). Deamidation events appear to be highly selective events for individual antibodies. For example, analysis of several monoclonal antibodies that bind the *her2/neu* gene product demonstrated asparagine 30 deamidation on one or both light chains and

asparagine 55 on the heavy chain (Harris et al. 2001). Deamidation events lead to more acidic forms of the antibody through the acquisition of additional carboxylic acid groups. Conversely, aspartic acid residues can also undergo modification to a succinimide moiety that results in a basic antibody isoform of the antibody by removal of a carboxylic acid group (Harris et al. 2001). In general, deamidation events appear to be relatively slow but are accelerated by unfolding of the antibody (Chelius et al. 2005). Initial detection of deamidation in antibody preparations is typically identified by differences in charge distribution or content using methods such as isoelectric focusing (IEF) or high-performance cation-exchange chromatography (Harris et al. 2001).

High performance chromatography can then be used to separate succinimide, isoaspartic, and aspartic acid isoforms of tryptic digest fragments of the antibody, which can be unambiguously characterized by tandem mass spectroscopy (MS). Correlation between tryptic digest tandem MS results and some other more readily accessible method, such as IEF, can provide a rapid format to follow antibody deamidation events. Using these techniques, asparagine deamidation events residues appear to occur more frequently than glutamine deamidation, and specific asparagine residues appear to be selectively targeted for this event (Kroon et al. 1992). Deamidation of asparagine is frequently associated with rearrangement events that lead to the formation of isoaspartic acid (Zhang and Czupryn 2003), and this outcome is correlated to amino acids adjacent to the asparagine prone for deamidation (Chelius et al. 2005) that provide a method for prediction of potential deamidation sites (see Box below). In particular, asparagine-glycine sequences can demonstrate accelerated deamidation rates since glycine residues lack a side-chain structure that would otherwise act to decreased conformation interference for backbone-associated isoaspartyl formation (Radkiewicz et al. 2001).

Amino acid[a] sequences predicted to deamidateSNG, LNG, LNN, and ENN
(Note these have a following amino acid of G or N)
and those that are less prone to deamidation
GNT, GNS, GNV, TNY, SNY, SNF, SNT, SNK, SNL, WNS, FNW, FNS, FNR HNA, HNH, LNW, CNV, NNF, DNA, and YNP

[a]Standard single amino acid letter nomenclature

Nonenzymatic parameters of asparagine and glutamine deamidation in proteins have been defined in detail for factors such as pH, temperature, and ionic strength (Robinson and Robinson 2004; Robinson et al. 2004). The primary sequence dependence of these deamidation events can be explained by a simple steric and catalytic model (Robinson and Robinson 2004; Robinson et al. 2004). Prediction of deamidation events based upon three-dimensional structures has also been described, but the data set for these studies are not yet sufficient to produce a general model (Robinson and Robinson 2001a). That asparagine and glutamine deamidation appear to be a constant phenomenon of proteins and correlate with their turnover provides the basis for the hypothesis that the presence and distribution of these amino acids within a protein can act as a molecular clock for its biological turnover (Robinson and Robinson 2001b, c). For the formulation scientist, empiric assessment of factors such as pH and ionic strength provide the best strategy to identify a formulation that

minimizes deamidation events. In general, deamidation does not result in a decrease in potency, and it may be hard to detect as the charge difference is small. At times, however, there can be a detrimental effect on potency through the introduction of an unfavorable negative charge that can have further ramification on biological function, particularly when deamidation occurs in the binding regions (Huang et al. 2005). As particularly reactive residues are identified, it may be possible to have the antibody engineered to remove the problematic amino acid or to change adjacent residues to reduce its reactivity.

4.3. Aggregation

Liquid formulations of protein therapeutics frequently exhibit a decrease in concentration because of adsorptivity to container walls at low concentration and can show aggregation events at high concentrations. Initial preparations of antibody drugs were administered in acute situations by IV infusion that could allow for medium protein concentration (1–10 mg/ml) formulations not dramatically affected by adherence or aggregation losses. As antibody-based drugs became more widely used in chronic care, high concentration formulations that would allow for clinically acceptable SC injection volumes became desirable, and aggregation became an important concern for designing formulations. Along with aggregation events, protein solutions at concentrations >50 mg/ml may become sufficiently viscous as to no longer readily pass through the gauge of a needle that would be comfortable for patients' use. Some antibodies demonstrate high concentration viscosity issues, while others do not. For example, the antirespiratory syncytial viral antibody Synagis® is formulated at 100 mg/ml protein and is administered successfully by IM injection. Thus, addressing viscosity, adsorptive loss and aggregation in any specific antibody formulation will likely be performed on a case-by-case basis.

As protein–protein contact frequency increases at high concentrations, the opportunity for stable aggregate formation increases proportionally. Proteins are folded in such a way as to internalize hydrophobic domains and surface-expose more hydrophilic domains in a thermodynamically stable situation. As folded proteins undergo normal molecular motion transient surface exposure of hydrophobic domains can lead to protein–protein contacts that hide these surfaces in a more energetically favorable manner. The outcome of these events is the stabilization of these protein–protein contacts with the ultimate outcome of dimerization, trimerization, and so on – leading to extended aggregation events (Cleland et al. 1993). As protein concentration and temperature goes up, so does the probability of energetically favorable contacts, leading to aggregation with increased frequency and duration of reversible protein–protein contacts, which leads to a greater extent of stable (even irreversible) aggregation events. Aggregation (covalent, noncovalent, dissociable, and nondissociable) must be considered a likely degradation event for high concentration antibody formulations.

For some antibodies, reduced temperatures can incite reversible self-associations; these molecules are known as cryoimmunoglobulins (Middaugh et al. 1978). IgG3 cryoimmunoglobulins have been shown to self-associate through sugar structures of the Fc domain (Panka 1997). Self-association events involving IgG1 antibodies seem to occur primarily through weak ionic and hydrophobic interactions (Hall and Abraham 1984). More recent studies

have examined kinetic and thermodynamic aspects of antibody solution dimerization using a recombinant human monoclonal antibody that recognizes vascular endothelial growth factor (rhMab-VEGF) as a model (Moore et al. 1999). It was found that for this IgG1 class antibody, aggregation rates were greater in slightly alkaline (pH 7.5–8.5) compared to slightly acidic (pH 6.5–7.5) conditions. A high salt environment (1 M NaCl) also enhanced dimerization. Not surprisingly, self-association events were accelerated as the storage temperature was increased. One of the most striking aspects of these dimerization studies on rhMab-VEGF is that trastuzumab, another genetically engineered antibody with the same IgG1 framework and a 92% sequence homology with rhMab-VEGF, fails to demonstrate aggregation events under the same conditions.

A number of additives have been identified that can reduce the rate of protein aggregation (Cleland et al. 1993; Baynes and Trout 2004). A rather wide spectrum of agents can reduce protein aggregation rates: urea, guanidinium chloride, amino acids (in particular glycine and arginine), various sugars, polyalcohols, polymers (including polyethylene glycol and dextrans), surfactants, and even antibodies themselves. Studies have shown that different proteins benefit from different types of antiaggregating factors, consistent with the notion that the interfacial surfaces that drive interactions leading to aggregation are protein-specific. Conceptually, antiaggregating agents might fall into one of two categories: small agents that fit into channels or grooves and large agents that might interact with lower-curvature surfaces of the protein. In essence, the small agents would act to stabilize a protein from acquiring a conformation that might be more reactive toward aggregation, while a large agent might act to reduce the frequency of surface contacts that lead to an aggregation event. In the case of antibody formulation, either or both may be important. As we will discuss, agents found to effectively protect an antibody from aggregation may differ for various stress conditions; antibodies that are undergoing agitation and thermal stress in solution may differ from those of the same antibody as it undergoes lyophilization and reconstitution.

Protection from aggregation can be limited in antibody formulations by the addition of surface-active agents such as detergents, both charged and uncharged. As an interesting aside, such surface-active agents can help reduce protein loss because of adherence to surfaces that can occur with low concentration protein formulations. Polysorbate 20 and 80 (now available from a vegetal source) are examples of detergents that are widely used to reduce the rate of protein aggregation in high concentration antibody drug formulations. A precautionary note must be sounded, however, as detergents perform this function optimally at low concentrations (0.01–0.05%) and can act detrimentally to participate in protein unfolding at higher concentrations, e.g., 1%.

That antibody aggregation can be accelerated by several physical conditions provides the potential for multiple methods to determine if a particular antibody drug is prone to aggregation and to rapidly test formulations for their ability to impede aggregation. Agitation studies are done, in addition to thermal stability studies, to determine if aggregation can occur in a given formulation. Different test methods are used, employing a shaker or a stirring apparatus. A study done on an IgG1 antibody found that sizes of aggregates produced by the two methods were comparable (Mahler et al. 2005). It was concluded that a higher throughput test could be constructed using stirring analyzed by

absorbance measurement. In the work, the stirred samples exhibited much higher absorbance and second particle species in DLS, indicating that stirring stress produces a higher amount of smaller protein aggregates. While Mahler found polysorbate 80 protects against aggregation, the stirred samples had an increase in turbidity and more aggregate products were detected by DLS as compared to a surfactant-free formulation. Polysorbate 80 stabilizes small aggregates and prevents further progress in the aggregation process.

4.4. Fragmentation

Intact, full-length antibodies are composed of several segments that have natural flexure sites. One site, in particular, exists at the flexure point between the Fc and Fv domain. Cleavage at this hinge region is a common concern when assessing antibody drug stability (Harris 2005). Molecular sizing methods such as sodium dodecyl sulfate–polyacrylamide gel electrophoresis (SDS–PAGE) and size-exclusion high performance liquid chromatography (SE-HPLC) can be used to rapidly identify fragmentation events in antibody drugs (Page et al. 1995). Fragmentation of full-length antibody drugs is a common occurrence and invariably affects their function. In general, cleaved forms are present in such low amounts that it is likely that little change in efficacy would be seen (Cordoba et al. 2005). At the very least, the antibody drug may have some small reduction in efficacy following fragmentation or may be more prone to proteases, degradation, and clearance events that would limit the duration of its efficacy. At the worst, a fragmented antibody preparation may result in a different biodistribution and thus a different safety profile. This can be of particular concern if the antibody is being used to delivery a cytotoxic chemotherapeutic agent. Fortunately, the extent of fragmentation in an antibody can be easily limited in the formulated product.

5. Strategies to Stabilize Antibody Formulations

While liquid antibody formulations are less expensive, faster to develop and generally easier to prepare for administration than alternative formulation approaches, liquid antibody formulations are prone to oxidation, deamidation, aggregation, and fragmentation as discussed above. In each of these events, water is the common culprit: water mediates electron transfer during oxidation and deamidation events, and its required addition across a peptide bond can be a critical step in fragmentation. The thermodynamic stresses that lead to protein aggregation are caused by hydrophobic protein surfaces being exposed to water and trying to find a lower energy state by non-native protein–protein interactions. Thus, water is a big problem for stabilizing antibody-based drugs. Lyophilization or introduction into hydrophobic polymer systems can reduce the impact of water on antibody drug formulations.

5.1. Lyophilization

Although some antibodies have demonstrated a propensity to undergo precipitation as they are cooled from 37°C (Middaugh et al. 1978), antibodies are typically robust to freeze/thaw cycles (Sarciaux et al. 1999). Early studies reported that antibodies were stable to the freeze-drying (lyophilization)

process in the absence of excipients that function as cryoprotectants (Friedli 1987); however, with the technical advancement of certain analytical methodologies, it became evident that antibodies are generally damaged in some way as a result of lyophilization as demonstrated by extensive formation of insoluble aggregates (Sarciaux et al. 1999). More recently, studies have shown that freeze-drying antibodies to a specific percent of residual water (usually between 1 and 8%) allow for optimal stabilization in the dry state and stability during reconstitution (Breen et al. 2001). Higher moisture content in lyophilized antibody preparations correlates with increased aggregation (as seen by SEC) and asparagine deamidation and isomerization (as measured by HIC). Studies have also been performed to identify optimized lyophilization schedules where the secondary drying phase is performed at an elevated temperature (Ma et al. 2001). This technique allows the lyophilized cake to achieve optimum moisture content, allowing the final product to be conformationally stable (as measured by DSC) during extended storage. Solid-state structural studies can be used to monitor conformational changes and aggregation events during the storage of a lyophilized monoclonal antibody preparation (Andya et al. 2003). Improved native-like structure and a reduction in aggregation can be obtained by incorporation of a carbohydrate excipient in sufficient quantities to fulfill the hydrogen bonding requirements on the protein surface, suggesting a critical role for nonwater molecules to act as placeholders for water molecules during drying and in the dry state. That the addition of excess carbohydrate failed to improve the stabilizing function of this excipient reaffirms the conclusion that antibodies have a limited number of sites that must be protected in this fashion (Andya et al. 2003). A variety of carbohydrates or polyol compounds such as sucrose, trehalose, and mannitol have been shown to provide this stabilizing function (Cleland et al. 2001; Duddu and Dal Monte 1997).

The rate of rehydration when water is reintroduced during reconstitution of lyophilized formulations is a critical parameter. As water is removed during different drying stages of the lyophilization cycle and replaced by a shell of nonwater excipients, the antibody drug can undergo structural modifications that result in a non-native conformation as may be seen by differential scanning calorimetry (Breen et al. 2001). If the rate of rehydration is sufficiently slow to allow recovery of native conformation as water replaces nonwater excipient molecules, reconstitution will typically provide a satisfactory outcome for the antibody. If, however, the antibody does not have sufficient time or capacity to recover its native state during reconstitution, extensive aggregation can result. Efforts to protect monoclonal antibodies from the rigors of freeze-drying and reconstitution have been aided by a number of analytical methods that can examine protein modifications. In the solid state, circular dichroism (CD) and Fourier transform infrared (FTIR) spectroscopy may be used to evaluate the protein; after reconstitution in the liquid phase, SEC or SDS–PAGE have been utilized to gather information from lyophilization studies (Costantino et al. 1998a; Hsu et al. 1992). A microscopic apparatus to visually monitor freeze-drying events has even been described (Hsu et al. 1996). Excipients that have been reported to slow the reconstitution rate and thereby preventing such changes in the rehydrated antibody are glycerol (Chang et al. 2005; Gekko 1981) and polymeric materials such as polyethylene glycol (Arakawa et al. 1991).

Pharmaceutical scientists frequently use increased temperatures for accelerated formulation stability studies. Although such studies can be used to assess formulation parameters such as pH and ionic strength, antibodies lyophilized in the presence of a cryoprotective sugar excipient provide a more complicated picture. Lyophilized amorphous solids composed of a monoclonal antibody and a sugar cryoprotectant material such as sucrose or trehalose form glassy structures, liquids that are too viscous to flow. That antibody-excipient complexes exhibit a glass transition temperature (Tg) provides the basis for observations showing that these materials have unique properties above and below this value. Thus, in predicting shelf life in accelerated degradation studies, it is important to use testing temperatures that do not exceed the Tg threshold of the complex (Duddu and Dal Monte 1997). In general, lyophilized formulations containing trehalose may likely show less tendency toward antibody aggregation than those with sucrose, since trehalose preparations have a higher Tg (Duddu and Dal Monte 1997). With this in mind, a promising approach to assess secondary structural parameters in evaluating antibody formulation stability is the use of amide I band Raman spectroscopy. This method demonstrates a good correlation between structural protein perturbations immediately after lyophilization and the rate of aggregation during long-term storage under accelerated conditions (Sane et al. 2004).

5.2. Polymer Delivery Systems

Removal of water from antibody preparations, by either lyophilization or spray freeze-drying, provides a starting point for incorporation of this dried material into a hydrophobic polymer matrix such as polylactide-co-glycolide (PLGA) that can be made into microspheres generated through a solid-in-oil-in-water (S/O/W) encapsulation process (Wang et al. 2004). Although both mannitol and trehalose can stabilize human IgG during spray freeze-drying, the double-emulsion solvent evaporation method used to load spray freeze-dried human IgG into PLGA microspheres has been shown to produce extensive antibody aggregation (Wang et al. 2004). Such an outcome is likely the result of thermodynamic stress experienced at the water/organic solvent interface, and a variety of process methods and excipients can be used to minimize this concern (Jones et al. 1997).

One feature of PLGA microparticle preparations is their recognition by immune elements and their capacity to stimulate immunization against incorporated proteins (Gupta et al. 1998; Lavelle et al. 1999; O'Hagan et al. 1991). While this has clear advantages for vaccines, it poses a serious concern for therapeutic protein delivery. Hydrophobic microparticles have been reported to incite local inflammation at subcutaneous injection sites (Daugherty et al. 1997), events that may be partially mediated through macrophage recruitment (Luzardo-Alvarez et al. 2005). Not only is the potential for antibody formation increased with local inflammation, the resulting injection site reaction may also be clinically unacceptable.

In spite of some serious caveats, polymeric microspheres and delivery systems can be successful antibody formulations if administered to the appropriate sites, using certain types of polymers or by preparing microspheres or polymeric formulations by methods that are more protective of the antibody. An example of a certain delivery site that may have less proclivity toward an

inflammatory response is reported, where PLGA microspheres loaded with an antiVEGF antibody were injected into the intravitreal humor of the eye, an immune-privileged site, for the treatment of age related macular degeneration (AMD) (Mordenti et al. 1999). Resorbable polymers that show less potential to incite inflammation, e.g., have smoother surface characteristics, might be used to deliver antibodies in a sustained manner. Direct, local delivery of antibodies using carboxymethylcellulose aqueous gels can be an effective post-surgical anti-infective strategy (Poelstra et al. 2002). Antibodies covalently coupled to a biodegradable hyaluronic acid hydrogel through a labile hydrazone linkage have been used for the sustained delivery of antibodies to sites within the central nervous system (Tian et al. 2005). Introduction of dry powder IgG into ethylene-vinyl acetate copolymer (EVAc) has also been examined as a potential polymer-based antibody delivery system (Wang et al. 1999). Similar to PLGA systems, EVAc microspheres can extend the time course of IgG release. This property makes polymers loaded with antibodies interesting opportunities for injectable sustained release delivery formats but also for topical application at mucosal surfaces. For example, long-term vaginal delivery of an antibody can be achieved in a mouse model using polymer vaginal rings (Kuo et al. 1998; Saltzman et al. 2000). Formulations of a biomedical grade polyurethane hydrogel with an antibody coating have also been prepared and shown to release bioactive protein (Rojas et al. 2000). It is important to note that one complicating aspect of many of these approaches is the requirement of a polymer solubilization step using a solvent, such as methylene chloride or isopropanol, which can compromise protein drug stability. Sustained release formulation approaches such as microspheres prepared using water, such as the PROMAXX microspheres (Epic Therapeutics) or crystallization of proteins (Yang et al. 2003) can bypass the use of solvents that are incompatible with proteins and antibodies.

6. Formulation Issues for Alternative Forms of Antibody Delivery

To date, antibody development has focused primarily on injectable routes of administration: intravenous (IV), intramuscular (IM), and subcutaneous (SC). A long history of IV antibody infusions exists (Sgouris 1970), and the advantages are clear for antibody-based drugs that are used in cancer treatments in order to reach tumor sites that may be diffuse or not otherwise accessible. In fact, the majority of the approved antibody-based drugs are administered by IV infusion (Table 8-1) with the total dose administered approaching one gram of protein per treatment in some cases. For many antibody-based therapies, a critical safety concern involves the onset of acute or delayed systemic reactions following infusion (Cook-Bruns 2001; Crandall and Mackner 2003). Parameters and characteristics of the “infusion reaction” as well as treatment protocols have been well described with acute events commonly occurring within 10 min to 4 h and delayed events occurring 24 h to 4 days postdosing (Cheifetz and Mayer 2005). Although formation of antibodies to the administered antibody drug appear to be a risk factor for infusion reaction events (Baert et al. 2003), infusion reactions can occur following the initial exposure (Cheifetz and Mayer 2005), and these reactions do not appear to be due to

Table 8-1. Formulations of approved products.

Antibody product; company	Generic name; description	Delivery route	Formulation concentration	Buffer components; pH[a]	Excipients
Othroclone OKT3®; J & J-Ortho Biotech	Muromonab –CD3; Murine IgG2a, anti-CD3	IV	1 mg/ml	Na,K phosphate; pH 7	NaCl, polysorbate 80
Reopro®; Centocor-Lilly	Abciximab; Chimeric IgG1, anti-GPIIb/IIIa, Fab	IV	2 mg/ml	Na phosphate; pH 7.2	NaCl, polysorbate 80
Rituxan®; Idec-Genentech	Rituximab; Chimeric IgG1, anti-CD20	IV	10 mg/ml	Na citrate; pH 6.5	NaCl, polysorbate 80
Zenapax®; Roche	Daclizimab; Humanized IgG1, anti-CD25	IV	5 mg/ml	Na phosphate; pH 6.9	NaCl, polysorbate 80
Simulect; Novartis[b]	Basilixamab; Chimeric IgG, anti-CD25	IV	4 mg/ml	Na,K phosphate, glycine	NaCl, sucrose, mannitol, polysorbate 80
Synagis®[a]; MedImmune	Palivizumab; Humanized IgG1, anti-RSV	IM	100 mg/ml	Histidine, glycine	Mannitol
Remicade®[b]; Centocor	Infliximab; Chimeric IgG1, anti-TNFα	IV	10 mg/ml	Na phosphate; pH 7.2	Sucrose, polysorbate 80
Herceptin®[b]; Genectech	Trastuzumab; Humanized IgG1, anti-HER2	IV	21 mg/ml	Histidine; pH 6	Trehalose, polysorbate 20, benzyl alcohol[c]
Mylotarg®[b]; Wyeth	Gemtuzumab ozogamicin; Humanized IgG4, anti-CD33, immunotoxin	IV	4 mg/ml	Na phosphate	NaCl, sucrose, dextran 40

Campath®-1H; Millennium-ILEX	Alemtuzumab; Humanized IgG1, anti-CD52	IV	Unclear – 30 mg/vial	Na,K-phosphate pH 7	NaCl, KCl, NaEDTA, polysorbate 80
Zevalin®[d]; Biogen Idec	Ibritumomab tiuxetan; Murine IgG1, anti-CD20; radiolabeled (^{90}Y or ^{111}In)	IV[d]	1.6 mg/ml	Na Acetate, Na,K-phosphate pH 7	NaCl, human albumin
Humira®; Abbott	Adalimumab; Human IgG1, anti-TNFα	IV	50 mg/ml	Na phosphate, Na Citrate; pH 5.2	Mannitol, polysorbate 80
Xolair®[b]; Genentech	Omalizumab; Humanized IgG1, anti-IgE	SC	125 mg/ml	Histidine	Sucrose, polysorbate 20
Bexxar®; Corixam - GSK	Tositumomab-I131; Murine IgG2a, anti-CD20, radiolabeled (^{131}I)	IV	14 mg/ml	Na phosphate; pH 7.2	NaCl, maltose
Raptiva®; Genentech	Efalizumab; Humanized IgG1, anti-CD11a	SC	100 mg/ml	Histidine; pH 6.2	Sucrose, polysorbate 20
Erbitux®; Imclone Systems	Cetuximab; Chimeric IgG1, anti-EGFR	IV	2 mg/ml	Na phosphate; pH 7.2	NaCl
Avasatin®; Genentech	Bevacizumab; Humanized IgG1, anti-VEGF	IV	25 mg/ml	Na phosphate; pH 6.4	Trehalose, polysorbate 20
Tysabri; Biogen Idec	Natalizumab; Humanized IgG4, anti-α4-integrin	IV	20 mg/ml	Na phosphate; pH 6.1	NaCl; polysorbate 80

Ordered by approval dates in the US

RSV respiratory syncytial virus; *TNFα* tumor necrosis factor alpha; *EGFR* epidermal growth factor receptor; *VEGF* vascular endothelial growth factor; *NaEDTA* sodium edentate

[a]Lyophilized product, concentration, pH, etc. values are obtained after reconstitution

[b]Added as a preservative to generate a multi-dose vial configuration

[c]Kit where components are mixed just prior to administration

[d]Some lyophilized formulations do not stipulate a pH (or range) following reconstitution

IgE responses or mast cell activation (Cheifetz et al. 2003). Most importantly for the patient, there appear to be treatment protocols to provide retreatment of patients even after an infusion reaction event (Cheifetz and Mayer 2005) with concomitant administration of immunomodulation molecules (Baert et al. 2003). There are many unanswered questions about the mechanism and prevention of adverse infusion reaction events associated with IV infusion of antibody drugs. Certainly, one method is to explore IM and SC delivery when possible, although these delivery approaches may also have confounding aspects of tissue response and volume limitations.

Other routes are also amenable to antibody delivery. The increased number of antibody therapeutics on the market and the greater exploration of nonlife threatening indications being treated by antibodies, drive efforts to deliver these agents by routes other than IV infusion. These routes may be more effective, less invasive, provide easier delivery, permit self-administration, and thereby be more convenient and possibly have lower costs if less active agent can be used, as in the case where in the alternate route of administration delivers the therapeutic agent to the intended site directly. Interestingly, some studies have suggested that antibodies administered by IV infusion are more susceptible to proteolysis than via IM injection (Page et al. 1995) and sucrose-stabilized immunoglobulins have been associated with acute renal failure following IV infusion (Chapman et al. 2004). The antibody used to protect neonates from respiratory syncytial viral (RSV) infection (Synagis®) is one example of an antibody administered by IM injection. For reasons discussed above, the majority of antibody-based drugs have moved toward SC delivery with formulations efforts being focused to this end. Based upon the desired actions for a number of antibody-based drugs, however, routes of administration other than IV, IM, or SC may be desirable. These alternative routes can provide unique formulation and stability issues.

6.1. Oral

Uptake of antibodies from the intestinal lumen can occur through fetal Fc receptors (FcRn) expressed at the apical surface of enterocytes (Lencer and Blumberg 2005). This natural antibody uptake mechanism was initially identified in the gastrointestinal (GI) tract of neonatal rodents and its expression shown to vanish following "closure" of the intestine after weaning. It was found only recently that the continued expression of this receptor in the adult intestine was demonstrated, and this finding has prompted efforts to examine this receptor system as a means of delivery antibodies after oral administration. Although this pathway appears to be a viable route for the delivery of therapeutic antibodies, issues associated with antibody stability in the GI tract (Reilly et al. 1997) and competition from endogenous antibodies can dramatically reduce the efficiency of uptake after oral delivery. Outside of this specific mechanism, no other transcellular mechanism of efficient antibody transport across epithelial cell of the GI tract has been demonstrated to date. Topical application of antibodies to produce a desired clinical outcome has been shown, however, with the oral delivery of a chicken-derived (IgY) antibodies for treating and preventing infectious diseases of the GI tract (Reilly et al. 1997; Horie et al. 2004; Mine and Kovacs-Nolan 2002). It should be noted that IgY antibodies have been shown to not bind to (or be transported by) FcRn (Lencer and Blumberg 2005).

6.2. Respiratory Tract

Intranasal and pulmonary administration of protein therapeutics have shown more promising clinical outcomes than oral delivery. While the surfaces of both the respiratory tract and the gastrointestinal tracts are readily accessible, the respiratory tract is a far less hostile environment for an administered protein therapeutic. Nonetheless, there are physical clearance mechanisms in place to remove foreign particles, which act to reduce residence time dramatically following administration. In the case of nasal administration, the use of a cream emulsion and a polymer delivery system has been shown to significantly decrease the clearance rate for a monoclonal antibody when applied to the nasal mucosa (Walsh et al. 2004). This study provides one approach for the topical application of a therapeutic antibody designed to provide clinical benefit at the mucosal surface. It does not, however, suggest that an appreciable amount of an antibody might be absorbed into the systemic circulation from this site. The nasal mucosa affords only a small absorptive surface area compared to the epithelial linings of the lung.

Aerosol delivery of antibodies to the lung has been explored as either a liquid or dry powder formulation, both the cases in which the droplets or particles must be of sufficiently small size that they are respirable perhaps to the level of the deep lung but large enough that they are not readily exhaled or just impact the back of the throat (Ref). The size of particles that provide this performance has a mass mean aerodynamic diameter and density such that they enter the alveoli and remain in the lung. This size window has been reported to be between 1 and 5 μm depending on the formulation used and in one case, far larger, 20 μm where the particles are dense (<0.4 g/cm^3) and highly porous (Edwards et al. 1997).

Formulation efforts were made for producing fine dry powder particles of an antiIgE monoclonal antibody (E25) in the size range desired for delivery to the lung (Costantino et al. 1998b). These studies showed that sodium phosphate was capable of extending the usefulness of mannitol as a protective excipient in spray-dried antibody formulations and that mannitol can play a role both in maintaining protein stability as well as producing a suitable aerosol preparation. Further studies to assess carbohydrate excipients for spray-dried aerosol E25 formulations showed that excipient to protein ratios were critical. Degradation issues involved not only protein aggregation but also protein glycation or lactosylation, a protein modification event in which a reducing sugar can add covalently at a free amine (Andya et al. 1999). The ability to formulate and delivery an antibody-based drug to the lung provides the potential for systemic delivery of that protein via uptake through the FcRn expressed at this mucosal surface. Elegant studies showing the distribution and function as well as the application of this transport route for systemic deliver of an Fc-containing protein chimera have been demonstrated (Bitonti et al. 2004; Spiekermann et al. 2002). Thus, the potential or systemic delivery of antibody-based drugs via the respiratory tract looks promising.

6.3. Miscellaneous Delivery Sites of the Body

Unique aspects of antibody-polymer formulations designed for intravitreal injection (Mordenti et al. 1999) or topical vaginal delivery (Kuo et al. 1998; Saltzman et al. 2000) have been discussed above. Additionally, antibody

formulations using hyaluronic acid hydrogels for sustained brain delivery have been noted (Tian et al. 2005). These methods focus on strategies to administer large amounts of an antibody at a specific site in order to provide a sustained level to improve efficacy and/or to minimize injection frequency. Other strategies have been described to deliver antibodies to miscellaneous sites throughout the body, For example, an antitransferrin antibody (OX-26) has been described as a carrier for delivery of covalently attached therapeutic molecules across the blood–brain barrier following IV injection (Granholm et al. 1998). An antitumor necrosis factor antibody has been adsorbed onto cardiovascular stent wires for local neutralization of this cytokine in order to limit restenosis events following stent placement (Javed et al. 2002). A CMC gel containing antibodies to prevent postsurgical infections has been administered to the intraperitoneal cavity (Poelstra et al. 2002).

6.4. Intracellular Targeting

Some promising antibody drug targets are intracellular. Although techniques exist where a cell can synthesize an antibody and secrete it into the cell cytoplasm, successful use of this technology requires gene therapy. Instead, it is possible to chemically couple an antibody with a pH-sensitive polymer that functions to disrupt membranes at acidic pH. Many antibodies are internalized by cells through a receptor-mediated uptake process that leads to their delivery into early and then late endosomes. During endosomal maturation after receptor-antibody internalization, the pH of these vesicles will drop from near neutral to below pH 6. This approach was demonstrated in a format in which the pH-responsive polymer poly(propylacrylic acid) was covalently attached to a monoclonal antibody to facilitate its delivery to the cytoplasm of target cells (Lackey et al. 2002).

7. Other Delivery Issues

A wide range of novel drugs and drug conjugates are being developed using monoclonal antibodies and engineered antibody fragments (Wu and Senter 2005). For some of these novel therapeutic approaches to be successful, they require additional or nontraditional delivery strategies. A cursory discussion of some of these approaches as they relate to intracellular targeting, site placement, and engineered antibodies fragments follows.

7.1. Antibody Fragments

An entire spectrum of antibody fragments have been identified through protein engineering studies with many of these showing remarkable potential for unique and novel clinical opportunities (Holliger and Hudson 2005). These smaller recombinant antibody fragments, the monovalent antibody fragments, Fab and single chain Fv, and the engineered variants, diabodies, triabodies, minibodies, and single-domain antibodies that are less costly to manufacture while still retaining the targeting specificity of full length antibodies are an emerging form of antibody therapy. In fact, some may have greater efficacy and more applications than whole monoclonal antibodies. It may be anticipated that this new subset of antibodies are posing new formulation challenges; however,

to date, publications detailing stability studies and formulation development for these molecules are rare in the scientific literature, so formulation data on antibody fragments is scant. The single V domains have been found to be poorly soluble and have a tendency to aggregate (Holliger and Hudson 2005), but these problems are being overcome by the identification of mutants that minimize the hydrophobic interface and selected by phage display (Jespers et al. 2004). Five Fab molecules have been approved as of this writing with the one humanized Fab (ranibizumab rhFab) awaiting approval in the very near future, but many are in early clinical trials and most in preclinical development. One study has been described that focused on Fab fragments. In general, the binding of an antibody to an effector protein does not necessarily inactivate that target's function (Kawade 1985). When an antibody is effectively inactivating, however, the Fab fragments in the absence of an Fc domain can frequently function as highly potent binding agents capable of masking binding sites or enzymatic elements on macromolecules. For example, Fab fragments prepared from sheep antisnake venom antibodies (Digibind, from GSK) can be an effective antivenom. Storage of liquid formulations of such antivenoms in subtropical countries where refrigeration may not be possible provides a significant formulation challenge. Although lyophilized products can perform well under these conditions, a pH 4.0 (acetate buffer) formulation was also found to be stable and potent for at least 1 year at room temperature (Al-Abdulla et al. 2003), presumably room temperatures characteristic of the tropical and subtropical regions where the material would be used. Strikingly, this stable formulation did not require the presence of a protective carbohydrate excipient. To improve drug delivery, antibody fragments have been fused to many types of molecules, such as radionuclides, cytotoxic drugs, toxins, peptides and proteins, enzymes, and liposomes (Nakamura et al. 2004). An immunoliposome made with a Mab fragment is reported to deliver drugs to the brain such that a molecule is able to cross the formidable barrier of the blood brain barrier (Schnyder and Huwyler 2005).

7.2. Immunoconjugates

Arming antibodies with materials useful for detection or cell killing has become a prominent approach to increase the utility of these proteins, reviewed by Wu and Senter (2005). Antibodies provide a useful format for the production of radiopharmaceuticals for site- or tissue-specific localization using gamma scintigraphy (Bogard et al. 1989; Tuncay et al. 2000) or for enhanced cell killing. There are currently three approved antibody-radionuclide drugs: two are murine radiolabeled Ab for B cell lymphomas ibritumomab tuixetan (^{90}Y, Zevalin) and tositumomab (^{131}I Bexxar), and the third is a humanized, gemtuzumab ozogamicin (calicheamicin, Mylotarg) for leukemia. The presence of a high energy emitting radionuclide, however, will compromise long-term stability of any antibody formulation; not only would the released energies act to damage the protein, but there is also a strong preference to use short half-life isotopes for these procedures (Zimmer et al. 1989). Thus, in these instances, a stable formulation based upon the principles discussed above can provide a product that can be radiolabeled and then used soon after this step. One example of this approach is a lyophilized antibody formulation that is reconstituted and prepared by a kit method prior to patient dosing (Ferro-Flores and Lezama-Carrasco 1994).

Antibodies coupled with cytotoxins for targeted cell killing (Dyba et al. 2004) are particularly useful in antibody-based cancer therapies (Adams and Weiner 2005). Beyond the identification of a stable formulation for the antibody, such materials have several additional problems for the formulation scientist to solve: stability issues of the attached agent and stability of the linker used to join the attached agent to the antibody. In the case of a monoclonal antibody-vinca alkaloid conjugate, a pH range of 4.5–5.5 in a phosphate buffer showed improved solution stability compared to material stored at pH 6.5–7.4 as evidenced by antibody aggregation and hydrolysis of the chemical linker used to conjoin the alkaloid to the antibody (Riggin et al. 1991). In most cases, cytotoxic materials are coupled with antibodies using reversible chemistries to provide a release mechanism for maximal activity at the target site. Many of these antibody conjugates use a disulfide bond linkage that can be reduced by a novel redox enzyme present in endosomes and lysosomes of target cells (Saito et al. 2003). Slightly oxidizing conditions that would provide added stability of this linker in the formulation could, over time, act to cause detrimental oxidation events in the antibody and/or the linked compound. Other conjugates use an acid-labile linker (Mueller et al. 1990). In this case, formulation pH must be restricted to either neutral or alkaline conditions. Enzymatic separation of antibody and a cytotoxic material could also be achieved by coupling the two through an amino acid linker that is recognized as a substrate by a specific protease or peptidase (Heinis et al. 2004). Formulation instability of this linker sequences can be corrected to some extent by selective changes of the amino acids used.

Thus, the challenges of immunoconjugates include maintaining both drug and antibody potency and stability. While some antibodies are efficacious by themselves, many are much more therapeutically active after being armed with a toxin, drug, and radionuclide (Brannon-Peppas and Blanchette 2004). These changes make the resulting product more difficult to prepare, stabilize, and deliver. Yet, there is tremendous enthusiasm for these approaches as they provide the promise for some companies to transform their antibody into a potentially curative drug. For this reason, many antibodies are combined with a generic delivery system, such as a liposome, that can be used to delivery a variety or even multiple agents simultaneously through antibody-directed targeting (Park et al. 2004). Examples of such an approach include studies performed using an antibody directed against the Her2/*neu* antigen to deliver liposomes containing a chemotherapeutic (Park et al. 1995), antibodies used to deliver cationic liposomes for the administration of nucleic acid material for gene therapy (Stuart et al. 2000), and antibodies used in the targeted delivery of modified gelatin nanoparticles (Balthasar et al. 2005) that can be coupled through a disulfide linkage (Dinauer et al. 2005).

8. Conclusions: Challenges and Opportunities

As antibody-based drugs come to the forefront of therapeutics derived from biotechnology, they provide a range of new and exciting opportunities to treat a number of currently unmet medical needs. Successful clinical application of these novel agents requires the development of stable formulations that can be used for specific delivery methods. Antibodies, because of their endogenous nature, have

built-in features that may pose problems for stability as biotherapeutics, which function in the normal clearance of these proteins from the body (Robinson et al. 1970). Thus, despite our best efforts to prepare stable antibody-based drug formulations, the ultimate stability of these products may be limited to inherent mechanisms of degradation predesigned for the rate of clearance optimal for their function and turnover in the body. Protein engineering has led to significant advances in improving some of these parameters, and the trend would predict that additional advances will be made in the near future (reviewed in (Holliger and Hudson 2005)). Protein modifications can be engineered such that stability and efficacy can be improved in ways that cannot be achieved solely, if at all, with formulation alterations. While it is clear that more research is needed in the relatively new area of engineered antibody fragments for clinical use (Holliger and Hudson 2005), they have great potential for diagnostic and therapeutic application.

In general, successful antibody formulation designs are simply the best compromise of minimizing several competing degradation pathways. One approach is to find a pH where the minimal amount of degradation events such as deamidation and oxidation will occur. Another is to identify a buffer system that can stabilize the formulation at that pH without damaging the antibody. One common tactic taken to reduce the rate of many of these chemical degradation events is to prepare lyophilized or freeze-dried antibody preparation, but even these can be compromised by aggregation issues because of the thermodynamic stress that occurs during freezing, drying and reconstitution. A number of protective excipients, mostly carbohydrates, can reduce the propensity of antibodies to aggregate during these stressful events. Another issue is to produce a formulation that is compatible with delivery – neither hypotonic nor hypertonic solutions are well-tolerated upon injection. Added to this is the potential use of a surface active agent to help with liquid stability such as a nonionic detergent at a low concentration (Mahler et al. 2005) as well as the possible addition of preservatives required for multi-use systems (Gupta and Kaisheva 2003).

The future of antibody based drugs is likely to include more complex systems than those currently approved for use in man. Possibly the most critical aspect of generating a pharmaceutically successful formulation for antibody based drugs is understanding the critical aspects of stability for the protein or the materials associated with the protein. It has been known for some time that even a single amino acid change in the Fv region of an antibody can result in dramatic differences in antigen-binding specificity (Rudikoff et al. 1982). Also, alterations at specific amino acids in the Fc domain can dramatically change functional aspects of an antibody. Thus, these kinds of changes must be considered more important in the search for a successful formulation than those changes that do not appear to affect function. In the case of antibody or antibody-like agents being used to deliver a payload such as a toxin or chemotherapeutic, the stability of the material to be delivered and its continued association with the delivery antibody is crucial.

Acknowledgments: The authors wish to thank Reed Harris, Tom Patapoff, and Nancy Valente for their very insightful conversations and helpful suggestions. The review of the manuscript by Xanthe Lam, Brian Lobo, and Chung Hsu

is appreciated. The references cited in this review were not intended to be inclusive of all of the seminal publications in the ever-expanding area of antibody stability and formulation. The relatively small numbers of references cited were selected to highlight specific aspects within the scope of this review. We regret that we could not cite many excellent publications that have made important contributions to this field.

References

Adams GP, Weiner LM (2005) Monoclonal antibody therapy of cancer. Nat Biotechnol 23(9):1147–1157

Al-Abdulla I et al (2003) Formulation of a liquid ovine Fab-based antivenom for the treatment of envenomation by the Nigerian carpet viper (*Echis ocellatus*). Toxicon 42(4):399–404

Andya JD et al (1999) The effect of formulation excipients on protein stability and aerosol performance of spray-dried powders of a recombinant humanized anti-IgE monoclonal antibody. Pharm Res 16(3):350–358

Andya JD, Hsu CC, Shire SJ (2003) Mechanisms of aggregate formation and carbohydrate excipient stabilization of lyophilized humanized monoclonal antibody formulations. AAPS PharmSci 5(2):E10

Arakawa T, Kita Y, Carpenter JF (1991) Protein–solvent interactions in pharmaceutical formulations. Pharm Res 8(3):285–291

Atkinson EM, Klum W (2001) Formulations strategies for biopharmaceuticals – ensuring success to market. IDrugs 4(5):557–560

Baert F et al (2003) Influence of immunogenicity on the long-term efficacy of infliximab in Crohn's disease. N Engl J Med 348(7):601–608

Baker M (2005) Upping the ante on antibodies. Nat Biotechnol 23(9):1065–1072

Balthasar S et al (2005) Preparation and characterisation of antibody modified gelatin nanoparticles as drug carrier system for uptake in lymphocytes. Biomaterials 26(15):2723–2732

Baynes BM, Trout BL (2004) Rational design of solution additives for the prevention of protein aggregation. Biophys J 87(3):1631–1639

Bazin R et al (1994) Use of hu-IgG-SCID mice to evaluate the in vivo stability of human monoclonal IgG antibodies. J Immunol Methods 172(2):209–217

Bitonti AJ et al (2004) Pulmonary delivery of an erythropoietin Fc fusion protein in non-human primates through an immunoglobulin transport pathway. Proc Natl Acad Sci U S A 101(26):9763–9768

Bogard WC Jr et al (1989) Practical considerations in the production, purification, and formulation of monoclonal antibodies for immunoscintigraphy and immunotherapy. Semin Nucl Med 19(3):202–220

Brannon-Peppas L, Blanchette JO (2004) Nanoparticle and targeted systems for cancer therapy. Adv Drug Deliv Rev 56(11):1649–1659

Breen ED et al (2001) Effect of moisture on the stability of a lyophilized humanized monoclonal antibody formulation. Pharm Res 18(9):1345–1353

Chang LL et al (2005) Effect of sorbitol and residual moisture on the stability of lyophilized antibodies: implications for the mechanism of protein stabilization in the solid state. J Pharm Sci 94(7):1445–1455

Chapman SA et al (2004) Acute renal failure and intravenous immune globulin: occurs with sucrose-stabilized, but not with D-sorbitol-stabilized, formulation. Ann Pharmacother 38(12):2059–2067

Chatenoud L (2003) CD3-specific antibody-induced active tolerance: from bench to bedside. Nat Rev Immunol 3(2):123–132

Cheifetz A, Mayer L (2005) Monoclonal antibodies, immunogenicity, and associated infusion reactions. Mt Sinai J Med 72(4):250–256

Cheifetz A et al (2003) The incidence and management of infusion reactions to infliximab: a large center experience. Am J Gastroenterol 98(6):1315–1324
Chelius D, Rehder DS, Bondarenko PV (2005) Identification and characterization of deamidation sites in the conserved regions of human immunoglobulin gamma antibodies. Anal Chem 77(18):6004–6011
Cleland JL, Powell MF, Shire SJ (1993) The development of stable protein formulations: a close look at protein aggregation, deamidation, and oxidation. Crit Rev Ther Drug Carrier Syst 10(4):307–377
Cleland JL et al (2001) A specific molar ratio of stabilizer to protein is required for storage stability of a lyophilized monoclonal antibody. J Pharm Sci 90(3):310–321
Cook-Bruns N (2001) Retrospective analysis of the safety of Herceptin immunotherapy in metastatic breast cancer. Oncology 61(Suppl 2):58–66
Cordoba AJ et al (2005) Non-enzymatic hinge region fragmentation of antibodies in solution. J Chromatogr B Analyt Technol Biomed Life Sci 818(2):115–121
Corthesy B (2003) Recombinant secretory immunoglobulin A in passive immunotherapy: linking immunology and biotechnology. Curr Pharm Biotechnol 4(1):51–67
Costantino HR et al (1998a) Effect of excipients on the stability and structure of lyophilized recombinant human growth hormone. J Pharm Sci 87(11):1412–1420
Costantino HR et al (1998b) Effect of mannitol crystallization on the stability and aerosol performance of a spray-dried pharmaceutical protein, recombinant humanized anti-IgE monoclonal antibody. J Pharm Sci 87(11):1406–1411
Crandall WV, Mackner LM (2003) Infusion reactions to infliximab in children and adolescents: frequency, outcome and a predictive model. Aliment Pharmacol Ther 17(1):75–84
Daugherty AL et al (1997) Pharmacological modulation of the tissue response to implanted polylactic-co-glycolic acid microspheres. Eur J Pharmacol Biopharm 44(1637):89–102
Demarest SJ, Rogers J, Hansen G (2004) Optimization of the antibody C(H)3 domain by residue frequency analysis of IgG sequences. J Mol Biol 335(1):41–48
Dinauer N et al (2005) Selective targeting of antibody-conjugated nanoparticles to leukemic cells and primary T-lymphocytes. Biomaterials 26(29):5898–5906
Duddu SP, Dal Monte PR (1997) Effect of glass transition temperature on the stability of lyophilized formulations containing a chimeric therapeutic monoclonal antibody. Pharm Res 14(5):591–595
Dyba M, Tarasova NI, Michejda CJ (2004) Small molecule toxins targeting tumor receptors. Curr Pharm Des 10(19):2311–2334
Edwards DA et al (1997) Large porous particles for pulmonary drug delivery. Science 276(5320):1868–1871
Ewert S, Honegger A, Pluckthun A (2004) Stability improvement of antibodies for extracellular and intracellular applications: CDR grafting to stable frameworks and structure-based framework engineering. Methods 34(2):184–199
Ferro-Flores G, Lezama-Carrasco J (1994) A freeze dried kit formulation for the preparation of 99mTc-EHDP-MoAb-IOR CEA1 complex. Nucl Med Biol 21(7):1013–1016
Friedli HR (1987) Methodology and safety considerations in the production of an intravenous immunoglobulin preparation. Pharmacotherapy 7(2):S36–S40
Gekko K (1981) Mechanism of polyol-induced protein stabilization: solubility of amino acids and diglycine in aqueous polyol solutions. J Biochem 90(6):1633–1641
Grainger DW (2004) Controlled-release and local delivery of therapeutic antibodies. Expert Opin Biol Ther 4(7):1029–1044
Granholm AC et al (1998) A non-invasive system for delivering neural growth factors across the blood–brain barrier: a review. Rev Neurosci 9(1):31–55
Griffiths HR (2000) Antioxidants and protein oxidation. Free Radic Res 33(Suppl):S47–S58
Gupta S, Kaisheva E (2003) Development of a multidose formulation for a humanized monoclonal antibody using experimental design techniques. AAPS PharmSci 5(2):E8

Gupta RK, Chang AC, Siber GR (1998) Biodegradable polymer microspheres as vaccine adjuvants and delivery systems. Dev Biol Stand 92:63–78

Hall CG, Abraham GN (1984) Reversible self-association of a human myeloma protein. Thermodynamics and relevance to viscosity effects and solubility. Biochemistry 23(22):5123–5129

Harris RJ (2005) Heterogeneity of recombinant antibodies: linking structure to function. Dev Biol (Basel) 122:117–127

Harris RJ et al (2001) Identification of multiple sources of charge heterogeneity in a recombinant antibody. J Chromatogr B Biomed Sci Appl 752(2):233–245

Hasegawa G et al (2005) Synthesis and characterization of a novel reagent containing dansyl group, which specifically alkylates sulfhydryl group: an example of application for protein chemistry. J Biochem Biophys Methods 63(1):33–42

Heinis C, Alessi P, Neri D (2004) Engineering a thermostable human prolyl endopeptidase for antibody-directed enzyme prodrug therapy. Biochemistry 43(20):6293–6303

Hodoniczky J, Zheng YZ, James DC (2005) Control of recombinant monoclonal antibody effector functions by fc *N*-glycan remodeling in vitro. Biotechnol Prog 21(6):1644–1652

Holliger P, Hudson PJ (2005) Engineered antibody fragments and the rise of single domains. Nat Biotechnol 23(9):1126–1136

Horie K et al (2004) Suppressive effect of functional drinking yogurt containing specific egg yolk immunoglobulin on *Helicobacter pylori* in humans. J Dairy Sci 87(12):4073–4079

Hsu CC et al (1992) Determining the optimum residual moisture in lyophilized protein pharmaceuticals. Dev Biol Stand 74:255–270 discussion 271

Hsu CC et al (1996) Design and application of a low-temperature Peltier-cooling microscope stage. J Pharm Sci 85(1):70–74

Huang L et al (2005) In vivo deamidation characterization of monoclonal antibody by LC/MS/MS. Anal Chem 77(5):1432–1439

Idusogie EE et al (2001) Engineered antibodies with increased activity to recruit complement. J Immunol 166(4):2571–2575

Imai M et al (2005) Complement-mediated mechanisms in anti-GD2 monoclonal antibody therapy of murine metastatic cancer. Cancer Res 65(22):10562–10568

Jasin HE (1993) Oxidative modification of inflammatory synovial fluid immunoglobulin G. Inflammation 17(2):167–181

Javed Q et al (2002) Tumor necrosis factor-alpha antibody eluting stents reduce vascular smooth muscle cell proliferation in saphenous vein organ culture. Exp Mol Pathol 73(2):104–111

Jefferis R (2005) Glycosylation of recombinant antibody therapeutics. Biotechnol Prog 21(1):11–16

Jespers L et al (2004) Crystal structure of HEL4, a soluble, refoldable human V(H) single domain with a germ-line scaffold. J Mol Biol 337(4):893–903

Jones PT et al (1986) Replacing the complementarity-determining regions in a human antibody with those from a mouse. Nature 321(6069):522–525

Jones AJ et al (1997) Recombinant human growth hormone poly(lactic-co-glycolic acid) microsphere formulation development. Adv Drug Deliv Rev 28(1):71–84

Kawade Y (1985) Neutralization of activity of effector protein by monoclonal antibody: formulation of antibody dose-dependence of neutralization for an equilibrium system of antibody, effector, and its cellular receptor. Immunology 56(3):497–504

Kohler G, Milstein C (1975) Continuous cultures of fused cells secreting antibody of predefined specificity. Nature 256(5517):495–497

Kroon DJ, Baldwin-Ferro A, Lalan P (1992) Identification of sites of degradation in a therapeutic monoclonal antibody by peptide mapping. Pharm Res 9(11):1386–1393

Kuo PY, Sherwood JK, Saltzman WM (1998) Topical antibody delivery systems produce sustained levels in mucosal tissue and blood. Nat Biotechnol 16(2):163–167

Lackey CA et al (2002) A biomimetic pH-responsive polymer directs endosomal release and intracellular delivery of an endocytosed antibody complex. Bioconjug Chem 13(5):996–1001

Lam XM, Yang JY, Cleland JL (1997) Antioxidants for prevention of methionine oxidation in recombinant monoclonal antibody HER2. J Pharm Sci 86(11):1250–1255

Lavelle EC et al (1999) The stability and immunogenicity of a protein antigen encapsulated in biodegradable microparticles based on blends of lactide polymers and polyethylene glycol. Vaccine 17(6):512–529

Lencer WI, Blumberg RS (2005) A passionate kiss, then run: exocytosis and recycling of IgG by FcRn. Trends Cell Biol 15(1):5–9

Lonberg N (2005) Human antibodies from transgenic animals. Nat Biotechnol 23(9):1117–1125

Luzardo-Alvarez A et al (2005) Biodegradable microspheres alone do not stimulate murine macrophages in vitro, but prolong antigen presentation by macrophages in vitro and stimulate a solid immune response in mice. J Control Release 109(1–3):62–76

Ma JK et al (1998) Characterization of a recombinant plant monoclonal secretory antibody and preventive immunotherapy in humans. Nat Med 4(5):601–606

Ma X et al (2001) Characterization of murine monoclonal antibody to tumor necrosis factor (TNF-MAb) formulation for freeze-drying cycle development. Pharm Res 18(2):196–202

Mahler HC et al (2005) Induction and analysis of aggregates in a liquid IgG1-antibody formulation. Eur J Pharm Biopharm 59(3):407–417

Merluzzi S et al (2000) Humanized antibodies as potential drugs for therapeutic use. Adv Clin Path 4(2):77–85

Middaugh CR et al (1978) Physicochemical characterization of six monoclonal cryoimmunoglobulins: possible basis for cold-dependent insolubility. Proc Natl Acad Sci U S A 75(7):3440–3444

Mimura Y et al (1995) Microheterogeneity of mouse antidextran monoclonal antibodies. Electrophoresis 16(1):116–123

Mine Y, Kovacs-Nolan J (2002) Chicken egg yolk antibodies as therapeutics in enteric infectious disease: a review. J Med Food 5(3):159–169

Mire-Sluis AR (2001) Progress in the use of biological assays during the development of biotechnology products. Pharm Res 18(9):1239–1246

Moore JM, Patapoff TW, Cromwell ME (1999) Kinetics and thermodynamics of dimer formation and dissociation for a recombinant humanized monoclonal antibody to vascular endothelial growth factor. Biochemistry 38(42):13960–13967

Mordenti J et al (1999) Intraocular pharmacokinetics and safety of a humanized monoclonal antibody in rabbits after intravitreal administration of a solution or a PLGA microsphere formulation. Toxicol Sci 52(1):101–106

Morgan PE, Sturgess AD, Davies MJ (2005) Increased levels of serum protein oxidation and correlation with disease activity in systemic lupus erythematosus. Arthritis Rheum 52(7):2069–2079

Mueller BM, Wrasidlo WA, Reisfeld RA (1990) Antibody conjugates with morpholinodoxorubicin and acid-cleavable linkers. Bioconjug Chem 1(5):325–330

Nakamura T et al (2004) Antibody-targeted cell fusion. Nat Biotechnol 22(3): 331–336

O'Hagan DT et al (1991) Biodegradable microparticles as controlled release antigen delivery systems. Immunology 73(2):239–242

Page M et al (1995) Fragmentation of therapeutic human immunoglobulin preparations. Vox Sang 69(3):183–194

Panka DJ (1997) Glycosylation is influential in murine IgG3 self-association. Mol Immunol 34(8–9):593–598

Park JW et al (1995) Development of anti-p185HER2 immunoliposomes for cancer therapy. Proc Natl Acad Sci U S A 92(5):1327–1331

Park JW, Benz CC, Martin FJ (2004) Future directions of liposome- and immunoliposome-based cancer therapeutics. Semin Oncol 31(6 Suppl 13):196–205

Peterson NC (2005) Advances in monoclonal antibody technology: genetic engineering of mice, cells, and immunoglobulins. ILAR J 46(3):314–319

Poelstra KA et al (2002) Prophylactic treatment of gram-positive and gram-negative abdominal implant infections using locally delivered polyclonal antibodies. J Biomed Mater Res 60(1):206–215

Presta LG (2002) Engineering antibodies for therapy. Curr Pharm Biotechnol 3(3):237–256

Radkiewicz JL et al (2001) Neighboring side chain effects on asparaginyl and aspartyl degradation: an ab initio study of the relationship between peptide conformation and backbone NH acidity. J Am Chem Soc 123(15):3499–3506

Reichert JM et al (2005) Monoclonal antibody successes in the clinic. Nat Biotechnol 23(9):1073–1078

Reilly RM, Domingo R, Sandhu J (1997) Oral delivery of antibodies. Future pharmacokinetic trends. Clin Pharmacokinet 32(4):313–323

Riggin A et al (1991) Solution stability of the monoclonal antibody-vinca alkaloid conjugate, KS1/4-DAVLB. Pharm Res 8(10):1264–1269

Robinson NE, Robinson AB (2001a) Prediction of protein deamidation rates from primary and three-dimensional structure. Proc Natl Acad Sci U S A 98(8): 4367–4372

Robinson NE, Robinson AB (2001b) Deamidation of human proteins. Proc Natl Acad Sci U S A 98(22):12409–12413

Robinson NE, Robinson AB (2001c) Molecular clocks. Proc Natl Acad Sci U S A 98(3):944–949

Robinson NE, Robinson AB (2004) Prediction of primary structure deamidation rates of asparaginyl and glutaminyl peptides through steric and catalytic effects. J Pept Res 63(5):437–448

Robinson AB, McKerrow JH, Cary P (1970) Controlled deamidation of peptides and proteins: an experimental hazard and a possible biological timer. Proc Natl Acad Sci U S A 66(3):753–757

Robinson NE et al (2004) Structure-dependent nonenzymatic deamidation of glutaminyl and asparaginyl pentapeptides. J Pept Res 63(5):426–436

Rojas IA, Slunt JB, Grainger DW (2000) Polyurethane coatings release bioactive antibodies to reduce bacterial adhesion. J Control Release 63(1–2):175–189

Rudikoff S et al (1982) Single amino acid substitution altering antigen-binding specificity. Proc Natl Acad Sci U S A 79(6):1979–1983

Saito G, Swanson JA, Lee KD (2003) Drug delivery strategy utilizing conjugation via reversible disulfide linkages: role and site of cellular reducing activities. Adv Drug Deliv Rev 55(2):199–215

Saltzman WM et al (2000) Long-term vaginal antibody delivery: delivery systems and biodistribution. Biotechnol Bioeng 67(3):253–264

Sane SU, Wong R, Hsu CC (2004) Raman spectroscopic characterization of drying-induced structural changes in a therapeutic antibody: correlating structural changes with long-term stability. J Pharm Sci 93(4):1005–1018

Sarciaux JM et al (1999) Effects of buffer composition and processing conditions on aggregation of bovine IgG during freeze-drying. J Pharm Sci 88(12):1354–1361

Schnyder A, Huwyler J (2005) Drug transport to brain with targeted liposomes. NeuroRx 2(1):99–107

Sgouris JT (1970) Studies on immune serum globulin (IgG) and its modification for intravenous administration. Prog Immunobiol Stand 4:104–113

Shen FJ et al (1996) The application of tert-butylhydroperoxide oxidation to study sites of potential methionine oxidation in a recombinant antibody. In: Marshak D (ed) Techniques in protein chemistry VII. Academic, San Diego, pp 275–284

Shields RL et al (2001) High resolution mapping of the binding site on human IgG1 for Fc gamma RI, Fc gamma RII, Fc gamma RIII, and FcRn and design of IgG1 variants with improved binding to the Fc gamma R. J Biol Chem 276(9):6591–6604

Siberil S et al (2005) Selection of a human anti-RhD monoclonal antibody for therapeutic use: impact of IgG glycosylation on activating and inhibitory Fc gamma R functions. Clin Immunol 118(2–3):170–179

Spiekermann GM et al (2002) Receptor-mediated immunoglobulin G transport across mucosal barriers in adult life: functional expression of FcRn in the mammalian lung. J Exp Med 196(3):303–310

Stockwin LH, Holmes S (2003) Antibodies as therapeutic agents: vive la renaissance!. Expert Opin Biol Ther 3(7):1133–1152

Stuart DD, Kao GY, Allen TM (2000) A novel, long-circulating, and functional liposomal formulation of antisense oligodeoxynucleotides targeted against MDR1. Cancer Gene Ther 7(3):466–475

Tian WM et al (2005) Hyaluronic acid hydrogel as Nogo-66 receptor antibody delivery system for the repairing of injured rat brain: in vitro. J Control Release 102(1):13–22

Tuncay M et al (2000) In vitro and in vivo evaluation of diclofenac sodium loaded albumin microspheres. J Microencapsul 17(2):145–155

Walsh S et al (2004) Extended nasal residence time of lysostaphin and an anti-staphylococcal monoclonal antibody by delivery in semisolid or polymeric carriers. Pharm Res 21(10):1770–1775

Wang CH, Sengothi K, Lee T (1999) Controlled release of human immunoglobulin G. 1. Release kinetics studies. J Pharm Sci 88(2):215–220

Wang J, Chua KM, Wang CH (2004) Stabilization and encapsulation of human immunoglobulin G into biodegradable microspheres. J Colloid Interface Sci 271(1):92–101

Wright A, Morrison SL (1994) Effect of altered CH2-associated carbohydrate structure on the functional properties and in vivo fate of chimeric mouse-human immunoglobulin G1. J Exp Med 180(3):1087–1096

Wu AM, Senter PD (2005) Arming antibodies: prospects and challenges for immunoconjugates. Nat Biotechnol 23(9):1137–1146

Yang MX et al (2003) Crystalline monoclonal antibodies for subcutaneous delivery. Proc Natl Acad Sci U S A 100(12):6934–6939

Yasui H, Ito W, Kurosawa Y (1994) Effects of substitutions of amino acids on the thermal stability of the Fv fragments of antibodies. FEBS Lett 353(2):143–146

Zhang W, Czupryn MJ (2003) Analysis of isoaspartate in a recombinant monoclonal antibody and its charge isoforms. J Pharm Biomed Anal 30(5):1479–1490

Zhu L et al (2005) Production of human monoclonal antibody in eggs of chimeric chickens. Nat Biotechnol 23(9):1159–1169

Zimmer AM et al (1989) Stability of radioiodinated monoclonal antibodies: in vitro storage and plasma analysis. Int J Rad Appl Instrum B 16(7):691–696

Chapter 9

Challenges in the Development of High Protein Concentration Formulations

Steven J. Shire, Zahra Shahrokh, and Jun Liu

Abstract Development of formulations for protein drugs requiring high dosing (on the order of mg/kg) may become challenging for solubility limited proteins and for the SC route with <1.5 mL allowable administration volume that requires >100 mg/mL protein concentrations. Development of high protein concentration formulations also results in several manufacturing, stability, analytical, and delivery challenges. The high concentrations achieved by small scale approaches used in preformulation studies would have to be confirmed with manufacturing scale processes and with representative materials because of the lability of protein conformation and the propensity to interact with surfaces and solutes which render protein solubilities that are dependent on the process of concentrating. The concentration dependent degradation route of aggregation is the greatest challenge to developing protein formulations at these higher concentrations. In addition to the potential for nonnative protein aggregation and particulate formation, reversible self-association may occur, which contributes to properties such as viscosity that complicates delivery by injection. Higher viscosity also complicates manufacturing of high protein concentrations by filtration approaches. Chromatographic and electrophoretic assays may not accurately determine the non-covalent higher molecular weight forms because of the dilutions that are usually encountered with these techniques. Hence, techniques must be used that allow for direct measurement in the formulation without substantial dilution of the protein. These challenges are summarized in this review.

Keywords Protein formulation • High concentration • Pharmaceutical • Manufacturing • Analytical • Viscosity

Reprinted from Journal of Pharmaceutical Science 93, 1390, 2004, with permission from Elsevier.

From: *Current Trends in Monoclonel Antibody Development and Manufacturing,* Biotechnology: Pharmaceutical Aspects, DOI 10.1007/978-0-387-76643-0_9, Edited by: S.J. Shire et al.

1. Introduction

Over the past two decades, recombinant DNA technology has led to the commercialization of many protein therapeutics requiring successful formulations. The most conventional route of delivery for protein drugs has been intravenous (IV) administration because of poor bioavailability by most other routes, greater control during clinical administration, and faster pharmaceutical development. For products that require frequent and chronic administration, the alternate subcutaneous (SC) route of delivery is more appealing. Particularly when coupled with prefilled syringe and autoinjector device technology, SC delivery allows for home administration and improved compliance of administration, and may result in expanded product markets. Proteins such as monoclonal antibodies are often administered with frequent dosing regimens and at high doses (several mg/kg). Two antibodies, Rituxan® and Herceptin® that have been approved for the treatment of cancer are intravenously administered in hospitals, but several programs are underway for use of monoclonal antibodies to treat diseases that may require outpatient administration, and hence require the development of SC route of administration. Treatments with high doses, e.g. more than 1 mg/kg or 100 mg per dose, require development of formulations at concentrations exceeding 100 mg/mL because of the small volume (<1.5 mL) that can be given by the SC routes. For some proteins, that have limited solubility, achieving such high concentration formulations may require the use of solubility enhancers. Even for the IV delivery route, where large volumes can be administered, protein concentration of tens of mg/mL may be needed for high dosing regimens and this may pose solubility challenges for some proteins such as cytokines and enzymes. Development of formulations at high concentrations also poses stability, manufacturing, and delivery challenges related to the propensity of proteins to aggregate at the higher concentrations. These challenges and appropriate analytical techniques for assessing high concentration protein formulations will be discussed.

2. Solubility Considerations

A potential challenge to developing a protein formulation that enables the desired dosing is achieving the required protein concentration in solution. The desired protein concentration may be difficult to achieve for some enzymes and cytokines that have limited solubility. The principles governing protein solubility are more complicated than those for small synthetic molecules (Arakawa and Timasheff 1985; Middaugh and Volkin 1992), and thus overcoming the protein solubility issue takes different strategies. Operationally, solubility for proteins could be described by the maximum amount of protein in the presence of cosolutes whereby the solution remains visibly clear (i.e. does not show protein precipitates, crystals, or gels,), or does not sediment at $30{,}000 \times g$ centrifugation for 30 min (Schein 1990). The dependence of protein solubility on ionic strength, salt form, pH, temperature, and certain excipients has been mechanistically explained by changes in bulk water surface tension, and protein binding to water and ions versus self-association (Arakawa and Timasheff 1985; Schein 1990; Melander and Horvath 1977; Jenkins 1998). Binding of proteins to specific excipients or salts influences solubility through changes in protein conformation or masking of certain amino acids involved in self-interaction.

Proteins are also preferentially hydrated (and stabilized as more compact conformations) by certain salts, amino acids, and sugars, leading to their altered solubility (Jenkins 1998). Protein solubility could also depend on the level of purity of the protein preparation; for example, fibrinogen solubility was found to be dependent on the initial amount of protein because of the impurities and heterogeneity of the preparation (Leavis and Rothstein 1974). Hence, selection of a protein formulation based on preformulation work that uses materials from early process development runs may be a misguided decision and needs to be verified with representative larger scale preparations.

Determining the highest protein concentration achievable remains an empirical exercise because the lability of protein conformation and the propensity to interact with itself, with surfaces, and with specific solutes, all lead to protein solubilities that depend on the process of concentrating. Table 9-1 lists the various methods for concentrating a protein solution, with their advantages and practical limitations. Early in preformulation studies where material is limited, small-scale methods are needed to achieve high protein concentrations. The most mechanically gentle and rapid method involve osmotic pressure dependent microdialysis principles (Zhang and Hjerten 1997; Saul and Don 1984). One such method (Zhang and Hjerten 1997) very rapidly achieves several orders of magnitude increase in protein concentration simultaneous with buffer exchange using only ~0.1 mg protein. Though this approach is a useful tool for rank ordering of solubility in various formulation compositions, for some cytokines, it gave ten times higher solubilities than those reached by dialfiltration/ultrafiltration on a Centricon® system that may result in shear induced protein denaturation and lowered apparent solubility (Shahrokh et al. unpublished results). Another approach based on osmotically driven solute concentration involves dialysis against a hygroscopic material such as Sephadex or polyethylene glycols (Middaugh and Volkin 1992). This approach requires the use of high purity materials that do not result in protein degradation, and must be done with care to prevent overdrying and exposure to very large surface areas since water rapidly leaves the protein solution. In addition, as polyelectrolytes, proteins impact the distribution of diffusible ions across the dialysis membrane to maintain electroneutrality as dictated by the Donnan equilibrium (Bull 1971). This could lead to a potentially large change in the ion composition within the protein solution as it concentrates, and could be damaging to the protein. The alternative small-scale methods of solvent evaporation by vacuum or nitrogen flow, and precipitation by salts or solvents (Rothstein 1994; Tanabe et al. 2000; Glatz 1992), alter the formulation composition and may also result in protein degradation due to the time or materials used in the process. Precipitation and generation of protein powders by supercritical fluids has met some success in maintaining active or structurally native proteins, but this approach remains of limited practical use particularly for small scale studies (Moshashaee et al. 2003; Winters et al. 1996). Concentration of solutes by freezing (Webb et al. 2002) is another approach that could achieve a high protein concentration, but alteration in the solute composition may cause potential damage to the protein during freezing and thawing and difficulty in retrieving the frozen concentrate, all make this an impractical approach. Chromatographic methods that bind the protein and allow elution at lower volumes is another useful tool for concentrating proteins over a large range of scale; these methods include ion exchange or hydrophobic interaction chromatography, but require buffer exchange after concentration. Filtration is the most common approach for concentrating proteins, and unlike many of the methods discussed is amenable to scale-up for manufacturing. There are

Table 9-1. The commonly used methods of concentrating proteins.

Concentrating method	Scale	Benefits	Limitations	Used for solubility determination
Osmotic driven (dialysis) methods: – Against solutions – Against water absorbing materials	Few μLs to few mLs	Small-scale; mechanically gentle; rapid – Simultaneous buffer exchange	Concentrations achieved may not translate to manufacturing scale – Have to buffer exchange later	Yes
Solvent evaporation: – Vacuum, N_2 flow – Lyophilization	– Few μLs to few mLs – mLs	– Small-scale – Pharmaceutically relevant and scalable	– Slow (may lead to degradation); concentrates excipients – Must protect against drying induced degradation; concentrates excipients	Yes, only in solution composition reached at end of process
Precipitation (salt or solvent; SCF)	Few μLs to liters	Quick and scalable	– Solution composition not pharmaceutically relevant – May lead to irreversible degradation	No
Freezing	Few mLs to liters	– Tens of fold concentration is achieved quickly	– Concentrates excipients too – Process may damage protein	No
Chromatographic bind and elute	Few μLs to many mLs	– Wide range of scale	– Solution composition not pharmaceutically relevant – Conditions may damage protein	No
Filtration systems: – Centrifugal (Centricon) – Pressure (Amicon) – TFF	– Hundreds of μLs to tens of mLs – Hundreds of mLs to liters	– Moderate scale; may include buffer exchange – Manufacturing scale; may include buffer exchange	– Adsorption losses; shear induced degradation – Findings may not translate to manufacturing scale – Large scale impractical for early development phases – High viscosity or pore clogging may limit concentrations reached	Yes, if not material limited

numerous filtration systems, each with an extent of adsorption or shear-induced denaturation/aggregation that is dependent on surface area, contact materials, and flow mechanisms. The mechanical and interfacial forces imposed on protein's structure (hence its solubility) by small-scale methods may be different than those by the large-scale processes, and hence, the results obtained by such methods would have to be verified by representative manufacturing processes. The most commonly used methods for large scale manufacturing of high protein concentrations are further discussed under Sect. 9.4.

3. Stability Considerations

Although proteins are more complex than typical small molecule pharmaceuticals, a great deal is now known about the various chemical degradations that occur in proteins, and several reviews are available (Ahern and Manning MC editors 1992; Manning et al. 1989; Cleland et al. 1993). Many of the chemical reactions such as deamidation, aspartate isomerization, oxidation, peptide bond hydrolysis that occur in proteins are hydrolytically driven requiring the presence of water, and generally the kinetics follows lower order concentration dependency. Aggregation, on the other hand, requiring bimolecular collisions, and a high concentration dependency is expected to be the primary degradation pathway in high concentration protein formulations. The relationship of concentration to aggregate formation depends on the size of aggregates as well as the mechanism of association (Glatz 1992; Manning et al. 1989). Protein aggregation may result in covalent (e.g. disulfide-linked) association or noncovalent (reversible or irreversible) association. Irreversible aggregation by noncovalent association generally occurs via hydrophobic regions exposed by thermal, mechanical, or chemical processes that alter a protein's native conformation (Chi et al. 2003). When the protein-unfolding step is rate limiting, the kinetics of protein aggregation often shows pseudo-first order behavior (Chi et al. 2003) rather than the expected higher order concentration dependency. Further illustration of the importance of the aggregation mechanism on the relationship of concentration to aggregate formation is shown by the inverse concentration dependency of protein aggregation that results from interaction with air–water interfaces (Treuheit et al. 2002).

Protein aggregation may impact protein activity, pharmacokinetics and safety, for example due to immunogenicity (Cleland et al. 1993; Braun et al. 1997; Koren et al. 2002). Irreversible protein aggregation is recognized as a major degradation product in protein formulations, whereas reversible protein self-association is often overlooked. Reversible protein association is less studied, partly because of poor analytical methodologies (as will be discussed under Sect. 9.6) and partly because of the perception that aggregates will not be present after typical dilutions are made prior to administration. However, if the rate of dissociation is slow, then reversible aggregation may still impact activity, in vivo clearance and safety. Even under conditions where the rate of dissociation is rapid, the equilibrium at high protein concentration may be shifted toward a greater amount of aggregate due to molecular crowding effects (Minton 1992; Wilf and Minton 1981; Zimmerman and Minton 1993). In particular, as the protein concentration increases, the fraction of the total volume occupied by the protein increases. The resulting decrease in the effective volume available to the protein yields a higher apparent protein

concentration that in turn favors self-association. This non-ideal solution behavior of increasing the apparent thermodynamic association constant with increasing protein concentration may be shelf-life limiting, especially when the resulting aggregates are irreversible. In addition, after in vivo administration, the protein therapeutic may be placed into a crowded macromolecular environment, which shifts the equilibrium to the associated state even after dilution.

Macromolecular crowding, i.e. excluded volume effects, can also have an impact on the physical properties of protein such as viscosity and can have major impact on the ability to manufacture high protein concentration formulations (see Sect. 9.4) as well as on the ability to administer the protein drug by injection (Fig. 9-2a). In general, the viscosity of a macromolecule in solution can be expressed as a virial expansion, where the viscosity, η, can be related to the solvent viscosity, η_o, and concentration of the protein, c_p, in g/mL by a power series (Cantor and Schimmel 1980):

$$\eta = \eta_o \left(1 + k_1 c_p + k_2 c_p^2 + k_3 c_p^3 + \cdots\right) \tag{9.1}$$

wherein Eq. 9.1, k_1 is the intrinsic viscosity, which is related to the contribution from individual solute molecules and k_2 and higher order coefficients are related to effects from interactions of two, three, or more protein molecules. This equation can be rewritten in terms of the specific viscosity, $\eta_s = (\eta - \eta_o)/\eta_o$:

$$((\eta - \eta_o)/\eta_o)/c_p = \eta_s/c_p = k_1 + k_2 c_p + k_3 c_p^2 + \cdots \tag{9.2}$$

In the case of significant protein self-association that results in formation of soluble aggregates, the higher order terms will dominate and lead to large increases in viscosity as a function of concentration.

There are two key approaches to mitigating irreversible protein aggregation for improving the shelf life of high concentration protein formulations. One approach uses conditions that stabilize the native conformation of the protein, and the other, reduces molecular collisions that lead to aggregation. For the first approach, molar concentrations of osmolytes, such as sugars, are added that are preferentially excluded from the immediate environment of proteins, and result in preferential hydration (Arakawa and Timasheff 1982; Arakawa et al. 1991). This preferential hydration leads to an increase in the protein's chemical potential since the increased ordering of water in the hydration shell leads to an entropic decrease for the entire thermodynamic system consisting of protein and solvent water. Since a larger surface area such as that found in unfolded proteins requires a greater number of ordered water molecules for preferential hydration, the protein will assume a more compact folded form to resist the thermodynamically unfavorable decrease in the system's entropy. Thus, the protein will minimize the surface area available for hydration leading to stabilization of the more compact folded form, which then decreases the formation of protein aggregates. However, if the native state of the protein is capable of associating, forming aggregates of native conformers, then the addition of preferentially excluded osmolytes may actually increase the amount of protein aggregate since total surface area will be diminished following protein self association. The potential impact of reversible self-association on product shelf-life or protein physical parameters will depend on the rate of dissociation as well as the possible consequent formation of irreversible aggregates during storage at high concentration. The use of preferentially excluded osmolytes to

fix the aggregation problem is limited since addition of high concentrations of excipients may also add to the viscosity and osmolality of the formulation that may render it impractical for use as a parenteral solution. Also, as already noted, the addition of these osmolytes may actually increase the amount of reversible native associated protein.

The second approach to minimize aggregation is to restrict the mobility of proteins in order to reduce the number of collisions. Lyophilization with appropriate excipients may improve protein stability against aggregation by decreasing protein mobility and by restricting conformational flexibility with the added benefit of minimizing hydrolytic reactions consequent to removal of water (Pikal 1994). The addition of appropriate excipients, including lyoprotectants, prevents the formation of aggregates during the lyophilization process as well as during storage of the final product (Andya et al. 2003; Carpenter et al. 1997, 2002). A key parameter for effective protection is the molar ratio of the lyoprotectant to the protein (Cleland et al. 2001). Generally, molar ratios of 300:1 or greater are required to provide suitable stability, especially for room temperature storage. While this strategy achieves an optimal final formulation at moderate protein concentrations, if the lyophilizer is used to concentrate the protein, additional challenges can result as discussed below.

4. Manufacturing Considerations

Although it may be possible to create a formulation during development that has the desired solubility and stability, the design of processes that will allow for manufacturing of the formulation at a larger scale is critical for successful implementation of bench top experimental findings. Two commonly used processes will be discussed below.

4.1. Tangential Flow Filtration

The main technology for buffer exchange and concentrating proteins that has been used at commercial scale is Tangential Flow Filtration (TFF) (Genovesi 1983; Shiloach et al. 1988; van Reis and Zydney 2001). In this technology, the protein is circulated by pumping through a series of hollow fiber tubes, which allow for the passage of water and small molecules but not large macromolecules. Attainment of high concentration formulations by TFF systems can be difficult because the required membrane flux may dictate higher concentrations at the membrane boundary than the targeted concentration. As an example, when a protein is concentrated to 100 mg/mL, the concentration at the membrane may be as high as 125 mg/mL. Depending on a protein's propensity to interact with and unfold at the surface, this could lead to decreased flux and eventual membrane clogging. Proteins are often shear sensitive, resulting in denaturation (Thomas et al. 1979; Watterson et al. 1974), and the continuous circulation through tubings and pulsation of the pumps may generate sufficient shear or cavitation to result in protein unfolding and precipitation. Although it may be possible to filter out the precipitated protein during manufacture of bulk protein, the shear sensitivity of a protein also lead to formation of aggregates and particulates during filling of the final product that requires some sort of a pumping system. Typical filling systems include piston driven

and diaphragm pumps. Piston driven pumps tend to generate more shear than rolling diaphragm pumps and this needs to be considered when filling high concentration protein solutions.

Another parameter that could limit a TFF system's ability to concentrate a protein solution is the solution's high viscosity. The viscosity increase may result in such high back-pressures during the TFF process that it may exceed the capacity of the pumps. In addition, as viscosity increases, it becomes increasingly difficult to remove the final finished product from the TFF unit, leading to economically unacceptable losses. Though these limitations may be handled by appropriate TFF equipment redesign, equipment design can be an expensive proposition. Since the viscosity of a macromolecular solution is dependent on temperature, increased temperatures would improve the TFF process if the protein stability is not compromised. Alternatively, design of an appropriate formulation to decrease viscosity may help solve manufacturing process limitations. Hence, the formulation may need to be designed to ensure not only acceptable shelf life, but also compatibility with the manufacturing process.

Although TFF is the industry standard for concentrating macromolecules at large scale, there are alternatives. Rotating and vortex systems that enhance mass-transfer have recently been designed (van Reis and Zydney 2001; Gehlert et al. 1998). Alternatively, any drying technique with a subsequent reconstitution at lower volumes can be used as will be discussed below.

4.2. Drying Techniques for Generating High Concentration Protein Formulations

As discussed earlier in Solubility Considerations, a high concentration protein formulation can be achieved either by decreasing the solvent content while retaining the protein, for example using filtration systems, or by removal of solvent followed by reconstitution with the desired solvent volume. The latter can be achieved either by bulk processing or by dehydrating final product in vials. Bulk drying processes include spray drying (Masters 1985; Rouan 1996), fluid bed drying (Poupitch 1994; Wildfong et al. 2002), vacuum drying (Mattern et al. 1999; Miller et al. 1998) or lyophilization in tray units (Avis 1990). Crystallization has proven to be effective in the development of insulin formulations, and shows great promise for the development of stable monoclonal antibody dosage forms (Harris et al. 1995; Shenoy et al. 2001). For parenteral protein products, bulk drying processes require operation under aseptic conditions, and have been used primarily in the aerosol industry. The alternative approach of lyophilizing sterile filtered products in vials is a cost-effective approach for generating high concentration protein formulations.

To use the lyophilizer as a concentrator, a loading volume of protein, V_L, at loading concentration C_L is lyophilized and then reconstituted with a volume of diluent, V_R, where $V_R < V_L$. The final concentration of the drug product, C_F, will then be:

$$C_F = C_L V_L / (V_R + V_S) \tag{9.3}$$

where V_S is the volume contributed from the remaining solids. To determine the appropriate V_R that gives a desired C_F, one can estimate V_S from the sum of the partial molar volumes of all the excipients. However, the most accurate

way to achieve the target protein concentration is to reconstitute with a series of diluent volumes and empirically determine the appropriate reconstitution volume. In addition to reaching the desired concentration, sufficient volume needs to be used in the reconstitution process to ensure that the required volume for administration can be removed from the vial. Thus, experiments may need to be designed whereby V_L and/or C_L are also varied to define the required overrage in the final reconstituted product. These parameters can also have a major impact on the reconstitution properties of the final product. Fig. 9-1 shows the effect of loading concentration on reconstitution times and morphology of the lyophilized solid. Each vial was loaded with the same total mass of protein and formulation excipients (i.e., a lower C_L required a larger V_L to maintain the loading mass). Vials were reconstituted to a final concentration of 125 mg/mL and investigated for solution clarity and disappearance of all solids after 10 min. The right side of Fig. 9-1 shows that as the protein loading concentration is decreased, reconstitution occurs much more readily. Investigation of the morphology of the lyophilized solid by scanning electron microscopy (SEM; left side of Fig. 9-1) shows a very dense compact structure at 110 mg/mL compared to a loosely packed layer of flakes at 40 mg/mL. Thus, the ease of wetting of the cake is very likely related to the differences in this morphology. SEM analysis of intermediate concentrations (not shown) demonstrates a gradual transition from a dense solid to the more loosely packed structure.

The process described above allows for designing a formulation with appropriate stability and tonicity. Although isotonicity is not necessarily required for SC administration, it may be desirable for minimizing pain upon administration (Gatlin and Gatlin 1999). Isotonicity is difficult to achieve

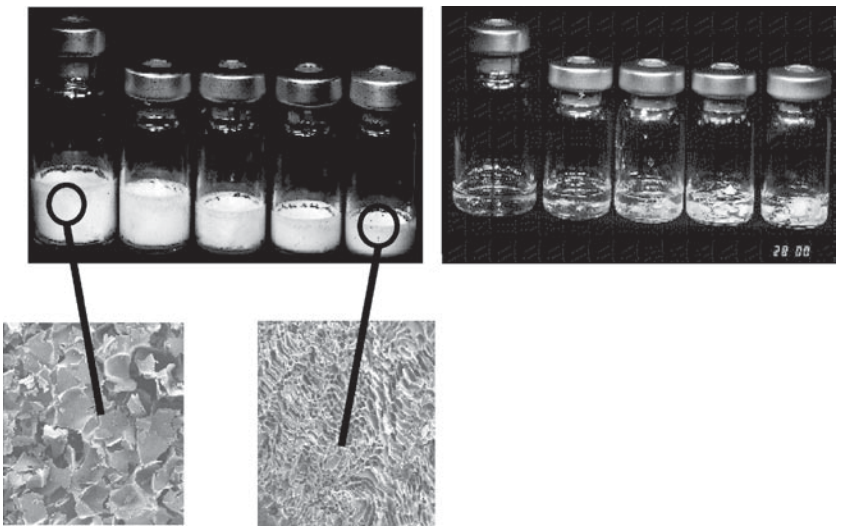

Fig. 9-1. Lyophilization of a monoclonal antibody as a function of loading concentration. *Upper left panel*: Loading concentration from left to right was 40, 60, 80, 100, and 110 mg/mL, respectively, while maintaining the same total mass of Mab and excipients. *Lower left panels*: Scanning electron microscopy of lyophilized solid for the 40 and 110 mg/mL Mab loading concentrations. *Right panel*: 10 min after reconstitution of vials in *upper left panel* to 125 mg/mL with sterile water for injection

Table 9-2. Concentration of excipient as a function of final reconstituted protein concentration and molar ratio of excipient to protein.

Excipient:protein molar ratio	**250:1**	**500:1**
C_F (mg/mL)	Excipient concentration (mM)	Excipient concentration (mM)
50	83	167
100	167	333
150	250	500
200	333	666

because both the protein and the excipients are concentrated during the reconstitution process. As shown in Table 9-2, excipient:protein molar ratios of 500:1 will result in hypertonic preparations if the final protein concentration is targeted for >100 mg/mL. If the desire is to achieve an isotonic formulation, then a choice of lower molar ratio of excipient:protein will result in a potentially less stable formulation. This was indeed the issue involving a rhuMAb preparation where the hypertonic formulation at 500:1 excipient: protein molar ratio gave a significantly more stable preparation at controlled room temperature (30°C), but the stabilities at 250 and 500:1 molar ratios were comparable at 2–8°C storage. In the case of this particular antibody where the target product profile and frequency of administration allowed for 2–8°C storage, stability was traded off for appropriate tonicity, and the 250:1 molar ratio was selected.

5. Cost of Goods and Delivery Considerations

Though high concentration formulations have the cost saving advantage of decreasing bulk storage space or number of product fills, they have undesirable overall cost of goods because of unrecoverable volumes from ultrafiltration units, fill vessels, and product containers. As an example, whereas the required volume overrage in vials containing moderate protein concentrations is typically <10% of the fill volume, the overrage for a >100 mg/mL protein formulation could be as high as 30% because of greater adherence of the viscous solution to product container surfaces. Unrecoverable product losses in the final dosage form could be minimized by decreasing product contact surface areas, for example with the use of smaller or narrower based vials, or by using prefilled syringe configurations where the solution can be pushed off the surfaces with the plunger head.

Protein formulation at high concentrations may also have physical properties that impact the ability to easily deliver the protein drug. For example, higher viscosity preparations may be difficult to administer by injection. Syringes for SC injection are often equipped with 26 or 27 gauge needles. If the viscosity of a high concentration formulation is sufficiently high, then it may impact the ability to load and deliver from a syringe, and unless the viscosity can be reduced by appropriate formulation excipients, the high concentration required for SC delivery may not be attainable. As an example, the protein concentration dependence of viscosity of an antibody is shown in Fig. 9-2a. The time required to load 1 mL of this formulation into a syringe equipped with 27 gauge needle correlates very well with the viscosity of the formulation.

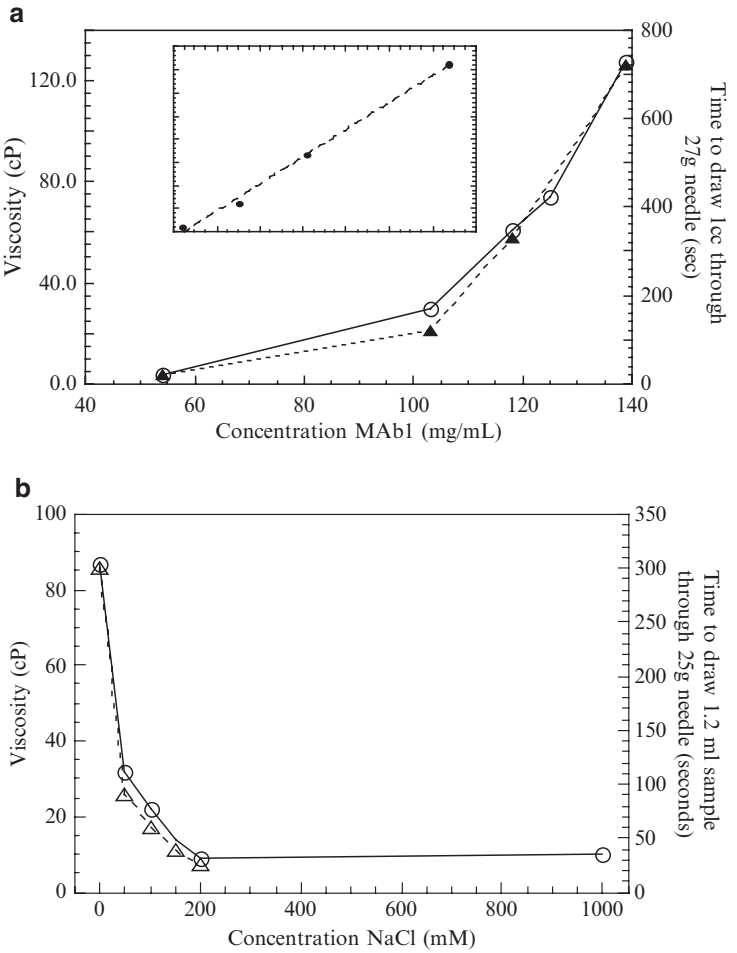

Fig. 9-2. (**a**) Viscosity (*solid line*, *open circles*) and syringe (27 gauge) loading time (dashed line, *solid triangles*) of a monoclonal antibody as a function of concentration. *Inset* is a linear regression fit of syringe (27 gauge) loading time vs. viscosity (loading time = −25.9 + 5.8 × viscosity, $R^2 = 0.995$). (**b**) Viscosity (*solid line*, *open circles*) and syringe (25 gauge) loading time of a monoclonal antibody at 125 mg/mL as a function of NaCl concentration

Adjustment of the formulation to contain NaCl greatly reduces viscosity (Fig. 9-2b), and yields reasonable time to draw the formulation into a syringe equipped with a 25 gauge needle. Thus, the alteration of the formulation excipients and the use of a slightly bigger needle yield reasonable time for withdrawal of a high concentration MAb formulation.

6. Analytical Considerations

Many of the analytical techniques currently available to explore covalent and conformational modifications in proteins (Jones 1993; Pearlman and Nguyen 1991) are easily adapted to the study of proteins at high concentration. Moreover, analytical techniques that characterize solid-state protein dosage

forms are useful in developing drying methods to produce a high protein concentration subsequent to reconstitution. These techniques include differential scanning calorimetry (DSC) (Hatley 1990), particularly modulated DSC technology (Breen et al. 2001; McPhillips et al. 1999), to determine glass transition temperatures and thermal phase transitions of the solid-state matrix at high protein concentrations, Fourier-transform infrared spectroscopy (FTIR) (Costantino et al. 1998; Prestrelski et al. 1993) and Raman spectroscopy to study the protein's secondary structure after drying and during storage, and fluorescence spectroscopy recently used to investigate possible tertiary structural alterations during the drying process (Sharma and Kalonia 2003).

Generally, the analytical technologies that are used to characterize proteins involve dilution to lower concentrations or exposure of the protein to solvent conditions that are very different than the initial formulation composition. This may have considerable impact on the results of the assay since a change in solvent composition or concentration may alter a protein's physical state in a way that is not representative of the initial conditions. This problem is especially important in the analysis of molecular weight/size distribution of proteins. SDS–PAGE, nongel sieving SDS–capillary electrophoresis, and matrix-assisted laser desorption ionization time-of-flight mass spectrometry (MALDI-TOF MS) are often used to obtain molecular weight information. These techniques are useful for detecting covalently linked aggregates, or SDS non-dissociable aggregates but can't be used to determine noncovalent protein association states. The often-used gel permeation or size exclusion chromatographic method (SEC) provides such information but has several problems. The protein's interaction with the chromatographic resin and its hydrodynamic volume may alter the elution times; the use of globular protein standards to estimate the molecular weight may thus be erroneous. When the interactions are ionic in nature due to the charge moieties on the resins, the addition of salts will decrease such interactions, but control experiments are then required to demonstrate that the increased ionic strength of the mobile phase did not perturb the size distribution of the protein. The impact of hydrodynamic volume leading to apparently larger proteins than actual size is especially noted for highly glycosylated proteins that have shapes different from the typical globular protein standards (Shire 1992; Lebowitz et al. 2002). The use of static light scattering detectors coupled with sizing chromatography (LC/LS) (Wen et al. 1996) allows for the absolute determination of molecular mass of a protein and its higher order aggregates and fragments during separation by gel sieving. Since measured elution times are no longer used to estimate molecular size, the problem of protein–resin interaction and molecular conformation are no longer important, provided the interactions do not prevent elution of the protein from the chromatographic column.

The most commonly used analytical technique for quantifying aggregates in pharmaceutical formulations is SEC with UV detection. In high concentration formulations where reversible protein self-association predominates, the determination of aggregate levels by the SEC method may be inconsistent and inaccurate. The SEC procedure involves a high dilution of the protein solution during injection onto the column that may lead to dissociation of aggregates with rapid dissociation rate constants. Moreover, to prevent detector saturation, high concentration protein solutions are generally diluted even prior to injection onto the SEC column. The rapid dissociation of a monoclonal antibody

upon dilution (Moore et al. 1999) yielded varying aggregate levels by SEC, depending on the time and temperature of analysis after sample dilution. To use SEC as an analytical tool for quantification of aggregates and estimation of formulation's shelf life and physical characteristics, it is imperative to have reproducible measurements. For a slower dissociating protein in the example shown in Fig. 9-3, reproducible quantification of aggregates in an 80 mg/mL formulation is achieved by limiting the analysis time to less than 24 h and by controlling the most critical parameters, the protein concentration after dilution and sample temperature (a fivefold decrease in dissociation rate was observed for every 10°C decrease in temperature of the auto-sampler compartment of the HPLC). The clinically relevant aggregate level for a protein that undergoes reversible self-association is that which remains after dilution in the IV solution for administration (if applicable) and after initial dilution in blood volume at 37°C. This may have to be determined separately from the routine stability testing of the pharmaceutical product, particularly when dissociation rate is slower than practical for routine analyses.

Technologies such as static and dynamic light scattering (Bloomfield 1981; Georgalis and Saenger 1999; Pecora 1972; Schurr 1977) and analytical ultracentrifugation (Bloomfield 1981; Georgalis and Saenger 1999; Pecora 1972; Schurr 1977) provide more representative information about protein self-association states at high protein concentrations because they maintain the concentration during analysis and can also be performed at high concentration. Another technique uses preparative centrifuges coupled with a specially designed microfractionator to obtain sedimentation equilibrium measurements of molecular weight in concentrated as well as multicomponent protein systems (Minton 1989). Limitations of the light scattering methods are that they are not quantitative and that they are subject to multiple scattering artifacts at high protein concentrations. Although sedimentation equilibrium centrifugal analysis can be used to characterize an aggregating system, the analysis requires fitting of data to several exponentials and is model dependent (Johnson and Straume 1994). Sedimentation velocity analysis has been greatly improved and algorithms are now available to determine small amounts of

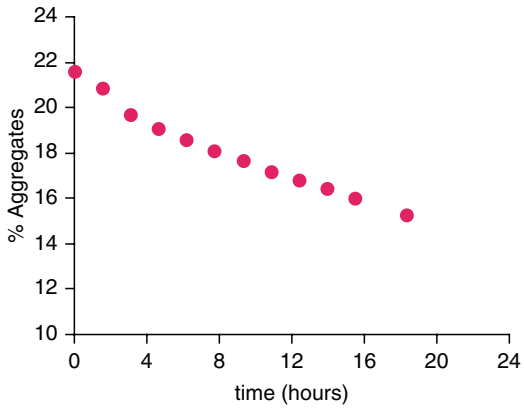

Fig. 9-3. Dissociation of aggregates in an 80 mg/mL protein formulation at 30°C upon dilution to 0.1 mg/mL. At 5°C, the dissociation rate is too small to detect any changes in the initial aggregate level during this time frame

protein aggregates and sedimentation coefficients (Schuck 1998; Schuck et al. 2002). The determination of the sedimentation coefficient can provide valuable information regarding overall shape of the protein when coupled with computations of hydrodynamic bead models (de la Torre 1992; Liu et al. 1995). However, correction of apparent molecular weights and sedimentation coefficients due to nonideality at high protein concentrations is difficult to achieve.

7. Summary and Conclusions

Protein properties such as self-association/aggregation, solubility, and viscosity pose challenges to developing pharmaceutically and economically acceptable formulations at high concentration. In addition to maintaining suitable stability, protein properties at high concentration may impact the ability to administer the drug, to manufacture at large scale, and also the yields of the two processes. Analytical methodologies to investigate protein properties at high concentration are also limited and must be considered with caution as they are impacted by the very property under investigation. Very little work has been published on high concentration protein formulation development and this review has touched on the key issues with examples of the potential solutions to the issues. Achieving a suitable formulation requires an integrated approach whereby a stable formulation is developed that can also be successfully administered and economically manufactured.

Acknowledgments: The authors wish to thank Dr. Robert Van Reis, Department of Recovery Sciences, Genentech Inc, for input on the TFF technologies, and Dr. Chung Hsu, Department of Pharmaceutical R&D, Genentech Inc., for discussions on bulk drying processes.

References

Ahern TJ, Manning MC (eds) (1992) Stability of protein pharmaceuticals. Part A: Chemical and physical pathways of protein degradation. Plenum, New York, p 434

Andya JD, Hsu CC, Shire SJ (2003) Mechanisms of aggregate formation and carbohydrate excipient stabilization of lyophilized humanized monoclonal antibody formulations. AAPS PharmSci 5(2):E10

Arakawa T, Timasheff SN (1982) Stabilization of protein structure by sugars. Biochemistry 21:6536–6544

Arakawa T, Timasheff SN (1985) Theory of protein solubility. Methods Enzymol 114:49–77

Arakawa T, Kita Y, Carpenter JF (1991) Protein–solvent interactions in pharmaceutical formulations. Pharm Res 8(3):285–291

Avis KE (1990) Parenteral preparations. In: Gennaro AR (ed) Remington's pharmaceutical sciences, 18th edn. Mack Publishing Company, Easton, PA, pp 1545–1569

Bloomfield VA (1981) Quasi-elastic light scattering applications in biochemistry and biology. Annu Rev Biophys Bioeng 10:421–450

Braun A, Kwee L, Labow MA, Alsenz J (1997) Protein aggregates seem to play a key role among the parameters influencing the antigenicity of interferon alpha (IFN-alpha) in normal and transgenic mice. Pharm Res 14(10):1472–1478

Breen ED, Curley JG, Overcashier DE, Hsu CC, Shire SJ (2001) Effect of moisture on the stability of a lyophilized humanized monoclonal antibody formulation. Pharm Res 18(9):1345–1353

Bull HB (1971) An introduction to physical biochemistry. F.A. David Company, Philadelphia, p 174

Cantor CR, Schimmel PR (1980) Biophysical chemistry: Part II: Techniques for the study of biological structure and function. W. H. Freeman and Company, San Francisco, p 503

Carpenter JF, Pikal MJ, Chang BS, Randolph TW (1997) Rational design of stable lyophilized protein formulations: some practical advice. Pharm Res 14(8): 969–975

Carpenter JF, Chang BS, Garzon-Rodriguez W, Randolph TW (2002) Rational design of stable lyophilized protein formulations: theory and practice. Pharm Biotechnol 13:109–133

Chi EY, Krishnan S, Randolph TW, Carpenter JF (2003) Physical stability of proteins in aqueous solution: mechanism and driving forces in nonnative protein aggregation. Pharm Res 20(9):1325–1336

Cleland JL, Powell MF, Shire SJ (1993) The development of stable protein formulations: a close look at protein aggregation, deamidation and oxidation. Crit Rev Ther Drug Carrier Syst 10(4):307–377

Cleland JL, Lam X, Kendrick B, Yang J, Yang TH, Overcashier D, Brooks D, Hsu C, Carpenter JF (2001) A specific molar ratio of stabilizer to protein is required for storage stability of a lyophilized monoclonal antibody. J Pharm Sci 90(3):310–321

Costantino HR, Chen B, Griebenow K, Hsu CC, Shire SJ (1998) Fourier-transform infrared spectroscopic investigation of the secondary structure of aqueous and dried recombinant human deoxyribonuclease I. Pharm Pharmacol Commun 4:391–395

de la Torre JG (1992) Sedimentation coefficients of complex biological particles. In: Harding SE, Rowe AJ, Horton JC (eds) Analytical ultracentrifugation in biochemistry and polymer science. The Royal Society of Chemistry, Cambridge, England, pp 333–345

Gatlin LA, Gatlin CAB (1999) Formulation and administration techniques to minimize injection pain and tissue damage associated with parenteral products. In: Gapta PK, Brazeau GA (eds) Injectable drug development: techniques to reduce pain and irritation. Interpharm Press, Denver, pp 401–421

Gehlert G, Luque S, Belfort G (1998) Comparison of ultra- and microfiltration in the presence and absence of secondary flow with polysaccharides, proteins, and yeast suspensions. Biotechnol Prog 14(6):931–942

Genovesi CS (1983) Several uses for tangential-flow filtration in the pharmaceutical industry. J Parenter Sci Technol 37(3):81–86

Georgalis Y, Saenger W (1999) Light scattering studies on supersaturated protein solutions. Sci Prog 82(Pt 4):271–294

Glatz CE (1992) Modeling of aggregation-precipitation phenomena. In: Ahern TJ, Manning MC (eds) Stability of protein pharmaceuticals. Plenum, New York, pp 135–166

Harris LJ, Skaletsky E, McPherson A (1995) Crystallization of intact monoclonal antibodies. Proteins 23(2):285–289

Hatley RHM (1990) International symposium on biological product freeze-drying and formulation, Bethesda, MD, pp 105–122

Jenkins WT (1998) Three solutions of the protein solubility problem. Protein Sci 7(2):376–382

Johnson ML, Straume M (1994) Comments on the analysis of sedimentation equilibrium experiments. In: Schuster TM, Laue TM (eds) Modern analytical ultracentrifugation. Birkhauser, Boston, pp 37–63

Jones AJS (1993) Analytical methods for the assessment of protein formulations and delivery systems. In: Cleland JL, Langer R (eds) Formulation and delivery of peptides and proteins. American Chemical Society, Washington, DC, pp 22–45

Koren E, Zuckerman LA, Mire-Sluis AR (2002) Immune responses to therapeutic proteins in humans-clinical significance, assessment and prediction. Curr Pharm Biotechnol 3(4):349–360

Leavis PC, Rothstein F (1974) The solubility of fibrinogen in dilute salt solutions. Arch Biochem Biophys 161(2):671–682

Lebowitz J, Lewis MS, Schuck P (2002) Modern analytical ultracentrifugation in protein science: a tutorial review. Protein Sci 11(9):2067–2079

Liu J, Lester P, Builder S, Shire SJ (1995) Characterization of complex formation by humanized anti-IgE monoclonal antibody and monoclonal human IgE. Biochemistry 34(33):10474–10482

Manning MC, Patel K, Borchardt RT (1989) Stability of protein pharmaceuticals. Pharm Res 6(11):903–918

Masters K (1985) Spray drying handbook. Wiley, New York

Mattern M, Winter G, Kohnert U, Lee G (1999) Formulation of proteins in vacuum-dried glasses. II. Process and storage stability in sugar-free amino acid systems. Pharm Dev Technol 4(2):199–208

McPhillips CDQM, Royall PG, Hill VL (1999) Characterization of the glass transition of HPMC using modulated differential scanning calorimetry. Int J Pharm 180:83–90

Melander W, Horvath C (1977) Salt effect on hydrophobic interactions in precipitation and chromatography of proteins: an interpretation of the lyotropic series. Arch Biochem Biophys 183(1):200–215

Middaugh CR, Volkin DB (1992) Protein solubility. In: Ahern TJ, Manning MC (eds) Stability of protein pharmaceuticals. Plenum, New York, pp 109–134

Miller DP, Anderson RE, de Pablo JJ (1998) Stabilization of lactate dehydrogenase following freeze thawing and vacuum-drying in the presence of trehalose and borate. Pharm Res 15(8):1215–1221

Minton AP (1989) Analytical centrifugation with preparative ultracentrifuges. Anal Biochem 176:209–216

Minton AP (1992) Confinement as a determinant of macromolecular structure and reactivity. Biophys J 63(4):1090–1100

Moore JM, Patapoff TW, Cromwell ME (1999) Kinetics and thermodynamics of dimer formation and dissociation for a recombinant humanized monoclonal antibody to vascular endothelial growth factor. Biochemistry 38(42):13960–13967

Moshashaee S, Bisrat M, Forbes RT, Quinn EA, Nyqvist H, York P (2003) Supercritical fluid processing of proteins: lysozyme precipitation from aqueous solution. J Pharm Pharmacol 55(2):185–192

Pearlman R, Nguyen TH (1991) Analysis of protein drugs. In: Lee VH (ed) Peptide and protein drug delivery. Marcel Dekker, New York, pp 247–301

Pecora R (1972) Quasi-elastic light scattering from macromolecules. Annu Rev Biophys Bioeng 1:257–276

Pikal MJ, Pikal MJ (1994) Freeze-drying of proteins: process, formulation and stability. In: Cleland JL, Langer R (eds) Formulation and delivery of proteins and peptides. American Chemical Society, Washington, DC, pp 120–133

Poupitch G (1994) Fluid bed drying in the laboratory. Am Biotechnol Lab 12(4):30–34

Prestrelski SJ, Tedeschi N, Arakawa T, Carpenter JF (1993) Dehydration-induced conformational transitions in proteins and their inhibition by stabilizers. Biophys J 65(2):661–671

Rothstein F (1994) Differential precipitation of proteins. Science and technology. Bioprocess Technol 18:115–208

Rouan SKE (1996) Biotechnology-based pharmaceuticals. In: Banker GS, Rhodes CT (eds) Modern pharmaceutics, 3rd edn. Marcel Dekker, New York, pp 843–873

Saul A, Don M (1984) A rapid method of concentrating proteins in small volumes with high recovery using Sephadex G-25. Anal Biochem 138(2):451–453

Schein CH (1990) Solubility as a function of protein structure and solvent components. Biotechnology 8(4):308–317

Schuck P (1998) Sedimentation analysis of noninteracting and self-associating solutes using numerical solutions to the Lamm equation. Biophys J 75(3):1503–1512

Schuck P, Perugini MA, Gonzales NR, Howlett GJ, Schubert D (2002) Size-distribution analysis of proteins by analytical ultracentrifugation: strategies and application to model systems. Biophys J 82(2):1096–1111

Schurr JM (1977) Dynamic light scattering of biopolymers and biocolloids. CRC Crit Rev Biochem 4(4):371–431

Sharma VK, Kalonia DS (2003) Steady-state trytophan fluorescence spectrscopy study to probe tertiary structure of proteins in solid powders. J Pharm Sci 92(4):890–899

Shenoy B, Wang Y, Shan W, Margolin AL (2001) Stability of crystalline proteins. Biotechnol Bioeng 73(5):358–369

Shiloach J, Martin N, Moes H (1988) Tangential flow filtration. Adv Biotechnol Processes 8:97–125

Shire SJ (1992) Analytical ultracentrifugation and its use in biotechnology. In: Schuster TM, Laue TM (eds) Modern analytical ultracentrifugation. Birkhauser, Boston, pp 261–297

Tanabe S, Tesaki S, Watanabe M (2000) Producing a low ovomucoid egg white preparation by precipitation with aqueous ethanol. Biosci Biotechnol Biochem 64(9):2005–2007

Thomas CR, Nienow AW, Dunnill P (1979) Action of shear on enzymes: studies with alcohol dehydrogenase. Biotechnol Bioeng 21(12):2263–2278

Treuheit MJ, Kosky AA, Brems DN (2002) Inverse relationship of protein concentration and aggregation. Pharm Res 19(4):511–516

van Reis R, Zydney A (2001) Membrane separations in biotechnology. Curr Opin Biotechnol 12(2):208–211

Watterson JG, Schaub MC, Waser PG (1974) Shear-induced protein–protein interaction at the air–water interface. Biochim Biophys Acta 356(2):133–143

Webb SD, Webb JN, Hughes TG, Sesin DF, Kincaid AC (2002) Freezing bulk-scale biopharmaceuticals using common techniques – and the magnitude of freeze-concentration. Biopharm 15(5):2–8

Wen J, Arakawa T, Philo JS (1996) Size-exclusion chromatography with on-line light-scattering, absorbance, and refractive index detectors for studying proteins and their interactions. Anal Biochem 240(2):155–166

Wildfong PL, Samy AS, Corfa J, Peck GE, Morris KR (2002) Accelerated fluid bed drying using NIR monitoring and phenomenological modeling: method assessment and formulation suitability. J Pharm Sci 91(3):631–639

Wilf J, Minton AP (1981) Evidence for protein self-association induced by excluded volume. Myoglobin in the presence of globular proteins. Biochim Biophys Acta 670(3):316–322

Winters MA, Knutson BL, Debenedetti PG, Sparks HG, Przybycien TM, Stevenson CL, Prestrelski SJ (1996) Precipitation of proteins in supercritical carbon dioxide. J Pharm Sci 85(6):586–594

Zhang R, Hjerten S (1997) A micromethod for concentration and desalting utilizing a hollow fiber with special reference to capillary electrophoresis. Anal Chem 69(8):1585–1592

Zimmerman SB, Minton AP (1993) Macromolecular crowding: biochemical, biophysical, and physiological consequences. Annu Rev Biophys Biomol Struct 22:27–65

Chapter 10

Protein Immobilization by Crystallization and Precipitation: An Alternative to Lyophilization

Karoline Bechtold-Peters

1. Introduction: Advantages and Limitations of Lyophilization

Of the 26 currently approved drug products containing monoclonal antibodies as active substance for therapy or in vivo diagnosis about a quarter are freeze-dried preparations that require reconstitution before use (product survey as of December 2008) (Wang et al. 2007).

cGMP compliant freeze drying units have been available for several decades and biopharmaceutical companies have at their disposal a selection of modern lyophilizers as part of their standard operating equipment. Lyophilizers are operated aseptically by being equipped with clean in place (CIP)/steam in place (SIP) technology, utilizing sterile air or sterile nitrogen, and by stoppering the vials still in the lyophilizer through collapsing shelves. Automated loading or unloading or the coupling of the lyophilizer to filling isolators are becoming common at the production scale.

Suitable cake forming agents such as sucrose, mannitol, glycine and trehalose are often used in the formulation. These sugars replace the water necessary to retain the native structure of the protein (Arakawa et al. 2001). In the literature it is often discussed whether the stabilization of protein originates from "glass dynamics," thus from immobilization in the glasslike state, or from the preservation of the native structure through "specific interaction" between sugars and protein (Chang et al. 2005a).

Finally, there exists extensive process-technical knowledge on how to operate the lyophilization process as standard operation in such a way that after freezing and water removal during primary and secondary drying the protein is not damaged. Various in-process control options are frequently used including the measurement of the product temperature by thermocouples, the monitoring of the drying process indirectly through pressure measurement by means of capacitive sensors, heat conductivity manometers or the pressure rise method (Tang et al. 2005) or directly by mass spectroscopy, drying balances or NIR (Presser 2003).

From: *Current Trends in Monoclonal Antibody Development and Manufacturing,*
Biotechnology: Pharmaceutical Aspects, DOI 10.1007/978-0-387-76643-0_10,
Edited by: S.J. Shire et al.

Despite its utility, the freeze drying process is also afflicted with substantial disadvantages and restrictions, and increasing interest exists in alternative stabilization and immobilization procedures. Freeze drying units are expensive investments. The removal of more than 90% of the mass of the initial solution for lyophilization is energy intensive. Lyophilization needs relatively long processing time of several days. The batch size is limited by the volume of the freeze-drier. Loading and loading rates have a substantial influence on the process, whereby careful scale up is needed and the transfer into larger scales is clearly more complex than with continuous procedures. These characteristics increase the price of a lyophilized product compared to liquid products.

Proteins can also undergo degradation during freeze-drying leading to losses in biological activity. During freezing, the physical environment of a protein changes dramatically leading to the development of stress that impacts protein stability (Bhatnagarab et al. 2007). Low temperature, freeze-concentration, and ice formation are chief stress factors resulting during cooling and freezing and may require addition of a cryoprotectant (Chen et al. 2003). Because of the increase in solute concentrations, freeze-concentration can also facilitate second order reactions, crystallization of buffer or non-buffer components, phase separation, and redistribution of solutes.

Furthermore the dehydration creates stress for the protein which must be antagonized by lyoprotectants. In particular, removing water generally decreases the chemical reaction rates since most of them are hydrolytically driven, but removal of too much water can also negatively affect the protein conformation. The aforementioned appropriate lyoprotectants may serve as "water replacements." Altogether it can be summarized that "freeze-drying is not an innocuous process and needs to be understood and used carefully" (Roy and Gupta 2004).

Because of the porous structure and the high content of amorphous material in lyophilized products, the reconstitution times are generally short. However, under the influence of temperature and moisture the product cake can sinter so that attention is to be directed towards appropriate processing conditions, adequate residual moisture of the lyophilizate, packaging tightness and proper residual moisture of the stopper (Earle et al. 1991). Physical and mechanical stability of freeze dried products is limited, they are – dependent on the formulation – more or less strongly hygroscopic products (Shamblin et al. 1998), which are to be stored absolutely below their glass temperature and efficiently protected against moisture (Franks 1998). The water content of the lyophilizate directly affects the glass temperature Tg of the dried product and hence the chemical and physical stability of the protein (Breen et al. 2001). Often the development of the dried formulations requires even a balance between chemical and physical stability (Chang et al. 2005b).

2. Alternative Immobilization and Drying Methods Appropriate for Biomolecule Processing

In order to stabilize a protein in an analogous way to lyophilization (i.e., dehydration, and restriction of the molecular mobility), other drying and precipitation procedures are available. These are summarized in Table 10-1 and will be presented in the remainder of the chapter.

A variant of freeze drying as drying procedures utilizing ice sublimation is spray-freeze drying. The process involves spraying the protein solution through nozzles into a freezing agent like liquid nitrogen or liquid propane. The protein as well as the excipients are suddenly frozen and then loaded into the freeze-drier onto precooled (e.g., −40°C) plates. The ice is them sublimated under vacuum. Compared to conventional freeze drying, spray-freeze drying results in ultraporous particles that exhibit no shrinkage or change in morphology during drying (Gieseler 2003, 2004; Figure 10-1) with very

Table 10-1. Options for protein immobilization procedures.

Immobilization principle	Processes
Predominantly by sublimation of ice	• Lyophilization
	• Spray-freeze drying
By evaporation of liquid water	• Spray drying
	• Vacuum drying
	• Other evaporative drying methods
By extraction of water, crystallization or precipitation of the molecule	• Crystallization
	• Precipitation
	• Supercritical drying
Immobilization on carriers or crosslinking between molecules	• Covalent bonding
	• Adsorptive bonding
	• Ligand bonding
	• Intra-/intermolecular bonding

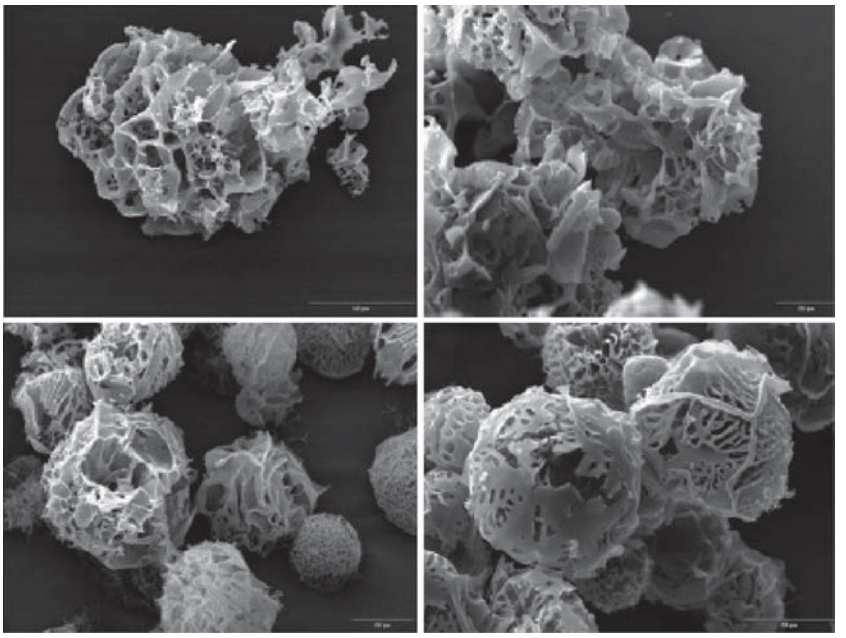

Fig. 10-1. SEM images illustrating the textural characteristics of spray-freeze dried trehalose produced by spraying the stock solution into liquid propane (*top row*) or liquid nitrogen (*bottom row*) (Gieseler 2004)

favorable dispersion properties. However, the process is more time-consuming and complex in operation.

Methods by which the solvent evaporates under the influence of temperature are spray drying or vacuum drying.

For the processing of full size antibodies suitable drying temperatures during spray drying are 90–130°C inlet temperature and 50–90°C outlet temperature (Maury et al. 2005a; Schüle et al. 2007). The temperature to which the proteins are exposed is reduced by evaporative cooling. Furthermore the protein is exposed to the increased temperatures for only a few milliseconds. Schüle et al. (2007) show that an IgG1 antibody could be spray-dried with different concentrations of mannitol as a matrix. After reconstitution, the native state was perfectly restored. In the dried state, however, the secondary structure as demonstrated on the basis of the amide I bands using ATR-FTIR was reversibly changed. The process conditions during the spray drying must be selected in such a way that low residual water contents, of less than 1%, are achieved. Potentially an after-drying step can be introduced in order to achieve optimal stability during storage (Schüle et al. 2008). Improved stability could also be achieved by an admixture of glycine, trehalose or sucrose to the matrix of mannitol (Schüle 2005a). Without the addition of a matrix former like sorbitol, substantially aggregated antibody was obtained after the spray drying process which continued during storage (Maury et al. 2005a).

In contrast to lyophilization, spray drying is a continuous procedure. Scale up can be achieved by increasing processing times instead of enlargement of the equipment. The spray drying can be accomplished under aseptic conditions, if a parenteral product is to be manufactured. However, such equipment with CIP/SIP systems is not standard. Following the spray drying the proteinaceous powder must next be dispensed under aseptic conditions, or stored temporarily as an intermediate bulk. Suitable powder filling machines are well-known from antibiotics production. As is the case with lyophilized products, the main part of the spray-dried proteinaceous product is amorphous and therefore metastable requiring storage far below the glass transition temperature. During the storage, recrystallization of matrix components (Schüle 2005a) can occur and result in negative effects on morphology, functionality and activity of the product.

Yield is a crucial output parameter for spray drying and often a major concern with the scale-down of this method for development or early clinical phases. Appropriate design of spray-drying chambers and cyclones has been used to improve the yields and decrease the fines lost in the exhaust air filter or due to adherence to equipment walls (Maury et al. 2005b; Maa et al. 1998; Schüle 2005b).

Vacuum drying is another type of evaporative procedure that does not use a freezing step. VitriLife® has developed a vacuum drying process which brings the solution to be dried to controlled boiling under reduced atmospheric pressure. In January 2003, AVANT acquired the exclusive rights to VitriLife®, a patented method for the industrial-scale preservation of biological solutions and suspensions, such as proteins, enzymes, viruses, bacteria and other cells. VitriLife® has the potential to cut production costs and improve product stability at room temperature or higher (Figure 10.2). Thus, its application may eliminate the need for costly cold-chain distribution and storage of vaccines – the major challenge to vaccine affordability in many areas of the world facing

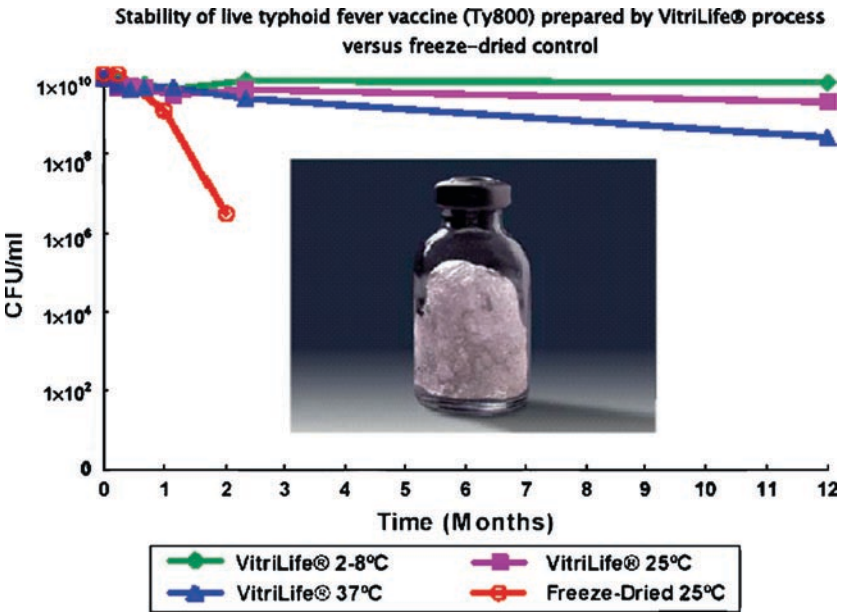

Fig. 10-2. Stabilization of vaccine by the VitriLife process (source: website of Avant Immunotherapeutics)

endemic disease. AVANT is presently developing the VitriLife® process to incorporate it into AVANT's bacterial vaccines program (website of Avant Immunotherapeutics).

3. Extraction of Water by Crystallization and Precipitation

Another method to remove water from a protein is by precipitation and extraction. Crystallization, precipitation, and supercritical procedures will be described in detail as principal topic of the next section. Such procedures extract the water from the macromolecule by transfer of the proteins into an environment where they are not soluble. Precipitation processes which take place very fast and result in a relatively unordered structure, differ from crystallization processes which are much slower and transfer the protein into a highly ordered structure with three-dimensional arrangement. Suitable agents for the initiation of reversible precipitation or crystallization of proteins are listed in Table 10-2 and can be divided into three classes:

- Organic solvents
- Polyhydroxy compounds (Figure 10-3)
- Salts (salting out method according to the Hofmeister series, Hofmeister 1888)

Further procedures for protein precipitation are:

- Precipitation close to the isoelectric point of protein (pH adjustment)
- Water extraction by supercritical fluids

In addition, proteins may be chemically crosslinked, e.g., by glutaraldehyde, to form nondissolvable or slowly dissolvable crystals.

Table 10-2. Agents initiating precipitation or crystallization.

Agents to cause proteins or peptides to reversibly precipitate or crystallize:	Examples (selection)
Organic solvents	2-methyl-2,4-pentanediol (MPD), acetone, propanol, ethanol, isopropanol
Polyhydroxy compounds	polyethylene glycol (PEG), MPEG, cyclodextrins
Salts ("salting out method")	Ammonium sulfate, see Hofmeister series
Precipitation close to isoelectric point of protein	pH adjustment at IP
Supercritical fluids	Supercritical carbon dioxide (containing various amounts of modifiers such as ethanol)

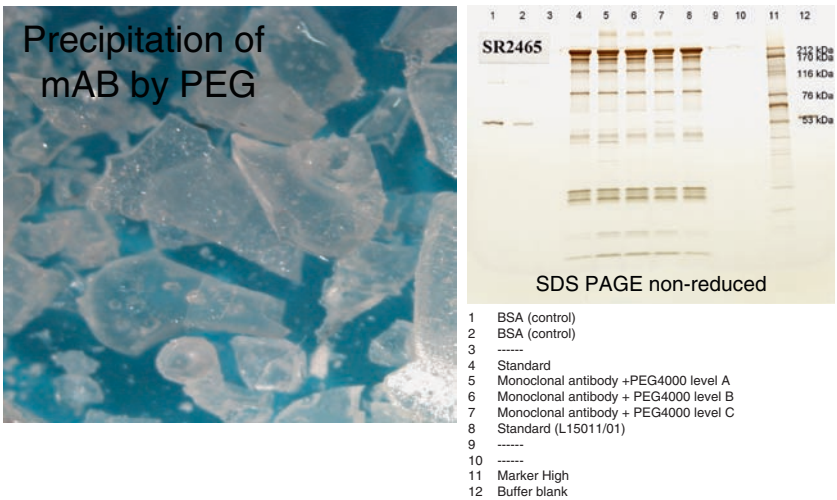

Fig. 10-3. Precipitation of a monoclonal antibody by PEG

With many crystallization and precipitation procedures, the completion of the process results in a protein suspension which opens up new possibilities for protein formulation. Highly concentrated protein preparations of >100 mg/mL in a liquid can result, which are attractive for high-dose monoclonal antibody products. The challenge consists of avoiding uncontrolled protein aggregation during storage. If the aggregation is forestalled in a controlled and reversible way by crystallization or precipitation, a stable formulation alternative can result. This is also an alternative to the patented approach to reconstitute lyophilized drugs with smaller solvent volumes and produce high concentration liquid formulations that are stable over short time periods (Andya et al. 2006).

Table 10-3. Types of insulin preparations (Brange et al. 1992).

Classification after timing of action	Name of Preparation	Abbreviation used in text and in figure 10-8
Rapid-acting	Acid regular	
	Neutral regular	
Short-acting	Insulin zinc suspension, amorphous	IZS amorph.
Intermediate-acting	Insulin zinc suspension, mixed	IZS mixed
	Isophane insulin (NPH)[a]	NPH
Long-acting	Insulin zinc suspension crystalline	IZS cryst.
	Protamine zinc insulin	PZI
Biphasic-acting	Biphasic insulin	

[a]Neutral protamine Hagedorn

An important consideration for the direct use of suspensions of precipitated or crystalline proteins is the biocompatibility of the precipitant and/or mother liquid or the possibility to replace these by another nonsolvent and/or nonsolvent mixture. Such protein suspensions can exhibit substantially reduced viscosities compared to highly concentrated solutions and thus produce less injection pain. Finally, the addition of surfactants for stabilization against storage-related aggregate formation can be avoided which may be advantageous for reduction of toxicity and immunogenicity (Matheus and Mahler 2005).

Such preparations may exhibit a slow dissolution, which results in a controlled release effect upon injection. Commercially available insulin preparation are available that rereal a prolonged duration of action. These products contain insulin or insulin analogues complexed by zinc (IZS), protamine sulfate (NPH, Isophane) or zinc-protamine sulfate (PZI). The duration of insulin release or the creation of a biphasic release profile can be achieved by varying the composition of the mixture of amorphous or crystalline zinc insulin or of non-retarded and protamine-bound insulin (Brange et al. 1992; Hermansen et al. 2002) (Table 10-3).

Whether the extraction process is a precipitation or crystallization depends more on the process parameters such as temperature and the protein concentration and less on the type of added reagents. High protein and precipitant concentrations lead to precipitation while lower protein and precipitant concentrations allow for a possible nucleation and subsequent crystal growth (Figures 10-4a and b).

An automated microbatch technique was used to establish a phase diagram for crystallization (Asherie 2004). The concentrations of the protein, carboxypeptidase G2 and precipitant, polyethylene glycol (PEG) 4000, were varied, while pH and temperature were kept constant. The phase diagram consists of

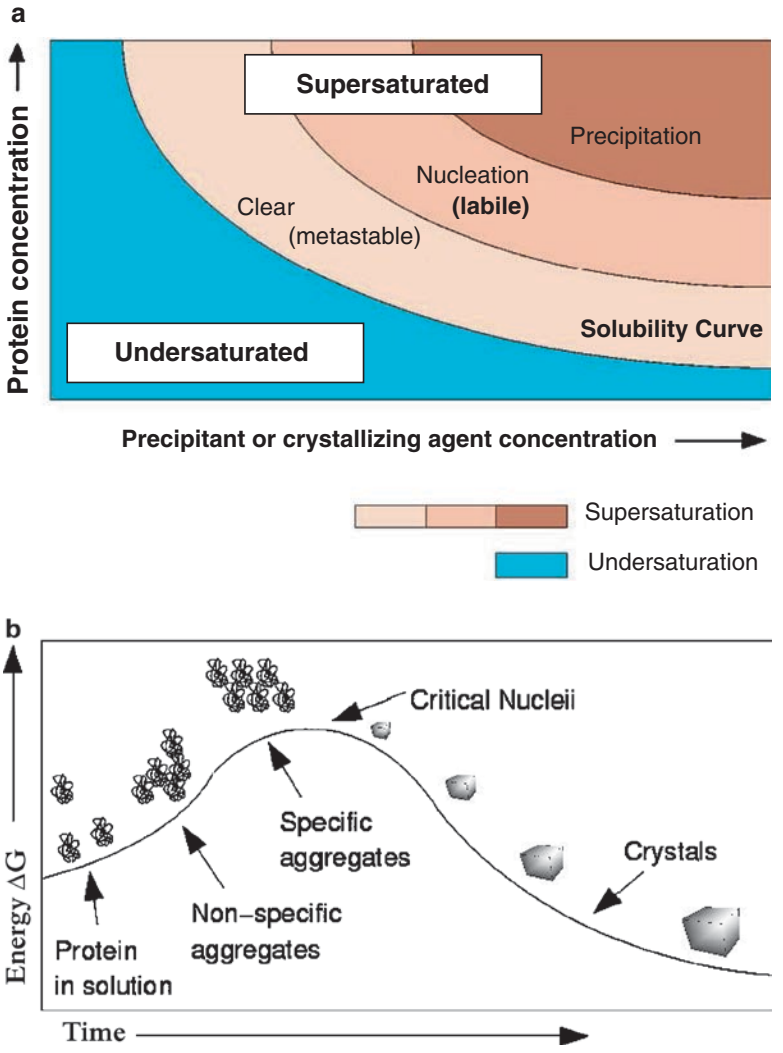

Fig. 10-4. (**a**) Phase diagram showing zones for crystal nucleation, growth and precipitation (source: adjusted from McCoy AJ, University of Cambridge). (**b**) Phase diagram for a typical protein (source: McCoy AJ, University of Cambridge)

an undersaturation and a supersaturation zone, the latter being subdivided into the metastable, nucleation, and precipitation zones. In the metastable zone, crystals may grow but nucleation of crystals does not occur. It is the best zone for growth of X-ray diffraction quality crystals because of the avoidance of uncontrolled nucleation, but nuclei must be introduced artificially into the system. Hence, for manufacturing purposes, working in the labile zone is more appropriate. The probability of nucleation increases with increasing supersaturation. At very high supersaturation conditions, nuclei formation is slower than the amorphous precipitation of the protein.

3.1. Crystallization

McPherson defines eight categories of protein crystallization additives (McPherson and Cudney 2006):

- ligands with physiological or biochemical relevance such as coenzymes, by which the protein conformation changes and is mostly stabilized,
- preservatives from the class of reducing or metal ion complexing materials such as EDTA (ethylene diamine tetraacetic acid) or DTT (dithiothreitol) or also bactericidals such as chlorbutanol or phenol,
- solubilization agents and detergents such as quaternary ammonium salts, sulfobetaines, and chaotropes,
- small admixtures (1–5%) of organic solvents such as DMSO or acetone,
- osmolytes, cosolvents, and cosmotropes at high concentration (1-molar and higher) such as sugars, proline, glycine, or TMAO (trimethyl amine oxide); their mode of action consists of changing the interaction of the protein surface with the solvent water or the hydration layer and possibly the water structure,
- intramolecular or intermolecular bridge formers, i.e., multivalent materials, which cause a reversible crosslinking between charged or polar groups on the protein surface like molecules with aliphatic residues of various chain lengths containing diamino or dicarboxyl groups. The protein is stabilized by additional intramolecular bridges, while the intermolecular bridges promote interactions in the crystal lattice,
- nucleation enhancers at small concentrations such as PEG or other polymers. The micro droplets of the polymeric phase serve to concentrate the protein locally and provide an interface for nucleation to occur. This category should probably also include cubic phases and surface which promote epitaxy and heterogeneous nucleation.

In combinatorial studies with 81 different proteins, including many enzymes such as bacterial lipase, but in addition, 9 monoclonal antibodies such as Rituximab, McPherson and Cudney (2006) tested 200 possible crystallization accelerators.

In the study under employment of the Sitting Drop Method (Figure 10-5), the crystallization accelerators were mixed 1:1 in water with 30% PEG 3350 in 0.1 M HEPES (4-(2-hydroxyethyl)-1-piperazineethanesulfonic acid) or with 50% Tacsimate (1.36 M malonic acid, 0.25 M ammonium citrate tribasic, 0.12 M succinic acid, 0.3 M DL-malic acid, 0.4 M sodium acetate, 0.5 M

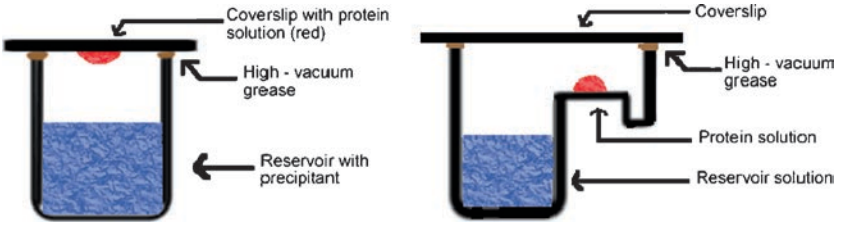

Fig. 10-5. Hanging drop (*left hand*) and sitting drop (*right hand*) methods for growing of large protein crystals for structure elucidation (source: Kogoy JM)

sodium formate, and 0.16 M ammonium tartrate dibasic). A total of 65 proteins or 85% could be crystallized. In particular, the crystallization was difficult for the monoclonal antibodies. A complete antibody, IDEC 151, could be crystallized with a mixture of Tacsimate and the nucleotides d(pT)12 and d(pT)4, serum albumin (rabbit) with PEG 3350 and pentaglycine plus triglycine (Figure 10-6). Good results were achieved in the study for example with a mixture consisting of suberic, sebacic, hexadecanedioic, and dodecanedioic acid as well as with a mixture additionally containing fumaric, pimelic, malic, glutaric, and oxamic acid.

Obviously, molecules rich in charged groups, particularly negatively charged carboxyl groups, might be of general utility. This is consistent with the expectations regarding the reversible crosslinking of proteins in a lattice. The results suggest furthermore that sulfonyl groups and phosphate groups might also promote crystallization.

Surely, not all substances examined in the study as potential crystallization promoters can be used for pharmaceutical purposes, e.g., Streptomycin, however, McPherson's work can provide a good starting point (McPherson 1978; McPherson 1982; McPherson et al. 1984; McPherson and Shlicta 1988; McPherson 1999; McPherson 2001).

Small scale crystallization studies can utilize micromethods such as Sitting, Sandwich, or the Hanging Drop Method or dialysis in dialysis buttons. However, for an industrial scale procedure, other methods must be employed. In industrial procedures, the protein solution is first concentrated, if necessary buffer components are removed by diafiltration, and then the precipitation agent or mixture added or the pH value adjusted to the precipitation pH (Shenoy 2002). The separation of the crystals can take place via filtration or centrifugation, Often the crystal cake must be washed to remove salts. Crystal screening kits like Wizard and Cryo, both from Emerald Biostructures, or Crystal Screen from Hampton Research have been used to facilitate batch crystallization processes (Shenoy 2002).

An important process parameter during protein crystallization is temperature, whereby there are proteins with direct (lower temperature facilitates nucleation) as well as with retrograde (higher temperature facilitates nucleation) temperature-dependent solubility behavior. Zhu et al. (2006) defined the "relative crystallizability of proteins" as integral of the area between the

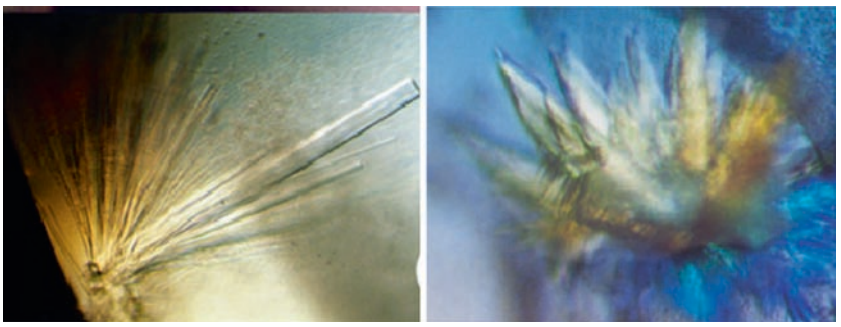

Fig. 10-6. Light microscope photographs of crystalline IDEC 151, a full-size IgG antibody with 151 kDa molecular weight (*left*), and of rabbit serum albumin (*right*) (McPherson and Cudney 2006)

nucleation and the precipitation curve and recommend for crystallization optimization, the generation of two-dimensional phase diagrams.

Because of the glycosylation and the flexibility in certain regions of antibodies, crystallization is far more challenging than for enzymes. Nevertheless several examples exist, where antibody crystallization was achieved.

Hagewiesche et al. (2006) describe in their patent application the crystallization of full-size antibodies or antibody fragments by the addition of salts of divalent cations, in particular of zinc chloride in sodium acetate buffer pH 4.7–5.7. The addition of organic solvents was not necessary and did not increase crystal yield. Bevacizumab (anti-VEGF) was described as a positive example. Depending upon the concentration of zinc chloride and sodium acetate, free crystals or concentrated crystal gels formed, while with anti-CD20, anti-HER2, anti-CD11a, and anti-2C4 antibodies, no crystalline products with birefringence were formed.

In a patent application entitled "The crystallization of anti-EGFR antibodies" (Matheus and Mahler 2005), Mab C225 Cetuximab and Mab h425 EMD 72000, were crystallized in the batch mode by addition of PEG 4000 or 8000, saturated ammonium sulphate solution or 50 vol% ethanol in citrate buffer pH 5.5 or phosphate buffer pH 8.0. The resulting crystals showed birefringing characteristics under the microscope and were stained with Coomassie blue dye. The FT-IR analysis did not show changes in the amide I-2-region compared with the initial solution after redispersion and relatively high yields were reached.

The crystallization of antibodies in complexes with protein A (*Staphylococcus aureus*), protein L (*Peptostreptococcus magnus*) or protein G (*Streptococcus*) offers the possibility of a generic method (Stura et al. 2001) but is unsuitable for a pharmaceutical application in a drug product for several reasons.

Altus describes the crystallization of full antibodies, single chain Fv fragments and Fab fragments in its patent application (Shenoy 2002), with Rituximab, Trastuzumab, and Infliximab as examples. At first using commercial crystallization kits, the suitable conditions are determined in a microbatch screening. Antibody crystals obtained through vapor diffusion technologies are introduced into the batch processes as seeds. Crystallization inducers include PEG 300–8000, glycerol, MPD (2-methyl-2,4-pentanediole), 2-ethoxyethanole, 1,2-propanediole (propyleneglycol), imidazole, 2-propanol, calcium actetate, sodium sulfate, lithium sulfate, usually in mixture, together with sodium acetate, HEPES, TRIS, CHES (2-[N-cyclohexylamino] ethanesulfonic acid), MES and other buffering substances. The presence of polysorbate 80 did not inhibit the crystallization process, and the total time was approximately 24 h. Protein crystals were also included in polymeric matrices such as SAIB (in ethanol). The yields at batch scale amounted to >80% (no information as regards the scale). No degradation was observed by SDS-PAGE, HPLC, and Western Blot and binding activity was retained (Miller 2001). Examples of the crystal morphologies obtained are shown in Figure 10-7a (Yang et al. 2003).

The main disadvantage of crystallization to transfer proteins into the solid state lies in the lack of generic approaches. Typically the optimal crystallization conditions for the individual protein must be discovered in extensive pretests at a microbatch scale using microtubes or microvessels (Shenoy 2002). Basically with the protein size, degree of glycosylation, and the percentage of flexible loops, the difficulty in finding suitable crystallization agents increases.

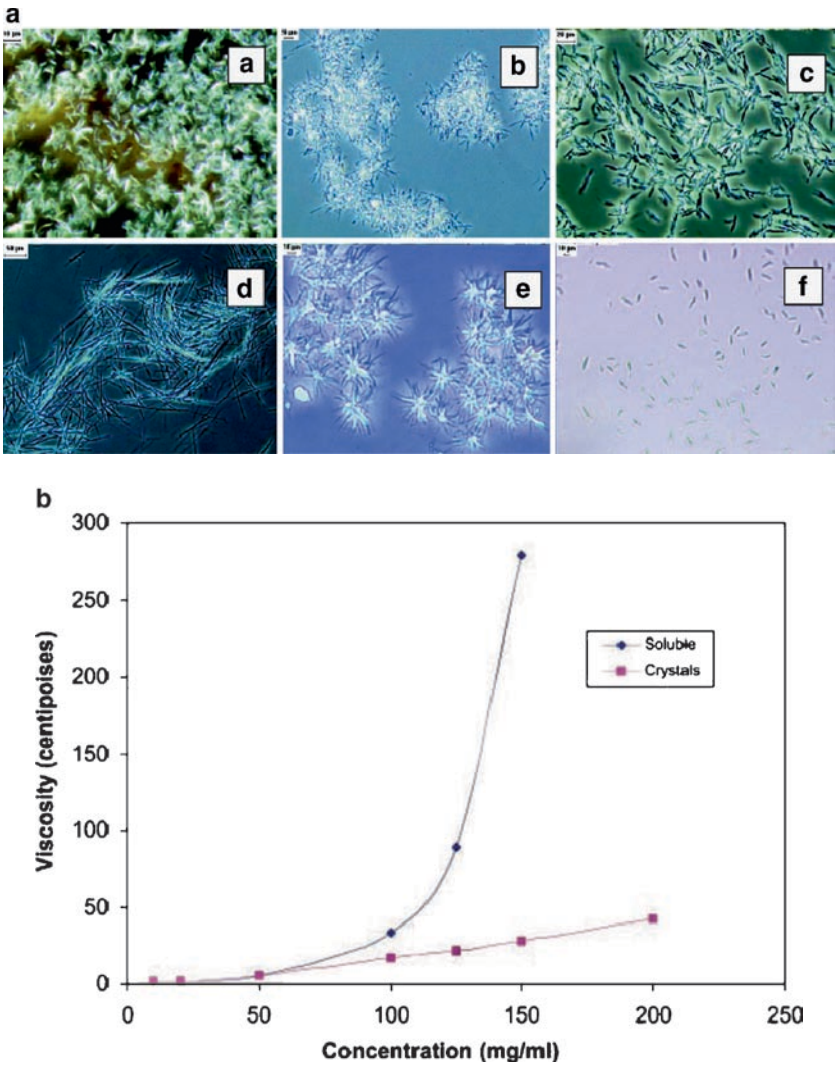

Fig. 10-7. (**a**) Microscopic aspect of diverse crystallized mAbs; Crystals of rituximab (A,B), trastuzumab (C,D) and infliximab (E,F) using 12–35% PEG 400 + 0–10% PEG 8000 (A–E) or 10% isopropanol for induction of crystallization (Yang et al. 2003; Copyright 2003 National Academy of Sciences, USA). (**b**) Viscosity of an increasingly concentrated infliximab solution in polysorbate 80- sucrose-phosphate buffer compared to a crystalline suspension in 10% ethanol, 10% PEG 3350, 0.1% polysorbate 80, 50 mM trehalose and 50 mM phosphate buffer (Yang et al. 2003; Copyright 2003 National Academy of Sciences, USA)

On the other hand, protein crystallization can offer some advantages when compared with other dehydration techniques. Additional purification can be obtained by the exclusion of impurities from the crystal lattice, if these impurities do not inhibit the crystallization. Genentech developed a purification process for a recombinant therapeutic protein via crystallization (Bean and Matthews 2007). The crystallization step could be scaled up and integrated

into production with high yields and excellent purity. The crystallized protein could also be stored as a bulk drug substance.

Modulating the rate of dissolution of the crystals by adjustment of protein crystal size and morphology can also alter the pharmacokinetics of a crystal suspension (Miller 2001; Yang et al. 2003).

Protein crystals are useful in the production of low viscosity, high concentration formulations for s.c. administration, through a 26-gauge needle (Yang et al. 2003). As Figure 10-7b demonstrates, even concentrations as high as 200 mg/mL show a viscosity of only about 50 cP when Infliximab is prepared as crystal suspension, compared with >250 cP in a 150 mg/mL solution.

Crystallization can also improve storage stability (Shenoy et al. 2001). Brange et al. (1992) examined the stability of insulin in neutral solution with respect to deamidation at Asn^{B3} through formation of isoAsp and Asp derivatives. The transformation at B3 was clearly reduced in the crystalline state (zinc insulin, NPH = Isophane) in comparison to the amorphous or dissolved state, which was explained by the reduced flexibility of the tertiary structure and thus reduced formation of the cyclic imide (Figure 10-8). Comparable mechanisms can be exploited for monoclonal antibodies: The stability of a monoclonal antibody crystal was examined at a 100 mg/mL concentration

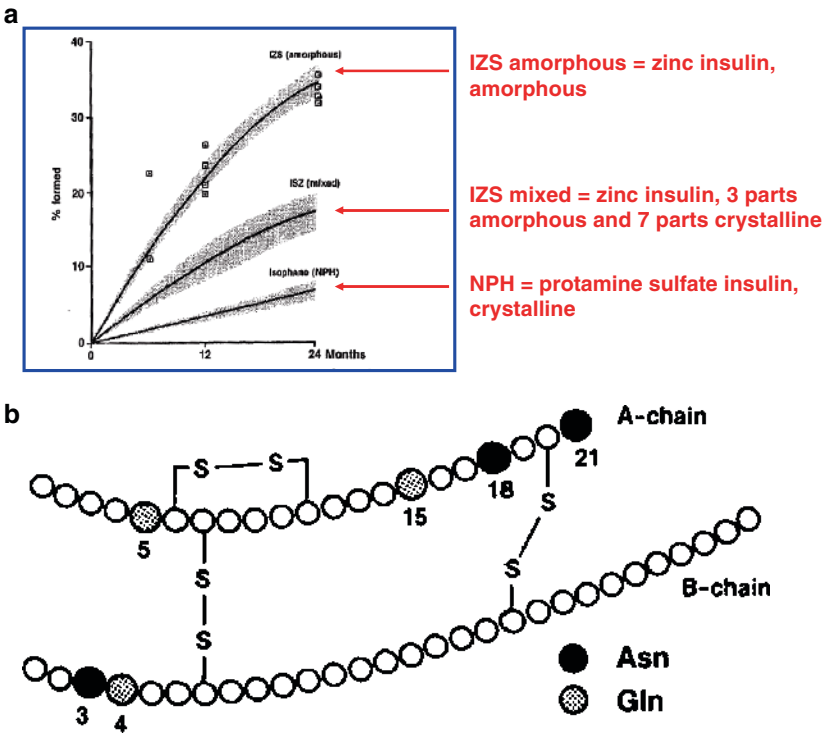

Fig. 10-8. Improved insulin stability by transition into crystalline state. (**a**) Time course of formation of hydrolysis products during storage at 25°C of different types of pharmaceutical insulin suspensions (all porcine insulin). IZS amorphous, IZS mixed and Protamine Sulfate Insuline. (**b**) Primary structure of insulin with indications of the amino acid residues prone to deamidation (Brange et al. 1992)

and after the incubation at room temperature for a month. The integrity of the antibody was well maintained as demonstrated by SDS-PAGE (Miller 2001).

3.2. Precipitation: Protein Coated Microcrystals

Protein coated microcrystals (PCMC) (Figure 10-9), and DNA coated microcrystals (DCMC) develop, if an aqueous buffered solution of a protein in which a carrier material is solved like the amino acids valine, glutamine or histidine, or a sugar is introduced rapidly into a water-miscible organic solvent such as propan-1-ol, propan-2-ol, ethanol, ethyl lactate, 2-methyl-2,4-pentanediol, or 1,5-pentanediol. The carrier material, its concentration and the organic solvent must be selected in such a way that the carrier material precipitates to a large extent as soon as the mixture is prepared. Protein solution and carrier material solution can also be added separately in a three line system which had proven to be the best option in experiments with bovine IgG because of better control of the protonation state (Partridge et al. 2006; Moore and Vos 2006).

In a related patent application (Moore et al. 2000), it is emphasized that the desired rapid protein dehydration is only achieved if the aqueous phase is added to a surplus of organic solvent and not the other way round as typical for protein crystallization procedures described in Sect. "Crystallization." The rapid removal of the water causes the protein to precipitate in amorphous form and as fine particles, since for kinetic reasons, no crystal growth can occur after nucleation. The resulting water content after addition of the aqueous solutions to the precipitation agent should not exceed 10% (Moore et al. 2004).

The carrier material, which is present in the aqueous phase at a concentration close to its saturation point preferentially forms crystals. The amorphous protein settles on the hydrophobic surfaces of the crystals and prevents the further increases in crystal size, due to Ostwald ripening. The resulting protein coated microcrystals are relatively small with diameters ranging from 1 to 100 μm.

For small scale studies, the procedure can be performed as batch process while for larger batches at pilot to production scale the continuous mode using static or dynamic mixers is preferred. Because of the short process times needed for protein dehydration, kilograms of PCMC can be manufactured within a few hours. After the precipitation process, the PCMC can be separated from the aqueous solvent mixture by decanting, filtration, or sedimentation procedures and washed, dried, or resuspended in another nonsolvent mixture.

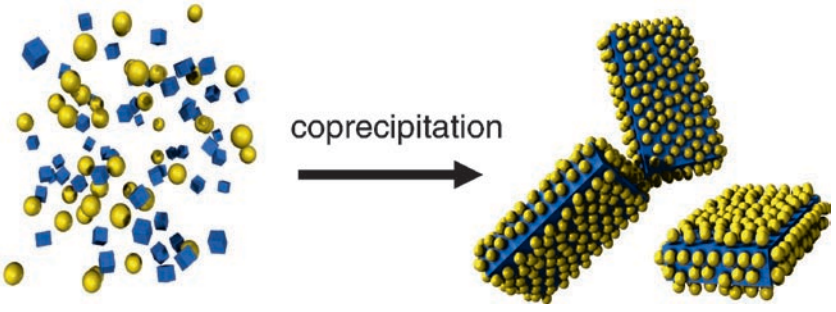

Fig. 10-9. Schematic drawing of coated microcrystals (source: website of XstalBio)

The investigation by Atomic Force Measurement (AFM) of trypsinogen-DL-valin PCMC showed that the protein fraction accumulates in the form of larger aggregates on the surfaces of the carrier material. The aggregates could deform and shift during the contact mode of the measuring procedure indicating that a strong bond to the carrier material is unlikely.

A crucial question is whether the processing into PCMC adversely affects the protein integrity and bioactivity. Water molecules, which are necessary for the preservation of the protein structure, could be extracted in the rapid dehydration process. Contrary to lyophilized or spray dried products, no embedding into an amorphous or partly amorphous matrix in the presence of water substitutes occurs. In addition, the induced protein aggregation could be irreversible. Investigations with a special solid state circular dichroism technology in the range of 190–310 nm wavelength showed only small structural changes of the model protein Subtilisin Carlsberg immobilized on K_2SO_4 in the comparison to the aqueous solution (Partridge et al. 2005a, b) (Figure 10-12). On the other hand, with Subtilisin immobilized on valine, it was seen that with final water contents of <5% the storage stability was worsened, since structural water molecules needed for the long term preservation of the conformation were removed (Partridge et al. 2005a, b). With a highly effective therapeutic cytokine, different formulations and process modes were tested and the developing PCMC placed in stability chambers after drying. In this case, the PCMC were very stable when using amino acids as a carrier: No changes in bioactivity or monomer content after reconstitution was observed with the protein either immediately after processing or after 2 months of storage at 40°C (Figure 10-10a and b). The stabilization of PCMC outside a glass matrix is explained by "solvent annealing," whereby during the rapid dehydration process polar solvent molecules are able to lower the barrier between conformational states and allow the protein to anneal to a stable (local) dry-state conformation (Partridge et al. 2005a, b).

Also physical stability was very good. After 2 months of storage at 25°C and 60% relative humidity, no change in aerodynamic particle size was found (Figure 10-10c). The physical stability of particle size and morphology also under influence of moisture represents a substantial advantage in relation to amorphous spray-dried particles.

Protein loading rates ranged from <<1% up to 40%. Besides the carrier material and the employed solvent, the type of protein and the loading rate have an influence on the developing particle size as well as on the morphology of the particles (Partridge et al. 2007; Figure 10-11). Further process parameters such as water content, pH value, temperature, and mixing conditions can further influence the particle characteristics (Partridge et al. 2005a, b; Lyle et al. 2006).

The careful adjustment of pH during crystallization is an important process parameter (Partridge et al. 2005a, b; Partridge et al. 2007). The PCMC process is a technology which has potentially broad applications and is suitable for a very wide spectrum of biomolecules from small proteins and nucleotides to monoclonal antibodies (Kreiner et al. 2005) (Table 10-4). In addition to applications as an alternative to lyophilization or spray drying, applications using PCMC in downstream processing involving molecular imprinting or for stabilization of biocatalysts in solvents are conceivable (Brown et al. 2006; Kreiner et al. 2001).

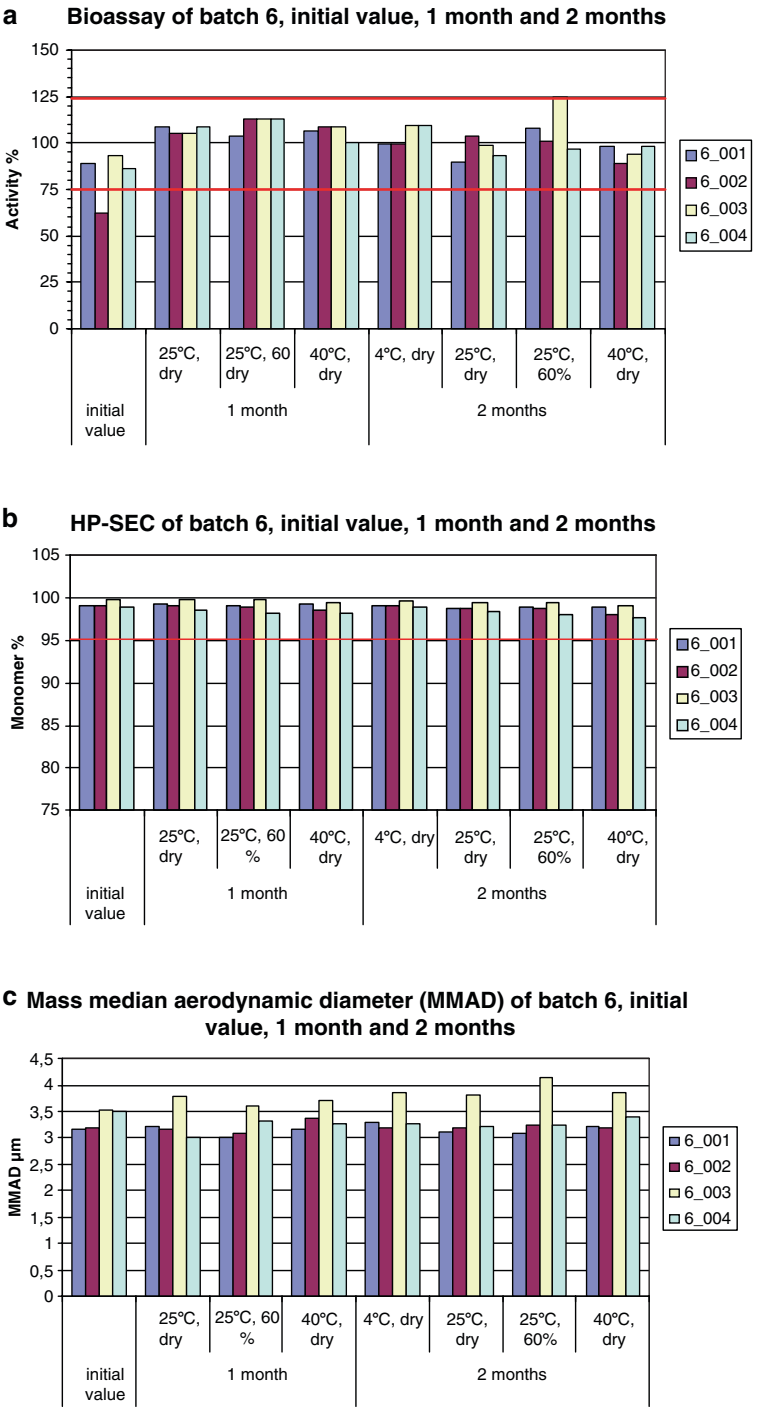

Fig. 10-10. PCMC with a cytokine as precipitated protein and DL-valine as carrier. Biological activity (**a**), monomers/aggregates via HP-SEC (**b**) and aerodynamic properties as mass mean aerodynamic diameter (**c**) after storage at various temperatures (Bechtold-Peters 2005)

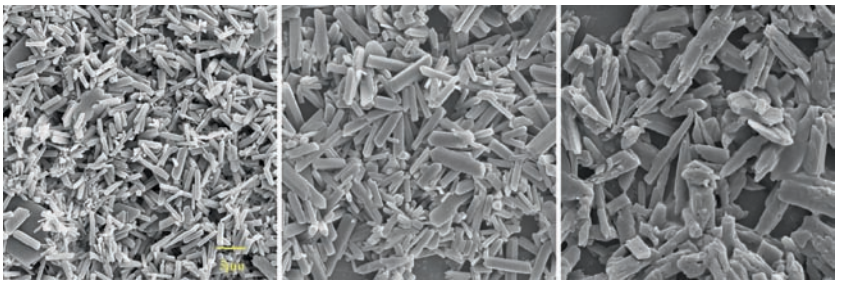

Fig. 10-11. Variation of protein payload 0.11% (*left*), 11.7% (*middle*) and 28.6% (*right*) increases crystal size and impacts on morphology of the crystals. Model protein cytochrome C (Partridge et al. 2007)

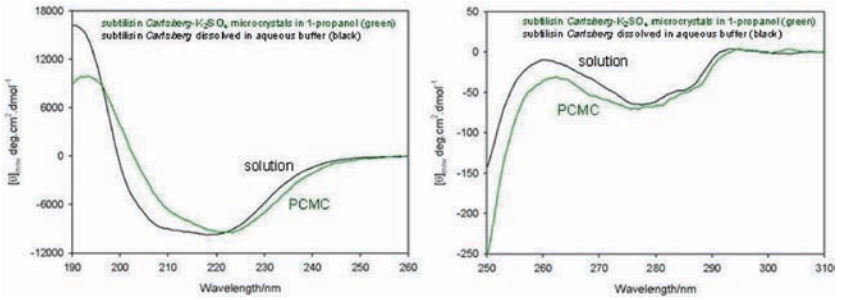

Figure 10-12. CD spectra of subtilisin Carlsberg coated onto K_2SO_4 microcrystals and suspended in propanol similar to CD spectra of the enzyme in aqueous solution (Partridge et al. 2005a, b)

Table 10-4. Macromolecules successfully transformed into PCMC at XstalBio or Boehringer Ingelheim.

Protein class	Example
Small proteins	Insulin Lysozyme, Cytochrome-c
Medium proteins	Adenosine deaminase Hyaluronidase α-1-Antitrypsin
	Glucose oxidase
	Proteases such as trypsin and trypsinogen
	Lipases
	Cytokines
Large proteins	Various antibodies (therapeutic and model antibodies) of the IgG-type
	BSA, Ovalbumine
	Lactate dehydrogenase
	Catalase
Vaccines	Tetanus toxoid, diptheria toxoid, rPA (anthrax) Adenylate cyclase toxin
DNA, RNA	Oligonucleotides, plasmids

3.3. Precipitation: Technospheres

A well characterized small organic molecule, 3,6-bis(N-fumaryl-N-(n-Butyl) amino)-2,5-diketopiperazine (FDKP), was found to self-assemble into microspherical particles (Figure 10-13). The basic solution of FDKP generates microspherical aggregates, when the pH of the solution is reduced. The microspherical aggregates rapidly dissociate back into single small molecules when the solution pH is raised with a base or under physiological conditions in the blood stream at neutral pH. The technique is described in US patent 5,503,852 (Steiner et al. 1996; Kaur et al. 2007).

This reversible microsphere formation process has applications in drug delivery because both low molecular weight drugs and proteins, can be encapsulated into the microsphere matrix. For example, glucagon, usually a very fast degrading peptide which must be administered immediately after the reconstitution of the lyophilized product, could be formulated into a sufficiently stable solution for infusion. Currently, the use of the technology is more focused on pulmonary delivery of insulin, PTH, or GLP-1 (Pfützner et al. 2002, 2003), but parenteral applications have also been published (Lian et al. 2000). Undisclosed data demonstrate excellent physical stability of the generated particles even at elevated temperatures and humidity.

3.4. Precipitation: Supercritical or Near-Critical Procedures

Super- or near-critical precipitation procedures can be differentiated into procedures in which a substance dissolved in dense gas precipitates by expansion (RESS = rapidly expansion of supercritical solutions) or in which only the solvent of the substance is removed by supercritical extraction (GAS = gas antisolvent). The latter are called antisolvent procedures and lead to

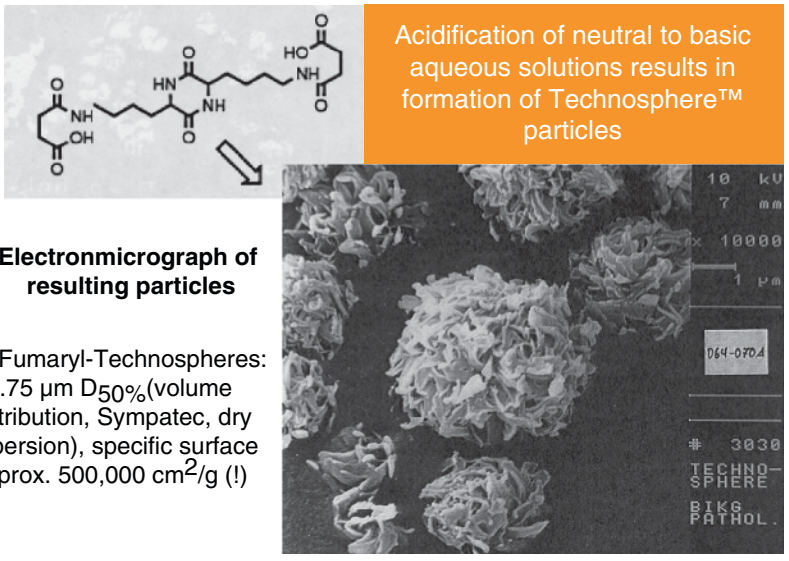

Fig. 10-13. Technospheres™ – mechanism of formation and scanning electron microscopical picture of resulting particles (Bechtold-Peters 2005)

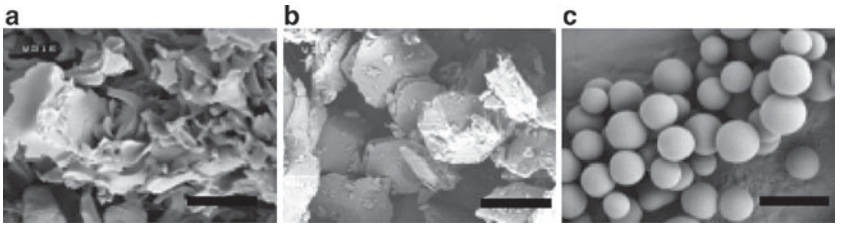

Fig. 10-14. Insulin produced by (**a**) isoelectric point solution precipitation (200 µm), (**b**) lyophilization (12 µm) and (**c**) the GAS process (2 µm) (Thiering et al. 2000)

discrete, spherical particles as shown in Figure 10-14. Since proteins are too hydrophilic to dissolve in the commonly used supercritical CO_2 (supercritical temperature 31°C at approx. 73 bar) under moderate conditions (<60°C, <300 bar) (Foster et al. 2003), only anti-solvent processes are suitable for these types of molecules.

Antisolvent procedures include Solution Enhanced Dispersion by Supercritical Fluids (SEDS), Aerosol Solvent Extraction System (ASES), Precipitation using Compressed Antisolvent (PCA), or Supercritical Antisolvent System with Enhanced Mass Transfer (SAS-EM). These all involve atomization of protein solutions through suitable nozzles and result in a particulate product. A good overview over existing supercritical precipitation techniques and related basic equipment designs is given by Vemavarapu et al. (2005) and Jung and Perrut (2001). The particle size spectrum ranges from submicron (Thiering et al. 2000) without spraying up to several microns (Jovanovic et al. 2008a, b) for sprayed product. Protein particles size, size distribution, and morphology depend on the conditions selected including temperature, pressure, and composition of the supercritical fluid (Jung and Perrut 2001). The conditions usual for the processing of sensitive active substances such as proteins can be selected to be sufficiently mild (Thiering et al. 2000). Often modifiers such as ethanol or methanol must be added to the carbon dioxide in order to improve the dissolution power of the supercritical fluid under constant pressure-temperature conditions. Finally, supercritical gas is also suitable for extraction of residual solvents in product derived from other manufacturing procedures such as the protein coated microcrystals described in Sect. “Precipitation: Protein Coated Microcrystals.”

Although most publications deal with rather small proteins such as lysozyme (14 kDa), insulin (6 kDa), or myoglobin (17 kDa) as model proteins (Thiering et al. 2000; Jovanovic et al. 2004, 2008b), there exist a few studies, using monoclonal antibodies. Supercritical carbon dioxide was used as an antisolvent for producing recombinant human immunoglobulin G (rIgG) particulate powders. In a PGSS-type process (particles from gas saturated solutions), liquid CO_2 was premixed with ethanol to create a single-phase, modified supercritical fluid (SCF). The modified SCF was then vigorously mixed with a pharmaceutically acceptable, aqueous formulation of rIgG, and the mixture was immediately atomized into a pressurized vessel where rapid expansion of the modified SCF extracted the aqueous phase, resulting in the precipitation of the protein powder. Attempts to characterize particle size and

morphology were confounded due to the extremely deliquescent nature of the powders, causing them to rapidly absorb moisture and become gummy. Operational conditions were optimized to a point which yielded powders that were completely soluble, and had SEC profiles indistinguishable from those of the starting solution. Antigen binding activities of the powders, however, were ≤50% of expected levels, revealing the need for improvement of this SCF processing approach for rIgGs (Nesta et al. 2000).

In a more successful study, Jovanovic et al. (2008a) showed that by adjusting the process conditions of an ASES-type process, polyclonal human serum IgG could be supercritically dried without significant formation of insoluble or soluble aggregates. Dimer formation and monomeric content were comparable to freeze-dried product. The successful precipitation and extraction conditions were 37°C/100 bar for pure CO_2 or 20°C (below the critical temperature)/100 bar for CO_2 modified by addition of 25% ethanol. Aqueous solutions of the IgG containing either trehalose or HP-β-cyclodextrin were sprayed into the pressure chamber with sub- or supercritical carbon dioxide. Addition of a buffer not soluble in the supercritical CO_2 turned out to be necessary for the recovery of soluble protein. Excellent storage stability data even at 40°C were obtained as Figure 10-15 reveals (Jovanovic et al. 2008a). An intensive study was performed by Bouchard et al. (2008) to evaluate various matrix formers for their physical stability and suitability as excipients after supercritical fluid processing under conditions comparable to those described earlier.

Solution Enhanced Dispersion by Supercritical fluids (SEDS) has been also used to produce dry particulate formulations of two antibody fragments, D1.3Fv and 4D5Fab (Sarup et al. 2000). Loss of activity was experienced with both of the antibody fragments. Activity loss was reduced by choice of solvent and temperature.

Finally, several years ago, a technology called supercritical carbon dioxide-assisted aerosolization coupled with bubble drying was developed by Sievers et al. This process involves mixing an aqueous stream containing the drug and any water soluble excipients and a stream of supercritical CO_2 inside a low dead volume tee. The emulsion is allowed to expand out of the capillary restrictor, resulting in the aerosolization of the aqueous solution. Sievers and coworkers show as examples how lysozyme and lactate dehydrogenase were dried in the presence of sucrose as stabilizer using this process. LDH could be stabilized throughout the nebulization, drying, and rehydration processes with the addition of sucrose. Almost complete preservation of activity was achieved with the further addition of a surface active agent, such as Tween 20, to the aqueous formulation prior to processing (Sellers et al. 2001).

4. Immobilization on Carriers: An Outlook into Adjacent Areas

In the strict sense, the PCMC technology already described under Sect. “Precipitation: Protein Coated Microcrystals” falls into this area of protein immobilization, since amorphous protein is fixed onto a carrier.

In this section, however, an outlook will be given into such procedures in which the proteins are held to the carrier by stronger forces such as covalent bonding, crosslinking or embedding into a polymeric structure. The examples

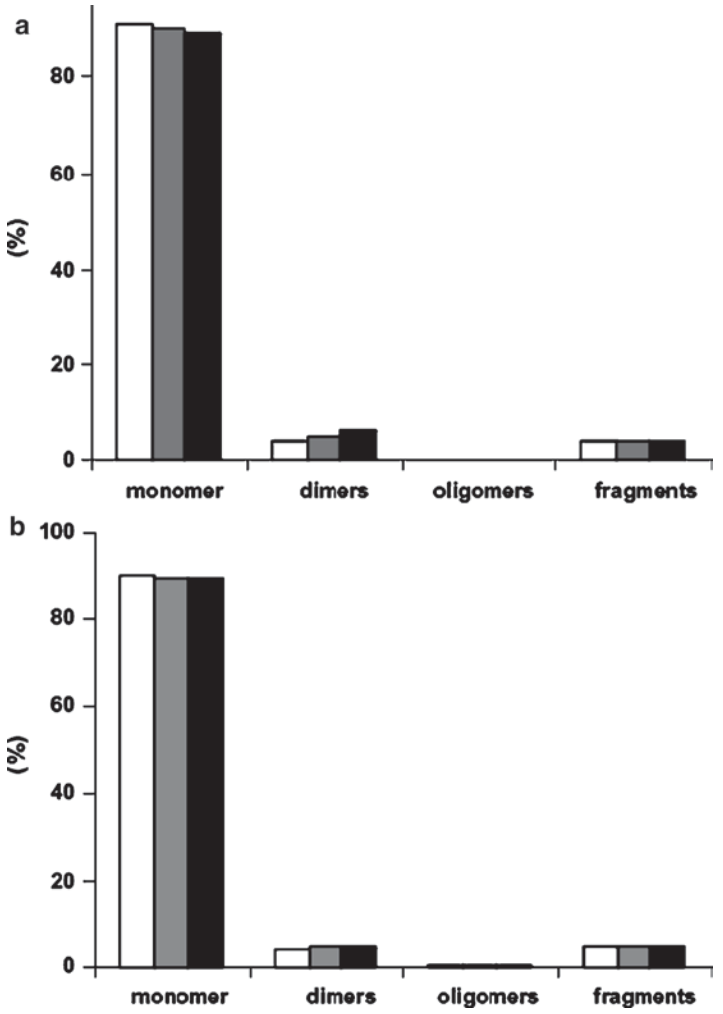

Fig. 10-15. GPC results of SFE dried IgG formulations containing (**a**) HP-ß-CD or (**b**) trehalose (conditions 37°C/100 bar, unmodified carbon dioxide): freshly prepared (*white bars*), stored for 4 weeks at 4°C (*grey bars*) or 40°C (*black bars*). Y-axis represents percentage of total AUC (Jovanovic et al. 2008a)

falling into this category are less likely to be used in pharmaceutical product applications and are more amenable to applications in analytics (chip technology) as well as in industrial enzymes.

A variety of protein immobilization techniques have revolutionized our analytical capabilities in biological research and quality control of biotech-derived compounds:

Antibody immobilization onto a surface while preserving the biologically reactive configuration has been achieved, for example, via self-assembled molecular monolayers (SAM) and plasma-based colloidal lithography creating chemical nanopatterns on the surface of a biosensor. An array of 100-nm wide motifs with hexagonal 2-D crystalline structure was created and shown to have COOH-terminated nanospots in a CH3-terminated matrix (Valsesia et al. 2006). It could

be shown that an ELISA test based on such an array had a signal four times higher as compared with the signal of the nonconstructed functional surface.

In another paper, a new method for immobilization of single proteins for spFRET studies by utilizing streptavidin-biotin and protein L-antibody interactions on glass coverslips coated with PEG is described (Pal et al. 2005). Single-molecule fluorescence studies with high signal/noise ratio are enabled by this method. A bacterial transport protein and the cytoplasmic region of a mammalian transporter were immobilized with high specificity.

Finally, a patent application by Remacle and Michel (2005) claims that incorporating polyols such as mannitol into solutions for spotting onto analytical arrays increases the time-dependent and thermal stability of the proteins spotted onto the support thus conserving the micro-array for quantitative multiparametric analysis after a long storage period. Appropriate arrays were PCR Creative chips (epoxide chemistry), Diaglass (aldehyde chemistry), or Oligo Slides (epoxide chemistry).

A summary of options for enzyme stabilization by immobilization is shown in Figure 10-16 (Gianfreda and Scarfi 1991). In the paper referenced, immobilization is considered an excellent method for enzyme stabilization. Several techniques, on the basis of chemical binding or physical retention, have been developed:

- Binding of enzyme molecules to carriers by covalent bonds, e.g., Carboxypeptidase A to styrene-maleic anhydride support (Dua et al. 1985)
- Binding of enzyme molecules to carriers by adsorptive interactions
- Entrapment into gels, beads, or fibers
- Crosslinking or co-crosslinking with bifunctional reagents, e.g., as CLECs (crosslinked enzyme crystals), CLEAs (crosslinked enzyme aggregates) or so-called Spherezymes (Cao et al. 2003; Sheldon 2007; Brady et al. 2008)
- Encapsulation in microcapsules or membranes

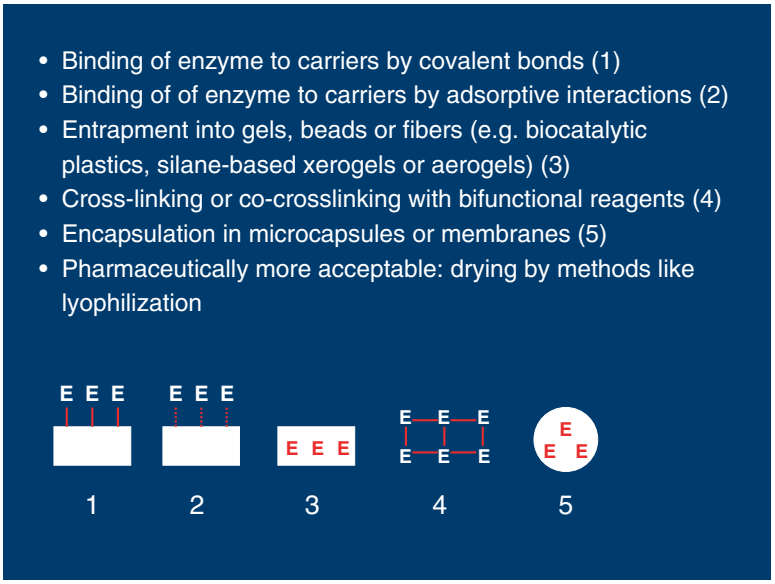

Fig. 10-16. Protein immobilization principles used for (industrial) enzymes (adapted from Gianfreda and Scarfi 1991)

By definition, an immobilized enzyme is a protein physically localized in a certain region of space or converted from a water-soluble mobile state to a water-insoluble immobile one (Gianfreda and Scarfi 1991). Biotechnical applications of immobilized biocatalysts include several fields of general interest beyond pharmaceutical technology, in particular: clinical chemistry (biomarker), enzymatic analysis of organic compounds, food processing, cleaning agents, waste management, enzymatic conversions of petrochemicals, synthetic organic chemistry and energy applications. Finally, immobilized enzymes very closely simulate the state of enzymatic proteins within the intracellular microenvironment of living cells.

- If a considerable conformational change of the enzyme occurs during pH inactivation, then stabilization of the enzyme can be achieved by tightening the structure by means of covalent (mono or multipoint) bindings to an insoluble support or by "cage effects" inside a polymeric gel. Bi- or polyfunctional agents such as glutaraldehyde, diimidate, or dithiols introduce intramolecular crosslinkages into one or more regions of the protein molecule and increase the rigidity of the protein structure. This conformational stabilization is usually encountered in nature where proteins are stabilized by the introduction of intramolecular linkages such as S-S covalent bonds or noncovalent salt bridges.
- If the polymeric support is a polyelectrolyte, local pH value or buffer properties can be obtained and the pH value of the enzyme microenvironments can be very close to the maximum enzyme stability pH. Furthermore, if a polyionic support is used, the concentration of charged ionic groups of the enzyme–adsorbed microenvironment is very high (similar to a concentrated salt solution) and the solubility of oxygen gas, is therefore, reduced by the salting out effect (Gianfreda and Scarfi 1991).
- If the enzymatic reaction to be achieved must take place in an organic solvent environment, forming a suspension of the enzyme in an undissolved state in the organic solvent can be one of the options (Laane 1987). It is assumed that only a small amount of water (a few molecules) is essential to maintain the native, catalytically active conformation of the enzyme. If the organic solvent does not remove the essential water layer, the enzyme will remain "frozen" in its active conformation retaining unaltered catalytic activity (Laane 1987). On the other hand, the sufficiently dehydrated enzymes have high conformation rigidity, and free water molecules usually required in enzyme inactivation processes are lacking. A very nice report on biocatalysis in the industrial production is given by Braun et al. (2006). Here, further possibilities for biocatalysis in organic solvents including enzymatic reactions in liquid crystals are listed.

Acknowledgments: Udo Heinzelmann, Torsten Schultz-Fademrecht and Beate Fischer, Boehringer Ingelheim Pharma GmbH&Co.KG, as well as Johann Patridge, Jan Vos und Barry Moore, XstalBio Ltd.

References

Andya J, Cleland JL, Hsu CC, Lam XM, Overcashier DE, Shire SJ, Yang JYF, Wu SSY (2006) Protein formulation. US Patent US2006275306

Arakawa T, Prestrelski SJ, Kenney WC, Carpenter JF (2001) Factors affecting short-term and long-term stabilities of proteins. Adv Drug Deliv Rev 46:307–326

Asherie N (2004) Protein crystallization and phase diagrams. Methods 34:266–272

Bean BA, Matthews TC (2007) Crystallization of therapeutic proteins and antibodies at Genentech: purification and bulk storage applications. 234th ACS National Meeting, Boston, 19–23 August 2007

Bechtold-Peters K (2005) Precipitation technologies – alternative approach to formulation of proteins for inhalation. Presentation at the AAPS workshop on nasal and pulmonary delivery: technology and future directions, San Francisco Marriott, CA, 9–10 June 2005

Bhatnagarab BS, Bogner RH, Pikal MJ (2007) Protein stability during freezing: separation of stresses and mechanisms of protein stabilization. Pharm Dev Technol 12:505–523

Bouchard A, Jovanic N, Hofland GW, Jiskoot W, Mendes E, Crommelin DJA, Wirkamp GJ (2008) Supercritical fluid drying of carbohydrates: selection of suitable excipients and process conditions. Eur J Pharm Biopharm 68:781–794

Brady D, Jordaan J, Simpson C, Chetty A, Arumugam C, Moolman FS (2008) Spherezymes: a novel structured self-immobilisation enzyme technology. BMC Biotechnol. doi:10.1186/1472-6750-8-8

Brange J, Lankjaer L, Havelund S, Vølund A (1992) Chemical stability of insulin. 1. Hydrolytic degradation during storage of pharmaceutical preparations. Pharm Res 9:715–726

Braun M, Teichert O, Zweck A (2006) Übersichtsstudie Biokatalyse in der industriellen Produktion, VDI, Zukünftige Technologien Nr. 57

Breen ED, Curley JG, Overcashier DE, Hsu CC, Shire SJ (2001) Effect of moisture on the stability of a lyophilized humanized monoclonal antibody formulation. Pharm Res 18:1345–1353

Brown SL, Cormack PAG, Coyle M, Vos J, Moore BD (2006) Biomolecular imprinting using PCMC to produce highly selective binding sites in synthetic polymers. Poster at the AAPS NBC 2006, Boston, MA, 18–21 June 2006

Cao L, van Langen L, Sheldon RA (2003) Immobilised enzymes: carrier-bound of carrier-free? Curr Opin Biotechnol 14:387–394

Chang LL, Shepherd D, Sun J, Ouellette D, Grant KL, Tang XC, Pikal MJ (2005a) Mechanism of protein stabilization by sugars during freeze-drying and storage: native structure preservation, specific interaction, and/or immobilization in a glassy matrix? J Pharm Sci 94:1427–1444

Chang LL, Shepherd D, Sun J, Tang XC, Pikal MJ (2005b) Effect of Sorbitol and residual moisture on the stability of lyophilized antibodies: implications for the mechanism of protein stabilization in the solid state. J Pharm Sci 94:1445–1455

Chen B, Bautista R, Yu K, Zapata GA, Mulkerrin MG, Chamow SM (2003) Influence of histidine on the stability and physical properties of a fully human antibody in aqueous and solid form. Pharm res 12:1952–1959

Dua RD, Kumar S, Vasudevan O (1985) Carboxypeptidase – a immobilization on activated styrene-maleic anhydride systems. Biotechnol Bioeng 27:675–680

Earle JP, Bennett PS, Larson KA, Shaw R (1991) The effects of stopper drying on moisture levels of haemophilus influenzae conjugate vaccine. International symposium on biological product freeze-drying and formulation, Bethesda, USA, 1990. Develop Biol Standard 74:203–210

Foster NR, Dehghani F, Charoenchaitrakool KM, Warwick B (2003) Application of dense gas techniques for the production of fine particles. AAPS PharmSci 5:article 11

Franks F (1998) Freeze-drying of bioproducts: putting principles into practice. Eur J Pharm Biopharm 45:221–229

Gianfreda L, Scarfi MR (1991) Enzyme stabilization: state of the art. Mol Cell Biochem 100:97–128

Gieseler H (2003) Microbalance study of drying rate and morphology of spray freeze-dried powders. Poster at the annual conference of the AAPS 2003. Salt Lake City, UT, 23–30 October 2003

Gieseler H (2004) Product morphology and drying behaviour delineated by a new freeze-drying microbalance. Thesis, University of Nuremberg-Erlangen

Hagewiesche A, Fukami J, Cromwell M, Dinges R (2006) Crystallization of antibodies or fragments thereof. PCT application WO 2006/012500

Hermansen K, Vaaler S, Madsbad S, Dalgaard M, Zander M, Begtrup K, Soendergaard K (2002) Postprandial glycemic control with biphasic insulin aspart in patients with type 1 diabetes. Metabolism 51:896–900

Hofmeister F (1888) Arch Exp Pathol Pharmacol 24:247–260

Jovanovic N, Bouchard A, Hofland GW, Wirkamp GJ, Crommelin DJA, Jiskoot W (2004) Stabilization of proteins in dry powder formulations using supercritical fluid technology. Pharm Res 21:1955–1969

Jovanovic N, Bouchard A, Hofland GW, Witkamp GJ, Crommelin DJA, Jiskoot W (2008a) Stabilization of IgG by supercritical fluid drying: optimization of formulation and process paramaters. Eur J Pharm Biopharm 68:183–190

Jovanovic N, Bouchard A, Sutter M, Van Speybroeck M, Hofland GW, Witkamp GJ, Crommelin DJA, Jiskoot W (2008b) Stable sugar-based protein formulations by supercritical fluid drying. Int J Pharm 346:102–108

Jung J, Perrut M (2001) Particle design using supercritical fluids: literature and patent survey. J Supercritical Fluids 20:179–219

Kreiner M, Moore BD, Parker MC (2001) Enzyme-coated microcrystals: a 1-step method for high activity biocatalyst preparations. Chem Commun 1096–1097, doi: 10.1039/b100722j

Kaur N, Zhou B, Breitbeil F, Hardy K, Kraft KS, Trantcheva I, Phanstiel OA (2007) Delineation of diketopiperazine self-assembly processes: understanding the molecular events involved in N′-(Fumaroyl)diketopiperazine of L-Lys (FDKP) interactions. Mol Pharm 5:294–315

Kogoy JM (2008) http://www.bio.davidson.edu/courses/MolBio/MolStudents/spring2003/Kogoy/protein.html. Accessed June 2008

Kreiner M, Fuglevand G, Moore BD, Parker MC (2005) DNA-coated microcrystals. Chem Commun 2675–2676

Laane C (1987) Medium-engineering for bio-organic synthesis. Biocatalysis 1: 17–22

Lian H, Steiner SS, Sofia RD, Woodhead JH, Wolf HH, White HS, Shen GS, Rhodes CA, McCabe RT (2000) A self-complementary, self-assembling microsphere system: application for intravenous delivery of the antiepileptic and neuroprotectant compound felbamate. J Pharm Sci 89:867–875

Lyle C, Vos J, Partridge J, Moore BD (2006) Hyaluronidase: formulation and stability of dry powder hyaluronidase-coated micro-crystals. Poster at the AAPS NBC 2006, Boston, MA, 18–21 June 2006

Maa YF, Nguyen PA, Sit K, Hsu CC (1998) Spray-drying performance of a bench-top spray dryer for protein aerosol powder preparation. Biotechnol Bioengineer 60:301–309

Matheus S, Mahler HC (2005) Solid forms of anti-EGF-antibodies. PCT application WO 2005/051355

Maury M, Murphy K, Kumar S, Mauerer A, Lee G (2005a) Spray-drying of proteins: effects of sorbitol and trehalose on aggregation and FT-IR amide I spectrum of an immunoglobulin G. Eur J Pharm Biopharm 59:251–261

Maury M, Murphy K, Kumar S, Shi L, Lee G (2005b) Effect of process variables on the powder yield of spray-dried trehalose on a laboratory spray-dryer. Eur J Pharm Biopharm 59:565–573

McCoy AJ (2008) http://www.structmed.cimr.cam.ac.uk/Course/Crystals/Theory/phases.html. Accessed June 2008

McPherson A (1978) The growth and preliminary investigation of protein and nucleic acid crystals by X-ray diffraction techniques. In: Glick D (ed) Methods of Biochemical Analysis. Academic, New York, pp 249–345

McPherson A (1982) Preparation and analysis of protein crystals. Wiley, New York 371

McPherson A, Friedman ML, Halsall HB (1984) Crystallization of alpha 1-acid glycoprotein. Biochem Biophys Res Commun 124:619–624

McPherson A, Shlicta P (1988) Heterogeneous and epitaxial nucleation of protein crystals on mineral surfaces. Science 239:385–387

McPherson A (1999) Crystallization of biological macromolecules. Cold Spring Harbor Laboratory Press, New York, p 586

McPherson A (2001) A comparison of salts for the crystallization of macromolecules. Protein Sci 10:418–422

McPherson A, Cudney B (2006) Searching for silver bullets: an alternative strategy for crystallizing macromolecule. J Struct Biol 156:387–406

Miller D (2001) Crystallization of intact monoclonal antibodies. Poster at the IBC's antibody production and donstream processing conference 2001, San Diego, CA, January 31–February 2, 2001

Moore BD, Parker MC, Halling PJ, Partridge J (2000) Rapid dehydration of proteins. PCT application WO 00/69887

Moore BD, Parker MC, Partridge J, Vos J, Kreiner MM, Stevens HNE, Flores MV (2004) Pharmaceutical composition. PCT application WO 2004/062560

Moore BD, Vos J (2006) Process for preparing microcrystals. PCT application WO 2006/010921

Nesta DP, Elliott JS, Warr JP (2000) Supercritical fluid precipitation of recombinant human immunoglobulin from aqueous solutions. Biotechnol Bioeng 67:457–464

Pal P, Lesoine JF, Lieb AM, Novotny L, Knauf PA (2005) A novel immobilization method for single protein spFRET sudies. Biophys J. doi:10.1529/biophysj.105.062794

Partridge J, Lyle C, Vos J, Parker MC, Moore BD (2005) Antibody-coated microcrystals. Poster at the annual conference of the AAPS 2005, Nashville, TN, 5–10 November 2005

Partridge J, Ganesan A, O'Farell N, Parker MC, Moore BD (2005) Stabilization without sugars. Poster at the annual conference of the AAPS 2005, Nashville, TN, 5–10 November 2005

Partridge J, Vos J, Lyle C, Parker MC, Moore BD (2006) Continuous flow coprecipitation of IgG-coated microcrystals using a novel three-line system. Poster at the AAPS NBC 2006, Boston, MA, 18–21 June 2006

Partridge J, Lyle C, Vos J, Moore BD (2007) Protein coated microcrystal dry powder formulations with payloads of 30 %w/w to 0.01 %w/w. Poster at the AAPS NBC 2007, San Diego, CA, 24–27 June 2007

Pfützner A, Flacke F, Pohl R, Linkie D, Engelbach M, Woods R, Forst T, Beyer J, Steiner SS (2003) Pilot study with technosphere/PTH(1–34) – a new approach for effective pulmonary delivery of parathyroid hormone (1–34). Horm Metab Res 35:319–323

Pfützner A, Mann AE, Steiner SS (2002) Technosphere/insulin – a new approach for effective delivery of human insulin via the pulmonary route. Diabetes Technol Ther 4:589–594

Press release dated May 6, 2006 on: http://www.xstalbio.com/site/press/boehringer/page. Accessed June 2008

Presser I (2003) Innovative online measurement procedures for optimization of freeze-drying processes. Thesis written in German, University of Munich

Remacle J, Michel G (2005) Method for stabilizing proteins on a microarray. US patent application US 2005/0112687
Roy I, Gupta MN (2004) Freeze-drying of proteins: some emerging concerns. Biotechnol Appl Biochem 39:165–177
Sarup L, Servistas MT, Sloan R, Hoare M, Humphreys CO (2000) Shorter communication: investigation of supercritical fluid technology to produce dry particulate formulations of antibody fragments. Food Bioproduct Process 78:101–104
Schüle S, Schultz-Fademrecht T, Bassarab S, Bechtold-Peters K, Garidel P, Friess W (2005) Development of an huIgG 1 Formulation for Inhalative Application. Poster at the AAPS NBC 2005, San Diego, CA, 24–27 June 2005
Schüle S (2005) Stabilization of antibodies in spray-dried powders for inhalation, Chapter 3.3.2. Thesis, University of Munich
Schüle S, Friess W, Bechtold-Peters K, Garidel P (2007) Conformational analysis of protein secondary structure during spray-drying of antibody/mannitol formulations. Eur J Pharm Biopharm 65:1–9
Schüle S, Schultz-Fademrecht T, Garidel P, Bechtold-Peters K, Friess W (2008) Stabilization of IgG1 in spray-dried powders for inhalation. Eur J Pharm Biopharm 69:793–807
Sellers SP, Clark GS, Sievers RE, Carpenter JF (2001) Dry powders stable protein formulations from aqueous solutions prepared using supercritical CO_2-assisted aerosolization. J Pharm Sci 90:785–797
Shamblin SL, Hancock BC, Zografi G (1998) Water vapor sorption by peptides, proteins and their formulations. Eur J Pharm Biopharm 45:239–247
Sheldon RA (2007) Enzyme immobilisation: the quest for optimum performance. Adv Synth Catal 349:387–394
Shenoy B, Wang Y, Shan W, Margolin AL (2001) Stability of Crystalline Proteins. Biotechnol Bioeng 73:358–369
Shenoy B (2002) Crystals of whole antibodies and fragments thereof and methods for making and using them. PCT application WO 02/072636
Steiner SS, Rhodes CA, Shen GS, McCabe RT (1996) Method for making self-assembling diketopiperazine drug delivery system. US patent US5,503,852
Stura EA, Graille M, Charbonnier JB (2001) Crystallization of macromolecular complexes: combinatorial complex crystallization. J Cryst Growth 232:573–579
Tang XC, Nail SL, Pikal MJ (2005) Freeze-drying process design by manometric temperature measurement: design of a smart freeze-dryer. Pharm Res 22:685–700
Thiering R, Dehghani F, Foster NR (2000) Micronization of model proteins using compressed carbon dioxide. Proceedings of the 5th international symposium on supercritical fluids, Atlanta, GA
Valsesia A, Colpo P, Meziani T, Lisboa P, Lejeune M, Rossi F (2006) Immobilization of antibodies on biosensing devices by nanoarrayed self-assembled monolayers. Langmuir 22:1763–1767
Vemavarapu C, Mollan MJ, Lodaya M, Needham TE (2005) Design and process aspects of laboratory scale SCF particle formation systems. Int J Pharm 292:1–6
Wang W, Singh S, Zeng DL, King K, Nema S (2007) Antibody structure, instability and formulation. J Pharm Sci 96:1–26
Website of Avant Immunotherapeutics, http://www.avantimmune.com. Accessed June 2008
Website of XstalBio, http://www.xstalbio.com. Accessed June 2008
Yang MX, Shenoy B, Disttler M, Patel R, McGrath M, Pechenov S, Margolin AL (2003) Crystalline monoclonal antibodies for subcutaneous delivery. Proc Natl Acad Sci USA 100:6934–6939
Zhu DW, Garneau A, Mazumdar M, Zhou M, Xu GJ, Lin SX (2006) Attempts to rationalize protein crystallization using relative crystallizability. J Struct Biol 154:297–302

Part V

Analytics and Specification Setting for MABS

Chapter 11

Characterizing High Affinity Antigen/ Antibody Complexes by Kinetic and Equilibrium Based Methods

Andrew W. Drake, David G. Myszka, and Scott L. Klakamp

Abbreviations

pM	picomolar
nM	nanomolar
fM	femtomolar
mAb	monoclonal antibody
K_D	equilibrium dissociation constant
k_a	association rate constant
k_d	dissociation rate constant
Fc	Flow cell
RU	resonance units
Da	Dalton
cy5	Indodicarbocyanine
pAb	polyclonal antibody
surfactant P-20	poly(oxyethylene)(20)-sorbitane monolaureate

1. Introduction

The development and application of monoclonal antibodies as drugs requires accurate and precise characterization of the antigen/antibody binding constants. Anticipating the required affinity for a therapeutically efficacious monoclonal antibody (mAb) is complex. Generally, the equilibrium dissociation constant for the antigen/mAb complex should be less than 100–1,000 picomolar (pM), depending upon the nature of the target, the desired function of the antibody, and the localized concentration of the antigen in the diseased tissue, among other factors. Measurement of the equilibrium dissociation constant (K_D), association rate constant (k_a), and dissociation rate constant (k_d) for these high affinity antibodies is difficult because of three independent reasons: (1) the time

Reprinted from Analytical Biochemistry 328 , Drake, A.W., Myszka, D.G., and Klakamp, S.L., "Characterizing high-affinity antigen/antibody complexes by kinetic- and equilibrium-based methods", 35-43, 2004, with permission from Elsevier.

From: *Current Trends in Monoclonel Antibody Development and Manufacturing,* Biotechnology: Pharmaceutical Aspects, DOI 10.1007/978-0-387-76643-0_11,
Edited by: S.J. Shire et al.

for the antigen/antibody complex to reach equilibrium can be very long, on the order of days (2) usually, the k_d for such a tight complex is extremely low, requiring long periods of data collection in order to discern enough information to predict complex stability, and (3) in cases where the k_d is easily measurable (greater than $5 \times 10^{-4}\,s^{-1}$), the k_a can be very fast, greater than $1 \times 10^{7}\,M^{-1}s^{-1}$.

Two biophysical methods that are gaining acceptance for characterizing high affinity interactions are Biacore and KinExA. With Biacore, one reactant is immobilized onto a biosensor chip and the other reactant is flowed across the surface, while the binding of the two reactants is followed in real time by surface plasmon resonance (Karlsson and Falt 1997; Myszka 1997; Morton and Myszka 1998; Myszka 1999; Rich and Myszka 2001; Rich and Myszka 2002; Roskos et al. 2007). For most high affinity interactions the association rate constant k_a and dissociation rate constant k_d are determined directly, and the K_D is calculated by the quotient of the rate constants, k_d/k_a.

KinExA®, which is short for the Kinetic Exclusion Assay, differs from Biacore in that it is a solution-based method and requires a secondary fluorescent reporter molecule (Blake et al. 1996, 1999; Chiu et al. 2001; Ohmura et al. 2001; Jones et al. 2002). The KinExA instrument is a flow spectrofluorimeter in which equilibrated solutions of an antigen/antibody complex are flowed over a bead pack with immobilized antigen or another mAb capture reagent. Detection of the free mAb from the equilibrated solution once flowed through the resin is accomplished with a secondary species-specific polyclonal antibody (pAb) that is fluorescently labeled. The KinExA instrument is also capable of determining directly the k_a by quantitating the decrease of free mAb as a function of time as an antigen/antibody solution approaches equilibrium. The k_d cannot be directly measured by KinExA instead, it is calculated from the product of $k_a \times K_D$.

In this chapter, we compare Biacore and KinExA for their ability to determine binding constants for very stable antibody/antigen complexes. We characterized a set of three different antigens and two different mAbs that span an affinity range of nanomolar (nM) to picomolar (pM). We show that if proper experimental methods for both Biacore and KinExA are used, the kinetic and thermodynamic binding constants measured between surface-based and solution-based biophysical methods are similar.

2. Materials and Methods

2.1. Instrumentation

All surface plasmon resonance experiments were performed using Biacore 2000 and Biacore 3000 optical biosensors (Biacore, Inc., Piscataway, NJ). All Kinetic Exclusion Assays were performed using a KinExA 3000 instrument (Sapidyne Instruments, Inc., Boise, ID).

2.2. Reagents

A corporate partner provided antigen-1 (Ag-1), which is a monomeric protein of molecular weight (MW) = 47 KDa. Antigens 2 and 2′ (Ag-2 and Ag-2′) are monomeric polypeptides of MW = 9.4 and 4.1 KDa, respectively and were purchased from Bachem Peninsular Labs (San Carlos, CA). Antibodies (mAbs-1 and -2) were fully human mAbs produced from XenoMouse® mice (see below). Alum (1452-250) was purchased from Superfos Biosector A/S (Vedbaek, Denmark). Bovine serum albumin (BSA) fraction V (BP1605-

100) was purchased from Fisher Scientific (Pittsburgh, PA). DMEM culture medium (51444) was obtained from JRH Biosciences (Lenexa, KS). Titermax (T-2684) and OPI media supplement (O-5003) were purchased from Sigma Chemical Co. (St. Louis, MO). Fetal Bovine Serum (SH30070.03) was purchased from Hyclone (Logan, UT). A penicillin-streptomycin (400-109) solution was obtained from Gemini Bio-Products (Woodland, CA). IL-6 (1131567) was purchased from Roche (Mannheim, Germany). All other general reagents were purchased from Sigma-Aldrich, Inc (St. Louis, MO).

All antigen and mAb samples for Biacore and KinExA analysis were prepared in vacuum-degassed HBS-P buffer (0.01 M HEPES, 0.15 M NaCl, 0.005% surfactant P-20, Biacore Inc., Uppsala, Sweden) with 100 μg/mL bovine serum albumin (BSA). Biacore amine-coupling reagents, 1-ethyl-3-(3-dimethylaminopropyl) carbodiimide (EDC), N-hydroxysuccinimide (NHS), and ethanolamine were purchased from Biacore, Inc. Biacore aldehyde-coupling reagents (sodium periodate 21,004-8, carbohydrazide C1,100-6, and sodium cyanoborohydride 15,615-9) were purchased from Aldrich (Milwaukee, WI). Biacore surface-regeneration reagents were phosphoric acid (Aldrich 34,524-5) and glycine (10 mM, pH 2.0, Biacore, Inc.). Research grade CM5 and B1 biosensor chips were purchased from Biacore, Inc.

The KinExA detection antibody was Cy5-labeled goat anti-human IgG, Fcγ specific (Jackson ImmunoResearch Laboratories, Inc., West Grove, PA, 109-175-008) diluted 250- to 5,000-fold in HEPES buffer (0.01 M HEPES, 0.15 M NaCl, pH 7.2) from a 0.5 mg/mL stock (1× PBS, pH 7.4). The solid phase particles used for the KinExA experiments were NHS-activated Sepharose 4 Fast Flow beads (Pharmacia Biotech AB, Uppsala, Sweden, 17-0906-01). Prior to reacting the sepharose beads with antigen, a bead stock aliquot of 1.5 mL in a microcentrifuge tube was spun down and washed at least six times with cold deionized H_2O. After rinsing the beads twice with sodium carbonate buffer (0.05 M, pH 9.3), antigen (~20 μg) in sodium carbonate buffer was added to the sepharose. The sepharose/antigen tube was either rocked overnight at 4°C or for at least 4 h at room temperature. After rocking, the sepharose was spun and rinsed twice with 1 M Tris buffer, pH 8.3. The antigen-coated beads were then rocked for 1 h at room temperature in 1 M Tris buffer with 2% BSA.

2.3. Generation of Fully Human Monoclonal Antibodies from XenoMouse® Strains

XenoMouse strains were produced as described previously by Mendez et al. (1997). MAb-1 was prepared using hybridoma technology (Yang et al. 1999; Davis et al. 2003). Briefly, animals aged 8–10 weeks were immunized in the footpad with 10 μg of soluble Ag-1 emulsified in Titermax (25 μL/mouse) for the first injection. The animals were boosted twice per week with 10 μg Ag-1 emulsified with 100 μg Alum. Lymphocytes from the lymph nodes of the animals were fused with P3 myeloma cells by an Electrocell Fusion protocol (Davis et al. 2003). The hybridoma cell line was grown in T75 flasks with 15% FBS, penicillin/streptomycin (100 U/mL/100 μg/mL), OPI media supplement (0.15 g oxaloacetate, 0.05 g pyruvate, 8.2 mg bovine insulin), and 10 U/mL of IL-6 in DMEM medium until 95% cell death to produce a hybridoma exhausted supernatant (Yang et al. 1999). These exhaust supernatants were purified using Protein A.

MAb-2 was produced using XenoMax technology with Ag-2′ for generation of antigen-specific monoclonal antibodies, which combines the use of

B cells from hyperimmunized XenoMouse mice with the culture, screening, and antibody recovery processes of the SLAM technology (Babcook et al. 1996).

2.4. Biacore Measurements

Standard EDC/NHS and carbohydrate coupling was used to covalently immobilize mAbs to a CM5 or B1 sensor chip (BIAapplications Handbook 1998). To minimize mass transport and crowding, mAbs were immobilized at levels that gave a maximum antigen binding response (R_{max}) of no more than 50–100 RU. A reference flow cell on each chip was activated and blocked with no mAb immobilization to serve as a control.

All Biacore kinetic experiments were conducted at 25°C. For each experiment, a series of six to eight antigen concentrations was prepared using two-fold dilutions. Antigen samples were randomly injected over the biosensor surface in triplicate at 100 μL/min. Several buffer blanks were injected intermittently over the course of an experiment for double referencing (Myszka 1999). Each sample and blank were injected for 60–90 s. Dissociation was followed for 5 min. The mAb-1 biosensor surface was regenerated with a 9 s pulse of 146 mM phosphoric acid. Regeneration of the mAb-2 biosensor surface with Ag-2 as the analyte was with a 15 s pulse of 14.6 mM phosphoric acid. Regeneration of the mAb-2 surface with Ag-2′ as the analyte was with a 12 s pulse of 10 mM glycine, pH 2.0. Dissociation data for Ag-2 and Ag-2′ were acquired by alternating three additional injections of the highest antigen concentration with three additional blank injections and following the dissociation phase for 3–4 h.

All Biacore sensorgrams were processed using Scrubber software (Version 1.1f, BioLogic Software, Australia). Sensorgrams were first zeroed on the y-axis and then x-aligned at the beginning of the injection. Bulk refractive index changes were removed by subtracting the reference flow cell responses. The average response of all blank injections was subtracted from all analyte and blank sensorgrams to remove systematic artifacts between the experimental and reference flow cells (Myszka 1999).

CLAMP biosensor data analysis software (Version 3.40, BioLogic Software, Australia) was used to determine k_a and k_d from the processed data sets. Data from all flow cells were globally fit to a 1:1 bimolecular binding model that included a mass transport term (Myszka et al. 1998). The K_D was calculated from the quotient k_d/k_a.

2.5. KinExA Equilibrium Measurements

All KinExA experiments were conducted at room temperature (~22°C). For all equilibrium experiments, antigen was serially diluted into solutions having a constant mAb binding site concentration. For K_D-controlled experiments, the mAb binding site concentration was less than or equal to $3 \times K_D$. An antibody-controlled experiment was performed on the Ag-2′/mAb-2 complex where the mAb-2 binding site concentration was held ~20-fold above K_D while the Ag-2′ concentration range remained identical to the K_D-controlled experiments. Antigen/antibody samples were then allowed to reach equilibrium. For complexes having pM K_Ds, samples were equilibrated at room temperature for as long as 3 days. The sample flow rate for all experiments was 0.25 mL/min and the labeling antibody flow rate was 0.5 mL/min. During a K_D-controlled

experiment, 5 mL of each sample was drawn through the flow cell. A sample volume of 500 μL was analyzed for the antibody-controlled experiment. Two replicates of each sample were measured for all equilibrium experiments. The equilibrium titration data were fit to a 1:1 binding model using KinExA software (Version 2.4, Sapidyne Instruments).

2.6. KinExA Kinetic Measurements

The k_a of the Ag-1/mAb-1 complex was measured by the "injection method" (KinExA 3000 manual 1998). Here, 0.5 mL of mAb-1 at a constant concentration was injected with 0.5 mL of several serially diluted concentrations of Ag-1. The mixing time (17.5 s) for each reaction was dictated by the time required for the KinExA instrument to deliver the solution to the flow cell at a flow rate of 0.5 mL/min. The resulting exponential function of free mAb as a function of antigen concentration was fit in the KinExA software to a reversible bimolecular rate equation. The k_d was calculated from the product $k_a \times K_D$.

Equilibrium approached more slowly in the binding reactions of Ag-2 and Ag-2′ to mAb-2 allowing the "direct method" to be utilized to determine k_a. In this method, the reduction of free antibody concentration was followed as a function of time as an antigen/mAb reaction approached equilibrium. With the "direct method", 1.5 mL of antigen/mAb solution was drawn through the flow cell for each data point at a flow rate of 0.25 mL/min. The labeling antibody flow rate was 0.5 mL/min. The time between data points was 12 min. The resulting exponential function of free mAb as a function of time was fit in the KinExA software to a reversible bimolecular rate equation. As before, the k_d was calculated from the product $k_a \times K_D$.

3. Results

3.1. Antigen-1/Antibody-1 Interaction

MAb-1 was immobilized by amine coupling (see Sect. 11.2) to one flow cell (Fc) of two different Biacore CM5 biosensor chips. Another Fc on each chip served as a control surface for refractive index changes and nonspecific binding by Ag-1, and reacted identical to the experimental Fc, but had no protein immobilized. Surface capacities of mAb-1 on each chip ranged from 440–480 RU, giving a binding response of ~50 RU with Ag-1 (MW = 47 KDa). Triplicate injections of 3.2–101 nM Ag-1 are shown in Fig. 11-1a for a representative Biacore experiment. Three independent Biacore experiments (three antibody immobilized Fcs) were performed with two different CM5 biosensor chips resulting in an average $k_a = 4.6(0.1) \times 10^5\,M^{-1}s^{-1}$, $k_d = 1.2(0.1) \times 10^{-3}\,s^{-1}$, and $K_D = 2.5(0.5)$ nM. The values in parentheses represent the 95% confidence intervals.

Three independent KinExA equilibrium titrations were performed on the mAb-1 system with twelve equilibrated solutions each with 0.033–152 nM Ag-1 and with the total concentration of mAb-1 held constant at 0.54 nM binding site. Each solution was equilibrated for 5 h before free mAb-1 was measured. The binding isotherm fit well to a 1:1 stoichiometric equilibrium model, (Fig. 11-1b shows a representative experiment), and yielded a $K_D = 1.3(0.3)$ nM. With an antigen/mAb complex possessing a K_D near nM, it is not pos-

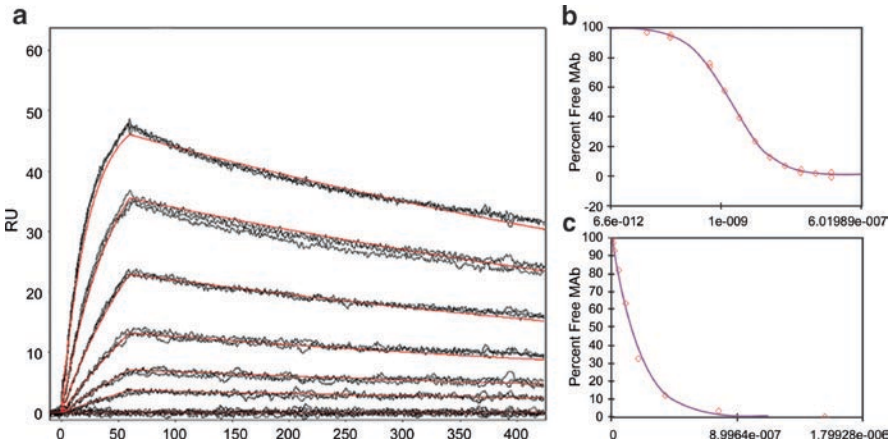

Fig. 11-1. (**a**) Globally fit (red line) Biacore data of antigen-1 binding to immobilized mAb-1. Ag-1 was injected in triplicate from 3.2–101 nM. Dissociation was followed for 5 min, $k_a = 4.2 \times 10^5\,M^{-1}s^{-1}$, $k_d = 1.2 \times 10^{-3}\,s^{-1}$, $K_D = 2.8$ nM (**b**) KinExA titration with 0.54 nM mAb-1 binding site with Ag-1 ranging from 0.033–152 nM, $K_D = 1.3$ nM (**c**) KinExA on-rate "injection method" with 47 nM mAb-1 binding site reacting with 0.75–1,530 nM Ag-1, $k_a = 3.3 \times 10^5\,M^{-1}s^{-1}$

sible to determine the k_a of this interaction by following a solution of antigen and mAb to equilibrium ("direct method") because equilibrium is reached too quickly. Therefore, the k_a is determined by an alternative KinExA method called the "injection method". Fig. 11-1c shows a representative experiment of this type in which 0.75–1,530 nM Ag-1 is mixed rapidly (17.5 s) with 47 nM mAb-1 binding site. The data from three independent experiments were described well by a monoexponential fit that resulted in an average $k_a = 3.3(0.6) \times 10^5\,M^{-1}s^{-1}$. The product of $k_a \times K_D$ gave a $k_d = 4.3(0.7) \times 10^{-4}\,s^{-1}$ for the Ag-1/mAb-1 system.

3.2. Antigen-2/Antibody-2 Interaction

MAb-2 was immobilized by aldehyde coupling (see Sect. 11.2) to three flow cells of a B1 biosensor surface and was used to measure the binding of Ag-2 (9.4 KDa). Surface capacities of mAb-2 ranged from 612 to 749 RU giving an Ag-2 binding response of less than 50 RU. Fig. 11-2a shows triplicate injections of 0.63–40 nM Ag-2 over the mAb surfaces at 25°C for a typical experiment. Owing to the slow k_d observed for Ag-2 dissociation, we followed the dissociation phase for 3 h in triplicate (sensorgrams at right in Fig. 11-2a) with a high concentration of Ag-2 (81 nM). The sensorgrams were reproducible and were fit globally (with local R_{max} values floated for each Fc) for all the Fcs from a single experiment. The binding responses gave an excellent fit to a 1:1 kinetic interaction model with a term for mass transport. In all, five independent experiments, fourteen mAb immobilized Fcs in total, on four different B1 chips were used to determine the binding constants of this interaction. The results of the Biacore kinetic analysis (Table 11-1), yielded an average $k_a = 6.6(1.5) \times 10^5\,M^{-1}s^{-1}$, $k_d = 2.1(0.5) \times 10^{-5}\,s^{-1}$, and $K_D = 33(11)$ pM, calculated from k_d/k_a.

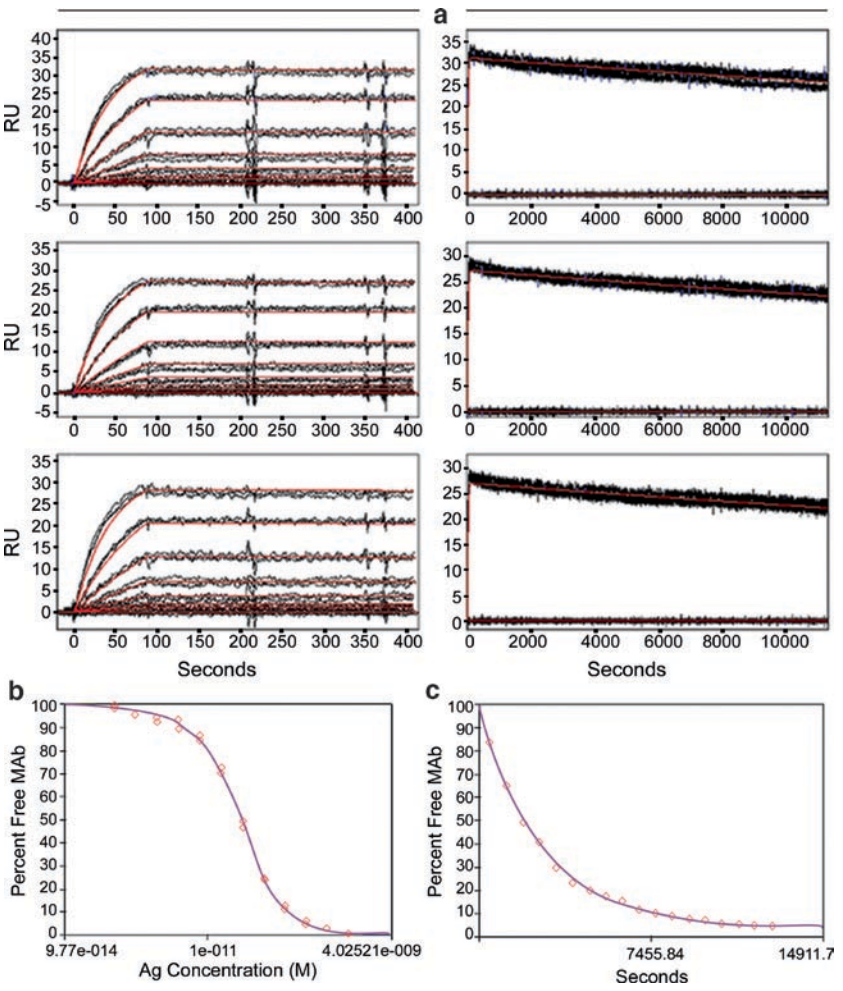

Fig. 11-2. (**a**) Biacore data for antigen-2 binding to immobilized mAb-2. The data was globally fit (*red line*) over three independent flow cells. On-rate data (*left column*) shows triplicate Ag-2 injections ranging from 0.63–40 nM. Off-rate data (*right column*) shows triplicate Ag-2 injections of 81 nM with dissociation followed for 3 h, $k_a = 5.8 \times 10^5\,M^{-1}s^{-1}$; $k_d = 1.8 \times 10^{-5}\,s^{-1}$; $K_D = 31$ pM. (**b**) KinExA titration of 20 pM mAb-2 binding site at equilibrium with 0.49–1,000 pM Ag-2, $K_D = 12$ pM (**c**) KinExA on-rate experiment utilizing the "direct method" with 404 pM Ag-2 reacting with 102 pM mAb-2 binding site every 12 min for ~3.5 h, $k_a = 1.0 \times 10^6\,M^{-1}s^{-1}$

KinExA required two different types of experiments to determine the K_D and kinetic parameters for the Ag-2/mAb-2 interaction. Fig. 11-2b shows a typical equilibrium titration experiment for the Ag-2/mAb-2 complex. These solutions require ~35 h to reach equilibrium at room temperature (*vide infra*). In each titration, free mAb-2 was quantitated in duplicate for twelve solutions at equilibrium with total Ag-2 concentration ranging from 0.49–1,000 pM, and with total mAb-2 concentration constant at 20 pM binding site in all the solutions. In total, five equilibrium titrations were performed for this complex with the average $K_D = 12(1)$ pM (see Table 11-1). All the experiments fit a 1:1 equilibrium binding model well.

Table 11-1. Equilibrium dissociation constants and rate constants for antigen/monoclonal antibody complexes.

Interaction[a]	Method	k_a ($M^{-1}s^{-1}$)[b]	k_d (s^{-1})[b]	K_D (pM)[b]
Antigen-1/mAb-1	Biacore	$4.6\ (0.1)\times10^{5}$	$1.2\ (0.1)\times10^{-3}$	2,500 (500)
Antigen-1/mAb-1	KinExA	$3.3\ (0.6)\times10^{5}$	$4.3\ (0.7)\times10^{-4}$	1,300 (300)
Antigen-2/mAb-2	Biacore	$6.6\ (1.5)\times10^{5}$	$2.1\ (0.5)\times10^{-5}$	33 (11)
Antigen-2/mAb-2	KinExA	$1.1\ (0.2)\times10^{6}$	$1.3\ (0.3)\times10^{-5}$	12 (1)
Antigen-2′/mAb-2	Biacore	$2.7\ (0.6)\times10^{6}$	$1.6\ (0.2)\times10^{-5}$	6.2 (0.8)
Antigen-2′/mAb-2	KinExA	$2.8\ (0.5)\times10^{6}$	$1.1\ (0.2)\times10^{-5}$	4.0 (1.9)

[a]Binding reaction between the stated antigen and its respective mAb
[b]Errors in parentheses are ±95% confidence intervals

To determine the k_a for this interaction by KinExA, a solution containing 102 pM binding site (2× mAb-2 concentration) and 404 pM Ag-2 was followed to equilibrium in three independent experiments. Free mAb was quantitated as a function of time after mixing of Ag-2 and mAb-2, and the resulting monoexponential function was fit to determine k_a. Fig. 11-2c shows a typical on-rate kinetic experiment. The average of the three independent experiments yielded a value for $k_a = 1.1(0.2)\times10^{6}\ M^{-1}s^{-1}$. The product of $k_a \times K_D$ gives the $k_d = 1.3(0.3)\times10^{-5}\ s^{-1}$.

3.3. Antigen-2′/Antibody-2 Interactions

We also investigated the kinetics of Ag-2′ binding to mAb-2. Ag-2′ is a peptide fragment of Ag-2. Mab-2 was immobilized by amine coupling on three Fcs of a CM5 biosensor chip while the fourth Fc, with no mAb immobilized, served as a control surface. Surface densities of mAb-2 varied from 1,650 to 2,300 RU giving an antigen-2′ binding response from 58 to 91 RU. Fig. 11-3a shows the results of triplicate injections of 0.18–23 nM Ag-2′ over the mAb surfaces at 25°C for a typical experiment. Ag-2′ dissociated from mAb-2 very slowly, similar to that seen with Ag-2. To measure the k_d accurately for this interaction, we followed the dissociation for 4 h at 23 nM Ag-2′ as shown in Fig. 11-3a. All the sensorgrams gave an excellent fit to a 1:1 kinetic interaction model with a term for mass transport. The experiment was performed independently on four CM5 biosensor chips (twelve mAb immobilized Fcs in total) and all three flow cells from each independent experiment were fit globally as described for Ag-2 above, resulting in an average k_a, k_d, and K_D of $2.7(0.6)\times10^{6}\ M^{-1}s^{-1}$, $1.6(0.2)\times10^{-5}\ s^{-1}$, and 6.2(0.8) pM, respectively.

The Ag-2′/mAb-2 complex was characterized on KinExA using one dual curve analysis (Fig. 11-3b) in addition to two more K_D-controlled titration experiments. For the dual curve analysis, Ag-2′ was varied from 40 fM–3.1 nM with mAb-2 at a concentration of 9.3 pM binding site for the K_D-controlled and 140 pM for the antibody-controlled titration. It took ~35 h to reach equilibrium for the K_D-controlled titration and 9 h for the mAb-controlled experiment. The three titration experiments resulted in an average $K_D = 4.0(1.9)$ pM, and an active binding site concentration of 73 pM binding site (52% activity) was calculated from the single dual curve analysis.

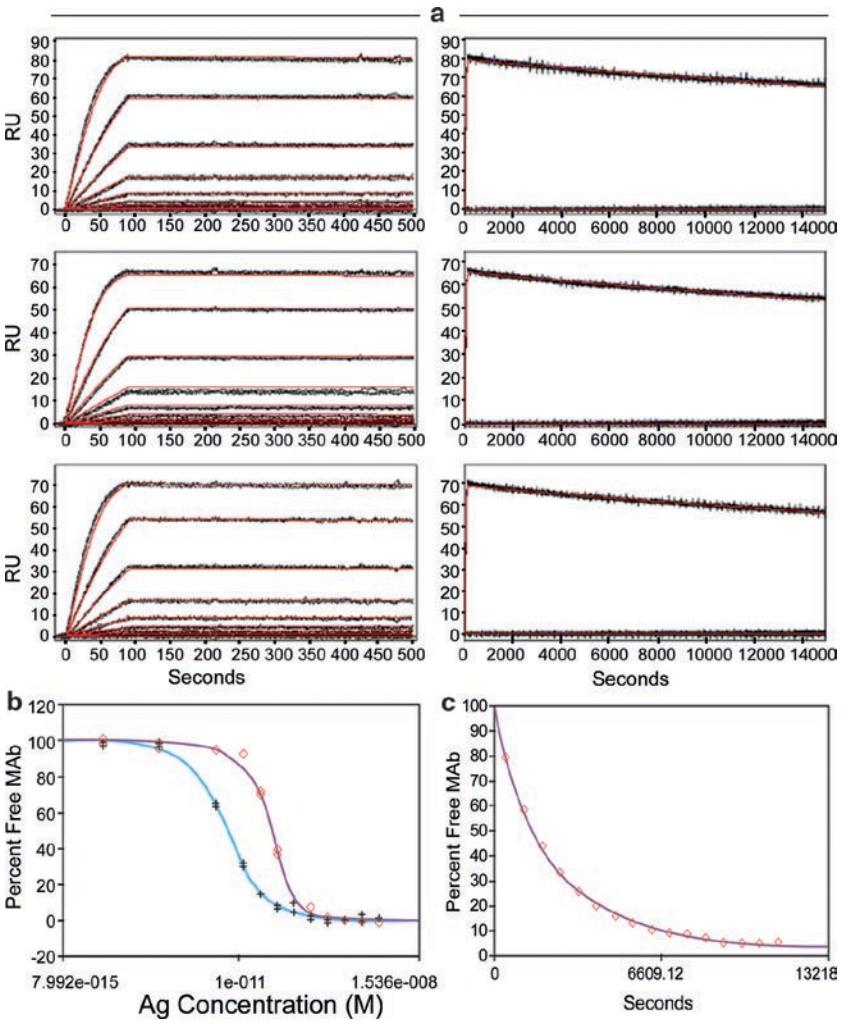

Fig. 11-3. (**a**) Biacore data of antigen-2′ binding to immobilized mAb-2. The data was globally fit (*red line*) over three independent flow cells. On-rate data shows triplicate Ag-2′ injections ranging from 0.18–23 nM. Off-rate data shows triplicate Ag-2′ injections of 23 nM with a 4 h dissociation time, $k_a = 2.7 \times 10^6\,M^{-1}s^{-1}$; $k_d = 1.6 \times 10^{-5}\,s^{-1}$; $K_D = 6.1$ pM (**b**) Dual curve equilibrium KinExA titration of 140 pM (*top curve*) and 9.3 pM (*bottom curve*) mAb-2 binding site with 40 fM–3.1 nM Ag-2′, $K_D = 3.8$ pM (**c**) KinExA on-rate "direct method" with 208 pM Ag-2′ reacting with 86 pM mAb-2 binding site every 12 minutes for ~3 h, $k_a = 2.5 \times 10^6\,M^{-1}s^{-1}$

A representative KinExA solution phase k_a determination for Ag-2′/mAb-2 is given in Fig. 11-3c. Because this complex has a slow k_d and takes several hours to reach equilibrium, it was possible to perform a "direct method" KinExA experiment. Ag-2′ was mixed at a concentration of 208 pM with 86.3 pM mAb-2 (binding site concentration), and free mAb concentration was followed as a function of time as described for Ag-2 above. Four independent kinetic experiments were performed with the resulting $k_a = 2.8(0.5) \times 10^6\,M^{-1}s^{-1}$ and $k_d = 1.1(0.2) \times 10^{-5}\,s^{-1}$.

4. Discussion

Improvements in antibody generation technology have permitted us to reach more deeply into the antibody repertoire and to discover antibodies with exceptionally high affinity for antigen targets. This has presented new challenges in terms of characterizing kinetic and equilibrium constants for antibody/antigen complexes that have affinities in the picomolar and sometimes femtomolar range. Two technologies that are often utilized to characterize antibody/antigen interactions are Biacore and KinExA. While both of these instruments can be used to measure the amount of complex formed for a given reaction, there are some general differences between them in how they work. Biacore is often considered a surface-based technology, since in the majority of applications complex formation is monitored directly to a ligand immobilized on a surface. While the method is label free, there has been a criticism that the surface imposes mass transport effects and steric hindrance that will significantly alter the binding constants (Schuck 1996; Fong 2002). KinExA is a solution-based method that relies on capturing and a post-reaction labeling step to quantitate the amount of complex formed during a reaction. While experiments may be set up to monitor the time course of a reaction, similar to Biacore, which measures reactions in real-time, KinExA typically samples reactions with much larger time steps and may miss some details in the reaction kinetics. We utilized Biacore and KinExA in combination to compare how well each system could analyze a set of antibody/antigen interactions that range in affinity from nM to pM.

As shown in Table 11-1, we found a very good agreement between the rate constants determined by Biacore and KinExA. On average the association and dissociation kinetic rate constants varied by only ~33% and ~44%, respectively, between the two techniques. It is often speculated that surface-based methods would yield slower association rates because of mass transport limitations. The results for the Ag-2′/mAb-2 system, which has the highest association rate of the three systems studied, showed that the association rate constants measured from Biacore and KinExA were identical within experimental error at $2.7(0.6)\times10^{6}\,M^{-1}s^{-1}$ and $2.8(0.5)\times10^{6}\,M^{-1}s^{-1}$, respectively. We also note that the association rate constant is faster for Ag-2′ than for Ag-2, while the dissociation rate constants are similar. This may reflect the fact that the diffusion of Ag-2′ to mAb-2 is faster that for Ag-2, but more likely suggests that there may be conformational differences in the peptides prior to binding. However, once the two different proteins are bound, it is likely that the residues involved in complexation are the same, resulting in similar k_ds. We also note that the dissociation data for the Ag-1/mAb-1 complex in Fig. 11-1a does deviate slightly at the highest concentration from an ideal 1:1 binding interaction model. However, at this highest antigen concentration (101 nM), we were 50–100× the K_D of the interaction, and in many cases fitting deviations are seen when the analyte concentration is this far over the K_D. This is especially true with K_Ds in the nM range because most likely the specific binding interaction is closer to the K_D of any nonspecific binding interactions that may be present with Ag-1 binding to mAb-1. In contrast, with Ag-2 and Ag-2′ we were 1,000–4,000× over the K_D at our highest antigen concentration, respectively. However, Ag-2 and Ag-2′ are much smaller monomeric proteins than Ag-1 and in addition, have much tighter K_Ds than Ag-1 meaning that even

at 23 nM (the highest Ag concentration injected) this would have probably been significantly below any K_D corresponding to a nonspecific interaction, if any are even possible between Ag-2 or Ag-2′ and mAb-2.

The greatest difference (2.7-fold) observed in the dissociation rate constants was for the weakest antigen/antibody interaction, while the parameters for the other interactions were within or near the 95% confidence interval. A slight bias for a slower dissociation rate and a tighter dissociation equilibrium constant by KinExA could be partially related to temperature effects. The KinExA experiments were conducted at room temperature (22°C; KinExA has no automated temperature control), while the Biacore studies were performed at a slightly higher temperature (25°C). On average, the equilibrium dissociation constants (K_D) for all three systems varied by only ~49% across a ~ 1,000-fold range of affinity (nM to pM). For characterization of high affinity therapeutic mAbs, this is very good when one considers that the average 95% confidence interval for each antigen/antibody system measured by Biacore and KinExA was ~24%.

As with any biophysical technique, successful implementation of the technology hinges on a properly designed and executed experiment. In the case of Biacore, we demonstrated that accurate and precise kinetics could be measured for antigen/mAb complexes possessing a pM K_D if proper experimental methods were used. Frequently, Biacore studies with mAbs are performed incorrectly by immobilizing antigen on the biosensor chip and flowing mAb as the analyte. The rationale for performing these experiments in this orientation is easily understood because there are often multiple mAbs to be screened against one antigen. However, at standard antigen immobilization densities the antibodies are able to crosslink on the surface. This cross-linking will yield apparent enhanced affinities by slowing the dissociation rate. In addition, protein complexes that truly possess pM affinity dissociate very slowly, displaying a few percent decay in the amount of complex over time, which makes direct measurement of their dissociation rates challenging. To overcome this obstacle, we showed how it is possible to follow the dissociation reaction for 3–4 h on Biacore to collect enough dissociation information to determine k_ds that are very slow. To obviate mass transport artifacts, steric hindrance, or aggregation, antibody immobilization levels were kept low in most cases giving an antigen R_{max} no greater than 50–100 RU. Finally, a high flow rate of 100 μL/min was used to minimize mass transport effects and to deliver a more consistent analyte plug across the surface during injection.

KinExA has its own experimental criteria to consider. This methodology is well suited for the measurement of the binding parameters of antigen/mAb complexes because of the requirement of having a fluorescently labeled detection reagent after free mAb has been captured on the bead pack; many fluorescently labeled species-specific polyclonal antibodies are available commercially. To perform a rigorous KinExA experiment several considerations need to be considered. Firstly, it is important to give the samples sufficient time to reach equilibrium. For example, with an antigen/antibody complex with a k_a and k_d of $7 \times 10^5\,M^{-1}s^{-1}$ and $2 \times 10^{-5}\,s^{-1}$, respectively, and with antigen and antibody at 29 pM each, it requires 35 h to reach equilibrium. Secondly, to measure accurately an antigen–antibody complex with a pM dissociation constant, it is essential to have the antibody binding site concentration less than or equal to three- to tenfold the K_D. It turns out that the shape of a KinExA

titration curve is not dependent on the absolute mAb concentration in solution, but on the ratio of mAb concentration to the K_D for the interaction. If the mAb concentration is near the K_D, the shape of the titration curve is very sensitive to changes in K_D and becomes "K_D-controlled." If the antibody concentration is much higher than the K_D, the resulting titration curve is sensitive to antibody concentration and is "mAb-controlled," and the shape changes little with K_D. Both types of equilibrium curves, K_D- and mAb-controlled, can be fit simultaneously to yield both the K_D and active mAb concentration. Dual curve analysis also provides extra assurance that the correct binding model is, indeed, a 1:1 stoichiometric interaction because with both curves it is easier to see deviations of the actual data from the theoretical fit. In addition, the dual curve fitting algorithm is similar to global fitting in Biacore, in that the fitted parameters, K_D and mAb binding site concentration, have to describe both curves simultaneously. In fact, many times we perform one dual curve analysis on each new interaction system we study to verify model correctness and accuracy, and then collect any additional replicates with solely K_D-controlled titration curves.

There are two key differences between running Biacore and KinExA experiments. The first, the fact that Biacore uses a surface for direct binding measurements while KinExA reactions occur in solution phase, is obvious. The similar binding constants obtained by Biacore and KinExA suggest that immobilization of the antibodies onto the surface did not affect their binding activity under the conditions used in these studies. Day et al. (2002) have also demonstrated equivalent kinetic and thermodynamic parameters for a small molecule-protein interaction determined both with Biacore and with solution-based techniques including isothermal titration calorimetry and stopped flow fluorescence. The general conclusion is that the non-crosslinked dextran matrix that was used in all of these Biacore studies may help maintain the molecules in a solution-like environment. The second key difference between Biacore and KinExA experiments relates to the time course of the study. Because of limited injection volumes, the available contact times for Biacore are on the order of one to ten minutes. In order to register complex formation in this short time frame, one is often required to work at antigen concentrations that are in excess of the equilibrium dissociation constant of the system. For example, in the case of Ag-2′ the lowest concentration that we tested by Biacore was 180 pM, 30-fold over its measured affinity of 6 pM. With KinExA we are able to work at concentrations well below the K_D since the reactions are able to equilibrate as long as is required before sampling in the instrument.

Certainly, we do not mean to imply that all rate constants and equilibrium dissociation constants for molecular interactions, especially those with pM K_Ds, determined by biosensors will match those obtained from solution-based techniques. However, our results illustrate that the frequently raised concern that surface-based techniques are inaccurate because of the surface itself should be carefully reconsidered. Finally, as with any analytical technique, the quality of the results is directly related to the quality of the experimental design and data analysis methods.

Acknowledgments. The computer algorithm for the simulation of the time to equilibrium for a 1:1 reversible interaction was graciously provided to us by Steve Lackie and Tom Glass of Sapidyne, Inc, Boise, ID.

References

Babcook JS, Leslie KB, Olsen OA, Salmon RA, Schrader JW (1996) A novel strategy for generating monoclonal antibodies from single, isolated lymphocytes producing antibodies of defined specificities. Proc Natl Acad Sci USA 93:7843–7848

Biacore, Inc. (1998) BIA applications handbook, version AB. Uppsala, Sweden

Blake DA, Chakrabarti P, Khosraviani M, Hatcher FM, Westhoff CM, Goebel P, Wylie DE, Blake RC II (1996) Metal binding properties of a monoclonal antibody directed toward metal-chelate complexes. J Biol Chem 271:27677–27685

Blake RC II, Pavlov AR, Blake DA (1999) Automated kinetic exclusion assays to quantify protein binding interactions in homogeneous solution. Anal Biochem 272:123–134

Chiu Y-W, Li QX, Karu AE (2001) Selective binding of polychlorinated biphenyl congeners by a monoclonal antibody: analysis by kinetic exclusion fluorescence immunoassay. Anal Chem 73:5477–5484

Davis CG, Jia X-C, Feng X, Haak-Frendscho M (2003) Production of human antibodies from transgenic mice. In: Lo BKC (ed) Methods in molecular biology. Humana Press, Totowa, NJ, pp 191–200

Day YSN, Baird CL, Rich RL, Myszka DG (2002) Direct comparison of binding equilibrium, thermodynamic, and rate constants determined by surface- and solution-based biophysical methods. Protein Sci 11:1017–1025

Fong C-C, Wong M-S, Fong W-F, Yang M (2002) Effect of hydrogel matrix on binding kinetics of protein-protein interactions on sensor surface. Anal Chim Acta 456:201–208

Jones RM, Yu H, Delehanty JB, Blake DA (2002) Monoclonal antibodies that recognize minimal differences in the three-dimensional structures of metal-chelate complexes. Bioconjug Chem 13:408–415

Karlsson R, Fält A (1997) Experimental design for kinetic analysis of protein-protein interactions with surface plasmon resonance biosensors. J Immunol Methods 200:121–133

Mendez MJ, Green LL, Corvalan JRF, Jia X-C, Maynard-Currie CE, Yang X-D, Gallo ML, Louie DM, Lee DV, Erickson KL et al (1997) Functional transplant of megabase human immunoglobulin loci recapitulates human antibody response in mice. Nat Genet 15:146–156

Morton TA, Myszka DG (1998) Kinetic analysis of macromolecular interactions using surface plasmon resonance biosensors. Methods Enzymol 295:268–294

Myszka DG (1997) Kinetic analysis of macromolecular interactions using surface plasmon resonance biosensors. Curr Opin Biotechnol 8:50–57

Myszka DG (1999) Improving biosensor analysis. J Mol Recognit 12:279–284

Myszka DG, He X, Dembo M, Morton TA, Goldstein B (1998) Extending the range of rate constants available from biacore: interpreting mass transport-influenced binding data. Biophys J 75:583–594

Ohmura N, Lackie SJ, Saiki H (2001) An immunoassay for small analytes with theoretical detection limits. Anal Chem 73:3392–3399

Rich RL, Myszka DG (2001) Survey of the year 2000 commercial optical biosensor literature. J Mol Recognit 14:273–294

Rich RL, Myszka DG (2002) Survey of the year 2001 commercial optical biosensor literature. J Mol Recognit 15:352–376

Roskos L, Klakamp S, Liang M, Arends R, Green L (2007) Molecular engineering II: antibody affinity. In: Dübel S (ed) Handbook of therapeutic antibodies. Wiley-VCH, Weinheim, Germany, pp 145–169

Sapidyne instruments, Inc. (1998) KinExA 3000 instrument manual. Boise, ID

Schuck P (1996) Kinetics of ligand binding to receptor immobilized in a polymer matrix, as detected with an evanescent wave biosensor. I. A computer simulation of the influence of mass transport. Biophys J 70:1230–1249

Yang X-D, Corvalan JRF, Wang P, Roy CMN, Davis CG (1999) Fully human anti-interleukin-8 monoclonal antibodies: potential therapeutics for the treatment of inflammatory disease states. J Leukoc Biol 66:1–10

Chapter 12

Analytical Characterization of Monoclonal Antibodies: Linking Structure to Function

Reed J. Harris, Edward T. Chin, Frank Macchi, Rodney G. Keck, Bao-Jen Shyong, Victor T. Ling, Armando J. Cordoba, Melinda Marian, Don Sinclair, John E. Battersby, and Andy J.S. Jones

Abbreviations

ADCC	Antibody-dependent cellular cytotoxicity
ASU	Succiminide at an aspartate residue
CDC	Complement-dependent cytotoxicity
CDR	Complementarity-determining regions
CHO	Chinese hamster ovary
Fab	Fragment antigen binding
Fc	Fragment crystallizable
Fuc	Fucose
Gal	Galactose
GlcNAc	*N*-Acetylglucosamine
HIC	Hydrophobic interaction chromatography
IEC	Ion exchange chromatography
IgG1	Immunoglobulin gamma subclass 1
IsoAsp	Isoaspartate
MALDI-TOF/MS	Matrix-assisted laser desorption/ionization time-of-flight mass spectrometry
Man	Mannose
VH	Variable region of the heavy chain

1. Introduction

The basic structural features of antibodies, including their primary structures (Edelman et al. 1969), were established well before the concept of therapeutic antibodies was conceived. These molecules are now known to bear multiple sources of microheterogenity that can have a dramatic effect on in vivo and in vitro properties. Rituximab (Rituxan®), Trastuzumab (Herceptin®) and omalizumab (Xolair®) are three examples of therapeutic IgG1/kappa subclass antibodies produced by Genentech, Inc.; these molecules are the main

From: *Current Trends in Monoclonal Antibody Development and Manufacturing,* Biotechnology: Pharmaceutical Aspects, DOI 10.1007/978-0-387-76643-0_12, Edited by: S.J. Shire et al.

subject of this discussion on the impacts of common and unique antibody modifications on functional properties.

2. Fc Glycosylation

Three-dimensional models of IgG1-type antibodies show that the conserved Fc glycans are sequestered in the interior of the Fc where they are an integral part of the overall structure (Deisenhofer 1981; Jefferis and Lund 2002). The main oligosaccharide forms are biantennary fucosylated complex type structures with zero, one or two galactose residues on their non-reducing termini, and are referred to as G0, G1, and G2, respectively, along with some minor forms as depicted in Fig. 12-1a, b. The published impacts of

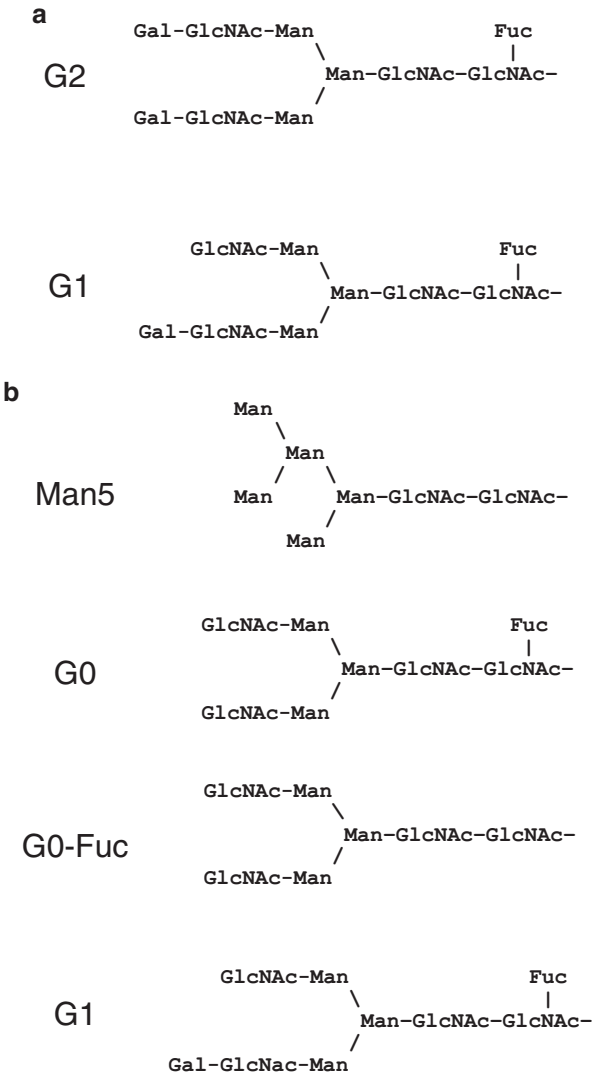

Fig. 12-1. (**a**) Schematic of omalizumab Fc glycans with Gal residues on a non-reducing terminus. (**b**) Schematic of omalizumab Fc glycans with GlcNAc or Man residues on a non-reducing terminus

Table 12-1. Literature review of Fc glycosylation heterogeneity impacts on effector functions.

Impact on	Citation	Synopsis
CDC	Tsuchiya et al. (1989)	Degalactosylation partially reduces C1q binding
	Boyd et al. (1995)	Gal removal reduces CDC
	Hodoniczky et al. (2005)	Gal removal reduces CDC
	Gazzano-Santoro et al. (1997)	Galactosylation of rituximab correlates with in vitro CDC
	Wright and Morrison (1998)	G0 (Lec8) MAb is equivalent to G0/G1/G2 mixture (Lec2) for CDC and C1q binding
	Tao and Morrison (1989)	Non-glycosylated and oligomannose IgG are deficient in CDC
	Boyd et al. (1995)	Deglycosylated IgG is defective in CDC
ADCC	Boyd et al. (1995)	Galactose removal has no effect; non-glycosylated forms are defective
	Wright and Morrison (1997)	Non-glycosylated forms are defective
	Umana et al. (1999)	Addition of bisecting GlcNAc enhances ADCC
	Hodoniczky et al. (2005)	Addition of bisecting GlcNAc enhances ADCC
	Shields et al. (2002)	Core fucose inversely correlates with ADCC
	Shinkawa et al. (2003)	Core fucose inversely correlates with ADCC, biGlcNAc has small effect, Gal has no effect
	Ferrara et al. (2006)	ADCC is enhanced even when one heavy chain has the non-fucosylated form

Table 12-2. Impacts of Fc glycosylation variability on effector functions and serum clearance.

Asn297 glycans	CDC	ADCC	Clearance
Non-glycosylated	Defective	Defective	No effect
Higher Gal	May improve	No effect	No effect
Oligomannose	Defective	Improves	No effect
Non-fucosylated	?	Higher	No effect
Bisecting GlcNAc	May increase	No effect	?

galactosylation, fucosylation, oligomannose forms, and non-glycosylation on effector functions are listed in Table 12-1, and an expanded summary that also lists impacts on clearance is presented in Table 12-2.

The absence of galactose has been reported to correlate with reductions in the affinity of complement protein C1q for the Fc region, thus affecting complement-dependent cytotoxicity (Gazzano-Santoro et al. 1997; Hodoniczky et al. 2005). The galactosylation-CDC correlation reflects the conditions of this in vitro assay, and a relationship between rituximab galactosylation and efficacy has not yet been established. Galactosylation of Fc glycans does not affect in vitro antibody-dependent cellular cytotoxicity (Boyd et al. 1995; Shinkawa et al. 2003).

Only a small percentage of serum IgGs lack core fucose on the Fc glycans (Jefferis et al. 1995). Non-fucosylation correlates with increases in FcγRIIIa binding and in vitro ADCC activity (Rothman et al. 1989; Shields et al. 2002). The correlation between the higher-affinity Val158 FcγRIIIa binding phenotype and rituximab efficacy suggests that ADCC is an important aspect of rituximab's

mechanism of action (Cartron et al. 2002; Weng and Levy 2003). Introduction of the GnTIII gene into a transfected CHO cell line produced an antibody with bisecting GlcNAc residues and reduced fucosylation that exhibited higher in vitro ADCC activity (Umana et al. 1999); a subsequent study attributed the increased ADCC activity to non-fucosylation (Shinkawa et al. 2003). The core fucose of Fc glcyans hinders binding of FcγRIIIa due to interference between a receptor oligosaccharide and the core fucose of the Fc glycans Ferrara et al. (2006); one consequence of this model is that ADCC may be enhanced even when only one heavy chain is non-fucosylated. More recent studies have established that sialyated Fc oligosaccharides can reduce in vitro ADCC (Kaneka et al. 2006).

Oligomannose forms are also produced at low levels using production cell lines such as Chinese hamster ovary (CHO) cells. The oligomannose forms are defective with respect to CDC, but exhibit elevated ADCC activity consistent with their non-fucosylation (Kanda et al. 2006, 2007; Li et al. 2006). Non-glycosylated IgG is defective with respect to both CDC and ADCC activity, and may have a reduced ability to resist proteolysis (Wright and Morrison 1998; Raju and Scallon 2006).

3. The Role of Fc Glycans on the Clearance of IgG1-Type Antibodies

Serum IgGs are protected from catabolism by FcRn (Junghans and Andersen 1996). FcRn binding is not affected by Asn297 (Fc) glycosylation type or by site occupancy (Tao and Morrison 1989). Serum clearance for many glycoproteins can be mediated by lectin-type receptors that recognize terminal sugar moieties such as the asialoglycoprotein receptor, which recognizes terminal Gal (Ashwell and Hartford 1982), and the mannose receptor, which recognizes terminal Man and GlcNAc (Stahl 1992). Fc oligosaccharides with terminal Gal that are present on omalizumab are given in Fig. 12-1a, and Fc oligosaccharides with terminal Man or GlcNAc are depicted in Fig. 12-1b.

The sequestration of the Asn297 oligosaccharides in the interior of the Fc suggests that they lack accessibility to such glycan-specific receptors, but we also have noted that Fc glycans can be readily removed by endoglycosidases such as PNGaseF or EndoH, so the carbohydrate receptor accessibility of these glycans is uncertain. Wright and Morrison (1994) provided an example where a chimeric antibody produced in the CHO lec1 cell line, which only adds oligomannose forms, have faster serum clearance in a mouse model relative to other CHO glycan types. Dong et al. (1999) described antibody whose uptake by dendritic cells was mediated by terminal GlcNAc (i.e., the G0 form). In addition, the Asn297 oligosaccharides can modulate the overall structure of the Fc (Krapp et al. 2003; Mimura et al. 2000), potentially mediating interactions with Fcγ receptors, which could in turn affect serum clearance.

We needed to determine the possible effects of glycosylation heterogeneity on the clearance of omalizumab, an IgG1/kappa antibody that binds to the FcεRI epitope of human IgE. We administered omalizumab to mice via the tail vein at approximately the human dose (5 mg/kg), and took samples at four time-points to measure serum concentrations and to examine the remaining omalizumab Fc oligosaccharides. The final time-point at 4 days had approximately 34% of the omalizumab concentration of the first (15 min) time-point. If any terminal saccharide had mediated accelerated clearance relative to other

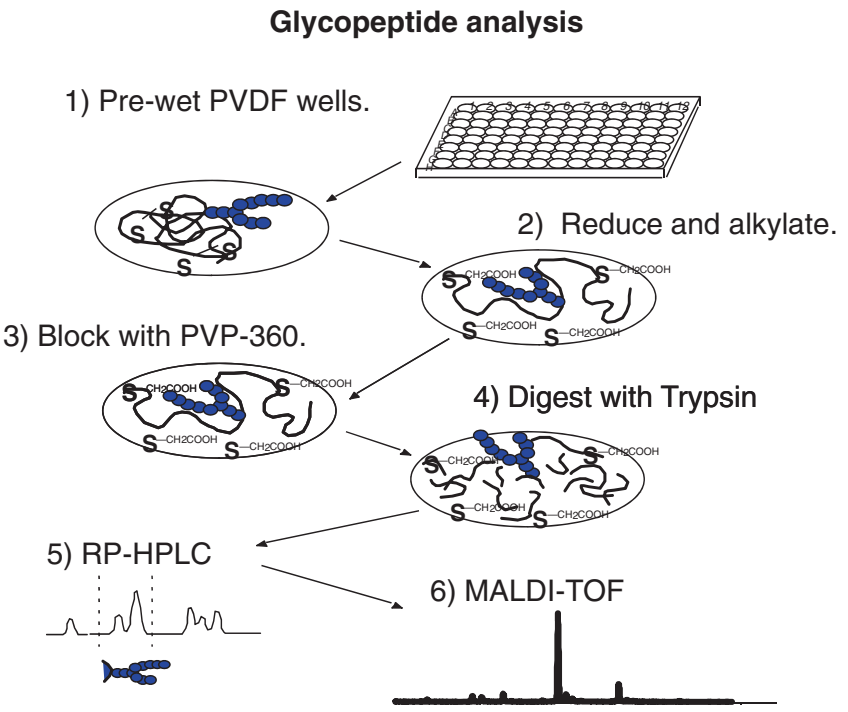

Fig. 12-2. Experimental design for omalizumab glycan distribution study. Wells coated with Immobilon P PVDF in a Millipore MultiScreen system were wetted with 100 µL of methanol, and then the liquid was drawn through the PVDF membrane by aspiration. Omalizumab that had been re-purified from murine pharmacokinetic study serum samples were reduced for 1 h at 37°C with dithiothreitol in 6 M guanidine, 360 mM Tris, 3 mM EDTA, pH 8.6, and then S-carboxymethylated by addition of iodoacetamide. The solutions were removed by aspiration, the wells were washed with water and then blocked with 1% polyvinylpyrolidone-360. Samples were digested with 0.5 µg of Promega sequencing grade trypsin in 0.1 M Tris, 10% acetonitrile, pH 8 for 4 h at 37°C. The supernatant fractions were transferred to polypropylene test tubes; the wells were washed twice with 0.1% TFA with the wash supernatants added to the supernatants. Samples were concentrated approximately twofold using a Savant Speed-Vac for the RP-HPLC step. The glycopeptide fraction was then purified by RP-HPLC, and a 2-min wide glycopeptide fraction was collected manually. Glycopeptide fractions were dried by vacuum, then reconstituted with 50% acetonitrile/0.1% TFA solution; 5 µL was transferred to stainless steel plate, mixed with 0.5 µL of a matrix solution (containing 2 mg/mL trihydroxyacetophenone (THAP) in 25% acetonitrile, 75% 13 mM ammonium citrate), dried again, and then analyzed using a PerSeptive Biosystems Voyager Elite MALDI-TOF mass spectrometer operating in the positive ion mode

forms, then we would have observed a shift in the glycan distribution away from the rapidly-clearing forms.

The experimental design is summarized in Fig. 12-2. Omalizumab was re-purified using an immobilized anti-human-kappa light chain antibody affinity column as described in Battersby et al. (2001), followed by reversed-phase chromatography; the material was S-carboxymethylated, digested with trypsin, and then the glycopeptide was collected from the RP-HPLC map. MALDI-TOF mass spectrometry was used to analyze the tryptic glycopeptide. The distribution of oligosaccharides did not change over the course of clearance (Fig. 12-3), demonstrating that the types of Fc glycans found on CHO-produced IgGs do not

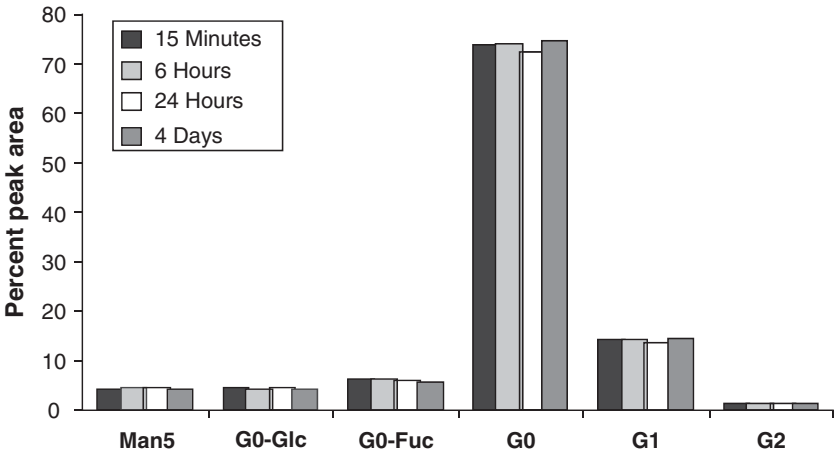

Fig. 12-3. Relative percent peak areas for omalizumab tryptic glycopeptides 15 min, 6 h, 24 h or 4 days after tail vein administration in mice

influence clearance in this model system. This lack of effect should be relevant for human subjects, as the lectin-type receptors are generally conserved in mice and humans. Subsequent studies performed elsewhere in mice and human subjects have confirmed the results we obtained for the main Fc oligosaccharide forms (Huang et al. 2006; Millward et al. 2007; Jones et al. 2007).

To summarise, Fc glycans may be a critical product quality attribute if ADCC activity is required for activity, in that case, fucosylation and site occupancy may need to be monitored. Other types of variability in the distribution of the main Fc oligosaccharide types should not affect in vivo properties, based on current understandings. Significant changes in Fc glycan distribution may raise concerns about other unseen molecular variability, as glycosylation is often viewed as a marker of the metabolic state of the cells used for production. For this reason, regulatory officials may require a demonstration of Fc glycosylation consistency even for antibodies whose Fc glycan distribution should not affect activity or clearance.

4. Heavy Chain C-Terminal Lysine Processing

The heavy chain gene encodes a terminal -Pro-Gly-Lys sequence (Ellison et al. 1982), but the C-terminal Lys is subject to removal by basic carboxypeptidases in the bloodstream and in mammalian production cultures (Harris 1995). There is no evidence that the presence or absence of terminal Lys affects in vitro activity, and any activity effect is unlikely given that the C terminus is oriented away from Fc receptor epitopes (Sondermann and Osthuizen 2002).

Lys heterogeneity does affect net charge, so it is possible that the presence or absence of terminal Lys could affect pharmacokinetic parameters, especially for subcutaneous injected products where the material needs to migrate through the cationic non-vascular spaces to reach the draining lymphatic system. For intravenous administration, Lys variability is unlikely to have a pharmacokinetic effect because distribution will be rapid, and the remaining Lys residues will be rapidly removed by serum carboxypeptidases (Skidgell 1988). C-terminal

Lys levels can be assayed directly by peptide mapping after cyanogen bromide cleavage (Harris 1995) or indirectly by comparing basic forms with and without carboxypeptidase B sample treatment (Weitzhandler et al. 2001).

5. Hinge-Region Fragmentation

IgG1-type antibodies in liquid formulations undergo fragmentation in the hinge region –KSCDKTHTC– sequence (Cordoba et al. 2005). This fragmentation is not caused by trace levels of proteases, but may instead be due to kinetics, where the relatively dense Fab and Fc modules put strain on the flexible hinge region that reduces the activation energy for polypeptide bond hydrolysis. Cohen et al. (2007) also described a distinct (beta-elimination) mechanism for cleavage at the -Ser-Cys- bond.

6. Glycation

Glycation is the product of glucose forming a Schiff base with Lys side chains, and then undergoing the Amadori rearrangement to a stable ketoamine (Furth 1988). We began to observe +162 Da adducts in electrospray mass spectrometry profiles of our therapeutic antibodies as our signal-to-noise ratio improved, especially for the light chains after chemical reduction of disulfide bonds, as shown in Fig. 12-4. The +162 Da forms can be isolated using TSK-boronate chromatography, which resolves glycated from non-glycated forms (Quan et al. 2008). Higher glycation levels correlate with glucose exposure in production cultures, similar to the clinical observation for serum IgGs and hemiglobin with diabetic patients. Certain Lys residues may be more susceptible to glycation due to their local charge environment (Zhang et al. 2008).

Glycation is not considered a critical quality attribute for omalizumab, as there are no Lys residues in its CDRs, and potency studies with glycated and non-glycated forms isolated by TSK-boronate chromatography demonstrated comparable in vitro potencies. We do not believe that glycation presents a safety risk to our patients, as serum-derived IgG molecules are also known to be glycated (Lapolla et al. 2000).

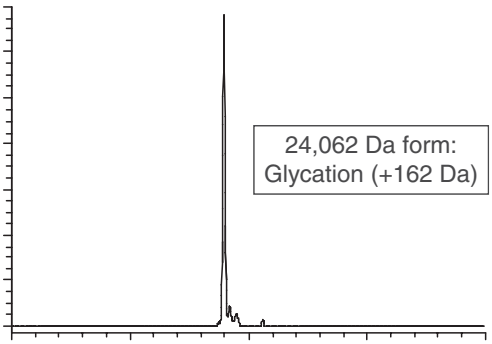

Fig. 12-4. Electrospray mass spectrometric analysis of the omalizumab light chain after reduction with DTT. The main form has a molecular mass of 23,900 Da; the 23,923 and adjacent (unlabeled) mass forms are sodium and potassium adducts, respectively. The 24,062 Da form is consistent with glycation (+162 Da)

7. Unpaired Cysteines

IgG1 antibodies have 32 conserved cysteines that normally form 16 disulfide bonds (Edelman et al. 1969). Analyses using Ellman's reagent (DTNB) indicated the presence of about 1 mol of free cysteine per mol of antibody (Henry Costantino unpublished). Ellman's analysis of Fab fractions collected from the papain/HIC assay discussed below showed that the alternate fractions contained free thiol forms.

The Fab-1 and Fab-2 fractions of Fig. 12-5 were collected into test tubes containing iodoacetamide with 6 M guanidine and 50 mM Tris, pH 8. The samples were subsequently sulfitolyzed and digested with trypsin to resolve the Fab-2 peptides containing the formerly unpaired cysteines (now present as carboxymethylcysteine) from the disulfide-bonded cysteines (now present a sulfo-cysteine). The peptide mapping experiments established that the unpaired cysteines in the Fab-2 fraction were Cys22 and Cys96, which were expected to form the VH-loop disulfide bond. The Fab-2 (unpaired cysteine) fraction exhibits reduced potency in an IgE-receptor binding inhibition assay.

Electrospray mass spectrometric analysis of Fab fractions confirmed that the unpaired Cys-containing forms were not partially mixed disulfides such as cysteinylated or glutathione-modified forms (Table 12-3). Evidently, the

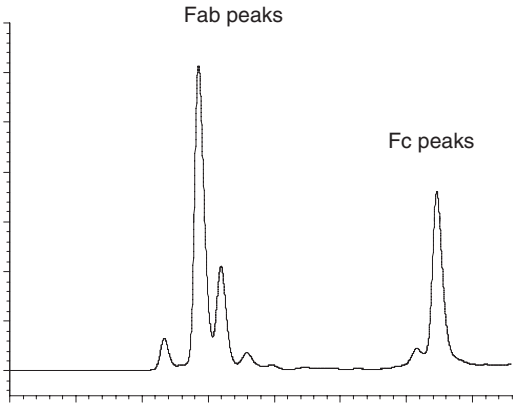

Fig. 12-5. Hydrophobic interaction chromatography after papain digestion of omalizumab. The molecular characteristics of the numbered Fab peaks are described in Table 12-3. Fc peaks are labeled a, b and c. Clip refers to a peak resulting from a papain cleavage artifact

Table 12-3. Characteristics of omalizumab HIC Fab fractions.

	Non-reduced Fab mass (Da)	Reduced light chain mass (Da)	Reduced heavy chain (1-228) mass (Da)	Present at Asp32 position	Nature of Cys22-Cys96 disulfides
Expected mass	48,201	23,900	24,303		
Fab peak 1	48,200	23,900	24,303	Asp	Disulfide
Fab peak 2	48,204	23,900	24,305	Asp	Thiol
Fab peak 3	48,201	23,901	24,303	isoAsp	Disulfide
Fab peak 4	–	23,900	24,305	isoAsp	Thiol
Fab peak 5	48,188	23,882	24,305	Asu	Disulfide
Fab peak 6	–	23,882	24,305	Asu	Thiol

omalizumab molecule forms a final structure before these cysteines can form the correct disulfides. The papain/HIC profile is remarkably well-maintained for production lots, with some gradual oxidation of the unpaired cysteines occurring in the accelerated stability studies. Complete disulfide formation may also be facilitated by the addition of copper to the culture medium (Chaderjian et al. 2005).

8. Aspartate Isomerization

Deamidation is a well-established degradative mechanism for proteins and peptides; this process usually proceeds via a succinimide intermediate, and results in aspartate and isoaspartate at former asparagine positions (Geiger and Clarke 1987). Deamidation is readily detected due to its change in charge characteristics, that can be detected by cation exchange chromatography or isoelectric focusing methods. Aspartate residues can also undergo isomerization to isoaspartate via the succinimide intermediate.

Isomerization of Asp32 within CDR-H1 of omalizumab converts the Fab to an inactive form, believed to be due to the change in charge orientation for the isoAsp form (Cacia et al. 1996). In theory, six Fab forms could be present (Asp, isoAsp or Asu at Asp32, with or without the VH disulfide). We modified the published (Cacia et al. 1996) papain/HIC method to allow resolution of all six Fab forms (Fig. 12-5, Table 12-3). The isoAsp32 fractions were assigned by tryptic peptide mapping. The Asu fractions were lower in mass by approximately 18 Da due to the succinimide form (Table 12-3). Collection of the isoAsp32 form using the modified HIC method confirmed that Asp32 isomerization compromises potency. The isoAsp32 and unpaired cysteine modifications may have a less dramatic effect on the activity of intact omalizumab compared to the Fab fragments, as the alternate Fab branch of the intact antibody may be unmodified and thus, retain full potency for this antibody, which does not require divalent binding for its activity.

For trastuzumab, the conversion of Asp102 residues in CDR-H3 to isoAsp allows chromatographic resolution by cation exchange chromatography; the Asu102 form can also be resolved (Harris et al. 2001). The trastuzumab form bearing one isoAsp102 residue is essentially inactive in the BT-474 anti-proliferation assay. It is interesting that the conversion of Asp to isoAsp affects the IEC elution, but does not change the pI as measured by isoelectric focusing slab gels, suggesting that charge presentation is responsible for the chromatographic resolution, and this structural change may also explain the loss of potency.

Asp32 isomerization to isoAsp was not detected by cation exchange chromatography for omalizumab; the succinimide (Asu) form can be resolved as a more basic form due to the loss of charge on the Asp side-chain (Fig. 12-6). Other forms were resolved due to Val-His-Ser- N-terminal extensions of the light or heavy chains (due to alternate cleavage of the signal peptide), or due to deamidation or sialylation in the Fc region (Table 12-4). None of these distinctions affected potency using an IgE-receptor inhibition assay similar to the one described in Cacia et al. (1996).

Asp isomerization has a dramatic effect on potency for both trastuzumab and omalizumab. This loss of potency results in the isoAsp forms being designated product-related impurities as defined in ICH Q6B, subject to direct or indirect control during lot release and stability testing.

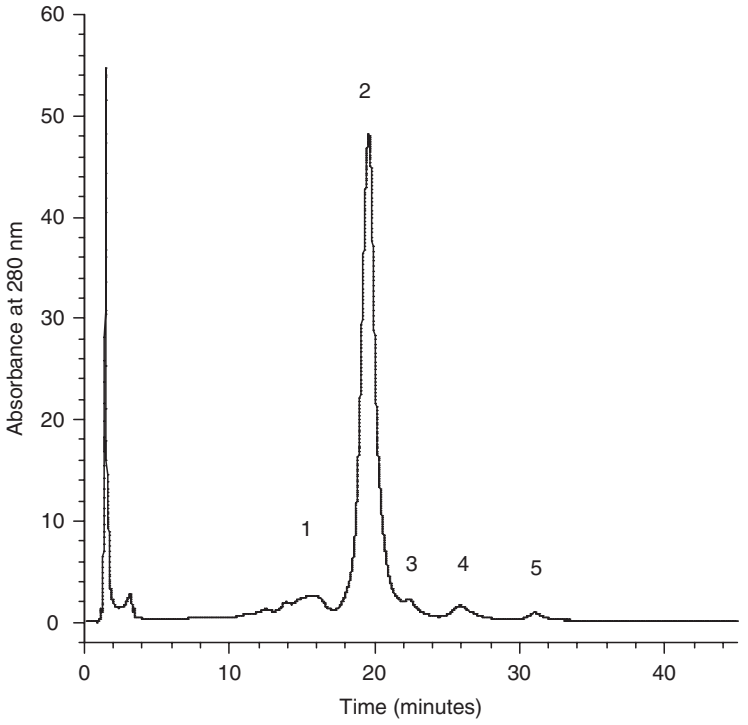

Fig. 12-6. Cation exchange chromatography of omalizumab. The molecular characteristics of the numbered peaks are described in Table 12-4

Table 12-4. Characteristics of omalizumab IEC fractions.

IEC peak	Structure	Potency (units/mg)
1	HC 375-396 deamidation or sialylated	1.1×10^4
2	Main peak	1.1×10^4
3	LC Asu32 or HC Met431 oxidation	0.9×10^4
4	Val-His-Ser- LC extension or Asu 74	0.8×10^4
5	Val-His-Ser- HC extension	1.2×10^4

9. Discussion

For cytotoxic antibodies that require ADCC, attention should be paid to levels of non-fucosylated forms and Fc site occupancy. For CDC-dependent antibodies, galactosylation may affect in vitro potency, and thus, it may need to be monitored for lot release testing even if its physiological significance is uncertain. Variability with respect to C-terminal Lys processing should not affect activity, but may influence pharmacokinetic properties, such as bioavailability, for subcutaneous administration products. There is no evidence that the distribution of the common Fc glycan types found on IgG1 antibodies produced in CHO cells will affect clearance.

Aspartate isomerization within CDRs is hard to detect using IEF-based methods, but it can have a deleterious effect on potency. A special irony for

the analytical chemist is that the isoaspartyl forms demonstrate the exquisite sensitivity of our chromatography and potency assays, as they are able to detect a single Asp to isoAsp change, but these molecular variants present us with development challenges such as instability, process constraints, and tight specification ranges. Assays using the Ellman's reagent can identify proteins with unpaired cysteines; in the case of omalizumab, these unpaired cysteines are found in the VH loop, with a significant potency loss.

Each therapeutic antibody presents us with both common and unique analytical challenges. Our licensed antibodies have validated chromatographic methods that provide key information about critical quality attributes. For omalizumab, the papain/HIC assay is able to resolve low-potency Fab forms with isoaspartyl and unpaired cysteine modifications; for trastuzumab, the key chromatographic assay is cation exchange chromatography. For rituximab, afucosylation and galactosylation may be relevant attributes. These experiences give us confidence that, we can successfully characterize these large molecules, but they also remind us that each product will require a comprehensive evaluation of the structural and functional aspects of the molecule.

References

Ashwell G, Hartford J (1982) Carbohydrate-specific receptors of the liver. Annu Rev Biochem 51:531–554

Battersby JE, Snedecor B, Chen C, Champion KM, Riddle L, Vanderlaan M (2001) Affinity-reversed-phase liquid chromatography assay to quantitate recombinant antibodies and antibody fragments in fermentation broth. J Chromatogr A 927:61–76

Boyd PN, Lines AC, Patel AK (1995) The effect of the removal of sialic acid, galactose and total carbohydrate on the functional activity of Campath-1H. Mol Immunol 32:1311–1318

Cacia J, Keck R, Presta L, Frenz J (1996) Isomerization fo an aspartic acid residue in the complementarity-determining region of a recombinant antibody to human IgE: identification and effect on binding activity. Biochemistry 35:1897–1903

Cartron G, Dacheux L, Salles G, Solal-Geligny P, Bardos P, Colombat P, Watier H (2002) Therapeutic activity of humanized anti-CD20 monoclonal antibody and polymorphism in IgG Fc receptor FcgRIIIa gene. Blood 99:754–758

Chaderjian WB, Chin ET, Harris RJ, Etcheverry TM (2005) Effect of copper sulfate on performance of a serum-free CHO cell culture process and the level of free thiol in the recombinant antibody expressed. Biotechnol Prog 21:550–553

Cohen SL, Price C, Vlasak J (2007) β-Elimination and peptide bond hydrolysis: two distinct mechanisms of human IgG1 hinge fragmentation upon storage. J Am Chem Soc 129:6976–6977

Cordoba AJ, Shyong BJ, Breen D, Harris RJ (2005) Non-enzymatic hinge region fragmentation of antibodies in solution. J Chromatogr B 818:115–121

Deisenhofer J (1981) Crystallographic refinement and atomic models of a human Fc fragment and its complex with fragment B of Protein A from *Staphylococcus aureus* at 2.9- and 2.8-Angstrom resolution. Biochemistry 20:2361–2370

Dong X, Storkus WJ, Salter RD (1999) Binding and uptake of agalactosyl IgG by mannose receptor on macrophages and dendritic cells. J Immunol 163:5427–5434

Edelman GM, Cunningham BA, Gall WE, Gottleib PD, Rutishauser U, Waxdal MJ (1969) The covalent structure of an entire γG immunoglobulin molecule. Proc Natl Acad Sci U S A 63:78–85

Ellison JW, Berson BB, Hood LE (1982) The nucleotide sequence of a human immunoglobulin Cγ1 gene. Nucleic Acids Res 10:4071–4079

Ferrara C, Stuart F, Sondermann P, Brünker P, Umana P (2006) The carbohydrate at FcgRIIIa Asn-162. An element required for high affinity binding to non-fucosylated IgG glycoforms. J Biol Chem 281:5032–5036

Furth AJ (1988) Methods for assaying nonenzymatic glycosylation. Anal Biochem 175:347–360

Gazzano-Santoro H, Ralph P, Ryskamp TC, Chen AB, Mukku VR (1997) A non-radioactive complement-dependent cytotoxicity assay for anti-CD20 monoclonal antibody. J Immunol Methods 202:163–171

Geiger T, Clarke S (1987) Deamidation, isomerization, and racemization at asparaginyl and aspartyl residues in peptides. Succinimide-linked reactions that contribute to protein degradation. J Biol Chem 262:785–794

Harris RJ (1995) Processing of C-terminal lysine and arginine residues of proteins isolated from mammalian cell culture. J Chromatogr 705:129–134

Harris RJ, Kabakoff B, Macchi FD, Shen FJ, Kwong M, Andya JD, Shire SJ, Bjork N, Totpal K, Chen AB (2001) Identification of multiple sources of charge heterogeneity in a recombinant antibody. J Chromatogr 752:233–245

Hodoniczky J, Zheng YZ, James DC (2005) Control of recombinant monoclonal antibody effector functions by Fc *N*-glycan remodeling in vitro. Biotechnol Prog 21:1644–1652

Huang L, Biolsi S, Bales KR, Kuchibhotla U (2006) Impact of variable domain glycosylation on antibody clearance: an LC/MS characterization. Anal Biochem 249:197–207

Jefferis R, Lund J (2002) Interaction sites on human IgG-Fc for FcγR: current models. Immunol Lett 82:57–65

Jefferis R, Lund J, Goodall M (1995) Recognition sites on human IgG for Fcγ receptors: the role of glycosylation. Immunol Lett 44:111–117

Jones AJ, Papac DI, Chin EH, Keck R, Baughman SA, Lin YS, Kneer J, Battersby JE (2007) Selective clearance of glycoforms of a complex glycoprotein pharmaceutical caused by terminal *N*-acetylglucosamine is similar in humans and cynomolgus monkeys. Glycobiology 17:529–540

Junghans RP, Andersen CL (1996) The protection receptor for IgG catabolism is the beta2-microglobulin-containing neonatal intestinal transport receptor. Proc Natl Acad Sci U S A 93:5512–5516

Kanda Y, Yamane-Ohnuki N, Sakai N, Yamano K, Nakano R, Inoue M, Misaka H, Iida S, Wakitani M, Konno Y et al (2006) Comparison of cell lines for stable production of fucose-negative antibodies with enhanced ADCC. Biotechnol Bioeng 94:680–688

Kanda Y, Yamada T, Mori K, Okazaki A, Inoue M, Kitajima-Miyama K, Kuni-Kamochi R, Nakano R, Yano K, Kakita S et al (2007) Comparison of biological activity among nonfucosylated therapeutic IgG1 antibodies with three different N-linked Fc oligosaccharides: the high-mannose, hybrid, and complex types. Glycobiology 17:104–118

Kaneka Y, Nimmerjahn F, Ravetch JV (2006) Anti-inflammatory activity of immunoglobulin G resulting from Fc sialylation. Science 313:670–673

Krapp S, Mimura Y, Jefferis R, Huber R, Sondermann P (2003) Structural analysis of human IgG-Fc glycoforms reveals a correlation between glycosylation and structural integrity. J Mol Biol 325:979–989

Lapolla A, Fedele D, Garbeglio M, Martano L, Tonani R, Seraglia R, Favretto D, Fedrigo MA, Traldi P (2000) Matrix-assisted laser desorption ionization mass spectrometry, enzymatic digestion, and molecular modeling in the study of nonenzymatic glycation of IgG. J Am Soc Mass Spectrom 11:153–159

Li H, Sethuraman N, Stadheim TA, Zha D, Prinz B, Ballew N, Bobrowicz P, Choi BK, Cook WJ, Cukan M et al (2006) Optimization of humanized IgGs in glycoengineered *Pichia pastoris*. Nat Biotechnol 24:210–215

Millward TA, Heitzmann M, Bill K, Längle U, Schumacher P, Forrer K (2007) Effect of constant and variable domain glycosylation on pharmacokinetics of therapeutic antibodies in mice. Biologicals 36:41–47

Mimura Y, Church S, Ghirlando R, Ashton PR, Dong S, Goodall M, Lund J, Jefferis R (2000) The influence of glycosylation on the thermal stability and effector function expression of human IgG1-Fc: properties of a series of truncated glycoforms. Mol Immunol 37:697–706

Quan C, Alcala E, Petkovska I, Matthews D, Canova-Davis E, Taticek R, Ma S (2008) A study in glycation of a therapeutic recombinant humanized monoclonal antibody: where it is, how it got there, and how it affects charge-based behavior. Anal Biochem 373:179–191

Raju TS, Scallon B (2006) Fc glycans terminated with *N*-acetylglucosamine residues increase antibody resistance to papain. Biochem Biophys Res Commun 341:797–803

Rothman RJ, Perussia B, Herlyn D, Warren L (1989) Antibody-dependent cytotoxicity mediated by natural killer cells is enhanced by castanospermine-induced alterations of IgG glycosylation. Mol Immunol 26:1113–1123

Shields RL, Lai J, Keck R, O'Connell LY, Hong K, Meng YG, Weikert SHA, Presta LG (2002) Lack of fucose on human IgG1 N-linked oligosaccharide improves binding to human FcgRIII and antibody-dependent cellular toxicity. J Biol Chem 277:26733–26740

Shinkawa T, Nakamurai K, Yamane N, Shoji-Hosaka E, Kanda Y, Sakurada M, Uchida K, Anazawa H, Sato M, Yamasaki M et al (2003) The absence of fucose but not the presence of galactose or bisecting *N*-acetylglucosamine of human IgG1 complex-type oligosaccharides shows the critical role for enhancing antibody-dependent cellular cytotoxicity. J Biol Chem 278:3466–3473

Skidgell RA (1988) Basic carboxypeptidases: regulators of peptide hormone activity. Trends Pharmacol Sci 9:299–334

Sondermann P, Osthuizen V (2002) Mediation and modulation of antibody function. Biochem Soc Trans 30:481–486

Stahl PD (1992) The mannose receptor and other macrophage lectins. Curr Opin Immunol 4:49–52

Tao M-H, Morrison SL (1989) Studies of aglycosylated chimeric mouse–human IgG. J Immunol 143:2595–2601

Tsuchiya N, Endo T, Matsuta K, Yoshinoya S, Aikawa T, Kosuge E, Takeuchi F, Miyamotot T, Kobata A (1989) Effects of galactose depletion from oligosaccharide chains on immunological activities of human IgG. J Rheumatol 16:285–290

Umana P, Jean-Mariet J, Moudry R, Amstutz H, Bailey JE (1999) Engineered glycoforms on an antineuroblastoma IgG1 with optimized antibody-dependent cellular cytotoxic activity. Nat Biotechnol 17:176–180

Weitzhandler M, Farnan D, Rohrer JS, Avdalovic N (2001) Protein variant separations using cation exchange chromatography on grafted, polymeric stationary phases. Proteomics 1:179–185

Weng W-K, Levy R (2003) Two immunoglobulin G fragment C receptor polymorphisms independently predict response to rituximab in patients with follicular lymphoma. J Clin Oncol 21:3940–3947

Wright A, Morrison SL (1994) Effect of altered CH2-associated carbohydrate structure on the functional properties an in vivo fate of chimeric mouse–human immunoglobulin G1. J Exp Med 180:1087–1096

Wright A, Morrison SL (1997) Effect of glycosylation on antibody function: implications for genetic engineering. Trends Biotechnol 15:26–32

Wright A, Morrison SL (1998) Effect of C2-associated carbohydrate structure on Ig effector function: studies with chimeric mouse-human IgG1 antibodies in glycosylation mutants of Chinese hamster ovary cells. J Immunol 160:3393–3402

Zhang B, Yang Y, Yuk I, Pai R, McKay P, Eigenbrot C, Dennis M, Katta V, Francissen KC (2008) Unveiling a glycation hot spot in a recombinant humanized monoclonal antibody. Anal Chem 80:2379–2390

Chapter 13

Analysis of Irreversible Aggregation, Reversible Self-association and Fragmentation of Monoclonal Antibodies by Analytical Ultracentrifugation

James D. Andya, Jun Liu, and Steven J. Shire

1. Introduction: Classes of Protein Aggregates and Protein Aggregation and Pharmaceutical Development

Since the emergence of recombinant DNA technology from the lab to commercialization, biotechnology protein drugs have garnered an increased share of new molecular entities (NMEs) in development pipelines (Mullin 2004). Monoclonal antibodies have rapidly become one of the major shares of this market with about 25% of biotech products in development. As with any other protein pharmaceutical monoclonal antibodies can degrade both by chemical and physical pathways. One of the most important pathways for protein physical degradation is the generation of protein aggregates. The ability of proteins to aggregate has been recognized from the early beginnings in protein biochemistry, and has become an important degradation pathway that can have a major impact on the safety and efficacy of protein drugs.

The aggregation of proteins can lead to decreases in activity and changed pharmacokinetics thus leading to alteration of efficacy. The safety profiles of protein therapeutics can also be altered. In particular, aggregation has been linked to increased immunogenicity (Hermeling et al. 2006). The later is not fully understood, often resulting in confusion as to what levels and types of aggregate are acceptable for protein drugs. Part of the confusion is that the term "protein aggregation" means different things to different people. Often protein aggregation is thought of as the result of protein unfolding whereby, the exposure of interior hydrophobic amino acid residues generates aggregated forms that are essentially irreversible, and which may lead to decreased solubility manifested as protein precipitates. In actuality, the picture is much more complex as shown in Fig. 13-1. Properly folded protein native structure is in a dynamic equilibrium with an ensemble of unfolded forms, and the amount of unfolded protein is governed by the overall equilibrium constant

From: *Current Trends in Monoclonal Antibody Development and Manufacturing,* Biotechnology: Pharmaceutical Aspects, DOI 10.1007/978-0-387-76643-0_13, Edited by: S.J. Shire et al.

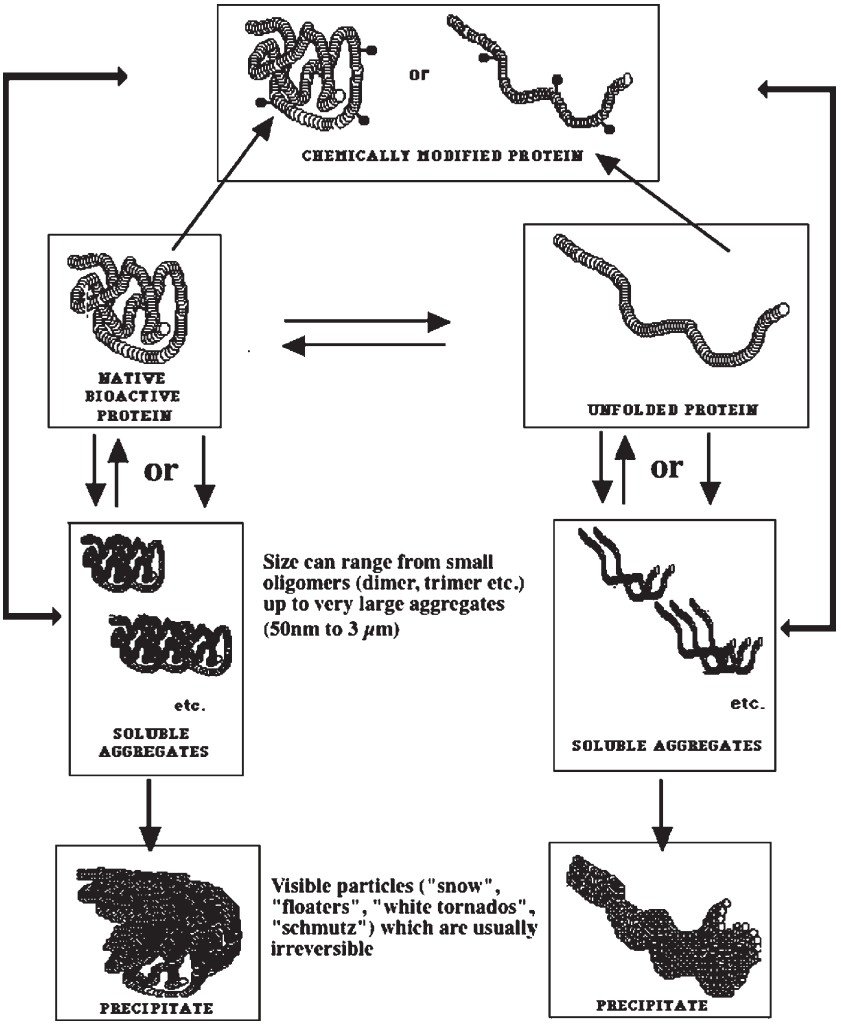

Fig. 13-1. Possible routes for the formation of soluble and insoluble protein aggregates

and hence free energies of the different species. This equilibrium is dictated by solution conditions such as pH, ionic strength and temperature. The unfolded forms under the appropriate conditions may begin to aggregate and, depending on the strength of the forces between molecules, may not easily reverse back through the dynamic unfolded to native equilibrium pathway. As these unfolded protein aggregates increase in size, the solubility may reach a point whereby precipitates are formed, and the whole complex is no longer in solution equilibrium with the soluble unfolded forms of the protein. These soluble and insoluble complexes that essentially are irreversible, or at least require long time to reverse are often thought of as protein aggregates. However, it should be recognized that properly folded native forms of the protein under appropriate conditions can in fact also associate and form aggregates that are irreversible or slowly dissociate to monomers. Another point to consider is that, such aggregates of native species may have a major impact on immunogenic response. It is generally recognized that large protein aggregates can

elicit an immune response, but the antibodies that are generated from unfolded protein likely will not cross react to a large extent with properly folded protein. Assemblies of native protein, on the other hand probably can generate antibodies that will react with the properly folded protein, which may neutralize function and activity of the protein drug. In addition, such aggregates may present a surface of repeating protein structures, and hence epitopes much like a virus and have been termed virus-like structures. The classic work of Dintzis et al. (1989), Vogelstein et al. (1982), shows how such assemblages can result in enhanced T cell independent immune responses. Clearly, not only the amount of aggregate but also the type of aggregate, will dictate the severity of immune responses and hence can impact safety and efficacy.

In addition to the irreversibility of native protein aggregates is the possibility of reversible aggregation, that is concentration dependent and often referred to as protein self-association. This is often thought to be less of an issue upon therapeutic administration, because it is expected that following dilution upon administration, these types of aggregates will dissociate back to the native monomeric protein. However, these aggregates will be introduced into a crowded environment whether in the blood or in the subcutaneous space. The impact of molecular crowding may kinetically and thermodynamically enhance the association as discussed by Minton (2005), (Zhou et al. 2008). Reversible association can also lead to altered solution properties such as viscosity which has implications for manufacturing, stability and delivery of high concentration protein drugs developed for subcutaneous administration. Protein self-association behavior may also be difficult to measure analytically, since the conditions of an assay can influence the observed size distribution.

Since the impact of the different complexes is not well understood, generally the safest course of action during protein drug development is to attempt to minimize all aggregate forms, and hence there is a need for rapid and accurate analytical methods to assess both reversible and irreversible forms of protein aggregates.

2. Methods for Analysis of Protein Size Distribution

Size exclusion chromatography has been the main workhorse in the industry for analysis of protein size distribution. The chromatography is fairly rapid, easy to use and HPLC equipment is found in virtually every pharmaceutical analytical laboratory. However, there are several issues and concerns in the use of this analytical approach. The hydrodynamic volume of the different species rather than molecular mass dictates the chromatographic separation. Often globular protein standards are used to assign mass values and molecules with huge asymmetry will run aberrantly when compared to these standards. In addition, different protein molecules may interact very differently with the column matrix. This can result in huge errors in determinations of molecular weight as shown by work on highly glycosylated proteins, where the extended sugar residues lead to greater hydrodynamic volumes and thus greater apparent molecular mass (Shire 1994). Coupling light scattering detection with the chromatography to get weight average molecular weight across the elution profile can circumvent this problem. However, reversible protein self-association may be difficult to analyze by SEC because of the dilution that occurs during the chromatography. In addition, preferential interactions with the column matrix may result in the removal of aggregated species from the

effluent resulting in lack of detection of the aggregated protein. Adding organic solvents or salts to decrease these matrix–protein interactions often mitigates this problem, but then raises the possibility that such manipulations impact the true size distribution. All of these concerns have prompted regulatory agencies to request the evaluation of protein size distribution data using orthogonal biophysical techniques such as, field flow fractionation (FFF), light scattering or analytical ultracentrifugation (AUC). The latter has rapidly emerged as the main technology for investigating the robustness of size exclusion chromatographic analysis, since it is a separation based technology that yields a size distribution that depends on a well-defined physical parameter, the sedimentation coefficient, and gives comparable resolution as SEC (Fig. 13:2). Since the separations occur in solution phase, the problems of interaction with solid support matrices is eliminated. AUC can also be carried out under a variety of solution conditions. Therefore, it is possible to directly test protein under conditions used in an SEC analysis. In addition, centrifugation may be carried out directly in a protein formulation buffer provided that, complications

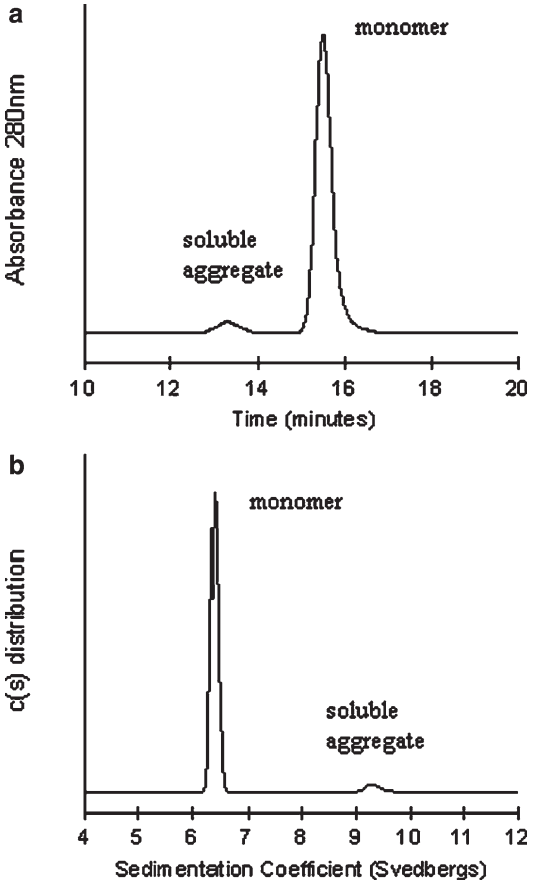

Fig. 13-2. Native size distribution analysis of a degraded antibody sample by (**a**) SEC and (**b**) AUC. AUC was carried out in the SEC mobile phase and the data was analyzed by the Lamm equation modeling program, SEDFIT. A similar amount of soluble aggregate of 5% was determined by both methods

of possible electrostatic interactions and sedimentation of excipients are taken into account. Finally, the dilution of samples during the centrifugation only occurs due to the wedge shape of the sectors in an analytical ultracentrifuge cell. Thus the typical dilutions during an SEC experiment which may be as much as 3–5-fold will be greater than by AUC, and thus with fast dissociation kinetics may be not be able to detect reversible self-association (Shire 1994). Although for the reasons discussed above, it remains necessary to use AUC as an orthogonal method to confirm SEC results, SEC remains the primary method of choice because of its high precision and ease of use. In particular, AUC requires an expensive piece of equipment and personnel who are trained in its use as well as analysis of the data.

3. What is Analytical Ultracentrifugation?

A modern analytical ultracentrifuge is a centrifuge capable of good temperature and rotational speed control, and is equipped with optical systems that allow for direct measurement of concentration gradients of sedimenting molecules generated by a high centrifugal force up to ~300,000 × g. The original design of the instrument by Thé Svedberg (Svedberg and Rinde 1924), and subsequent advances by Pickels (1950, 1952) served as the basis for the design of the first commercially available analytical ultracentrifuge, the Model E by the Beckman, Spinco Division. The development of the Model E was a great accomplishment and resulted in classic work that laid the foundations for modern protein chemistry and molecular biology. The early experiments on hemoglobin conducted by Svedberg and Fåhraeus (1926) demonstrated conclusively that, proteins were actually homogeneous macromolecular entities and the semi-conservative replication of DNA was elucidated by Meselson and Stahl in their classic centrifuge experiments (Meselson and Stahl 1958). Since those classic experiments, many labs became expert and proficient in using the Model E. However, the maintenance and ease in using of this instrument were very challenging, and the field was generally restricted to a set of dedicated and technical experts who not only used the technology to quantitatively solve biological problems, but also contributed to the evolution of the Model E. These contributions have included development of refractive optics (Philpot and Cook 1948) and the UV absorption scanner as well as software for analysis and hardware, and software to allow for instrument control and computer data acquisition (Schachman and Edelstein 1966; Williams 1976). With the introduction of the XLA and XLI analytical ultracentrifugation, technology became more accessible to the non-specialized user. In particular, the new instrument can attain a maximum speed of 60,000 rpm and is equipped with a highly precise and stable temperature control system. The absorption optics use a highly stable, UV-enhanced xenon flashlamp as the light source and a toroidal diffraction grating monochromator to provide the wavelength range from 190 to 800 nm (Giebler 1992). The Rayleigh optical system which is extremely useful for analyzing the sedimentation of non-absorbing macromolecules in solution uses a 30 mW, 675 nm laser as the light source (Furst 1997). In addition, the new centrifuge has improved computer interfacing allowing for computer control of the experiment and dependable data acquisition.

4. Analytical Ultracentrifugation Theory

A change in mass concentration, c , of solute molecules with diffusion coefficient D and sedimentation coefficient s in a two component system as a function of time under an applied centrifugal force $\omega^2 r$ is given by the Lamm equation (Lamm 1929; Cantor and Schimmel 1980):

$$\frac{dc}{dt} = \left(\frac{1}{r}\right)\frac{d\left\{r\left[D(dc/dr) - cs\omega^2 r\right]\right\}}{dr} \tag{13.1}$$

when an analytical ultracentrifuge is run at high rotor speeds resulting in high centrifugal forces, the sedimenting molecules undergo mass transport and the experiment is referred to as sedimentation velocity whereby, different non-interacting sedimenting molecules form unique concentration boundaries. The sedimentation coefficient of a macromolecular species shown in the Lamm equation is usually expressed in Svedberg units ($1S = 10^{-13}$ s), and is the velocity of the concentration boundary divided by the applied centrifugal force, and is directly related to the molecular mass M and the translational diffusion coefficient, D by the Svedberg equation:

$$s = \frac{v}{\omega^2 r} = \frac{M(1-\bar{v}\rho)D}{RT} \tag{13.2}$$

where v is the rate of sedimentation, ω the angular velocity, r the radial distance from the center of rotation, M the molecular mass, $\bar{v}$ the partial specific volume of solute, ρ the density of solvent, R the gas constant and D the diffusion coefficient. As can be seen by the Svedberg equation during the sedimentation velocity experiment, macromolecules are separated based on not only the molecular mass, but also on the shape, since the diffusion coefficient is inversely related to the frictional coefficient of the molecule. In theory, the sedimentation coefficient of each species can be determined by analyzing the rate of movement of a midpoint in the boundaries, or more rigorously the migration of the second moment of the boundary. In the case where the sedimenting molecules are interacting, depending on the kinetics of the interaction, the sedimentation boundaries do not represent single species but rather a mixture of species in a reaction boundary. Theories have been developed to describe these boundaries, and in some cases the stoichiometries and equilibrium constants of interacting systems (Stafford 1997) can be evaluated. For non-interacting species, the velocity and shape of the moving boundary can be used to determine the sedimentation coefficient (s) and diffusion coefficient (D) of the individual macromolecular species. However, such analysis only yields an average s value for a complicated system composed of multiple sedimenting species. The diffusional spreading of the boundaries can also obscure the presence of other species. These problems can be at least addressed in part by several more sophisticated sedimentation velocity methods, including the Van Holde and Weischet method (Van Holde and Weischet 1978; Demeler et al. 1997), and the whole boundary curve fitting method (Philo 1994). The sedimentation coefficient and diffusion coefficient determined from these methods can be used to study more about the shape and size of the sedimenting species (Byron 1997; Laue 1997). The time derivative method (Stafford 1992, 1997) developed by Stafford although useful for investigating relatively large

complexes, is not correct for diffusional spreading and thus has limited use in resolving distribution of smaller non-interacting aggregates. Recent advances in fitting data directly to the Lamm equation which have been incorporated in the program SEDFIT (Schuck 2000) have addressed some of these issues, and in particular, since diffusion is taken into account, the analyses are capable of resolving non-interacting species including dimers and higher order structures. A nice summary of the strategy used in SEDFIT to numerically solve the Lamm equation has been provided in a recent review (Berkowitz 2006).

Although there is considerable resolving power when using the centrifuge, it is important to verify that the different species observed are truly different molecular mass complexes. Resolution of peaks by SEDFIT does not necessarily relate to different size complexes, but may be related to aggregates with different conformation and hence different frictional coefficient. This issue can be addressed by running the centrifuge at lower rotor speeds, where under those conditions, the rate of sedimentation in the centrifugal field is opposed by the rate of diffusion, and eventually when they reach equilibrium, a time invariant exponential concentration gradient of solute is established throughout the centrifuge cell. The concentration distribution at equilibrium can be rigorously described with thermodynamic theory, and has been widely used to determine the molecular weight, stoichiometry, binding affinity and virial coefficient. For an ideal, non-interacting multiple-component system, the concentration distribution at equilibrium can be described as

$$C(r) = \delta + \sum_{i=1}^{n} c_i(r_o) \exp\left\{\frac{M_i(1-\bar{v}\rho)\omega^2(r^2 - r_o^2)}{2RT}\right\} \tag{13.3}$$

where $C(r)$ is the concentration at radial position, r, $c_i(r_0)$ the concentration of the ith species at an arbitrary radial reference position, r_0, δ the baseline offset, M_i the molecular weight of ith species, T the temperature in Kelvin, ω the angular velocity, $\bar{V}$ the partial specific volume of solute, ρ the density of solvent and R the gas constant. The derivation of this equation results directly from the Lamm equation since at sedimentation equilibrium there is no net transport, and the contributions from sedimentation and diffusion in the brackets are equal to each other, i.e., for one component:

$$D(\mathrm{d}c / \mathrm{d}r) = cs\omega^2 r \tag{13.4}$$

Grouping of terms, insertion of the Svedberg equation, and integration results in Eq. 13.2 for one ideal sedimenting component. For such a system containing only a single sedimenting ideal species, the molecular weight measurement can be made by simply fitting the data of concentration as a function of radius position. For more complicated systems, in principle Eq. 13.3 can be further modified to allow the sedimentation equilibrium data to be fit to models, that incorporate self or hetero association systems as well as corrections for thermodynamic nonideality by including virial coefficients as fitting parameters (McRorie and Voelker 1993).

5. Application of Analytical Ultracentrifugation

Analytical ultracentrifugation is a method to analyze protein concentration gradients during high speed centrifugation. The instrumentation consists of a sample cell with optical grade quartz or sapphire windows, a rotor that

maintains cell position and orientation during centrifugation, a temperature controlled high speed centrifuge, that is capable of speeding up to 60,000 rpm and an absorbance or interference optical system to monitor protein sedimentation during the run. A sedimentation velocity analysis involves loading protein and buffer blank samples into a double sectored cell that, along with a reference cell for radial position calibration, is placed into a 4- or 8-hole rotor. For analysis of a monoclonal antibody, centrifugation is typically carried out at speeds of 40,000–60,000 rpm. Protein sedimentation during centrifugation is observed by taking continuous radial absorbance scans during the run, and a sedimentation velocity experiment takes approximately 3 to 4 hours. The resulting data are a series of boundary scans obtained as protein moves during centrifugation according to the forces of sedimentation and diffusion. An example of raw centrifugation data is shown in Fig. 13-3, where boundary scans are shown from the analysis of a monoclonal antibody sample with 1 and 6% soluble aggregate. The boundary consists of a transition region that defines protein movement down the cell and a plateau region. Absorbance in the plateau region decreases during centrifugation because of the sector shaped cell which minimizes convection effects. Fig. 13-3 also shows that resolution of components in a protein mixture may be observed in the boundary as in this case separation of soluble aggregate and antibody monomer occurred near the plateau region.

Various data analysis programs have been developed to analyze protein size distribution from the concentration gradient during centrifugation, in terms of sedimentation rates. In a final state, sedimentation velocity data is visualized as a sedimentation coefficient distribution function, that looks very much like a typical chromatogram from an SEC experiment (Fig. 13-2). An easily employed method for data analysis that involves no modeling assumptions is the time derivative or DC/DT. In this analysis, the $g(s^*)$ sedimentation coefficient distribution function is calculated using a subset of boundary scans that are pair-wise subtracted to define components and remove time-independent

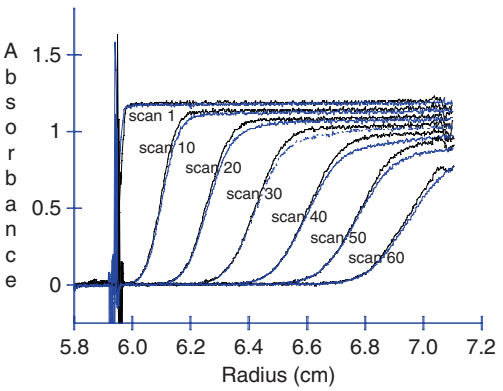

Fig. 13-3. Protein boundary scans obtained during sedimentation velocity analysis of a monoclonal antibody samples containing 1 and 6% soluble aggregate. The sample with higher amount of aggregate is visualized by increased sedimentation near the plateau region of the boundary scans

noise. An example of using DC/DT to analyze an antibody sample consisting of a mixture of 20% FAB and 80% full-length antibody is shown in Fig. 13-4. Although separated species in the mixture are observed, the resolution is not optimal. A limitation of the DC/DT analysis is that, the method does not account for diffusion during sedimentation and utilizes only a subset of scans taken during the run.

More recently, data analysis programs such as SEDFIT have been developed that employ least squares fitting to directly solve the Lamm equation. The analysis involves an iterative application of several parameters that characterize meniscus position, protein size and shape to best fit the experimental boundary data. Lamm equation modeling better accounts for protein physical parameters such as molecular weight, conformation and diffusion that influence the concentration gradient during centrifugation. The result is vastly improved resolution. As shown in Fig. 13-4, the application of SEDFIT to the antibody sample prepared with 20% FAB and 80% full length antibody results in excellent resolution of the protein components, that equals or exceeds that of chromatography methods. The availability of Lamm equation modeling programs, such

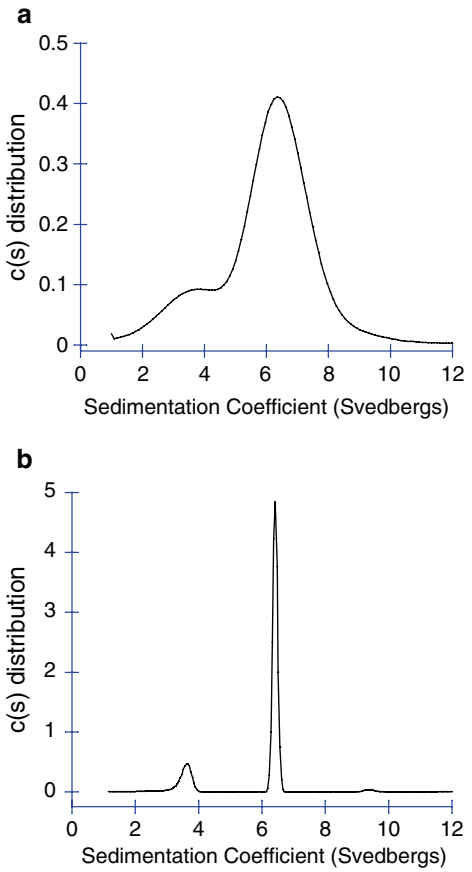

Fig. 13-4. AUC SV of a mixed 20% FAB and 80% full-length antibody sample with data analysis carried out using (**a**) DC/DT and (**b**) SEDFIT

as SEDFIT, has helped to establish AUC sedimentation velocity as the method of choice for use as an orthogonal test of native protein size distribution.

An advantage of measuring native protein size distribution by AUC is the ability to detect reversible self-association. This physical property can be observed in both sedimentation velocity and equilibrium analysis. For example, Fig. 13-5 shows SEC and AUC sedimentation velocity of a monoclonal antibody sample carried out in the same buffer system (i.e., SEC mobile phase). SEC analysis showed a single monomer peak at 99.6% with a small amount of aggregate species. However, a difference in size distribution heterogeneity was observed during AUC sedimentations velocity in the SEC mobile phase buffer. Evidence of reversible self-association was obtained in further studies in PBS buffer, that showed the weight-average sedimentation coefficient for the sample was dependent on protein concentration during the analysis (Fig. 13-6). In addition, sedimentation equilibrium data showed that the observed weight average of the molecular weight of the antibody increased with increased protein concentration (Fig. 13-7). Therefore, in this case using AUC as an orthogonal method for protein size distribution resulted in the detection of reversible self-association behavior that was difficult to be measured by the commonly used SEC method alone.

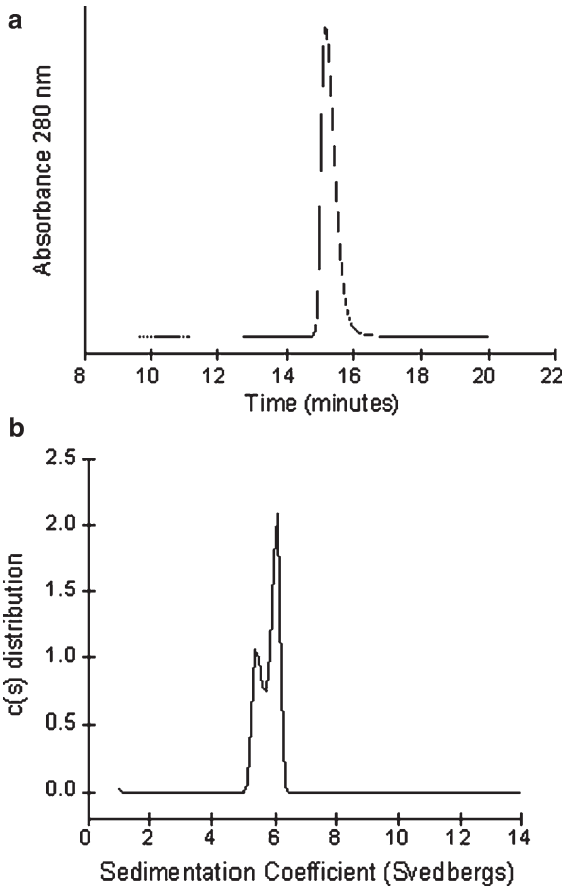

Fig. 13-5. Size distribution analysis of a full-length monoclonal antibody carried out using (**a**) SEC and (**b**) AUC sedimentation velocity in identical buffer systems

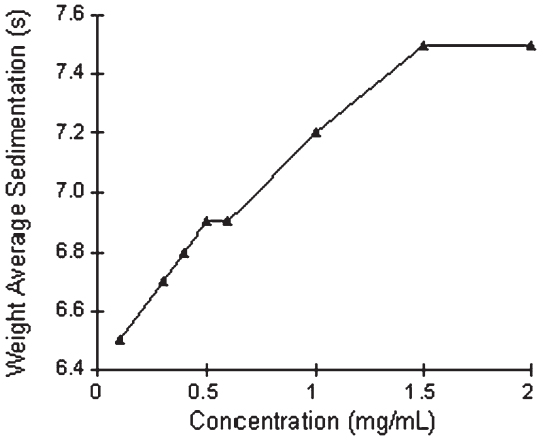

Fig. 13-6. Weight average sedimentation coefficient versus protein concentration observed during AUC sedimentation velocity analysis of a monoclonal antibody shown in Fig. 13-5 in PBS buffer

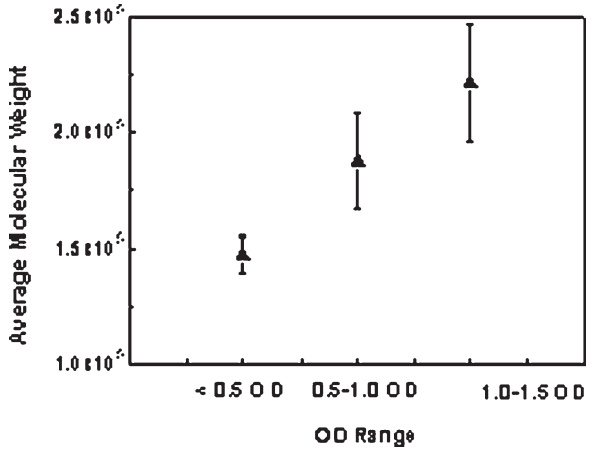

Fig. 13-7. Weight average molecular weight determined by sedimentation equilibrium of the antibody sample shown in Fig. 13-5 in PBS buffer

6. Method Optimization to Evaluate Trace Amounts of Aggregate

6.1. Assay Precision and Reproducibility

As discussed above, AUC sedimentation velocity analyzed by SEDFIT is well suited as an orthogonal method to measure protein size distribution. However, establishing the precision and reproducibility to measure small amounts of aggregate species is important to its utility in the analysis of pharmaceutical proteins, such as a monoclonal antibody, that may contain low amounts of aggregate species. An analysis of an antibody aggregate system, including dimer and higher order species, using simulated data suggested that sedimentation velocity resulted in a limit of quantitation of from 0.2 to 0.6% depending

on the aggregate species and the amount of random noise introduced to the analysis (Gabrielson et al. 2007). However, as discussed further below, AUC of actual samples is influenced by not only random noise but also errors that are intrinsic to the instrumentation such as systemic noise, cell alignment, the measurement of radial position and wavelength. These factors, which can influence assay precision and accuracy, may be difficult and impossible to reproduce using the simulated data. For example, our initial attempts to apply SEDFIT to measure aggregate with pharmaceutical antibody samples were not encouraging. Fig. 13-8 shows the triplicate analysis using AUC sedimentation velocity in three centrifuge cells in single 4-hole rotor. The data were analyzed by SEDFIT following the simple procedure of calculating the $c(s)$ distribution profile by floating meniscus position and protein shape parameters. The results showed the quantitation of the main aggregate species that was presumable antibody dimer which was not reproducible. In addition, other aggregate and fragment species appeared that may be artifacts. Improving the precision and reproducibility of SEDFIT to determine small amounts of antibody aggregate required an optimization of both the experimental setup and analysis procedures.

6.2. Instrument, Cell Condition and Signal Noise

As shown previously in Fig. 13-3, the physical separation of dimer from antibody monomer can be observed as small changes in absorbance near the plateau region of the boundary. Therefore, any error or noise in the absorbance scans can affect the resolution of trace amounts of aggregate species. Noise in an AUC experiment has been characterized as systematic and random (Liu et al. 2006). Systematic noise includes time-invariant and radial-invariant noise that can be removed by analysis programs such as DC/DT and SEDFIT. Random noise is more difficult to identify and control. Sources may include intrinsic noise from the optical system as well as errors in the precise measurement of radial position and maintaining the wavelength during the run.

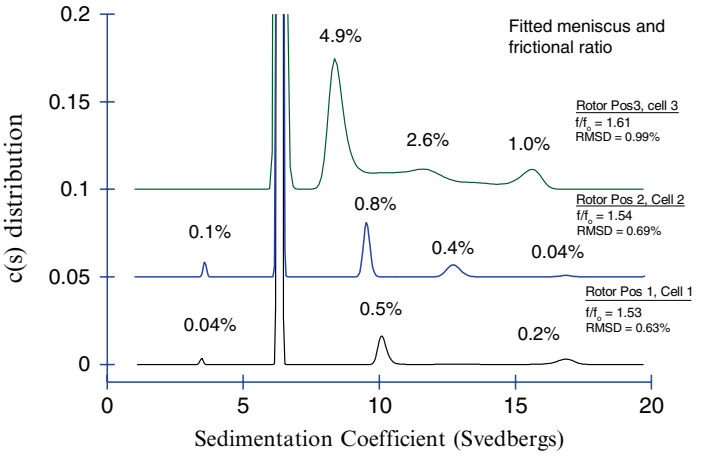

Fig. 13-8. Triplicate AUC sedimentation velocity analysis of an antibody sample containing approximately 1% aggregate by SEC

To study wavelength stability during centrifugation, we devised a test that involved taking repeat scans of a small molecule with a suitable absorbance spectrum during centrifugation at slow speeds, where no net movement of the molecule occurs (i.e., 3,000 rpm). For this analysis, the amino acid tryptophan was added to a standard 1.2 cm AUC cell. Absorbance was monitored at a wavelength of 230 nm, which is a spectral region where absorbance changes significantly with a small change in wavelength. As shown in Fig. 13-9, variability was observed in the absorbance measured between some of the successive scans that can only be caused by a drift of wavelength. A comparison of the magnitude of the absorbance variability with the known tryptophan absorbance spectra allowed us to calculate that a wavelength change of 1–2 mm occurred in some of the scans during the analysis. Wavelength variability can introduce a systematic error, that cannot be corrected by analysis software and may affect assay precision. For example, a test using simulated data of an antibody with 1% dimer, where an error of 5% change in OD was introduced to 10% of the scans showed that quantitation of aggregate species dropped from 1.0 to 0.8% (Liu et al. 2006). Given the surprising nature of this error, each centrifuge involved in measuring small amounts of protein aggregate should be checked for characterization of wavelength drift. In addition, to minimize the influence of wavelength drift on the analysis, the absorbance of a protein sample should be measured at 278–280 nm, which is a peak position where slight changes in wavelength have less of an effect on the absorbance value.

In addition to the wavelength issue, cell alignment to the center of rotation has been found to be an important source for assay variability. The cell alignment usually is achieved by aligning the score mark on the bottom of the cell housing with the mark on the rotor. Misalignment of cell can lead to convection and disturbance of the moving boundary. A recent study by Arthur and his colleagues (Arthur et al. 2006) showed that, cell misalignment can be a major source of variability for their model protein systems. They have shown significant change of aggregate distribution even with an alignment off by just 0.5°. Misalignment due to visual error can be avoided by using an alignment tool provided by Spin Analytical (Spin Analytical, NH). The other factors, such as quality of the centerpiece and precision of the keyway slot can also contribute to the variability of measurement. Recent work by Pekar and colleagues showed that the precision and accuracy of quantification appear

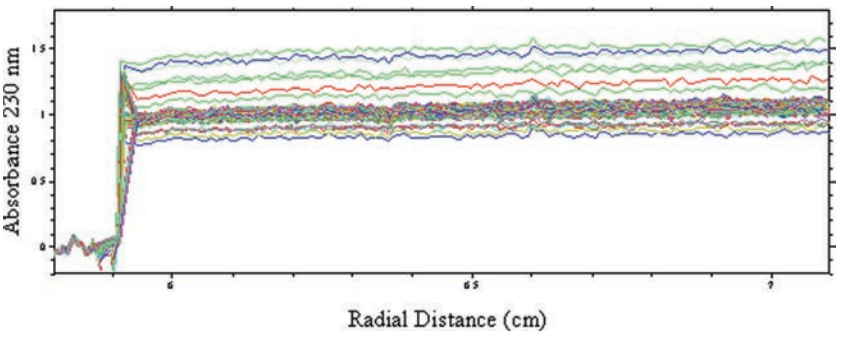

Fig. 13-9. Radial absorbance scans of L-tryptophan at 230 nm during slow speed centrifugation (3,000 rpm). For this analysis, 200 scan were collected using a 1.2 cm cell

to be highly dependent on the quality of the centerpiece (Pekar et al. 2007). A careful evaluation of the centerpiece by microscope and experimental data is critical to obtain relevant and reproducible results for measuring protein size distribution.

Another source of variability can be the intrinsic noise associated with photometric detection. This error can be minimized by experimental setup to maintain a good signal-to-noise level, as is appropriate for any spectrophotometric measurement of a protein solution. For example, to improve the signal-to-noise level, we routinely load our AUC cells to achieve a total absorbance of 1.0. To illustrate the importance of experimental configuration, Fig. 13:10 shows a case where the signal to nose level was purposely reduced by under loading at a concentration, where spectrophotometer noise can significantly affect the signal or by overloading the cell with protein at a concentration that is outside the linear range of the spectrophotometer . In both cases a worsening of the signal-to-noise resulted in changes in the distribution profile of minor components.

6.3. Meniscus Position

The precise measurement of radial position is important to the precision and accuracy of detecting minor components in an AUC sedimentation velocity experiment. This is illustrated in an analysis of the meniscus, which is the position defined as the top of the liquid column in the sample sector of the AUC cell. The meniscus is visualized by loading the assembled AUC cells with approximately 25–50 μL less volume of the protein in the sample sector than the amount of buffer in the reference sector. The slight difference in volume is observed as a sharp absorbance spike in the radial absorbance spectra that corresponds to the starting point of sedimentation. AUC instrumentation is designed to obtain precise radial position measurements every 0.001 cm with an error of ±0.001 cm. As shown in Fig. 13-11, when the absorbance spike that defines the meniscus position from multiple scans is analyzed on this scale, it is not immediately clear as, where the true meniscus position occurs.

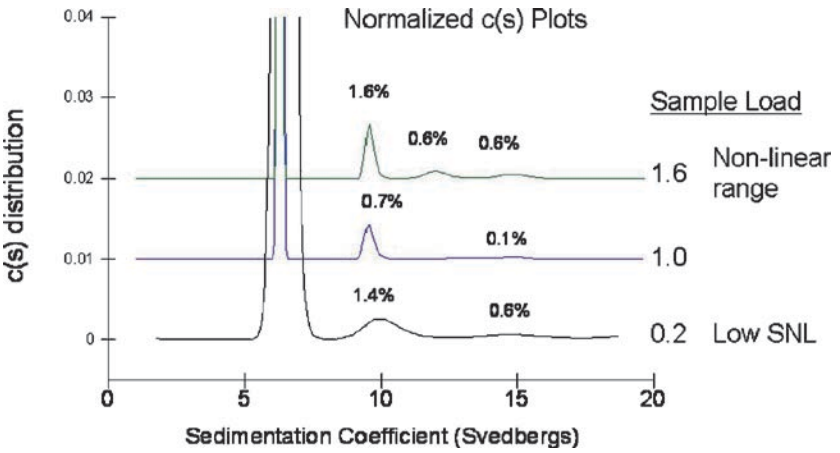

Fig. 13-10. Effect of signal to noise level on antibody aggregate upon under-loading

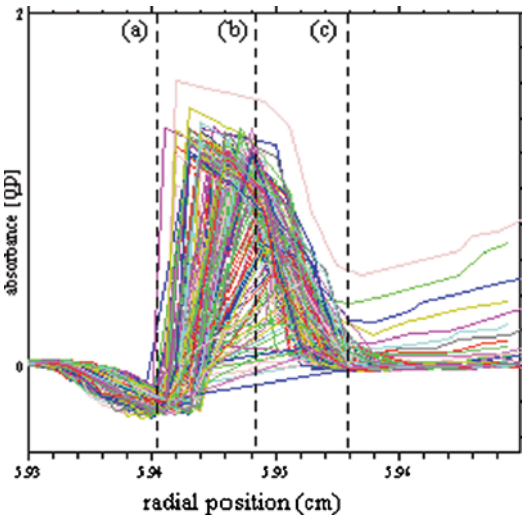

Fig. 13-11. Meniscus potion during the AUC sedimentation velocity analysis of a monoclonal antibody where (**a**) and (**c**) represent the lower and upper range, (**b**) is the calculated midpoint position of the absorbance spike

Determining the optimal position of the meniscus is a key parameter in the analysis of sedimentation velocity data with SEDFIT. When this parameter is floated, the program iteratively evaluates different positions and selects the best value based on the minimal RMS error of the fit. Fig. 13-12 shows an example of the fitting error observed as a function of meniscus position during centrifugation of a monoclonal antibody. The meniscus position that minimized fitting error was slightly off from the center position determined externally by simply measuring the start and end of the absorbance spike. The corresponding influence of meniscus position on the protein size distribution of a monoclonal antibody is shown in Fig. 13-13. Little effect is observed on the sedimentation determined for antibody monomer; however, a slight change in meniscus position significantly influences the sedimentation and quantitation of minor component species. For example, a meniscus position too far to the right of the center position results in less aggregate, and the introduction of presumably artifactual fragment species. Conversely, a meniscus position placed left of the center position results in overestimated amount of aggregate species and may also introduce artifacts. In our experience with data analysis, floating the meniscus position to minimize fitting error resulted in significant variability in the quantitation of small amounts of aggregate species between replicate samples. For example, this was the primary source of error in the replicate data shown in Fig. 13-8. To improve the fit, we routinely set the meniscus to the center position determined externally by measuring the absorbance spike.

6.4. Frictional Ratio

As discussed above, protein separation during centrifugation occurs because of differences in molecular weight and conformation. Protein shape affects translation movement, and is characterized by the frictional coefficient that is

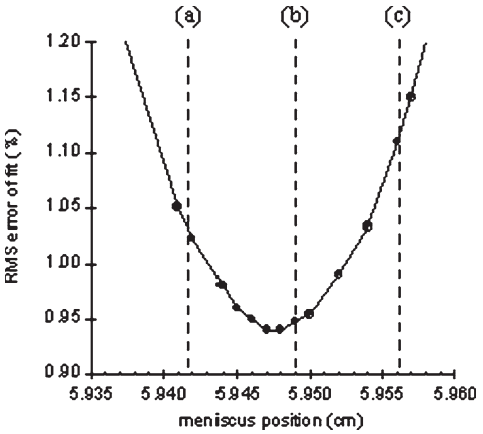

Fig. 13-12. Effect of meniscus position and RMS error of fit during SEDFIT analysis. The relative meniscus position is represented by lines denoted by (**a**) and (**c**) the lower and upper range and (**b**) is the calculated midpoint position

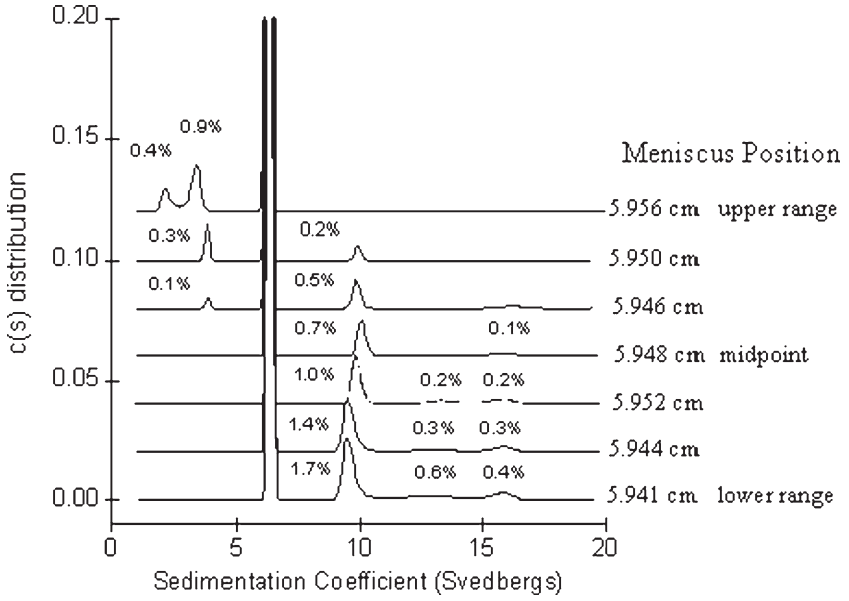

Fig. 13-13. Effect of meniscus position on the determined $c(s)$ sedimentation coefficient distribution

inversely related to diffusion as defined by the Svedberg equation. Therefore, incorporation of a shape factor is an important parameter in Lamm equation modeling of sedimentation velocity data. To account for molecular conformation, the SEDFIT program defines the frictional ratio as the translational friction of the protein divided by that of a sphere of equal mass (Schuck 2000). Therefore, this factor simply characterizes how much of the molecule departs from a spherical conformation. In the data analysis routine, the program iteratively applies various frictional ratio values along with other parameters to

arrive at a best fit solution to the experimental data. The determined frictional ratio will vary with different proteins depending on their relative shape. For example, in the separate analysis of monoclonal antibody Fab and full-length molecules, a best fit of the data was obtained by applying a frictional ratio of 1.27 and 1.56, respectively.

Determining an optimized frictional ratio becomes more complicated in samples containing multiple species and minor components. In the simplest analysis routine, SEDFIT determines a weight average frictional ratio to best fit the data. As shown in Fig. 13-14, this parameter can significantly affect the sedimentation value and quantitation of minor species such as soluble aggregate in an antibody preparation. In these samples, the weight average frictional ratio is dominated by the monomer, and this may introduce analysis errors in the minor component analysis, especially, if the shape differs significantly from that of the monomer (Schuck 2000). An improved fit may be obtained by analyzing the data in a bimodal mode, where frictional ratio values are fitted to different regions of sedimentation. Alternately, known molecular weight and sedimentation coefficient value of individual species

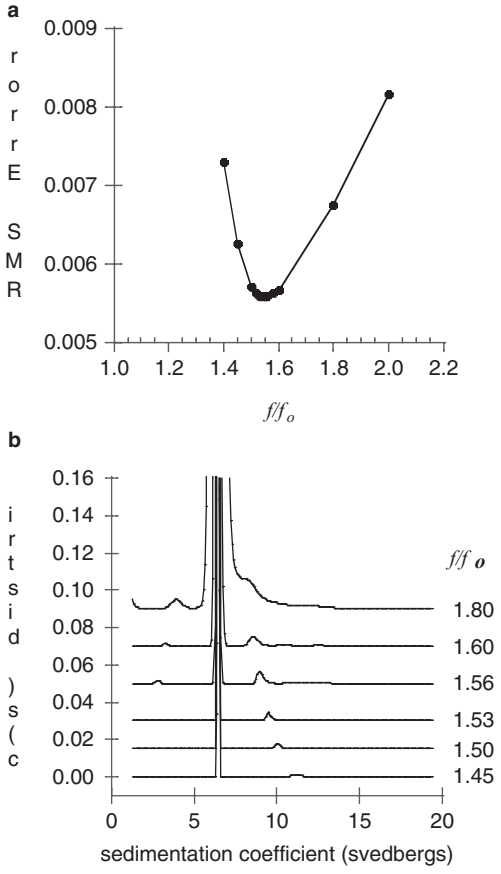

Fig. 13-14. Effect of f/f_o on antibody size distribution profile determined by SedFit were (**a**) shows the effect of f/f_o on fitting error and (**b**) shows the corresponding normalized $c(s)$ distribution profile. An optimal $f/f_o = 1.56$ was determined to best fit the data

can be used to calculate the frictional ratio of components and these numbers can be applied to the analysis. This analysis strategy is illustrated by a study of monoclonal antibody Fab and full-length mixtures that were prepared containing 2, 5, 10 and 20% Fab whose sedimentation velocity data were analyzed using the three methods described above. Table 13-1 shows a comparison of the weight average frictional ratio from the samples determined by best fitting the experimental data, and by calculating the value from prior knowledge of the separate components. Improved quantitation of the minor component in the mixture was obtained as a better estimate of the protein frictional ratio was applied to the data.

Given the importance of the frictional ratio to the accuracy and precision of a SEDFIT analysis, it is important to test the shape factor model that is used in data analysis. An example is shown in Fig. 13-15 where a monoclonal antibody sample containing approximately 0.9% dimer species by SEC was measured by AUC sedimentation velocity. In this case, the experiment was configured to obtain continuous scans of a single cell and the sample was measured in triplicate. For data analysis, the meniscus position was set to the midpoint of the absorbance spike and not floated. The frictional ratio applied to the data was analyzed using two methods. First, the $c(s)$ distribution function was calculated using the weight-average value that minimized RMS fitting error, and this resulted in a dimer value of $0.8 \pm 0.1\%$ and two higher molecular weight species of less than 0.2%. The data were also analyzed in bimodal mode by assigning a frictional ratio to the monomer that was calculated using the known sedimentation coefficient and molecular weight of the monoclonal antibody, and floating the frictional ratio for the aggregate species. In this case, a similar amount of dimer of $0.7 \pm 0.1\%$ along with the two higher molecular weight species of less than 0.2% was determined. Testing the parameters in this fashion gives improved confidence in the fitting model that is used to analyze the data.

7. Summary of Experimental Configurations to Improve Reproducibility

The analytical ultracentrifuge is a powerful orthogonal method to monitor native protein size distribution. The application of the technique to measure protein aggregate at levels expected in a pharmaceutical antibody preparation requires extra care in instrument maintenance, experimental setup and data analysis. For example, the instrument should be in good working order and

Table 13-1. Quantitation of FAB and full-length antibody mixtures by SEC and AUC sedimentation velocity.

Sample Mixtures[a]		Weight average f/fo		Peak area Bimodel f/fo		Assigned f/fo	
FAB (%)	**Full-length (%)**	**FAB (%)**	**Full-length (%)**	**FAB (%)**	**Full-length (%)**	**FAB (%)**	**Full-length (%)**
2	98	1	99	2	98	2	98
5	95	4	96	5	95	5	95
10	90	8	92	10	90	10	90
20	80	18	82	20	80	20	80

[a]Quantitation of sample mixtures determined by SEC

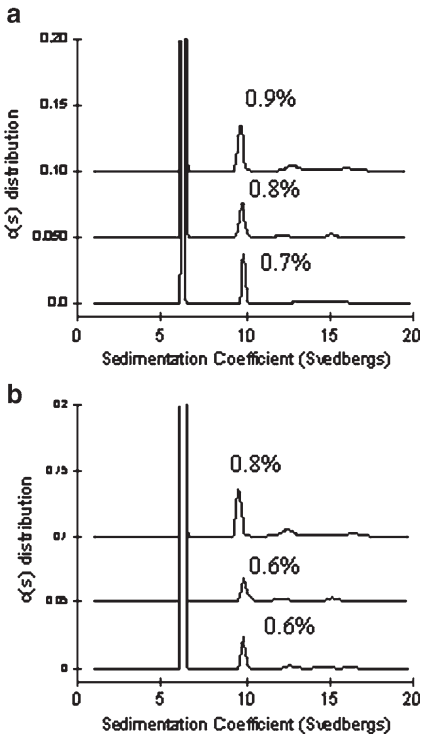

Fig. 13-15. AUC sedimentation velocity of a monoclonal antibody sample with data analyzed by SEDFIT. The sample was run in triplicate and data analysis that was carried out by setting the midpoint position of the absorbance spike as the meniscus position. In addition, SEDFIT analysis was carried out by (**a**) floating the frictional ratio and (**b**) assigning a frictional ratio of 1.53 to the monomer and floating the value for aggregate species. The first analysis method resulted in an estimated amount of dimer of $0.8 \pm 0.1\%$ and the second method resulted in a dimer level of $0.7 \pm 0.1\%$. In each case two higher molecular species were observed at a level of 0.1% or less

regularly checked for wavelength, radial position and temperature calibration. The experiment should be carried out under conditions that provide good signal to noise for the optical system. To minimize the effects of wavelength drift, data should be collected at a wavelength, where the absorbance does not change appreciably with 1–2 nm change in wavelength. For protein molecules this means monitoring the absorbance at 279–280 nm. The configuration of the experiment in terms of number of scans taken can also affect the precision of the analysis, where more scans can lesson the influence of random noise and wavelength drift and results in an improved analysis. Increasing the number of scans can be achieved by sedimentation at a reduced temperature, using a larger step size or simply, at the cost of an already low level of sample throughput, carrying out several continuous scans of a single cell.

Improved reproducibility can also be achieved by selection of data analysis parameters using SEDFIT. The program allows for subtraction of time-invariant and radial-invariant noise, and this option should be selected in the analysis procedure. In addition, close attention should be paid to the meniscus position. In our experiments we do not float this parameter, but rather set the meniscus to

the determined midpoint position of the absorbance spike. Finally, an improved analysis can be obtained by better modeling the components in the protein sample. For example, if the shape of aggregate species differs significantly from that of the monomer, then a bimodal analysis of assigning or fitting frictional ratio values to different regions of the sedimentation coefficient distribution profile may improve the results. Therefore, to improve the fitting model, it may be of value to isolate protein components and measure the physical properties of sedimentation and frictional ratio in separate experiments. These values can then be incorporated into the SEDFIT analysis to improve the assessment of complicated multi-component systems.

References

Arthur KK, Babrielson JP, Kendrick BS, Stone MR (2006) Detection of protein aggregates by sedimentation velocity analytical ultracentrifugation (SV-AUC): sources of variability and their relative importance. Presented at workshop on protein aggregation, Breckenridge, CO, 26–27 Sept 2006

Berkowitz SA (2006) Role of analytical ultracentrifugation in assessing the aggregation of protein biopharmaceuticals. AAPS J 8:E590–E605

Byron O (1997) Construction of hydrodynamic bead models from high-resolution X-ray crystallographic or nuclear magnetic resonance data. Biophys J 72:408–415

Cantor CR, Schimmel PR (1980) Describing transport in the ultracentrifuge: the Lamm equation. In: Bartlett AC (ed) Biophysical chemistry, Part II techniques for the study of biological structure and function. W.H. Freeman and Company, San Francisco, CA, pp 596–603

Demeler B, Saber H, Hansen JC (1997) Identification and interpretation of complexity in sedimentation velocity boundaries. Biophys J 72:397–407

Dintzis RZ, Okajima M, Middleton MH, Greene G, Dintzis HM (1989) The immunogenicity of soluble haptenated polymers is determined by molecular mass and hapten valence. J Immunol 143:1239–1244

Furst A (1997) The XL-I analytical ultracentrifuge with Rayleigh interference optics. Eur Biophys J 35:307–310

Gabrielson J, Randilph T, Kendrick B, Stoner M (2007) Sedimentation velocity analytical ultracentrifugation and SEDFIT/*c*(*s*): limits of quantitation for a monoclonal antibody system. Anal Biochem 361:24–30

Giebler RA (1992) New analytical ultracentrifuge with a novel precision absorption optical system. In: Harding SE, Rowe AJ, Horton JC (eds) Analytical ultracentrifugation in biochemistry and polymer science. Royal Society of Chemistry, Cambridge, England, pp 16–25

Hermeling S, Schellekens H, Maas C, Gebbink MFBG, Crommelin DJA, Jiskoot W (2006) Antibody response to aggregated human interferon alpha2b in wild-type and transgenic immune tolerant mice depends on type and level of aggregation. J Pharm Sci 5:1084–1096

Lamm O (1929) Die differentialgleichung der ultazentrifugierung. Ark Mat Astr Fys Part B 21B:1–4

Laue TM (1997) Advances in sedimentation velocity analysis. Biophys J 72:395–396

Liu J, Andya JD, Shire SJ (2006) A critical review of analytical ultracentrifugation and field flow fractionation methods for measuring protein aggregation. AAPS J 8:E580–E589

McRorie DK, Voelker PJ (1993) Self-associating systems in the analytical ultracentrifuge. Beckman Instruments, Inc., Fullerton, CA 100 pp

Meselson M, Stahl FW (1958) The Replication of DNA in *Escherichia coli*. Proc Natl Acad Sci U S A 44:671–682

Minton AP (2005) Influence of macromolecular crowding upon the stability and state of association of proteins: predictions and observations. J Pharm Sci 94:1668–1675
Mullin R (2004) Biopharmaceuticals. Chem Eng News 82:9
Pekar A, Sukumar M (2007) Quantitation of aggregates in therapeutic proteins using sedimentation velocity analytical ultracentrifugation: practical considerations that affect precision and accuracy. Anal Biochem 367:225–237
Philo J (1994) Measuring sedimentation, diffusion, and molecular weights of small molecules by direct fitting of sedimentation velocity concentration profiles. In: Schuster TM, Laue TM (eds) Modern analytical ultracentrifugation. Birkhausser, Boston, pp 156–170
Philpot JSL, Cook GH (1948) Research 1:234
Pickels EG (1950) Mach Des 22:102
Pickels EG (1952) Methods Med Res 5:107
Schachman HK, Edelstein SJ (1966) Ultracentrifuge studies with absorption optics. IV. Molecular weight determinations at the microgram level. Biochemistry 5:2681–2705
Schuck P (2000) Size-distribution analysis of macromolecules by sedimentation velocity ultracentrifugation and Lamm equation modeling. Biophys J 78:1606–1619
Shire SJ (1994) Analytical ultracentrifugation and its use in biotechnology. In: Schuster TM, Laue TM (eds) Modern analytical ultracentrifugation. Birkhausser, Boston, pp 261–297
Stafford WFI (1992) Boundary analysis in sedimentation transport experiments: a procedure for obtaining sedimentation coefficient distributions using the time derivative of the concentration profile. Anal Biochem 203:295–301
Stafford WFI (1997) Sedimentation velocity spins a new weave for an old fabric. Curr Opin Biotechnol 8:14–24
Svedberg T, Fåhraeus RA (1926) New method for determining the molecular weight of the proteins. J Am Chem Soc 48:430
Svedberg T, Rinde H (1924) The ultra-centrifuge, a new instrument for the determination of size and distribution of size of particle in amicroscopic colloids. J Am Chem Soc 46:2677–2693
Van Holde KE, Weischet W (1978) Boundary analysis of sedimentation-velocity experiments with monodisperse and paucidisperse solutes. Biopolymers 17:1387–1403
Vogelstein B, Dintzis RZ, Dintzis HM (1982) Specific cellular stimulation in the primary immune response: a quantized model. Proc Natl Acad Sci U S A 79:395–399
Williams RCJ (1976) Improvement in precision of sedimentation-equilibrium experiments with an on-line absorption scanner. Biophys Chem 5:19–26
Zhou H-X, Rivas GM, Minton AP (2008) Macromolecular crowding and confinement: biochemical, biophysical, and potential physiological consequences. Annu Rev Biophys 37:375–397

Chapter 14

Biophysical Signatures of Monoclonal Antibodies

N. Harn, T. Spitznagel, M. Perkins, C. Allan, S. Shire, and C. R. Middaugh

1. Introduction

Monoclonal antibodies are the most common protein that is being developed by many companies as therapies against a wide range of diseases (Andreakos et al. 2002; Campbell and Marcus 2003; Trikha et al. 2002; Untch et al. 2003). With increasing interest in the use of monoclonal antibodies therapeutics, it is apparent that the combination of specificity and safety offered by these proteins will continue to drive the biotechnology industry forward in the coming years (Gelfand 2001; Brekke and Sandlie 2003). As is the case with any drug, a successful MAb formulation is dependant upon many factors, including understanding their biophysical properties to help describe their behavior and physical stability. While a wide variety of physical characterizations of monoclonal antibodies are routinely performed from basic research through their pharmaceutical development, little systematic information exists regarding the range of values commonly encountered during such studies. A new investigator is thus faced with some uncertainty concerning what might be considered "normal" values for the many different types of measurements. As will be shown below, despite the primary structure similarity of IgG molecules (with the exception of heavy chain subtype and hyper-variable regions, of course), generally, there is significant variation in the results of such studies. The primary purpose of this study is to establish the range of values obtained from a variety of biophysical measurements and not to examine in depth the origin or nature of such differences, although a brief discussion of these issues will be provided. Therefore, the identity of the 12 IgG molecules that were obtained from three of the leading producers of IgG monoclonal antibodies will not be provided. Rather, they are each moved into and maintained in identical buffer conditions (pH 7.4 PBS) and are identified by a simple letter designation. Spectroscopic, calorimetric, electrophoretic and solubility methods are employed for the analysis of MAbs and illustrate the diversity of their biophysical characteristics which pertain to a wide variety of pharmaceutically relevant structural, physical, and thermal stability parameters. Secondary structure is probed employing both FTIR and far-UV

From: *Current Trends in Monoclonel Antibody Development and Manufacturing,*
Biotechnology: Pharmaceutical Aspects, DOI 10.1007/978-0-387-76643-0_14,
Edited by: S.J. Shire et al.

CD spectroscopy. Tertiary structure is examined using intrinsic fluorescence and high-resolution second derivative UV absorbance spectroscopy, while DLS is performed to gather information pertaining to protein hydrodynamic size. Other physical parameters of immediate pharmaceutical interest such as thermal unfolding temperatures, isoelectric point and heterogeneity and apparent solubility are obtained from DSC, capillary isoelectric focusing and PEG precipitation methods, respectively.

2. Materials and Methods

2.1. Materials

Twelve recombinant monoclonal antibodies (referred to as MAb A-L) were supplied by MedImmune (Gaithersburg, MD), Human Genome Sciences (Gaithersburg, MD), and Genentech (San Francisco, CA) in their respective pharmaceutical formulations. Each antibody was dialyzed against two, 2-h 200:1 volume exchanges of pH 7.4 phosphate buffered saline (PBS, Fischer Scientific, St. Louis, MO) followed by a third exchange that lasted overnight. When dialysis was complete, pH and concentration were confirmed. All concentrations were determined from A_{280nm} measurements performed by an Agilent 8453 UV spectrophotometer (Palo Alto, CA). The values of the extinction coefficients ranged from 1.34 to 1.70 mL/mg cm with an average value of 1.51 mL/mg cm. Antibody concentrations were similar for each antibody and optimized for each technique as described below.

2.2. FTIR Spectroscopy

Fourier transform infrared spectroscopy was performed to monitor the secondary structure of the MAbs. Data was collected with a Nicolet™ Magna-IR 560 instrument equipped with an MCT/A detector and a 45° ZnSe ATR trough plate. Samples were held for 10 min at room temperature before collecting a spectrum. A resolution of 4 cm^{-1} was obtained upon co-adding 256 interferograms and subtracting contributions from the ATR crystal. Protein concentrations ranged from 18 to 26 mg/mL. To remove buffer contributions, raw protein absorbance spectra were processed by complete subtraction of the water association band near 2,300 cm^{-1}. The resultant spectrum was then smoothed with a 9-point Savitzky–Golay function, and a second derivative spectrum was subsequently calculated. Similar results were obtained employing a transmission geometry and are not reported here.

To determine relative secondary structure amounts, the zero-order FTIR spectrum was Fourier self-deconvoluted with OMNIC™ 5.0 software with sensitivity (K) and bandwidth factors of 1.5 and ~20, respectively. The deconvoluted spectrum was subsequently fit across the Amide I region using 5–7 Guassian peaks and the second derivative peak positions as guides for initial peak placement in Grams A/I™ fitting software. Secondary structure amounts were reported as the area of the fitted peak relative to the total area of the deconvoluted spectrum. Secondary structure type was assigned by comparison of the peak positions determined upon fitting to the peak positions previously reported in the literature (van de Weert et al. 2001; van Stokkum et al. 1995; Susi and Byler 1986).

2.3. Circular Dichroism Spectropolarimetry

Secondary structure was also analyzed employing a Jasco-720 spectropolarimeter (Tokyo, Japan). Because chloride interference from the PBS solution did not permit data collection below 200 nm, CD spectra were obtained in the far-UV region by scanning from 260 to 200 nm. The representative spectra are the result of three accumulations, obtained by scanning at 20 nm/min with 2-s response time at each 1-nm increment. The instrument was set to 1 nm bandwidth during data collection and protein concentrations ranged from 0.17 to 0.22 mg/mL. A 1 mm path length sample cell was employed throughout the study. To normalize spectral differences due to protein concentration, the molar ellipticity (deg/M cm) was calculated from raw data (Cd_{mdeg}) and plotted at each wavelength.

$$[\Theta] = \Theta/(10cl)$$

where [Θ] is the molar ellipticity in mdeg/M cm, Θ is CD signal in mdeg, c is the molar concentration, and l is the path length in cm.

2.4. High Resolution Second Derivative UV-Absorbance Spectroscopy

The absorbance spectrum of each antibody was collected with a diode-array spectrometer with 1 nm diode spacing. Data for each spectrum was collected over a 25-s integration period. Resolution was enhanced to 0.01 nm using interpolation and derivative analysis (Kueltzo and Middaugh 2003, 2005). Second derivative spectra were calculated based upon a fifth degree Savitzky–Golay polynomial, 9-point filter length window and fit to a cubic function. The second derivative spectra were then splined using 99 interpolated points between each 1-nm data point. The negative peak positions of the aromatic residues were monitored between 250 and 300 nm for indication of differences in the polarity of their environments (Kueltzo and Middaugh 2005; Kueltzo et al. 2003). The concentration range of samples was between 0.17 and 0.22 mg/mL.

2.5. Fluorescence Spectroscopy

The tryptophan emission spectrum of each antibody was collected employing a QuantaMaster™ fluorometer (Photon Technologies Incorporated Monmouth, NJ) that was equipped with a 75W Xenon arc lamp and a Model 810 PMT detector. The tryptophan emission spectrum was collected from 305 to 450 nm upon excitation with 295 nm light, and corrected spectra were produced by reference to a standard solution. Emission spectra were subtracted using a buffer spectrum and smoothed employing a 7-point Savitzky–Golay function, effectively eliminating the Raman band of water. Emission peak maxima were determined from the point at which the first derivative of the emission intensity spectrum crossed the wavelength axis. The concentration range of the samples was 0.17–0.22 mg/mL.

2.6. Dynamic Light Scattering

The mean hydrodynamic diameter of each of the 12 antibodies was determined with a Brookhaven™ light scattering instrument (Brookhaven, NY) equipped with a BI200SM goniometer and a BI-9000AT correlator. Samples

were passed through a 0.22-μm filter to remove any large aggregates or precipitates prior to analysis and determination of protein concentration, which ranged from 1.79 to 1.94 mg/mL. Light scattering was observed at 90° upon passing a 50 mW helium/neon laser at a wavelength of 532 nm into the sample. Data of five consecutive 30-s runs was averaged, and the size reported was obtained employing a cumulant analysis of the auto-correlation function. Nonlinear least squares (multicomponent) analysis was able to resolve small amounts of a high molecular weight fraction, but the size and amount of this fraction was not highly reproducible, so it is not reported here.

2.7. Differential Scanning Calorimetry

The thermal stability of the monoclonal antibodies was examined by collecting DSC thermograms of each antibody and monitoring the thermal transition midpoints (T_ms) of the observed endotherms. Differential changes in heat capacity were monitored with increasing temperature using a Microcal™ capillary auto-VP-DSC (Northhampton, MA) by heating the samples from 10 to 100°C at a rate of 1°C/min. Protein concentrations ranging from 0.96 to 1.14 mg/mL were employed. The resulting protein-buffer thermograms were processed by subtracting a corresponding buffer–buffer scan and subsequently fitting a baseline to the trace. The T_ms were recorded at each peak maxima observed in the thermograms using Origin™ 7.0 software.

2.8. Capillary Isoelectric Focusing

The isoelectric points (pI) of the MAbs were determined employing a Convergent Biosciences™ cIEF280 capillary isoelectric focusing instrument (Toronto, ON, Canada). Samples contained ~0.1 mg/mL MAb, 1% w/v methylcellulose, 0.05% v/v pI markers (pIs 3.78 and 9.50) and 4% Pharmalytes™ brand ampholytes (Amersham Biosciences) ranging from pIs of 3–10. A 20-μL injection of the sample was used to fill the entire capillary prior to applying voltage. A 1,200 V voltage was applied for 3 min to initiate the separation of the proteins. A second, higher voltage (3,000 V) was then applied for 12 min to provide an enhanced resolution of the separation. The instrument's CCD camera then measured the A_{280nm} across the entire capillary to provide the final electropherogram. After data was collected, the positions of the two pI markers were indexed for interpolation of peak values of the included MAbs. Due to a lack of availability of higher pI markers, some MAb peaks overlap and their exact pIs could not be calculated.

2.9. PEG Precipitation (Solubility)

The apparent thermodynamic activity of saturated solutions of each antibody, a measure of their relative solubilities, was determined using a polyethylene glycol precipitation assay (Middaugh et al. 1979). This analysis was performed by diluting a 40% w/v solution of 8,000 MW PEG into polypropylene tubes over the range of 4–13% w/v as described previously (Middaugh et al. 1979). Stock monoclonal antibody solution and PBS buffer were added to produce a final volume of 0.4 mL containing 2 mg/mL of protein. After equilibrating the samples overnight at 25°C, the samples were centrifuged at 8,000 *g* for 15 min to remove precipitated protein. The concentration of the MAb in the supernatant was determined using an Agilent 8453 UV-Visible

spectrophotometer. The log of experimental supernatant concentration was plotted against PEG concentration. The negatively linear portion of the resultant straight line (R^2: 0.9891–0.9993) was extrapolated to zero PEG concentration, to obtain the apparent saturation thermodynamic activity of the protein in the presence of PEG. These values were used to compare the apparent solubilities of the MAbs.

3. General Biophysical Properties of Monoclonal Antibodies

3.1. FTIR Spectroscopy

The infrared spectrum of proteins potentially provides a wealth of information regarding relative content and type of secondary structures. All zero and second order IR absorbance spectra obtained for the 12 antibodies exhibited the expected large content of intramolecular β-sheet, with the major deconvoluted peak position ranging from 1,639 to 1,635 cm^{-1} (Fig. 14-1) (van de Weert et al. 2001; van Stokkum et al. 1995; Byler and Susi 1986). Other resolved second derivative peaks indicative of intramolecular β-sheet (1,672 cm^{-1}), intermolecular β-sheet (1,695 and 1615 cm^{-1}), β-turn (1,686 cm^{-1}), and α-helix or random structure (1,650 cm^{-1}) were apparent to differing degrees in each of the antibodies. Applying the fitting procedures described above, the relative content of intramolecular β-sheet ranged from 54% (MAb B) to 74% (MAb K) with the latter value probably being the most realistic. The relative amounts of intermolecular β-sheet were calculated to be in the range of 10% (MAb D) to 21% (MAb H). Native α-helix estimates range from 11% (MAb E) to 22% (MAb D). Both of the latter two values are clearly too high. The helical values probably reflect contributions from disordered structure while the intermolecular β-sheet estimates may reflect uncorrected side-chain contributions as well as some small amounts of aggregated protein (Venyaminov and Kalnin 1990a, b).

3.2. Circular Dichroism Spectropolarimetry

To compliment FTIR spectroscopy, secondary structure analysis was also performed employing circular dichroism spectropolarimetry. The circular dichroism spectrum of these MAbs was characterized by the existence of a large negative band near 218 nm and a positive band from 200 to 205 nm (Fig. 14-2) (Vermeer and Norde 2000). The large negative band at 218 nm is characteristic of the large β-sheet content of these antibody domains, and its assignment is well established. The other characteristic β-sheet band typically occurs at <200 nm and is positive. While data could not be collected below this wavelength due to the high salt concentration in the buffer, there is clear evidence of positive ellipticity at 200–205 nm. The apparent peak seen ca. 205 nm for most of the antibodies is an artifact due to saturation of the instrument's photomultiplier from excessive absorption of light by chloride ion. The values of the ellipticity minimum at 218 nm ranged from 3.750 to 6.010 deg/cm dmol with an average value of 4.100 deg/cm dmol. Antibodies B, H, J, and K produced spectra that contain a shoulder near 225 nm. Another spectral signature of antibodies E, F and L was a small positive shoulder that occurred near 235 nm. These spectral contributions are thought to arise from either additional sheet contributions, β-turns, disulfide bonds or most probably

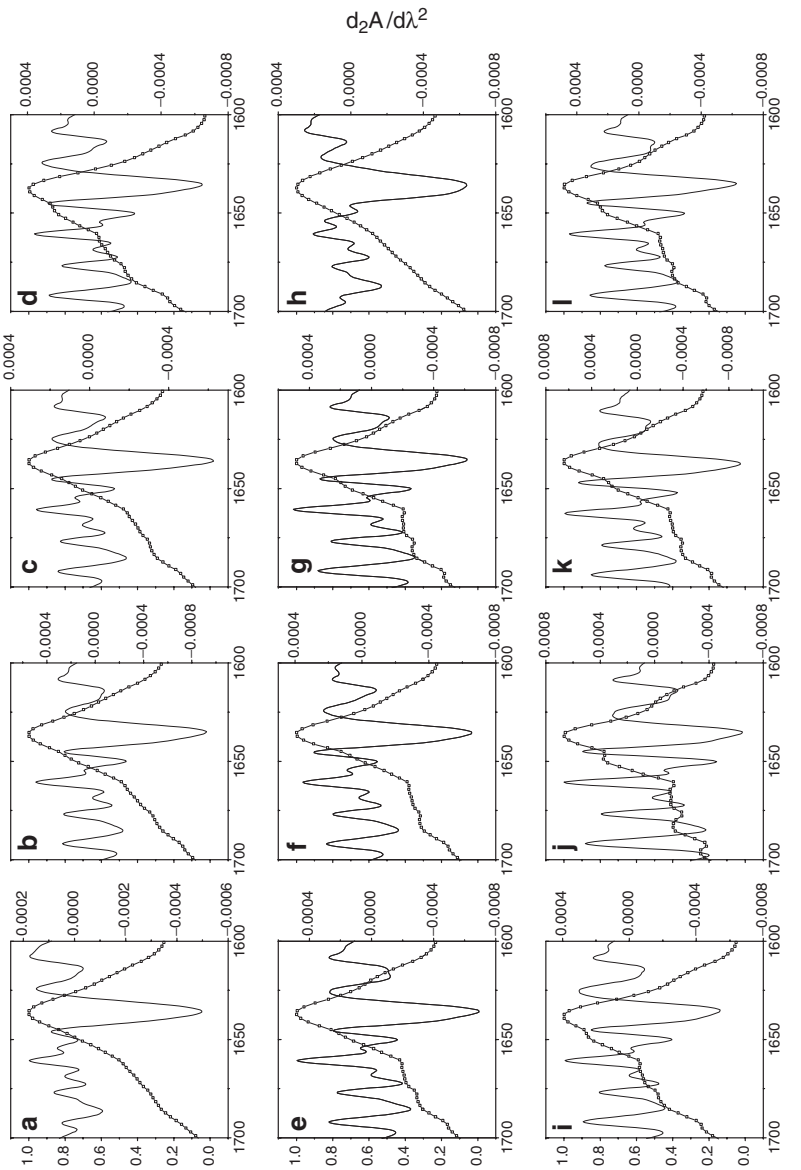

Fig. 14-1. (–□–) Normalized zero-order ATR-FTIR spectra of MAbs a-l. (—) Second derivative spectra of MAbs a-l. Spectra were obtained employing a ZnSe ATR plate with sample concentrations ranging from 18 to 26 mg/mL. After sufficient equilibration at room temperature, 256 single beam interferograms were collected and converted to absorbance spectra on a Nicolet™ 560 MagnaIR. A spectrum of pH 7.4 PBS was subtracted to remove water contributions in the Amide I region prior to smoothing and calculation of the second derivative spectrum

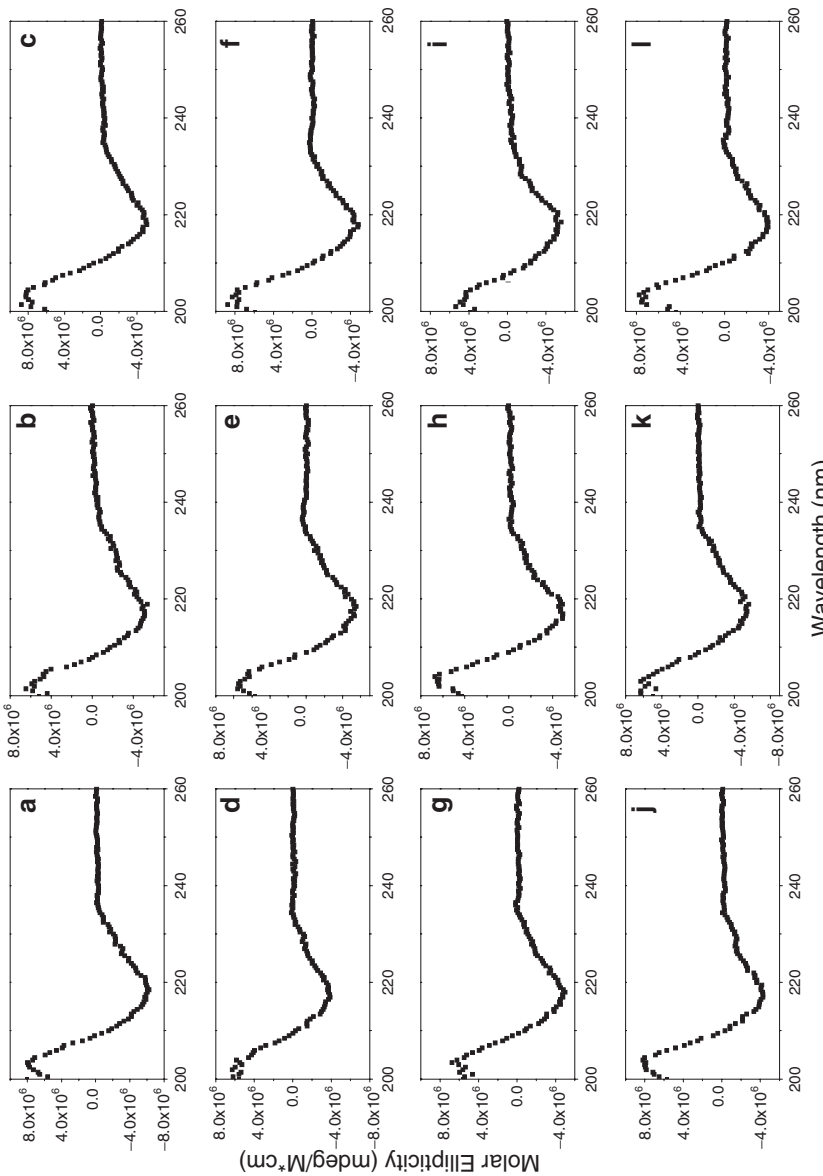

Fig. 14-2. CD spectra of MAbs a-l. After sufficient equilibration at 25°C, CD spectra were collecting in the far-UV region with 2-s response time at each 1-nm data point. After three accumulations that were scanned at 20 nm/min, each spectrum was subtracted with a pH 7.4 PBS buffer spectra. Molar ellipticity was calculated from the following expression: $[\Theta] = \Theta/(10cl)$, where $[\Theta]$ is the molar ellipticity in mdeg/M cm, Θ is CD signal in mdeg, c is the molar concentration, and l is the path length in cm. MAb concentrations ranged from 0.17 to 0.22 mg/mL, and a 1 mm path length cell was employed for CD measurements

aromatic side chains in particularly optically active environments, or some combination thereof (Byler and Susi 1986; Narhi et al. 1993; Philo et al. 1993; Radziejewski et al. 1992).

3.3. High Resolution Derivative UV-Absorbance Spectroscopy

UV absorbance spectroscopy measurements are routinely made to determine MAb protein concentration. It has been shown, however, that upon resolving the individual bands of the aromatic amino acids in the 250–300 nm UV region, important structural information can also be determined by these measurements (Kueltzo and Middaugh 2005; Mach et al. 1995; Mach and Middaugh 1994). The resolved absorbance bands, typically obtained through calculation of the second or fourth derivative, indicate the average environmental polarity of the three individual aromatic amino acid side chains in a protein. Because the three aromatic residues are dispersed globally throughout

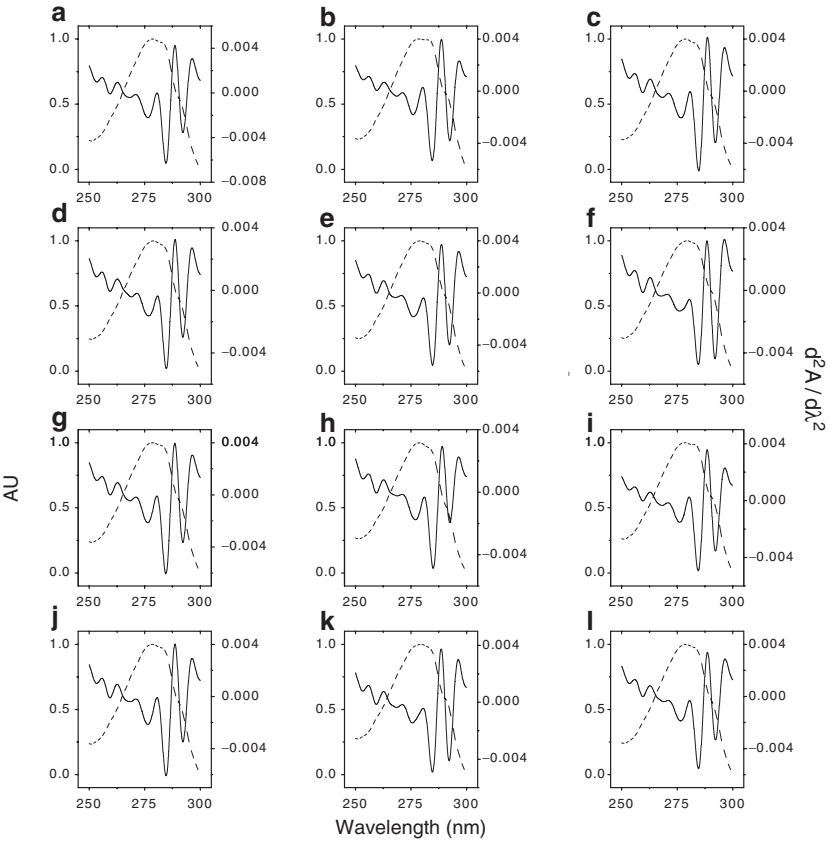

Fig. 14-3. (--) Normalized zero-order absorbance spectra of MAbs a-l. (—) High resolution second derivative spectra of MAbs a-l. Absorbance spectra were obtained employing a 25 s integration time on a diode array UV absorbance instrument containing 1 nm spacing of each diode. Subsequent data analysis employing calculation of a second derivative and interpolation between data points produced theoretical peak resolution of the aromatic amino acid side chains on the order of 0.01 nm. MAb concentrations ranged from 0.17 to 0.22 mg/mL, and a 1 cm path length cell was used to obtain a spectrum at 25°C

a protein's structure, they provide a different picture from that provided by intrinsic fluorescence spectroscopy (see below). Average peak positions at 25°C of fully exposed model amino acids are ~252.8 nm (Phe), ~258.5 nm (Phe), ~265.7 nm (Phe), ~277.5 nm (Tyr), ~283.8 nm (Tyr/Trp), and ~290.6 nm (Trp) (Kueltzo et al. 2003). The collection of absorbance data employing diode detectors and subsequent analysis permits extremely precise measurements of peak position to be made, and thus it becomes a sensitive way to monitor the tertiary structure of the IgG molecules (standard error as low as 0.01 nm) (Kueltzo and Middaugh 2005; Kueltzo et al. 2003; Fan et al. 2005). The zero and second order spectra of each antibody are represented in Fig. 14-3. A plot of the individual second derivative peak positions vs. antibody is presented in Fig. 14-4 with the range of peak values listed on the right. The absolute values differ from one instrument to another by as much as 0.1 nm, and this should be taken in account when using this data. Relative to the model amino acid peak positions, the lowest second derivative absorbance peak observed of the MAbs for Phe_{1-3}, Try/Trp, and Trp were red-shifted 0.53, 0.86, 2.3, 0.71, and 1.46 nm, respectively. Only the Tyr peak is blue shifted, and it differs by 1.66 nm from the model amino acid peak. Significant peak shifts have been reported as low as 0.05 nm, and among the antibodies here, the range of values

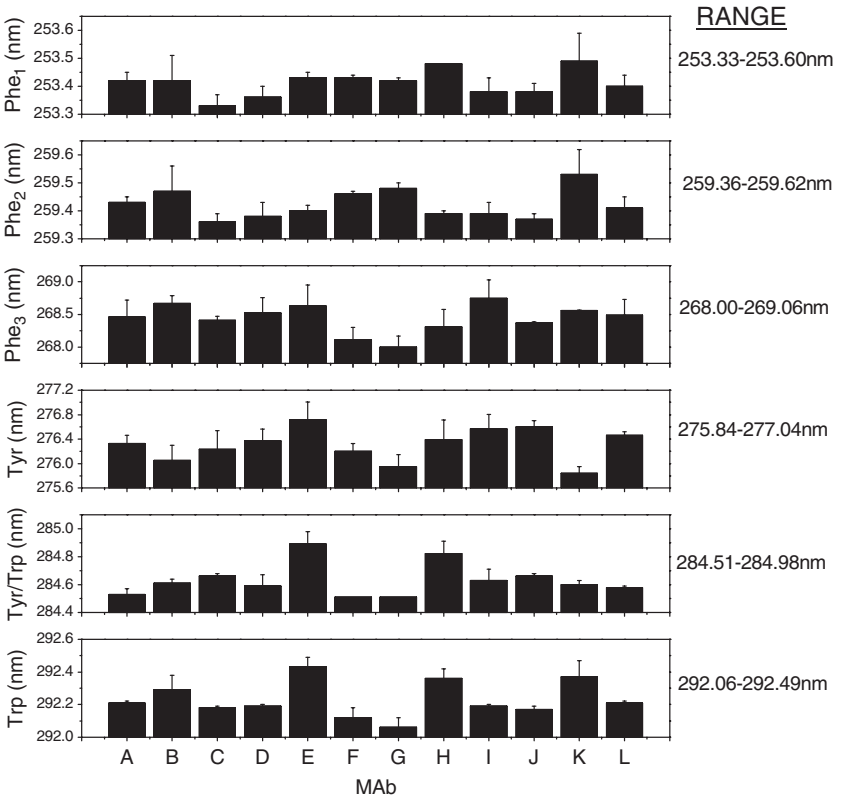

Fig. 14-4. Second derivative peak positions of Phe, Tyr and Trp of MAbs A-L (±standard error of three trials). Phe peaks occur at ~253, 259, and ~268 nm. A resolved Tyr peak is exhibited at ~276 nm, while a combination of Tyr and Trp is manifested near 284 nm. A resolved Trp peak occurs at 292 nm. The range of peak values is listed on the *right side* of the figure

varies from ~0.3 to over 1.2 nm (Kueltzo and Middaugh 2005; Kueltzo et al. 2003; Fan et al. 2005). Although many aromatic residues are present in highly conserved sites in the sequence of antibodies, it is seen here that either small differences in content or variations in the polarity of their local environment are sufficient to produce significant spectral differences. Thus, this technique serves to both distinguish individual antibodies and as a source of signals for conformational studies.

3.4. Fluorescence Spectroscopy

A second useful technique employed to probe the tertiary structure of antibodies is intrinsic fluorescence emission spectroscopy using Trp residues as structural probes. Due to low quantum yields of Phe, this amino acid is not usually examined in fluorescence spectroscopy. Although Tyr produces somewhat more fluorescence emission upon excitation, its emission spectrum tends to be difficult to detect in Trp containing proteins due to low levels of emission and resonance energy transfer to indole side-chains. Because Trp residues often have large fluorescence yields and their excitation at 295–305 nm produces a spectrum with little interference from Tyr residues, it is most commonly used as an internal probe of protein structure. Highly buried Trp residues may have emission peak maxima <320 nm when excited with 295 nm light. In contrast, Trp residues that are completely exposed to aqueous solvent produce emission peak maxima >350 nm. The Trp emission fluorescence spectrum of the 12 antibodies is shown in Fig. 14-5. The range of emission peak maxima was 13 nm, from 330 to 343 nm. As also observed in high resolution second

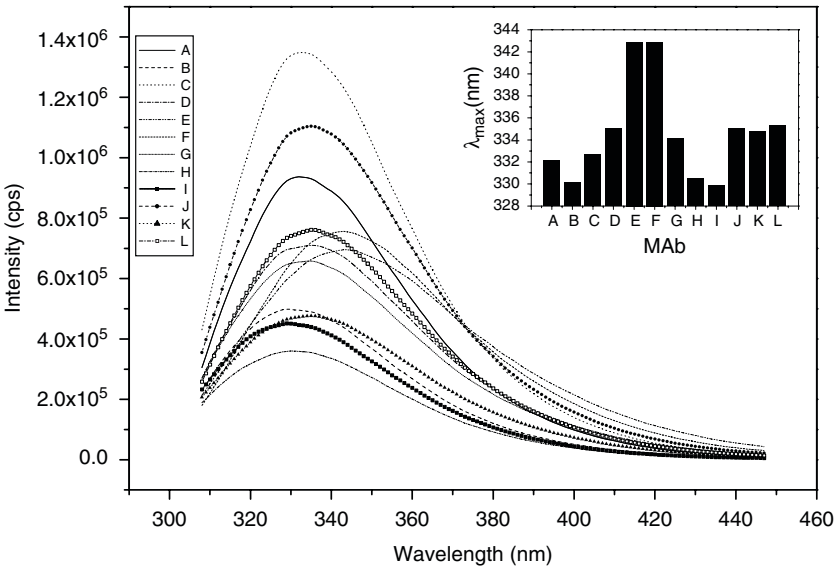

Fig. 14-5. Trp emission spectrum of MAbs A-L. Emission intensity was collected from 305 to 450 nm at 1-nm intervals upon excitation with 295 nm light. Spectra were subtracted employing a spectrum of pH 7.4 PBS to remove the contribution of the Raman peak of water. *Inset*: Emission peak maxima of MAbs A-L (±standard error of three trials). Peak positions were determined at the point at which the first derivative of the emission spectrum crossed the wavelength axis. MAb concentrations ranged from 0.17 to 0.22 mg/mL

derivative UV-absorbance spectroscopy, the average environment experienced by the Trp residues differs significantly. It must always be remembered that the fluorescence spectrum of a large protein like an immunoglobulin, reflects the average emission of many residues. In the case of IgG molecules, however, many of the Trp are conserved. For example, a Trp is often located near the disulfide bond in immunoglobulin variable domains, which frequently tends to quenching of its fluorescence (Ohage and Steipe 1999; Martsev et al. 2002). While this might be expected to simplify comparative fluorescence spectroscopy of IgG molecules, the frequent occurrence of the indole side-chain within hyper-variable regions potentially adds an increased degree of spectral variability. Fluorescence emission is also affected, among other factors, by details of the local environment of the indole ring including hydrogen bonding of the ring nitrogen (Lakowicz 1999; Burstein et al. 1973). Changes in Tyr content and environment can also alter Trp emission through variation in energy transfer events. Nevertheless, small changes in structure can still often be seen through changes in Trp emission.

3.5. Dynamic Light Scattering

Dynamic light scattering experiments provide an estimate of hydrodynamic size through mathematical analysis of a correlation function, reflecting the fluctuations in intensity of scattered light due to Brownian motion. The hydrodynamic diameters of the monoclonal antibodies determined from a cumulant analysis of the auto-correlation function are listed in Fig. 14-6. The values

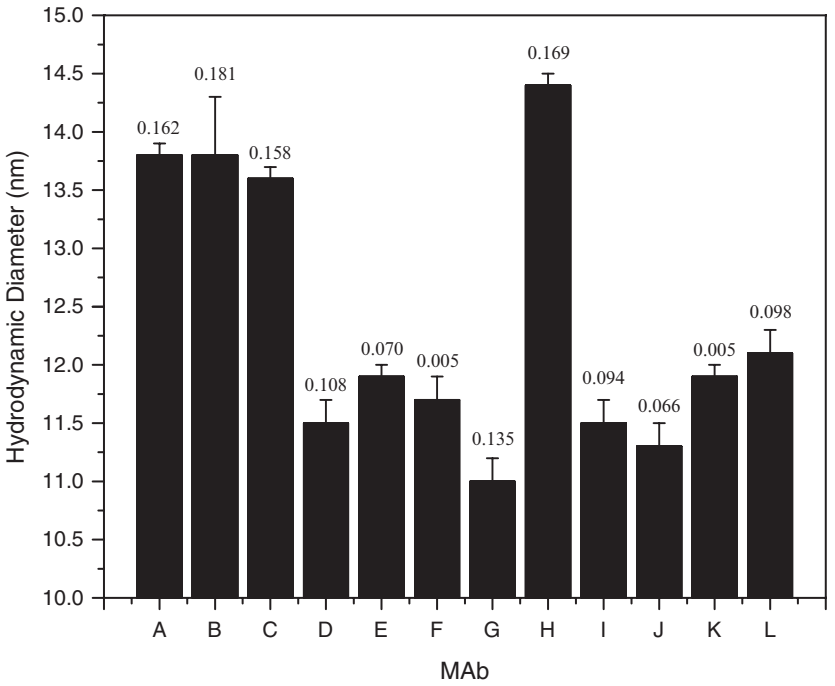

Fig. 14-6. Hydrodynamic diameter determined by DLS of MAbs A-L (±standard deviation of 5, 30 s runs). Diameters were obtained through a cumulant analysis of the auto-correlation function obtained on samples ranging from 1.79 to 1.96 mg/mL of antibody. Polydispersity values are listed above each bar

range from 11.0 to 14.4 nm. Treatment of the scattering data employing this type of analysis can produce misleading results for heterogeneous systems. Because this type of analysis is performed by fitting a single exponential to the correlation function that is weighted by an intensity average of the scattered light, systems with more than one size particle, such as aggregated IgG molecules can dramatically influence the analysis and ultimately the average size obtained can be in significant error. Polydispersity indices (PDI) of these measurements varied from 0.005 to 0.181 and indicate some size heterogeneity. Those antibodies with diameters >13 nm also produced higher PDI, suggesting the possible influence from larger particles. This is, in fact, expected since dimers and trimers are present to varying extents in each of the formulations. As indicated in the experimental section, a nonlinear least squares analysis of data from each protein finds such an aggregation peak, but it is not quantitatively reproducible due to the instability of the mathematical analysis. The cumulant analysis, however, still provides a sensitive way to detect the presence of associated species. The most frequent value measured was between 11 and 12 nm, and is comparable to other reported values of immunoglobulin diameters (Sukumar et al. 2004; Armstrong et al. 2004).

3.6. Differential Scanning Calorimetry

To characterize the thermal stability of the MAbs, differential scanning calorimetry was performed. Representative thermograms obtained for each antibody are shown in Fig. 14-7. All T_m values were above 60°C and as high

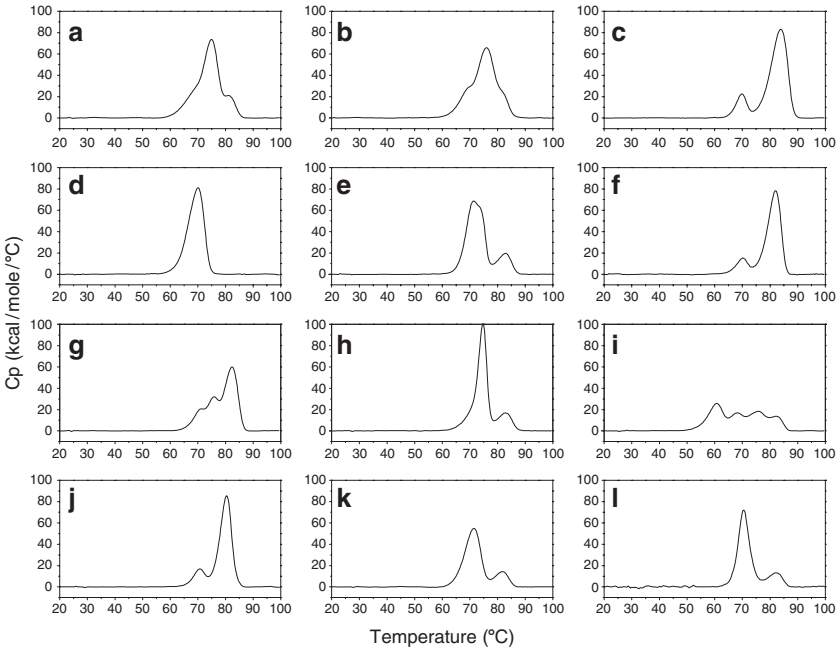

Fig. 14-7. Representative DSC thermograms of MAbs a-l. Thermograms are the result of heating from 10 to 100°C at 1°C/min with a Microcal™ capillary auto-DSC. Subtraction of a MAb-buffer scan with a buffer–buffer scan and subsequent normalization to protein concentration produced the representative thermograms. MAb concentrations ranged from 0.96 to 1.14 mg/mL

as 83°C, suggesting significant thermal stability of each immunoglobulin. Although previous literature frequently suggests two conformational transitions corresponding to the F_c and F_{ab} regions of the molecule, the thermograms of these 12 antibodies exhibit from one to four distinct transitions (Vermeer and Norde 2000; Souillac 2005). These results suggest that the stability of these domains is surprisingly variable among this representative group of IgG molecules. This also emphasizes the utility of this approach for various pharmaceutical applications given the uniqueness of the behavior of each antibody and the complexity seen in many cases.

3.7. Capillary Isoelectric Focusing

The isoelectric points of each MAb were measured employing a capillary electrophoresis based isoelectric focusing system equipped with an on-column imaging system. Measurements of pIs in this manner can greatly increase resolution (as low at 0.03 pI units). Upon focusing, immunoglobulins typically display a series of closely spaced bands often referred to as a "spectrotype." As shown in Fig. 14-8, three to five peaks are typically seen, although in some cases as many as seven to nine bands can be resolved (not observed here (Perkins et al. 2000)). From the electropherograms, it is observed that the pIs of these molecules range from 7.29 (MAb D) to at least 9.50 (MAb E), the latter overlapping with the highest pI marker (Fig. 14-8). The observation of multiple isoforms has been primarily linked to deamidation of side chain asparagine residues (Perkins et al. 2000; Tsai et al. 1993; Mimura et al. 1995).

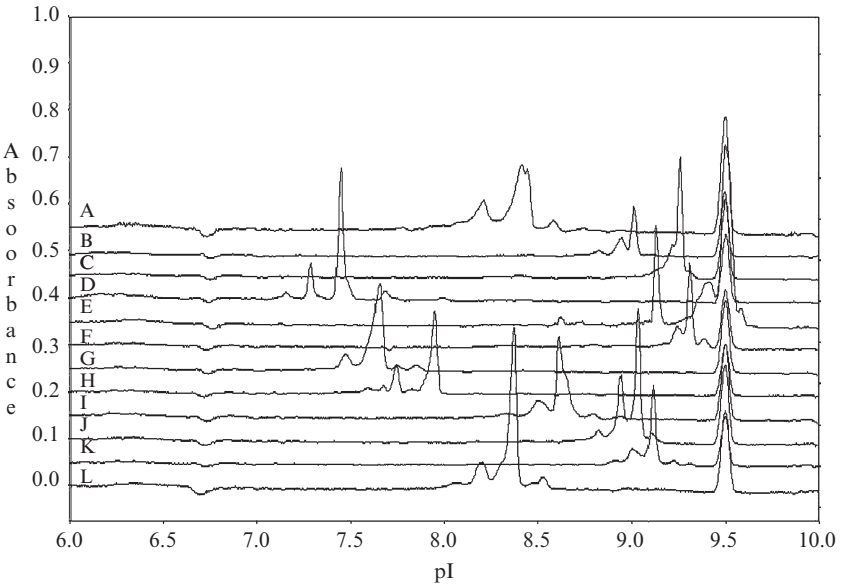

Fig. 14-8. Representative electropherograms demonstrating the pI(s) of MAbs A-L. Isoelectric focusing experiments were performed employing a capillary electrophoresis instrument equipped with a CCD camera that measures absorbance at 280 nm for detection of separated protein bands. Calibration with pI markers at 3.47 and 9.50 permitted determination of the protein pIs in the electropherogram. MAb concentrations were ~0.1 mg/mL prior to focusing

4. Solubility

With the recent interest in the development of highly concentrated monoclonal antibody formulations, the ability to compare solubility is important to the identification of lead candidates for development of these formulations (Sukumar et al. 2004; Shire et al. 2004; Liu et al. 2005; Minton 2005). It is well known that the solubility of immunoglobulins can vary greatly from virtually insoluble to hundreds of g/L (Middaugh et al. 1979). To compare the apparent solubility of these MAbs, a method which determines the differential solubility in the presence of increasing concentrations of the inert solute PEG was employed (Middaugh et al. 1979). This data is extrapolated to zero PEG content and an "apparent thermodynamic activity" of the IgG is obtained. While the exact meaning of these numbers is unclear, they provide a relatively unbiased way of comparing the solubility of the 12 proteins. The apparent saturation thermodynamic activities (a_{apparent}) at 25°C of these MAbs in the presence of PEG ranged from 94 mg/mL (MAb A) to ~1,200 mg/mL (MAb F), but most were between 150 and 300 mg/mL (Fig. 14-9). Thus, the values range over a factor of ten, but all

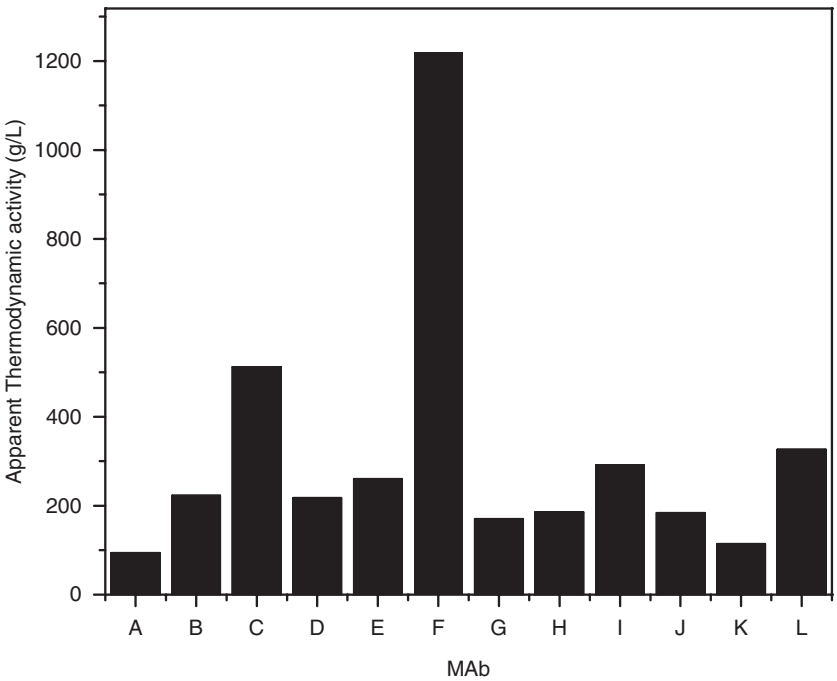

Fig. 14-9. Apparent saturation thermodynamic activity in PEG solutions of MAbs A-L at 25°C. Apparent activities were determined upon precipitation of the protein with 8,000 MW PEG as previously described (Middaugh et al. 1979). The negatively linear portion of a plot of apparent activity vs. PEG concentration (% w/v) was fitted, and the *y*-intercept was taken as the apparent thermodynamic activity of each MAb in the absence of PEG. The values permit a comparison of apparent solubilities of each antibody. R^2 values ranged from 0.9891 to 0.9993. A total of 20 mg of each protein were used for this study

appear to be relatively soluble. It must be remembered, however, that the antibodies employed in this study have been carefully selected previously for pharmaceutical development and are therefore, probably not representative of a more randomly selected population.

5. Discussion

A wide variety of monoclonal antibodies are currently being developed for the treatment of a broad range of diseases. A comprehensive understanding of the structure and stability of these molecules is necessary to achieve MAb formulations that maintain safety and retain potency when administered to patients after storage for 2–3 years. The development of monoclonal antibody formulations is aided by a number of orthogonal biophysical analyses which characterize relevant aspects of the physical nature of the proteins under various conditions. Although specific results of such measurements for specific antibodies are described in the scientific literature, a comprehensive study of a set of multiple antibodies that display a broad range of biophysical characteristics under identical solution conditions is not available. The work described in this chapter establishes an initial database for comparative use. Even though the monoclonal IgGs of this study possess significant sequence homology, it is clear that the differences present can have a profound impact on the various physical properties measured here. These differences are due to the intrinsic nature of a particular MAb and not necessarily related to the pharmaceutical properties of the molecules. By viewing the range of values commonly encountered, scientists can be better equipped to understand the significance of differences due to environmental factors (e.g. pH, ionic strength, etc.) and differences due to the intrinsic nature of the MAb itself.

To demonstrate the range of biophysical signatures of MAbs, spectroscopic calorimetric, electrophoretic and solubility methods were performed on a set of 12 monoclonal antibodies under identical solution conditions. A simple phosphate buffered saline solution was selected due to its common use. It should be recognized, however, that other buffers (e.g. histidine) are often used in actual pharmaceutical formulations. The secondary structure sensitive methods (CD and FTIR spectroscopy) suggested that the MAbs consisted largely of β-sheet structure, a previously well-established fact. There are, however, detectable differences especially in the FTIR spectra that suggest minor differences among the molecules. This technique is not at present sufficient to provide definitive information about the significance of these differences. Nevertheless, the Amide I FTIR spectrum is sufficient to provide a confirmation of the overall structural integrity of IgG monoclonal antibodies. Tertiary structure analyses based upon probing the environments of the various aromatic amino acids by derivative absorbance and fluorescence spectroscopies demonstrate that a distinct fingerprint is available for each protein studied here. Combined especially with structural perturbation (e.g. by temperature, pH, ionic strength, redox potential, agitation, freeze/thaw stress, etc.), it is clear that these methods provide a sensitive way to monitor the conformational stability of immunoglobulins. Similarly, by measuring their hydrodynamic

radius employing DLS, the size of the antibodies can also be used as a sensitive measure of physical stability (e.g. aggregation) even if precise size estimates cannot be readily obtained.

DSC is an especially valuable technique for monitoring the thermal stability of MAbs and the differential unfolding of some Ab domains can be seen over a remarkably wide temperature range. A typical IgG molecule contains 12 individual domains (6 assuming identity through heavy chain/light chain symmetry). Domain/domain interactions are coupled with the unfolding behavior of many of the domains, but the presence of up to four distinct transitions illustrates the potential power of DSC to at least partially dissect the domain structure of these molecules. It is quite remarkable how small alterations in sequence can have such a dramatic impact on the strength of inter/intramolecular interactions that ultimately dictate the thermal unfolding and stability of these complex molecules.

The wide range in values and patterns seen upon the isoelectric analysis of these proteins also stakes a strong claim for the importance of this technique. While most of the other approaches used in this study reflect non-covalent phenomena, this technique primarily sees a form of chemical degradation, primarily deamidation (Perkins et al. 2000; Tsai et al. 1993; Mimura et al. 1995). While such events may or may not have an effect on the binding properties and pharmacokinetic behavior of an individual antibody, the ease with which it can be monitored by this simple technique argues for its extended use and inclusion in future databases.

As an immediate consequence of its relevance to the development of highly concentrated MAb formulations, a measure of solubility of monoclonal antibodies would seem to be a desirable parameter. Because many antibodies will gel, phase separate or form amorphous suspensions when concentrated, conventional equilibrium solubility measurements are often difficult or impossible. The PEG precipitation method employed here, while providing an indirect measure of solubility does have a reasonable theoretical basis (Middaugh et al. 1979), is easy to perform and is especially useful in comparative studies. The wide range in apparent solubilities observed here is entirely consistent with previous studies (Lawson et al. 1988), and supports the more widespread use of this approach.

Due to the obvious importance of the biophysical characterization of monoclonal antibody formulations to their pharmaceutical development, having an understanding of the range of properties these proteins exhibit is useful. When new immunoglobulins are introduced into the development process, the ability to recognize normal from more aberrant behavior requires an understanding of those properties that are intrinsic to the MAb, and those that may reflect the presence and consequences of external factors. Thus, the data reported here can serve as the beginning of a comparative database for MAbs that should help to better understand the critical properties of these important therapeutic proteins.

Acknowledgments: We thank MedImmune, Human Genome Sciences, and Genentech for the generous gift of the large quantities of monoclonal antibodies used in these studies.

References

Andreakos E, Taylor PC, Feldmann M (2002) Monoclonal antibodies in immune and inflammatory diseases. Curr Opin Biotechnol 13:615–620

Armstrong JK, Wenby RB, Meiselman HJ, Fisher TC (2004) The hydrodynamic radii of macromolecules and their effect on red blood cell aggregation. Biophys J 87:4259–4270

Brekke OH, Sandlie I (2003) Therapeutic antibodies for human diseases at the dawn of the twenty-first century. Nat Rev Drug Discov 2:52–62

Burstein EA, Vedenkina NS, Ivkova MN (1973) Fluorescence and the location of tryptophan residues in protein molecules. Photochem Photobiol 18:263–279

Byler DM, Susi H (1986) Examination of the secondary structure of proteins by deconvolved FTIR spectra. Biopolymers 25:469–487

Campbell P, Marcus R (2003) Monoclonal antibody therapy for lymphoma. Blood Rev 17:143–152

Fan H, Ralston J, Dibiase M, Faulkner E, Russell Middaugh C (2005) Solution behavior of IFN-beta-1a: an empirical phase diagram based approach. J Pharm Sci 94:1893–1911

Gelfand EW (2001) Antibody-directed therapy: past, present, and future. J Allergy Clin Immunol 108:S111–S116

Kueltzo LA, Middaugh CR (2003) Structural characterization of bovine granulocyte colony stimulating factor: effect of temperature and pH. J Pharm Sci 92:1793–1804

Kueltzo LA, Middaugh CR (2005) Ultraviolet absorption spectroscopy. In: Wim Jiskoot DJAC (ed) Methods for structural analysis of protein pharmaceuticals, vol 3. AAPS Press, Arlington, VA, pp 1–25

Kueltzo LA, Ersoy B, Ralston JP, Middaugh CR (2003) Derivative absorbance spectroscopy and protein phase diagrams as tools for comprehensive protein characterization: a bGCSF case study. J Pharm Sci 92:1805–1820

Lakowicz JR (1999) Principles of fluorescence spectroscopy. Kluwer/Plenum, New York, p 698

Lawson EQ, Brandau DT, Trautman PA, Middaugh CR (1988) Electrostatic properties of cryoimmunoglobulins. J Immunol 140:1218–1222

Liu J, Nguyen MD, Andya JD, Shire SJ (2005) Reversible self-association increases the viscosity of a concentrated monoclonal antibody in aqueous solution. J Pharm Sci 94:1928–1940

Mach H, Middaugh CR (1994) Simultaneous monitoring of the environment of tryptophan, tyrosine, and phenylalanine residues in proteins by near-ultraviolet second-derivative spectroscopy. Anal Biochem 222:323–331

Mach H, Volkin DB, Burke CJ, Middaugh CR (1995) Ultraviolet absorption spectroscopy. Methods Mol Biol 40:91–114

Martsev SP, Dubnovitsky AP, Vlasov AP, Hoshino M, Hasegawa K, Naiki H, Goto Y (2002) Amyloid fibril formation of the mouse V(L) domain at acidic pH. Biochemistry 41:3389–3395

Middaugh CR, Tisel WA, Haire RN, Rosenberg A (1979) Determination of the apparent thermodynamic activities of saturated protein solutions. J Biol Chem 254:367–370

Mimura Y, Kabat EA, Tanaka T, Fujimoto M, Takeo K, Nakamura K (1995) Microheterogeneity of mouse antidextran monoclonal antibodies. Electrophoresis 16:116–123

Minton AP (2005) Influence of macromolecular crowding upon the stability and state of association of proteins: predictions and observations. J Pharm Sci 94:1668–1675

Narhi LO, Rosenfeld R, Talvenheimo J, Prestrelski SJ, Arakawa T, Lary JW, Kolvenbach CG, Hecht R, Boone T, Miller JA et al (1993) Comparison of the biophysical characteristics of human brain-derived neurotrophic factor, neurotrophin-3, and nerve growth factor. J Biol Chem 268:13309–13317

Ohage E, Steipe B (1999) Intrabody construction and expression. I. The critical role of VL domain stability. J Mol Biol 291:1119–1128

Perkins M, Theiler R, Lunte S, Jeschke M (2000) Determination of the origin of charge heterogeneity in a murine monoclonal antibody. Pharm Res 17:1110–1117

Philo JS, Rosenfeld R, Arakawa T, Wen J, Narhi LO (1993) Refolding of brain-derived neurotrophic factor from guanidine hydrochloride: kinetic trapping in a collapsed form which is incompetent for dimerization. Biochemistry 32:10812–10818

Radziejewski C, Robinson RC, DiStefano PS, Taylor JW (1992) Dimeric structure and conformational stability of brain-derived neurotrophic factor and neurotrophin-3. Biochemistry 31:4431–4436

Shire SJ, Shahrokh Z, Liu J (2004) Challenges in the development of high protein concentration formulations. J Pharm Sci 93:1390–1402

Souillac PO (2005) Biophysical characterization of insoluble aggregates of a multi-domain protein: an insight into the role of the various domains. J Pharm Sci 94:2069–2083

Sukumar M, Doyle BL, Combs JL, Pekar AH (2004) Opalescent appearance of an IgG1 antibody at high concentrations and its relationship to noncovalent association. Pharm Res 21:1087–1093

Susi H, Byler DM (1986) Resolution-enhanced Fourier transform infrared spectroscopy of enzymes. Methods Enzymol 130:290–311

Trikha M, Yan L, Nakada MT (2002) Monoclonal antibodies as therapeutics in oncology. Curr Opin Biotechnol 13:609–614

Tsai PK, Bruner MW, Irwin JI, Ip CC, Oliver CN, Nelson RW, Volkin DB, Middaugh CR (1993) Origin of the isoelectric heterogeneity of monoclonal immunoglobulin h1B4. Pharm Res 10:1580–1586

Untch M, Ditsch N, Hermelink K (2003) Immunotherapy: new options in breast cancer treatment. Expert Rev Anticancer Ther 3:403–408

van de Weert M, Haris PI, Hennink WE, Crommelin DJ (2001) Fourier transform infrared spectrometric analysis of protein conformation: effect of sampling method and stress factors. Anal Biochem 297:160–169

van Stokkum IH, Linsdell H, Hadden JM, Haris PI, Chapman D, Bloemendal M (1995) Temperature-induced changes in protein structures studied by Fourier transform infrared spectroscopy and global analysis. Biochemistry 34:10508–10518

Venyaminov S, Kalnin NN (1990a) Quantitative IR spectrophotometry of peptide compounds in water (H_2O) solutions. I. Spectral parameters of amino acid residue absorption bands. Biopolymers 30:1243–1257

Venyaminov S, Kalnin NN (1990b) Quantitative IR spectrophotometry of peptide compounds in water (H_2O) solutions. II. Amide absorption bands of polypeptides and fibrous proteins in alpha-, beta-, and random coil conformations. Biopolymers 30:1259–1271

Vermeer AW, Norde W (2000) The thermal stability of immunoglobulin: unfolding and aggregation of a multi-domain protein. Biophys J 78:394–404

Part VI

Pharmacokinetics and Immunogenicity

Chapter 15

Impact of Fc Glycosylation on Monoclonal Antibody Effector Functions and Degradation by Proteases

T. Shantha Raju

1. Introduction

Antibodies (Abs) are soluble serum glycoproteins that are involved in innate immunity. These soluble serum glycoproteins are categorized into five major classes, as IgA, IgD, IgE, IgG and IgM, of which IgGs are the major components (Spiegelberg and Dainer 1979). IgGs contain four polypeptide chains, two identical light chains and two identical heavy chains. The light and heavy chains of IgGs are covalently linked through interchain disulfide bonds. IgGs contain four distinct domains, a variable domain and three constant domains: CH_1, CH_2 and CH_3 domains (Edelman et al. 1969; Jefferis 1991). Variable and CH_1 domains together constitute the Fab portion of IgGs whereas, CH_2 and CH_3 domains constitute the Fc portion of IgGs. Fab and Fc portions are connected through a highly flexible hinge region that connects the two heavy chains through interchain disulfide bonds.

IgGs are further subdivided into four isotypes as IgG_1, IgG_2, IgG_3 and IgG_4. Major differences between these four isotypes of IgGs are in the number and arrangements of interchain disulfide bonds in the hinge region connecting the two heavy chains (Edelman et al. 1969; Spiegelberg and Dainer 1979; Jefferis 1991). IgG_1 and IgG_4 isotypes contain two disulfide bonds each in the hinge region, whereas IgG_2 contain four disulfide bonds and IgG_3 contains thirteen disulfide bonds in the hinge region (Raju 2003). In addition to these differences, position of disulfide bonds linking the two light chains to the two heavy chains in the upper hinge region or in the CH_1 domain also differs with isotypes.

In humans, among the four IgG isotypes, IgG_1 isotype exhibits substantial amount of antibody effector functions (Liu et al. 1987; Wright and Morrison 1997) including antibody dependent cellular cytotoxicity (ADCC) and complement dependent cytotoxicity (CDC). All the four IgG isotypes are N-glycosylated in the CH_2 domain (Mizuochi et al. 1982). Structure and function of these Fc glycans may vary with the IgG isotypes (Raju et al. 2000; Hamako et al. 1993). These Fc glycans affects antibody binding to Fc receptors and binding to complement activating factors such as C1q protein (Wright and Morrison 1997; Scallon et al. 2007a, b). Until recently, little was

From: *Current Trends in Monoclonel Antibody Development and Manufacturing,* Biotechnology: Pharmaceutical Aspects, DOI 10.1007/978-0-387-76643-0_15, Edited by: S.J. Shire et al.

known about the impact of Fc glycans on antibody stability. In this chapter, we discuss some of the recent data that show the importance of Fc glycans on antibody stability with respect to an increase in antibody resistance to proteases (Raju and Scallon 2006; Raju and Scallon 2007).

2. Biosynthesis of Fc Glycans

Biosynthesis of N-Glycans of IgGs in the Fc follows the same classical biosynthetic pathway of other well-characterized glycoproteins, in which oligosaccharyltransferase transfers a preassembled $Glc_3Man_9GlcNA_2$ oligosaccharide *en bloc* from dolichol phosphate to Asn 297 of the nascent polypeptide (IgGs heavy chain) in the endoplasmic reticulum (ER) (Kornfeld and Kornfeld 1985). Following this transfer, glucosidases mediate the removal of three Glc residues from the oligosaccharide chain to form $Man_9GlcNAc_2$ oligosaccharide linked to the polypeptide chain (Schachter 1974, 1984). The next step in the process is the removal of a single mannose residue by mannosidase I to form $Man_8GlcNAc_2$ oligosaccharide on the polypeptide. At this stage, the entire polypeptide chain translocates from the ER into the *cis*-Golgi. In the *cis*-Golgi, three more mannose residues are removed by mannosidases to form $Man_5GlcNAc_2$ oligosaccharide. The $Man_5GlcNAc_2$ oligosaccharide is the precursor for the initiation of biosynthesis of the complex and hybrid type oligosaccharides. Once the polypeptide chain containing $Man_5GlcNAc_2$ oligosaccharide translocates into the medial-Golgi, the N-acetylglucosaminyltransferase – I (GnT-I) enzyme mediates the transfer of GlcNAc from UDP-GlcNAc to the O-2 position of the terminal Man residue in the $\alpha 1 \rightarrow 3$ branch of the $Man_5GlcNAc_2$ oligosaccharide (Schachter 1986a, b; Campbell and Stanley 1984; Stanley et al. 1996). After the addition of GlcNAc, further removal of two more Man residues from the $\alpha 1 \rightarrow 6$-branch is mediated by mannosidases to give the $Man_3GlcNAc_3$ oligosaccharide. Subsequent transfer of a GlcNAc residue from UDP-GlcNAc to the newly generated terminal Man residue at O-2 in the $\alpha 1 \rightarrow 6$-branch is mediated by N-acetylglucosaminyltransferase – II (GnT-II). After the assembly of the complex core oligosaccharide containing two terminal GlcNAc residues in the two arms of the biantennary oligosaccharide with a composition of $Man_3GlcNAc_4$, addition of a Gal, bisecting GlcNAc, NANA (or NGNA) and core Fuc residues occurs in the trans-Golgi mediated by the respective transferases from the respective nucleotide sugars as shown in Fig. 15-1 (Kornfeld and Kornfeld 1985; Schachter 1986a, b, 2000).

3. Heterogeneity of Fc Glycans

As described above, biosynthesis of N-glycans is a complex process due to the involvement of many different enzymes including glycosyltransferases, glycosidases, nucleotide sugar synthetases, transporters etc (Schachter 2000; Raju et al. 1996). Because of the involvement of many different enzymes and substrates/acceptors, glycoprotein glycans are highly heterogeneous. These heterogeneous glycans often contain complex bi-, tri-, and tetraantennary oligosaccharides with or without core Fuc (Schachter 2000).

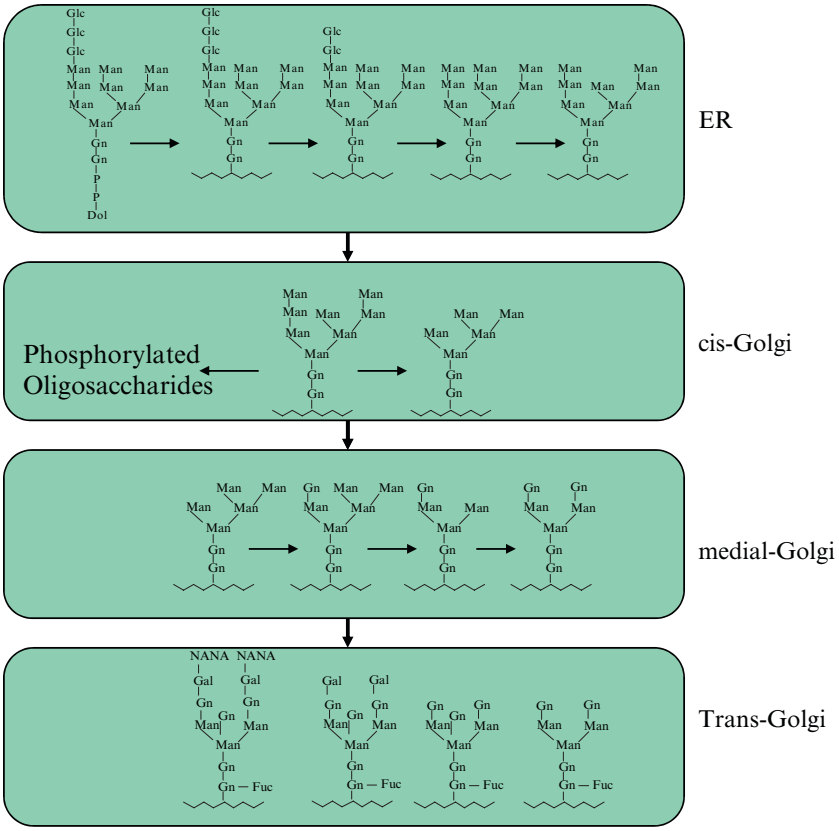

Fig. 15-1. Biosynthesis of N-Glycans. Processing of oligosaccharides to a complex biantennary structure is shown. The newly synthesized species $Glc_3Man_9GlcNAc_2$ is transferred from dolichyl diphosphate to the Asn-X-Ser/Thr sequence where is X is any amino acid residue except Pro. Arrows indicate sequence as the glycoprotein passes through the endoplasmic reticulum. After removal of the three terminal glucoses, the glycoprotein moves to the *cis*-Golgi, where it undergoes a series of steps through which mannose residues are trimmed by Alpha-mannosidases. Processing can stop at this point or proceed to yield $Man_5GlcNAc_2$. Newly synthesized glycoprotein then exits the Golgi and is transported to the cell membrane or is secreted. Symbols: glucose (Glc); mannose (Man); N-acetylglucosamine (Gn); fucose (Fuc); galactose (Gal); sialic acid (NANA)

In addition, some of these glycans may also contain bisecting GlcNAc residues (Campbell and Stanley 1984). Besides complex oligosaccharides, glycoproteins may also contain high mannose and hybrid oligosaccharides due to incomplete processing and/or biosynthesis during the transport of nascent polypeptide chains through the ER and Golgi compartments (Kornfeld and Kornfeld 1985). Some glycoproteins may also contain phosphorylated and/or sulfated N-glycans (Zhou et al. 2004). Hence, N-glycans found in glycoproteins are often a microheterogeneous mixture of complex, high mannose and hybrid oligosaccharides (Raju et al. 1996). Such microheterogeneity of glycans is also due to the competition between various glycosyltransferases and glycosidases for the available acceptors or substrates within the ER and Golgi compartments (Stanley et al. 1996).

Fc glycans of IgGs are not different than the glycans found in cell surface and serum glycoproteins with the exception of complex oligosaccharides, in which only biantennary oligosaccharides with or without core fucose and bisecting GlcNAc are found in IgGs (Mizuochi et al. 1982; Rudd et al. 1991). To date, no complex tri- and tetraantennary oligosaccharides are found in the Fc region of IgGs (Parekh et al. 1989; Kobata 2000; Rifai et al. 2000; Ritchie et al. 2002). However, this simplicity of Fc glycans is abolished by the compounded microheterogeneity of complex biantennary oligosaccharides due to the presence and/or the absence of multiple terminal sugars such as sialic acid, Gal and GlcNAc, bisecting GlcNAc, and core Fuc residues (Raju et al. 2000). Often, Fc glycans contain exposed GlcNAc and Man residues of the core branch due to incomplete sialylation and also due to under galactosylation (Raju et al. 2001). In addition, IgG glycans in the Fc may also contain variable amounts of high mannose and hybrid type oligosaccharides (Kobata 2000). Hence, Fc glycans of IgGs are often more heterogeneous than the glycans found in serum and cell surface glycoproteins.

4. Human IgG Glycosylation

Fc glycans of human IgGs have been studied extensively and thoroughly characterized (Mizuochi et al. 1982; Rademacher et al. 1986; Kobata 2000). Major glycans of human IgGs are complex biantennary structures with core fucose and are terminated with 0, 1 or 2 Gal residues (abbreviated as G0, G1 and G2 structures, respectively; *see* Fig. 15-2). The G1 structure is a mixture of two-branched isomers in which Gal is on either $\alpha 1 \rightarrow 3$- or $\alpha 1 \rightarrow 6$- arm (Fig. 15-2). In addition, human IgGs also contains ~10% of glycans that are missing core Fuc and ~10% of glycans contain bisecting GlcNAc (Raju et al. 2000). Human IgGs may also contain minor amounts of high mannose structures (~2–5% of glycans) and hybrid structures (<1%).

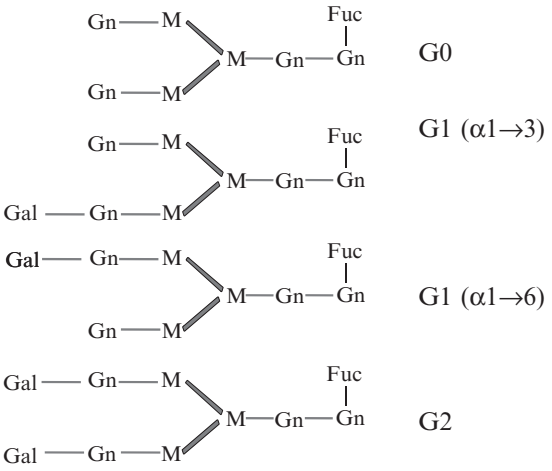

Fig. 15-2. Structure of Major N-Glycans Found in human IgG. These structures differ only in the amount of terminal Gal content (Gn = N-acetylglucosamine; *see* Fig. 15-1 for other sugar residues)

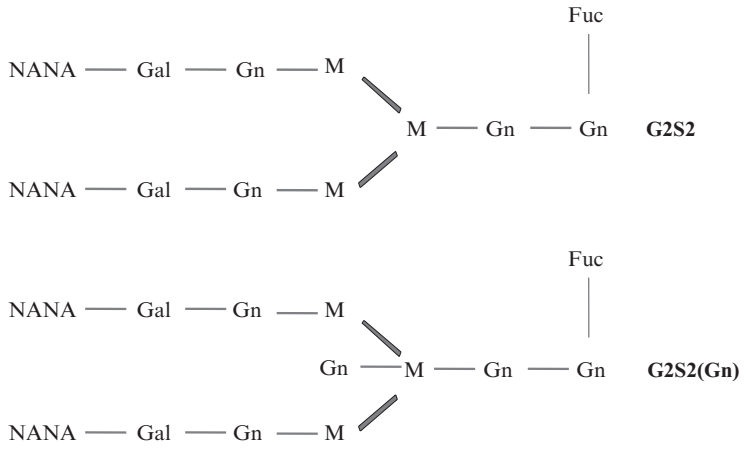

Fig. 15-3. Structure of largest N-Glycans found in human IgG. These structures differ in the absence [G2S2] or in the presence [G2S2(Gn)] of bisecting N-acetylglucosamine only

Largest N-linked oligosaccharide structures found in human IgGs are the acidic oligosaccharides that are core fucosylated and sialylated complex biantennary oligosaccharides with [G2S2(Gn) structure] or without (G2S2 structure) a bisecting GlcNAc residue (Fig. 15-3). These structures are present in human IgGs as minor components (<1% of total glycans; Rademacher et al. 1986). The terminal sialic acid residues present in human IgGs are reported to be mainly $\alpha 2 \rightarrow 6$-linked to the penultimate Gal residues of N-glycans (Jassal et al. 2001). This is in contrast to glycans present in serum and cell surface glycoproteins, in which majority of glycans contain $\alpha 2 \rightarrow 3$-linked sialic acid residues (Varki 1996).

5. Species Specificity of IgG Glycans

Microheterogeneity of IgG glycans present in the Fc may vary with the species (Raju et al. 2000). As described above, human IgG glycans are complex biantennary structures with heterogeneity due to the presence and/or absence of galactose, core fucose, bisecting GlcNAc and terminal sialic acid residues. In contrast, majority of glycans found in chicken serum IgGs are high mannose type oligosaccharide (Hamako et al. 1993; Raju et al. 2000). In addition, chicken serum IgGs also contain significant amounts of core fucosylated complex biantennary oligosaccharides with bisecting GlcNAc residues (Raju et al. 2000). However, acidic glycans found in both human and chicken IgGs contain only N-acetylneuraminic acid (NANA) residues (Raju et al. 2000). In contrast, serum IgGs from mouse, cow, goat, sheep, horse and rhesus contain only N-glycolylneuraminic acid (NGNA) residues. However, serum IgGs of dog, guinea pig, rat, rabbit and cat contain a mixture of both NANA and NGNA, albeit, in different proportions (Raju et al. 2000). The difference between NANA and NGNA is the presence of an additional oxygen atom in NGNA as shown in Fig. 15-4. In addition, serum IgGs of mouse, sheep, cow, goat etc may also contain terminal Gal $\alpha 1 \rightarrow 3$ Gal epitopes (Galili 1999; Vanhove et al. 1998). Also, variations in core fucosylation of Fc glycans with

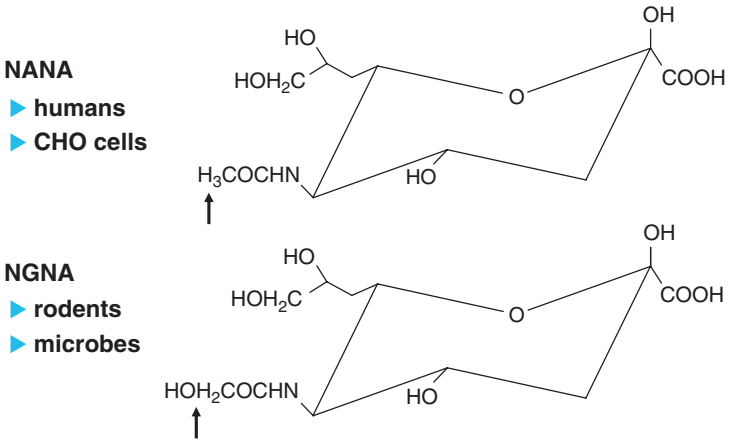

Fig. 15-4. Chemical structure of NANA and NGNA. These two variants of sialic acid residues differ only with one oxygen atom as indicated by arrow. NANA is found in human and chicken whereas NGNA was found in rodents and microbes. NGNA is also found in cow, sheep, goat etc

species were observed (Raju et al. 2000). Additionally, Fc glycans of IgGs with bisecting GlcNAc was only found in human, chicken, rhesus, cow, guinea pig, sheep, goat, rat, mouse and rabbit but not found in dog, horse and cat (Raju et al. 2000).

6. Disease Specific Glycosylation of IgGs

The microheterogeneity of human IgG glycans may also vary with age and gender (Endo et al. 1993; Yamada et al. 1997). Such variations are often indicative of disease status (Yamada et al. 1997; Routier et al. 1997; Routier et al. 1998; Tsuchiya et al. 1994). For example, serum IgGs of rheumatoid arthritis patients contain less galactosylated glycans (i.e., more amounts of G0 structures) than the glycans from normal healthy people (Endo et al. 1993; Tsuchiya et al. 1994; Field et al. 1994; Rademacher et al. 1995). Serum IgGs from patients with other autoimmune diseases are also found to be less galactosylated compared to normal healthy individuals (Takahashi et al. 1987; Opdenakker et al. 2006; Arnold et al. 2007). Although no single reason has been attributed to this anomaly in IgG glycosylation of patients with autoimmune disorders, several investigations has been shown that there are multiple reasons for which a combination of over expression of either IgG degrading proteases or glycosidases are the possible cause (Malhotra et al. 1995; Popko et al. 2006). Additionally, it has been shown that β1,4-galactosyltransferase, an enzyme mediates the transfer of Gal residue from UDP-Gal to penultimate GlcNAc residue at O-4 position in β-configuration, is poorly expressed in patients with autoimmune disorders (Keusch et al. 1995; Alavi and Axford 1995).

7. Glycosylation in Recombinant IgGs

Biotechnology companies are currently producing recombinant IgGs (rIgGs) using recombinant DNA technology (Parekh et al. 1989; Pollock et al. 1999). About 21 of these rIgGs are currently being marketed as human therapeutics

to treat life-threatening diseases including cancer (Presta 2006; Presta 2007; Raju 2003, 2008). Several hundred more rIgGs are in clinical trials for development as human therapeutics. Majority of the marketed (and those are in human clinical trials) rIgGs are produced using in vitro cell culture methods. Different biotechnology companies use different host cell lines to produce rIgGs (Parekh et al. 1989). A significant number of rIgGs are produced using Chinese hamster ovary (CHO) cells as host. Murine hybridoma cell lines such as NS/0, SP2/0 etc. are also being used as host cell lines to produce rIgGs (Scallon et al. 2007a, b). During the manufacturing process, expression level of rIgGs can vary from the cell lines and culture conditions (Parekh et al. 1989; Andersen et al. 2000). For low expressing cells, several strategies are described to amplify the cell lines to improve expression level of rIgGs (Dorai et al. 2007). Some cell lines have been amplified to produce greater than 4 g of rIgG per liter of culture medium. Cell culture conditions are also manipulated to improve the expression level of rIgGs.

Integrity of polypeptide chains of rIgGs seems to be largely unchanged in the various host cell lines. However, significant changes in glycosylation pattern of rIgGs have been noticed (Scallon et al. 2007a, b). Glycosylation of rIgGs has been shown to vary by the cell line, which is analogous to variations in glycosylation of serum IgGs from different animal species (Raju et al. 2000). Glycosylation of rIgGs can also vary with the culture conditions and with expression levels (Raju et al. 2001; Parekh et al. 1989). Hence, glycosylation of rIgGs produced under different culture conditions will vary from batch to batch.

Glycosylation machinery of CHO cells is very similar to the human glycosylation machinery (Stanley et al. 1996) – with several minor differences. Among these minor differences, notable one is that normal CHO cells do not contain N-acetylglucosaminyltransferase-III (GnT-III), an enzyme that mediates the transfer of bisecting GlcNAc (Fig. 15-5) to complex N-glycans (Campbell and Stanley 1984). Since the amount of bisecting GlcNAc-containing oligosaccharides in human IgG is ~10% (Raju et al. 2000), the absence of bisecting GlcNAc-containing oligosaccharides in antibodies produced using CHO cells as hosts may affect bioactivity.

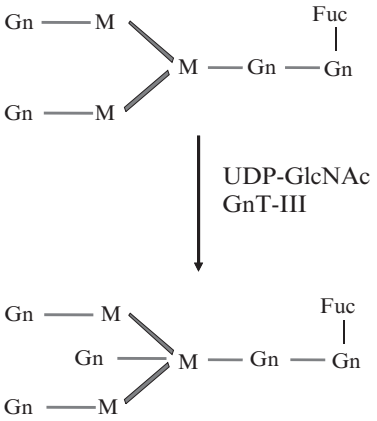

Fig. 15-5. Biosynthesis of bisecting GlcNAc containing N-glycans. N-Acetylglucosaminyltransferase-III mediates the transfer of GlcNAc from UDP-GlcNAc to G0 oligosaccharide

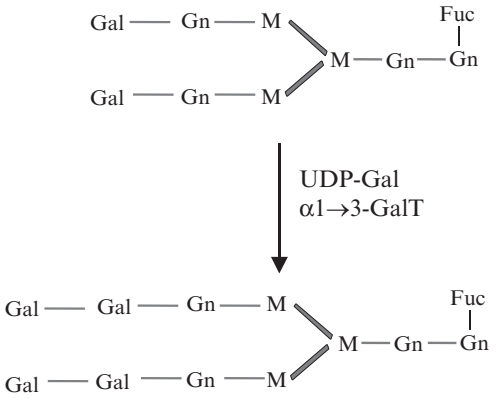

Fig. 15-6. Biosynthesis of α-Gal containing N-Glycans. α1→3-Galactosyltransferase mediates the transfer of Gal from UDP-Gal to G2 oligosaccharide

Another difference between CHO cell derived IgG and human IgG is in the nature of sialic acid linkages. As mentioned earlier, human IgGs may contain α2→6-linked sialic acid residues, whereas the CHO cell derived antibodies contain α2→3-linked sialic acid residues (Shah et al. 1998). However, the amount of sialylated oligosaccharides in both human and CHO cell derived antibodies is very small (<5% of glycans contain sialic acid residues) (Raju et al. 2000; Hamako et al. 1993).

Similar to IgGs derived from human serum, rIgGs produced in CHO cells mainly contain core fucosylated biantennary complex oligosaccharides terminated with 0, 1, or 2 Gal residues (*see* Fig. 15-2). The relative proportions of G0, G1, and G2 oligosaccharides vary from batch to batch and are dependent on cell culture conditions (Umana et al. 1999a, b; Mimura et al. 2001a, b).

Glycosylation of rIgGs produced using cell lines derived from mouse and other mammals is also very similar to glycosylation of human IgGs (Raju et al. 2000; Hamako et al. 1993). However, several significant differences might affect product quality as well as bioactivity. Most mouse-derived cell lines contain α1→3-galactosyltransferase that mediates the transfer of Gal residues from UDP-Gal in α-configuration to the internal and/or exposed Gal residues (Fig. 15-6; Galili 1999; Vanhove et al. 1998). Another difference is that the rIgGs produced using mouse cell lines contain glycans with NGNA (Varki 1996). More than 95% of human and CHO cell derived antibody oligosaccharides contain core Fuc residues (Raju et al. 2001). However, about 10–40% of the mouse cell derived IgGs glycans do not seem to contain core Fuc residues.

8. Antibody Effector Functions and IgG Glycosylation

IgGs exhibit antibody effector functions in which these molecules mediate target cell killing by either ADCC or CDC mechanisms (Wright and Morrison 1997). It has been shown that Fc glycosylation is required for IgGs to exhibit measurable ADCC or CDC activities (Morrison et al. 2002). Aglycosylated (or the enzymatically deglycosylated) antibodies do not show in vitro ADCC or

CDC activities (Wright and Morrison 1994; Wright et al. 2000; Morrison et al. 2002). This is because Fc glycans affect the antibody binding to Fc receptors that is required for ADCC activity. Similarly, glycosylated antibodies bind to C1q protein, whereas aglycosylated (or enzymatically deglycosylated) antibodies do not bind to C1q protein (Jefferis 1993). Since C1q is the first component of the complement cascade, binding to C1q protein is required for CDC activity of antibodies (Burton et al. 1980; Duncan and Winter 1988). Hence, Fc glycans play important role in defining the IgGs cell killing mechanisms. Additionally, several terminal sugars have been shown to dramatically affect the ADCC and/or CDC activity (Umana et al. 1999a, b; Shields et al. 2002; Scallon et al. 2007a, b). For example, non-fucosylated or partially fucosylated antibodies have been shown to exhibit dramatically improved ADCC activities than the completely fucosylated antibodies (Scallon et al. 2007a, b; Presta 2002). This increase in ADCC activity of non-fucosylated antibodies is due to increased binding of FcγRIIIa receptor (Mimura et al. 2001a, b; Scallon et al. 2007a, b). Terminal sialylation of Fc glycans also affect ADCC activity in a very similar way (Scallon et al. 2007a, b). Increased sialylation results in decreased ADCC activity of antibodies due to decrease in binding of FcγRIIIa receptor (Scallon et al. 2007a, b). Although Fc glycans do not appear to affect antibody binding to antigens, terminal sialylation may affect the binding of antibodies to immobilized antigens largely due to an avidity affect on antigen–antibody interactions (Scallon et al. 2007a, b). In contrast to the core Fuc and terminal sialic acid residues, presence of bisecting GlcNAc has been shown to increase ADCC activity of antibodies (Umana et al. 1999a, b). This increase in ADCC activity of bisecting GlcNAc containing antibodies is also due to increased binding to FcγRIIIa receptor (Umana et al. 1999a, b; Mimura et al. 2001a, b; Davies et al. 2001).

Although non-galactosylated antibodies bind to C1q protein, their relative binding affinity is significantly less than the binding affinities of galactosylated antibodies (Hodoniczky et al. 2005). Hence, the extent of galactosylation of IgGs affects the C1q binding and affects the CDC activity. However, ADCC does not appear to be dependent on the extent of galactosylation of antibodies (Hodoniczky et al. 2005; Scallon et al. 2007a, b).

9. IgG Cleaving Proteases

IgGs are globular proteins and hence they are more resistant to proteases than the normal serum proteins and glycoproteins. Under physiological conditions, common proteases such as trypsin, chymotrypsin, pronase, etc do not appear to cleave IgGs (Raju and Scallon 2006). Further, IgGs concentration in the serum is very high (~10 mg/ml serum) and hence they are capable of escaping degradation by proteases that may be present in the serum at very low concentration. However, certain specific proteases such as matrix metalloproteases (MMPs such as MMP3, MMP12 etc), neutrophil elastase, cathepsin etc can cleave IgGs in the Fc and/or in the hinge region (Zhu and Yu 2006). Some of these proteases have been shown to be overexpressed under certain disease conditions (Kageyama et al. 2000). These proteases cleave IgGs into Fab or F(ab')2 and Fc or truncated Fc fragments (Kotajima et al. 1998). Some of the proteases that cleave IgGs into these fragments are shown in Table 15-1.

Table 15-1. List of proteases that cleave IgGs into Fab and F(ab')2 fragments.

Proteases	Common sources	Reaction products	Comments
Gelatinase A (MMP[a]-2)	Human	F(ab')2	Requires Ca^{++}
Stromelysin (MMP-3)	Human	F(ab')2	Requires Ca^{++}
Matrilysin (MMP-7)	Human	F(ab')2	Requires Ca^{++}
Gelatinase B (MMP-9)	Human	F(ab')2	Requires Ca^{++}
Macrophage elastase (MMP-12)	Human	F(ab')2	Requires Ca^{++}
Neutrophil elastase	Human	Fab	Inflammatory enzyme
Cathepsin G	Human	F(ab')2	Inflammatory enzyme
IdeS[b]	Bacteria	F(ab'2)	Found in infectious agents
Staphylokinase	Bacteria	Fab	Found in infectious agents
Streptokinase	Bacteria	Fab	Found in infectious agents
Pepsin	Human, Pig etc	F(ab'2)	Requires acidic pH. nonspecific
Papain	Papaya Plants	Fab, F(ab')2	Requires L-cysteine for activity
Ficin	Fig latex	Fab, F(ab')2	Requires L-cysteine for activity

[a]*MMP* matrix metalloproteinases
[b]*IdeS* IgG degrading enzyme of *Streptococcus pyogenes* (*see* Hess et al. 2007)

In addition to the proteases expressed in human that cleave IgGs under physiological conditions, some proteases expressed in microorganisms also can degrade IgGs into specific fragments. One such enzyme is IdeS (IgG degrading enzyme of *Streptococcus equi ssp. equi*) that cleaves IgGs into F(ab')2 and truncated Fc fragments (Hess et al. 2007). IdeS cleaves IgGs at a much faster rate than MMPs and other physiologically relevant proteases. In addition to IdeS, other bacterial enzymes such as staphylokinase and streptokinase also degrade IgGs, but these enzymes specificity is different as they digest IgGs into Fab and Fc fragments.

Physiologically relevant proteases like MMPs and bacterial enzymes like IdeS cleave IgGs under physiological pH. However, pepsin cleaves IgGs into F(ab')2 under acidic conditions. Pepsin is also a non-specific enzyme and hence the enzyme digestions need to be controlled to obtain F(ab')2 fragments (Raju and Scallon 2006). Although the Fab portion of IgGs is more resistant to protease digestions than the Fc portion, under acidic conditions pepsin can even digest the Fab portion into smaller peptides (Bennett et al. 1997).

Papain is a sulfhydryl protease from papaya plants that cleaves IgGs into Fab or F(ab')2 and Fc or truncated Fc fragments as shown in Fig. 15-7. In the presence of cysteine, papain cleaves IgGs into Fab and Fc fragments (Bennett et al. 1997). In the absence of cysteine, preactivated papain cleaves IgGs into F(ab')2 and truncated Fc fragments. Hence, IgGs contain two papain digestion sites, one in the upper hinge region and the other in the lower hinge region. In addition there are secondary papain digestions sites in the CH_2 and CH_3 domains (Bennett et al. 1997). Hence, papain digestion reactions need to be controlled to produce proper fragments from IgGs. Similar to papain, ficin from fig latex also cleaves IgGs into fragments. Both papain and ficin are sulfhydryl proteases that possess similar properties similar to physiologically relevant proteases such as MMPs.

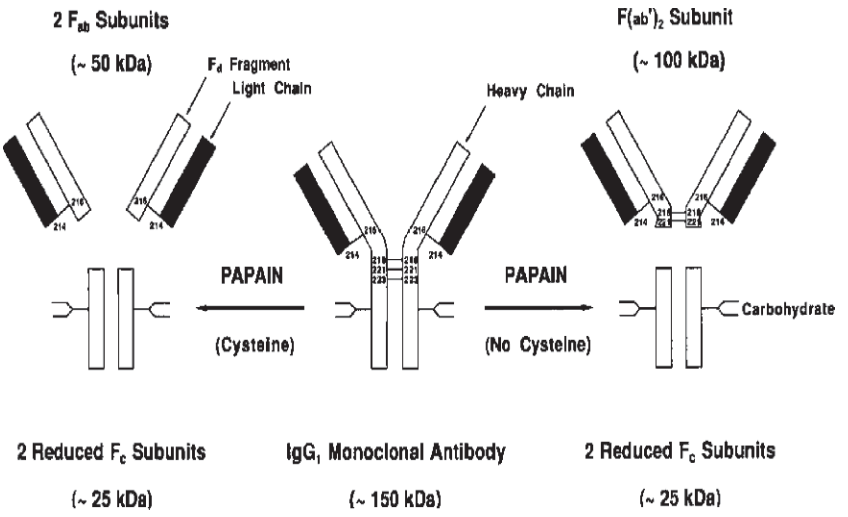

Fig. 15-7. Papain digestion sites in IgGs. In the presence of L-cysteine papain digests IgGs into Fab and Fc fragments. In the absence of L-cysteine, preactivated papain digests IgGs into F(ab')2 and truncated Fc fragments

10. Fc Glycosylation Increases Antibody Resistance to Papain

As described above, the role of Fc glycans on antibody functions has been thoroughly investigated. But, until recently, not much was known about the effect of Fc glycans on the antibody stability with particular reference to protease resistance. Glycans have been shown to increase resistance of glycoproteins to proteolysis (Bennett et al. 1997). Since Fc glycans are sequestered in the space between the two CH_2 domains of heavy chains, their effect on the antibody resistance to proteases may be different than the effect of glycans on glycoproteins, in which the glycans are exposed on the surface. Further, Fc glycans are sequestered in and around the region of cleavage sites of papain and MMPs. Using papain as a model, enzyme an investigation was carried out to compare the protease resistance of glycosylated and deglycosylated antibodies along with their corresponding Fc fragments (Raju and Scallon 2006). It was discovered that glycosylated IgGs and their corresponding Fc fragments are more resistant to papain digestions than the respective deglycosylated IgGs and Fc fragments. Glycosylated IgGs and the corresponding Fc fragments showed increased resistance to papain digestions, both at the primary papain digestion sites as well as at the secondary papain digestion sites suggesting that the Fc glycosylation increases antibody resistance to proteases (Chuang and Morrison 1997; Raju and Scallon 2006).

11. Role of Terminal Sugars on Antibody Resistance to Papain

Complex N-glycans of cell surface glycoproteins are usually terminated with sialic acid residues. However, as described earlier, complex N-glycans that are found in Fc of IgGs are a heterogeneous mixture of oligosaccharides with

multiple terminal sugars. Presence of terminal sugars such as sialic acid and core fucose may negatively affect the antibody functions and the presence of terminal Gal and/or bisecting GlcNAc may affect the antibody functions positively. Recently, it has been shown that different terminal sugars have differential effect on the antibody resistance to a protease (Raju and Scallon 2007). In this study, homogeneous antibody glycoforms terminated with either GlcNAc (G0 glycoform), or Gal (G2 glycoform) or NANA residues (G2S2 glycoforms) were prepared by in vitro glycoengineering methods (Raju et al. 2001). Papain digestion of these homogeneous glycoforms indicated that the G0 glycoform of IgGs was more resistant to protease digestion than the G2 and G2S2 glycoforms (Raju and Scallon 2007). A similar pattern was seen for intact IgGs, as well as for Fc fragments, suggesting that the IgGs containing terminal GlcNAc residues in their Fc glycans are more resistant to proteases. These observations suggested that, in addition to impacting the antibody effector functions, terminal sugars might also play a role defining the antibody resistance to proteases, hence affecting the antibody stability (Raju and Scallon 2007).

12. Effect of Fc Glycans on Antibody Structure

Human IgG Fc fragments of G2 and G0 (*see* Fig. 15-8 for structure of G2) glycoforms have been co-crystallized in complexation with miniZ peptide, an engineered 2-helix version (Z34C) of the B domain of protein A, and their X-ray crystal structures were resolved at 1.65 and 2.3 Å, respectively. The miniZ peptide complexation with Fc was used to increase the resolution of the Fc crystal structure, resulting in the creation of high-resolution structures

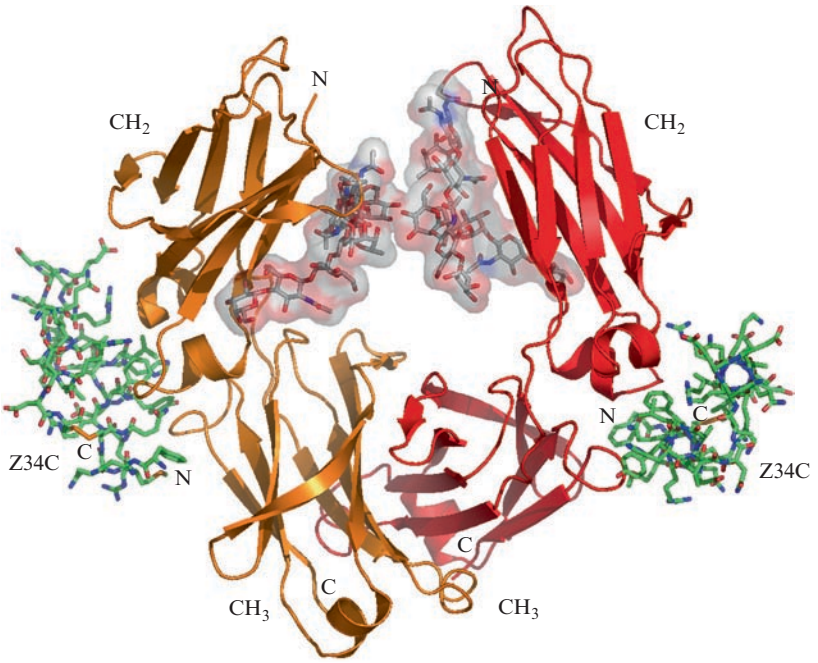

Fig. 15-8. Crystal structure of G2-miniZ complex. X-ray crystal structure of IgG Fc fragment of G2 glycoform in complexation with miniZ peptide at 1.65 Å is shown

of the homogeneous glycoforms of Fc (Kelley et al. 1992; Braisted and Wells 1996; Starovasnik et al. 1997; Deisenhofer 1981; Sauer et al. 1995).

The crystal structures of both glycoforms show that the Fc fragment of IgG_1 is a disulfide-linked dimer of two identical heavy chains consisting of CH_2 and CH_3 domains. Each heavy chain portions is related by a nearly perfect twofold axis. The G2 and G0 complex with miniZ (G2-miniZ) crystallized as a single Fc fragment bound to one miniZ molecule in the asymmetric unit. The difference between the CH_2 and CH_3 domains results from high temperature factors associated with two loops located near the bottom of the CH_2 domain, one of which is bound to the oligosaccharide moiety. The CH_3 domain has a lower overall temperature factor due to its packing contact with a symmetry related chain, but does contain two loop regions that are solvent exposed and have high temperature factors.

13. G2 Oligosaccharide Structure

The G2-miniZ complex contains two identical complex biantennary oligosaccharides, each consisting of 4 GlcNAc, 3 Man, 2 Gal, and 1 Fuc. The sugar residues, from GlcNAc linked to Asn297 up to the mannose core and along the $\alpha1\rightarrow6$-branch up to the Gal residue have low temperature factors. The GlcNAc and Gal residues in the $\alpha1\rightarrow3$-branch are not as well resolved as with the Gal in the $\alpha1\rightarrow6$-branch. The Gal and GlcNAc residues in the $\alpha1\rightarrow3$-branch possibly have multiple conformations. The Fuc attached to the GlcNAc that in turn linked to Asn297 also has high temperature factors and may also adopt multiple conformations. A total of six hydrogen bonds (H-bonds) between sugar residues and amino acid residues were observed in G2-miniZ complex (Fig. 15-9a). The core GlcNAc residue linked to Asn297 forms a H-bond with the Arg 301. The second GlcNAc in the core region H-bonds with Lys246. The Gal residue present in the $\alpha1\rightarrow6$ branch H-bonds with the Lys 246 and Thr260 and the GlcNAc residue carrying Gal residue in the $\alpha1\rightarrow6$ branch H-bonds with the Asp 265. The sugars from both Fc monomers have very little contact with each other except there is a carbohydrate-carbohydrate type interaction between the two Man residues (*see* Fig. 15-10) in the $\alpha1\rightarrow3$-branch of two oligosaccharides, which are in a buried surface (Raju 2008).

14. The Carbohydrate Structure Comparison of G2 and G0 Complexes

When either the CH_2 or the CH_3 domains are superimposed, the relative orientation of the core and $\alpha1\rightarrow6$-branch sugar residues remains constant for the G2 and G0 complexes suggesting very little freedom of motion. In the crystal structures, the $\alpha1\rightarrow3$-branch moves by as much as 0.83 Å when comparing the GlcNAc residue in the G2 and G0 complexes. The mannose from chain A in the $\alpha1\rightarrow3$-branch has little hydrophobic contact with the $\alpha1\rightarrow3$-mannose from chain B (Fig. 15-10). In the G2, Gal O2 H-bonds to Thr 260 OG1 and is also 2.8 Å from the carbonyl oxygen of Pro244. In G0, Lys 246 no longer hydrogen bonds to GlcNAc (Fig. 15-9b). Since the Gal is gone in the $\alpha1\rightarrow6$-branch, the stretch from Pro244 to Pro 247 would be slightly

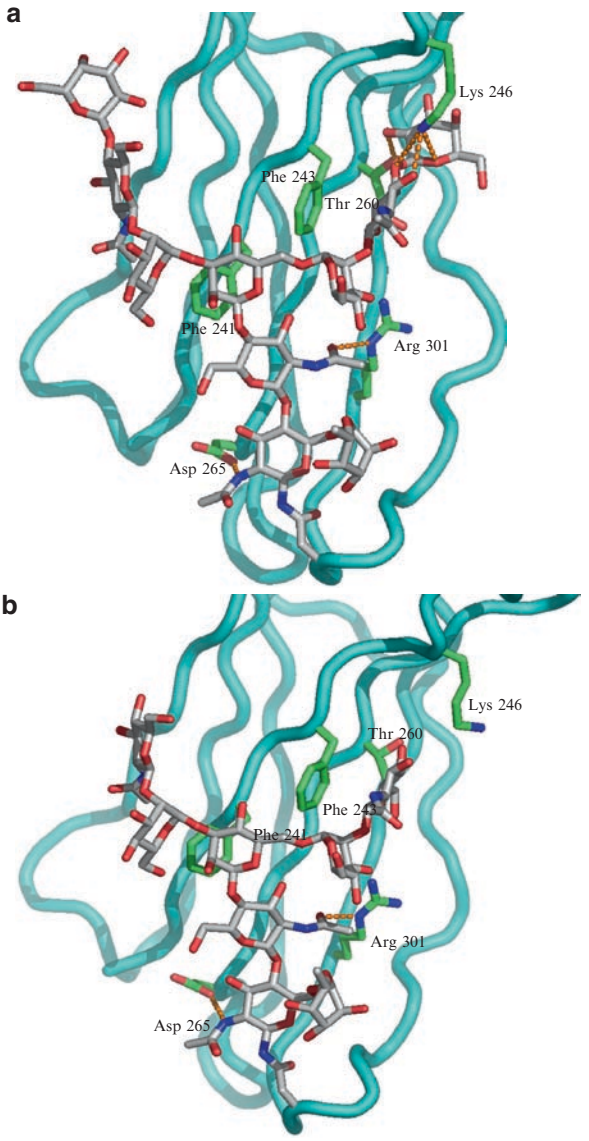

Fig. 15-9. (**a**) Hydrophilic interactions between G2 Oligosaccharide and amino acid residues. The X-ray crystal structural analysis shows six hydrogen bonds formed between the sugar residues and amino acid residues. (**b**) Hydrophilic interactions between G0 oligosaccharide and amino acid residues. The X-ray crystal structural analysis shows only two hydrogen bonds formed between the sugar residues and amino acid residues

destabilized in the G0-miniZ complex. Water now occupies the space near where the Gal O-2 resided and now bridges the carbonyl oxygen of Pro244 to Thr 260, which would provide some stabilizing energy. In the absence of Gal and GlcNAc residues, the G-2-miniZ complex also has similar structural properties like the G0-miniZ complex.

In the X-ray structures, as the carbohydrate structure is truncated, tertiary structure of the Fc appears to be affected as evidenced by the loss of

resolution in the X-ray structure and the uniform increase in B-factors (Krapp et al. 2003). An NMR study using selective 13C labeling of the glycans in a murine IgG2b supports the interpretations from the X-ray data (Gilhespy et al. 1994; Yamaguchi et al. 1998). In this NMR study, researchers concluded that the mobility of the carbohydrate chain is comparable to that of the polypeptide backbone chain with the exception of the galactose residue at the nonreducing end of the $\alpha 1 \rightarrow 3$ branch, which is extremely mobile and that agalactosylation does not induce any significant change in the mobility (Yamaguchi et al. 1998).

15. Conclusions

The importance of IgG glycosylation in the Fc has been studied for several decades and the literature is replete with information on the impact of Fc glycans on biological activity of IgGs. In addition to these aspects, this chapter discusses a new aspect of Fc glycans and their impact on antibody resistance to proteases. It is now clear that the Fc glycans increase antibody resistance to proteases (Raju and Scallon 2006). Structural analyses of Fc by X-ray and NMR studies show a hydrophobic interaction between the two core Man residues in the $\alpha 1 \rightarrow 3$-branch of two complex oligosaccharides (*see* Fig. 15-10) (Laskowski et al. 1996; Wormald et al. 1997; Yamaguchi et al. 1998; Krapp et al. 2003). This hydrophobic interaction seems to be necessary to maintain proper Fc conformation to provide increased resistance to proteases (Raju 2008). Fc glycosylation is also necessary for IgGs to exhibit ADCC and CDC activities underscoring the importance of hydrophobic interaction between the two Man residues (Raju 2008). Without this hydrophobic interaction, the antibody molecule may bulge a little, which in turn increase the hydrodynamic

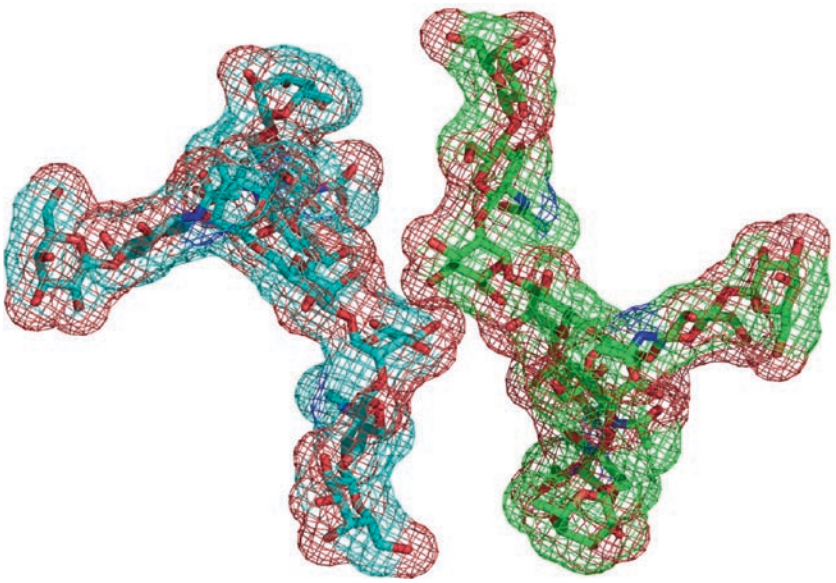

Fig. 15-10. Carbohydrate–carbohydrate interactions between the two Fc N-glycans. The X-ray crystal structural analysis shows a hydrophobic interaction between the two-mannose residues present in the $\alpha 1 \rightarrow 3$-branch or each oligosaccharide chain

volume thus altering the confirmation in the CH_2 domain. This structural perturbation may be responsible for the increased protease sensitivity, and loss of ADCC and CDC activities of aglycosylated (or deglycosylated) antibodies. Along with the X-ray and NMR structural analysis, studies from differential scanning microcalorimetry of glycosylated and aglycosylated mouse IgG2b-Fc revealed significant differences in the stability of both CH_2 and CH_3 domains between the glycosylated and aglycosylated forms (Tishchenko 1998). The free energy of stabilization of the aglycosylated CH_2 domain was decreased suggesting it to be less structured, in agreement with its observed increased susceptibility to proteases (Tishchenko 1998; Simonson and Brunger 1992).

Interestingly, similar conclusions could be drawn from comparative studies of galactosylated (G2) and agalactosylated (G0) glycoforms of human IgG1-Fc fragments, with a lower enthalpy for the G0 glycoform, relative to the G2 glycoform, being evident, possibly reflecting the loss of hydrophilic interactions between oligosaccharides and CH_2 domains (Ghirlando et al. 1999; Tao and Morrison 1989). These data have been interpreted as supporting the proposal that in the absence of a $\alpha 1 \rightarrow 6$ branch galactose residue the oligosaccharide chain is more mobile (Corper et al. 1997; Ghirlando et al. 1999). The contribution of Phe 241 and Phe 243, Asp 265 and Arg 301 may provide the majority of the stabilization for CH_2 oligosaccharide interaction, and the remaining stabilization energy comes from the Gal (in $\alpha 1 \rightarrow 6$-branch) interactions with Lys 246 and Thr 260 residues (*see* Fig. 15-10). These hydrophilic and hydrophobic interactions between galactose and amino acid residues may play a role in increasing the binding affinity of galactosylated antibodies to C1q protein. But such interactions might also increase the accessibility of amino acid residues to proteases, thus decreasing the resistance of galactosylated antibodies to proteases. Although no solution or crystal data is available for sialylated antibodies, it is tempting to speculate that the molecular interactions between sialic acid residues and amino acid residues are the reasons for decreased resistance of sialylated antibodies to proteases. Sialic acid is negatively charged and bulkier than most monosaccharides found in animal glycoproteins. The charge and bulkiness might also affect the Fc conformation and hence affect antibody stability and biological activity. Minor structural variations in Fc glycans not only affect the antibody functions but also antibody resistance to proteases and hence antibody stability.

References

Alavi A, Axford J (1995) Evaluation of beta 1,4-galactosyltransferase in rheumatoid arthritis and its role in the glycosylation network associated with this disease. Glycoconj J 12:206–210

Andersen DC, Bridges T, Gawlitzek M, Hoy C (2000) Multiple cell culture factors can affect the glycosylation of Asn-184 in CHO-produced tissue-type plasminogen activator. Biotechnol Bioeng 70(1):25–31

Arnold JN, Wormald MR, Sim RB, Rudd PM, Dwek RA (2007) The impact of glycosylation on the biological function and structure of human immunoglobulins. Annu Rev Immunol 25:21–50

Bennett KL, Smith SV, Truscott RJ, Sheil MM (1997) Monitoring papain digestion of a monoclonal antibody by electrospray ionization mass spectrometry. Anal Biochem 245:17–27

Braisted AC, Wells JA (1996) Minimizing a binding domain from protein A. Proc Natl Acad Sci USA 93(12):5688–5692

Burton DR, Boyd J, Brampton AD, Easterbrook S, Emanuel EJ, Novotny J, Rademacher TW, van Schravendijk MR, Sternberg MJ, Dwek RA (1980) The Clq receptor site on immunoglobulin G. Nature 288(5789):338–344

Campbell C, Stanley P (1984) A dominant mutation to ricin resistance in chinese hamster ovary cells induces UDP-GlcNAc: Glycopeptide beta-4-N-acetylglucosaminyltransferase-III activity. J Biol Chem 259(21):13370–13378

Chuang PD, Morrison SL (1997) Elimination of N-linked glycosylation sites from the human IgA1 constant region: Effects on structure and function. J Immunol 158:724–732

Corper AL, Sohi MK, Bonagura VR, Steinitz M, Jefferis R, Feinstein A, Beale D, Taussig MJ, Sutton BJ (1997) Structure of human IgM rheumatoid factor Fab bound to its autoantigen IgG Fc reveals a novel topology of antibody–antigen interaction. Nat Struct Biol 4(5):374–381

Davies J, Jiang L, Pan LZ, LaBarre MJ, Anderson D, Reff M (2001) Expression of GnT-III in a recombinant anti-CD20 CHO production cell line: Expression of antibodies with altered glycoforms leads to an increase in ADCC through higher affinity for Fc gamma RIII. Biotechnol Bioeng 74(4):288–294

Deisenhofer J (1981) Crystallographic refinement and atomic models of a human Fc fragment and its complex with fragment B of Protein A from *Staphylococcus aureus* at 2.9 Å and 2.8 Å resolution. Biochemistry 20(9):2361–2370

Dorai H, Li K, Huang CC, Bittner A, Galindo J, Carmen A (2007) Genome-wide analysis of mouse myeloma cell lines expressing therapeutic antibodies. Biotechnol Prog 33(4):911–920

Duncan AR, Winter G (1988) The binding site for C1q on IgG. Nature 332(6166): 738–740

Edelman GM, Cunningham BA, Gall WE, Gottlieb PD, Rutishauser U, Waxdal MJ (1969) The covalent structure of an entire gammaG Immunoglobulin molecule. Proc Natl Acad Sci USA 63(1):78–85

Endo T, Oda O, Yamanaka N, Maeda K, Yoshida M, Kobata A (1993) Alterations in the carbohydrate structures of an abnormal protein from sera of patients with rheumatoid arthritis. Arch Biochem Biophys 307(1):119–125

Field MC, Amatayakul C, Rademacher TW, Rudd PM, Dwek RA (1994) Structural analysis of the N-glycans from human immunoglobulin A1: Comparison of normal human serum immunoglobulin A1 with that isolated from patients with rheumatoid arthritis. Biochem J 299(Pt 1):261–275

Galili U (1999) Evolution of alpha 1,3-galactosyltransferase and of the alpha-gal epitope. Subcell Biochem 32:1–23

Ghirlando R, Lund J, Goodall M, Jefferis R (1999) Glycosylation of human IgG-Fc: Influences on structure revealed by differential scanning micro-calorimetry. Immunol Lett 68(1):47–52

Gilhespy M, Partridge J, Jefferis R, Homans SW (1994) A novel 13C isotopic labeling strategy for probing the structure and dynamics of glycan chains in situ on glycoproteins. Glycobiology 4(4):485–489

Hamako J, Matsui T, Ozeki Y, Mizuochi T, Titani K (1993) Comparative studies of asparagine-linked sugar chains of immunoglobulin G from eleven mammalian species. Comp Biochem Physiol B 106(4):949–954

Hess JL, Porsch EA, Shertz CA, Boyle MD (2007) Immunoglobulin cleavage by the streptococcal cysteine protease IdeS can be detected using Protein G capture and mass spectrometry. J Microbiol Methods 70(2):284–291

Hodoniczky J, Zheng YZ, James DC (2005) Control of recombinant monoclonal antibody effector functions by Fc N-glycan remodeling in vitro. Biotechnol Prog 21(6):1644–1652

Jassal R, Jenkins N, Charlwood J, Camilleri P, Jefferis R, Lund J (2001) Sialylation of human IgG-Fc carbohydrate by transfected rat alpha2, 6-sialyltransferase. Biochem Biophys Res Commun 286(2):243–249

Jefferis R (1991) Structure–function relationships in human immunoglobulins. Neth J Med 39(3–4):188–198

Jefferis R (1993) The glycosylation of antibody molecules: Functional significance. Glycoconj J 10(5):358–361

Kageyama Y, Miyamoto S, Ozeki T, Hiyohsi M, Suzuki M, Nagano A (2000) Levels of rheumatoid factor isotypes, metalloproteinase-3 and tissue inhibitor of metalloproteinase-1 in synovial fluid from various arthritides. Clin Rheumatol 19:14–20

Kelley RF, O'Connell MP, Carter P, Presta L, Eigenbrot C, Covarrubias M, Snedecor B, Bourell JH, Vetterlein D (1992) Antigen binding thermodynamics and antiproliferative effects of chimeric and humanized anti-P185HER2 antibody Fab fragments. Biochemistry 31(24):5434–5441

Keusch J, Lydyard PM, Isenberg DA, Delves PJ (1995) β1,4-Galactosyltransferase activity in B cells detected using a simple ELISA-based assay. Glycobiology 5:365–370

Kobata A (2000) A journey to the world of glycobiology. Glycoconj J 17:443–464

Kornfeld R, Kornfeld S (1985) Assembly of asparagine-linked oligosaccharides. Annu Rev Biochem 54:631–664

Kotajima L, Aotsuka S, Fujimani M, Okawa-Takatsuji M, Kinoshita M, Sumiya M, Obata K (1998) Increased levels of matrix metalloproteinase-3 in sera from patients with active lupus nephritis. Clin Exp Rheumatol 16:409–415

Krapp S, Mimura Y, Jefferis R, Huber R, Sondermann P (2003) Structural analysis of human IgG-Fc glycoforms reveals a correlation between glycosylation and structural integrity. J Mol Biol 325(5):979–989

Laskowski RA, Rullmannn JA, MacArthur MW, Kaptein R, Thornton JM (1996) AQUA and PROCHECK-NMR: Programs for checking the quality of protein structures solved by NMR. J Biomol NMR 8(4):477–486

Liu AY, Robinson RR, Hellstrom KE, Murray ED, Chang CP, Hellstrom I (1987) Chimeric mouse-human IgG1 antibody that can mediate lysis of cancer cells. Proc Natl Acad Sci USA 84(10):3439–3443

Malhotra R, Wormald MR, Rudd PM, Fischer PB, Dwek RA, Sim RB (1995) Glycosylation changes of IgG associated with rheumatoid arthritis can activate complement via the mannose-binding protein. Nat Med 1(3):237–243

Mimura Y, Lund J, Church S, Dong S, Li J, Goodall M, Jefferis R (2001a) Butyrate increases production of human chimeric IGg in CHO-K1 cells whilst maintaining function and glycoform profile. J Immunol Methods 247(1–2):205–216

Mimura Y, Ghirlando R, Sondermann P, Lund J, Jefferis R (2001b) The molecular specificity of IgG-Fc interactions with Fc gamma receptors. Adv Exp Med Biol 495:49–53

Mizuochi T, Taniguchi T, Shimizu A, Kobata A (1982) Structural and numerical variations of the carbohydrate moiety of immunoglobulin G. J Immunol 129(5):2016–2020

Morrison SL, Mohammed MS, Wims LA, Trinh R, Etches R (2002) Sequences in antibody molecules important for receptor-mediated transport into the chicken egg yolk. Mol Immunol 38(8):619–625

Opdenakker G, Dillen C, Fiten P, Martens E, Van Aelst I, Van den Steen PE, Nelissen I, Starckx S, Descamps FJ, Hu J, Piccard H, Van Damme J, Wormald MR, Rudd PM, Dwek RA (2006) Remnant epitopes, autoimmunity and glycosylation. Biochim Biophys Acta 1760(4):610–615

Parekh RB, Dwek RA, Rudd PM, Thomas JR, Rademacher TW, Warren T, Wun TC, Hebert B, Reitz B, Palmier M, Ramabhadran T, Tiemeier DC (1989) N-Glycosylation and in vitro enzymatic activity of human recombinant tissue plasminogen activator expressed in chinese hamster ovary cells and a murine cell line. Biochemistry 28(19):7670–7679

Pollock DP, Kutzko JP, Birck-Wilson E, Williams JL, Echelard Y, Meade HM (1999) Transgenic milk as a method for the production of recombinant antibodies. J Immunol Methods 231(1–2):147–157

Popko J, Marciniak J, Zalewska A, Maldyk P, Rogalski M, Zwierz K (2006) The activity of exoglycosidases in the synovial membrane and knee fluid of patients with rheumatoid arthritis and juvenile idiopathic arthritis. Scand J Rheumatol 35(3):189–192

Presta LG (2002) Engineering antibodies for therapy. Curr Pharm Biotechnol 3(3):237–256

Presta LG (2006) Engineering of therapeutic antibodies to minimize immunogenicity and optimize function. Adv Drug Deliv Rev 58(5–6):640–656

Presta L (2007) Evolving an anti-toxin antibody. Nat Biotechnol 25(1):63–65

Rademacher TW, Homans SW, Parekh RB, Dwek RA (1986) Immunoglobulin G as a glycoprotein. Biochem Soc Symp 51:131–148

Rademacher TW, Jones RH, Williams PJ (1995) Significance and molecular basis for IgG glycosylation changes in rheumatoid arthritis. Adv Exp Med Biol 376:193–204

Raju TS (2003) Glycosylation variations with expression systems and their impact on biological activity of therapeutic immunoglobulins. BioProcess Int 1(4):44–53

Raju TS (2008) Terminal sugars of Fc glycans influence antibody effector functions of IgGs. Curr Opin Immunol 20(4):471–478

Raju TS, Scallon BJ (2006) Glycosylation in the Fc domain of IgG increases resistance to proteolytic cleavage by papain. Biochem Biophys Res Commun 341(3):797–803

Raju TS, Scallon B (2007) Fc glycans terminated with N-acetylglucosamine residues increase antibody resistance to papain. Biotechnol Prog 33(4):964–971

Raju TS, Lerner L, O'Connor JV (1996) Glycopinion: Biological significance and methods for the analysis of complex carbohydrates of recombinant glycoproteins. Biotechnol Appl Biochem 24(Pt 3):191–194

Raju TS, Briggs JB, Borge SM, Jones AJ (2000) Species-specific variation in glycosylation of IgG: Evidence for the species-specific sialylation and branch-specific galactosylation and importance for engineering recombinant glycoprotein therapeutics. Glycobiology 10(5):477–486

Raju TS, Briggs JB, Chamow SM, Winkler ME, Jones AJ (2001) Glycoengineering of therapeutic glycoproteins: In vitro galactosylation and sialylation of glycoproteins with terminal N-acetylglucosamine and galactose residues. Biochemistry 40(30):8868–8876

Rifai A, Fadden K, Morrison SL, Chintalacharuvu KR (2000) The N-Glycans determine the differential blood clearance and hepatic uptake of human immunoglobulin (Ig)A1 and IgA2 isotypes. J Exp Med 191(12):2171–2182

Ritchie GE, Moffatt BE, Sim RB, Morgan BP, Dwek RA, Rudd PM (2002) Glycosylation and the complement system. Chem Rev 102(2):305–319

Routier FH, Davies MJ, Bergemann K, Hounsell EF (1997) The glycosylation pattern of humanized IgGI antibody (D1.3) expressed in CHO cells. Glycoconj J 14(2):201–207

Routier FH, Hounsell EF, Rudd PM, Takahashi N, Bond A, Hay FC, Alavi A, Axford JS, Jefferis R (1998) Quantitation of the oligosaccharides of human serum IgG from patients with rheumatoid arthritis: A critical evaluation of different methods. J Immunol Methods 213(2):113–130

Rudd PM, Leatherbarrow RJ, Rademacher TW, Dwek RA (1991) Diversification of the IgG molecule by oligosaccharides. Mol Immunol 28(12):1369–1378

Sauer E, Kleywegt GJ, Uhlen M, Jones TA (1995) Crystal structure of the C2 fragment of streptococcal Protein G in complex with the Fc domain of human IgG. Structure 3(3):265–278

Scallon BJ, Tam SH, McCarthy SG, Cai AN, Raju TS (2007a) Higher levels of sialylated Fc glycans in immunoglobulin G molecules can adversely impact functionality. Mol Immunol 44(7):1524–1534

Scallon B, McCarthy S, Radewonuk J, Cai A, Naso M, Raju TS, Capocasale R (2007b) Quantitative in vivo comparisons of the Fc gamma receptor-dependent agonist activities of different fucosylation variants of an immunoglobulin G antibody. Int Immunopharmacol 7(6):761–772

Schachter H (1974) The subcellular sites of glycosylation. Biochem Soc Symp 40:57–71
Schachter H (1984) Glycoproteins: Their structure, biosynthesis and possible clinical implications. Clin Biochem 17(1):3–14
Schachter H (1986a) Biosynthetic controls that determine the branching and microheterogeneity of protein-bound oligosaccharides. Adv Exp Med Biol 205:53–85
Schachter H (1986b) Biosynthetic controls that determine the branching and microheterogeneity of protein-bound oligosaccharides. Biochem Cell Biol 64(3): 163–181
Schachter H (2000) The joys of HexNAc. The synthesis and function of N- and O-glycan branches. Glycoconj J 17(7–9):465–483
Shah P, Reece-Ford M, Dong S, Goodall M, Pidaparthi S, Jefferis R, Jenkins N (1998) Physiological influences on recombinant IgG glycosylation. Biochem Soc Trans 26(2):S114
Shields RL, Lai J, Keck R, Connell LY, Hong K, Meng YG, Weikert SH, Presta LG (2002) Lack of fucose on human IgG1 N-linked oligosaccharide improves binding to human Fcgamma RIII and antibody-dependent cellular toxicity. J Biol Chem 277(30):26733–26740
Simonson T, Brunger AT (1992) Thermodynamics of protein-peptide interactions in the ribonuclease-S system studied by molecular dynamics and free energy calculations. Biochemistry 31(36):8661–8674
Spiegelberg HL, Dainer PM (1979) Fc receptors for IgG, IgM and IgE on human leukaemic lymphocytes. Clin Exp Immunol 35(2):286–295
Stanley P, Raju TS, Bhaumik M (1996) CHO cells provide access to novel Nglycans and developmentally regulated glycosyltransferases. Glycobiology 6(7):695–699
Starovasnik MA, Braisted AC, Wells JA (1997) Structural mimicry of a native protein by a minimized binding domain. Proc Natl Acad Sci USA 94(19):10080–10085
Takahashi N, Ishii I, Ishihara H, Mori M, Tejima S, Jefferis R, Endo S, Arata Y (1987) Comparative structural study of the N-linked oligosaccharides of human normal and pathological immunoglobulin G. Biochemistry 26(4):1137–1144
Tao MH, Morrison SL (1989) Studies of aglycosylated chimeric mouse-human IgG. Role of carbohydrate in the structure and effector functions mediated by the human IgG constant region. J Immunol 143(8):2595–2601
Tishchenko VM (1998) Effect of immunoglobulin G1 Pro 290 residue on structural and biological characteristics of its SH2 domain. Bioorg Khim 24(6):465–467
Tsuchiya N, Endo T, Shiota M, Kochibe N, Ito K, Kobata A (1994) Distribution of glycosylation abnormality among serum IgG subclasses from patients with rheumatoid arthritis. Clin Immunol Immunopathol 70(1):47–50
Umana P, Jean M, Bailey JE (1999a) Tetracycline-regulated over expression of glycosyltransferases in chinese hamster ovary cells. Biotechnol Bioeng 65(5):542–549
Umana P, Jean M, Moudry R, Amstutz H, Bailey JE (1999b) Engineered glycoforms of an antineuroblastoma IgG1 with optimized antibody-dependent cellular cytotoxic activity. Nat Biotechnol 17(2):176–180
Vanhove B, Charreau B, Cassard A, Pourcel C, Soulillou JP (1998) Intracellular expression in pig cells of anti-alpha1, 3-galactosyltransferase single-chain FV antibodies reduces Gal alpha1, 3-Gal expression and inhibits cytotoxicity mediated by anti-Gal xenoantibodies. Transplantation 66(11):1477–1485
Varki A (1996) “Unusual” modifications and variations of vertebrate oligosaccharides: Are we missing the flowers for the trees? Glycobiology 6(7):707–710
Wormald MR, Rudd PM, Harvey DJ, Chang SC, Scragg IG, Dwek RA (1997) Variations in oligosaccharide–protein interactions in immunoglobulin G determine the site-specific glycosylation profiles and modulate the dynamic motion of the Fc oligosaccharides. Biochemistry 36(6):1370–1380

Wright A, Morrison SL (1994) Effect of altered CH2-associated carbohydrate structure on the functional properties and in vivo fate of chimeric mouse–human immunoglobulin G1. J Exp Med 180(3):1087–1096

Wright A, Morrison SL (1997) Effect of glycosylation on antibody function: Implications for genetic engineering. Trends Biotechnol 15(1):26–32

Wright A, Sato Y, Okada T, Chang K, Endo T, Morrison S (2000) In vivo trafficking and catabolism of IgG1 antibodies with Fc associated carbohydrates of differing structure. Glycobiology 10(12):1347–1355

Yamada E, Tsukamoto Y, Sasaki R, Yagyu K, Takahashi N (1997) Structural changes of immunoglobulin G oligosaccharides with age in healthy human serum. Glycoconj J 14(3):401–405

Yamaguchi Y, Kato K, Shindo M, Aoki S, Furusho K, Koga K, Takahashi N, Arata Y, Shimada I (1998) Dynamics of the carbohydrate chains attached to the Fc Portion of immunoglobulin g as studied by NMR spectroscopy assisted by selective 13C labeling of the glycans. J Biomol NMR 12(3):385–394

Zhou Q, Park SH, Boucher S, Higgins E, Lee K, Edmunds T (2004) N-Linked oligosaccharide analysis of glycoprotein bands from isoelectric focusing gels. Anal Biochem 335(1):10–16

Zhu J, Yu DT (2006) Matrix metalloproteinase expression in the spondyloarthropathies. Curr Opin Rheumatol 18:364–368

Chapter 16

Immunogenicity Assessment of Antibody Therapeutics

P. Stas, Y. Gansemans, and I. Lasters

1. Introduction

Therapeutic antibodies currently make out a considerable part of the therapeutic proteins sales world-wide, with a broad range of drugs currently on the market and with antibodies making out a large fraction of ongoing clinical trials. From the therapeutic antibodies currently on the market, it has become clear that all are immunogenic to a certain extend. Their immunogenicity is characterized as the fraction of patients and subjects treated that mount anti-drug-antibodies (ADA) against the therapeutic antibody.

Therapeutic antibodies are currently mainly addressing disease in the cancer and inflammatory field, while selected antibodies are developed to treat viral diseases.

Immunogenicity was originally believed to be mainly linked with murine antibodies. Indeed, the first generation and diagnostic antibodies were initially murine antibodies, typically showing a high immunogenicity. With the advent of novel technologies developing chimeric and fully human or humanized antibodies, in conjunction with optimized production, purification and formulation technologies, the immunogenicity of several therapeutic antibodies could be reduced to a certain extend. Classification of the therapeutic antibodies (Hwang and Foote 2005) shows an overall reduction of immunogenicity related to fully human antibodies compared to murine antibodies.

However, it has become clear that fully human and humanized antibodies do also show significant immunogenicity levels. Moreover, while several therapeutic antibodies were originally developed for an oncology setting, where immunogenicity might be a lesser important drug characteristic, these drugs have shown their therapeutic use in inflammatory and auto-immune diseases. In the latter setting, their chronic use in combination with a different patient population shows significantly different immunogenicity related to the drug. Indeed, some of the currently available fully human antibodies lead to significant immunogenicity in patients over time.

From: *Current Trends in Monoclonel Antibody Development and Manufacturing,*
Biotechnology: Pharmaceutical Aspects, DOI 10.1007/978-0-387-76643-0_16,
Edited by: S.J. Shire et al.

The growing insights and data gathered on immunogenicity has lead to the development of an EMEA guideline to address immunogenicity and the development of a related immunogenicity risk management plan. While the European guidance is addressing protein therapeutics in general, it forms a solid basis for the assessment of immunogenicity related to antibody therapeutics, addressing both the likelihood and the severity of the drug-related immunogenicity.

2. Immunogenicity Drivers

Multiple factors contribute to a potential immunogenicity of protein therapeutics (EMEA 2008). Immunogenicity drivers can be patient/disease related, as well as related to the drug itself.

2.1. Patient and Disease Related Immunogenicity Drivers

Immunogenicity is influenced by genetic factors that influence the immune response, such as the patients HLA haplotype, but also genetic factors related to a gene defect play a role. For example, the use of FactorVIII as a substitution product, will differentiate in immunogenicity in healthy people, where the protein is endogenous, as compared to patients with reduced FactorVIII level or even lacking the protein, which influences immunological tolerance. Immunogenicity is observed against proteins with amino acid sequences identical to fully human proteins, and can be influenced by gene polymorphisms.

Immunogenicity against a protein therapeutic can be age-related, as for e.g., the protein turn-over is different in youngsters when compared to adults. This has led to different observed immunogenicity of e.g., infliximab in the treatment of rheumatoid arthritis and juvenile arthritis at a comparable dose.

Disease related factors strongly influence immunogenicity. Generally, therapeutic antibodies used in an oncology setting are typically less immunogenic than usage of the same antibodies in inflammatory and autoimmune diseases. Immunomodulating factors will influence the observed immunogenicity of the therapeutic antibodies, as some of them have an immunostimulating or immunoreducing activity. Moreover, concomitant treatment further influences the observed immunogenicity. For example, the use of the disease modifying anti-rheumatic drug (DMARD) MTX significantly reduces the observed immunogenicity both for adalimumab and infliximab (Baert et al. 2003). Moreover, immunogenicity can be influenced by previous exposure to similar or related proteins.

Further factors that influence the immunogenicity are the duration of treatment, the route of administration and treatment modalities. Therapeutic antibodies used in a repeated dosing scheme, or with intermittent dosing scheme changes, have a higher likelihood to induce immunogenicity in patients as opposed to short dosing schemes to treat acute indications. In general, the observed immunogenicity against antibody therapeutics will increase as patients groups are subjected to the drug over longer periods (Goldstein et al. 1986; Schroeder et al. 1989). Long term usage of adalimumab leads to 18% immunogenicity, as opposed to 5–12% immunogenicity in shorter studies. Intravenous administration reduces the likelihood of an immune response as opposed to subcutaneous and intramuscular injection, where a different

immunological subsystem is triggered through the Langerhals and dermal dendritic cells.

2.2. Product Related Immunogenicity Drivers

Protein therapeutics are high molecular weight molecules with complex chemical structures and are often subject to post-translational modification. The production process and the producing organism alter the protein therapeutic in a subtle way, which consistently leads to a subtle variability in the end product. Suitable bioanalytical methods should be employed to characterize glycosylation, deamidation, oxidation, and other factors (EMEA 2008), and to identify the presence of degradation products and alternative glycosylation patterns, thereby ensuring an end product variability within acceptable variability limits. The composition of the formulation of the protein therapeutic should best maintain the conformation of the therapeutic, and should involve the use of excipients. As the formulation and the source of the excipients can alter immunogenicity, any formulation change should be strictly evaluated.

A major contributor to immunogenicity is the degree of "foreignness" of a protein to the host. It is indeed more likely to observe high immunogenicity to a bacterium derived protein therapeutic such as staphylokinase, as compared to a protein that shows high homology to a circulating, endogenous protein, such as EPO. Over the past 20 years, the immunogenicity of antibody therapeutics has been reduced significantly by developing fully human and humanized therapeutics, as compared to the first and second generation murine and chimeric therapeutic antibodies (Hwang and Foote 2005).

Aggregate and immune-complex formation are major drivers of an immune response and hence immunogenicity. Firstly, aggregates can be more readily taken up by antigen presenting cells, leading to a humoral immune response with strong T-cell support. Secondly, some aggregate variants showing repeated structure, are able to crosslink B-cell receptors, thereby inducing B-cell proliferation and activate a T-cell independent immune response (Bachmann et al. 1993).

Factors leading to aggregate formation include formulation, production processes, storage conditions and/or the physicochemical characteristics of the protein drug itself. In some cases, drug handling has been reported as leading to the formation of (transient) aggregates, for instance when using sub-optimal dilution agents or upon fast dilution of the drug.

Upon immune responses against aggregated drug, proper characterization of the antibody response should be performed, identifying whether the ADA response is directed against the aggregate and/or the free, non-aggregated protein.

Immunogenicity has been reported to be driven by endotoxins, lipids and production method related DNA. With production and purification processes improving over time, leading to end products of higher purity and homogeneity, the incidence of anaphylactic shock or allergy due to the protein therapeutic has strongly decreased over time. However, recent novel production organisms have shown altered immunogenicity profiles.

2.3. Immunogenicity Incidence Versus Severity

When assessing the risk related to immunogenicity, both the likelihood as well as the severity of the observed immunogenicity should be addressed. In some cases, the likelihood to mount an immune response towards a protein therapeutic is high, while no severe adverse effects occur rare cases of immunogenicity

can indeed lead to severe side effects, as has been reported by the use of recombinant EPO, leading to anti-drug antibodies (ADA) cross reacting with endogenous EPO, hence leading to PRCA in a number of patients treated (Casadevall et al. 2002).

Upon developing any protein therapeutic, a risk management should be developed addressing the likelihood, incidence and expected adverse effects related to the immunogenicity.

While the current guidelines are developed for protein therapeutics in general, some of the aspects have to be taken into account in the development of antibody therapeutics.

In general, the effects of ADA against therapeutic antibodies result in altered drug efficacy and pharmacokinetics. Eventually, the advent of ADA against a therapeutic protein could lead to elimination of the drug in the patient and hence the deletion and/or inefficacy of the drug.

Immunogenicity can be further reduced by taking special care to the formulation, the avoidance of aggregates or degradation products, and controlling the development of immunocomplexes.

Recent developments focusing on Fc engineering and antibody-fusion protein might increase the risk for immunogenicity of the antibody therapeutic. In view of amino acids substitutions in the antibody constant parts, the possibility of raising cross-reactive antibodies with endogenous Fc should get the necessary attention. It is unlikely however that the tolerance against the Fc can be broken.

3. Strategies to Identify Anti-drug Antibodies

Fig. 16-1 depicts a comprehensive strategy to address immunogenicity during the different developmental stages of a therapeutic antibody.

As immunogenicity is defined as the fraction of patients developing ADA, the actual measurement of immunogenicity can only be performed after administration of the drug to patients. However, in silico and in vitro tools can be used to compare and predict eventual immunogenicity.

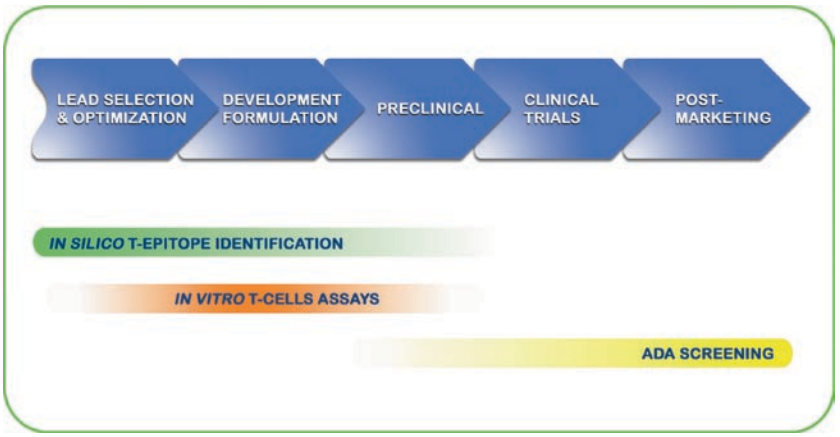

Fig. 16-1. A comprehensive assessment of the immunogenicity risk throughout the drug development process involves early stage in silico methods, in vitro methods during development and formulation, and a combination of anti-drug antibody screening methods during pre-clinical, clinical and postmarketing stage

Several whitepapers and guidance have been developed to address the measurement of ADA in patients and at pre-clinical level (EMEA 2008; Gupta et al. 2007; Koren et al. 2008; Mire-Sluis et al. 2004a, b; Shankar et al. 2008).

A tiered approach has been suggested where different assays identify and characterize ADA levels and types upon (repeated) administration of a drug. Typically, the first step is to develop a screening assay to identify potential ADA responses in patient samples. This assay should be validated to its intended use, and avoid false negatives while allowing for a number of false positive samples. A confirmatory assay should be able to differentiate the false positive from the real positive samples, thereby identifying all positive patient responses. Eventually, assays should be developed to further characterize the ADA response, by identifying the neutralizing nature of the ADA and determining the ADA isotypes Fig. 16-2.

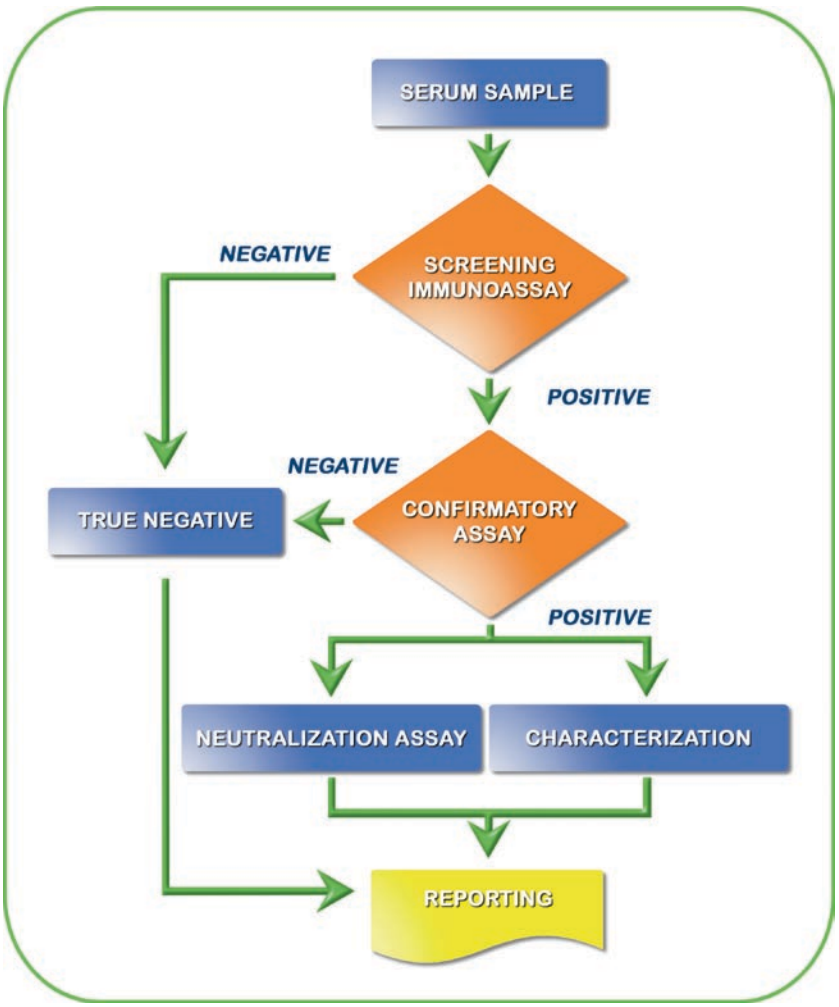

Fig. 16-2. Tiered approach to measure ADA against protein therapeutics

ADA assays generally involve techniques such as direct, indirect and bridging ELISA, complemented with surface plasma resonance, chemiluminescence and/or radio-precipitation based assays. In specific cases, cell-based assays are used to determine the neutralizing capacity of the ADA response.

During the development of assays for ADA against therapeutic antibodies, "drug interference" effect should be avoided, and specific antibodies should be measured. Measurement of ADA in the presence of the therapeutic antibody can show difficult, and the high concentration of non-specific antibodies in the patients should be taken into account. Especially the differentiation between neutralizing and non-neutralizing specific ADA can be challenging. For antibodies with long half life, a long wash-out period should be selected (Mire-Sluis et al. 2004).

Table 16-1 compiles published data on immunogenicity of therapeutic antibodies. The table shows that due to different assays used and their respective sensitivities, the observed immunogenicity data cannot be easily compared throughout studies. Moreover, studies often comprise a small number of patients, whereas different studies often rely on different treatment schemes based on the individual medical history and disease state of the patients. Therefore, care must be taken not to over-interpret immunogenicity data.

An example of the variability of observed immunogenicity amongst similar clinical studies is alemtuzumab, a humanised anti-CD52 antibody used in the treatment of rheumatoid arthritis (RA), where 6 clinical studies performed between 1995 and 2005 report ADA levels between 0 and 75% (Isaacs et al. 1992; Weinblatt et al. 1995; Isaacs et al. 1996a, b; Reiff 2005). Combining the data results in an immunogenicity of 45% in 120 patients, whereas the usage of alemtuzumab in the treatment of B-cell chronic lymphocytic leukemia (B-CLL) results in only 1.9% HAHA response for a group of 167 subjects. This suggests the influence of the disease state on the antigenic response.

Similarly, the chimeric antibody rituximab, targeting the B-cell differentiation antigen CD20, does not elicit an ADA response when treating patients suffering from B-CLL (Piro et al. 1999; Davis et al. 2000). This may be explained by the combination of three factors: the antibody causing B cell depletion, the patient having a B-cell lymphoma and the concomitant use of immunosuppressive drugs. Immunogenicity of rituximab on the treatment of auto-immune diseases like systemic lupus erythomatosus or primary Sjogren's syndrome, results in immunogenicity levels reaching respectively 65 and 27%, with concomitant use of immunosuppressive drugs (Looney et al. 2004; Pijpe et al. 2005).

Reported immunogenicity on the fully human therapeutic protein adalimumab, targeting TNF-alpha, in the treatment of RA was reported between 1 and 12% (van de Putte et al. 2004; Weinblatt et al. 2003; Package insert; Keystone et al. 2004), with one outlier study reporting 85% (Bender et al. 2007). Further monitoring of patients with long term treatment was reported to reach up to 18%.

4. Non-clinical Immunogenicity Testing

Immunogenicity testing guidances are mainly geared towards the standardization and validation of assays for the detection and characterization of ADA.

Table 16-1. Reported immunogenicity of therapeutic antibodies.

Name	Type	Target	Indication	ADA (%)	Subjects	Imm-Sup	References
HuBrE-3	Humanized	400 kDa breast epithelial mucin	Breast cancer	14	7	+	Kramer et al. (1998)
hu-A33	Humanized	A33	Colorectal cancer (CRC)	73	11		Welt et al. (2003a, b)
hu-A33	Humanized	A33	Colorectal cancer (CRC)	33	12		Scott et al. (2005)
hu-A33	Humanized	A33	Colorectal cancer (CRC)	54	44	+	Ritter et al. (2001)
hu-A33	Humanized	A33	Colorectal cancer (CRC)	59	13	+	Welt et al. (2003a, b)
Tysabri/natalizumab	Humanized	a4 integrin	Crohn's disease	7	181	+	Ghosh et al. (2003)
MLNO2	Humanized	a4b7	Ulcerative colitis	44	118		Feagan et al. (2005)
Eculizumab	Humanized	C5	Paroxysmal nocturnal hemoglobinuria (PNH)	0.2	43	+	Hillmen et al. (2006)
Cantuzumab-mertansine	Humanized	Can	Colorectal cancer (CRC)	0	37		Tolcher et al. (2003)
Hu23F2G	Humanized	CD11/CD18	Multiple sclerosis	0	24		Bowen et al. (1998)
Raptiva/efalizumab	Humanized	CD11a	Psoriasis	2.3	501		Menter et al. (2005)
Raptiva/efalizumab	Humanized	CD11a	Psoriasis	4	292	+	Papp et al. (2006)
Raptiva/efalizumab	Humanized	CD11a	Psoriasis	6	1,063		PI
B43-Genistein	Murine	CD19	Acute lymphoblastic leukemia (ALL)	33	9	+	Uckun et al. (1999)
Bexxar/tositumomab	Murine	CD20	Non-Hodgkin's lymphoma (NHL)	9	55	+	Kaminski et al. (2001)
Rituxan/rituximab	Chimeric	CD20	Non-Hodgkin's lymphoma (NHL)	0	58		Davis et al. (2000)
Rituxan/rituximab	Chimeric	CD20	Non-Hodgkin's lymphoma (NHL)	0	37		Piro et al. (1999)
Rituxan/rituximab	Chimeric	CD20	Systemic lupus erythematosus	65	17	+	Looney et al. (2004)
Rituxan/rituximab	Chimeric	CD20	Primary Sjogren's syndrome (PSS)	27	15	+	Pijpe et al. (2005)

(continued)

Table 16-1. (continued)

Name	Type	Target	Indication	ADA (%)	Subjects	Imm-Sup	References
Zevalin/ibritumomab-tiuxetan	Murine	CD20	Non-Hodgkin's lymphoma (NHL)	3	211		PI
Epratuzumab	Humanized	CD22	Primary Sjogren's syndrome (PSS)	19	16		Steinfeld et al. (2006)
OKT3	Murine	CD3	Graft rejection	54	82	+	McIntyre et al. (1996)
HuM291/vasilizumab	Humanized	CD3	Graft vs. host disease (GVHD)	0	13	+	Carpenter et al. (2002)
HuM195	Humanized	CD33	Acute promyelocytic leukemia	5	21	+	Jurcic et al. (2000)
Mylotarg/ gemtuzumab-ozogamicin	Humanized	CD33	Acute myeloid leukemia	0	142		PI
cM-T412	Chimeric	CD4	Rheumatoid arthritis (RA)	75	12		Choy et al. (1998)
hMAb BIWA 4/bivatuzumab	Humanized	CD44v6	Head and neck squamous cell carcinoma	10	20	+	Börjesson et al. (2003)
hMAb BIWA 4/bivatuzumab	Humanized	CD44v6	Head and neck squamous cell carcinoma	0	10		Colnot et al. (2003)
Bivatuzumab mertansine	Humanized	CD44v6	Head and neck squamous cell carcinoma	0	7		Tijink et al. (2006)
BIWI 1/bivatuzumab mertansine	Humanized	CD44v6	Squamous cell carcinoma	0	31		Sauter et al. (2007)
Mab BIWA 1	Murine	CD44v6	Head and neck squamous cell carcinoma	92	12		Stroomer et al. (2000)
Campath-1H/alemtuzumab	Humanized	CD52	Rheumatoid arthritis (RA)	63	40		Weinblatt et al. (1995)
Campath-1H/alemtuzumab	Humanized	CD52	Rheumatoid arthritis (RA)	10	10		Reiff (2005)
Campath-1H/alemtuzumab	Humanized	CD52	Rheumatoid arthritis (RA)	75	4		Reiff (2005)
Campath-1H/alemtuzumab	Humanized	CD52	Rheumatoid arthritis (RA)	29	31		Reiff (2005)
Campath-1H/alemtuzumab	Humanized	CD52	Rheumatoid arthritis (RA)	53	30		Reiff (2005)
Campath-1H/alemtuzumab	Humanized	CD52	Rheumatoid arthritis (RA)	0	5		Reiff (2005)
Campath-1H/alemtuzumab	Humanized	CD52	B-CLL	1.9	211		PI

Erbitux/cetuximab	Chimeric	EGFR	Cancer	5	1,001		PI
ch14.18	Chimeric	Ganglioside GD2	Neuroblastoma	0	9		Handgretinger et al. (1995)
Reopro/abciximab	Chimeric	GPIIb/IIIa	Coronary angioplasty	4	500		Tcheng et al. (2001)
Reopro/abciximab	Chimeric	GPIIb/IIIa	Coronary angioplasty	21	500		Tcheng et al. (2001)
Reopro/abciximab	Chimeric	GPIIb/IIIa	Coronary angioplasty	5	616		PI
Reopro/abciximab	Chimeric	GPIIb/IIIa	Coronary angioplasty	7	616		PI
Herceptin/trastuzumab	Humanized	HER2	Breast cancer	0.1	903		PI
Xolair/omalizumab	Humanized	IgE	Asthma	0	22		Djukanović et al. (2004)
Xolair/omalizumab	Humanized	IgE	Asthma	0	268	+	Busse et al. (2001)
Simulect/basiliximab	Chimeric	IL2R	Graft rejection	1	339	+	PI
Simulect/basiliximab	Chimeric	IL2R	Graft rejection	1	138	+	PI
Zenapax/HAT/daclizumab	Humanized	IL2R	Graft rejection	8	12	+	Vincenti et al. (1997)
Zenapax/HAT/daclizumab	Humanized	IL2R	Graft rejection	14	123		PI
Zenapax/HAT/daclizumab	Humanized	IL2R	Graft rejection	34	61		PI
c-MOv18	Chimeric	R	Ovarian cancer	0	5	+	
c-Nd2	Chimeric	Pancreatic mucin	Pancreatic cancer	0	10		Sawada et al. (1999)
Denosumab	Human	RANKL	Osteoporosis/osteopenia	0.6	312		McClung et al. (2006)
Synagis/palivizumab	Humanized	RSV	Hematopoietic stem cell transplants	0	6		Boeckh et al. (2001)
Synagis/palivizumab	Humanized	RSV	Bronchopulmonary dysplasia	1	1,002		The Impact-RSV Study Group (2006)
Humicade/CDP571	Humanized	TNFa	Crohn's disease	7	111	+	Sandborn et al. (2001)
Humira/adalimumab	Human	TNFa	Rheumatoid arthritis (RA)	12	434	+	van de Putte et al. (2004)
Humira/adalimumab	Human	TNFa	Rheumatoid arthritis (RA)	1	209	+	Weinblatt et al. (2003)
Humira/adalimumab	Human	TNFa	Rheumatoid arthritis (RA)	87	15	+	Bender et al. (2007)

(continued)

Table 16-1. (continued)

Name	Type	Target	Indication	ADA (%)	Subjects	Imm-Sup	References
Humira/adalimumab	Human	TNFa	Rheumatoid arthritis (RA)	5	1,062	+	PI
Humira/adalimumab	Human	TNFa	Rheumatoid arthritis (RA)	0.7	419	+	Keystone et al. (2004)
Remicade/infliximab	Chimeric	TNFa	Rheumatoid arthritis (RA)	17.4	87	+/–	Maini et al. (1998)
Remicade/infliximab	Chimeric	TNFa	Rheumatoid arthritis (RA)	8	60	+	Lipsky et al. (2000)
Remicade/infliximab	Chimeric	TNFa	Crohn's disease	6	50	+/–	Present et al. (1999)
Remicade/infliximab	Chimeric	TNFa	Crohn's disease	27	237	+/–	Hanauer et al. (2002)
Remicade/infliximab	Chimeric	TNFa	Crohn's disease	6	101	+/–	Targan et al. (1997)
Remicade/infliximab	Chimeric	TNFa	Crohn's disease	9	199	+	Hanauer (1999)
Remicade/infliximab	Chimeric	TNFa	Crohn's disease	61	125	+	Baert et al. (2003)
Remicade/infliximab	Chimeric	TNFa	Crohn's disease	55	174	+/–	Vermeire et al. (2007)
Certolizumab pegol	Humanized	TNFa	Crohn's disease	12	73	+/–	Schreiber et al. (2005)
Certolizumab pegol	Humanized	TNFa	Crohn's disease	8	331	+/–	Sandborn et al. (2007)
Certolizumab pegol	Humanized	TNFa	Crohn's disease	9	668	+/–	Schreiber et al. (2007)
Avastin/bevacizumab	Humanized	VEGF	Solid tumors	0	25	+	Gordon et al. (2001)
Avastin/bevacizumab	Humanized	VEGF	Solid tumors	0	12	+	Margolin et al. (2001)
Vitaxin	Humanized		Late stage cancer	0	17		Gutheil et al. (2000)

ADA: antibody response to the therapeutic protein
Subjects: number of individuals included in the study
Imm-Sup "+" when immunosuppressive drugs were used during treatment
PI package insert

Table 16-2. Overview of clinical and non-clinical methods addressing immunogenicity of protein therapeutics, the information they provide and the required input.

	In silico methods	**Peptide binding assays**	**Peptide elution from APC**	**T-cell activation and proliferation assays**	**ADA screening**
Information					
Binding of the peptide to the HLA Class-II receptor	X	X	X	X	X
Antigen processing by the APC	–	–	X	X	X
Activation of the T-helper cell	–	–	–	X	X
Presence of anti-drug antibodies	–	–	–	–	X
Input required	• Lead sequence	• Peptides	• Protein and/or derived peptides	• Highly pure proteins • Immunograde peptides • PBMC from >50 donors	• Clinical grade protein • Patient serum
Cost	Low	Medium	High	High	Medium

EMEA guidance EMEA/CHMP/BMWP/14327/2006 which came into force in April 2008 mentions regarding the non-clinical assessment of immunogenicity that "*therapeutic proteins show species differences in most cases. Thus, human proteins will be recognized as foreign proteins by animals. For this reason, the predictivity of non-clinical studies for evaluation of immunogenicity is considered low. Non-clinical studies aiming at predicting immunogenicity in humans are normally not required. However, ongoing consideration should be given to the use of emerging technologies (novel in vivo, in vitro and in silico models), which might be used as tools*."

The need for non-clinical immunogenicity studies will depend strongly on the risk profile of the drug. High-risk drugs, such as proteins having a non-redundant, endogenous human counterpart, might need more non-clinical characterization than low-risk protein therapeutics such as therapeutic fully human antibodies.

To date, no systems are available to estimate ADA in a pre-clinical or research setting, prior to the first dose in humans. Though regulatory requirements include monitoring of the development of ADA during pre-clinical development in animal models, the observed immunogenicity is difficult to map to the eventual immunogenicity measured in humans. ADA measurement in animal models are mostly used to support and document adverse effects, PK and PD data during non-clinical and toxicology studies.

For the prediction or relative assessment of immunogenicity prior to clinical trials, other methodologies are to be used.

4.1. T_h Epitopes

Raising a persistent antibody response against an antigen requires at least three cell-types: B-cells producing antigen specific antibodies, T helper-lymphocytes and professional antigen presenting cells. Professional antigen presenting cells such as dendritic cells and langerhals cells take up antigens, such as the therapeutic antibodies, and digest them into peptides that are subsequently presented on the cell surface in conjunction with HLA Class-II receptors. The HLA-peptide complex can then be recognized by the T-cell receptor on $CD4^+$-T helper cells, triggering the production of cytokines that on their turn activate B-cells to produce antibodies. Fig. 16-3 shows the conformation of such as peptide, or T-cell epitope, bound to an HLA Class-II receptor.

Tolerance mechanisms and negative selection of Th-cells reacting to peptides derived from self-proteins, or circulating proteins, ensure that typically immune responses are only raised against antigens linked with a danger signal.

Typically, a persistent humoral response requires a T-cell memory, allowing the organism to respond rapidly and repeatedly to antigens. As B-cells are also antigen presenting cells, they are able to internalize and digest the antigen which is binding to the membrane bound antibodies, present the peptides in HLA context and thereby attracting specific Th-cells to produce the cytokines needed to further activate the B-cell and increase the antigen specific antibody production.

It is generally believed that the absence of T-helper epitopes in antigens hinders the generation of a strong immune reaction, since it does not allow for building up a T-cell memory. As mentioned before, T-cell independent mechanism exist, which typically lead to low-affinity antibodies and which do not show an immune memory, hence asustainable ADA response.

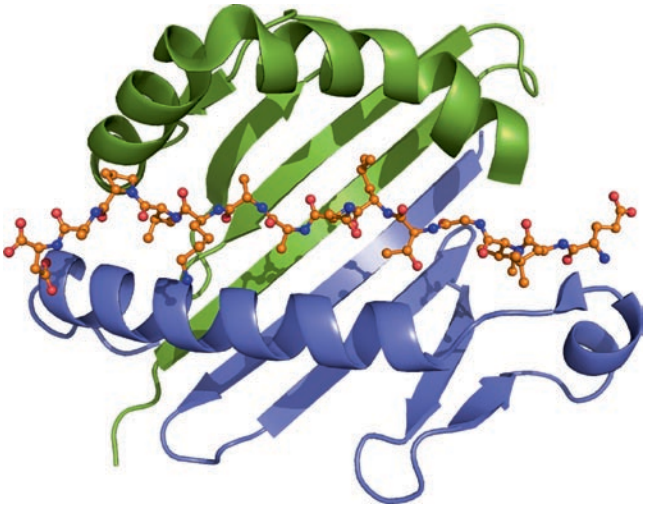

Fig. 16-3. HLA Class II DRB1*0101 binding area, with α and β chains in resp. *blue* and *green*, and a bound peptide in *orange* (PDB-code 1KLU)

The HLA Class-II receptor shows a high level of polymorphism, as the system has to be able to present a wide variety of different peptides.

Typically, preclinical methods will evaluate the therapeutic antibodies for their T-cell epitope content, as this allows to perform a relative comparison of the expected immunogenicity between comparable therapeutic proteins. Moreover, T-cell epitopes can be readily estimated and tested by a range of in silico and in vitro methods.

4.2. T-cell Dependant Immunogenicity Assessment

T-cell epitopes can be identified though in silico and in vitro methods. The in silico methods typically address the binding of peptides to HLA receptors, whereas in vitro methods have been developed to measure the binding of peptides to HLA, the activation of T-cells or to identify the peptides generated by the antigen-presenting cells. The type of method to be used highly depends on the development phase of the therapeutic antibody.

4.2.1. In Silico Methods

In silico methods allow to identify T-cell epitopes in a rapid and low-cost way. Typically, these methods evaluate the primary structure of the protein therapeutic, assessing whether a specific peptide sequence can bind to a specific HLA receptor. These methods are optimally suited during early drug design, such as lead priotirization upon library screening, to provide guidance during protein engineering studies or to identify the safest mutations/substitutions during humanization and CDR-grafting studies. Moreover, the methods can be used in de-immunization strategies, i.e., to identify substitutions in protein therapeutics that remove T-cell epitopes.

The in silico methods exist in three different types: additive methods based on inference, non-additive methods based on inference, and structure-based

methods. The earliest predictive models were entirely statistical, where characterized epitope sequences were aligned and sequence motives were identified based on sequence alignments. Based on the motives, substitution matrices could be built, containing a "score" for each amino-acid at each position of 9-mer peptides. Adding the scores for each peptide sequence gave the binding score assessment of the peptide to certain HLA. While this model works reasonably well for HLA Class I (Peters et al. 2003), the approach has been shown to be less accurate for HLA Class-II receptors, which drives the humoral response. Applying novel statistical methods, generated tools including Rankpep, Propred, Tepitope, Epimatrix, Bimas and Syphpeiti (Hammer et al. 1994; Rammensee et al. 1999; Sturniolo et al. 1999; Borras-Cuesta et al. 2000; Singh and Raghava 2001; Reche et al. 2004; Peters and Sette 2005). Other methods by inference have been developed based on artificial neural networks, hidden Markov models (Mamitsuka 1998) and support vector machines (SVMs) (Zhao et al. 2003).

More recent methods include structure-based information, and have been successfully applied to both Class I and Class II receptors. Rather than being based on the sequence information alone, these methods use information of molecular interactions between peptide and molecule, using force-fields, solvation parameters or other structure-derived properties (Desmet et al. 2005). Compared to the previous generation methods, the structure based methods allow to address a wider variety of HLA polymorphism, thereby addressing a wider population. While the latest methods by inference work reasonably well compared to the first generation tools, they do not attain the general accuracy level of the structure based methods (Van Walle et al. 2007).

4.2.2. In Vitro Methods

Whereas the in silico methods allow to identify the binding of peptides to HLA receptors, thereby replacing the classical in vitro HLA binding assays, recent in vitro methods allow to address the processing of the antigen by the antigen presenting cell and the activation of T-cells by the HLA peptide complex.

Techniques to experimentally identify T cell epitopes typically rely on the elution of peptides from antigen presenting cells, analyzing the elution profiles with mass spectroscopy (Falk et al. 1991; Davenport et al. 1997).

T cell activation and proliferation assays measure whether a therapeutic protein or peptide can elicit an immune response. Typically, therapeutic antibody or derived peptides are used to prime human peripheral blood mononuclear cells (PBMC), derived from healthy donors or patients. After a number of days of culture, the cells are restimulated with autologous monocytes and whole antigen or peptides to restimulate the specific T-helper cells. The activated T-cells are then characterized based on cytokine production, using ELISpot assays, or more optimally measuring activation markers and cytokines with flow cytometric methods.

While the latter methods offer the highest information content, care has to be taken to work with highly pure antigen, if possible in a close to final formulation. Indeed, excipients, aggregates and production system related factors can strongly influence the read-outs. Moreover, due to the HLA polymorphism, samples of at least 50 healthy donors should be included in each study Fig. 16-4.

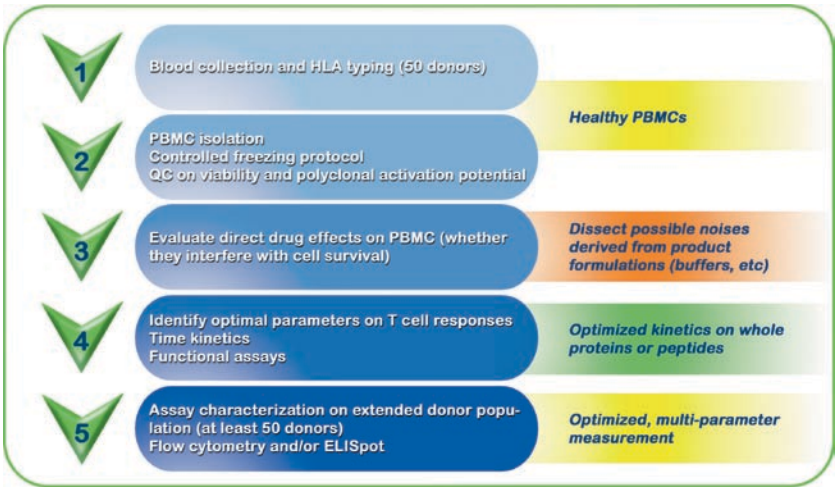

Fig. 16-4. Typical project lay-out addressing T-cell responses in donors or patient

5. Conclusions

With all therapeutic antibodies showing some level of immunogenicity, both the likelihood and severity of an immune response should be monitored throughout the product development. Whereas the actual ADA response can only be addressed during clinical development or post-marketing, research and non-clinical assessment of expected immunogenicity employ different methods.

Table 16-2 gives an overview of the available techniques, the information they provide and the moment in the development cycle they bring most added value.

In the development process of therapeutic antibodies, the combination of in silico tools, in vitro T-cell activation assays and eventually ADA screening and characterization will allow a full assessment of the drug immunogenicity.

In silico methods are optimally suited to compare relative immunogenicity in a set of drug lead candidates or variants, supporting the lead selection and optimization during early drug lead screening, protein engineering and drug optimization.

In vitro methods will further characterize the expected immunogenicity, assisting the drug development and taking into account other immunogenicity drivers such as aggregates, formulation and production system related factors. Moreover, in vitro methods are optimally suited to compare immunogenicity in comparability studies, manufacturing changes and/or in the development of biosimilar drugs.

In vivo methods allow the direct measurement of ADA against the protein therapeutic, and have to be developed prior to or during the clinical trials. They further support the patient monitoring and post-marketing surveillance of the therapeutic antibody.

References

Bachmann MF, Rohrer UH, Kundig TM, Burki K, Hengartner H, Zinkernagel RM (1993) The influence of antigen organization on B cell responsiveness. Science 262:1448–1451

Baert F, Noman M, Vermeire S, Van Assche G, D'Haens G, Carbonez A, Rutgeerts P (2003) Influence of immunogenicity on the long-term efficacy of infliximab in Crohn's disease. N Engl J Med 348:601–608

Bender NK, Heilig CE, Droll B, Wohlgemuth J, Armbruster FP, Heilig B (2007) Immunogenicity, efficacy and adverse events of adalimumab in RA patients. Rheumatol Int 27:269–274

Boeckh M, Berrey MM, Bowden RA, Crawford SW, Balsley J, Corey L (2001) Phase 1 evaluation of the respiratory syncytial virus-specific monoclonal antibody palivizumab in recipients of hematopoietic stem cell transplants. J Infect Dis 184:350–354

Borras-Cuesta F, Golvano J, Garcia-Granero M, Sarobe P, Riezu-Boj J, Huarte E, Lasarte J (2000) Specific and general HLA-DR binding motifs: Comparison of algorithms. Hum Immunol 61:266–278

Bowen JD, Petersdorf SH, Richards TL, Maravilla KR, Dale DC, Price TH, St John TP, Yu AS (1998) Phase I study of a humanised anti-CD11/CD18 monoclonal antibody in multiple sclerosis. Clin Pharmacol Ther 64:339–346

Börjesson PK, Postema EJ, Roos JC, Colnot DR, Marres HA, van Schie MH, Stehle G, de Bree R, Snow GB, Oyen WJ et al (2003) Phase I therapy Study with 186Re-labeled humanised monoclonal antibody BIWA 4 (bivatuzumab) in patients with head and neck squamous cell carcinoma. Clin Cancer Res 9:3961s–3972s

Busse W, Corren J, Lanier BQ et al (2001) Omalizumab, anti-IgE recombinant humanized monoclonal antibody, for the treatment of severe allergic asthma. J Allergy Clin Immunol 108:184–190

Carpenter PA, Appelbaum FR, Corey L, Deeg HJ, Doney K, Gooley T, Krueger J, Martin P, Pavlovic S, Sanders J et al (2002) A humanised non-FcR-binding anti-CD3 antibody, visilizumab, for treatment of steroid-refractory acute graft-versus-host disease. Blood 99:2712–2719

Casadevall N, Nataf J, Viron B, Kolta A, Kiladjian JJ, Martin-Dupont P, Michaud P, Papo T, Ugo V, Teyssandier I, Varet B, Mayeux P (2002) Pure red-cell aplasia and antierythropoietin antibodies in patients treated with recombinant erythropoietin. N Engl J Med 346(7):469–475

Choy EHS, Schantz A, Pitzalis C, Kingsley GH, Panayi GS (1998) The pharmacokinetics and human anti-mouse antibody response in rheumatoid arthritis patients treated with a chimeric anti-CD4 monoclonal antibody. Br J Rheumatol 37:801–802

Colnot DR, Roos JC, de Bree R, Wilhelm AJ, Kummer JA, Hanft G, Heider KH, Stehle G, Snow GB, van Dongen GA (2003) Safety, biodistribution, pharmacokinetics, and immunogenicity of 99mTc-labeled humanised monoclonal antibody BIWA 4 (bivatuzumab) in patients with squamous cell carcinoma of the head and neck. Cancer Immunol Immunother 52:576–582

Davenport MP, Smith KJ, Barouch D, Reid SW, Bodnar WM, Willis AC, Hunt DF, Hill AV (1997) HLA Class I binding motifs derived from random peptide libraries differ at the COOH terminus from those of eluted peptides. J Exp Med 185:367–371

Davis TA, Grillo-López AJ, White CA, McLaughlin P, Czuczman MS, Link BK, Maloney DG, Weaver RL, Rosenberg J, Levy R (2000) Rituximab anti-CD20 monoclonal antibody therapy in non-Hodgkin's lymphoma: Safety and efficacy of re-treatment. J Clin Oncol 18:3135–3143

Desmet J, Meersseman G, Boutonnet N, Pletinckx J, De Clercq K, Debulpaep M, Braeckman T, Lasters I (2005) Anchor profiles of HLA-specific peptides: Analysis by a novel affinity scoring method and experimental validation. Proteins 58:53–69

Djukanović R, Wilson S, Kraft M, Jarjour N, Steel M, Chung F, Bao W, Fowler-Taylor A, Matthews J, Busse W, Holgate S, Fahy J (2004) Effects of treatment with

anti-immunoglobulin E antibody omalizumab on airway inflammation in allergic asthma. Am J of Resp Crit Care Med 170:583–593

European Agency for the Evaluation of Medicinal Products (EMEA) (2008) Guideline on immunogenicity assessment of biotechnology-derived therapeutic proteins. EMEA/CHMP/BMWP/14327/2006, April 2008

Falk K, Roetzschke O, Stefanovic S, Jung G, Rammensee HG (1991) Allele-specific motifs revealed by sequencing of self-peptides eluted from MHC molecules. Nature 351:290–296

Feagan BG, Greenberg GR, Wild G, Fedorak RN, Paré P, McDonald JW, Dubé R, Cohen A, Steinhart AH, Landau S et al (2005) Treatment of ulcerative colitis with a humanised antibody to the alpha4beta7 integrin. N Engl J Med 352:2499–2507

Ghosh S, Goldin E, Gordon FH, Malchow HA, Rask-Madsen J, Rutgeerts P, Vyhnálek P, Zádorová Z, Palmer T, Donoghue S et al (2003) Natalizumab for active Crohn's disease. N Engl J Med 348:24–32

Goldstein G, Fuccello AJ, Norman DJ, Shield CF III, Colvin RB, Cosimi AB (1986) OKT3 monoclonal antibody plasma levels during therapy and the subsequent development of host antibodies to OKT3. Transplantation 42:507–511

Gordon MS, Margolin K, Talpaz M, Sledge GW Jr, Holmgren E, Benjamin R, Stalter S, Shak S, Adelman D (2001) Phase I safety and pharmacokinetic study of recombinant human anti-vascular endothelial growth factor in patients with advanced cancer. J Clin Oncol 19:843–850

Gutheil JC, Campbell TN, Pierce PR, Watkins JD, Huse WD, Bodkin DJ, Cheresh DA (2000) Targeted antiangiogenic therapy for cancer using Vitaxin: A humanised monoclonal antibody to the integrin alphavbeta3. Clin Cancer Res 6:3056–3061

Hammer J, Bono E, Gallazzi F, Belunis C, Nagy Z, Sinigaglia F (1994) Precise prediction of major histocompatibility complex class II-peptide interaction based on peptide side chain scanning. J Exp Med 180:2353–2358

Hanauer SB (1999) Review article: Safety of infliximab in clinical trials. Aliment Pharmacol Ther 13:16–22

Hanauer SB, Feagan BG, Lichtenstein GR, Mayer LF, Schreiber S, Colombel JF, Rachmilewitz D, Wolf DC, Olson A, Bao W et al (2002) Maintenance infliximab for Crohn's disease: The ACCENT I randomised trial. Lancet 359:1541–1549

Hillmen P, Young NS, Schubert J, Brodsky RA, Socié G, Muus P, Röth A, Szer J, Elebute MO, Nakamura R et al (2006) The complement inhibitor eculizumab in paroxysmal nocturnal hemoglobinuria. N Engl J Med 355:1233–1243

Hwang W, Foote J (2005) Immunogenicity of engineered antibodies. Methods 36:3–10

Isaacs JD, Manna VK, Rapson N, Bulpitt KJ, Hazleman BL, Matteson EL, St Clair EW, Schnitzer TJ, Johnston JM (1996a) CAMPATH-1H in rheumatoid arthritis–an intravenous dose-ranging study. Br J Rheumatol 35:231–240

Isaacs JD, Watts RA, Hazleman BL, Hale G, Keogan MT, Cobbold SP, Waldmann H (1992) Humanised monoclonal antibody therapy for rheumatoid arthritis. Lancet 340:748–752

Isaacs JD, Wing MG, Greenwood JD, Hazleman BL, Hale G, Waldmann H (1996b) A therapeutic human IgG4 monoclonal antibody that depletes target cells in humans. Clin Exp Immunol 106:427–433

Jurcic JG, Deblasio T, Dumont L, Yao TJ, Scheinberg DA (2000) Molecular remission induction with retinoic acid and anti-CD33 monoclonal antibody HuM195 in acute promyelocytic leukemia. Clin Cancer Res 6:372–380

Kaminski MS, Zelenetz AD, Press OW, Saleh M, Leonard J, Fehrenbacher L, Lister TA, Stagg RJ, Tidmarsh GF, Kroll S et al (2001) Pivotal study of iodine I 131 tositumomab for chemotherapy-refractory low-grade or transformed low-grade B-cell non-Hodgkin's lymphomas. J Clin Oncol 19:3918–3928

Keystone EC, Kavanaugh AF, Sharp JT, Tannenbaum H, Hua Y, Teoh LS, Fischkoff SA, Chartash EK (2004) Radiographic, clinical, and functional outcomes of treatment with adalimumab (a human anti-tumor necrosis factor monoclonal antibody) in patients with

active rheumatoid arthritis receiving concomitant methotrexate therapy: A randomized, placebo-controlled, 52-week trial. Arthritis Rheum 50:1400–1411

Kramer EL, Liebes L, Wasserheit C, Noz ME, Blank EW, Zabalegui A, Melamed J, Furmanski P, Peterson JA, Ceriani RL (1998) Initial clinical evaluation of radiolabeled MX-DTPA humanised BrE-3 antibody in patients with advanced breast cancer. Clin Cancer Res 4:1679–1688

Lipsky PE, van der Heijde DM, St Clair EW, Furst DE, Breedveld FC, Kalden JR, Smolen JS, Weisman M, Emery P, Feldmann M et al (2000) Infliximab and methotrexate in the treatment of rheumatoid arthritis. Anti-Tumor Necrosis Factor Trial in Rheumatoid Arthritis with Concomitant Therapy Study Group. N Engl J Med 343:1594–1602

Looney RJ, Anolik JH, Campbell D, Felgar RE, Young F, Arend LJ, Sloand JA, Rosenblatt J, Sanz I (2004) B cell depletion as a novel treatment for systemic lupus erythematosus: A phase I/II dose-escalation trial of rituximab. Arthritis Rheum 50:2580–2589

Maini RN, Breedveld FC, Kalden JR, Smolen JS, Davis D, Macfarlane JD, Antoni C, Leeb B, Elliott MJ, Woody JN et al (1998) Therapeutic efficacy of multiple intravenous infusions of anti-tumor necrosis factor alpha monoclonal antibody combined with low-dose weekly methotrexate in rheumatoid arthritis. Arthritis Rheum 41:1552–1563

Mamitsuka H (1998) Predicting peptides that bind to MHC molecules using supervised learning of Hidden Markov Models. Proteins 33:460–474

Margolin K, Gordon MS, Holmgren E, Gaudreault J, Novotny W, Fyfe G, Adelman D, Stalter S, Breed J (2001) Phase Ib trial of intravenous recombinant humanised monoclonal antibody to vascular endothelial growth factor in combination with chemotherapy in patients with advanced cancer: Pharmacologic and long-term safety data. J Clin Oncol 19:851–856

McClung MR, Lewiecki EM, Cohen SB, Bolognese MA, Woodson GC, Moffett AH, Peacock M, Miller PD, Lederman SN, Chesnut CH et al (2006) Denosumab in postmenopausal women with low bone mineral density. N Engl J Med 354:821–831

McIntyre JA, Kincade M, Higgins NG (1996) Detection of IGA anti-OKT3 antibodies in OKT3-treated transplant recipients. Transplantation 61:1465–1469

Menter A, Gordon K, Carey W, Hamilton T, Glazer S, Caro I, Li N, Gulliver W (2005) Efficacy and safety observed during 24 weeks of efalizumab therapy in patients with moderate to severe plaque psoriasis. Arch Dermatol 141:31–38

Mire-Sluis AR, Barrett YC, Devanarayan V, Koren E, Liu H, Maia M, Parish T, Scott G, Shankar G, Shores E et al (2004) Recommendations for the design and optimization of immunoassays used in the detection of host antibodies against biotechnology products. J Immunol Methods 289:1–16

Papp KA, Miller B, Gordon KB, Caro I, Kwon P, Compton PG, Leonardi CL, Efalizumab Study Group (2006) Efalizumab retreatment in patients with moderate to severe chronic plaque psoriasis. J Am Acad Dermatol 54:S164–S170

Peters B, Sette A (2005) Generating quantitative models describing the sequence specificity of biological processes with the stabilized matrix method. BMC Bioinformatics 6:132

Peters B, Tong W, Sidney J, Sette A, Weng Z (2003) Examining the independent binding assumption for binding of peptide epitopes to MHC-I molecules. Bioinformatics 19:1765–1772

Pijpe J, van Imhoff GW, Spijkervet FK, Roodenburg JL, Wolbink GJ, Mansour K, Vissink A, Kallenberg CG, Bootsma H (2005) Rituximab treatment in patients with primary Sjögren's syndrome: An open-label phase II study. Arthritis Rheum 52:2740–2750

Piro LD, White CA, Grillo-López AJ, Janakiraman N, Saven A, Beck TM, Varns C, Shuey S, Czuczman M, Lynch JW et al (1999) Extended Rituximab (anti-CD20

monoclonal antibody) therapy for relapsed or refractory low-grade or follicular non-Hodgkin's lymphoma. Ann Oncol 10:655–661

Present DH, Rutgeerts P, Targan S, Hanauer SB, Mayer L, van Hogezand RA, Podolsky DK, Sands BE, Braakman T, DeWoody KL et al (1999) Infliximab for the treatment of fistulas in patients with Crohn's disease. N Engl J Med 340:1398–1405

Rammensee H, Bachmann J, Emmerich NP, Bachor OA, Stevanovic S (1999) SYFPEITHI: Database for MHC ligands and peptide motifs. Immunogenetics 50:213–219

Reche PA, Glutting JP, Zhang H, Reinherz EL (2004) Enhancement to the RANKPEP resource for the prediction of peptide binding to MHC molecules using profiles. Immunogenetics 56:405–419

Reiff A (2005) A review of Campath in autoimmune disease: Biologic therapy in the gray zone between immunosuppression and immunoablation. Hematology 10:79–93

Ritter G, Cohen LS, Williams C, Richards EC, Old LJ, Welt S (2001) Serological analysis of human anti-human antibody responses in colon cancer patients treated with repeated doses of humanised monoclonal antibody A33. Cancer Res 61:6851–6859

Sandborn WJ, Feagan BG, Hanauer SB, Present DH, Sutherland LR, Kamm MA, Wolf DC, Baker JP, Hawkey C, Archambault A et al (2001) An engineered human antibody to TNF (CDP571) for active Crohn's disease: A randomized double-blind placebo-controlled trial. Gastroenterology 120:1330–1338

Sandborn WJ, Feagan BG, Stoinov S, Honiball PJ, Rutgeerts P, Mason D, Bloomfield R, Schreiber S, PRECISE 1 Study Investigators (2007) Certolizumab pegol for the treatment of Crohn's disease. N Engl J Med 357:228–238

Sauter A, Kloft C, Gronau S, Bogeschdorfer F, Erhardt T, Golze W, Schroen C, Staab A, Riechelmann H, Hoermann K (2007) Pharmacokinetics, immunogenicity and safety of bivatuzumab mertansine, a novel CD44v6-targeting immunoconjugate, in patients with squamous cell carcinoma of the head and neck. Int J Oncol 30:927–935

Sawada T, Nishihara T, Yamamoto A, Teraoka H, Yamashita Y, Okamura T, Ochi H, Ho JJ, Kim YS, Hirakawa K (1999) Preoperative clinical radioimmunodetection of pancreatic cancer by 111 In-labeled chimeric monoclonal antibody Nd2. Jpn J Cancer Res 90:1179–1186

Schreiber S, Rutgeerts P, Fedorak RN, Khaliq-Kareemi M, Kamm MA, Boivin M, Bernstein CN, Staun M, Thomsen OO, Innes A et al (2005) A randomized, placebo-controlled trial of certolizumab pegol (CDP870) for treatment of Crohn's disease. Gastroenterology 129:807–818

Schreiber S, Khaliq-Kareemi M, Lawrance IC, Thomsen OØ, Hanauer SB, McColm J, Bloomfield R, Sandborn WJ, PRECISE 2 Study Investigators (2007) Maintenance therapy with certolizumab pegol for Crohn's disease. N Engl J Med 357:239–250

Schroeder TJ, First MR, Hurtubise PE, Marmer DJ, Martin DM, Mansour ME, Melvin DB (1989) Immunologic monitoring with Orthoclone OKT3 therapy. J Heart Transplant 8:371–380

Scott AM, Lee FT, Jones R, Hopkins W, MacGregor D, Cebon JS, Hannah A, Chong G, U P, Papenfuss A et al (2005). A phase I trial of humanised monoclonal antibody A33 in patients with colorectal carcinoma: Biodistribution pharmacokinetics and quantitative tumor uptake. Clin Cancer Res 11:4810–4817

Singh H, Raghava GP (2001) ProPred: Prediction of HLA-DR binding sites. Bioinformatics 17:1236–1237

Steinfeld SD, Tant L, Burmester GR, Teoh NK, Wegener WA, Goldenberg DM, Pradier O (2006) Epratuzumab (humanised anti-CD22 antibody) in primary Sjögren's syndrome: An open-label phase I/II study. Arthritis Res Ther 8:R129

Stroomer JW, Roos JC, Sproll M, Quak JJ, Heider KH, Wilhelm BJ, Castelijns JA, Meyer R, Kwakkelstein MO, Snow GB et al (2000) Safety and biodistribution of

99mTechnetium-labeled anti-CD44v6 monoclonal antibody BIWA 1 in head and neck cancer patients. Clin Cancer Res 6:3046–3055

Sturniolo T, Bono E, Ding J, Raddrizzani L, Tuereci O, Sahin U, Braxenthaler M, Gallazzi F, Protti MP, Sinigaglia F et al (1999) Generation of tissue-specific and promiscuous HLA ligand databases using DNA microarrays and virtual HLA class II matrices. Nat Biotechnol 17:555–561

Targan SR, Hanauer SB, van Deventer SJ, Mayer L, Present DH, Braakman T, DeWoody KL, Schaible TF, Rutgeerts PJ (1997) A short-term study of chimeric monoclonal antibody cA2 to tumor necrosis factor alpha for Crohn's disease. Crohn's Disease cA2 Study Group. N Engl J Med 337:1029–1035

Tcheng JE, Kereiakes DJ, Lincoff AM, George BS, Kleiman NS, Sane DC, Cines DB, Jordan RE, Mascelli MA, Langrall MA et al (2001) Abciximab readministration: Results of the ReoPro Readministration Registry. Circulation 104:870–875

The Impact-RSV Study Group (2006) Palivizumab, a humanized respiratory syncytial virus monoclonal antibody, reduces hospitalization from respiratory syncytial virus infection in high-risk infants. Pediatrics 102:531–537

Tijink BM, Buter J, de Bree R, Giaccone G, Lang MS, Staab A, Leemans CR, van Dongen GA (2006) A phase I dose escalation study with anti-CD44v6 bivatuzumab mertansine in patients with incurable squamous cell carcinoma of the head and neck or esophagus. Clin Cancer Res 12:6064–6072

Tolcher AW, Ochoa L, Hammond LA, Patnaik A, Edwards T, Takimoto C, Smith L, de Bono J, Schwartz G, Mays T et al (2003) Cantuzumab mertansine, a maytansinoid immunoconjugate directed to the CanAg antigen: A phase I, pharmacokinetic, and biologic correlative study. J Clin Oncol 21:211–222

Uckun FM, Messinger Y, Chen CL, O'Neill K, Myers DE, Goldman F, Hurvitz C, Casper JT, Levine A (1999) Treatment of therapy-refractory B-lineage acute lymphoblastic leukemia with an apoptosis-inducing CD19-directed tyrosine kinase inhibitor. Clin Cancer Res 5:3906–3913

Van Walle I, Gansemans Y, Parren PW, Stas P, Lasters I (2007) Immunogenicity screening in protein drug development. Expert Opin Biol Ther 7:405–418

van de Putte LB, Atkins C, Malaise M, Sany J, Russell AS, van Riel PL, Settas L, Bijlsma JW, Todesco S, Dougados M et al (2004) Efficacy and safety of adalimumab as monotherapy in patients with rheumatoid arthritis for whom previous disease modifying antirheumatic drug treatment has failed. Ann Rheum Dis 63:508–516

Vermeire S, Noman M, Van Assche G, Baert F, D'Haens G, Rutgeerts P (2007) Effectiveness of concomitant immunosuppressive therapy in suppressing the formation of antibodies to infliximab in Crohn's disease. Gut 56:1226–1231

Vincenti F, Lantz M, Birnbaum J et al (1997) A phase I trial of humanized anti-interleukin 2 receptor antibody in renal transplantation. Transplantation 63:33–38

Weinblatt ME, Maddison PJ, Bulpitt KJ, Hazleman BL, Urowitz MB, Sturrock RD, Coblyn JS, Maier AL, Spreen WR, Manna VK et al (1995) CAMPATH-1H, a humanised monoclonal antibody, in refractory rheumatoid arthritis. An intravenous dose-escalation study. Arthritis Rheum 38:1589–1594

Weinblatt ME, Keystone EC, Furst DE, Moreland LW, Weisman MH, Birbara CA, Teoh LA, Fischkoff SA, Chartash EK (2003) Adalimumab, a fully human anti-tumor necrosis factor alpha monoclonal antibody, for the treatment of rheumatoid arthritis in patients taking concomitant methotrexate: The ARMADA trial. Arthritis Rheum 48:35–45

Welt S, Ritter G, Williams C Jr, Cohen LS, John M, Jungbluth A, Richards EA, Old LJ, Kemeny NE (2003a) Phase I study of anticolon cancer humanised antibody A33. Clin Cancer Res 9:1338–1346

Welt S, Ritter G, Williams C Jr, Cohen LS, Jungbluth A, Richards EA, Old LJ, Kemeny NE (2003b) Preliminary report of a phase I study of combination chemotherapy and humanised A33 antibody immunotherapy in patients with advanced colorectal cancer. Clin Cancer Res 9:1347–1353

Zhao Y, Pinilla C, Valmori D, Martin R, Simon R (2003) Application of support vector machines for T-cell epitopes prediction. Bioinformatics 19:1978–1984

Further reading to be recommended in addition to the EMEA 2008 guidance includes

Gupta S, Indelicato SR, Jethwa V, Kawabata T, Kelley M, Mire-Sluis AR, Richards SM, Rup B, Shores E, Swanson SJ, Wakshull E (2007) Recommendations for the design, optimization, and qualification of cell-based assays used for the detection of neutralizing antibody responses elicited to biological therapeutics. J Immunol Methods 321(1–2):1–18

Koren E, Smith HW, Shores E, Shankar G, Finco-Kent D, Rup B, Barrett YC, Devanarayan V, Gorovits B, Gupta S, Parish T, Quarmby V, Moxness M, Swanson SJ, Taniguchi G, Zuckerman LA, Stebbins CC, Mire-Sluis A (2008) Recommendations on risk-based strategies for detection and characterization of antibodies against biotechnology products. J Immunol Methods 333(1–2):1–9

Mire-Sluis AR, Barrett YC, Devanarayan V, Koren E, Liu H, Maia M, Parish T, Scott G, Shankar G, Shores E et al (2004) Recommendations for the design and optimization of immunoassays used in the detection of host antibodies against biotechnology products. J Immunol Methods 289:1–16

Rosenberg AS, Worobec A (2004a) A risk-based approach to immunogenicity concerns of therapeutic protein products – Part 1 – considering consequences of the immune response to a protein. Biopharm Int 17:22–26

Rosenberg AS, Worobec A (2004b) A risk-based approach to immunogenicity concerns of therapeutic protein products – Part 2 – considering host-specific and product-specific factors impacting immunogenicity. Biopharm Int 17:34–42

Rosenberg AS, Worobec A (2005) A risk-based approach to immunogenicity concerns of therapeutic protein products – Part 3 – effects of manufacturing changes in immunogenicity and the utility of animal immunogenicity studies. Biopharm Int 18:32–36

Shankar G, Pendley C, Stein KE (2007) A risk-based bioanalytical strategy for the assessment of antibody immune responses against biological drugs. Nat Biotechnol 25:555–561

Shankar G, Devanarayan V, Amaravadi L, Barrett YC, Bowsher R, Finco-Kent D, Fiscella M, Gorovits B, Kirschner S, Moxness M, Parish T, Quarmby V, Smith H, Smith W, Zuckerman LA, Koren E (2008) Recommendations for the validation of immunoassays used for detection of host antibodies against biotechnology products. J Pharm Biomed Anal 48(5):1267–1281

Van Walle I, Gansemans Y, Parren PW, Stas P, Lasters I (2007) Immunogenicity screening in protein drug development. Expert Opin Biol Ther 7:405–418

Part VII

Armed Antibodies and New Classes of Antibodies

Chapter 17

Production of Monoclonal Antibodies in *E. coli*

Dorothea E. Reilly and Daniel G. Yansura

Abbreviations

ADCC	Antibody dependent cellular cytotoxicity
bp	Base pairs
C1q	Subcomponent of C1, a complement activator
CDC	Complement dependent cytotoxicity
CHO	Chinese hamster ovary
E. coli	*Escherichia coli*
ELISA	Enzyme-linked immunosorbent assay
FcRn	Neonatal Fc receptor
IPTG	Isopropyl β-D-thiogalactopyranoside
IV	Intravenous
kDa	Kilodaltons
PBS	Phosphate buffered saline
SEC	Size-exclusion chromatography
TIR	Translation initiation region

1. Introduction

The number of monoclonal antibodies approved for use as therapeutic agents by regulatory agencies has increased in the past several years. Monoclonal antibodies are predicted to become an increasingly larger part of biopharmaceutical products, and perhaps dominate the market share by the end of the decade (Walsh 2006). Mammalian expression systems, such as Chinese Hamster Ovary cells (CHO), are currently the preferred system for producing full-length monoclonal antibodies. Fungal systems could become more of a contender for the production of antibodies if titers can be increased (Andersen and Reilly 2004). However, with fungal production systems, there may be concerns about potential non-native mammalian N-linked or O-linked glycosylation that could result in immunogenic responses in humans. Technology developed in recent years (Hamilton et al. 2003) could help to alleviate this concern.

From: *Current Trends in Monoclonel Antibody Development and Manufacturing,* Biotechnology: Pharmaceutical Aspects, DOI 10.1007/978-0-387-76643-0_17, Edited by: S.J. Shire et al.

The expression of full-length monoclonal antibodies in *E. coli* is a more recent development (Simmons et al. 2002; Mazor et al. 2007), and could result in significant production advantages over mammalian cell based systems. An *E. coli* system offers the advantages of speed, with much faster cell growth and the ability to rapidly make new production cell lines when compared to mammalian cell systems. In addition, production processes using *E. coli* do not present the concern of adventitious agents that exists for mammalian cell systems, thereby alleviating the need for viral removal steps and the validation that is required for those steps.

Finally, the lack of glycosylation in *E. coli* produced antibodies eliminates clinical complications associated with effector functions (Routledge et al. 1995; Friend et al. 1999). Most therapeutic applications do not require these activities, as blocking some type of protein-protein interaction is the primary and only function of many antibodies.

2. *E. coli* Challenges

The production of full-length monoclonal antibodies in *E. coli* presents a number of challenges due to the size and complexity of the molecule. The protein mass of approximately 150 kDa represents a barrier, although it is partially mitigated by the fact that it represents two smaller light chains and two larger heavy chains. It is probably much easier for these smaller subunits to fold at least somewhat on their own than it would be for one long continuous polypeptide of this size to achieve the correct structural conformation. Nonetheless, the folding of the individual chains prior to full assembly represents another hurdle for *E. coli* due to the number of internal disulfide bonds, two for light chain and four for heavy chain. In general, most host secreted-proteins contain only one or two cystine bridges, and the enzymes responsible for their formation become somewhat limited, when expressing heterologous proteins with numerous cysteines (Joly and Laird 2007). Finally, the four subunits must assemble into the complete quaternary structure, which largely occurs by means of favorable light-heavy and heavy-heavy chain interactions. The complex at this step should be fairly stable and the formation of the last disulfide bonds between heavy and light chains as well as between the two heavy chains at the hinge region completes the assembly. In the end this represents the biosynthesis of a large protein with sixteen disulfide bonds and four subunits (Fig. 17-1), which is quite a marvel for *E. coli*.

3. Expression Construct Design

The design of the expression construct and its DNA sequence controls or affects almost every step in the biosynthesis of the antibody, from transcription, to translation, secretion and folding. A replicating plasmid such as one based on pBR322 (Bolivar et al. 1977) is generally used for this purpose, as the copy number is held at about fifty per cell, and the DNA is readily available for further manipulation. While the individual components on the plasmid control specific biosynthetic steps, the overall goal is to create a system where each step is coupled to the next while avoiding any bottlenecks. Since antibodies vary from one molecule to the next, their intrinsic translation, secretion and folding abilities will also be different as well. It is therefore prudent to

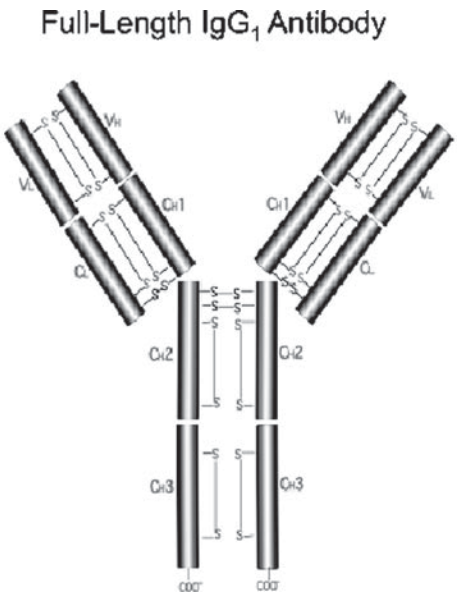

Fig. 17-1. The structure of a humanized IgG1 monoclonal antibody showing the four covalently linked subunits, two light chains and two heavy chains. Each chain has both variable (V_L and V_H) and constant (C_L and C_H) domains. There are a total of sixteen disulfide bonds in a human IgG1 immunoglobulin

incorporate in the construct some flexibility, so that one can manipulate the expression of each of the components, and be able to adjust these for each specific antibody.

4. Promoters

Essentially any promoter with a tight control can be used to drive the transcription of the heavy and light chains of the antibody. The list commonly includes the *tac, lac, ara* and *phoA* as well as others (Makrides 1996). The strength of the promoter in itself is actually not that important, but the overall downstream translation level of each chain is critical for maintaining a balanced system and avoiding secretion and folding problems. Strong promoters for example will most likely have to be coupled with weak translation initiation regions in order to achieve this goal (Simmons and Yansura 1996; Pluckthun et al. 1996). The expression of heterologous proteins targeted to the *E. coli* periplasm puts a stress on the host cell most likely due to competition for the somewhat limited secretory pathway components. This is why a tightly controlled promoter such as the *phoA* is necessary if one is to avoid toxicity problems prior to an induction. Ideally one would like to build up cell mass without complications until the optimal time for turning on the promoter.

5. Signal Sequences

Although it is possible to form disulfide bonds in the cytoplasm in thioredoxin and glutaredoxin mutant hosts (Derman et al. 1993; Prinz et al. 1997; Bessette et al. 1999), secretion of the antibody chains to the oxidizing environment

of the periplasm is usually the best choice (Joly and Laird 2007; Humphreys 2007). There are a large number of signal sequences that could possibly be used, but just a small subset of these have actually been reported in the literature for antibody expression. These include the PelB, STII, PhoA and the OmpA leader peptides. While these have successfully been used for the periplasmic secretion of both light chain and heavy chain for producing antibody fragments, only the STII and the PelB signal sequences have so far been used to secrete the full-length IgG1 heavy chain (Simmons et al. 2002; Mazor et al. 2007).

6. Control of Each Chain

In order to successfully achieve the significant expression and folding of a full-length antibody in the *E. coli* periplasm, it is important to fine-tune the translation level of each chain. High-level expression of any of the chains can result in the secretory backup of these polypeptides and the buildup of precursor chains in the cytoplasm. This will result in cellular stress responses and a significant drop in the accumulation of the fully folded antibody. The second problem is associated with unbalanced translation of the two chains resulting in poor folding and assembly of the heterotetrameric protein. An approximately 1:1 to 1.5:1 ratio of light:heavy chain has been observed to be optimal for folding in the periplasm (Simmons et al. 2002), although the optimal ratio may vary from antibody to antibody.

The easiest way to control the translation of each chain is through the translation initiation region (TIR). This region represents the 5′ end of the mRNA that influences its binding to the small ribosomal subunit to begin the translation process. It covers approximately the sequence from 10 base pairs (bp) upstream of the Shine-Dalgarno through the first six codons of the coding sequence (McCarthy and Gualerzi 1990). While only the Shine-Dalgarno and the Met codon actually make contact with the ribosomal 16 S rRNA and the Met tRNA respectively, the surrounding sequences strongly influence this binding by means of the resulting RNA secondary structure (De Smit and Van Duin 1990). One can in principle make changes in any part of the TIR to manipulate the translation initiation rate. However we have found it easier to just change the first six codons of the signal sequence, and empirically screen for the desired translation level (Simmons and Yansura 1996).

Full-length antibodies have been expressed in *E. coli* using either separate cistrons with individual promoters for each chain (Simmons et al. 2002) or a bicistronic setup with a single promoter (Mazor et al. 2007). In theory, each system should be able to work as well as the other in terms of providing just the right level of translation of heavy and light chains. However if the antibody one is trying to express has problems with a secretory backup or the ratio of the individual chains is not optimal, then it is much easier to adjust the translation with a separate cistron system. With a bicistronic construct, the translation of the second gene (usually heavy chain) is controlled by the TIR and translation of the first gene as well as the re-initiation coupling of the later coding sequence. The sequence and translation of the second gene can also influence the translation of the first cistron although to a lesser extent. This makes it difficult to adjust

the translation of one chain without inadvertently changing the translation of the other at the same time. The use of a separate cistron system avoids this and allows for the independent manipulation of each chain.

7. Chaperone Over-Expression

While the antibody chains probably have some ability to fold by themselves, the host-cell chaperones most likely help facilitate this activity. There are a number of chaperones in the periplasm including the peptidyl prolyl isomerases SurA, PpiA, PpiD and FkpA, the anti-aggregation Skp (Baneyx and Palumbo 2003) (Thome and Muller 1991), and the disulfide oxido-reductases DsbA and DsbC (Joly et al. 1998; Qiu et al. 1998; Jeong and Lee 2000; Bessette et al. 2001). In addition to their catalytic role, some of these proteins such as FkpA and DsbC have additional anti-aggregation activities. The over-expression of some of these chaperones has been reported in the literature to improve the folding of particular antibodies (Bothmann and Pluckthun 1998; Hayhurst and Harris 1999; Bothmann and Pluckthun 2000).

For full-length antibodies with their multiple disulfide bonds, we have found that the over-expressing DsbA and DsbC in particular have been quite beneficial. Since DsbA is the primary oxidizing agent and DsbC the isomerizing agent for disulfide bonds, it can be beneficial to over-express both in order to promote the formation of the correct covalent bridges. The positive effect of using these two chaperones is more evident when producing antibodies at high cell densities in a fed-batch fermention than in batch shake flask cultures. This difference in effect is likely due to more optimal growth conditions in fermentor cultures where pH and glucose feeding are controlled, and a consistent dissolved oxygen concentration can be maintained.

8. Optimized Construct

The final construct for scaling up the production of a full-length antibody in a fermentor will encode for the expression of light chain, heavy chain and most likely the co-expression of the chaperones DsbA and DsbC. In addition, there will be an antibiotic resistance marker for plasmid retention as well as a plasmid origin of replication. Fig. 17-2 shows an example of what a typical plasmid might look like.

9. Host Strains

A variety of *E. coli* strains may be suitable for the production of antibodies, although in general strains that are deficient in periplasmic proteases, have been successfully used to obtain higher titers of antibodies. Suitable strains include W3110 derivatives such as 33D3 (W3110 kan^R Δ *fhuA* (Δ tonA) *ptr3 lacIq lacL8 ompt*Δ (nmpc-fepE)-*degP*) (Simmons et al. 2002) or 62B8 (W3110 Δ *fhuA phoA ilvG2096* (Val^r) *manA degP* Δ*prc sprW148R*) (Chen et al. 2004). Other combinations of protease deletions can also be beneficial for the accumulation of full-length monoclonal antibodies in *E. coli*.

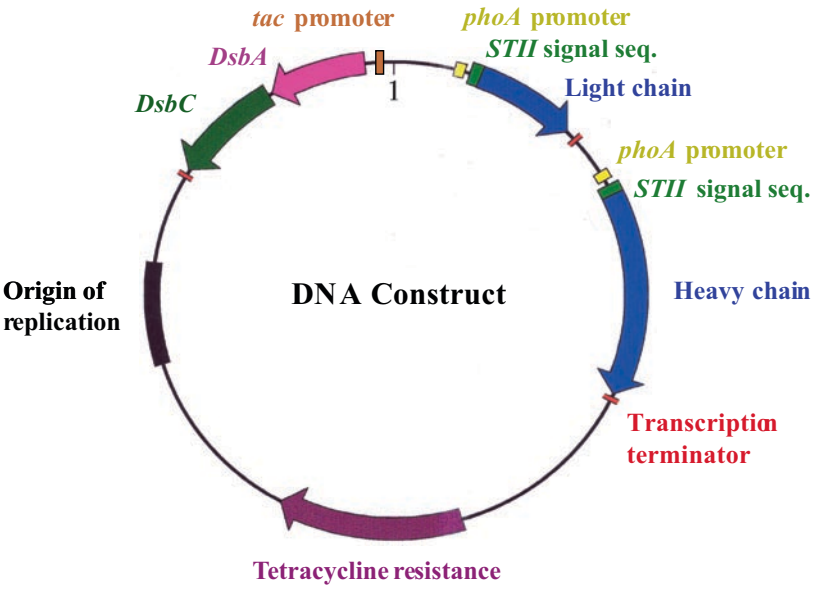

Fig. 17-2. A typical plasmid map showing the light and heavy chain coding sequences as well as the *phoA* promoters, *STII* signal sequences and downstream transcriptional terminators that control their expression. Also shown are the chaperonin genes *DsbA* and *DsbC*, the antibiotic resistance gene and the plasmid origin of replication

10. Fermentation Scale Up

Production of full-length antibodies in *E. coli* can be achieved at a variety of scales, from small volumes in shake flasks up to very large volumes in fermentors. When expressing a full-length antibody using a plasmid such as the one shown in Fig. 17-2, the fermentation medium is designed such that the inorganic phosphate initially present in the medium is consumed by the growing culture and over time phosphate is depleted (Chen et al. 2004). This results in the induction of the *phoA* promoter and transcription of the light chain and heavy chain genes.

A growth medium such as C.R.A.P. (Simmons et al. 2002) is suitable for small-scale cultures grown in shake tubes or flasks. For larger scale cultures grown in fermentors, it is possible to achieve high cell density cultures with the proper design of the growth medium. One suitable medium initially contains 8.9 mM glucose, 14.3 mM $MgSO_4$, 143 μM $FeCl_3$, 46 μM each of $ZnSO_4$, $CuSO_4$, and H_3BO_4, 42 μM each $CoCl_2$, $NaMoO_4$, and $MnSO_4$, 40.6 mM $(NH_4)_2SO_4$, 16 mM K_2HPO_4, 10 mM NaH_2PO_4, 3.6 mM sodium citrate, 12 mM KH_2PO_4, 29 g/L casein hydrolysate, 14.3 g/L yeast extract, and either 15–20 mg/L tetracycline or 50–70 mg/L ampicillin. Additional salts are fed to the culture during the course of the fermentation in order to achieve high cell density (Simmons et al. 2002). A concentrated glucose solution is continuously fed using a computer controlled feed algorithm.

Large-scale fermentation cultures are initiated with a Luria Broth (LB) shake flask culture that has been grown for approximately 16 h at 30°C with shaking. The fermentor culture is also grown at 30°C with agitation and aeration.

A typical fermentation culture depletes phosphate at around 20–30 h after reaching a maximum OD_{550} of approximately 200–250. Fermentations are typically allowed to continue for 70–80 h, ensuring anywhere from 40–60 h of antibody production.

Soluble folded antibody expressed during the course of the fermentation will be translocated to the periplasmic compartment of the *E. coli* cells, and must be extracted for analysis and purification. For small-scale analyses samples were extracted using a buffer and conditions similar to the method described by Battersby et al. (2001) and titers were determined using the dual-column chromatographic method (Battersby et al. 2001). For large-scale purifications, the cell lysis method and purification have previously been described (Simmons et al. 2002).

As noted above, the translation of the light chain and heavy chain can be individually controlled by using separate cistrons for each chain, and also by varying the TIR strengths for each chain. In an initial attempt to increase the titers of a full-length antibody, the TIRs for both light chain and heavy chain were increased. As shown in Fig. 17-3, when both light chain and heavy chain each had TIR strengths of 1, a titer of approximately 100 mg/L was obtained. Doubling the TIR strengths for both chains also resulted in a titer of approximately 100 mg/L.

SDS-PAGE and immunoblot analysis of reduced *E. coli* cell pellets from the fermentation culture suggested that when the relative TIR strengths for both light chain and heavy chain were increased from 1 to 2, there was a concomitant increase in the expression of both chains. The titer result suggests that most of the light chain and heavy chain produced by the cells does not end up in properly folded and soluble antibody. To further investigate this, a modified version of a reversed-phase chromatography assay described by Chen et al. (2004) was used to quantify the total amounts of light chain and heavy chain produced during the course of the fermentation. Analyses using this assay showed that less than 15% of either the light chain or heavy chain ended up in the fully assembled antibody.

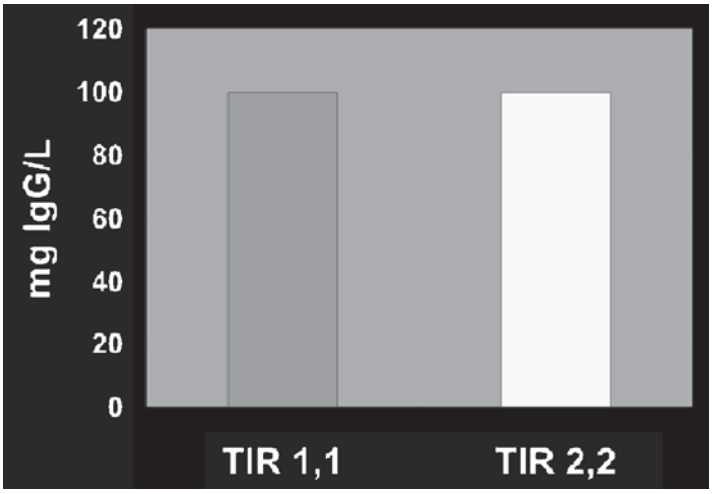

Fig. 17-3. Increasing the TIRs and ultimately the translation of both chains does not in itself increase the level of folded and assembled antibody

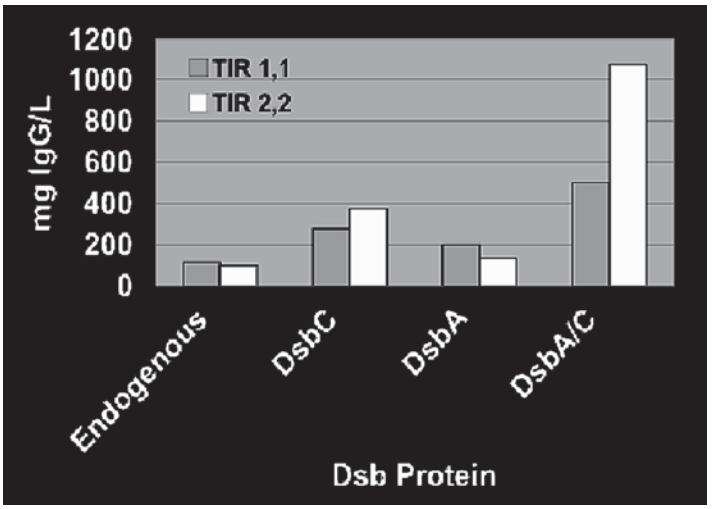

Fig. 17-4. Manipulating the antibody expression by means of light and heavy chain TIR changes and the coexpression of DsbA, DsbC and the combination DsbA and DsbC. In order to fully take advantage of the increased light and heavy chain translation with higher TIRs, both DsbA and DsbC must be over-expressed

As mentioned previously, full-length antibodies have sixteen disulfide bonds, far more than any endogenous *E. coli* protein. In order to test whether co-expressing DsbA and/or DsbC could improve the folding and assembly of the antibody chains, resulting in higher titers of full-length antibodies, fermentations were done where either DsbA, DsbC, or both DsbA and DsbC were co-expressed with light chain and heavy chain. The genes for DsbA, DsbC, or DsbA and C were inserted into a compatible plasmid under the control of the *tacII* promoter (De Boer et al. 1983). IPTG was added to the fermentation culture to induce the expression of the Dsb protein(s) shortly before the expected time of phosphate depletion.

The results from a representative series of fermentations are shown in Fig. 17-4. Co-expression of DsbA with either the TIR 1 or TIR 2 antibody plasmid resulted in a two-fold increase in the titer of the soluble and assembled antibody, from approximately 100 mg/L up to 200 mg/L. This is only a modest gain in folding and assembly efficiency. Co-expression of DsbC with the antibody resulted in antibody titers in the range from 300–350 mg/L, a larger increase in titer than seen with DsbA co-expression. However, there still isn't much of a titer difference between the TIR 1 construct and the TIR 2 construct, although there is roughly twice as much light chain and heavy chain available for antibody formation from the TIR 2 construct, as mentioned above.

The largest boost in titers was observed when both DsbA and DsbC were co-expressed with the antibody chains in a high-cell density fermentation. In this experiment, the TIR 1 antibody construct gave an antibody titer of approximately 500 mg/L, while the TIR 2 antibody construct gave a titer of approximately 1,050 mg/L. These results suggest that both the disulfide oxidase activity of DsbA and the disulfide isomerase activity of DsbC are important for the folding and assembly of full-length antibodies in *E. coli*.

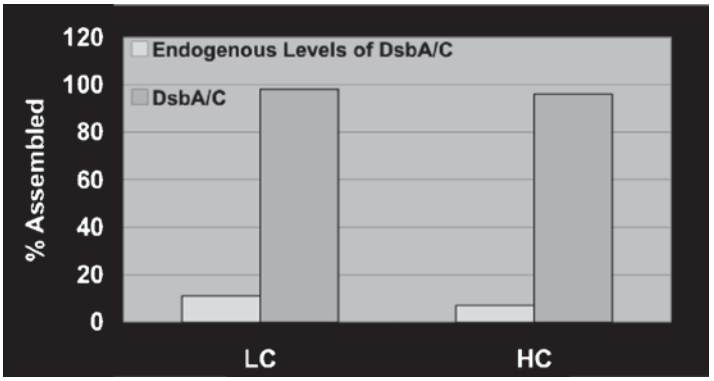

Fig. 17-5. Increasing the expression of DsbA and DsbC over endogenous levels in the periplasm dramatically improves the folding and assembly efficiency of both antibody chains

Fig. 17-5 also shows that light and heavy chain folding and assembly efficiencies are increased from less than 15% to approximately 95% in the example when both DsbA and DsbC are co-expressed.

11. Antibody Characterization

Antibody was purified from *E. coli* fermentation cell paste as previously described (Simmons et al. 2002). Frozen paste was resuspended in buffer, cells mechanically lysed, and the suspension centrifuged to remove debris. Protein A was used as the capture step, and antibody eluted from the column was further purified using ion exchange chromatography. Extensive biochemical characterization was done on antibody preparations that were derived from *E. coli* in order to demonstrate that they had the properties expected of a full-length aglycosylated antibody.

As previously shown (Simmons et al. 2002), an *E. coli*-derived antibody co-migrated with a CHO-derived antibody on SDS-PAGE. In addition, mass spectrometry, cation exchange chromatography, and amino acid analysis also gave results consistent with a fully assembled full-length antibody. In addition, an ELISA assay comparing binding of a CHO-derived antibody with an *E. coli*-derived antibody demonstrated no difference in antigen binding. Fig. 17-6 shows that an *E. coli*-derived antibody co-migrates with the same antibody produced in CHO cells on size exclusion chromatography (SEC) when run under native conditions. SEC was performed using PBS as the running buffer.

Extensive functional and biological characterization was also done on several *E. coli* derived antibodies. Pharmacokinetic studies were done in Sprague Dawley rats to determine the in vivo clearance characteristics. Animals were given a single IV bolus of antibody and serum samples were taken out to 42 days for analysis by an ELISA assay. The data from this study is shown in Fig. 17-7. The initial or alpha clearance appears to be identical to that seen with the CHO-derived version of the antibody, while the terminal or beta clearance appears to be somewhat faster for the *E. coli*-derived version of the antibody. The overall clearance of the CHO-derived antibody was approximately 8.3 ± 0.6 mL/kg/day versus 12.5 ± 3.1 mL/kg/day for the *E. coli*-derived antibody.

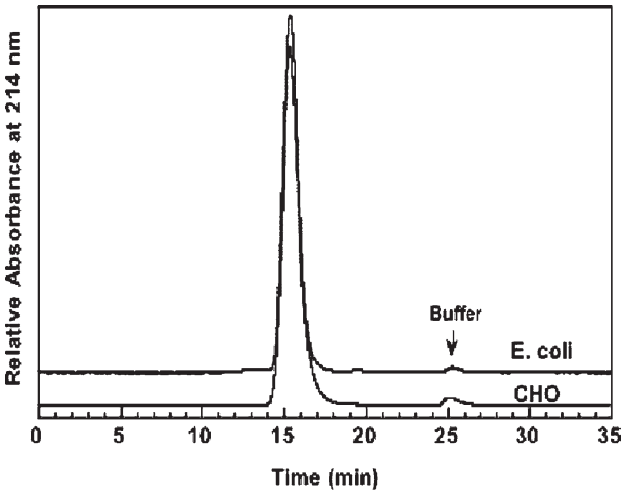

Fig. 17-6. *E. coli* produced antibodies have the same size as mammalian produced proteins as judged by native size exclusion chromatography

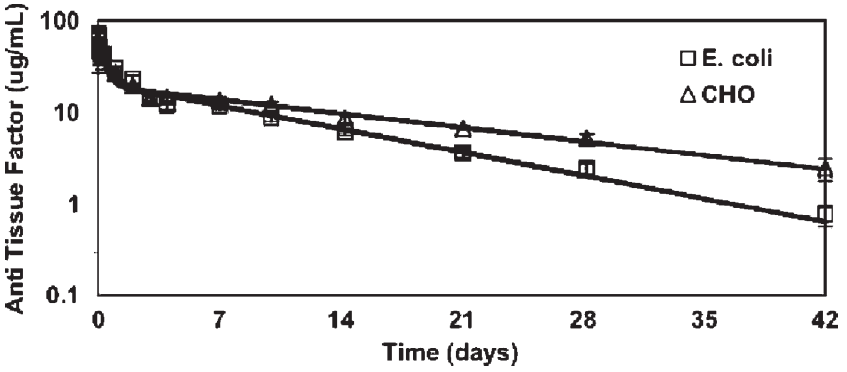

Fig. 17-7. A comparison of the clearance rates in Sprague Dawley rats of mammalian and *E. coli* produced antibodies. While the alpha phases appear to be identical, the beta clearance for the aglycosylated *E. coli* produced antibody is slightly faster

The *E. coli*-derived antibodies were also compared to CHO-derived antibodies for in vitro binding to a series of Fc Gamma receptors as well as to C1q using standard protocols (Simmons et al. 2002). The binding of the full-length aglycosylated antibody to Fc Gamma R1 is shown in Fig. 17-8 and the binding to Fc Gamma RIIIa (F158) is shown in Fig. 17-9. Although there is detectable binding to Fc Gamma RI, the IC_{50} is down multiple orders of magnitude compared to the CHO-derived antibody. In the case of binding to Fc Gamma Receptor IIIa, binding is negligible for the *E. coli*-derived antibody. A similar result was obtained showing negligible binding of the *E. coli*-derived antibody to C1q. All of this data strongly suggests that both ADCC and CDC would be minimal with the aglycosylated antibodies produced by *E. coli*.

An in vivo study was also done to demonstrate that an *E. coli*-derived anti-ligand antibody is efficacious in animal models, where neither ADCC nor CDC is required for biological activity. For this study, nude mice were

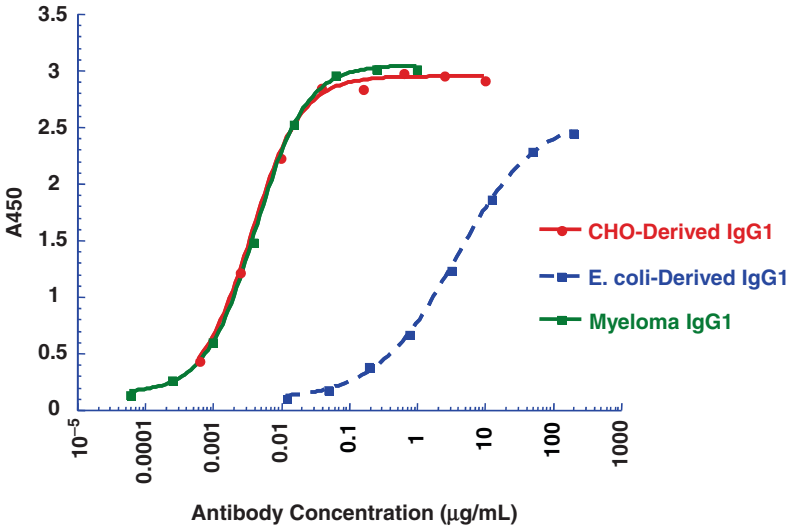

Fig. 17-8. The mammalian produced antibodies show strong binding to the FcγR1a receptor, while the *E. coli* derived antibodies show at least two logs weaker binding. The loss of binding with the aglycosylated *E. coli* antibodies results in the lack of any significant ADCC response. Such effector responses are often not needed for therapeutic uses and can lead to undesirable side effects in a clinical situation

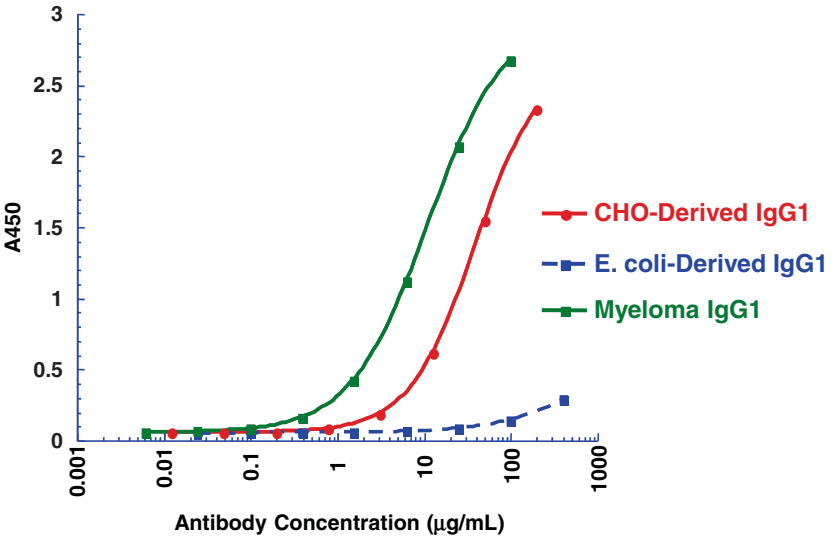

Fig. 17-9. A comparison of mammalian and *E. coli* derived antibodies in terms of their binding to the high affinity FcγRIIIa (F158) receptor. The reduced binding of the *E. coli* antibodies results in a significant loss of any ADCC response

subcutaneously inoculated with a tumor cell line 3 days prior to receiving an IV infusion of either the *E. coli*-derived antibody or the CHO-derived version of the antibody. IV dosing was repeated every 7 days. The time for each tumor to grow to 200 mm^3 was extrapolated from tumor growth curves and the results

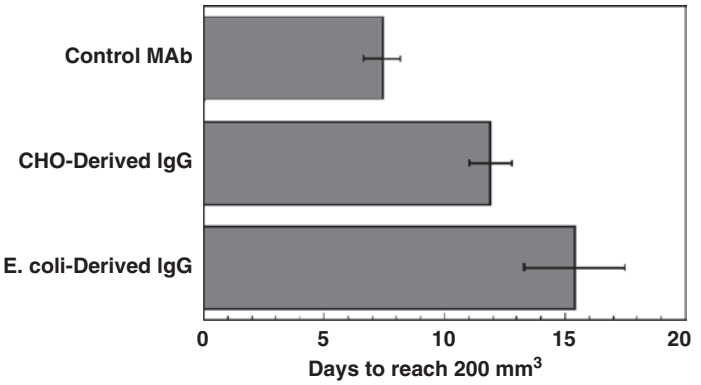

Fig. 17-10. A mouse xenograft efficacy model for tumor growth inhibition comparing the mammalian and *E. coli* produced antibodies. The blocking of a protein-protein interaction rather than an effector function activity such as ADCC is responsible for tumor growth inhibition

are shown in Fig. 17-10. From this data it is apparent that the time for tumors to reach the target volume is roughly equal for both the CHO-derived and the *E. coli*-derived antibodies, demonstrating that the aglycosylated antibody is just as efficacious as the glycosylated antibody in this animal model.

12. Conclusion

Full-length monoclonal antibodies can readily be produced in *E. coli* with some attention to the design of the plasmid, choice of host strain and fermentation conditions. These proteins have the expected properties of aglycosylated antibodies with normal bivalent antigen binding, lack of effector functions (ADCC and CDC) and a long circulating serum half-life (Tao and Morrison 1989). The lack of effector functions is not detrimental for most therapeutic applications where the blocking of receptor-ligand interactions is the primary mechanism of action.

There are situations where *E. coli* may become the preferred production host over the presently used mammalian cells. The current production yields for most mammalian produced monoclonal antibodies is in the 1–2 g/L range with the suggestion that future increases are possible. Some of the better behaving *E. coli* produced monoclonal antibodies now have titers in the same 1–2 g/L range which makes them competitive to mammalian produced antibodies. Since the *E. coli* genetics and biochemistry are better understood and it is easier and faster to engineer *E. coli* cells than mammalian cells, it is reasonable to assume that technology and yields will certainly improve over time. Some of the reported expression levels of 8.5 g/L for IGF-1 (Joly et al. 1998) and 4.5 g/L for an anti-CD18 $F(ab')_2$ antibody fragment (Andersen and Simmons 2004) provide support for such optimism.

The first inroads for *E. coli* produced monoclonal antibodies, however, may actually be the introduction of novel therapeutic forms that are difficult to produce in mammalian cells. The recently reported One-Armed anti-c-Met antibody (Martens et al. 2006) is an example of such a molecule with specific properties. It is a monovalent monoclonal antibody with a long serum half-life,

which can be readily made in *E. coli* at high levels. The successful use of the knobs into holes technology for hetero-dimerization of heavy chain (Merchant et al. 1998) in this molecule has since provided an opening for the production of novel bispecific antibodies (in preparation). The addition of *E. coli* as an alternative host for the production of monoclonal antibodies is now providing a broadened base for new and interesting therapeutic proteins.

Acknowledgments: The authors would like to thank Lisa A. Damico, Sean Kelley, and David Xie for the use of unpublished data on the pharmacokinetic analyses of the antibodies, Ralph Schwall for efficacy studies, Gloria Meng and An Song for binding studies, Amy Lim for SEC data, and Michael W. Laird for help with the manuscript preparation.

References

Andersen D, Reilly DE (2004) Production technologies for monoclonal antibodies and their fragments. Curr Opin Biotechnol 15:456–462

Andersen DC, and Simmons LC (2004) A system for antibody expression and assembly. European Patent: EP1427744

Baneyx F, Palumbo JL (2003) Improving heterologous protein folding via molecular chaperone and foldase co-expression. In: Vaillancourt PE (ed) Methods in molecular biology, vol 205, *E. coli* gene expression protocols. Humana press, Totawa, N J, pp 171–197

Battersby JE, Snedecor B, Chen C, Champion KM, Riddle L, Vanderlaan M (2001) Affinity-reversed-phase liquid chromatography assay to quantitate recombinant antibodies and antibody fragments in fermentation broth. J Chromatogr A 927:61–76

Bessette PH, Aslund F, Beckwith J, Georgiou G (1999) Efficient folding of proteins with multiple disulfide bonds in the *Escherichia coli* cytoplasm. Proc Natl Acad Sci USA 96:13703–13708

Bessette PH, Qiu JI, Bardwell JCA, Swartz JR, Georgiou G (2001) Effect of sequences of the active-site dipeptides of DsbA and DsbC on *in vivo* folding of multidisulfide proteins in *Escherichia coli*. J Bacteriol 183(3):980–988

Bolivar F, Rodriguez RL, Greene PJ, Betlach MC, Heyneker HL, Boyer HW, Crosa JH, Falkow S (1977) Construction and characterization of new cloning vehicles. Gene 2:95–113

Bothmann H, Pluckthun A (1998) Selection for a periplasmic factor improving phage display and functional periplasmic expression. Nat Biotechnol 16:376–380

Bothmann H, Pluckthun A (2000) The periplasmic *Escherichia coli* peptidylprolyl cis, trans-isomerase FkpA. J Biol Chem 275(22):17100–17105

Chen C, Snedecor B, Nishihara JC, Joly JC, McFarland N, Andersen DC, Battersby JE, Champion KM (2004) High-level accumulation of a recombinant antibody fragment in the periplasm of *Escherichia coli* requires a triple-mutant (*degP prc spr*) host strain. Biotechnol Bioeng 85(5):463–474

De Boer HA, Comstock LJ, Vasser M (1983) The *tac* promoter: a functional hybrid derived from the *trp* and *lac* promoters. Proc Natl Acad Sci USA 80:21–25

De Smit MH, van Duin J (1990) Secondary structure of the ribosome binding site determines translational efficiency: a quantitative analysis. Proc Natl Acad Sci USA 87:7668–7672

Derman AI, Prinz WA, Belin D, Beckwith J (1993) Mutations that allow disulfide bond formation in the cytoplasm of *Escherichia coli*. Science 262:1744–1747

Friend PJ, Hale G, Chatenoud L, Rebello P, Bradley J, Thiru S, Phillips JM, Waldmann H (1999) Phase I study of an engineered aglycosylated humanized CD3 antibody in renal transplant rejection. Transplantation 68(11):1632–1637

Hamilton SR, Bobrowicz P, Bobrowicz B, Davidson RC, Li H, Mitchell T, Nett JH, Rausch S, Stadheim TA, Wischnewski H, Wildt S, Gerngross TU (2003) Production of complex human glycoproteins in yeast. Science 301:1244–1246

Hayhurst A, Harris WJ (1999) *Escherichia coli* skp chaperone coexpression improves solubility and phage display of single-chain antibody fragments. Protein Expr and Purif 15:336–343

Humphreys DP (2007) Periplasmic Expression of Antibody Fragments. In: Ehrmann M (ed) The periplasm. ASM press, Washington DC, pp 361–388

Jeong KJ, Lee SY (2000) Secretory production of human leptin in *Escherichia coli*. Biotechnol Bioeng 67(4):398–407

Joly JC, Laird MW (2007) Practical applications for periplasmic protein accumulation. In: Ehrmann M (ed) The periplasm. ASM Press, Washington DC, pp 345–360

Joly JC, Leung WS, Schwartz JR (1998) Overexpression of *Escherichia coli* oxidoreductases increases recombinant insulin-like growth factor-I accumulation. Proc Natl Acad Sci USA 95:2773–2777

Makrides SC (1996) Strategies for Achieving High-Level Expression of Genes in *Escherichia coli*. Microbiol. Rev. 60 (3):512–538

Martens T, Schmidt NO, Eckerich C, Fillbrandt R, Merchant M, Schwall R, Westphal M, Lamszus K (2006) A novel one-armed anti-c-Met antibody inhibits glioblastoma growth *in vivo*. Clin Cancer Res 12:6144–6152

Mazor Y, Blarcom TV, Mabry R, Iverson BL, Georgiou G (2007) Isolation of engineered, full-length antibodies from libraries expressed in *Escherichia coli*. Nat Biotechnol 25:563–565

McCarthy JEG, Gualerzi C (1990) Translational control of prokaryotic gene expression. Trends Genet 6(3):78–85

Merchant AM, Zhu Z, Yuan JQ, Goddard A, Adams CW, Presta LG, Carter P (1998) An efficient route to human bispecific IgG. Nat Biotechnol 16:677–681

Pluckthun A, Krebber A, Krebber C, Horn U, Knupfer U, Wenderoth R, Nieba L, Proba K, Riesenberg D (1996) Producing antibodies in *Escherichia coli*: from PCR to fermentation. In: McCafferty J, Hoogenboom HR, Chiswell DJ (eds) Antibody engineering: a practical approach. Oxford university press, New York, N Y, pp 203–251

Prinz WA, Aslund F, Holmgren A, Beckwith J (1997) The role of the thioredoxin and glutaredoxin pathway in reducing protein disulfide bonds in the *Escherichia coli* cytoplasm. J Biol Chem 272(25):15661–15667

Qiu JI, Schwartz JR, Georgiou G (1998) Expression of active human tissue-type plasminogen activator in *Escherichia coli*. Appl Environ Microbiol 64(12):4891–4896

Routledge EG, Falconer ME, Pope H, Lloyd IS, Waldmann H (1995) The effect of aglycosylation on the immunogenicity of a humanized therapeutic CD3 monoclonal antibody. Transplantation 60:847–853

Simmons LC, Yansura DG (1996) Translational level is a critical factor for the secretion of heterologous proteins in *Escherichia coli*. Nat Biotechnol 14:629–634

Simmons LC, Reilly D, Klimowski L, Raju TS, Meng G, Sims P, Hong K, Shields RL, Damico LA, Rancatore P, Yansura DG (2002) Expression of full-length immunoglobulins in *Escherichia coli*: rapid and efficient production of aglycosylated antibodies. J Immunol Methods 263:133–147

Tao MH, Morrison SL (1989) Studies of aglycosylated chimeric mouse-human IgG. J Immunol 143:2595–2601

Thome BM, Muller M (1991) Skp is a periplasmic *Escherichia coli* protein requiring SecA and SecY for export. Mol Microbiol 5(11):2815–2821

Walsh G (2006) Biopharmaceutical Benchmarks 2006. Nat Biotechnol 24:769–776

Chapter 18

Recent Advancements in the Use of Antibody Drug Conjugates for Cancer Therapy

Peter D. Senter

1. Introduction

Monoclonal antibodies (mAbs) have demonstrated considerable utility in the clinical treatment of cancer (Reichert et al. 2005; Reichert and Valge-Archer 2007). While the activities of unmodified mAbs such as Rituxan® (rituximab) in non-Hodgkin's lymphoma, Panorex® (edrecolomab) in colorectal carcinoma, Herceptin® (trastuzamab) for metastatic breast cancer and Avastin® (bevacizumab) for colorectal and lung cancer are substantial, these agents are rarely curative. As a result, considerable attention has turned to enhancing antibody activity by appending cytotoxic drugs to them, thereby generating antibody drug conjugates (ADCs) capable of site-selective drug delivery. The rationale for this approach is that by delivering cancer drugs to tumor cells, it may be possible to both enhance therapeutic efficacy and spare normal tissues from chemotherapeutic damage. In the past few years, significant progress has been made in this field of research (Damle 2004; Wu and Senter 2005; Kovtun and Goldmacher 2007; Carter and Senter 2008; Chari 2008). Critical parameters for ADC development have been identified which include the choice of target antigen, the ability of the ADC to get localized to target tissues, the fate of the antibody once bound to its cognate antigen, the stability of the linker used to attach the drug to the antibody both in the systemic circulation and inside the target cell, and the potency and mechanism of action of the released drug. Other important considerations include the methods used to generate ADCs, the composition and heterogeneity of the resulting product, and the effects that chemical modification have on such antibody properties as pharmacokinetics, biodistribution, antigen binding and effector functions. This review will describe several aspects of ADC development, with an emphasis on how addressing key parameters have led to promising agents that have advanced into clinical trials.

2. Optimization of ADC Drug and Linker Components

Early work in antibody-mediated drug targeting surrounded the use of clinically approved drugs, since much was known about how they could be chemically manipulated and the agents were readily available. Drugs such as doxorubicin,

From: *Current Trends in Monoclonal Antibody Development and Manufacturing,*
Biotechnology: Pharmaceutical Aspects, DOI 10.1007/978-0-387-76643-0_18,
Edited by: S.J. Shire et al.

methotrexate, mitomycin, 5-fluorouracil, and vinca alkaloids were typically used (Pietersz et al. 1994), and little attention was paid to particular aspects of the mAb carrier, the mode and stoichiometry of drug attachment and the mechanism of drug release. As a result, the activities of these agents were marginal, and few of them were extensively investigated.

An example of an earlier generation ADC is BR96-doxorubicin (Fig. 18-1). This conjugate is directed against the Le^Y tetrasaccharide antigen on human carcinomas, and is comprised of the clinically approved drug doxorubicin, which was known to be active in a broad array of tumors. The appeal of using such a drug was that although it lacked high potency, it was active in breast

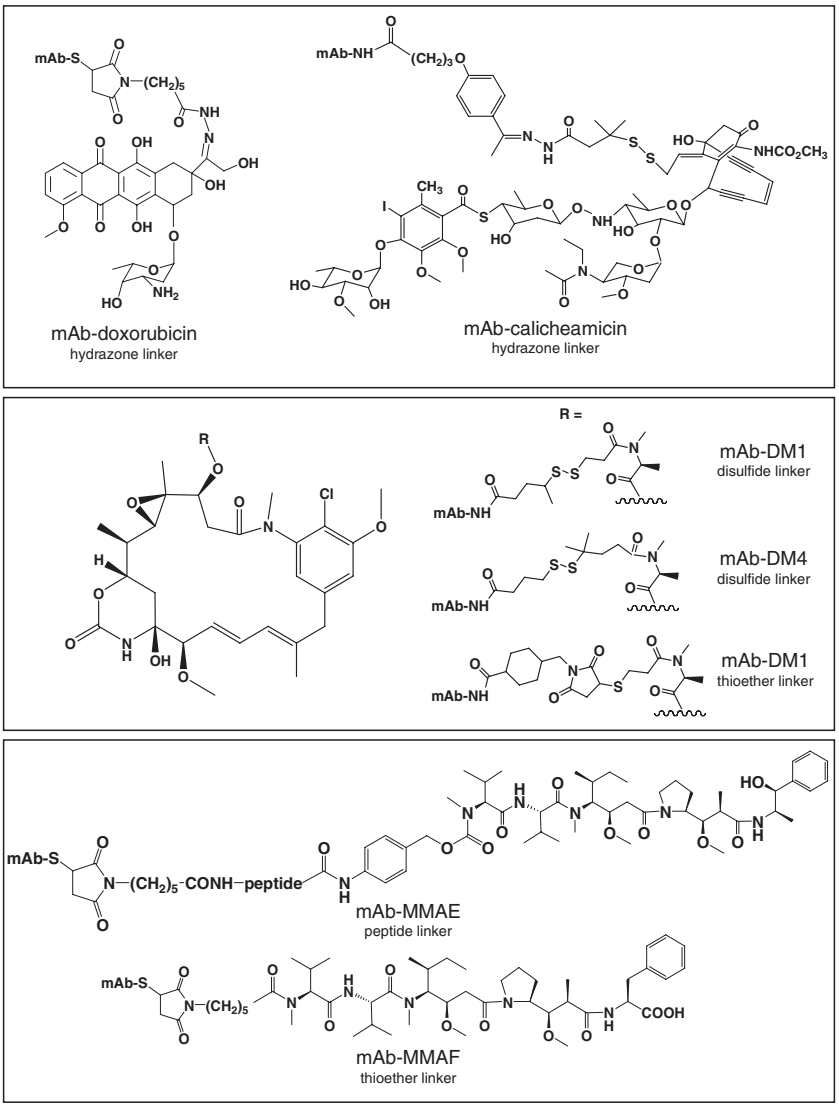

Fig. 18-1. Structures of antibody drug conjugates for cancer therapy. The drugs used to prepare the conjugates range from doxorubicin to highly potent agents like the auristatin analogues MMAE and MMAF

cancer, which was known to be LeY positive (Trail et al. 1993, 2003). Once the ADC binds to cell surface antigens, it internalizes within acidic endosomal and lysosomal vesicles. As a result, an acid-labile hydrazone linker was developed for this ADC which was relatively stable at neutral pH, but unstable at pH 5, allowing for intracellular release of the active drug. BR96-doxorubicin contained 8 drugs/mAb, which were attached to mAb thiol groups generated through intrachain disulfide bond reduction (Table 18-1).

Treatment of tumor bearing mice and rats with BR96-doxorubicin led to immunologically specific tumor cures, albeit at doses in excess of 100 mg/kg. The drug component of BR96-doxorubicin has low potency, and it is therefore not surprising that the ADC doses required for activity were very high. In a Phase I clinical trial, the MTD of BR96-doxorubicin was approximately 700 mg/m^2, with dose limiting toxicities of gastrointestinal origin (Saleh et al. 2000).In a subsequent Phase II trial, the toxicities were attributed to normal gut expression of LeY (Tolcher et al. 1999). In both the trials, little antitumor activity was obtained, and the measured half-life of systemic drug release was only 43 h. It became apparent that BR96-doxorubicin was significantly hampered due to the low drug potency component, the unstable linker used, and the presence of target antigen on highly sensitive non-tumor cells.

The results with low potency ADCs such as BR96-doxorubicin prompted significant efforts towards utilizing drugs with much higher potencies than doxorubicin for targeted delivery. The natural product calicheamicin has been the subject of extensive investigation for drug delivery, due to its ability to bind to the minor groove and effect cell kill at concentrations well below that of standard chemotherapeutic agents (Damle and Frost 2003; Damle 2004). As with BR96-doxorubicin, an acid labile hydrazone linker was used to link the drug to mAb carriers (Fig. 18-1), with a similar half-life for drug release from the ADC in the range of 48–72 h (Boghaert et al. 2007). Pronounced antitumor activities have been obtained with mAb-calicheamicin ADCs on epithelial cancers at doses as low as approximately 2 mg (mAb component)/kg (Boghaert et al. 2004, 2008; Hamann et al. 2005). The enhanced potency of this ADC compared to the corresponding doxorubicin conjugate reflects the relative activities of the drug components. This is apparent from in vitro assays, in which the ADCs differ in potency by as much as 1,000-fold (Trail et al. 1997; Boghaert et al. 2004). Other promising ADCs using calicheamicin are directed against the CD22 (DiJoseph et al. 2004a, b, 2005) and 5T4 (Boghaert et al. 2008) antigens, recognizing B-cell lymphomas and epithelial tumors, respectively.

The sole clinically approved ADC to date, gemtuzumab ozogamicin (Mylotarg®), consists of an anti-CD33 mAb linked to calicheamicin through an acid-labile hydrazone linker (Bross et al. 2001; Hamann et al. 2002). This ADC is clinically used for the treatment of acute myeloid leukemia at doses of 9 mg/m^2 given twice at 2 week intervals (Bross et al. 2001; Larson et al. 2005). Complete remissions were obtained in approximately 30% of the patients treated with gemtuzumab ozogamicin, with side effects including myelosuppression and hepatic veno-occlusive disease. Although the effects of calicheamicin ADCs are in many cases antigen-specific, it has been reported that gemtuzumab ozogamicin elicits potent antitumor activity in an antigen-independent manner on solid tumor in vivo (Boghaert et al. 2006). The effects were attributed to passive targeting, and required the use of an

Table 18-1. ADCs for cancer therapy. The examples included have demonstrated significant levels of activity in several preclinical models, and in some cases, clinical trials.

ADC		**Drug component**			**Linker component**	
mAb-drug	Antigen/tumor	Drug component	Mechanism of activity	Free drug potency (M)	Cleavable unit/mechanism for drug release	Leading reference
BR96-doxorubicin	LeY/carcinomas	Doxorubicin	Topoisomerase II	10^{-7}	Hydrazone/low pH	Trail et al. (1993)
mAb-calicheamicin	CD33/leukemiaCD22/ lymphomas	Calicheamicin	DNA minor groove binder	10^{-10}–10^{-9}	Hydrazone/low pH	Damle (2004)
	LeY/carcinomas					
	5T4/carcinomas					
mAb-DM1	CD56/lungCanAg/ colorectal	Maytansine	Tubulin depolymerization	10^{-11}–10^{-9}	Disulfide/reduction	Chari (2008)
	CD33/leukemia					
	PSMA/prostate					
	CD79/lymphoma					
mAb-DM4	CanAg/colorectal	Maytansine	Tubulin depolymerization	10^{-12}–10^{-11}	Disulfide/reduction	Chari (2008)
	Her2/neu					
	α_v Integrin/carcinomas					
mAb-MMAE	CD30/Hodgkin's disease	Auristatin	Tubulin depolymerization	10^{-11}–10^{-9}	Peptide/enzymatic hydrolysis	Doronina et al. (2003), Carter and Senter (2008)
	PSMA/prostate					
	GPNMB/melanoma					
mAb-MMAF	CD70/renal cellCD22/ lymphoma	Auristatin	Tubulin depolymerization	10^{-8}–10^{-7}	Peptide/enzymatic hydrolysis Thioether/ mAb degradation	Doronina et al. (2006), Carter and Senter (2008)
	CD79/lymphoma					

acid-labile hydrazone linker. Therefore, it is possible that non-specific drug release through linker instability contributes to the activities of gemtuzumab ozogamicin in these models. It is not clear that these effects would extend to AML, although gemtuzumab ozogamicin has been shown to exhibit activity in AML patients whose cancer cells do not apparently display the CD33 antigen (Jedema et al. 2004; Boghaert et al. 2006). To summarize, the results with mAb-calicheamicin conjugates demonstrate the importance of drug potency in developing ADCs with broad spectrum activity. In addition, the approval of gemtuzumab ozogamicin represents a breakthrough in the field.

Maytansinoids (Chari 2008) and auristatins (Doronina et al. 2003, 2006) are other classes of highly potent drugs that have been widely utilized for ADC development. These drugs are significantly more potent than most drugs used in cancer chemotherapy, and act by binding to tubulin at the same site as the vinca alkaloids and inhibiting tubulin polymerization. Maytansinoids are derived from a natural product, while the auristatins are totally synthetic.

The methodology used for linking maytansinoids to antibody carriers involved the use of a disulfide bond in the linker (Fig. 18-1). In vivo stability of disulfide bonds can be greatly enhanced though steric hindrance, as shown with immunotoxins (Thorpe et al. 1987, 1988). The use of disulfide linkers exploits the observation that the intracellular concentration of thiols, such as glutathione and cysteine, are much higher than those in plasma. A series of maytansinoid-disulfide linker derivatives with varying degrees of steric hindrance were developed, from which DM1 and DM4 were selected as lead agents for antibody attachment (Widdison et al. 2006). ADCs were made by modifying antibody lysines with a bifunctional crosslinking reagent, and then adding thiol-containing DM1 or DM4. The resulting ADCs contained a mean of 3–4 drugs/antibody, and displayed high in vitro potency in an immunologically specific manner, as demonstrated with the humanized antibody, huC242 against CanAg, a tumor-selective carbohydrate epitope on MUC-1, a membrane-associated mucin (Liu et al. 1996; Kovtun et al. 2006; Kovtun and Goldmacher 2007). As with the hydrazone-linked ADCs described earlier, the disulfide bond in huC242-DM1 is unstable, with a half life of approximately 24 h. HuC242-DM4, having a more hindered disulfide, is more stable with a reported half life of approximately 102 h (Chari 2008). The more hindered disulfide ADCs have been shown to have superior antitumor activity in preclinical models (Widdison et al. 2006; Chen et al. 2007a; Chari 2008). There are several other examples of maytansinoid ADCs that have promising preclinical activities (Henry et al. 2004; Tassone et al. 2004a, b; Aboukameel et al. 2007; Legrand et al. 2007; Polson et al. 2007).

Use of peptide-based linker technologies may present significant advantages over those that are hydrolytically or reductively labile, since hydrolysis is enzymatic, and enzymes can be selected for preferential expression within tumor cells or solid tumor masses. ADCs comprised of drugs such as doxorubicin (Dubowchik and Firestone 1998), mitomycin C (Dubowchik et al. 1998), camptothecin (Walker et al. 2002), tallisomycin (Walker et al. 2004) , and auristatin family members (Walker et al. 2002; Doronina et al. 2003, 2006; Francisco et al. 2003) have been prepared using peptide sequences for intracellular drug release. Of these, the auristatins are of particular interest, because they are highly potent, totally synthetic, stable, and are amenable to chemical modification strategies to allow for linker attachment.

An auristatin derivative, monomethyl auristatin E (MMAE), was modified with dipeptide linkers, and the resulting drug derivatives were linked to antibody thiol groups (Doronina et al. 2006), generating conjugates of uniform composition (Fig. 18-1). The antibodies used were directed against the CD30 antigen on Hodgkin's disease and the Le^Y antigen on carcinomas. In vitro studies demonstrated that peptide-linked ADC were highly potent with 10–100-fold greater immunologically dependent cell kill compared to corresponding hydrazone based ADCs. The half-lives of drug release in vivo were 6 and 10 days in mice and cynomolgus macaques, respectively (Sanderson et al. 2005), longer than previously described linkers. Furthermore, the more stable peptide-linked MMAE ADCs were less toxic than corresponding hydrazone-linked ADCs (Doronina et al. 2003). The peptide that was selected for further studies was comprised of valine-citrulline (Val-Cit), since it was shown to be stable in plasma, but labile towards enzymes such as cathepsin B, which is highly expressed lysosomal enzyme (Doronina et al. 2003).

mAb-Val-Cit-MMAE ADCs had pronounced antitumor activities in xenografts models, leading to cures of established tumors at very small fractions of the maximum tolerated doses (Doronina et al. 2003) (Fig. 18-2). Subsequently, auristatin ADC technology has been successfully applied to antibodies recognizing a wide range of tumor antigens, including BCMA (Ryan et al. 2007), CD19 (Benjamin et al. 2007), CD20 (Law et al. 2004), CD70 (Law et al. 2006), CD79 (Polson et al. 2007), E selectin (Bhaskar et al. 2003), EphB2 (Mao et al. 2004), glycoprotein NMB (Tse et al. 2006), melanotransferrin/p97 (Chen et al. 2007b), MUC16 (Chen et al. 2007b), PSMA (Ma et al. 2006), and TMEFF2 (Afar et al. 2004).

Since auristatins are totally synthetic, integral structural modifications can be made that significantly alter the properties of the drug. One such auristatin, MMAF, terminates with a negatively charged phenylalanine residue that impairs cell membrane permeability (Doronina et al. 2006). Consequently, ADCs containing MMAF that facilitate drug uptake by antigen-positive cells are >2,000-fold more potent than the free drug itself. MMAF linked to an anti-CD70 antibody through a peptide linker was active against renal cell carcinoma xenografts and also circumvented multidrug resistance mechanisms (Law et al. 2006).

A finding that ran counter to expectations was that the cleavable peptide (Val-Cit) in MMAF ADCs could be entirely eliminated (Fig. 18-1), without diminishing activity. ADCs in which the drug was directly attached to anti-CD30 and anti-Le^Y antibodies through thioether adducts retained activity (Doronina et al. 2006). Mass spectrometry showed that the released drug was a cysteine-adduct of the linker-MMAF derivative, presumably resulting from antibody degradation within lysosomes. A closely related drug, MMAE was not active when attached in this manner, indicating that ADCs requiring antibody degradation for drug release are highly dependent on the nature of the drug for activity. Similar results were obtained with a thioether adduct of DM4 which was appended to lysine residues on the humanized antibody, huC242 (Erickson et al. 2006) (Fig. 18-1). In this case, the released drug upon cell incubation was a lysine-DM1 derivative in which the lysine residue was the attachment residue on the antibody delivery vehicle. The resulting ADC was active in vitro, but had little in vivo activity compared to the corresponding disulfide. It is not yet clear what the requirements are for effective cell kill

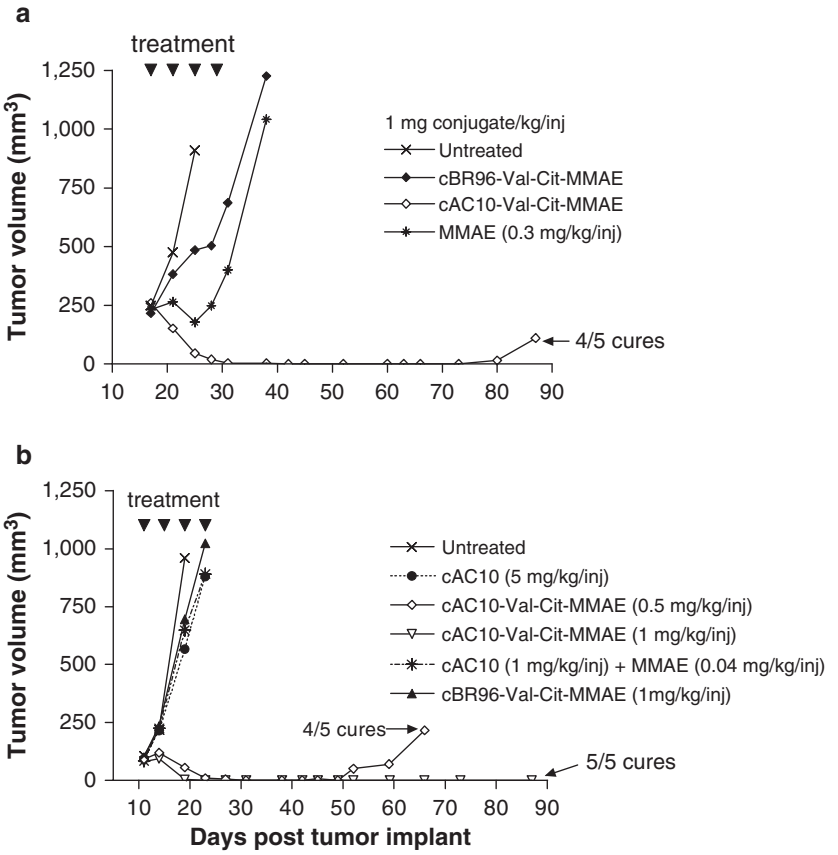

Fig. 18-2. In vivo therapeutic effects of auristatin ADCs in mice with subcutaneous human tumor xenografts. Animals with Karpas 299 anaplastic large cell lymphoma xenografts were treated with cAC10 (anti-CD30 on Karpas 299 tumor cells) or BR96 (anti-LewisY negative control) ADCs according to the schedule shown by the *arrows* and the doses (antibody component) indicated in the legend. The activities are (**a**) immunologically specific and (**b**) more pronounced than mAb+unconjugated drug mixtures. The amount of unconjugated drug in (**b**) is equal to the amount of drug conjugated in the 1 mg/kg ADC group. Adapted from Doronina et al. (2003)

using linker technologies that require antibody degradation for drug release, but it is apparent that activity is less predictable than that is obtained using cleavable linker technologies.

The anti-CD70 ADC with a thioether linkage to MMAF had a similar half-life of 7 days for drug release in vivo (Alley et al. 2008) as the corresponding peptide-linked ADC (Sanderson et al. 2005). Ex vivo plasma stability studies revealed a shared mechanism for drug release from these ADCs involving a fragmentation reaction involving the maleimide linkage to antibody thiols. Thus, the weakest link in the antibody-MMAF thioether adduct is the thioether formed when the maleimido drug derivative is condensed with antibody thiols. A new generation of ADCs was subsequently made that had used an acetamide-thiol adduct in place of the thioether (Fig. 18-1). Circulating ADC did not lose any detectable drug over 2 weeks in vivo. The tolerability, efficacy, and intratumoral drug concentrations resulting from ADCs that

were indefinitely stable in vivo were no different from the corresponding maleimido-thioether adducts. Thus, extending the stability of the ADCs beyond that of the 6–10 day half-life of the previously described peptide-based ADCs does not result in detectable therapeutic improvements. The effects of increasing drug retention half-life in this manner will undoubtedly require clinical testing in order to establish the impact on efficacy and tolerability.

3. Optimization of the Conjugation Technology

The ADCs described thus far have been produced through the reaction of drugs or chemical crosslinking reagents with solvent accessible reactive amino acids such as lysine and cysteine on the antibody. The process used to covalently attach the drug to the antibody delivery vehicle can have a major impact on activity, since antibody modification may compromise binding, aggregation state, pharmacokinetics, and biodistribution. For example, linker technologies have been developed to attach as many as 16 doxorubicin molecules/antibody, but many of the resulting ADCs were largely aggregated and had impaired antigen binding (King et al. 2002). The other extreme involves the attachment of drugs that self-associate such as calicheamicin to antibodies. In order to avoid aggregation, the clinically approved ADC gemtuzumab ozogamicin was prepared with an average of 2–3 drugs/antibody, but half the antibody in the preparation contains no drug at all (Hamann et al. 2002). The heterogeneity of calicheamicin containing ADCs has recently been reduced by additives in the conjugation process (Hollander et al. 2008). Conjugation technology is a critical aspect in generating effective ADCs, and optimization strategies can vary with the drug, linker, and the antibody used.

The first anti-CD30-valine-citrulline-MMAE ADCs were formed by reducing the interchain disulfides on the cAC10 antibody and attaching the drugs to the resulting cysteine residues (Doronina et al. 2003; Francisco et al. 2003). These ADCs contained 8 drugs/antibody, and were highly uniform in composition, since there were only four reducible disulfides in the antibodies used. While the binding properties of the resulting ADC were well preserved, subsequent studies demonstrated that the pharmacokinetic properties of the antibody delivery vehicle were altered in a significant way. The 8-loaded ADC cleared much more rapidly from the circulation than the unmodified antibody (Hamblett et al. 2004). This led to the development of cAC10-Val-Cit-MMAE with 4 drugs/antibody. Although the in vitro potency of the 4-loaded ADC was half that of the 8-loaded version, the in vivo potencies of these agents were the same. To understand the basis for this, pharmacokinetic studies were undertaken, and it was found that the clearance rate of the 8-loaded ADC was approximately twice that of the 4-loaded counterpart, and tumors therefore experienced comparatively longer exposure to ADCs with lower drug loading levels. Importantly, the maximum tolerated doses of the ADCs were dependent on drug loading, such that twice as much 4-loaded ADC could be administered as 8-loaded. The results from this work demonstrated that drug loading was a key parameter for tolerability, and optimal therapeutic windows required careful attention to the amount of drug attached to the mAb. cAC10-Val-Cit-MMAE, with a mean loading of 4 drugs/antibody, now known as SGN-35, is currently in a dose-escalation Phase I clinical trial for the treatment of Hodgkin's disease (Younes et al. 2007). Significant antitumor activities, including partial and complete remissions have been obtained.

Recently, significant attention has been directed towards the use of recombinant strategies for the production of ADCs with predetermined sites for drug attachment. The first example of this approach involved engineered forms of cAC10, in which intrachain cysteines were replaced with serines (McDonagh et al. 2006). The ADCs produced from these antibodies had two or four molecules of MMAE/antibody, and were produced in high yields with unprecedented levels of product uniformity (Sun et al. 2005; McDonagh et al. 2006). The engineered ADCs were compared with those derived from the parent anti-CD30 IgG1 for binding affinity, cytotoxic activity and for in vivo tolerability, pharmacokinetics and efficacy. It was found that all the ADCs with 4 drugs/antibody were equally active and tolerated, independent of the site of drug substitution. These results provided evidence that the number of drugs/antibody influences the therapeutic window to a greater extent than the site to which the drugs are attached. More recently, an approach involving the generation of recombinant antibodies bearing introduced cysteines for drug conjugation has led to well-defined ADCs with pronounced levels of efficacy and tolerability (Junutula et al. 2008a, b). It is apparent that recombinant approaches will play a role for ADCs in clinical development.

4. Conclusion

Significant advancements have been made in ADC technology since the clinical trials with low potency, clinically approved anticancer drugs. Several drug classes have been described that are suitable as use within ADCs, including calicheamicin, maytansinoids, and the auristatins described here. These highly potent drugs help compensating for the low percentage of the injected ADC that actually binds and is retained within tumor cells. New linker technologies have been developed for these agents that allow them to remain associated with the mAb for extended periods of time and to be released under carefully defined conditions. Conjugation technologies have advanced to a point, where both the site and stoichiometry of drug attachment is controlled, and the resulting ADCs are well-defined. ADCs that incorporate these improvements have demonstrated levels of activity and immunological specificity that were previously unattainable. Several such ADCs have advanced into clinical trials and are show promising levels of activity.

There are many unresolved issues surrounding ADC technology. The impact that antibody affinity, internalization rate, antigen recycling, intracellular compartmentalization, antibody isotype, and ADC pharmacokinetics have on efficacy is largely unexplored. Little is known about how various conjugation methodologies affect activity. The use of antigen-binding non-IgG carriers (Binz et al. 2005) for drug delivery has hardly been touched upon. However, in spite of the unknown, it is apparent from the progress in the past few years that ADCs are poised to have an impact on cancer therapy.

References

Aboukameel A, Goustin A-S, Mohammad R, Zuany-Amorim C, Bissery M-C, Al-Katib AM (2007) Superior anti-tumor activity of the CD19-directed immunotoxin, SAR3419 to rituximab in non-Hodgkin's xenograft animal models: preclinical evaluation. Blood 110: Abstract 2339

Afar DE, Bhaskar V, Ibsen E, Breinberg D, Henshall SM, Kench JG, Drobnjak M, Powers R, Wong M, Evangelista F et al (2004) Preclinical validation of

anti-TMEFF2-auristatin E-conjugated antibodies in the treatment of prostate cancer. Mol Cancer Ther 3:921–932

Alley SC, Benjamin DR, Jeffrey SC, Okeley NM, Meyer DL, Sanderson RJ, Senter PD (2008) The contribution of linker stability to the activities of anticancer immunoconjugates. Bioconjug Chem, 19, 759–765

Benjamin D, Morris-Tilden C, Stone I, Jonas M, Sutherland MK, Miyamoto J, Brown L, Westendorf L, Meyer D, Carter P (2007) Humanized anti-CD19 auristatin antibody-drug conjugates display potent antitumor activity in preclinical models of B-cell malignancies. AACR-NCI-EORTC Conference on Molecular Targets and Cancer Therapeutics: Abstract B60

Bhaskar V, Law DA, Ibsen E, Breinberg D, Cass KM, DuBridge RB, Evangelista F, Henshall SM, Hevezi P, Miller JC et al (2003) E-Selectin up-regulation allows for targeted drug delivery in prostate cancer. Cancer Res 63:6387–6394

Binz HK, Amstutz P, Pluckthun A (2005) Engineering novel binding proteins from nonimmunoglobulin domains. Nat Biotechnol 23:1257–1268

Boghaert ER, Sridharan L, Armellino DC, Khandke KM, DiJoseph JF, Kunz A, Dougher MM, Jiang F, Kalyandrug LB, Hamann PR et al (2004) Antibody-targeted chemotherapy with the calicheamicin conjugate hu3S193-*N*-acetyl γ calicheamicin dimethyl hydrazide targets Lewis^{Y} and eliminates Lewis^{Y}-positive human carcinoma cells and xenografts. Clin Cancer Res 10:4538–4549

Boghaert ER, Khandke K, Sridharan L, Armellino D, Dougher M, Dijoseph JF, Kunz A, Hamann PR, Sridharan A, Jones S et al (2006) Tumoricidal effect of calicheamicin immuno-conjugates using a passive targeting strategy. Int J Oncol 28:675–684

Boghaert ER, Khandke KM, Sridharan L, Dougher M, Dijoseph JF, Kunz A, Hamann PR, Moran J, Chaudhary I, Damle NK (2007) Determination of pharmacokinetic values of calicheamicin-antibody conjugates in mice by plasmon resonance analysis of small (5 mul) blood samples. Cancer Chemother Pharmacol, 61, 1027–1035

Boghaert ER, Sridharan L, Khandke KM, Armellino D, Ryan MG, Myers K, Harrop R, Kunz A, Hamann PR, Marquette K et al (2008) The oncofetal protein, 5 T4, is a suitable target for antibody-guided anti-cancer chemotherapy with calicheamicin. Int J Oncol 32:221–234

Bross PF, Beitz J, Chen G, Chen XH, Duffy E, Kieffer L, Roy S, Sridhara R, Rahman A, Williams G et al (2001) Approval summary: gemtuzumab ozogamicin in relapsed acute myeloid leukemia. Clin Cancer Res 7:1490–1496

Carter PJ, Senter PD (2008) Antibody–drug conjugates for cancer therapy. Cancer J 14: 154–169

Chari RV (2008) Targeted cancer therapy: conferring specificity to cytotoxic drugs. Acc Chem Res 41:98–107

Chen Q, Millar HJ, McCabe FL, Manning CD, Steeves R, Lai K, Kellogg B, Lutz RJ, Trikha M, Nakada MT et al (2007a) α_v Integrin-targeted immunoconjugates regress established human tumors in xenograft models. Clin Cancer Res 13:3689–3695

Chen Y, Clark S, Wong T, Dennis MS, Luis E, Zhong F, Bheddah S, Koeppen H, Gogineni A, Ross S et al (2007b) Armed antibodies targeting the mucin repeats of the ovarian cancer antigen, MUC16, are highly efficacious in animal tumor models. Cancer Res 67:4924–4932

Damle NK (2004) Tumour-targeted chemotherapy with immunoconjugates of calicheamicin. Expert Opin Biol Ther 4:1445–1452

Damle NK, Frost P (2003) Antibody-targeted chemotherapy with immunoconjugates of calicheamicin. Curr Opin Pharmacol 3:386–390

DiJoseph JF, Armellino DC, Boghaert ER, Khandke K, Dougher MM, Sridharan L, Kunz A, Hamann PR, Gorovits B, Udata C et al (2004a) Antibody-targeted chemotherapy with CMC-544: a CD22-targeted immunoconjugate of calicheamicin for the treatment of B-lymphoid malignancies. Blood 103:1807–1814

DiJoseph JF, Goad ME, Dougher MM, Boghaert ER, Kunz A, Hamann PR, Damle NK (2004b) Potent and specific antitumor efficacy of CMC-544, a CD22-targeted immunoconjugate of calicheamicin, against systemically disseminated B-cell lymphoma. Clin Cancer Res 10:8620–8629

DiJoseph JF, Popplewell A, Tickle S, Ladyman H, Lawson A, Kunz A, Khandke K, Armellino DC, Boghaert ER, Hamann P et al (2005) Antibody-targeted chemotherapy of B-cell lymphoma using calicheamicin conjugated to murine or humanized antibody against CD22. Cancer Immunol Immunother 54:11–24

Doronina SO, Toki BE, Torgov MY, Mendelsohn BA, Cerveny CG, Chace DF, DeBlanc RL, Gearing RP, Bovee TD, Siegall CB et al (2003) Development of potent monoclonal antibody auristatin conjugates for cancer therapy. Nat Biotechnol 21:778–784

Doronina SO, Mendelsohn BA, Bovee TD, Cerveny CG, Alley SC, Meyer DL, Oflazoglu E, Toki BE, Sanderson RJ, Zabinski RF et al (2006) Enhanced activity of monomethylauristatin F through monoclonal antibody delivery: effects of linker technology on efficacy and toxicity. Bioconjug Chem 17:114–124

Dubowchik GM, Firestone RA (1998) Cathepsin B-sensitive dipeptide prodrugs. 1. A model study of structural requirements for efficient release of doxorubicin. Bioorg Med Chem Lett 8:3341–3346

Dubowchik GM, Mosure K, Knipe JO, Firestone RA (1998) Cathepsin B-sensitive dipeptide prodrugs. 2. Models of anticancer drugs paclitaxel (Taxol), mitomycin C and doxorubicin. Bioorg Med Chem Lett 8:3347–3352

Erickson HK, Park PU, Widdison WC, Kovtun YV, Garrett LM, Hoffman K, Lutz RJ, Goldmacher VS, Blättler WA (2006) Antibody–maytansinoid conjugates are activated in targeted cancer cells by lysosomal degradation and linker-dependent intracellular processing. Cancer Res 66:4426–4433

Francisco JA, Cerveny CG, Meyer DL, Mixan BJ, Klussman K, Chace DF, Rejniak SX, Gordon KA, DeBlanc R, Toki BE et al (2003) cAC10-Val-CitMMAE, an anti-CD30-monomethyl auristatin E conjugate with potent and selective antitumor activity. Blood 102:1458–1465

Hamann PR, Hinman LM, Hollander I, Beyer CF, Lindh D, Holcomb R, Hallett W, Tsou HR, Upeslacis J, Shochat D et al (2002) Gemtuzumab ozogamicin, a potent and selective anti-CD33 antibody–calicheamicin conjugate for treatment of acute myeloid leukemia. Bioconjug Chem 13:47–58

Hamann PR, Hinman LM, Beyer CF, Greenberger LM, Lin C, Lindh D, Menendez AT, Wallace R, Durr FE, Upeslacis J (2005) An anti-MUC1 antibody–calicheamicin conjugate for treatment of solid tumors. Choice of linker and overcoming drug resistance. Bioconjug Chem 16:346–353

Hamblett KJ, Senter PD, Chace DF, Sun MM, Lenox J, Cerveny CG, Kissler KM, Bernhardt SX, Kopcha AK, Zabinski RF et al (2004) Effects of drug loading on the antitumor activity of a monoclonal antibody drug conjugate. Clin Cancer Res 10:7063–7070

Henry MD, Wen S, Silva MD, Chandra S, Milton M, Worland PJ (2004) A prostate-specific membrane antigen-targeted monoclonal antibody–chemotherapeutic conjugate designed for the treatment of prostate cancer. Cancer Res 64:7995–8001

Hollander I, Kunz A, Hamann PR (2008) Selection of reaction additives used in the preparation of monomeric antibody–calicheamicin conjugates. Bioconjug Chem 19:358–361

Jedema I, Barge RM, van der Velden VH, Nijmeijer BA, van Dongen JJ, Willemze R, Falkenburg JH (2004) Internalization and cell cycle-dependent killing of leukemic cells by Gemtuzumab Ozogamicin: rationale for efficacy in CD33-negative malignancies with endocytic capacity. Leukemia 18:316–325

Junutula JR, Bhakta S, Raab H, Ervin KE, Eigenbrot C, Vandlen R, Scheller RH, Lowman HB (2008a) Rapid identification of reactive cysteine residues for site-specific labeling of antibody-Fabs. J Immunol Methods 332:41–52

Junutula JR, Raab H, Clark S, Bhakta S, Leipold DD, Weir S, Chen Y, Simpson M, Tsai SP, Dennis MS et al (2008b) Site-specific conjugation of a cytotoxic drug to an antibody improves the therapeutic index. Nat Biotechnol 26:925–932

King HD, Dubowchik GM, Mastalerz H, Willner D, Hofstead SJ, Firestone RA, Lasch SJ, Trail PA (2002) Monoclonal antibody conjugates of doxorubicin prepared with branched peptide linkers: inhibition of aggregation by methoxytriethyleneglycol chains. J Med Chem 45:4336–4343

Kovtun YV, Goldmacher VS (2007) Cell killing by antibody–drug conjugates. Cancer Lett 255:232–240

Kovtun YV, Audette CA, Ye Y, Xie H, Ruberti MF, Phinney SJ, Leece BA, Chittenden T, Blättler WA, Goldmacher VS (2006) Antibody–drug conjugates designed to eradicate tumors with homogeneous and heterogeneous expression of the target antigen. Cancer Res 66:3214–3221

Larson RA, Sievers EL, Stadtmauer EA, Lowenberg B, Estey EH, Dombret H, Theobald M, Voliotis D, Bennett JM, Richie M et al (2005) Final report of the efficacy and safety of gemtuzumab ozogamicin (Mylotarg) in patients with CD33-positive acute myeloid leukemia in first recurrence. Cancer 104:1442–1452

Law CL, Cerveny CG, Gordon KA, Klussman K, Mixan BJ, Chace DF, Meyer DL, Doronina SO, Siegall CB, Francisco JA et al (2004) Efficient elimination of B-lineage lymphomas by anti-CD20-auristatin conjugates. Clin Cancer Res 10:7842–7851

Law CL, Gordon KA, Toki BE, Yamane AK, Hering MA, Cerveny CG, Petroziello JM, Ryan MC, Smith L, Simon R et al (2006) Lymphocyte activation antigen CD70 expressed by renal cell carcinoma is a potential therapeutic target for anti-CD70 antibody–drug conjugates. Cancer Res 66:2328–2337

Legrand O, Vidriales MB, Thomas X, Dumontet C, Vekhoff A, Morariu-Zamfir R, Lambert J, San Miguel JF, Marie J-P (2007) An open label, dose escalation study of AVE9633 administered as a single agent by intravenous (IV) infusion weekly for 2 weeks in 4-week cycle to patients with relapsed or refractory CD33-positive acute myeloid leukemia (AML). Blood 110: Abstract 1850

Liu C, Tadayoni BM, Bourret LA, Mattocks KM, Derr SM, Widdison WC, Kedersha NL, Ariniello PD, Goldmacher VS, Lambert JM et al (1996) Eradication of large colon tumor xenografts by targeted delivery of maytansinoids. Proc Natl Acad Sci U S A 93:8618–8623

Ma D, Hopf CE, Malewicz AD, Donovan GP, Senter PD, Goeckeler WF, Maddon PJ, Olson WC (2006) Potent antitumor activity of an auristatin-conjugated, fully human monoclonal antibody to prostate-specific membrane antigen. Clin Cancer Res 12:2591–2596

Mao W, Luis E, Ross S, Silva J, Tan C, Crowley C, Chui C, Franz G, Senter P, Koeppen H et al (2004) EphB2 as a therapeutic antibody drug target for the treatment of colorectal cancer. Cancer Res 64:781–788

McDonagh CF, Turcott E, Westendorf L, Webster JB, Alley SC, Kim K, Andreyka J, Stone I, Hamblett KJ, Francisco JA et al (2006) Engineered antibody–drug conjugates with defined sites and stoichiometries of drug attachment. Protein Eng Des Sel 19:299–307

Pietersz GA, Rowland A, Smyth MJ, McKenzie IF (1994) Chemoimmunoconjugates for the treatment of cancer. Adv Immunol 56:301–387

Polson AG, Yu SF, Elkins K, Zheng B, Clark S, Ingle GS, Slaga DS, Giere L, Du C, Tan C et al (2007) Antibody–drug conjugates targeted to CD79 for the treatment of non-Hodgkin lymphoma. Blood 110:616–623

Reichert JM, Valge-Archer VE (2007) Development trends for monoclonal antibody cancer therapeutics. Nat Rev Drug Discov 6:349–356

Reichert JM, Rosensweig CJ, Faden LB, Dewitz MC (2005) Monoclonal antibody successes in the clinic. Nat Biotechnol 23:1073–1078

Ryan MC, Hering M, Peckham D, McDonagh CF, Brown L, Kim KM, Meyer DL, Zabinski RF, Grewal IS, Carter PJ (2007) Antibody targeting of B-cell maturation antigen on malignant plasma cells. Mol Cancer Ther 6:3009–3018

Saleh MN, Sugarman S, Murray J, Ostroff JB, Healey D, Jones D, Daniel CR, LeBherz D, Brewer H, Onetto N et al (2000) Phase I trial of the anti-Lewis Y drug immunoconjugate BR96-doxorubicin in patients with lewis Y-expressing epithelial tumors. J Clin Oncol 18:2282–2292

Sanderson RJ, Hering MA, James SF, Sun MM, Doronina SO, Siadak AW, Senter PD, Wahl AF (2005) *In vivo* drug-linker stability of an anti-CD30 dipeptide-linked auristatin immunoconjugate. Clin Cancer Res 11:843–852

Sun MM, Beam KS, Cerveny CG, Hamblett KJ, Blackmore RS, Torgov MY, Handley FG, Ihle NC, Senter PD, Alley SC (2005) Reduction-alkylation strategies for the modification of specific monoclonal antibody disulfides. Bioconjug Chem 16:1282–1290

Tassone P, Goldmacher VS, Neri P, Gozzini A, Shammas MA, Whiteman KR, Hylander-Gans LL, Carrasco DR, Hideshima T, Shringarpure R et al (2004a) Cytotoxic activity of the maytansinoid immunoconjugate B-B4-DM1 against CD138+ multiple myeloma cells. Blood 104:3688–3696

Tassone P, Gozzini A, Goldmacher V, Shammas MA, Whiteman KR, Carrasco DR, Li C, Allam CK, Venuta S, Anderson KC et al (2004b) In vitro and in vivo activity of the maytansinoid immunoconjugate huN901-*N*2′-deacetyl-*N*2′-(3-mercapto-1-oxopropyl)-maytansine against CD56+ multiple myeloma cells. Cancer Res 64:4629–4636

Thorpe PE, Wallace PM, Knowles PP, Relf MG, Brown AN, Watson GJ, Knyba RE, Wawrzynczak EJ, Blakey DC (1987) New coupling agents for the synthesis of immunotoxins containing a hindered disulfide bond with improved stability in vivo. Cancer Res 47:5924–5931

Thorpe PE, Wallace PM, Knowles PP, Relf MG, Brown AN, Watson GJ, Blakey DC, Newell DR (1988) Improved antitumor effects of immunotoxins prepared with deglycosylated ricin A-chain and hindered disulfide linkages. Cancer Res 48:6396–6403

Tolcher AW, Sugarman S, Gelmon KA, Cohen R, Saleh M, Isaacs C, Young L, Healey D, Onetto N, Slichenmyer W (1999) Randomized phase II study of BR96-doxorubicin conjugate in patients with metastatic breast cancer. J Clin Oncol 17:478–484

Trail PA, Willner D, Lasch SJ, Henderson AJ, Hofstead S, Casazza AM, Firestone RA, Hellström I, Hellström KE (1993) Cure of xenografted human carcinomas by BR96-doxorubicin immunoconjugates. Science 261:212–215

Trail PA, Willner D, Knipe J, Henderson AJ, Lasch SJ, Zoeckler ME, TrailSmith MD, Doyle TW, King HD, Casazza AM et al (1997) Effect of linker variation on the stability, potency, and efficacy of carcinoma-reactive BR64-doxorubicin immunoconjugates. Cancer Res 57:100–105

Trail PA, King HD, Dubowchik GM (2003) Monoclonal antibody drug immunoconjugates for targeted treatment of cancer. Cancer Immunol Immunother 52: 328–337

Tse KF, Jeffers M, Pollack VA, McCabe DA, Shadish ML, Khramtsov NV, Hackett CS, Shenoy SG, Kuang B, Boldog FL et al (2006) CR011, a fully human monoclonal antibody–auristatin E conjugate, for the treatment of melanoma. Clin Cancer Res 12:1373–1382

Walker MA, Dubowchik GM, Hofstead SJ, Trail PA, Firestone RA (2002) Synthesis of an immunoconjugate of camptothecin. Bioorg Med Chem Lett 12:217–219

Walker MA, King HD, Dalterio RA, Trail P, Firestone R, Dubowchik GM (2004) Monoclonal antibody mediated intracellular targeting of tallysomycin S(10b). Bioorg Med Chem Lett 14:4323–4327

Widdison WC, Wilhelm SD, Cavanagh EE, Whiteman KR, Leece BA, Kovtun Y, Goldmacher VS, Xie H, Steeves RM, Lutz RJ et al (2006) Semisynthetic maytansine analogues for the targeted treatment of cancer. J Med Chem 49:4392–4408

Wu AM, Senter PD (2005) Arming antibodies: prospects and challenges for immunoconjugates. Nat Biotechnol 23:1137–1146

Younes A, Forero-Torres A, Bartlett N, Leonard JP, Rege B, Kennedy DA, Lorenz J, Sievers EL (2007) A novel antibody-drug conjugate, SGN-35 (anti-CD30-auristatin), induces objective responses in patients with relapsed or refractory Hodgkin lymphoma, preliminary results of a phase I tolerability study. 7th International Symposium on Hodgkin Lymphoma: Abstract PO99bis

Chapter 19

Antibody Radiolabeling

Corinne Bensimon and Russell Redshaw

1. Introduction

The concept of using radiolabeled antibodies in vivo dates back to 1949 when Pressman (1949) demonstrated that radiolabeled antibodies could be used to localize specific tissue. Using ^{131}I radiolabeled anti-carcinoembryonic antigen antibodies, Goldenberg et al. (1978) imaged human colonic carcinoma xenografts and in doing so, set in motion the field of radiolabeled antibodies for use in imaging and therapy.

Antibody based imaging entails either an antibody, bivalent fragment $F(ab')_2$, monovalent fragment Fab′ or antibody construct (minibody, diabody, tribody, etc.), with either a gamma or positron emitting radioisotope, having an appropriate energy, and an external camera system. A list of radioisotopes suitable for imaging is shown in Table 19-1.

Single-photon emission computed tomography (SPECT) imaging involves the use of a gamma scintillation camera where multiple images are taken, typically encompassing 180° or 360°. SPECT imaging is based on the Anger camera which uses NaI:Tl as the scintillation crystal, the thickness of the crystal allows for optimal resolution of gamma rays in the range of 100–200 keV. Gamma emitting isotopes with higher gamma energies, such as ^{111}In, are imaged through the placement of a collimator on the imaging camera. With positron emission tomography (PET) imaging, a positron, which is a beta-like nuclear particle that travels a few millimeters from its nucleus, collides with an electron and causes annihilation of particles creating two photons that travel in 180° opposite direction. The PET imaging system captures and registers photons arising from annihilation precisely, at the same time thereby providing exceptional sensitivity. Both SPECT and PET systems use computer algorithms to reconstruct multiple tomograms in coronal, sagittal, and transverse projections.

From: *Current Trends in Monoclonal Antibody Development and Manufacturing,*
Biotechnology: Pharmaceutical Aspects, DOI 10.1007/978-0-387-76643-0_19,
Edited by: S.J. Shire et al.

Table 19-1. Radioiostopes for use in antibody imaging.

Imaging modality	Radioisotope	Half-life	Energy	Method of production
SPECT	^{99m}Tc – Technetium	6.0 h	140 keV	Generator
SPECT	^{123}I – Iodine	13.2 h	159 keV	Cyclotron
SPECT	^{111}In – Indium	2.8 days	171 keV	Cyclotron
			245 keV	
SPECT	^{117m}Sn – Tin	13.6 days	159 keV	Cyclotron
PET	^{18}F – Fluorine	110 min	633 keV	Cyclotron
PET	^{68}Ga – Gallium	68 min	1.90 MeV	Generator
PET	^{64}Cu – Copper	12.7 h	578 keV	Cyclotron

Table 19-2. Antibodies that have received regulatory approval to market in various countries.

Antibody	Isotope	indication
CEA-Scan (arcitumomab)	^{99m}Tc	Detection of colorectal cancer metastases
Granuloscint (fanolesomab)	^{99m}Tc	Detection of infection
Leukoscan (salesomab)	^{99m}Tc	Detection of infection
Prostascint (capromab pendetide)	^{111}In	Detection of prostate metastases

Not all these imaging antibodies are approved for sale in the United States

Antibody based SPECT and PET are used to locate and image cancer, infectious, and cardiac disease. Several radiolabeled antibodies for diagnostic imaging have been commercialized (see Table 19-2).

Radiolabeled antibodies are being embraced as a valuable tool for use in drug research and development. The introduction of small animal SPECT and PET imaging systems has stimulated antibody (and other drug) developers to use radioimaging as a translational tool that effectively bridges in vivo information in experimental animal models with humans (Buchanan et al. 2007).

Achieving selective delivery of cytotoxic agents to diseased tissue and cells is a key objective to the development of better efficacious therapeutics. Antibody-mediated radiotherapy has now been clinically demonstrated in patients with non-Hodgkin's B-cell lymphoma (NHL) using antibodies directed against the cluster designation 20 antigen (CD 20). ^{131}I Bexxar (tositumab) and ^{90}Y Zevalin (ibritumomab tiuxetan) have provided durable response rates of 70–80% (Witzig et al. 2002; Kaminski et al. 2000). The use of radiolabeled antibodies to treat other hematological malignancies is being investigated; for example anti-CD 33 radiolabeled HuM195 antibody to treat myeloid leukemia (Jurcic 2005) and radiolabeled anti-muc-1 antibody to treat multiple myeloma (Supiot et al. 2002).

Use of radiolabeled antibodies to treat solid tumors has been extensively investigated and has not provided clinically high durable response rates (Goldenberg 2002; Goldenberg and Sharkey 2006; Reilly 1991). Numerous variables are involved, but it is recognized that the combination of modest tumor uptake and relatively long serum half-life of radiolabeled antibody results in dose limiting toxicity to normal organs and in particular to bone

marrow. To help over come this problem, pre-targeting has been proposed (see Reilly 2006). Liu et al. (2002) describes pre-targeting as follows: "Pre-targeting involves the administration of a non-radioactive tumor-specific agent carrying a molecular group with high affinity for a small effector molecule. After a suitable interval to allow for tumor targeting and clearance, the radiolabeled effector is administered. Thus, the pre-targeting method allows for the clearance of the tumor-specific antibody from normal tissues before the administration of the radiolabeled effector, and therefore can potentially overcome the intrinsic disadvantage of the lower ratios of tumor radioactivity that are characteristics of conventional targeting." Pre-targeting holds promise to further improve radioimaging and therapy applications for antibodies. A number of antibody pre-targeting approaches have been devised which are summarized in Table 19-3.

The role for radioimmunotherapy for the treatment of solid tumors continues to be investigated and it may ultimately become an adjuvant therapy to eradicate minimal or metastatic disease. Radioimmunotherapy is also under investigation for the treatment of infectious disease (Dadachova et al. 2005, 2006a,b; Casadevall et al. 2007).

As a therapeutic strategy radiolabeled antibodies have several attractive features that are described below:

- The radiolabel may not interfere with antibody biological activity: Antibody dependent complement-mediated cytotoxicity (CDC) and antibody dependent cellular toxicity (ADCC) and can be engineered not to affect antibody–antigen binding.
- For beta particle based radioimmunotherapy, the radiolabeled antibody does not need to be internalized – some beta particles have a range of up to 1.0 cm thereby allowing destruction of neighboring cells (referred to as the crossfire effect). For this reason radioimmunoconjugates are effective in heterogeneous tumor architecture.

Table 19-3. Pre-targeting strategies.

Pre-targeting method	Reference
Avidin–biotin	Paganelli et al. (1991)
Avidin–biotin 3-step method consisting of:	
Streptavidin–antibody (V_L) fusion (targeting protein)	Sato et al. (2005)
Thioglactoside clearing agent	Lin et al (2006)
Biotin–radioisotope conjugate	Axworthy et al. (2000)
Morpholino – use of complementary morpholino oligomers	Liu et al. (2002)
	He et al. (2007)
	Liu et al. (2006)
	Liu et al. (2007)
Bispecific antibody – Hapten peptide	Sharkey et al. (2005)
	Sharkey and Goldenberg (2006)
	Rossi et al. (2006)
	Moosmayer et al. (2006)

Table 19-4. Radioisotopes for therapeutic considerations.

Radionuclide	Half-life	Emission for therapy	Penetration range	Source of production
^{67}Cu – Copper	61.9 days	β	0.05–2.1 mm	Cyclotron
^{131}I – Iodine	8.02 days	β	0.08–2.3 mm	Reactor
^{177}Lu – Lutetium	6.7 days	β	0.04–1.8 mm	Reactor
^{188}Re – Rhenium	17.0 h	β	1.9–10.4 mm	Generator
^{90}Y – Yttrium	64 h	β	4.0–11.3 mm	Generator
^{211}At – Astatine	7.2 h	α	60 μm	Cyclotron
^{212}Bi – Bismuth	60.5 min	α	84 μm	Generator
^{225}Ac – Actinium	10.0 days	α	50–80 μm	Generator
^{123}I – Iodine	13.3 h	Auger	<100 nm	Cyclotron
^{125}I – Iodine	59.4 days	Auger	<100 nm	Reactor
^{111}In – Indium	3.0 days	Auger	<100 nm	Cyclotron

- Radiolabeling technology is well established and a variety of approaches are readily available.
- There is a selection of radioisotopes with therapeutic properties commercially available.
- Go/no go experimentation is relatively straightforward.

Radioimmunotherapy may be carried out by employing radioisotopes with a suitable beta or alpha particle, or Auger electron emission. A list of radionuclides for use in radioimmunotherapeutics is shown in Table 19-4.

Selection of a therapeutic radionuclide must factor the nature of the disease: tumor size and volume, stage of development, the amount of target receptor or antigen present at the diseased cell or tissue and normal tissue, the extent to which the antibody or antibody construct may penetrate the diseased tissue, and overall biodistribution to non-target tissue. Consideration should also be given to match the antibody biology; specifically, its distribution and pharmacokinetics, with the energy emission of the radionuclide for optimal therapeutic outcome; the goal being delivery of lethal radiation dose to the disease tissue with minimal radiation to non-target tissue. The highest linear energy transfer is observed with alpha particles which limit the cells' ability to repair DNA and are effective in hypoxic conditions (Volkert et al 1991). Alpha particles have a short path length and a higher energy, making them more lethal to cells, than beta emitters (McDevitt and Scheinberg 2002), however the range of alpha emitters is only a few cell diameters.

Beta particle emitting radionuclides have an effective killing range over several hundred cell diameters. ^{90}Y has a deeper penetration range (11.3 mm) than ^{177}Lu (1.8 mm).

The physical half-life of the radionuclide and the biological half-life of the antibody or, in the case of pretargeting, radiolabeled effector molecule, must be considered when designing the optimal radioimmunotherapeutic agent. One can also select a therapeutic radionuclide that, in addition to beta particle emissions for therapy possesses gamma energies suitable for imaging. ^{188}Re, ^{177}Lu, and ^{131}I are representative beta emitting radionuclides that have energies suitable for imaging and real-time dosimetry. Due to their short penetration

range, use of Auger electron emitting radionuclides for therapy is restricted to antibodies that internalize within the target cell nucleus. Auger electron therapy appears to be feasible with the HIV-1 tat to IgG radioimmunoconjugates engineered by Hu et al. (2006) and Cornelissen et al. (2007) that are internalized within the target cell nucleus.

Radionuclides commonly employed for antibody radiolabeling are halogens and metal elements; the following examines considerations of each in detail.

2. Radiolabeling Antibodies with Radiohalogens

The most commonly used halogens for antibody radiolabeling are iodine, bromine and fluorine isotopes. The advantage of halogens over metals is that they can be directly introduced onto an antibody via electrophilic substitution of the halogen onto antibody tyrosine residues. The main problem with halogenated antibodies is in vivo dehalogenation, as a result of enzymatic cleavage due to structural similarities between thyroid hormones and halogenated tyrosine-like residues of an antibody or its catabolites. In particular, dehalogenation with iodide results in significant and undesirable accumulation in both the thyroid and stomach tissues, and sub-optimal uptake at the antibody target.

Fluorine isotope (^{18}F) forms very strong C–F bonds and therefore the rate of dehalogenation in vivo is slower than iodine isotopes (Zumdahl (1997)). Bromine (^{77}Br) forms slightly stronger C–Br bonds than C–I bonds (Table 19-5). However dehalogenation in vivo remains problematic, but has the advantage of not accumulating in the thyroid. Iodine isotopes (^{123}I, ^{125}I, ^{131}I) are widely available and frequently used to label antibodies with high specific activity. Methods for halogenation are as follows:

2.1. Direct Radiolabeling with Radiohalogens

The most commonly used methods are described below:

Iodine monochloride method (Helmkamp et al. 1967; Doran and Spar 1980):

Radioiodine is equilibrated with stable iodine monochloride in dilute HCl. The mixture is then added to the antibody. The reaction is depends upon the pH and temperature. The disadvantage of this method is the presence of inactive iodide that will affect the binding properties of the labeled antibody.

2.1.1. Enzymatic Methods (Marchalonis 1969)

Lactoperoxidase is equilibrated with a nanomolar quantity of oxidant such as hydrogen peroxide. The solution is added to the mixture of antibody and

Table 19-5. Energy of C–halogens bonds.

Bond	Bond energy (kJ/mol)
C–F	485
C–Br	285
C–I	213

radioiodide. The hydrogen peroxide oxidizes iodide to form reactive iodine species that reacts with the tyrosine residue on the antibody. The method is very mild due to the small quantity of peroxide and does not cause denaturation of the antibody.

2.1.2. Chloramine-T (Hunter and Greenwood 1962), Iodobeads (Markwell 1982) and Iodogen (1,3,4,6-Tetrachloro-3α,6α-Diphenylglycouril) (Fraser and Speck 1978) Methods

The electropositive iodonium ion, is generated in situ by adding an oxidizing agent to the mixture of antibody and sodium iodide. The iodonium ion (I+) reacts mainly on the antibody tyrosine residues. The resonance effect of the *p*-hydroxyl group on the tyrosine residue directs the electrophilic substitution to the ortho position of the hydroxyl group. Addition of iodide to the histidine residue can also occur but phenylalanine residues are sufficiently deactivated relative to the tyrosine residue that no appreciable iodination can occur. The amount and the strength of the oxidizing agent used in a reaction must be carefully selected in order to minimize denaturation of the protein by breaking peptide and disulfide bonds. Range finding studies are carried out at different molar ratios iodide:iodogen and iodogen:antibody in order to optimize the labeling yield without compromising the immunoreactivity. Iodogen is usually coated on glass surface such as a vial or glass beads and is less oxidative than chloramine-T. The reaction is stopped by simply transferring the labeled antibody from the coated vials or beads to a purification column. Chloramine-T is soluble in most buffers used for radiolabeling. Therefore an antioxidant such as sodium metabisulfite, is needed to quench the reaction before purification of the labeled antibody. Iodobeads are modified chloramine-T molecules attached to polystyrene beads that are less oxidative than chloramine-T and eliminate the need to remove the chloramine-T from the final drug product.

2.2. Indirect Radiolabeling with Radiohalogens

Indirect labeling has the advantage of separating the antibody from the oxidant and therefore minimizing denaturation of the antibody. Chloramine-T or Iodogen are used for tyrosine-like moieties and *t*-butylhydroperoxide (TBHP) or *N*-chlorosuccinimide NCS for non-tyrosine-like moieties. The iodinated moiety is purified prior to the conjugation step to increase the specific activity of the final drug product and is conjugated to the antibody through the lysine residues. The moiety should provide fast and efficient radioiodination and rapid antibody coupling. Also, the moiety must be structurally different from iodotyrosine to preclude enzymatic deiodination. The most common moieties are Bolton Hunter reagent (*N*-hydroxysuccinimide ester of *p*-hydroxyphenylpropionic acid) and Wood reagent (*p*-hydroxylbenzimidate) (Fig. 19-1).

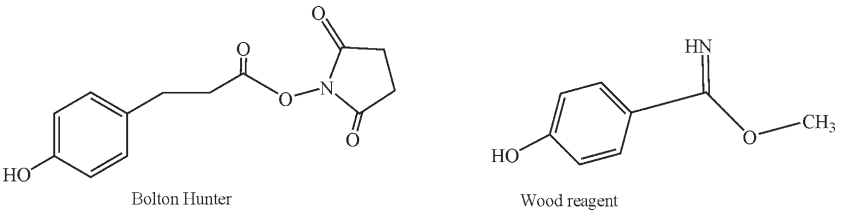

Fig. 19-1. Iodine chelates

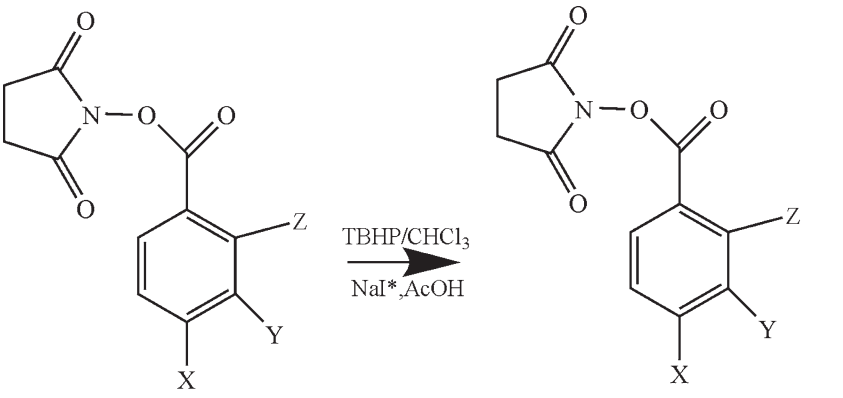

m-BuATE: X=H, Y-$SnBu_3$, Z=H
m-MeATE: X=H, Y=$SnMe_3$, Z=H
p-BuATE: X-$SnBu_3$, Y=H, Z=H
m-BuMATE: X=CH_3, Y=$SnBu_3$, Z=H
m-BuHATE: X=OH, Y=$SnBu_3$, Z=H
m-BuMeO_2ATE; X=Z=OCH_3, Y=$SnBu_3$

m-SIB: X=H, Y=I*, Z=H
m-SIB: X=H, Y=I*, Z=H
p-SIB; X=I*, Y=H, Z=H
m-SMIB; X=CH_3, Y=I*, Z=H
m-SHIB; X=OH, Y=I*, Z=H
m-SMeO_2IB; X=Z=OCH_3, Y=I*

Fig. 19-2. Iodination reaction of *N*-succinimidyl-(tri-*n*-butylstannyl)benzoate

The Bolton Hunter method (Bolton and Hunter 1973) is very susceptible to hydrolysis during iodination because of the succidinimyl functional group, but is easy to conjugate. The labeled Bolton Hunter reagent is less susceptible to in vivo dehalogenation than a labeled tyrosine using iodogen. On the other hand, Wood reagent (Wood et al. 1975) is more resistant to hydrolysis, but is more difficult to conjugate because of the imidoester group. Other iodine moieties have been investigated, for example *N*-succinimidyl-(tri-*n*-butylstannyl) benzoate (m-BuATE) (Fig. 19-2).

The radioiodination of m-BuATE is performed using an oxidant (*t*-butylhydroperoxide (TBHP) or *N*-chlorosuccinimide (NCS)) in a solution of 2% acetic acid in chloroform at pH 5.0–5.5 to form *N*-succinimidyl 3-iodobenzoate (m-SIB). m-SIB has the advantage of a carbon chain between the ester group and the aromatic ring shorter than Bolton Hunter. This reduces the hydrolysis of the *N*-succinimidyl group and results in improved conjugation yield to the antibody (70% labeling versus 30% for Bolton Hunter) (Vaidyanathan et al. 1993). Moreover, the m-SIB moiety is resistant to enzymatic degradation due to the structural differences with the tyrosine. The percentage of injected dose in the thyroid is reduced from 5.05% for the direct labeling to 0.36% for m-SIB, in normal mice, when conjugated to an IgG antibody after 5 days (Zalutsky and Narula 1987). Vaidynathan and Zalutsky (1990a) observed similar results with the anti-tenascin monoclonal antibody 81C6, where the thyroid uptake was 0.18% ID/g for m-SIB when compared to 0.44% for Bolton Hunter and 5.97% for Iodogen, after 3 days in normal mice. Under optimized oxidant conditions, Garg et al. (1989) showed that by changing the bulky butyl group on the stannyl in m-BuATE with a smaller methyl group such as *N*-succinimidyl-(tri-*n*-methylstannyl)benzoate (m-MeATE), the steric effect is reduced and the iodination yield of the moiety improves from 80 to 97% in 30 min. Wilbur et al. (1991) investigated the importance of the position of the butylstannyl group by comparing

N-succinimidyl-3(tri-*n*-butystannyl)benzoate (m-BuATE) and *N*-succinimidyl-4(tri-*n*-butylstannyl)benzoate (*p*-BuATE). The biodistribution in normal mice of the two radioiodinated moieties conjugated to NR-Lu-10 antibody fragment were similar, but higher kidney uptake was observed for *p*-SIB (15.6%) when compared to 0.52% for m-SIB. The resonance forms of the amide group on the aromatic ring create a lower electron density on the carbon in position four when compared to the carbon in position three. The reduced electron density on the carbon bearing the iodine atom increased the possibility of dehalogenation by nucleophilic attack. This theory was investigated further by increasing the electron density on the carbon bearing the iodine in order to improve the stability of the C–I bond. Electrodonating substituents of different strength were added in ortho of the stannyl group: an hydroxyl group was added to m-BuATE to form 4-hydroxy-3-(tri-*n*-butylstannyl)benzoate m-BuHATE (Vaidyanathan et al. 1993), a methyl group was added to form 4-methyl-3-(tri-*n*-butylstannyl)benzoate m-BuMATE (Garg et al. 1993) and a methoxy group was added to form 2,4-dimethoxy-3-(tri-*n*-butylstannyl) benzoate m-BuMeO$_2$ATE (Vaidynathan and Zalutsky 1990b). The increased electron density on the carbon 3 did not help the stability of the iodinated moiety in vitro (see Table 19-6). Furthermore a decrease of the iodination rate was observed from 80% for SIB to 60% for SMIB and 30% for SMeO$_2$IB.

A new type of iodine moiety was investigated to reduce the hydrolysis of the activated ester: 3(tri-*n*-tributylstannyl)phenylisothiocyanate (Fig. 19-3). The isothiocyanate eliminates hydrolysis during the iodination process; however the conjugation rate is slower by 12 h versus 15 min for the *N*-succinimidyl. A decrease in the thyroid uptake by a factor of 3–4 is observed in comparison to direct iodination in tumor bearing mice (Ram and Buchsbaum 1992, 1994).

Table 19-6. Comparison of SIB to SHIB, SMIB and SMeO2IB.

Antibody	Chelate	Iodinated chelate	Thyroid (%ID/g)	Liver (%ID/g)	Kidney (%ID/g)
Anti-tenacin 81C6	m-BuATE	SIB	0.3	1.85	0.24
	m-BuHATE	SHIB	0.5	2.12	0.27
Anti hAFP DU-PAN 1 (Fab′)	m-BuATE	SIB	0.12	0.34	1.09
	m-BuMATE	SMIB	0.32	0.35	2.27
Anti-CEA C110	m-BuATE	SIB	0.4	5.97	1.88
	m-BuMeO$_2$IB	SMeO$_2$IB	1.3	5.96	1.95

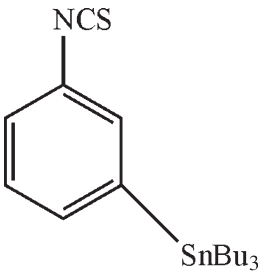

Fig. 19-3. 3(tri-*n*-Butylstannyl)phenylisothiocyanates

3. Radiolabeling of Antibodies with Radiometals

Radiometals can be introduced directly or indirectly to the antibody.

3.1. Direct Radiolabeling with Radiometals

Direct labeling is frequently carried out with ^{99m}Tc, ^{186}Re and ^{188}Re. The pertechnetate ion TcO_4^- and the perrhenate ion ReO_4^- have an oxidation state of +7 and are chemically very stable species. In order to perform direct antibody labeling with rhenium or technetium, the radiometal must first be reduced to a lower oxidation state, by the addition of a reducing agent. Various reducing agents such as: stannous chloride $SnCl_2 \cdot 2H_2O$ (Hnatowich et al. 1993), stannous tartrate (Pettit et al. 1980), or sodium borohydrate ($NaBH_4$) can be used for this purpose. In the lower oxidation state (+5), the reduced metals are chemically very reactive and coordinate to at least four donor atoms to form a stable complex. Donor groups such as thiol, amide, amino, and carbonyl are common with this class of metal ion. The probability of finding four or more atoms in that preferred arrangement in an antibody is very low and may lead to denaturation of the antibody. With thiol groups, a reduction of the disulfide bond on the antibody is needed using a low concentration of mild reducing agent such as 2-mercaptoethanol, prior to radiolabeling.

3.2. Indirect Radiolabeling with Radiometals

The following metallic radionuclides (e.g. ^{64}Cu, ^{68}Ga, ^{90}Y, ^{99m}Tc, ^{111}In, ^{153}Sm, ^{177}Lu, ^{186}Re, ^{188}Re and ^{225}Ac) can be indirectly labeled on the antibodies using bifunctional chelates that are conjugated to the antibody either before (post-metallation) or after addition (pre-metallation) of the metal ion. For the post-metallation method, the bifunctional ligand is first covalently attached to the antibody followed by purification and subsequent complexation with the metal ion (see Fritzberg et al. 1988). The advantage of this approach is generally a more stable immunoconjugate and the opportunity to substitute metal radionuclides for different applications. For example, ^{111}In is used for biodistribution studies while ^{90}Y is used for radioimmunotherapy with Zevalin (ibritumomab tiuxetan) an anti-CD 20 monoclonal antibody conjugated to MX-DTPA. With the pre-metallation method, the bifunctional ligand is first complexed with the appropriate radiometal, and then conjugated to the antibody. This approach is recommended when the labeling requires conditions that could denature the antibody, however it leads to radiolabeled antibodies with low specific activity.

Transchelation of the radionuclide to circulating proteins in the blood can be a major problem with chelated antibodies. Depending on the chelate and the radiometal, the transchelation may result in undesirable soft tissue uptake; in particular high liver accumulation.

3.2.1. Reactive Functional Group

The reactive functional group on the chelates must provide rapid conjugation to the antibody at neutral pH and room temperature (Fichna and Janecka 2003). The choice of functional group depends on the antibody and the presence of the following groups: amino, thiol and aldehyde (Fig. 19-4).

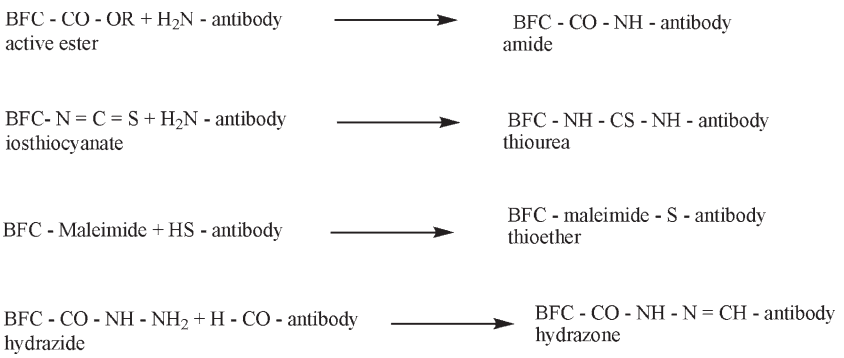

Fig. 19-4. Functional groups

The functional groups commonly used are activated ester, isothiocyanate, maleimide and hydrazide. Activated ester such as *N*-hydroxysuccinimide (NHS) reacts with the amino group of a lysine residue on the antibody to form an amide bond at mildly acid to neutral pH range. Activated esters are very reactive and water soluble making it easy to purify when the conjugated antibody is insoluble in water. Isothiocyanate reacts with the amino group of lysine residues on antibodies to form a thiourea bond at high pH 8–9, along with the occurrence of competing hydrolysis occurring. Therefore, this functional group is not applicable for antibodies sensitive to high pH. Maleimide reacts with thiol groups on the antibody to form thioether linkage at neutral pH. In alkaline conditions, the maleimide can be hydrolyzed into maleanic acid. Hydrazides react with aldehyde groups on the antibody to form hydrazone conjugates. This functional group is suitable for antibodies containing serine, threonine and hydroxylysine.

With bifunctional chelates, the position of the functional group on the aromatic ring attached to the chelator affects the stability of the conjugate. There are two kinds of substituents: nucleophilic and electrophilic. Nucleophilic groups (NH_2, OH, OCH_3) are ortho or para activating group and increases the electron density on those carbons while electrophilic groups (NO_2, SCN) decrease the electron density on those carbons. The variation in the electron density of the benzyl group has an impact on the stability of the chelate (Wilson et al. 1998). When ^{153}Sm is complexed with BA-DOTA, the loss of metal is 17% with a nucleophilic group in para position such as NH_2 versus 33% with an electrophilic group such as NO_2. For MeO-BA-DOTA complexed with ^{153}Sm, when two nucleophilic substituents are present: one in ortho (OCH_3) and one in meta (NH_2), the metal loss is 6%. However if the meta substituent is replaced by an electrophilic group such as NO_2, then the metal loss is 1%.

3.2.2. Linker

A linker is used to connect the bifunctional chelate to the antibody. The choice of linker depends on the pharmacokinetic requirements. The linker can be electrophilic, nucleophilic or neutral and have a significant effect on biodistribution. For example, increasing the hydrophilicity of the antibody with the linker can improve the renal clearance (Liu and Edwards 2001a) and reduces the accumulation to fatty tissues like the liver.

3.2.3. Bifunctional Chelates for ^{90}Y, ^{111}In, ^{153}Sm, ^{177}Lu

The chemistry of yttrium, indium, samarium and lutetium is very similar. The most prevalent oxidation state in aqueous solution is +3. Complexation with this series of metals favors ligands containing donor atoms such as oxygen, nitrogen and sulfur. Stable complexes are obtained with coordination numbers varying from 3 to 8 depending of the chelate. Two types of chelates are available: acyclic chelates (e.g. Bz-DTPA, 1B4M-DTPA, MX-DTPA, CHX-DTPA) and cyclic chelates (e.g. C-DOTA, PA-DOTA, 1B4M-DOTA, BA-DOTA, MeO-BA-DOTA) as shown in Figs. 19-5 and 19-6.

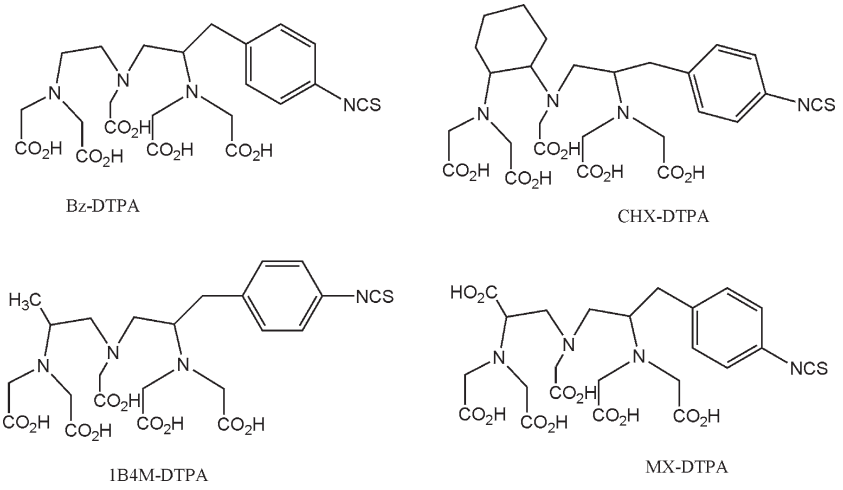

Fig. 19-5. Acyclic chelates

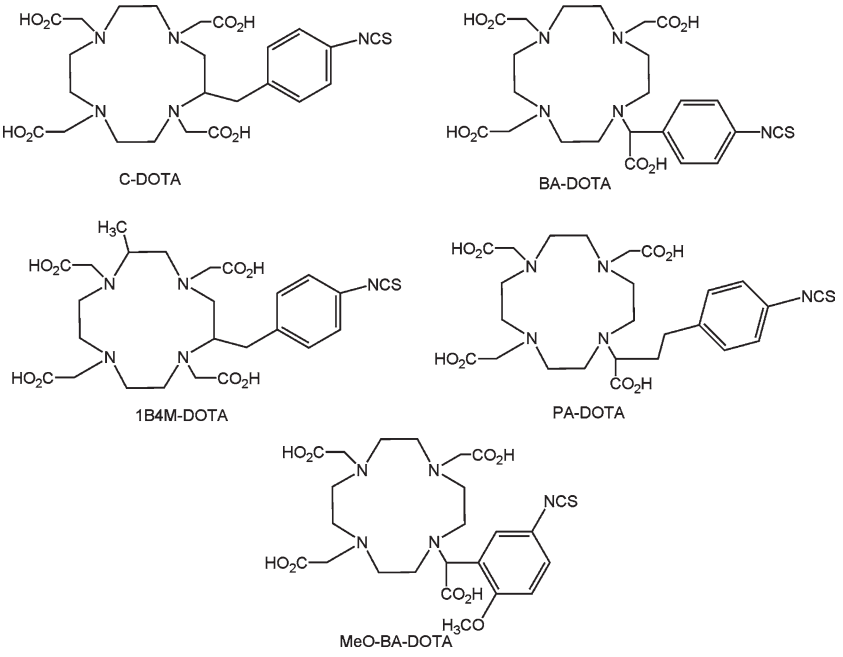

Fig. 19-6. Cyclic chelates

The choice of the bifunctional chelate depends on the oxidation state, the size of the radionuclide and the sensitivity of the antibody to elevated temperature. The size of the metallic ion is more critical for cyclic chelates.

In general, acyclic chelates react faster with metals than cyclic chelates. For acyclic chelates, the pre-organization of chelate and the denticity increase the stability of the metal complex. Stimmel (1995, 1998) demonstrated that acyclic chelates such as: CHX-A″-DTPA (Gansow and Brechbiel 1992) and MX-DTPA (Gansow and Brechbiel 1989) react instantaneously with ^{90}Y, ^{177}Lu and ^{153}Sm, up to a molar ratio chelate:metal 1:1. The chelation is affected minimally by traces of metal impurities in the radioisotope. The acyclic chelates are not stable at low pH, the nitrogens involved in chelation, are easily protonated resulting in the release of the radionuclide. The acyclic chelates are divided in two groups. The first group constituted of DTPA, Bz-DTPA is easily protonated at low pH and therefore this group is very unstable. The second group, MX-DTPA, 1B4M-DTPA, CHX-DTPA, has a better stability at low pH. The addition of substituents like a carboxyl group in MX-DTPA or a methyl group in IB4M-DTPA add some extra rigidity that makes the protonation of the nitrogen harder and therefore increases the stability in vivo.

In order to further improve the stability of the acyclic chelate, a cyclohexyl was added to the DTPA backbone. Camera et al. (1994) compared the in vivo stability of CHX-DTPA to 1B4M-DTPA. When conjugated to the anti-Ephrin-B3 monoclonal antibody, CHX-A-DTPA and 1B4M-DTPA showed similar bone uptake while CHX-B-DTPA showed a higher uptake in the femur. The stability of the four isomers of CHX-DTPA: CHX-A′-DTPA, CHX-A″-DTPA , CHX-B′-DTPA and CHXB″-DTPA with ^{90}Y was studied by Wu et al. (1997) who observed that the CHX-A group showed a better stability in serum and low pH than the CHX-B group. Milenic et al. (2002) labeled ^{177}Lu on CHX-A″-DTPA conjugated to the anti-B72.3 antibody CC49 and found that CHX-A″-DTPA was superior to PA-DOTA with respect to immunoreactivity, specific activity, and the in vivo pharmacokinetic data.

For cyclic chelates C-DOTA and PA-DOTA, the kinetics of complexation are slower (Stimmel et al. 1995; Stimmel and Kull 1998). The molar ratio chelate/isotope depends on the size of the metal. A molar ratio chelate:metal of 2:1 and 3:1 are achieved respectively with ^{177}Lu and ^{90}Y. As the metal ionic radius decreases, the reaction kinetics is faster and the stability of the complex decreases.

Metal contaminants have a significant impact on labeling yield. The rate of reaction for PA-DOTA is 45 min versus 15 min with C-DOTA for ^{90}Y, ^{153}Sm and ^{177}Lu. The benzyl group is connected directly to the carboxylic arm, creating some steric effects that slow down the reaction.

An hypothesis was made by Chappell et al. (2003), that the addition of substituents on the cyclic chelate may help to adopt a lower energy configuration that speeds up the labeling and gives a better in vivo stability in the serum and at low pH. The addition of a methyl (1B4M-DOTA) and a cyclohexyl (CHX-DOTA) was studied to verify this hypothesis. The chelates were conjugated to Herceptin and labeled with Lu-177. 1B4M-DOTA has a similar kinetic rate as C-DOTA and PA-DOTA. However, CHX-DOTA has faster kinetics but a lower yield than C-DOTA. The serum stability showed a loss of activity of 2.7, 1.8, 0.4 and 0.2% for CHX-DOTA, C-DOTA, 1B4M-DOTA and PA-DOTA respectively. The tumor uptake of 1B4M-DOTA (22.3 %ID/g) was equivalent

to the one of C-DOTA (24.3%ID/g), but PA-DOTA (18.1%ID/g) and CHX-DOTA (18.1%ID/g) was lower. The liver uptake was equivalent for 1B4M-DOTA (4.8%ID/g) and C-DOTA (4.8%ID/g), but was higher for CHX-DOTA (6.65%ID/g) and PA-DOTA (5.8%ID/g) (see Table 19-7).

The following are other macrocyclic chelators to be considered for radiometals whose size may not be optimal for DOTA and DTPA based ligands:

3.2.4. Bifunctional Chelates for ^{64}Cu

The chemistry of copper is restricted to two oxidation states (I and II). The redox and complexation chemistry of copper is well known. New chelates have been developed for copper to obtain faster kinetics and improved stability when compared to DOTA (Smith 2004). The chelates commonly used with ^{64}Cu and ^{67}Cu are DOTA, TETA, cross-bridged cyclam (Hubin and Meade 2002) and SarAr (Fig. 19-7).

With DOTA, the labeling reaction requires a pH of 5.5 at room temperature for a period between 30 and 45 min. Cross-bridged cyclam requires similar reaction time with a temperature of 75°C and a basic pH. SarAr can be labeled with a wide range of pH (from 4 to 9) at room temperature, with a reaction time of only 2 min. SarAr has also an excellent stability in acid, with no detectable loss of Cu. These chelates showed excellent stability in serum over 24 h (Table 19-8).

Table 19-7. Stability comparison of DOTA derivatives.

Chelate	Metal loss in serum (%)	Tumor uptake (%ID/g)	Liver uptake (%ID/g)
CHX-DOTA	2.7	18.1	6.65
PA-DOTA	0.2	18.1	5.8
IB4M-DOTA	0.4	22.3	4.8
C-DOTA	1.8	24.3	4.8

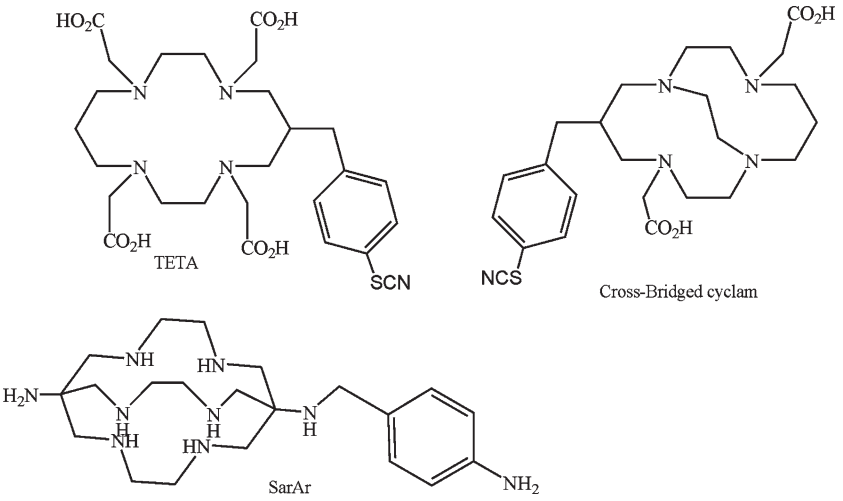

Fig. 19-7. Copper chelates

Table 19-8. Stability of copper chelates.

Chelate	pH	Time (min)	Temperature (°C)	Stability in serum (24 h)
DOTA	5.5	45	20–25	>99
TETA	5.5	30	20–25	98
Cross-bridged cyclam	>8.0	60	75	>99
SarAr	4–9	<2	20–25	>99.0

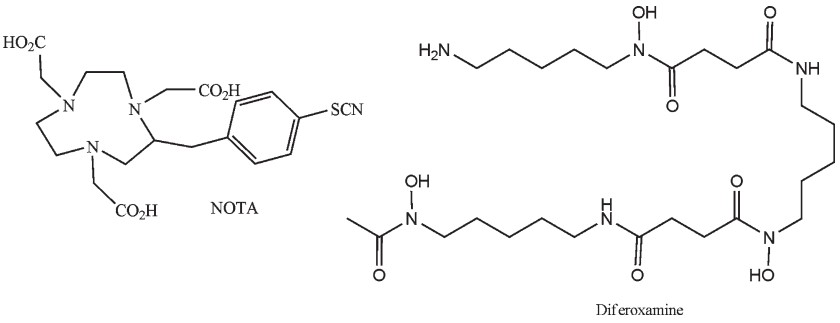

Fig. 19-8. Gallium chelates

3.2.5. Bifunctional Chelates for ^{68}Ga

Gallium coordination chemistry is similar to In(III). The cyclic chelators most often used for Ga(III) are NOTA, DOTA and TETA. Some acyclic chelators can also be used such as deferroxamine (Smith-Jones et al. 1994) (see Fig. 19-8). NOTA has been shown to be far superior to 1B4M-DTPA when conjugated to antibody T010 and labeled with ^{67}Ga (Lee et al. 1997), to DOTA and to TETA (Broan et al. 1991).

DTPA is a commonly used bifunctional chelate with ^{99m}Tc that has non desirable uptake in the liver. Hydrazinonicotinamide HYNIC (Rennen et al. 2000), diamine dimercaptide N_2S_2 (Luyt et al. 1999), and *N*-hydroxysuccinimide of mercaptoacetyl triglycine ester MAG3 (Hnatowich et al. 1998; Fritzberg et al. 1992) are alternate chelates for consideration with pertechnetate (or perrhenate) (see Fig. 19-9). Once these chelates have been conjugated to an antibody, the labeling is carried out by adding $^{99m}TcO_4^-$ in the presence of a reducing agent such as Sn^{2+} or by a ligand exchange with a weak ^{99m}Tc-chelate such as ^{99m}Tc-gluceptate, ^{99m}Tc-tartrate, or ^{99m}Tc-citrate.

3.2.6. New Bifunctional Chelates

Macrocyclics and MDS Nordion developed new chelates: PCTA and OXO (Fig. 19-10). The goal of these new chelates, presently under investigation, is to achieve kinetic properties superior to DOTA and achieve in vivo and in vitro stability similar to DOTA.

4. Manufacturing of Radiolabeled Antibodies

Depending on the half-life of the radionuclide, the type of decay, energy, nature of the antibody, and its stability, there are two approaches that can be made for preparing and manufacturing radioimmunoconjugates; a so-called

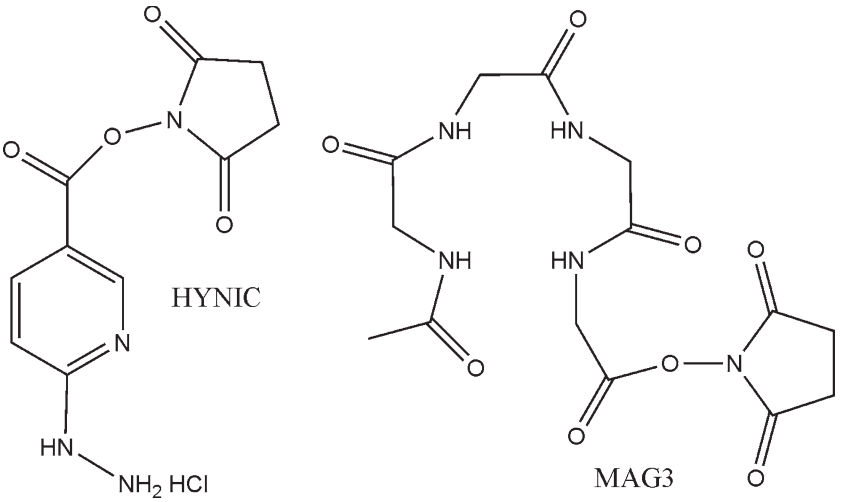

Fig. 19-9. Technetium chelates

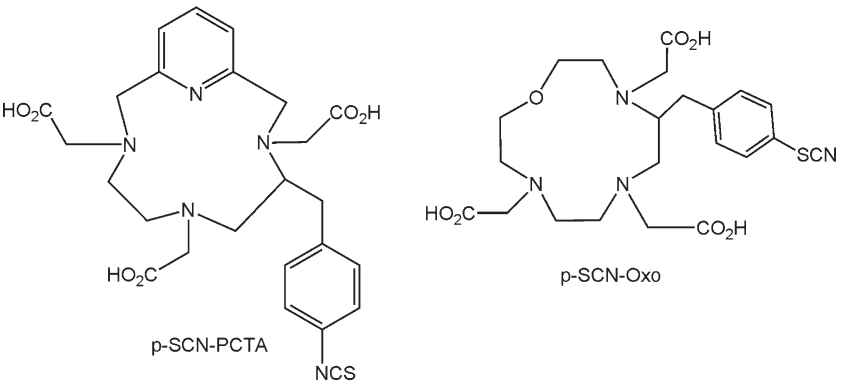

Fig. 19-10. PCTA and OXO chelates

"kit" approach whereby the antibody radiolabeling is carried out typically at a single dose level, either at the location where it will be used or at a radiopharmacy. The other approach is central manufacturing where the radiolabeling is carried out on a larger batch scale, usually not exceeding 100 Curies, using the same controls required for small scale parenteral drug manufacture, and individual doses are aseptically filled, packaged, and distributed to hospitals or clinics. Irrespective of the approach, all commercial radioimmunoconjugate manufacturing for human use must be carried out following current Good Manufacturing Practice in a validated facility using validated materials, processes, test methods, and equipment, and be in compliance with nuclear safety and environment regulations.

4.1. Radiolabeling of Antibodies with Kits

Radioimmunoconjugate kits can be conveniently stored until ready for use and are most suitable for short-lived radionuclides such as ^{99m}Tc, ^{68}Ga, and ^{64}Cu. Zevalin (ibritumomab tiuxetan) is the first radioimmunotherapeutic kit product

that consists of four vials: a reaction vial, a vial containing the anti-CD 20 antibody–MX DTPA conjugate, a diluent vial and a buffer vial.

A key advantage of the kit approach is that it can allow for the substitution of radionuclides that share similar chemistry. With Zevalin, the kit is first prepared with ^{111}In and the patient undergoes an imaging study to confirm distribution and tumor uptake. Assuming appropriate distribution in the patient, following 7 days from the imaging injection another Zevalin kit is formulated with ^{90}Y and the patient is given the therapy. Quality control testing for kits at the radiopharmacy consists of instant thin layer chromatography, dose calibrator measurement, pyrogen and sterility testing.

4.2. Central Radiolabeling of Antibodies

Central manufacturing of radioimmunoconjugates is most suitable for radionuclides with half-lives of at least 13 h, and where the conjugate can be formulated to achieve adequate stability to enable shipment from the manufacturer to the hospital or clinic. ^{131}I and ^{177}Lu are radionuclides with a half-life suitable for central manufacturing. A frequent stability objective for a central manufactured radioimmunotherapeutic is 5–6 days from the time of manufacture and some diagnostic radioimmunoconjugates have been formulated to have stability for more than 7 days. ^{131}I Bexxar (tositumab) is the first centrally manufactured therapeutic radioimmunoconjugate approved by the US FDA. A key advantage with central manufacturing is that the radioimmunoconjugate can be sent directly to the hospital or clinic and the radiopharmaceutical only requires handling to dispense and measure the dose, therefore radiation exposure to personnel is reduced in comparison to kits.

The following processes are involved with central manufacturing:

4.2.1. Radiolabeling

Depending on the radionuclide, the methods for radiolabeling have been previously described in this chapter.

4.2.2. Purification

Two methods are commonly used to purify radioimmunoconjugates: gel chromatography and ion exchange resin.

Gel chromatography separates component by size, with larger molecules eluting faster than smaller one. Fractions of eluate are collected, the radioactivity is measured for each fraction, and the components in each fraction are identified. The fractions containing the radiolabeled compound are pooled together. The length and the diameter of the size exclusion column are dependant on the volume of sample. With larger batch size, the column becomes too cumbersome to be used inside a hot cell.

Two kinds of ion exchange resins are available: cation exchange resin and anion exchange resin. An anion exchange resin will retain anions while cation exchange resin will retain cations. Anion exchange resins are commonly used to remove free iodine from iodine labeled antibody. The size of the ion exchange column is dependant of the amount of anions or cations that needs to be removed and is independent of the volume. The capacity of the resin is measured as milliequivalent of ions per gram of resin. As a rule of thumb, the

capacity of the size exclusion resin should be at least four times the amount of milliequivalent ions per gram that is needed to purify the labeled antibody.

4.2.3. Formulation

Antibody integrity is difficult to maintain in formulations consisting of alpha or beta emitting radionuclides. The factors that influence the stability of a radiolabeled antibody are related to the physical characteristics of the radionuclide: energy, type of decay, activity concentration, specific activity, storage temperature and the amount and type of stabilizer.

Activity concentration is defined as the amount of radioactivity per milliliter of solution. The total activity is the radioactivity per dose. The radiolytic decomposition increases with the activity concentration and the total activity.

Specific activity is defined as the radioactivity per gram of labeled antibody. High specific activity is required for biologically active antibodies. High specific activity could create an unstable product that can affect binding properties.

Storage temperature of the radioimmunoconjugate is also an important consideration. Lower temperature reduces the diffusion and the interaction of free radicals with the radiolabeled antibody and improves stability.

Emissions from the radionuclide attack the radiolabeled antibody or any other compound in close proximity, causing decomposition (Garrison 1987). Radiolysis causes the formation of free radicals, that are very reactive toward any organic molecules. Therefore, stabilizers must be included in the formulation to minimize radiolysis. The stabilizer must have antioxidant properties and be a free radical scavenger of type I and/or type II. A radical scavenger of type I neutralize free radicals formed as the results of absorption of ionization radiation by water molecules (i.e. $H^{\bullet}$ and $^{\bullet}OH$). A radical scavenger of type II neutralize free radicals formed as the results of absorption of ionization radiation by molecular oxygen (i.e. superoxide $O_2^{-\bullet}$ and singlet oxygen $^1O_2$).

Free radical scavengers such as human serum albumin (HSA), polyvinylpyrrolidone (Shochat et al. 1999), gentisic acid (Liu and Edwards 2001b) and ascorbic acid (Liu et al. 2003) have been used as stabilizers in radiolabeled antibodies.

4.2.4. Sterile Filtration

Radiolabeled antibodies are sensitive to heat and formulations cannot tolerate autoclaving. The radioimmunoconjugate is sterilized using a 0.2 μm membrane filter that removes organisms by a sieving mechanism. Dispensing is carried out aseptically in a validated Class 100 environment. A wide variety of filters for sterilization are available for different volume of batch size.

4.2.5. Quality Control

Radioimmunoconjugates are parenteral drugs and all quality control methods must be validated and carried out on validated test equipment.

4.2.5.1. Chemistry Testing

Chemistry testing on radioimmunocojugates includes the measurement of free radionuclide, radiochemical purity, pH and ionic strength, activity concentration and potency.

Free radionuclide is mostly measured by instant thin layer chromatography (ITLC). During the chromatographic process, the components of the sample are distributed between the adsorbent (stationary phase) and the solvent (mobile phase), depending on their affinity for either phase. Depending on the polarity, affinity to the stationary phase slows down the migration while affinity to the mobile phase speeds up the migration. The amount of free radionuclide is calculated as a ratio of the activity of the free radionuclide versus the total activity applied to the ITLC strip. The activity on the strip is measured using a scanner equipped with a radiation detector.

Radiochemical purity is measured by high performance liquid chromatography (HPLC), using a radiation detector. The separation between the components can be done either by mass with a size exclusion column or by polarity with a reverse phase column. The radiochemical purity of a radiopharmaceutical is the fraction of the activity representing the radiolabeled antibody compared to the degradation products and aggregates.

pH is measured using a pH meter and ideal pH should be around 7. Ionic strength or osmolality is also an important test and can be measured using an osmometer. Both pH meters and osmometers are available with microprobes reducing the size of the sample (50–70 μL) and the radiation dose to the operator.

Activity concentration measures the radioactivity per milliliter of solution. The activity concentration should also be measured at the end of the shelf life to ensure that the radiolabeled antibody remains intact.

4.2.5.2. Biological Testing

Immunoreactivity test is a measure of the binding property of the labeled antibody to an antigen that may be a receptor either on live cells, dead cell or receptor fragments. The labeling process may affect the binding property of the antibody to the antigen. The immunoreactivity is measured by determining the immunoreactive fraction (Lidmo et al. 1984) or by enzyme-linked immunosorbent assay (ELISA). The immunoreactive fraction is determined by linear extrapolation at infinite antigen-excess. The excess of antigen ensures that the true value of immunoreactive fraction is obtained as opposed to the apparent immunoreactive fraction. The ELISA assay combines the specificity of the antibodies with the sensitivity of an enzyme. The ELISA assay allows a direct comparison of the labeled antibody versus the unlabeled, without modifying the method to adapt to radioactive detection.

4.2.5.3. Sterility and Pyrogen Testing

United States Pharmacopeia (USP) 30 is followed for sterility and pyrogen testing. For sterility testing typically the membrane filtration method is used, and pyrogen testing may use either the gel-clot or colorimetric method.

References

Axworthy DB, Reno JM, Hylarides MD, Mallett RW, Theodore LJ, Gustavson LM, Su F, Hobson LJ, Beaumier PL, Fritzberg AR (2000) Cure of human carcinoma xenografts by a single dose of pretargeted yttrium 90 with negligible toxicity. Proc Natl Acad Sci U S A 97:1802–1807

Bolton AE, Hunter WM (1973) The labeling of proteins to high specific radioactivity by conjugation to a 125I- containing acylating agent. Biochem J 133:529–538

Broan CJ, Cox JPL, Craig AS, Kataky R, Parker D, Harrison A, Randall AM, Ferguson G (1991) J Chem Soc Perkin Trans 2:87–99

Buchanan L, Jurek P, Redshaw R (2007) Nuclear imaging drug development tools. GEN 27:23–25

Camera L, Kinuya S, Garmestani K, Wu C, Briechbiel MW, Pai LH, McMurry TJ, Gansow OA, Pastan I, Paik CH et al (1994) Evaluation of the serum stability and in vivo biodistribution of CHX-DTPA and other ligands for yttrium labeling of monoclonal antibodies. J Nucl Med 35:882–889

Casadevall A, Goldstein H, Dadachova E (2007) Targeting host cells harbouring viruses with radiolabeled antibodies. Expert Opin Biol Ther 7:595–597

Chappell LL, Ma D, Milenic DE, Garmestani K, Venditto V, Beitzel MP, Brechbiel MW (2003) Synthesis and evaluation of novel bifunctional chelating agents based on 1, 4, 7, 10-tetraazacyclododecane-*N*, *N*′, *N*″, *N*‴-tetraacetic acid for radiolabeling proteins. Nucl Med Biol 30:581–595

Cornelissen B, Hu M, McLarty K, Costantini D, Reilly RM (2007) Cellular penetration and nuclear importation properties of ^{111}In-labelled and ^{123}I-labeled HIV-1 Tat peptide immunocojugates in BT-474 human breast cancer cells. Nucl Med Biol 34:37–46

Dadachova, E. and Casadevall, A. (2005) Antibodies as delivery vehicles for radioimmunotherapy of infectious disease. Expert Opin. Drug Delivery 2(6):1075–1084

Dadachova E, Casadevall A (2006) Treatment of infection with radiolabeled antibodies. Q J Nucl Med Mol Imaging 50:193–204

Dadachova E, Patel MC, Toussi S, Apostolidis C, Morgenstern A, Brechbiel MW, Gorny MK, Zolla-Pazner S, Casadevall A, Goldenstein H (2006) Targeted killing of virally infected cells by radiolabeled antibodies to viral proteins. PLoS Med 3:2094–2103

Doran DM, Spar IL (1980) Oxidative iodine monochloride iodination technique. J Immunol Methods 39:155–163

Fichna J, Janecka A (2003) Synthesis of target-specific radiolabeled peptides for diagnostic imaging. Bioconjug Chem 14:3–17

Fraser PJ, Speck JC (1978) Protein and cell membrane iodinations with a sparingly soluble chloramide, 1, 3, 4, 6-tetrachloro-3a, 6a-diphenylglycoluril. Biochem Biophys Res Commun 80:849–857

Fritzberg AR, Berninger RW, Hadley SW, Wester DW (1988) Approaches to radiolabeling of antibodies for diagnosis and therapy of cancer. Pharm Res 5:325–334

Fritzberg AR, Kasina S, Rao TN, VanderHeyden JL, Srinivasan A (1992) Metal-radionuclide-labeled proteins and glycoproteins for diagnosis and therapy. US Patent 5,091,514

Gansow OA, Brechbiel MW (1989) Backbone polysubstituted chelate for forming a metal chelate protein conjugate. US Patent 4831175

Gansow OA, Brechbiel MW (1992) Bifunctional DTPA-type ligand. US Patent 05124471

Garg PK, Archer GE, Bigner DD, Zalutsky MR (1989) Synthesis of radioiodinated *n*-succinimidyl iodobenzoate: optimization for use in antibody labeling. Appl Radiat Isot 40:485–490

Garg PK, Garg S, Zalutsky MR (1993) *N*-Succinimidyl 4-methyl-3-(tri-*n*-butylstannyl) benzoate: synthesis and potential utility for the radioiodination of monoclonal antibodies. Nucl Med Biol 20:379–387

Garrison WM (1987) Reaction mechanisms in the radiolysis of peptides, polypeptides and proteins. Chem Rev 87:381–398

Goldenberg DM (2002) Targeted therapy of cancer with radiolabeled antibodies. J Nucl Med 43:693–713

Goldenberg DM, Sharkey RM (2006) Advances in cancer therapy with radiolabeled monoclonal antibodies. Q J Nucl Med Mol Imaging 50:248–264

Goldenberg DM, DeLand F, Kim E, Bennett S, Primus FJ, van Nagell JR, Estes N, DeSimone P, Rayburn P (1978) Use of radiolabeled antibodies to carcinoembryonic antigen for the detection and localization of diverse cancers by external photoscanning. N Engl J Med 298:1384–1386

He J, Liu G, Dou S, Gupta S, Rusckowski M, Hnatowich D (2007) An improved method for covalently conjugating morpholino oligomers to antitumor antibodies. Bioconjug Chem 18:983–988

Helmkamp RW, Contreras MA, Bale WF (1967) I-131 labeling of protein by iodine monochloride. Int J Appl Radiat Isot 18:737–746

Hnatowich DJ, Mardirossian G, Ruskowski M, Fogarasi M, Virzi F, Winnard P Jr (1993) Directly and indirectly technicium-99m-labeled antibodies-A comparison of in vitro and animal in vivo properties. J Nucl Med 34:109–119

Hnatowich DJ, Qu T, Chang F, Ley AC, Ladner RC, Rusckowsky M (1998) Labeling peptides with technitium-99m using a bifunctional chelator of a *N*-hydroxysuccinimde ester of mercaptoacetyltriglycine. J Nucl Med 39:56–64

Hu M, Chen P, Chan C, Scollard DA, Reilly RM (2006) Site-specific conjugation of HIV-1 Tat peptides to IgG: a potential route to construct radioimmunoconjugates for targeting intracellular and nuclear epitopes in cancer. Eur J Nucl Med Mol Imaging 33:301–310

Hubin TJ, Meade TJ (2002) Novel macrocyclics magnetic resonance imaging contrast agents. International Patent WO 02/006287.A2

Hunter WM, Greenwood FC (1962) Preparation of iodine-131 labeled human growth hormone of high specific activity. Nature 194:495–496

Jurcic JG (2005) Immunotherapy for acute myeloid leukemia. Curr Oncol Rep 7:339–346

Kaminski MS, Estes J, Zasadny KR, Francis IR, Ross CW, Tuck M, Regan D, Fisher S, Gutierrez J, Kroll S, Stagg R, Tidmarsh G, Wahl RL (2000) Radioimmunotherapy with ^{131}I tositumomab for relapsed refractory B-cell non-hodgkin lymphoma: updated results and long term follow-up of the University of Michigan Experience. Blood 96:1259–1266

Lee J, Garmestani K, Wu C, Brechbiel MW, Chang HK, Choi CW, Gansow OA, Carrasquillo JA, Paik CH (1997) In vitro and in vivo evaluation of structure–stability relationship of ^{111}In and ^{67}Ga-labeled antibodies via 1B4M and C-NOTA chelates. Nucl Med Biol 24:225–230

Lidmo T, Boven E, Cuttitta F, Fedorko J, Bunn PA (1984) Determination of the immunoreactive fraction of radiolabeled monoclonal antibodies of radiolabeled monoclonal antibodies by linear extrapolation to binding at infinite antigen excess. J Immunol Methods 72:77–89

Lin Y, Pagel JM, Axworthy D, Pantelias A, Hedin N, Press OW (2006) A genetically engineered anti-cd45 single-chain antibody–streptavidin fusion protein for pretargeted radioimmunotherapy of hematologic malignancies. Cancer Res 66:3884–3892

Liu S, Edwards DS (2001a) Bifunctional chelators for therapeutic lanthanide radiopharmaceuticals. Bioconjug Chem 12:7–34

Liu S, Edwards DS (2001b) Stabilization of ^{90}Y-labled DOTA-biomolecule conjugates using gentisic acid and ascorbic acid. Bioconjug Chem 12:554–558

Liu G, Mang'era K, Liu N, Gupta S, Rusckowski M, Hnatowich DJ (2002) Tumor pretargeting in mice using ^{99m}Tc-labeled morpholino, a DNA analog. J Nucl Med 43:384–391

Liu S, Ellars CE, Edwards DS (2003) Ascorbic acid: useful as a buffer agent and radiolytic stabilizer for metalloradiopharmaceuticals. Bioconjug Chem 14:1052–1056

Liu G, Dou S, Mardirossian G, He J, Zhang S, Liu X, Rusckowski M, Hnatowich D (2006) Successful radiotherapy of tumor in pretargeted mice by ^{188}Re radiolabeled phosphorodiamidate morpholino oligomer, a synthetic DNA analogue. Clin Cancer Res 12:4958–4964

Liu G, Dou S, Yin D, Squires S, Liu X, Wang Y, Rusckowski M, Hnatowich D (2007) A novel pretargeting method for measuring antibody internalization in tumor cells. Cancer Biother Radiopharm 22:33–39

Luyt LG, Jenkins HA, Hunter DH (1999) An N2H2 Bifunctional chelator for technitium-99m and rhenium complexation, conjugation and epimerization to a single isomer. Bioconjug Chem 10:470–479

Marchalonis JJ (1969) An enzymatic method for the trace iodination of immunoglobulins and other proteins. Biochem J 113:299–305
Markwell MAK (1982) A new solid state reagent to iodinate proteins. Anal Biochem 125:427–432
McDevitt MR, Scheinberg DA (2002) Ac-225 and her daughters: the many faces of shiva. Cell Death Differ 9:593–594
Milenic DE, Garmestani K, Chappell LL, Dadachova E, Yordanov A, Ma D, Schlom J, Brechbiel MW (2002) In vivo comparison of macrocyclic and acyclic ligands for radiolabeling of monoclonal antibodies with ^{177}Lu for radioimmunotherapeutic applications. Nucl Med Biol 29:432–442
Moosmayer D, Berndorff D, Chang C-H, Sharkey RM, Rother A, Borkowski S, Rossi EA, McBride WJ, Cardillo TM, Goldenberg DM, Dinkelborg LM (2006) Bispecific antibody pretargeting of tumor neovasculature for improved systemic radiotherapy of solid tumors. Clin Cancer Res 12:5587–5595
Paganelli G, Magnani P, Zito F, Villa E, Sudait F, Lopalco L, Rossetti C, Malcovati M, Chiolerio F, Seccamani E, Siccardi AG, Fazio F (1991) Three-step monoclonal antibody tumor targeting in carcinoembryonic antigen positive patients. Cancer Res 15:5960–5966
Pettit WA, Delard FH, Bennett SJ, Goldenberg DM (1980) Improved protein labeling by stannous tartrate reduction of pertechnatate. J Nucl Med 21:59–62
Pressman D (1949) The zone of localization of antibodies; the in vivo disposition of anti-mouse-kidney serum and anti-mouse-plasma serum as determined by radioactive tracers. J Immunol 63:375–388
Ram S, Buchsbaum DJ (1992) Development of 3-iodophenylisothiocyanate for radioiodination of monoclonal antibodies. Appl Radiat Isot 43:1387–1391
Ram S, Buchsbaum DJ (1994) Radioiodination of monoclonal antibodies D612 and 17-1A with 3-iodophenylisothiocyanate and their biodistribution in tumor-bearing nude mice. Cancer 73:808–815
Reilly RM (1991) Radioimmunotherapy of malignancies. Clin Pharm 10:359–375
Reilly RM (2006) Radioimmunotherapy of solid tumors: the promise of pretargeting strategies using bispecific antibodies and radiolabelled haptens. J Nucl Med 47:196–199
Rennen HJ, Boerman OC, Koendens EB, Oyen WJ, Corsten FH (2000) Labeling proteins with Tc-99m via hydrazinonicotinamide (HYNIC). Optimization of the comjugation reaction. Nucl Med Biol 27:599–604
Rossi AR, Goldenberg DM, Cardillo TM, McBride WJ, Sharkey RM, Chang CH (2006) Stably tethered multifunctional structures of defined composition made by the dock and lock method for use in cancer targeting. Proc Natl Acad Sci U S A 103:6841–6846
Sato N, Hassan R, Axworthy DB, Wong KJ, Yu S, Theodore LJ, Lin Y, Park L, Brechbiel MW, Pastan I, Paik CH, Carrasquillo JA (2005) Pretargeted radioimmunotherapy of mesothelin-expressing cancer using a tetravalent single-chain Fv–streptavidin fusion protein. J Nucl Med 46:1201–1209
Sharkey RM, Goldenberg DM (2006) Targeted therapy of cancer: new prospects for antibodies and immunoconjugates. CA Cancer J Clin 56:226–243
Sharkey RM, Cardillo TM, Rossi EA, Chang C-H, Karacay H, McBride WJ, Hansen HJ, Horak ID, Goldenberg DM (2005) Signal amplification in molecular imaging by pretargeting a multivalent bispecific antibody. Nat Med 11:1250–1255
Shochat D, Chan ASK, Buckley MJ, Colcher D (1999) Radioprotectant for peptides labeled with radioisotopes. US Patent 5,961,955
Smith SV (2004) Molecular imaging with copper-64. J Inorg Biochem 98:1874–1901
Smith-Jones PM, Stolz B, Bruns C, Albert R, Reist HW, Fridrich R, Maecke HR (1994) Galliuim-67/Galluim-68-[DFO]-Octreotide – a potential radiopharmaceutical for PET imaging of somatostatin receptor-positive tumors: synthesis and radiolabeling in-vitro and preliminary in-vivo studies. J Nucl Med 35:317–325

Stimmel JB, Kull FC Jr (1998) Samarium-153 and Lutetium-177 chelation properties of selected macrocyclic and acyclic ligands. Nucl Med Biol 25:117–125

Stimmel JB, Stockstill ME, Kull FC Jr (1995) Yttrium-90 chelation properties of tetraazatetraacetic acid macrocycles, diethyltriaminepentaacetic acid analogues and a novel terpyridine acyclic chelator. Bioconjug Chem 6:219–225

Supiot S, Faivre-Chauvet A, Couturier O, Heymann MF, Robillard N, Kraber-Bodéré F, Morandeau L, Mahé MA, Chérel M (2002) Comparison of the biological effects of MA5 and B-B4 monoclonal antibody labeled with Iodine-131 and Bismuth-213 on multiple myeloma. Cancer 94:1202–1209

Vaidynathan G, Zalutsky MR (1990a) Protein radiohalogenation: observations on the design of *N*-succinimidyl ester acylation agents. Bioconjug Chem 1:269–273

Vaidynathan G, Zalutsky MR (1990b) Radioiodination of antibodies via *N*-succinimidyl 2, 4-dimethoxy-3-(trialkylstannyl)benzoate. Bioconjug Chem 1:387–393

Vaidyanathan G, Affleck D, Zalutsky MR (1993) Radioiodination of proteins using *N*-succinimidyl 4-hydroxy-3-iodobenzoate. Bioconjug Chem 4:78–84

Volkert WA, Goeckler WF, Ehrhardt GJ, Ketring AR (1991) Therapeutic radionuclides: production and decay property considerations. J Nucl Med 32:174–185

Wilbur DS, Hadley SW, Grant LM, Hylarides MD (1991) Radioiodinated iodobenzoyl conjugates of a monoclonal antibody Fab fragment. In vivo comparisons with chloramine-T-labeled Fab. Bioconjug Chem 2:111–116

Wilson DA, Garlich JR, Fordyce WA, Frank RK, Simon J, Goeckler WF, Cheng RC, Kruper WJ, McMillan K (1998) Macrocyclic tetraazacyclodecane conjugates and their use as diagnostic and therapeutic agents. US Patent 5,756,065

Witzig TE, Gordon LI, Cabanillas F, Cruczman MS, Emmanouilides C, Joyce R, Pohlman BL, Bartlett NL, Wiseman GA, Padre N, Grillo-Lopez AJ, Multani P, White CA (2002) Randomized controlled trial of yttrium-90 labeled ibritumomab tiuxetan radioimmunotherapy versus rituximab immunotherapy for patients with relapsed or refractory low grade follicular or transformed B-cell non-Hodgkin's lymphoma. J Clin Oncol 20:2453–2463

Wood FT, Wu NM, Gerhart JC (1975) The radioactive labeling of proteins with an iodinated amidination reagent. Anal Biochem 69:339–349

Wu C, Kobayashi H, Sun B, Yoo TM, Paik CH, Gansow OA, Carrasquillo JA, Pastan I, Brechbiel MW (1997) Stereochemical influence on the stability of radiometal complexes in vivo. Synthesis and evaluation of the four stereoisomers of 2-(*p*-nitrobenzyl)-trans-CyDTPA. Bioorg Med Chem 5:1925–1934

Zalutsky MR, Narula AS (1987) A method for the radiohalogenation of proteins resulting in decreased thyroid uptake of radioiodine. Appl Radiat Isot 38:1051–1055

Zumdahl S (1997) Chemistry. Houghton Mifflin, Boston, MA, 1118 p

Index